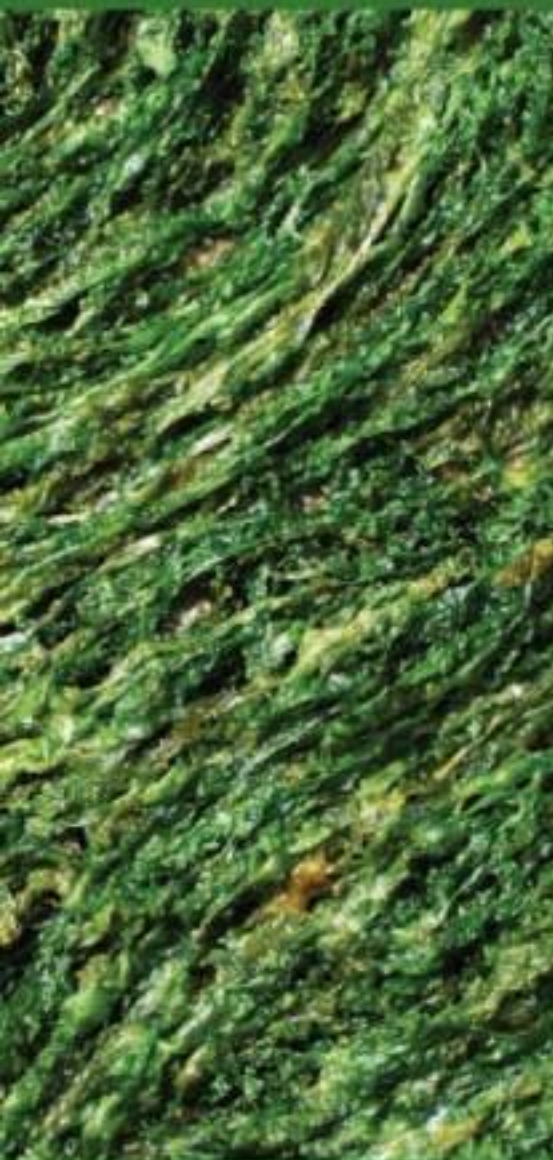


# PHYCOTOXINS

## Chemistry and Biochemistry



 **Blackwell**  
Publishing

**Luis M. Botana**  
*EDITOR*

# PHYCOTOXINS

Chemistry and Biochemistry

# PHYCOTOXINS

## Chemistry and Biochemistry

Luis M. Botana  
Editor

 **Blackwell**  
Publishing

**Dr. Luis M. Botana** is professor of Pharmacology, University of Santiago de Compostela, Spain. His group is a world leader in the development of new methods to monitor the presence of phycotoxins, having developed methods to date for saxitoxins, yessotoxin, pectenotoxin, ciguatoxins, brevetoxins, okadaic acid and dinophy-sistoxins. Dr. Botana is the editor of *Seafood and Freshwater Toxins: Pharmacology, Physiology and Detection*, to date the only comprehensive reference book entirely devoted to marine toxins.

©2007 Blackwell Publishing  
All rights reserved

Blackwell Publishing Professional  
2121 State Avenue, Ames, Iowa 50014, USA

Orders: 1-800-862-6657  
Office: 1-515-292-0140  
Fax: 1-515-292-3348  
Web site: [www.blackwellprofessional.com](http://www.blackwellprofessional.com)

Blackwell Publishing Ltd  
9600 Garsington Road, Oxford OX4 2DQ, UK  
Tel.: +44 (0)1865 776868

Blackwell Publishing Asia  
550 Swanston Street, Carlton, Victoria 3053, Australia  
Tel.: +61 (0)3 8359 1011

Authorization to photocopy items for internal or personal use, or the internal or personal use of specific clients, is granted by Blackwell Publishing, provided that the base fee is paid directly to the Copyright Clearance Center, 222 Rosewood Drive, Danvers, MA 01923. For those organizations that have been granted a photocopy license by CCC, a separate system of payments has been arranged. The fee codes for users of the Transactional Reporting Service is ISBN-13: 978-0-8138-2700-1/2007.

Printed on acid-free paper in the United States of America

First edition, 2007

Library of Congress Cataloging-in-Publication Data

Phycotoxins : Chemistry and biochemistry / edited by Luis Botana.—1st ed.  
p. cm.

Includes bibliographical references.

ISBN-13: 978-0-8138-2700-1 (alk. paper)

ISBN-10: 0-8138-2700-0 (alk. paper)

1. Algal toxins. I. Botana, Luis M. [DNLM: 1. Marine Toxins—chemistry. 2. Marine Toxins—metabolism. QW 630.5.M3 P578 2007]

RA1242.A36.P59 2007

615.9'45—dc22

2006032585

The last digit is the print number: 9 8 7 6 5 4 3 2 1

# Contents

Preface	vii
Contributors	ix
<b>1. Gambierol</b>	<b>1</b>
<i>Makoto Sasaki, Eva Cagide, and M. Carmen Louzao</i>	
<b>2. Brevetoxins: Structure, Toxicology, and Origin</b>	<b>19</b>
<i>Ambrose Furey, Keith O'Callaghan, Javier García Fernández, Mary Lehane, Mónica Fernández Amandi, and Kevin J. James</i>	
<b>3. Chemistry of Maitotoxin</b>	<b>47</b>
<i>Masayuki Satake</i>	
<b>4. Biochemistry of Maitotoxin</b>	<b>55</b>
<i>Laura A. de la Rosa, Emilio Alvarez-Parrilla, and Alejandro Martínez-Martínez</i>	
<b>5. Chemistry of Palytoxins and Ostreocins</b>	<b>75</b>
<i>Panagiota Katikou</i>	
<b>6. Biochemistry of Palytoxins and Ostreocins</b>	<b>95</b>
<i>Carmen Vale and Isabel R. Ares</i>	
<b>7. Chemistry of Cyanobacterial Neurotoxins — Anatoxin-a: Synthetic Approaches</b>	<b>119</b>
<i>Nuria Armesto Arbella, Keith O'Callaghan, Ambrose Furey, and Kevin J. James</i>	
<b>8. Anatoxin-a and Analogues: Discovery, Distribution, and Toxicology</b>	<b>141</b>
<i>Kevin J. James, Janet Crowley, Justine Duphard, Mary Lehane, and Ambrose Furey</i>	
<b>9. Pectenotoxins</b>	<b>159</b>
<i>Christopher O. Miles</i>	
<b>10. Chemistry, Origins, and Distribution of Yessotoxin and Its Analogues</b>	<b>187</b>
<i>Philipp Hess and John A.B. Aasen</i>	
<b>11. Pharmacology of Yessotoxin</b>	<b>203</b>
<i>Amparo Alfonso and Carmen Alfonso</i>	
<b>12. Chemistry of Diarrhetic Shellfish Poisoning Toxins</b>	<b>211</b>
<i>Paulo Vale</i>	

<b>13. The Molecular and Integrative Basis to Domoic Acid Toxicity</b>	<b>223</b>
<i>John S. Ramsdell</i>	
<b>14. Hepatotoxic Cyanobacteria</b>	<b>251</b>
<i>Ana Gago-Martinez</i>	
<b>15. Polycavernosides</b>	<b>275</b>
<i>Leo A. Paquette and Mari Yotsu-Yamashita</i>	
<b>16. Structural Assignment and Total Synthesis of Azaspiracid-1</b>	<b>297</b>
<i>Michael O. Frederick, Kevin P. Cole, Goran Petrovic, Eriketi Loizidou, and K.C. Nicolaou</i>	
<b>17. Biochemistry of Azaspiracid Poisoning Toxins</b>	<b>311</b>
<i>Natalia Vilarino</i>	
<b>18. Cyclic Imines: An Insight into this Emerging Group of Bioactive Marine Toxins</b>	<b>319</b>
<i>Jordi Molgó, Emmanuelle Girard, and Evelyne Benoit</i>	
Index	<b>337</b>

## Preface

Marine toxins are important to the scientific community because they pose many challenges. The first one is the obvious food safety issue, that requires a large investment in producing countries to regularly monitor the potential presence of these compounds in seafood. A second challenge is the potential these compounds offer as tools for research, since the variety of mechanistic actions is impressive. This book intends to offer a glimpse of this diversity of mechanisms of actions. The third challenge is the chemical structure of the compounds, from the simple domoic acid to the unusual structure of azaspiracid or the large molecule of palytoxin. Another goal to this editorial work is to provide an overall view on the chemical diversity of marine toxins. Not all the known toxins are included in this book, but only those that have been recently discovered or that still provide puzzles on their chemistry or pharmacology. Although to some groups the uncertainties are wide (how many yessotoxin analogs? are they toxic?), to others the mystery goes even to their structure (ovatatoxins?).

This book is the silent work of many great scientist who spared some of their very busy time to write their chapters. I express my admiration for their dedication and thank them for their contributions and their hard work.

I would like to thank Dr. Leo Nollet and Dr. Y. H. Hui for their editorial help, and the staff at Blackwell, especially Susan Engelken, for their excellent work.

Luis M. Botana  
2006

# Contributors

## **John A. B. Aasen (chapter 10)**

Norwegian School of Veterinary Sciences  
P.O. Box 8146  
N-0033, Oslo, Norway  
Email: John.Aasen@veths.no

## **Amparo Alfonso (chapter 11)**

Departamento de Farmacología  
Facultad de Veterinaria  
Universidad de Santiago de Compostela  
27002 Lugo Spain  
Ph: 34-982-252-242  
Email: ffmaar@lugo.usc.es

## **Carmen Alfonso (chapter 11)**

Departamento de Farmacología  
Facultad de Veterinaria  
Universidad de Santiago de Compostela  
27002 Lugo Spain  
Ph: 34-982-252-242  
Email: mcarmena@lugo.usc.es

## **Isabel R. Ares (chapter 6)**

Departamento de Farmacología  
Facultad de Veterinaria  
Universidad de Santiago de Compostela  
27002 Lugo Spain  
Ph: 34-982-252-242  
Email: miales@lugo.usc.es

## **Nuria Armesto Arbella (chapter 7)**

PROTEOBIO  
Mass Spectrometry Centre for Proteomics and Biotoxin Research  
Cork Institute of Technology  
Bishopstown, Cork, Ireland  
Ph: 353-21-4326701  
Fax: 353-21-4345191

## **Evelyne Benoit (chapter 18)**

Laboratoire de Neurobiologie Cellulaire et Moléculaire  
Unité Propre de Recherche 9040



Centre National de la Recherche Scientifique  
Institut Fédératif de Neurobiologie Alfred Fessard  
1 Avenue de la Terrasse  
Bâtiments 32–33  
91198 Gif-sur-Yvette Cedex, France  
Ph: 33-1-6982-3642  
Fax: 33-1-6982-4141

**Luis M. Botana (editor)**

Departamento de Farmacología  
Facultad de Veterinaria  
Universidad de Santiago de Compostela  
27002 Lugo Spain  
Ph: 34-982-252-242  
Email: luis.botana@lugo.usc.es

**Eva Cagide (chapter 1)**

Departamento de Farmacología  
Facultad de Veterinaria  
Universidad de Santiago de Compostela  
27002 Lugo Spain  
Ph: 34-982-252-242  
Email: evacaot@lugo.usc.es

**Kevin P. Cole (chapter 16)**

Scripps Institute  
Department of Chemistry  
University of California, San Diego  
10550 North Torrey Pines Road  
La Jolla, CA 92037, USA  
Ph: 858-784-2400  
Fax: 858-784-2469

**Janet Crowley (chapter 8)**

PROTEOBIO  
Mass Spectrometry Centre for Proteomics and Biotoxin Research  
Cork Institute of Technology  
Bishopstown, Cork, Ireland  
Ph: 353-21-4326701  
Fax: 353-21-4345191

**Laura A. de la Rosa (chapter 4)**

Departamento de Ciencias Básicas  
Instituto de Ciencias Biomédicas  
Universidad Autónoma de Ciudad Juárez  
Cd. Juárez, Chihuahua, Mexico  
Ph: 52-1613-7679  
Email: ldelaros@uacj.mx

**Mónica Fernández Amandi (chapter 2)**

Cork Institute of Technology  
Department of Chemistry  
Rossa Avenue  
Bishopstown, Cork, Ireland  
Ph: 353-21-4326701  
Fax: 353-21-4345191

**Michael O. Frederick (chapter 16)**

Scripps Institute  
Department of Chemistry  
University of California, San Diego  
10550 North Torrey Pines Road  
La Jolla, CA 92037, USA  
Ph: 858-784-2400  
Fax: 858-784-2469

**Ambrose Furey (chapters 2, 7, and 8)**

PROTEOBIO  
Mass Spectrometry Centre for Proteomics and Biotoxin Research  
Cork Institute of Technology  
Bishopstown, Cork, Ireland  
Ph: 353-21-4326701  
Fax: 353-21-4345191  
Email: afurey@cit.ie

**Ana Gago-Martinez (chapter 14)**

Departamento de Química Analítica y Alimentaria  
Universidad de Vigo  
Campus Universitario  
36310 Vigo, España  
Ph: 34-986-812284  
Cell: 34-619-016172  
Email: anagago@uvigo.es

**Javier García (chapter 2)**

Department of Chemistry  
Cork Institute of Technology  
Rossa Avenue  
Bishopstown, Cork, Ireland  
Ph: 353-21-4326701  
Fax: 353-21-4345191

**Emmanuelle Girard (chapter 18)**

Laboratoire de Neurobiologie Cellulaire et Moléculaire  
Unité Propre de Recherche 9040  
Centre National de la Recherche Scientifique  
Institut Fédératif de Neurobiologie Alfred Fessard

1 Avenue de la Terrasse  
Bâtiments 32–33  
91198 Gif-sur-Yvette Cedex, France  
Ph: 33-1-6982-3642  
Fax: 33-1-6982-4141

**Philipp Hess (chapter 10)**

Team Leader Biotoxin Chemistry  
Marine Institute  
Rinville, Oranmore  
Galway, Ireland  
Ph: 353-91-387200  
Fax: 353-91-387201  
Email: philipp.hess@marine.ie

**Kevin J. James (chapters 2, 7, and 8)**

PROTEOBIO  
Mass Spectrometry Centre for Proteomics and Biotoxin Research  
Cork Institute of Technology  
Bishopstown, Cork, Ireland  
Ph: 353-21-4326701  
Fax: 353-21-4345191  
Email: kjames@cit.ie

**Panagiota Katikou (chapter 5)**

National Reference Laboratory for Marine Biotoxins  
Institute of Food Hygiene  
Ministry of Rural Development and Food  
3A Limnou Street  
546 27 Thessaloniki, Greece  
Ph: 30-2310-552928  
Fax: 30-2310-566581  
Email: pkatikou@vet.auth.gr

**Mary Lehane (chapters 2 and 8)**

Department of Applied Sciences  
Limerick Institute of Technology  
Ireland  
Ph: 353-21-4326701  
Fax: 353-21-4345191

**Eriketi Loizidou (chapter 16)**

Scripps Institute  
Department of Chemistry  
University of California, San Diego  
10550 North Torrey Pines Road  
La Jolla, CA 92037, USA

Ph: 858-784-2400  
Fax: 858-784-2469

**M. Carmen Louzao (chapter 1)**

Departamento de Farmacología  
Facultad de Veterinaria  
Universidad de Santiago de Compostela  
27002 Lugo Spain  
Ph: 34-982-252-242  
Email: ffmclooj@lugo.usc.es

**Alejandro Martínez-Martínez (chapter 4)**

Departamento de Ciencias Básicas  
Instituto de Ciencias Biomédicas  
Universidad Autónoma de Ciudad Juárez  
Cd. Juárez, Chihuahua, Mexico  
Ph: 52-1613-7679

**Christopher O. Miles (chapter 9)**

AGResearch Ltd.  
Ruakura Research Centre  
East Street, Private Bag 3123  
Hamilton, New Zealand  
Ph: 64-7-838-5041  
Fax: 64-7-838-5189  
Email: chris.miles@agresearch.co.nz

**Jordi Molgó (chapter 18)**

Laboratoire de Neurobiologie Cellulaire et Moléculaire  
Unité Propre de Recherche 9040  
Centre National de la Recherche Scientifique  
Institut Fédératif de Neurobiologie Alfred Fessard  
1 Avenue de la Terrasse  
Bâtiments 32–33  
91198 Gif-sur-Yvette Cedex, France  
Ph: 33-169-82-3642  
Fax: 33-169-82-4141  
Email: Jordi.Molgo@nbcn.cnrs-gif.fr

**K. C. Nicolaou (chapter 16)**

Scripps Institute  
Department of Chemistry  
University of California, San Diego  
10550 North Torrey Pines Road  
La Jolla, CA 92037, USA  
Ph: 858-784-2400  
Fax: 858-784-2469  
Email: kcn@scripps.edu

**Keith O'Callaghan (chapters 2 and 7)**

PROTEOBIO

Mass Spectrometry Centre for Proteomics and Biotoxin Research

Cork Institute of Technology

Bishopstown, Cork, Ireland

Ph: 353-21-4326701

Fax: 353-21-4345191

**Leo A. Paquette (chapter 15)**

Evans Chemical Laboratories

Department of Chemistry

Ohio State University

100 West 18th Avenue

Columbus, OH 43210-1185, USA

Ph: 614-292-2520

Fax: 614-292-1685

Email: paquette.1@osu.edu

**Emilio Alvarez-Parrilla (chapter 4)**

Departamento de Ciencias Básicas

Instituto de Ciencias Biomédicas

Universidad Autónoma de Ciudad Juárez

Cd. Juárez, Chihuahua, Mexico

Ph: 52-1613-7679

**Goran Petrovic (chapter 16)**

Scripps Institute

Department of Chemistry

University of California, San Diego

10550 North Torrey Pines Road

La Jolla, CA 92037, USA

Ph: 858-784-2400

Fax: 858-784-2469

**John S. Ramsdell (chapter 13)**

Center for Coastal Environmental Health and Biomolecular Research

NOAA, National Ocean Service

219 Fort Johnson Road

Charleston, SC 29412, USA

Ph: 843-762-8510

Fax: 843-762-8700

Email: john.ramsdell@noaa.gov

**Makoto Sasaki (chapter 1)**

Graduate School of Life Sciences

Tohoku University

Tsutsumidori-Amamiya

Aoba-ku, Sendai 981-8555, Japan  
Ph: 022-717-8828  
Fax: 022-717-8897  
Email: msasaki@astr.bios.tohoku.ac.jp

**Masayuki Satake (chapter 3)**

Center for Marine Science  
University of North Carolina at Wilmington  
5600 Marvin K. Moss Lane  
Wilmington, NC 28409, USA  
Email: msatakenc@yahoo.co.jp

**Carmen Vale (chapter 6)**

Departamento de Farmacología  
Facultad de Veterinaria  
Universidad de Santiago de Compostela  
27002 Lugo Spain  
Ph: 34-982-252-242  
Email: mcvale@lugo.usc.es

**Paulo Vale (chapter 12)**

Laboratório de Biotoxinas Marinhas  
Departamento de Ambiente Aquático  
Instituto Nacional de Investigação Agrária e das Pescas  
IPIMAR  
Av. Brasília, 1449-006 Lisboa, Portugal  
Ph: 351-2130-27000  
Fax: 351-2130-15948  
Email: pvale@ipimar.pt

**Natalia Vilariño (chapter 17)**

Departamento de Farmacología  
Facultad de Veterinaria  
Universidad de Santiago de Compostela  
27002 Lugo Spain  
Ph: 34-982-252-242  
Email: nvilari@lugo.usc.es

**Mari Yotsu-Yamashita (chapter 15)**

Laboratory of Biophysical Chemistry  
Graduate School of Agricultural Science  
Tohoku University  
Tsutsumidori-Amamiyamachi  
Aoba-ku, Sendai 981-8555, Japan  
Ph: 81-22-717-8922  
Email: myama@biochem.tohoku.ac.jp

# 1 Gambierol

Makoto Sasaki, Eva Cagide, and  
M. Carmen Louzao

## Introduction

Gambierol (1) is a marine polycyclic ether toxin that was isolated by the Yasumoto group as a toxic constituent along with ciguatoxin congeners from the culture cells of *Gambierdiscus toxicus* collected at the Rangiroa Peninsula in French Polynesia. Its gross chemical structure including the relative stereochemistry has been determined by extensive two-dimensional (2D) nuclear magnetic resonance (NMR) experiments (Fig. 1.1; Satake, Murata, and Yasumoto 1993a). This intriguing toxin molecule consists of a transfused octacyclic polyether skeleton containing 18 stereogenic centers and a partially skipped triene side chain including a conjugated (*Z,Z*)-diene system, thus providing a formidable synthetic challenge. Subsequently, the absolute configuration has been established by derivatization and application of modified Mosher analysis (Morohashi, Satake, and Yasumoto 1998). The axial C5 hydroxy group was inverted to equatorial disposition by an oxidation/reduction sequence and then esterified with (*S*)- and (*R*)- $\alpha$ -methoxy- $\alpha$ -trifluoromethylphenylacetic acid (MTPA). NMR analysis of the derived MTPA esters unambiguously established the 6*S* configuration, allowing the absolute configuration of the whole molecule as shown in Fig. 1.1.

Gambierol (1) exhibits potent neurotoxicity against mice with minimal lethal dose (MLD) of 50  $\mu\text{g kg}^{-1}$  by intraperitoneal (i.p.) injection, and the neurological symptoms caused in mice resemble those shown by ciguatoxins. This finding implies the possibility that gambierol is also responsible for ciguatera seafood poisoning (Satake, Murata, and Yasumoto 1993a). Recently, Inoue et al. (2003) have described that gambierol (1) inhibits the binding of dihydrobrevetoxin B (PbTx-3) to voltage-gated sodium channels, although its binding affinity is significantly lower than those of brevetoxins and ciguatoxins. As is often the case with other polycyclic ether natural products, the extremely limited availability of gambierol (1) from natural sources has hampered detailed biological studies on this neurotoxin. Therefore, chemical total synthesis has been the only means to deliver useful quantities of this natural product. Consequently, considerable synthetic efforts toward gambierol (1) have been devoted, and to date three completed total syntheses have been independently reported by

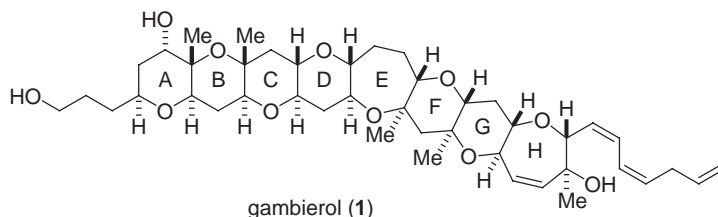


**Figure 1.1.** Structure of gambierol (1).

Fuwa et al. (2002a, 2002b), Kadota et al. (2003b, 2003c), Johnson, Majumder, and Rainier (2004, 2006), and Majumder et al. (2006). In this chapter, we discuss the chemical synthesis and biological properties of gambierol (1).

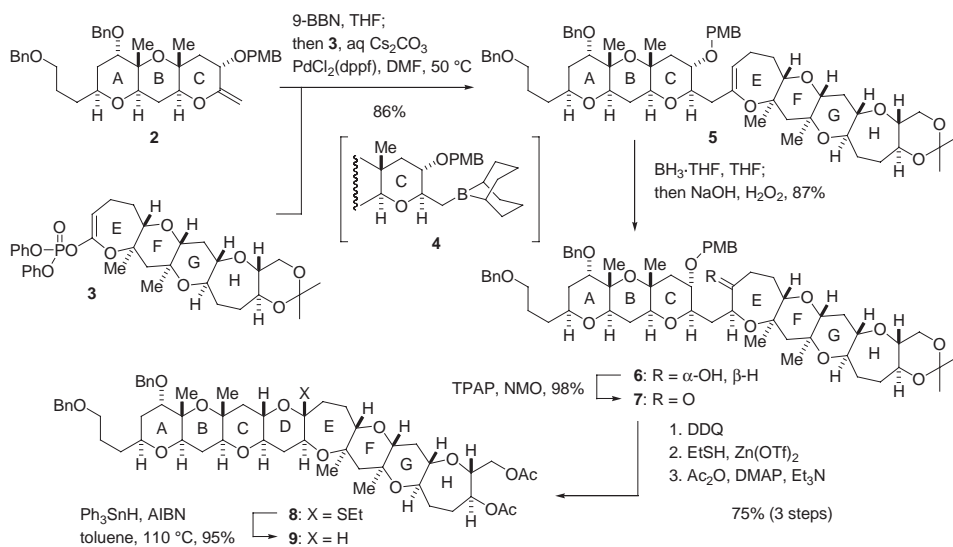
## Chemical Synthesis of Gambierol

### First Total Synthesis

In 2002, the first total synthesis of gambierol (1) was reported by Sasaki and co-workers (Fuwa et al. 2002a, 2002b). The convergent strategy employed for the synthesis of gambierol (1) is based on our developed Suzuki-Miyaura coupling chemistry (Sasaki et al. 1998, 1999, 2002; Sasaki and Fuwa 2004; Miyaura et al. 1986, 1989; Miyaura and Suzuki 1995; Chemler, Trauner, and Danishefsky 2001). The synthesis also features the stereoselective construction of the labile triene side chain through CuCl-accelerated Stille coupling at the final stage of the total synthesis.

Hydroboration of the ABC-ring exocyclic enol ether 2 (Fuwa et al. 2002a; Fuwa, Sasaki, and Tachibana 2001) with 9-borabicyclo[3.2.1] nonane (9-BBN) produced the corresponding alkylborane 4, which was coupled in situ with the EFGH-ring enol phosphate 3 (Fuwa et al. 2002a) in the presence of PdCl<sub>2</sub>(dppf) [dppf = 1,1'-bis(diphenylphosphino) ferrocene] and aqueous cesium carbonate in THF/DMF at 50°C to generate the desired cross-coupled product 5 in a gratifying 86% yield (Scheme 1.1). Given the structural complexity and size of the fragments, this remarkable yield demonstrates the power and reliability of the Suzuki–Miyaura cross-coupling reaction.

Subsequent hydroboration of endocyclic enol ether 5 proceeded stereoselectively to give alcohol 6, which was further oxidized with tetra-*n*-propylammonium perruthenate (TPAP) and *N*-methylmorpholine *N*-oxide (NMO) (Ley et al. 1994) to afford ketone 7. Oxidative removal of the *p*-methoxybenzyl (PMB) group followed by treatment with ethanethiol and zinc triflate effected cyclization of the D-ring

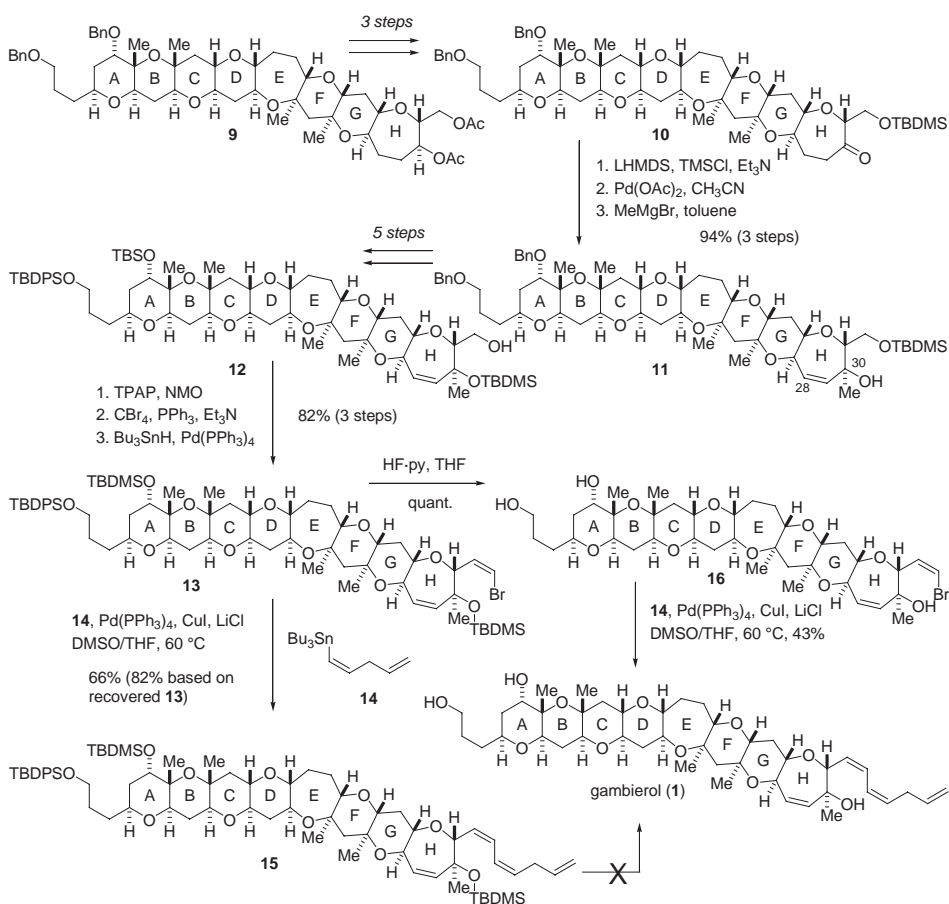


Scheme 1.1.



as the mixed thioketal to yield, after acetylation 8. Reduction of the ethylthio group was performed under radical conditions [ $\text{Ph}_3\text{SnH}$ , 2,2'-azobisisobutyronitrile (AIBN), toluene,  $110^\circ\text{C}$ ] (Nicolaou et al. 1989) to furnish the octacyclic polyether core 9 in 95% yield. Thus, the synthesis of the octacycle 9 was achieved in just seven steps from the coupling of two advanced intermediates 2 and 3.

For the functionalization of the H-ring, diacetate 9 was elaborated to ketone 10 in a three-step sequence (Scheme 1.2). Based on our preliminary model experiments, incorporation of the C28–C29 double bond was performed by means of the Ito-Saegusa protocol (Ito, Hirao, and Saegusa 1978). Thus, treatment of ketone 10 with lithium bis(trimethylsilyl)amide in the presence of chlorotrimethylsilane and triethylamine gave the corresponding enol silyl ether, which upon immediate exposure to palladium acetate in acetonitrile afforded the desired enone. Subsequent stereoselective introduction of the C30 axial methyl group was accomplished by treatment with methylmagnesium bromide in toluene at  $-78^\circ\text{C}$  (Feng and Murai 1992) to deliver tertiary alcohol 11 in 94% overall yield as a single stereoisomer. A further five-step sequence of protective group manipulations converted 11 into primary alcohol 12. Oxidation to the aldehyde and following Corey–Fuchs reaction (Corey and Fuchs



Scheme 1.2.

1972) afforded a dibromoolefin, which was reduced by the Uenishi protocol (Uenishi et al. 1998) to generate (*Z*)-vinyl bromide 13 in good overall yield.

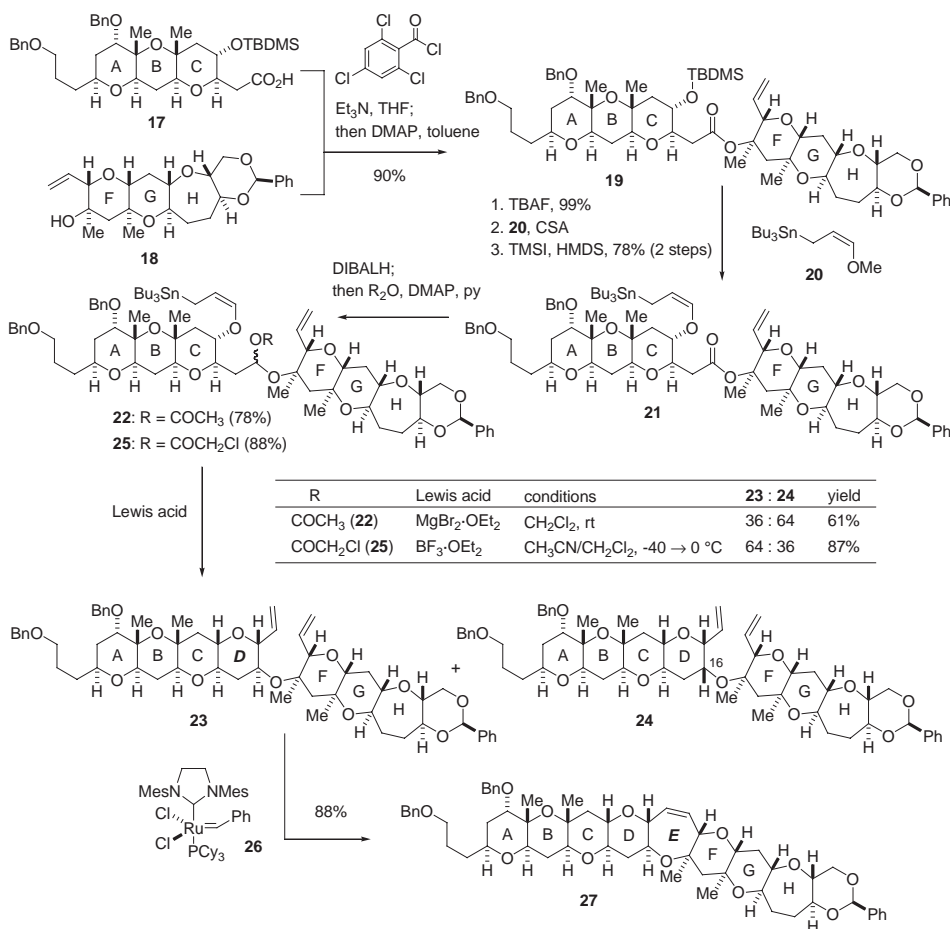
The final stages to complete the total synthesis required stereoselective installation of the triene side chain and global deprotection. The Stille coupling of (*Z*)-vinyl bromide 13 with (*Z*)-vinylstannane 14 (Shirakawa et al. 1999; Mastukawa et al. 1999) turned out to be troublesome due to the low reactivity of these substrates. After extensive experimentation, it was finally found that the Pd(PPh<sub>3</sub>)<sub>4</sub>/CuCl/LiCl-promoted modified Stille coupling conditions, originally developed by Han, Stolz, and Corey (1999), were quite suitable for the present case. Under the optimal conditions, the Stille coupling of 13 with 14 gave rise to fully protected gambierol (15) in 66% yield (82% yield based on recovered 13). However, all attempts to remove the silyl protective groups within 15 were unsuccessful. The sterically hindered C30 *tert*-butyldimethylsilyl (TBDMS) ether could not be cleaved under relatively mild conditions using various deprotection agents, including tetra-*n*-butylammonium fluoride (TBAF), HF·pyridine, Et<sub>3</sub>N·3HF, or tris(dimethylamino)sulfonium difluorotrimethylsilicate (TASF) (Noyori et al. 1980; Scheidt et al. 1998). In addition, isomerization or loss of the labile triene side chain was observed under harsh conditions.

This critical issue was overcome by carrying out global deprotection prior to introduction of the labile triene side chain. Treatment of (*Z*)-vinyl bromide 13 by excess HF·pyridine facilitated clean deprotection of the three silyl groups to deliver triol 16 in excellent yield. Finally, the Stille coupling of unprotected 16 with 14 under the established conditions [Pd(PPh<sub>3</sub>)<sub>4</sub>, CuCl, LiCl, DMSO/THF, 60°C] furnished (–)-gambierol (1) in 43% isolated yield. The spectroscopic data (<sup>1</sup>H NMR, <sup>13</sup>C NMR, HRMS, and CD) and mice lethality of synthetic gambierol were completely identical to those of the natural sample, thereby confirming the structure of gambierol including the absolute configuration. Thus, the first total synthesis of gambierol (1) was completed in 0.57% overall yield over a 71-step longest linear sequence. The total synthesis clearly demonstrated that the *B*-alkyl Suzuki–Miyaura coupling chemistry is an important and general fragment coupling process in polycyclic ether synthesis.

### Total Synthesis by the Yamamoto/Kadota Group

Shortly after the total synthesis of Sasaki and co-workers was published (Fuwa et al. 2002a, 2002b), the Yamamoto and Kadota group reported the second total synthesis of gambierol (1) (Kadota et al. 2003b, 2003c). The Yamamoto/Kadota synthesis was based on their developed convergent approach to polycyclic ether systems using an intramolecular cyclization of  $\gamma$ -alkoxyallylstannane to  $\alpha$ -acyloxy ether in conjunction with ring-closing metathesis (RCM) reaction (Kadota et al. 2001, 2003a; Kadota and Yamamoto 2005).

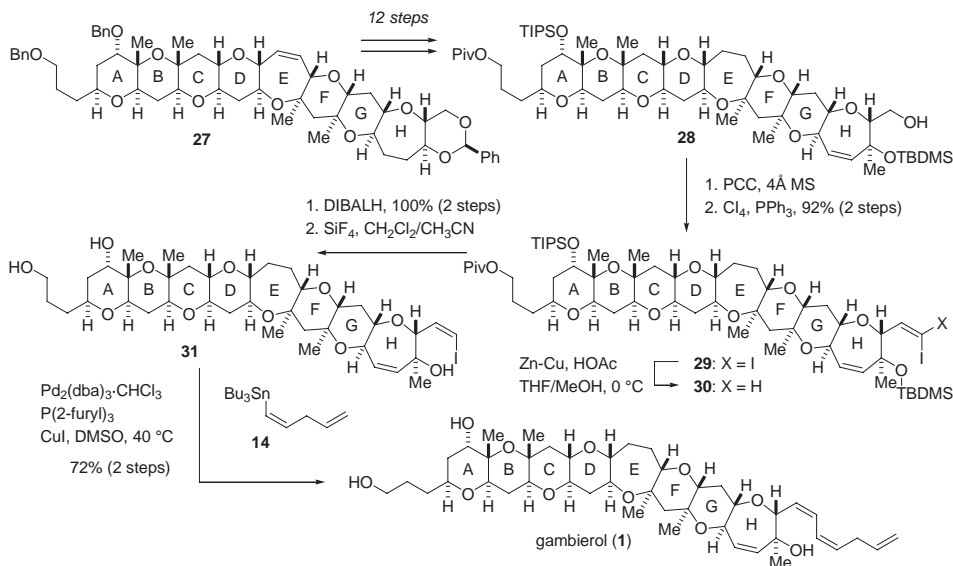
The synthesis commenced with coupling of the ABC- and FGH-ring fragments (17 and 18, respectively) through esterification to give 19 (Scheme 1.3). After removal of the TBDMS group with TBAF, the resultant alcohol was reacted with  $\gamma$ -methoxyallylstannane 20 in the presence of acid catalyst to yield a mixed acetal, which was then treated with iodotrimethylsilane and hexamethyldisilazane, leading to  $\gamma$ -alkoxyallylstannane 21. The ester 21 was then converted into  $\alpha$ -acetoxy ether 22 according to the method of Rychnovsky (Dahanukar and Rychnovsky 1996; Kopecky and Rychnovsky 2000, 2003). Thus, partial reduction of ester 21 with di-isobutylaluminum hydride (DIBALH), followed by in situ acetylation of the hemiacetal with acetic anhydride/4-(dimethylamino)pyridine/pyridine, gave 22 as an inseparable mixture of diastereomers in 78% yield. Treatment of 22 with magnesium bromide etherate (CH<sub>2</sub>Cl<sub>2</sub>, at room temperature) produced a mixture of the desired product 23 and its diastereomer 24, with the undesired 24 predominating (23:24 = 36:64). In contrast, reaction



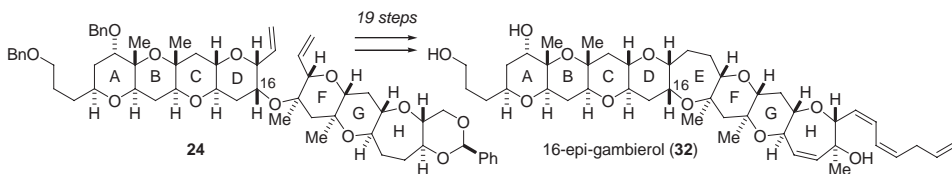
Scheme 1.3.

of  $\alpha$ -chloroacetoxy ether 25 with boron trifluoride etherate (20:1 CH<sub>3</sub>CN/CH<sub>2</sub>Cl<sub>2</sub>, -40°C to 0°C) led to the selective formation of 23 (23:24 = 64:36, 88% combined yield). This improved stereoselectivity is explained by the greater leaving ability of the  $\alpha$ -chloroacetoxy group to form the oxonium cation intermediate than that of the acetoxy group. The derived diene 23 was then subjected to RCM reaction using the second-generation Grubbs catalyst 26 (Scholl et al. 1999), leading to the octacyclic polyether 27 in high yield.

Functionalization of the H-ring of 27 was performed in a 12-step sequence similar to the Sasaki synthesis to afford primary alcohol 28 (Scheme 1.4). For the stereoselective introduction of the triene side chain, a simple and practical method for the synthesis of (*Z*)-iodoolefin has been developed (Kadota et al. 2003d). Thus, alcohol 28 was oxidized with pyridinium chlorochromate (PCC) to the aldehyde, which was then treated with Cl<sub>4</sub> and PPh<sub>3</sub> to yield di-iodoolefin 29 in high yield. Reduction of 29 with zinc-copper couple in the presence of acetic acid generated the desired (*Z*)-iodoolefin 30 exclusively. After a two-step deprotection, the derived triol 31 was subjected to the modified Stille coupling with (*Z*)-vinyl stannane 14. As expected, iodoolefin 31 showed higher reactivity than that of



Scheme 1.4.



Scheme 1.5.

the bromine counterpart, and the modified Stille coupling reaction with 14 [Pd<sub>2</sub>(dba)<sub>3</sub>·CHCl<sub>3</sub>, P(2-furyl)<sub>3</sub>, CuI, DMSO, 40 °C] proceeded smoothly to furnish gambierol (1) in 72% yield over the two steps. The longest linear sequence leading to 1 is 66 steps with 1.2% overall yield (102 total synthetic steps).

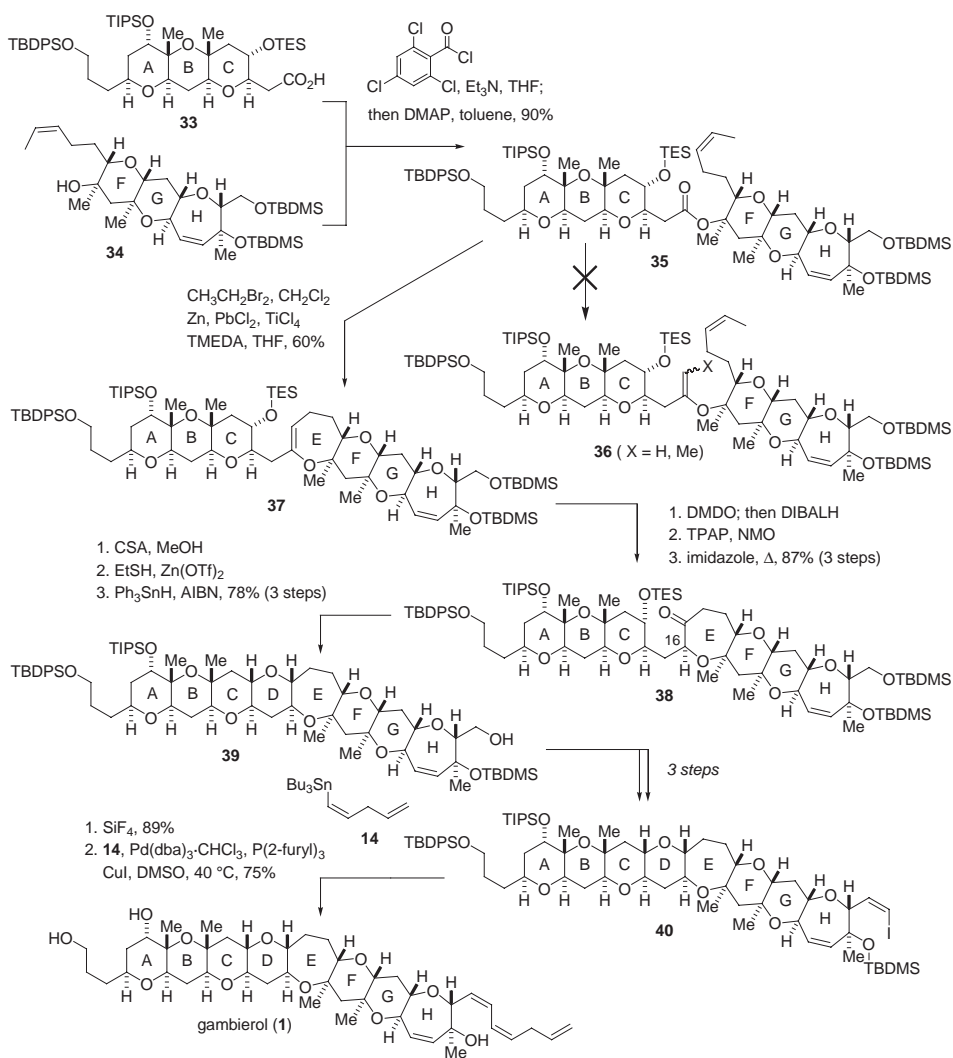
Similar transformations starting from the isomer 24 delivered 16-epi-gambierol (32), a non-natural analogue (Scheme 1.5). The epimer 32 exhibited no toxicity against mice at higher dose (14 mg/kg<sup>-1</sup>). This result indicates that the transfused polycyclic ether framework is essential to the toxicity (Kadota et al. 2003b).

### Total Synthesis by Rainier and Co-workers

Most recently, Rainier and co-workers accomplished a more convergent total synthesis of gambierol (1) (Johnson, Majumder, and Rainier 2004, 2006; Majumder et al. 2006). Their general strategy to fused polycyclic ether systems involves (a) synthesis of C-glycoside from coupling of cyclic enol ether with carbon nucleophiles and (b) tandem methylation/enol ether-olefin RCM. The synthesis commenced

with convergent union of the ABC- and FGH-ring fragments (33 and 34, respectively) through esterification by the Yamaguchi method to provide 35 (Scheme 1.6). Initial attempts to convert ester 35 into acyclic enol ether metathesis precursor 36 using the Takai-Utimoto titanium methylidene protocol (Okazoe and Takai 1987; Takai et al. 1994) were unsuccessful. After much experimentation, it was found that reaction of 35 with the titanium alkylidene, generated from 1,1-dibromoethane, led to the formation of seven-membered enol ether 37 in 60% yield. Furthermore, the expected acyclic enol ether product 36 (R = Me) was also obtained in 30% yield and could be converted to 37 in an unoptimized 60% yield by treating with the second-generation Grubbs catalyst 26.

Epoxidation of endocyclic enol ether 37 with dimethyl dioxirane (DMDO) followed by one-pot reduction with DIBALH produced a 10:1 mixture of alcohols, in which the major isomer possessed



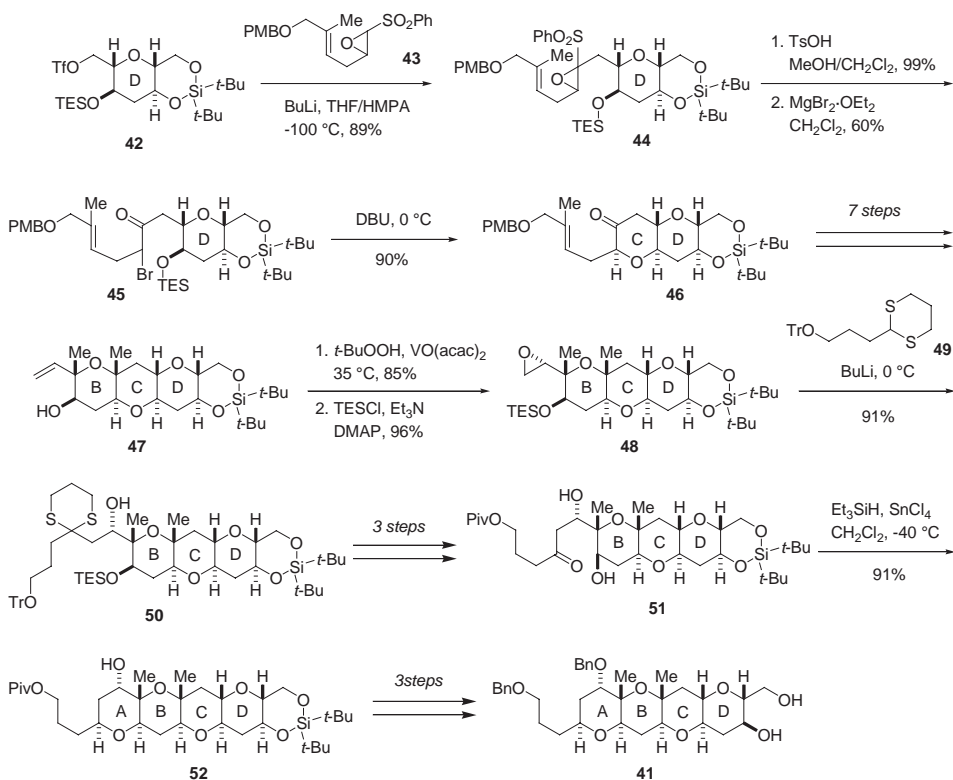
Scheme 1.6.

the correct stereochemistry at C16. Oxidation of these alcohols afforded ketone 38 and its C16 epimer, respectively. The minor diastereomer could be isomerized to 38 by treating with imidazole. Thus, the desired ketone 38 was obtained in 87% overall yield for the three steps. Subsequent construction of the D-ring was performed by reductive desulfurization of mixed thioketal in the same way as that adopted by the Sasaki group, leading to octacyclic ether 39. Stereoselective installation of the triene side chain was then carried out via (*Z*)-vinyl iodide 40 following Yamamoto's protocol to complete the total synthesis of gambierol (1).

The convergence aspect of the Rainier synthesis is particularly noteworthy in light of the use of fragment 34 furnished with the H-ring functionality. Thus, the longest linear sequence to the target was 44 steps from D-glucal with 1.2% overall yield.

### Synthesis of ABCD-ring Fragment by Mori and Co-workers

Very recently, Mori and co-workers reported the synthesis of the ABCD-ring fragment 41 of gambierol (1) (Furuta et al. 2005). Their synthesis features the oxiranyl anion strategy (Mori et al. 1996a, 1996b) to construct the C-ring and reductive etherification of  $\beta$ ,  $\delta$ -dihydroxy ketone to form the functionalized A-ring. The synthesis began with alkylation of the oxiranyl anion, derived from epoxy sulfone 43, with triflate 42, to afford 44 as a mixture of two diastereomers (Scheme 1.7). After removal of the



Scheme 1.7.

triethylsilyl (TES) group, treatment of the resultant alcohol with magnesium bromide etherate gave a 1:1 mixture of diastereomeric  $\alpha$ -bromo ketones 45. Subsequent treatment of this mixture with DBU generated ketone 46 with diastereomeric ratio (dr) = 94:6. A further seven-step sequence was required to form the B-ring of 47. The homoallylic hydroxy-directed epoxidation of 47 with *tert*-butyl hydroperoxide in the presence of vanadyl acetylacetonate [VO(acac)<sub>2</sub>] afforded the desired epoxide in high selectivity (dr = 93:7), which was then protected as the TES ether to give 48. Reaction of epoxide 48 with the lithium anion derived from 49 led to alcohol 50 in high yield, which was then converted into  $\beta,\gamma$ -dihydroxy ketone 51 in three steps. Upon treatment with triethylsilane and tin(IV) chloride, reductive etherification of 51 proceeded smoothly to afford 52 in 91% yield. A further two-step sequence was required to complete the synthesis of the ABCD-ring fragment 41.

## Diverted Synthesis of Gambierol Analogues for Structure-Activity Relationship Studies

There exist only a few reports concerning systematic structure–activity relationship studies of marine polycyclic ethers (Rein, Bade, and Gawley 1994; Rein et al. 1994; Gawley et al. 1995), mainly because of (a) extremely limited availability of these secondary metabolites from natural sources and (b) difficulties in chemical modification of the highly complex molecular structures. Our efficient and convergent chemical total synthesis realized the preparation of ample quantities of gambierol (1), while chemical modification of gambierol itself is seemingly quite difficult due to the presence of the labile functionalities, namely, the triene side chain and the C30 tertiary allylic alcohol. In this context, we envisioned that a variety of structural analogues could be accessed from an advanced intermediate, octacyclic polyether 9 (Scheme 1.1). Such concept has recently been termed “diverted total synthesis” by Njardarson et al. (2005).

We have synthesized 17 structural analogues of gambierol (1) and evaluated their toxicity against mice by *i.p.* injection to establish the structure-activity relationships (Fuwa et al. 2003, 2004). These studies revealed that structural elements required for exhibiting potent toxicity of gambierol (1) were (a) the C28–C29 double bond and (b) the unsaturated side chain with an appropriate length. In contrast to these important structural elements, the C1 and C6 hydroxy groups, the C30 axial-oriented methyl group, and the C34–C35 double bond are not essential but are preferred functional groups for exhibiting potent toxicity (Fig. 1.2).

The information gained from these structure-activity relationship studies should open the way for the design and synthesis of novel probe molecules, which are useful for further detailed biological studies of gambierol (1).

## Biology of Gambierol

Because of its structural novelty and toxicity, gambierol is quite interesting (Botana et al. 2004). However, detailed biological studies, including the precise biochemical mode of action, have been slowed down, partially due to the scarcity of this toxin from natural sources.

Gambierol exhibits potent toxicity against mice with a MLD of 50–80  $\mu\text{g kg}^{-1}$  by *i.p.* injection and 150  $\mu\text{g kg}^{-1}$  by peroral (*p.o.*) administration (Ito et al. 2003), doses that are even lower than for brevetoxins (PbTXs), such as PbTX-3 (200  $\mu\text{g kg}^{-1}$  *i.p.*) (Baden and Mende 1982). Based on the little difference between the two routes of administration, gambierol is considered to be absorbed efficiently from the intestine (Ito et al. 2003).



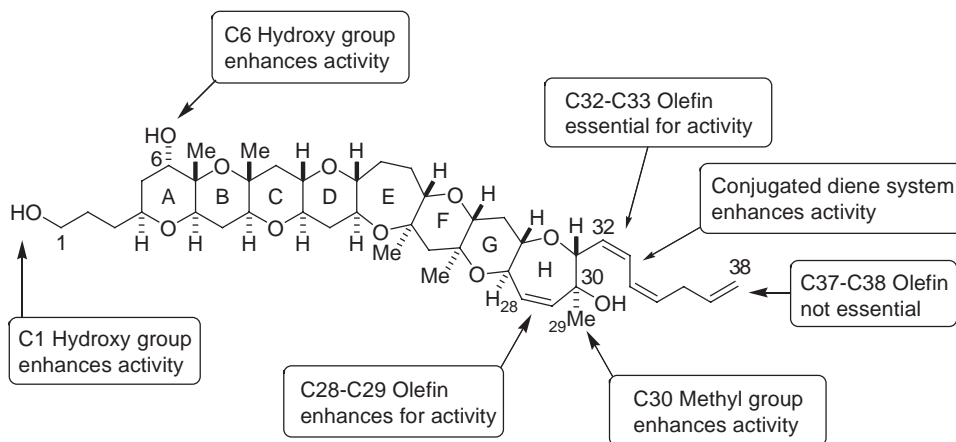


**Figure 1.2.** Structure-activity relationships of gambierol (1).

### Experimental Pathology (Morphological Response)

Gambierol and ciguatoxins (CTXs) have the same biogenetic origin (Satake, Murata, and Yasumoto 1993a). Ciguatoxins are the principal toxins responsible for ciguatera seafood poisoning (Murata et al. 1990; Lewis et al. 1991; Satake, Murata, and Yasumoto 1993b; Satake et al. 1997; Yasumoto et al. 2000). The symptoms of ciguatera vary somewhat geographically as well as between individuals, incidents, and the toxin congeners involved in the intoxication. They even may change temporally within an area (Van Dolah 2000b). Those symptoms generally include early gastrointestinal disturbance (nausea, vomiting, and diarrhea) followed by a variety of later neurological sequel (numbness of the peroral area and extremities, reversal of temperature sensation, muscle and joint aches, headache, itching, blurred vision, and paralysis) and cardiovascular alterations (tachycardia and hypertension) (Van Dolah 2000a, 2000b; Lewis 2001). Although in cases of severe toxicity, paralysis, coma, and death may occur, the corresponding fatality rate is low. However, the neurological symptoms last for weeks or even years (Yasumoto 2001). The minimum toxicity level to humans is estimated at  $0.5 \text{ ng kg}^{-1}$  (Legrand et al. 1992). The neurological symptoms caused in mice by gambierol resemble those shown by CTXs.

Neurosensory symptoms play an important role in ciguatera poisoning (Pearn 2001), although with maitotoxin and ciguatoxins (responsible for this disease) experimental animals showed no behavior that may be indicative of neurological effects (Lewis 2001). However, the use of gambierol elicited certain neurosensory-related reactions (scratching) in mice that Ito et al. (2003) suppose that humans might also present, although they do not know the specific symptoms and their duration. These pathological effects, as well as the biogenetic origin, imply the possibility that gambierol may be also responsible for ciguatera seafood poisoning.

Ito et al. (2003) studied the pathological effects on experimental mice after administrations of gambierol at  $60\text{--}150 \text{ } \mu\text{g kg}^{-1}$  and found that the worst condition periods of mice by gambierol were 1 hour via i.p. route, and 3 hours via p.o. If they could survive longer, recovery was likely, as well as the pathological changes.

**Symptoms:** With i.p. administration, the mice started to make small sounds and were crouching. Their bodies showed rapid respiratory throbbing and twitched frequently. Then, sometimes they



suddenly began to run and were wet around the mouth, chest, and forelegs with a nonblood liquid, although some of them showed blood-soaked faces, but this blood didn't come from the stomach. In addition, with p.o. administration, the mice started to scratch and hiccough. Abdominal swelling was prominent in all conditions, and an autopsy revealed gas accumulation in the intestines (Fig. 1.3). In lethal and serious conditions, some of the mice had congested or bleeding penises.

These symptoms suggest that the death of gambierol-treated mice is mainly due to dyspnea (Ito et al. 2003).

Postmortem examination: All treated mice showed congestion in the heart, with the right ventricles dilated with blood, and in the severe cases, the lungs, livers, and kidneys were also damaged (Ito et al. 2003).

At 2 hours after p.o. administration with  $140 \mu\text{g kg}^{-1}$  of gambierol, electron microscopy showed that the cardiac muscle fibers in the myocardium separated each other by edema and congestion (Figs. 1.4a and 1.4b), although the cell structure had no changes. Similar systemic congestions have been reported by palytoxin and ciguatoxins (Ito, Ohkusu, and Yasumoto 1996; Terao et al. 1991).

At 40–60 minutes, mice with severe damage (after administration of  $140\text{--}150 \mu\text{g kg}^{-1}$  of gambierol) showed narrowed alveolar lumens, which were filled with flocculent and/or fine granular substances in addition to surfactant (Figs. 1.4c and 1.4d). Alveolar macrophages as well as neutrophils and lymphocytes were also found frequently in those lumens when compared with the lung of control. Those immune-related cells were probably mobilized to remove gambierol from the alveolar lumens. After 2 days, bleeding and edema were observed outside of blood vessels near bronchioles.

Administration of gambierol elicited congestion in the liver, resulting in fatty changes around the central vein (Fig. 1.5a). A similar effect was obtained in the kidney, showing prominent congestion at the medulla.

The stomachs showed ulceration of mucosa, with bleeding on the surface and edema at submucosa (Fig. 1.5b). The intestines became dilated and lucent, containing gas and a yellowish liquid until 8 hours. The gas in the small intestine disappeared after 24 hours with  $100 \mu\text{g kg}^{-1}$  and after 48 h with  $140 \mu\text{g kg}^{-1}$ , with decreasing congestion.

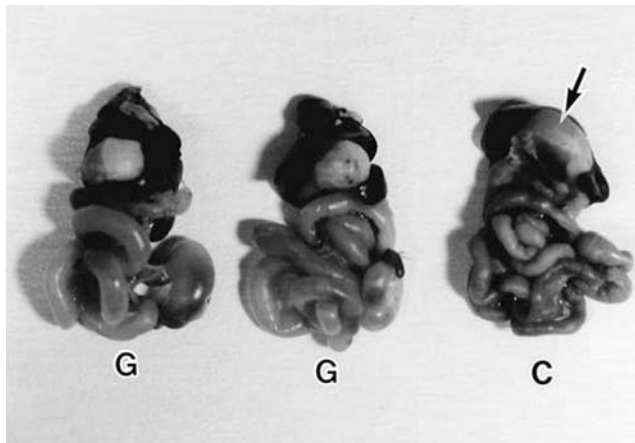


**Figure 1.3.** Internal organs of four-week-old mice 8 hours after p.o. administration of gambierol at  $100 \mu\text{g kg}^{-1}$  (Reprinted from Ito et al. 2003, with permission from Elsevier). G = Gambierol-treated mice had atrophic stomachs at this stage. The small intestine, cecum, and large intestine were swollen with gas. C = nontreated mouse organs, with arrow indicating the stomach.

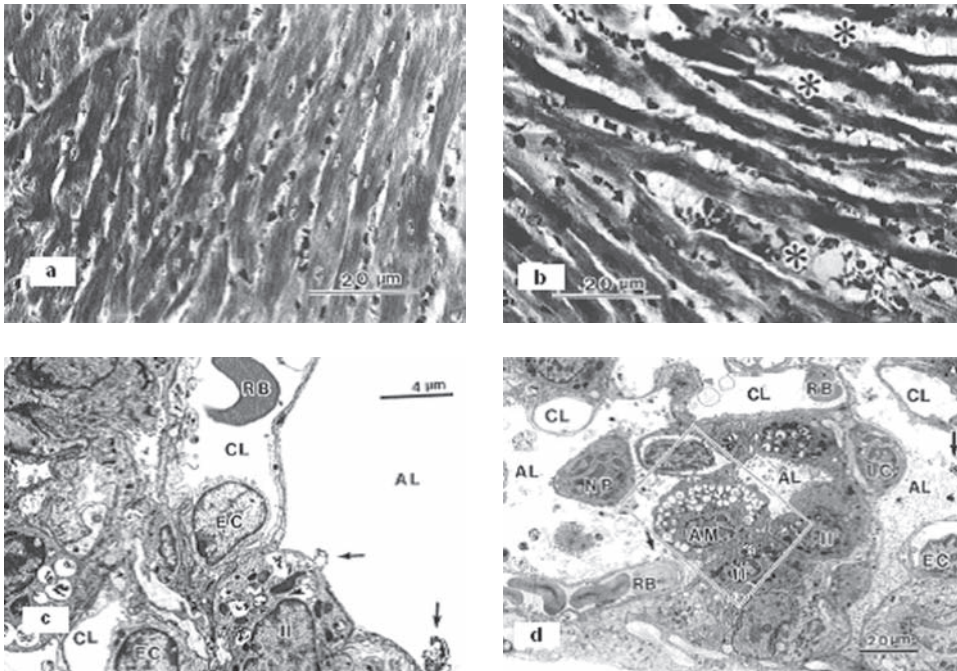


**Figure 1.4.** (a) The heart of control from nontreated mice and (b) 2 hours after p.o. administration of  $140 \mu\text{g kg}^{-1}$  gambierol. The myocardium showed separation of muscle fibers by edema (\*) and congestion. (c) The lung of control is shown, where the alveolar lumen (AL) is wide, and surfactant (arrows) can be seen on the epithelial surface. (d) A low-magnification image of the alveoli of a mouse in serious condition 40 minutes after p.o. administration of gambierol at  $140 \mu\text{g kg}^{-1}$ . Note the narrow alveolar lumens (AL) are filled with materials including surfactant (arrows). AM = alveolar macrophage in the alveolar lumen of the treated mice. II = type II alveolar cells. CL = capillary lumen. EC = endothelial cell. NP = neutrophil, RB = erythrocyte. (Reprinted from Ito et al. 2003, with permission from Elsevier)

### *Possible Pharmacological Targets for Gambierol*

Little information exists about the biological effects of gambierol, and molecular targets have not been fully elucidated yet. In any case, the biogenetic origin and pathological effects suggest that gambierol is also responsible for ciguatera poisoning (Ito et al. 2003).

So far, two possible targets have been suggested for gambierol: sodium channels (Inoue et al. 2003, Louzao et al. 2006) and potassium channels (Ghiaroni et al. 2005).

#### *Sodium Channels as a Possible Target for Gambierol*

In addition to have similar polyether structures, the molecular target of brevetoxins and ciguatoxins is the voltage-gated sodium channels of excitable membranes, a fundamental transmembrane protein involved in cellular excitability (Bidard et al. 1984; Poli, Mende, and Baden 1986; Lombet, Bidard, and Lazdunski 1987; Dechraoui et al. 1999; Baden and Adams 2000). These lipid-soluble cyclic polyethers bind specifically to receptor site 5 of the  $\alpha$ -subunit of the sodium channels (Catterall and Gainer 1985; Cestele and Catterall 2000), altering the channels' function; change the activation voltage for channel-opening to more negative values (Huang, Wu, and Baden 1984; Hogg, Lewis,

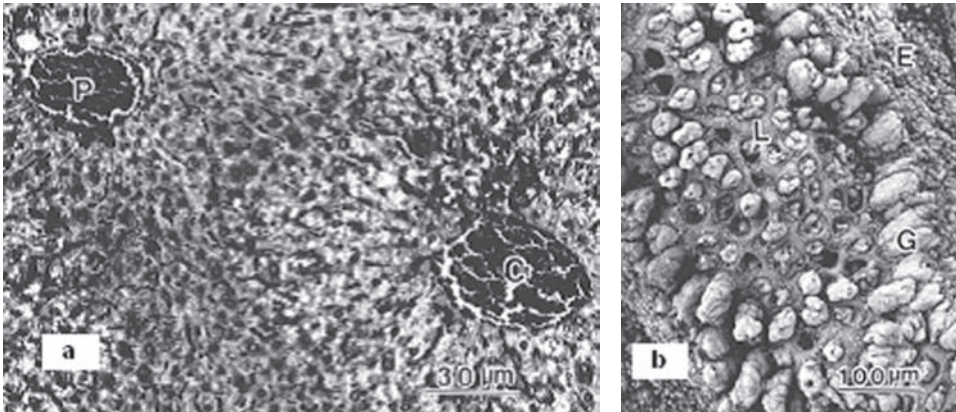


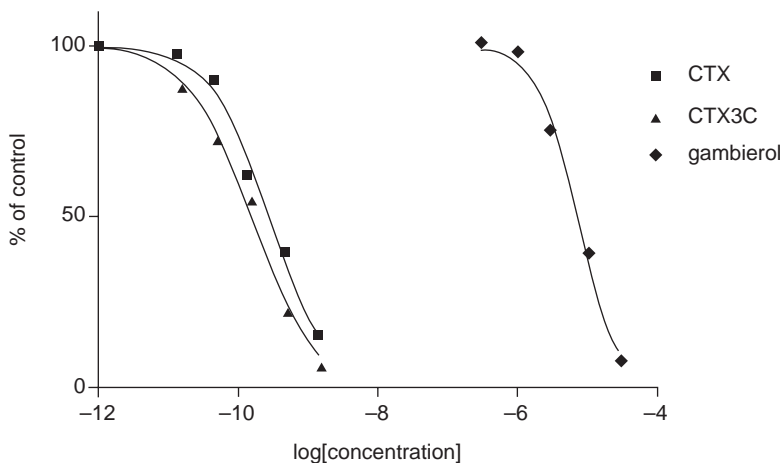
**Figure 1.5.** Histological changes in liver and stomach (Reprinted from Ito et al. 2003, with permission from Elsevier). (a) The liver 2 hour after p.o. gambierol at  $140 \mu\text{g kg}^{-1}$ , showing prominent congestions of sinusoidal capillaries at the periphery. P = portal veins. C = central vein. (b) Stomach alterations in the same conditions. Mucosa showed ulceration and erosion sporadically. E: surface epithelial cells, G: gastric glands, L: lamina propria.

and Adams 1998) and also extend the mean open time; inhibit the inactivation of opened channels, resulting in a persistent activation; and induce subconductance states (Baden and Adams 2000; Jeglitsch et al. 1998).

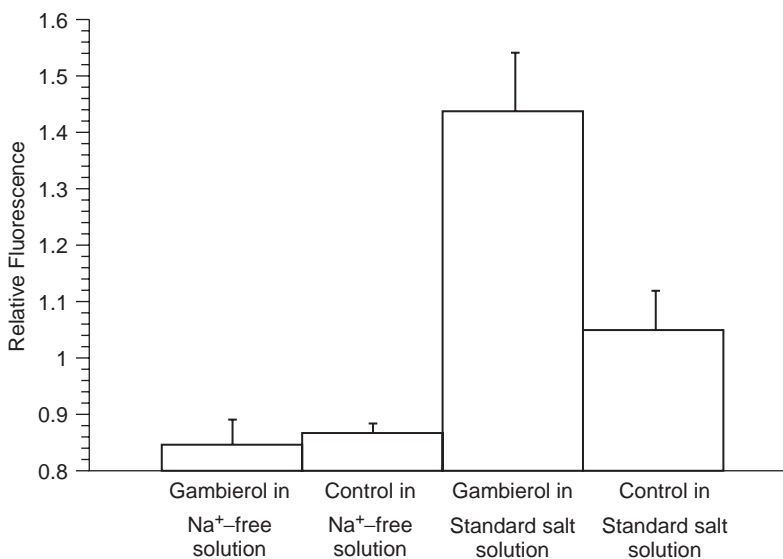
Electrophysiological studies of the mode of action of brevetoxins and ciguatoxins identify them as specific sodium channel activators (Lombet, Bidard, and Lazdunski 1987). Tritiated dihydrobrevetoxin-B ( $[^3\text{H}]\text{PbTx-3}$ ) has been used in homologous and heterologous displacement experiments to define site 5 toxins (Lewis et al. 1991; Lombet, Bidard, and Lazdunski 1987; Dechraoui et al. 1999; Yasumoto et al. 1995). In this way, by using rat brains synaptosomes, Inoue et al. (2003) showed that gambierol inhibited the binding of PbTx-3 to site 5 of the voltage-gated sodium channel, because this toxin was able to displace PbTx-3 from site 5 with concentrations in the micromolar range. This displacement was also found with CTXs (Fig. 1.6) at much lower concentrations.

Taking into account the similar molecular structure of brevetoxins, ciguatoxins and gambierol (polyether compounds), Inoue et al. (2003) suggest that the binding site of gambierol might be site 5, or at least overlap it. Although they do not exclude the possibility that gambierol may be allosterically modulating the sodium channels in order to displace  $[^3\text{H}]\text{PbTx-3}$ . They also investigated the relationship between the sizes of the polycyclic backbones and the binding affinities of the molecules, resulting in a linear relationship: the more number of fused rings, the more inhibitory activity. So they found that gambierol, having less fused rings than CTXs tested, also has a lower free energy of binding.

Experiments carried out by the Botana group with fluorescent dyes in neuroblastoma human cells confirmed the hypothesis that gambierol acts on sodium channels (Louzao et al. 2006). They used human excitable cells to associate gambierol effects with neurological symptoms, by using a potentiometric probe: the fluorescent dye bis-(1,3-dibutylbarbituric acid) trimethine oxonol, bis-oxonol [ $\text{DiBAC}_4(3)$ ] (Mohr and Fewtrell 1987; Louzao et al. 2001, 2003, 2004). In this way, they observed that  $30 \mu\text{M}$  gambierol induced a sodium-dependent depolarizing effect, because this toxin was able to increase bis-oxonol fluorescence when it was added in a  $\text{Na}^+$ -containing medium, and in contrast, this effect was abolished in a  $\text{Na}^+$ -free medium (Fig. 1.7).



**Figure 1.6.** Inhibition of binding of  $[^3\text{H}]\text{PbTx-3}$  to site 5 of the voltage-gated sodium channels by polyethers (Reprinted from Inoue et al. 2003, with permission from Elsevier).

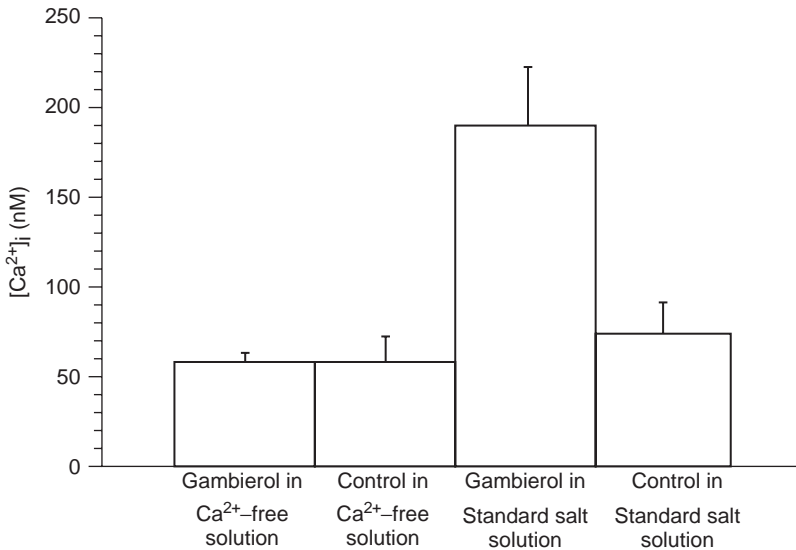


**Figure 1.7.** Influence of extracellular  $\text{Na}^+$  on  $30 \mu\text{M}$  gambierol-induced response. This effect was measured in a  $\text{Na}^+$ -free and  $\text{Na}^+$ -containing solution. Neuroblastoma cells were equilibrated with bis-oxonol. In the  $\text{Na}^+$ -free solution, there is no gambierol-evoked depolarizing effect, as there is in the  $\text{Na}^+$ -containing solution.

It is well known that site 5 of the voltage-gated sodium channel enhances membrane depolarization elicited by site 2 through positive allosteric coupling on the sodium channel complex (Catterall and Gainer 1985; Louzao et al. 2004). Louzao et al. (2006) found that gambierol was able to increase the effect of veratridine (an alkaloid activator of sodium channel site 2), when neuroblastoma cells were incubated with  $30 \mu\text{M}$  gambierol by nearly 10 minutes and then  $40 \mu\text{M}$  veratridine was added. They found that there was a significant depolarization difference at the beginning of the veratridine addition (Table 1.1). A further verification of gambierol target site was found when they added  $25 \text{ nM}$  CTX3C

**Table 1.1.** Effects of gambierol in combination with toxins acting on sodium channel

	Relative Fluorescence $\pm$ S.E.M.
Gambierol + Veratridine	1.83426 $\pm$ 0.19027
Control + Veratridine	1.15215 $\pm$ 0.12685
Gambierol + CTX3C	1.54139 $\pm$ 0.18234
Gambierol	1.42224 $\pm$ 0.10756
CTX3C	2.39761 $\pm$ 0.23611

**Figure 1.8.** Influence of extracellular Ca<sup>2+</sup> on 30  $\mu$ M gambierol-induced response. This effect was measured in a Ca<sup>2+</sup>-free and Ca<sup>2+</sup>-containing solution. Intracellular calcium was monitored in fura-loaded neuroblastoma cells. Gambierol produced no increment in cytosolic calcium when it was added in the Ca<sup>2+</sup>-free solution.

(a ciguatoxin congener that binds to site 5 of sodium channels) and 30  $\mu$ M gambierol together to neuroblastoma cells (Satake, Murata, and Yasumoto 1993b). As shown in Table 1.1, cell fluorescence decreased until reaching the gambierol-evoked depolarization level (Louzao et al. 2006). These results seem to confirm that gambierol is targeting the same site of the sodium channels as CTX3C (site 5) but acting as a partial agonist.

In addition, the Botana group observed that gambierol also stimulated a cytosolic calcium increment by using the dye Fura-2 acetoxymethyl ester (Fura-2, AM) (Grynkiewicz, Poenie, and Tsien 1985). Fig. 1.8 shows that gambierol induced no calcium increment when this cation was omitted from the incubation medium. This result indicates that extracellular calcium was the source of the gambierol-evoked cytosolic calcium increase (Louzao et al. 2006).

### *Potassium Channels as a Possible Target for Gambierol*

Recently, Ghiaroni et al. (2005) opened the possibility that gambierol could be acting as a voltage-gated potassium blocker. They used the patch-clamp technique in order to check the gambierol effect on mouse taste cells. Alteration of the activity of those excitable cells could be an explanation for the



dysgeusia (taste-altered sensations) involved in the sensory disturbances of ciguatera fish poisoning (Varkevisser et al. 2005). Ciguatoxins induce the ciguatera neurological disturbances by opening the voltage-gated sodium channels at resting potential, but surprisingly, Ghiaroni et al. (2005) did not observe a significant effect evoked by gambierol in sodium or chloride current ( $I_{Na}$  and  $I_{Cl}$ , respectively) of the voltage-clamped mouse taste cells at the concentrations tested (1 nM–1  $\mu$ M) and applying the toxin by 5 min as a maximum time.

In addition to voltage-gated sodium channels, voltage-gated potassium channels are also involved in membrane excitability (Bezanilla 2002; Choe 2002; Errington et al. 2005). Ghiaroni et al. (2005) checked the effect on voltage-gated potassium currents ( $I_K$ ), although not in isolation (after blocking  $I_{Na}$ ), and found that gambierol inhibited the potassium currents ( $I_K$ ) in the nanomolar range ( $IC_{50} = 1.8$  nM), but this reduction in current amplitude was different than the reduction induced by tetraethylammonium. That is, gambierol never abolished  $I_K$  completely; on average, they observe an approximately 60% reduction of  $I_K$  by 0.1  $\mu$ M gambierol, and this effect was irreversible. They also observed that gambierol slowed down the activation time of  $I_K$ .

In addition, Ghiaroni et al. (2005) checked whether gambierol also affected chloride currents, because  $I_{Cl}$  mediates action potential repolarization in taste cells, as well as  $I_K$  (Herness and Sun 1999), but it had no effect. Gambierol affected specifically only  $I_K$  on mouse taste cells.

It has been reported that P-CTX-1, the main ciguatoxin involved in ciguatera fish poisoning (Lewis et al. 1991; Satake, Murata, and Yasumoto 1993b), activates sodium channels as well as blocks potassium currents (Hidalgo et al. 2002; Birinyi-Strachan et al. 2005). Assuming that gambierol is a ciguatera toxin, it could act in both channels depending on the concentration.

10 nM P-CTX-1 showed no difference in sodium currents when applied for 1 minute in cultured rat myotubes. However, there was a sustained current at longer times of exposure (greater than 10 minutes), indicating that sodium channels remained open during the test pulse (Hidalgo et al. 2002). This pattern of action also occurred at higher toxin concentrations and shorter times of toxin exposure. However, when low-to-moderate concentrations of P-CTX-1 were applied, the toxin blocked potassium currents within a membrane potential dependency, which may indicate a voltage dependency for the inhibitory effect of the toxin. Therefore, in addition to activating sodium channels, as it does in other excitable tissues, in rat myotubes gambierol also interacts with potassium channels. This combined effect activates a calcium-release signal-transduction pathway in muscle cells, mediated by membrane depolarization and  $IP_3$ .

## References

- Baden, D.G., and Adams, D.J. 2000. In *Seafood and Freshwater Toxins: Pharmacology, Physiology and Detection*, ed. Botana, L.M. New York: Marcel Dekker, 505–532.
- Baden, D.G., and Mende, T.J. 1982. *Toxicon* 20, 457–461.
- Bezanilla, F. 2002. *J Gen Physiol* 120, 465–473.
- Bidard J.-N., Vijverberg, H.P.M., Frelin, C., Chungue, E., Legrand, A.-M., Bagnis, R., and Lazdunski, M. 1984. *J Biol Chem* 259, 8353–8357.
- Birinyi-Strachan, L.C., Gunning, S.J., Lewis, R.J., and Nicholson, G.M. 2005. *Toxicol Appl Pharmacol* 204, 175–186.
- Botana, L.M., Vieytes, M.R., Louzao, M.C., and Alfonso, A. 2004. In *Handbook of Food Analysis*, ed. Nollet, L. New York: Marcel Dekker, 911–930.
- Catterall, W.A., and Gainer, M. 1985. *Toxicon* 23, 497–504.
- Cestele, S., and Catterall, W.A. 2000. *Biochimie* 82, 883–892.
- Chemler, S.R., Trauner, D., and Danishefsky, S.J. 2001. *Angew Chem Int Ed* 40, 4544–4568.
- Choe, S. 2002. *Nat Rev Neurosci* 3, 115–121.
- Corey, E.J., and Fuchs, P.L. 1972. *Tetrahedron Lett* 13, 3769–3772.

- Dahanukar, V.H., and Rychnovsky, S.D. 1996. *J Org Chem* 61, 8317–8320.
- Dechraoui, M.Y., Naar, J., Pauillac, S., and Legrand, A.M. 1999. *Toxicol* 37, 125–143.
- Errington, A.C., Stohr, T., and Lees, G. 2005. *Curr Top Med Chem* 5, 15–30.
- Feng, A., and Murai, A. 1992. *Chem. Lett.* 1587–1590.
- Furuta, H., Hase, M., Noyori, R., and Mori, Y. 2005. *Org Lett* 7, 4061–4064.
- Fuwa, H., Kainuma, N., Satake, M., and Sasaki, M. 2003. *Bioorg Med Chem Lett* 13, 2519–2522.
- Fuwa, H., Kainuma, N., Tachibana, K., and Sasaki, M. 2002a. *J Am Chem Soc* 124, 14983–14992.
- Fuwa, H., Kainuma, N., Tachibana, K., Tsukano, C., Satake, M., and Sasaki, M. 2004. *Chem A-Eur J* 10, 4894–4909.
- Fuwa, H., Sasaki, M., Satake, M., and Tachibana, K. 2002b. *Org Lett* 4, 2981–2954.
- Fuwa, H., Sasaki, M., and Tachibana, K. 2001. *Org Lett* 3, 3549–3552.
- Gawley, R.E., Rein, K.S., Jeglitsche, G., Adams, D.J., Theodorakis, E.A., Tiebes, J., and Nicolaou, K.C. 1995. *Chem Biol* 2, 533–541.
- Ghiaroni, V., Sasaki, M., Fuwa, H., Rossini, G.P., Scalera, G., Yasumoto, T., Pietra, P., and Bigiani, A. 2005. *Toxicol Sci* 85, 657–665.
- Grynkiwicz, G., Poenie, M., and Tsien, R.Y. 1985. *J Biol Chem* 260, 3440–3450.
- Han, X., Stolz, B.M., and Corey, E.J. 1999. *J Am Chem Soc* 121, 7600–7605.
- Herness, M.S., and Sun, X.D. 1999. *J Neurophysiol* 82, 260–271.
- Hidalgo, J., Liberona, J.L., Molgo, J., and Jaimovich, E. 2002. *Br J Pharmacol* 137, 1055–1062.
- Hogg, R.C., Lewis, R.J., and Adams, D.J. 1998. *Neurosci Lett* 252, 103–106.
- Huang, J.M., Wu, C.H., and Baden, D.G. 1984. *J Pharmacol Exp Ther* 229, 615–621.
- Inoue, M., Hirama, M., Satake, M., Sugiyama, K., and Yasumoto, T. 2003. *Toxicol* 41, 469–474.
- Ito, E., Ohkusu, M., and Yasumoto, T. 1996. *Toxicol* 34, 643–52.
- Ito, Y., Hirao, T., and Saegusa, T. 1978. *J Org Chem* 43, 1011–1013.
- Ito, E., Suzuki-Toyota, F., Toshimori, K., Fuwa, H., Tachibana, K., Satake, M., and Sasaki, M. 2003. *Toxicol* 42, 733–740.
- Jeglitsch, G., Rein, K., Baden, D.G., and Adams, D.J. 1998. *J Pharmacol Exp Ther* 284, 516–525.
- Johnson, H.W.B., Majumder, U., and Rainier, J.D. 2004. *J Am Chem Soc* 127, 848–849.
- . 2006. *Chem A-Eur J* 12, in press.
- Kadota, I., Ohno, A., Matsuda, K., and Yamamoto, Y. 2001. *J Am Chem Soc* 123, 6702–6703.
- . 2003a. *J Am Chem Soc* 124, 3562–3566.
- Kadota, I., Takamura, H., Sato, K., Ohno, A., Matsuda, K., Satake, M., and Yamamoto, Y. 2003b. *J Am Chem Soc* 125, 11893–11899.
- Kadota, I., Takamura, H., Sato, K., Ohno, A., Mastuda, K., and Yamamoto, Y. 2003c. *J Am Chem Soc* 125, 46–47.
- Kadota, I., Ueno, H., Ohno, A., and Yamamoto, Y. 2003d. *Tetrahedron Lett* 44, 8645–8647.
- Kadota, I., and Yamamoto, Y. 2005. *Acc Chem Res* 38, 423–432.
- Kopecky, D.J., and Rychnovsky, S.D. 2000. *J Org Chem* 65, 191–198.
- . 2003. *Org Synth* 80, 177–183.
- Legrand, A.M., Fukui, M., Cruchet, P., and Yasumoto, T. 1992. *Bull Soc Pathol Exot* 85, 467–469.
- Lewis, R.J. 2001. *Toxicol* 39, 97–106.
- Lewis, R.J., Sellin, M., Poli, M.A., Norton, R.S., MacLeod, J.K., and Sheil, M.M. 1991. *Toxicol* 29, 1115–1127.
- Ley, S.V., Norman, J., Griffith, W.P., and Marsden, S.P. 1994. *Synthesis* 639–666.
- Lombet, A., Bidard, J.N., and Lazdunski, M. 1987. *FEBS Lett* 219, 355–359.
- Louzao, M.C., Cagide, E., Vieytes, M.R., Sasaki, M., Fuwa, H., Yasumoto, T., and Botana, L.M. 2006. *Cell Physiol and Biochem* 17, 257–268.
- Louzao, M.C., Rodriguez Vieytes, M., Garcia Cabado, A., Vieites Baptista De Sousa, J.M., and Botana, L.M. 2003. *Chem Res Toxicol* 16, 433–438.
- Louzao, M.C., Vieytes, M.R., Baptista de Sousa, J.M., Leira, F., and Botana, L.M. 2001. *Anal Biochem* 289, 246–250.
- Louzao, M.C., Vieytes, M.R., Yasumoto, T., and Botana, L.M. 2004. *Chem Res Toxicol* 17, 572–578.
- Majumder, U., Cox, J.M., Johnson, H.W.B., and Rainier, J.D. 2006. *Chem A-Eur J* 12, in press.
- Mastukawa, Y., Asao, N., Kitahara, N., and Yamamoto, Y. 1999. *Tetrahedron* 55, 3779–3790.
- Miyaura, N., Ishiyama, T., Ishikawa, M., and Suzuki, A. 1986. *Tetrahedron Lett* 27, 6369–6372.
- Miyaura, N., Ishiyama, T., Sasaki, H., Ishikawa, M., Satoh, M., and Suzuki, A. 1989. *J Am Chem Soc* 111, 314–321.
- Miyaura, N., and Suzuki, A. 1995. *Chem. Rev.* 95, 2457–2483.
- Mohr, F.C., and Fewtrell, C. 1987. *J Immunol* 138, 1564–1570.
- Mori, Y., Yaegashi, K., and Furukawa, H. 1996a. *J Am Chem Soc* 118, 8158–8159.
- Mori, Y., Yaegashi, K., Iwase, K., Yamamori, Y., and Furukawa, H. 1996b. *Tetrahedron Lett* 37, 2605–2608.

- Morohashi, A., Satake, M., and Yasumoto, T. 1998. *Tetrahedron Lett* 39, 97–100.
- Murata, M., Legrand, A.M., Ishibashi, Y., Fukui, M., and Yasumoto, T. 1990. *J Am Chem Soc* 112, 4380–4386.
- Nicolaou, K.C., Prasad, C.V.C., Hwang, C.-K., Duggan, M.E., and Veale, C.A. 1989. *J Am Chem Soc* 111, 5321–5330.
- Njardarson, J.T., Gaul, C., Shan, D., Huang, X.Y., and Danishefsky, S.J. 2004. *J Am Chem Soc* 126, 1038–1040.
- Noyori, R., Nishida, I., Sakata, J., and Nishizawa, M. 1980. *J Am Chem Soc* 102, 1223–1225.
- Okazoe, T., and Takai, K. 1987. *J. Org. Chem.* 52, 4410–4412.
- Pearn, J. 2001. *J Neurol Neurosurg Psychiatry* 70, 4–8.
- Poli, M.A., Mende, T.J., and Baden, D.G. 1986. *Mol Pharmacol* 30, 129–135.
- Rein, K.S., Bade, D.G., and Gawley, R.E. 1994. *J Org Chem* 59, 2101–2106.
- Rein, K.S., Gawley, R.E., Lynn, B., and Baden D.G. 1994. *J Org Chem* 59, 2107–2113.
- Sasaki, M., and Fuwa, H. 2004. *Synlett* 1851–1874.
- Sasaki, M., Fuwa, H., Inoue, M., and Tachibana, K. 1998. *Tetrahedron Lett* 39, 9027–9030.
- Sasaki, M., Fuwa, H., Ishikawa, M., and Tachibana, K. 1999. *Org. Lett* 1, 1075–1077.
- Sasaki, M., Ishikawa, M., Fuwa, H., and Tachibana, K. 2002. *Tetrahedron* 58, 1889–1911.
- Satake, M., Morohashi, A., Oguri, H., Oishi, T., Hiramata, M., Harada, N., and Yasumoto, T. 1997. *J Am Chem Soc* 119, 11325–11326.
- Satake, M., Murata, M., Yasumoto, T. 1993a. *J Am Chem Soc* 115, 361–362.
- . 1993b. *Tetrahedron Lett* 34, 1975–1978.
- Scheidt, K.A., Chen, H., Follows, B.C., Chemler, S.R., Coffey, D.S., Roush, W.R. 1998. *J Org Chem* 63, 6436–6437.
- Scholl, M., Ding, S., Lee, C.W., and Grubbs, R.H. 1999. *Org. Lett.* 1, 953–956.
- Shirakawa, E., Yamasaki, K., Yoshida, H., and Hiyama, T. 1999. *J Am Chem Soc* 121, 10221–10222.
- Takai, K., Kakiuchi, T., Kataoka, Y., and Utimoto, K. 1994. *J Org Chem* 59, 2668–2670.
- Terao K., Ito, E., Oarada, M., Ishibashi, Y., Legrand, A.-M., and Yasumoto, T. 1991. *Toxicon* 29, 633–643.
- Uenishi, J., Kawahama, R., Yonemitsu, O., and Tsuji, J. 1998. *J Org Chem* 63, 8965–8975.
- Van Dolah, F.M. 2000a. *Environ. Health Perspect* 108, 133–141.
- . 2000b. In *Seafood and Freshwater Toxins: Pharmacology, Physiology and Detection*, ed. Botana, L.M. New York: Marcel Dekker, 19–43.
- Varkevisser, B., Peterson, D., Ogura, T., and Kinnamon, S.C. 2005. *Chem Senses* 26, 499–505.
- Yasumoto, T. 2001. *Chem Rec* 1, 228–242.
- Yasumoto, T., Fukui, M., Sasaki, K., Sugiyama, K. 1995. *JAOAC Int* 78, 574–582.
- Yasumoto, T., Igarashi, T., Legrand, A.M., Cruchet, P., Chinain, M., Fujita, T., and Naoki, H. 2000. *J Am Chem Soc* 122, 4988–4989.



## 2 Brevetoxins: Structure, Toxicology, and Origin

Ambrose Furey, Javier García, Keith O'Callaghan,  
Mary Lehane, Mónica Fernández Amandi,  
and Kevin J. James

### Introduction

Neurotoxic shellfish poisoning (NSP) is caused by a group of polyether toxins, called the brevetoxins (BTX) produced by the marine dinoflagellate *Karenia brevis*. *K. brevis* is an unarmored alga. When mature, it is about 20–40  $\mu\text{m}$  in diameter (Gray et al. 2003). These algae have the ability to accumulate to high levels in filter-feeding bivalve molluscs. The neurotoxicity of the BTX is caused by their ability to bind to site 5 of the  $\text{Na}^+$  channels; these channels are fundamental to the optimum functioning of excitatory tissue (heart, neurons, and muscles). The BTXs act as depolarizers that open the voltage-gated  $\text{Na}^+$  channels in cell walls, altering the membrane properties of the affected cells and facilitating the inward flow of  $\text{Na}^+$  ions into the cell, resulting in persistent activation of the cell, eventually culminating in paralysis of the fatigued cells. The NSP victim, several hours following ingestion of the toxin, typically experiences severe gastrointestinal symptoms, hypotension, arrhythmias, numbness, tingling, and bronchi-constriction. Fortunately, there are no records of human deaths caused by BTX; however, in animals, progression of the symptoms to seizures, coma, and cardiac arrest leading to death, has been observed (Kirkpatrick et al. 2004, 2005; van Apeldoorn et al. 2001). Airborne blooms of *K. brevis* containing BTX have been demonstrated to induce upper and lower respiratory tract irritation (Pierce et al. 2005).

Two types of BTX have been characterised, designated type A and type B; type A consists of a flexible spine of 10-fused polyether rings; type B contains a rigid ladder of 11 rings. Additional analogues have been isolated from shellfish and these are postulated to be bioconversion products, the result of metabolism in the mollusc. In addition to the BTX, several phosphorous containing molecules were isolated from *K. brevis* that exhibit high ichthyotoxicity (Koley et al. 1995; Husain et al. 1996; Mazunder et al. 1997).

BTXs were once regarded as endemic to the Gulf of Mexico; however, since the early 1990s BTX or BTX-like toxins have been found in regions as diverse as the east coast of Florida, North Carolina, New Zealand, Asia, South Africa, North America, and Europe (Smith, Chang, and MacKenzie 1993; Hallegraeff 1995; Van der Vyver et al. 2000; van Apeldoorn et al. 2001; Hallegraeff and Hara 1995; Viviani 1992; Quilliam 1999; Rademaker et al. 1997, 1995; Khan, Arakawa, and Onoue 1996a, 1996b, 1997).

### Structure of the Brevetoxins

#### *Brevetoxins and Their Analogues*

Brevetoxins are methylated cyclic polyether toxins. There are two main types: type A comprised of a flexible backbone of 10 fused polyether rings, and type B with a rigid backbone of 11 polyether

rings. Type B is the more prevalent toxin in nature (Rein, Baden, and Gawley 1994; Rein et al. 1994; Gawley et al. 1995; and Baden et al. 2005). See Fig. 2.1.

Several new BTX analogues have recently been identified. PbTx-13 and PbTx-14 are likely to be artifacts of acid-catalysed methanol addition formed during the chemical purification process (see Fig. 2.2) (Baden et al. 2005; Bourdelais and Baden 2004). PbTx-11, PbTx-12, and PbTx-tbm (PbTx-2 lacking the side chain tail) are new toxins found both in cultures and in nature. The toxicology of these

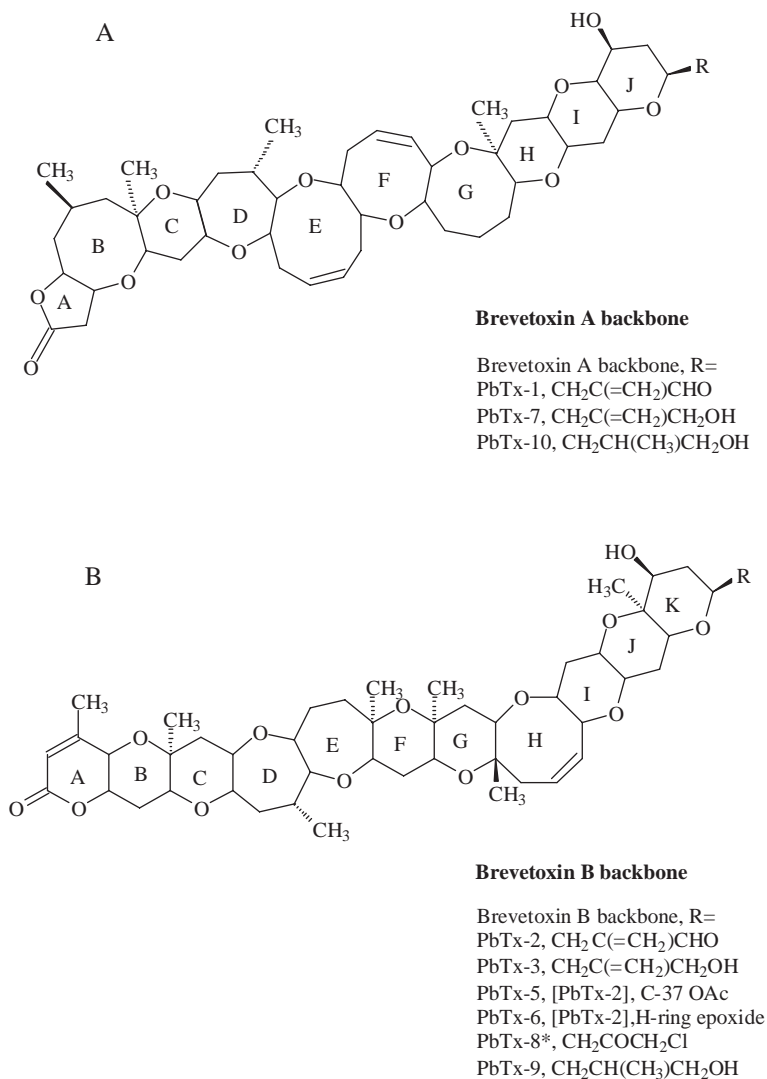


**Figure 2.1.** Brevetoxins are based on two different structural backbones, based on what are perceived to be the two parent molecules, PbTx-2 (brevetoxin B) and PbTx-1 (brevetoxin A). All other known derivatives are based on alteration of the R-side chain, epoxidation across the double bond in the H-ring of PbTx-2, or derivatization at the C-37 hydroxyl in PbTx-2. PbTx-8, the chloromethyl ketone derivative of PbTx-2, is an artifact of chloroform extraction and subsequent phosgene conversion of PbTx-2. Common features include trans-fused polyether ring systems consisting of five- to nine-membered rings. \* denotes likely chemical artifact from extraction (Baden et al. 2005).

compounds has yet to be studied. What is known is that they competitively bind to site 5 of the Na<sup>+</sup> channel (Bourdelaïs and Baden 2004; Abraham et al. 2005). Brevetoxin type compounds (see Fig. 2.3) have been isolated from cultures of *K. brevis* by Shimizu, Gupta, and Krishna Prasad (1990). These compounds do not cause antagonistic activity, and it is believed that their co-occurrence in nature may reduce the adverse effects of BTX containing sea sprays. The BTXs are characterized by four main regions in their structures: an electrophilic A-ring with a lactone group, the B-G rings comprised of six fused ether rings commonly referred to as the “spacer” region of the molecule (this region is slightly flexible), the H-K rings terminal, which is very rigid, and a variable side chain (see Fig. 2.1).

Synthesis studies have demonstrated that alterations that destroy the A-ring lactone or that reduce the rigidity of the H-K ring region will reduce significantly the toxicity of the molecule.

## Synthesis of Brevetoxins

### Brevetoxin B: Retrosynthetic Analysis and Strategy

Brevetoxin-B (PbTx-2, 1) is the first member of the marine polycyclic ethers to have been structurally elucidated and one of the most potent neurotoxins (Lin et al. 1989). Its highly complex

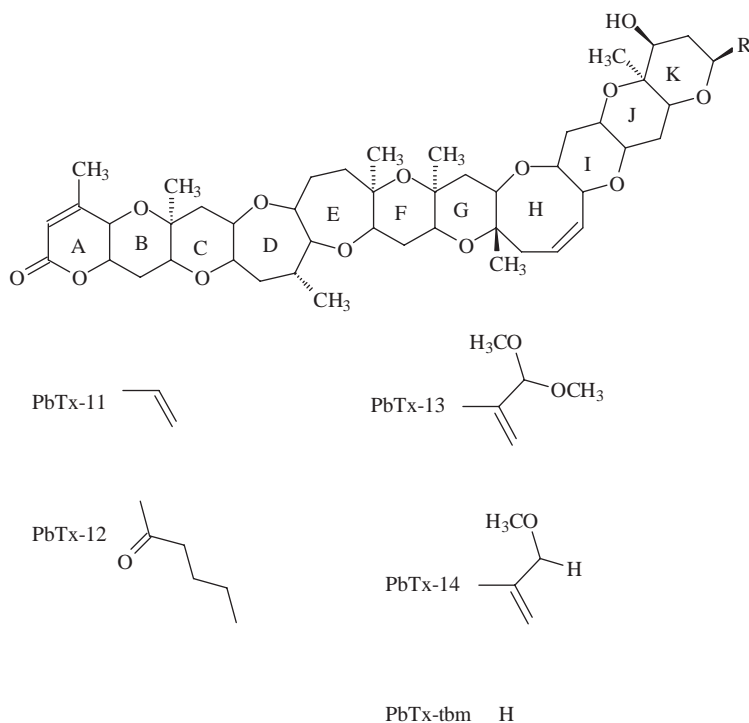


**Figure 2.2.** Five new brevetoxins, based on the PbTx-2 type backbone, have been purified and characterized: PbTx-11, a toxin with a shortened side chain; PbTx-12, the only natural ketone brevetoxin known; PbTx-13 and PbTx-14, which are both believed to be extraction artifacts formed in the presence of methanol reaction with the very active exomethylene-conjugated aldehyde of PbTx-2; and PbTx-tbm, a brevetoxin PbTx-2 backbone without any side chain, a form that is prevalent in senescent cultures (Baden et al. 2005).

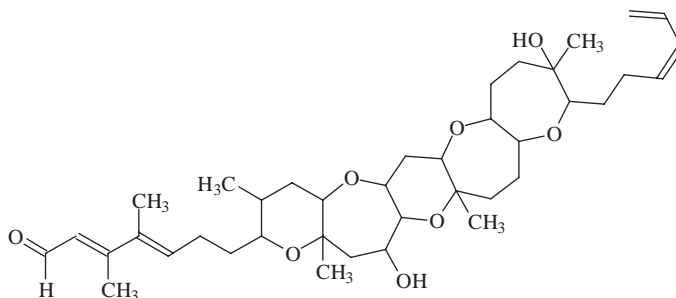
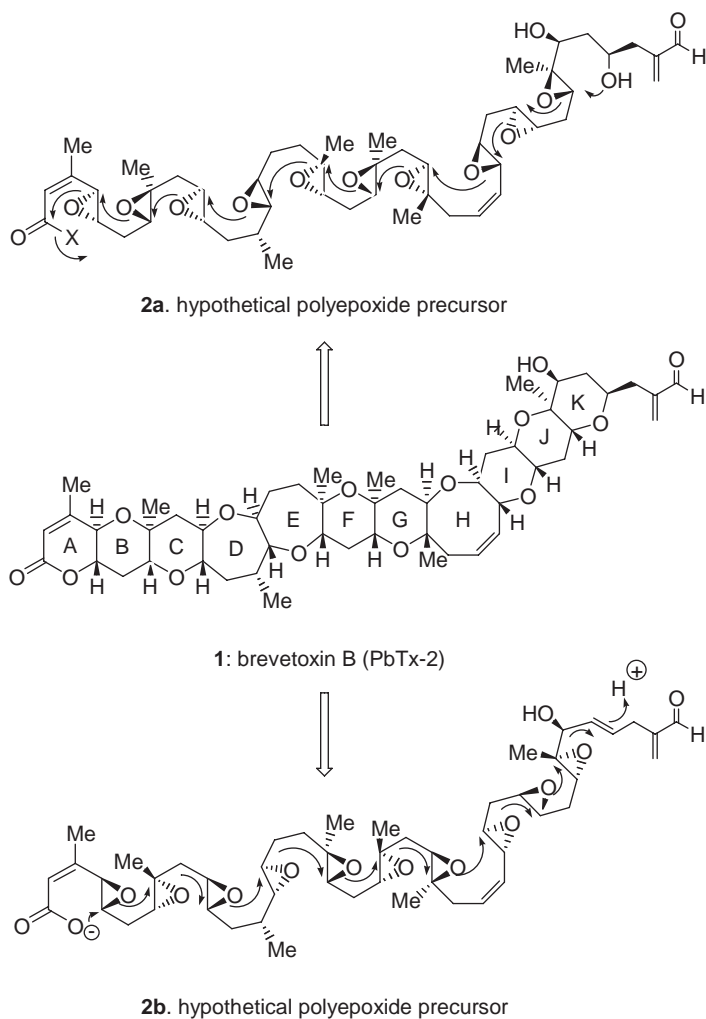


**Figure 2.3.** The brevenals are shorter transfused polyether molecules isolated from *K. brevis*. Consisting of a 6–7–6–7–7 ring motif, these materials bind with high affinity in brevetoxin receptor assays, and effectively act as inhibitors of brevetoxin binding and activity. Brevenal is the major constituent derived from cultures or the environment, with smaller amounts of brevenol (brevenal with the aldehyde reduced to the alcohol) (Baden et al. 2005).

molecular architecture is characterized by a novel array of ether oxygen atoms, regularly placed on a single carbon chain. This remarkable structure includes 11 rings, 23 stereogenic centers, and 3 carbon-carbon double bonds. This neurotoxin, whose mechanism of action involves the opening of sodium channels, exhibits intriguing regularity with regard to its ring fusions, which are all *trans*; each ring contains a single ether oxygen, which is separated by a C–C bond. All substituents flanking the ring oxygens are *syn* to each other except those on ring K, which are *anti*. With its complex structure, BTX B presented a formidable problem to synthetic organic chemistry. Not only did new methods need to be developed for the construction of the various cyclic ether moieties residing within its structure but the “right strategy” had to be devised for the global assembly of the molecule. A brief inspection of structure 1 leads to the idea of polyepoxide 2a or 2b (Scheme 2.1) serving as a potential precursors via “zip” type reactions (Krishna Prasad and Shimizu 1989; Nakanishi 1985; Lee et al. 1989; Townsend and Basak 1991). Although these hypothetical biosynthetic pathways bear a close resemblance to Cane, Celmer, and Westley’s (1983) unified proposal for the biosynthesis of the polyether ionophores such as monesin, the question as to whether nature employs any of these productive polycyclization cascades in the biosynthesis of BTX B has not yet been experimentally answered (Garson 1993). In spite of their appeal, these concerted polycyclizations would be very difficult to execute in the laboratory. In addition to the difficulties inherent in the stereoselective synthesis of the requisite polyepoxides, there would be no way to enforce the desired regiochemical course of the individual ring closures.

After several abortive attempts, the synthesis of BTX B (1) was finally achieved after 12 years of effort, and the total synthesis was reported in 1995 by K.C. Nicolaou and co-workers (Nicolaou et al. 1995a, 1995b, 1995c). Along with the accomplishment of the total synthesis, this work yielded an area of new synthetic technologies for the construction of cyclic ethers of various sizes.

Prominent among them are Scheme 2.2: (a) the region- and stereoselective routes to tetrahydrofuran, tetrahydropyran, and oxepane systems employing specifically designed hydroxyl epoxides; (b) the silver-promoted hydroxyl dithioacetal cyclisation to didehydrooxocanes; (c) the radical-mediated bridging of bis(thionolactones) to bicyclic systems; (d) the photo induced coupling of dithioesters to oxepanes; (e) the silico-induced hydroxy ketone cyclisation to oxepanes; (f) nucleophilic additions to thiolactones as an entry to medium and large ring ethers; (g) thermal cyclo additions of dimethyl acetylene dicarboxylate with cyclic enol ethers as an entry to medium size oxocyclic systems, and (h) the novel and unprecedented chemistry of dithiatopazine.

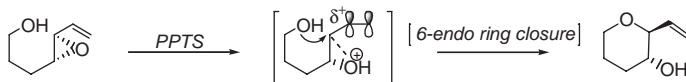


**Scheme 2.1.** Structure of brevetoxin B (1) and hypothetical polyepoxide precursors 2a and 2b.

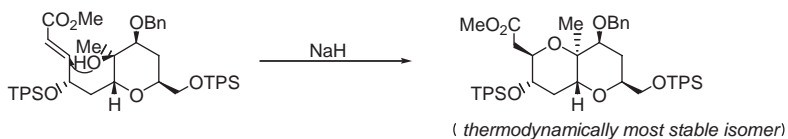
### *The Doubly Convergent Approach with Stepwise Formation of the Bis(oxepane) System: The Third Generation Strategy*

Schemes 2.3a–c outline the retro-synthetic production of BTX B (1). The final approach to PbTx-2 involved separate assembly of the ABCDEFG and IJK ring systems 4 and 5, their coupling, and final elaboration to the end. The didehydrooxocane ring in BTX B (ring H) was thus designated as the final ring to be constructed. Retro-synthetic cleavage of the indicated C–O bond in 1 and removal of the terminal electrophilic groupings reveal hydroxy dithioketal 3 as a plausible precursor. Tricyclic aldehyde 4 and heptacyclic phosphonium salt 5 can thus be defined as potential precursors to 3. The reliable and usually stereoselective Wittig reaction would be employed to accomplish the union of compounds 4 and 5 (Scheme 2.3a). Tricyclic aldehyde 4 was traced retro-synthetically to D-mannose 10.

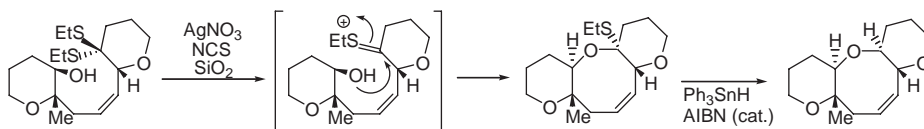
6-endo-Activated hydroxy epoxide cyclization



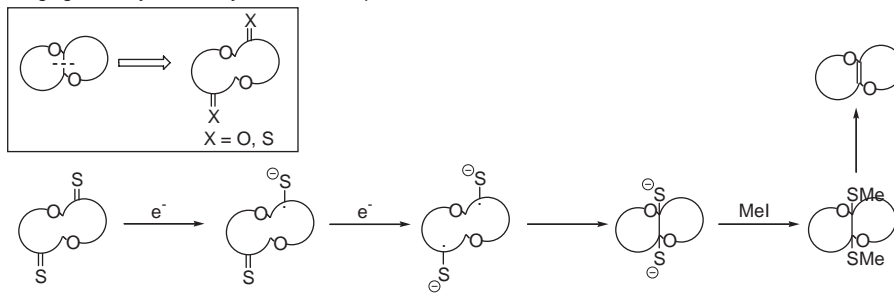
Intramolecular conjugate addition



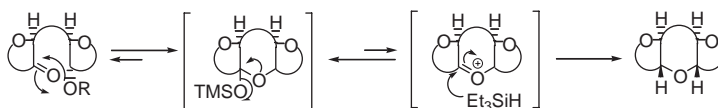
Hydroxy dithioketal cyclization: Construction of didehydrooxocane systems



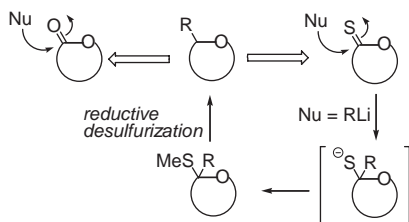
Bridging macrocycles to bicycles: the concept



The reductive hydroxy ketone cyclization

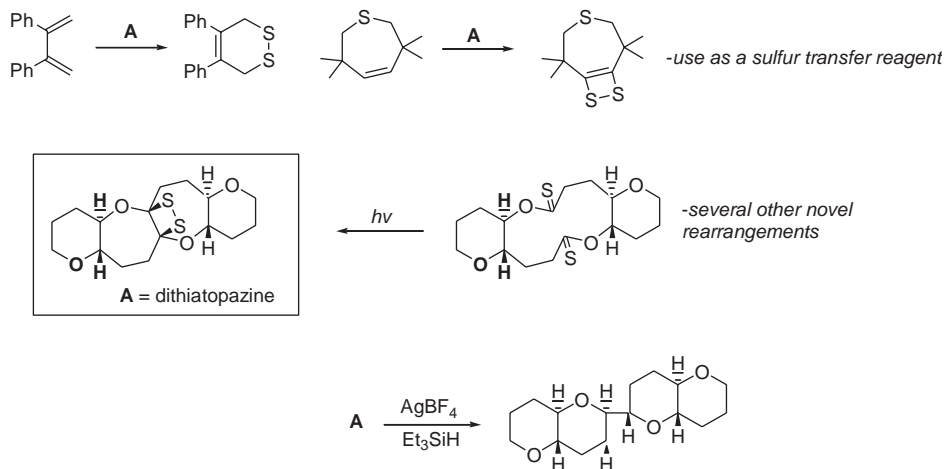


Construction of cyclic ethers from thiolactones



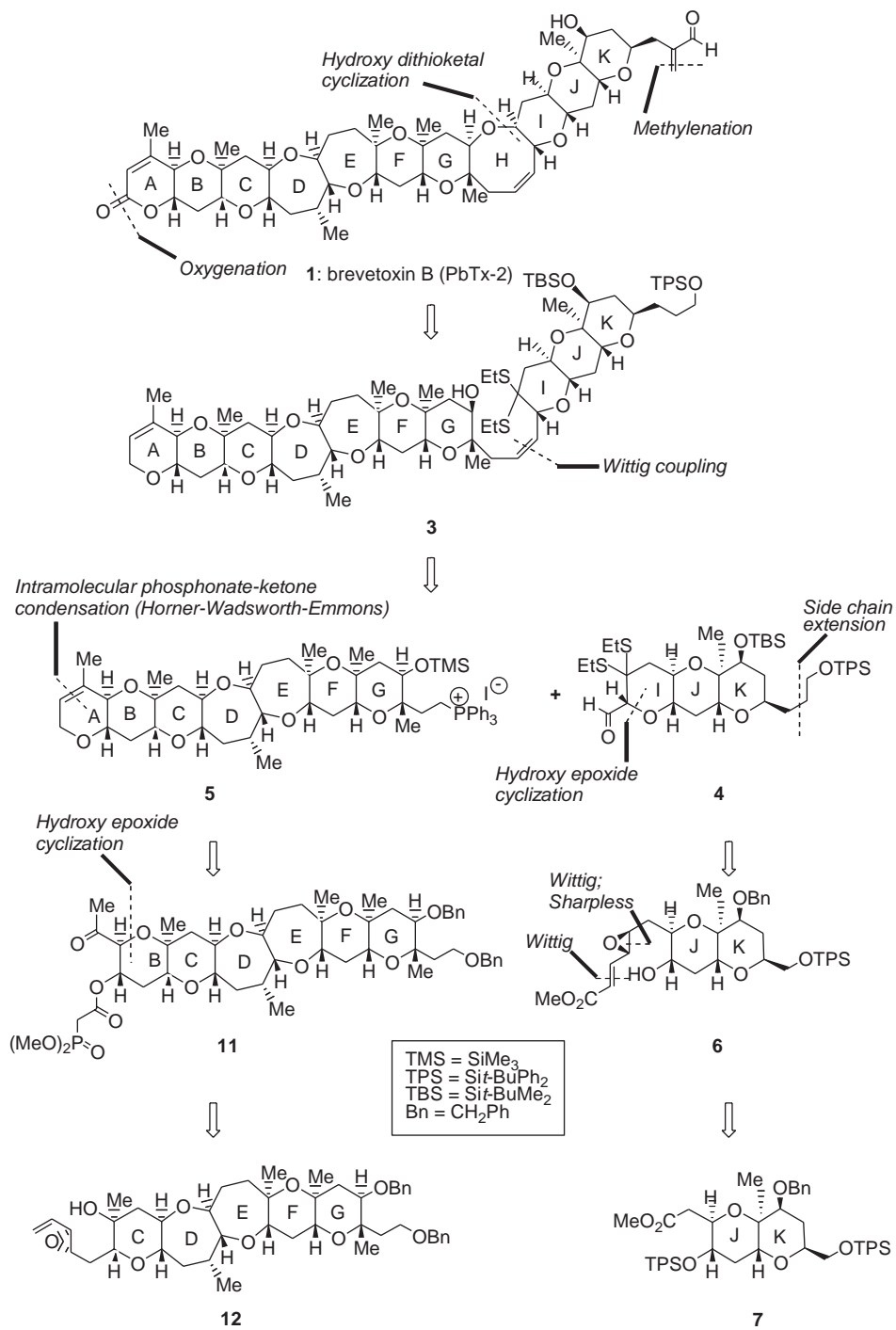
**Scheme 2.2.** Key synthetic methodologies developed for the formation of polycyclic ethers and fundamental discoveries.

## Novel chemistry of dithiatopazine



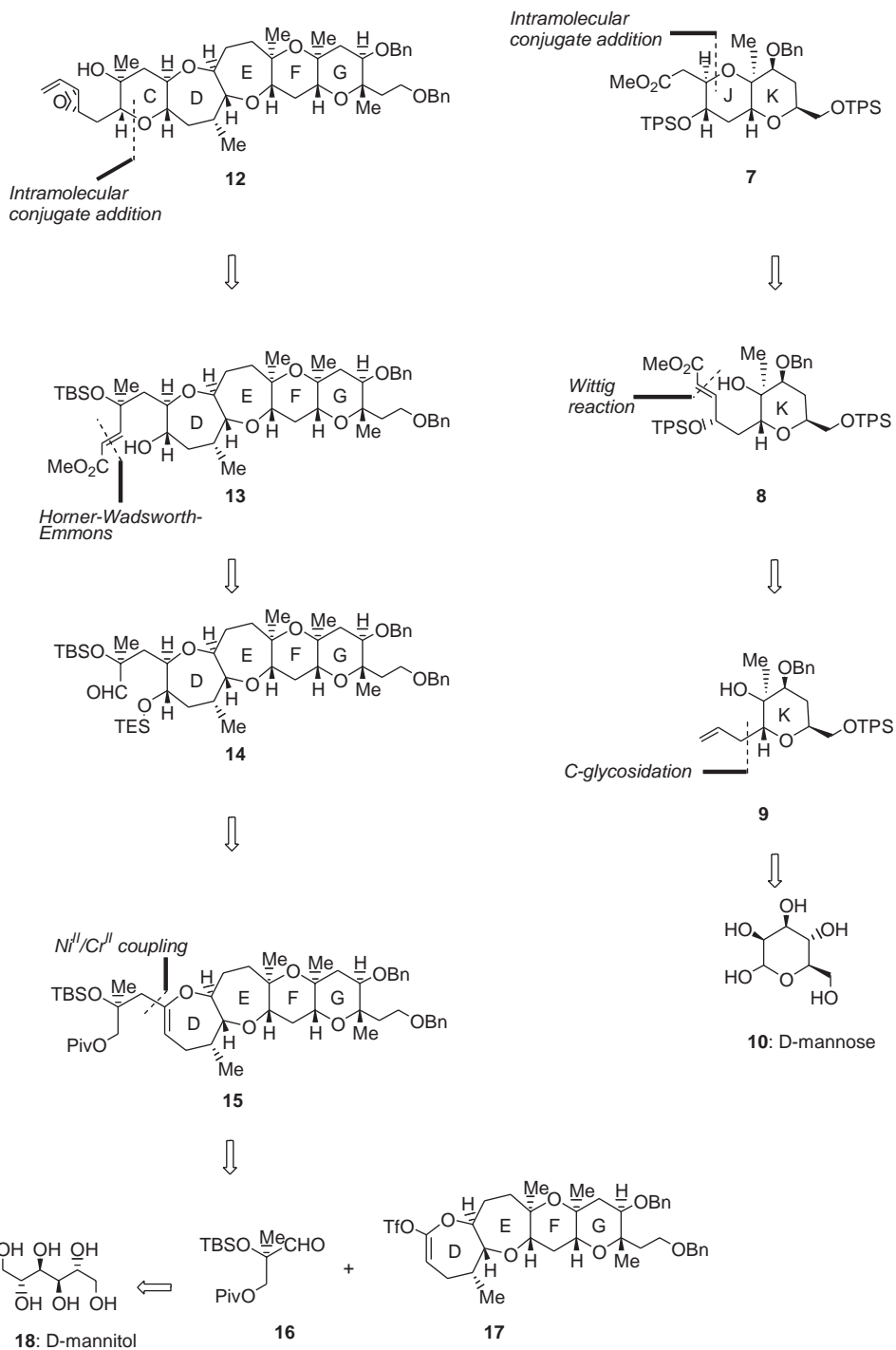
Scheme 2.2. (Continued)

In contrast with the IJK system 4, compound 5, Scheme 2.3a poses a much more difficult synthetic challenge. Keto phosphonate ester 11, revealed by that retro-synthetic disassembly of ring A in 5, could conceivably participate in an intra molecular Horner-Wadsworth-Emmons (HWE) reaction (Nicolaou et al. 1989b) on treatment with a suitable base. Deoxygenation of the A-ring lactone and a sequence of conventional functional group manipulations would then complete the synthesis of 5. Compound 11 can be dismantled in a productive fashion by cleavage of the indicated C-O bond. In the synthetic direction, a 6-*endo* activated hydroxy epoxide cyclization of 12 could accomplish the construction of pyran ring B. Retro-synthetic disassembly of the C-ring in compound 12 in the manner illustrated in Scheme 2.3b reveals an  $\alpha,\beta$ -unsaturated hydroxy ester 13 as a potential precursor. The free secondary hydroxyl group attached to ring D in 13 and the electrophilic  $\beta$ -carbon of the unsaturated ester moiety are in proximity. In such a favorable setting, the alkoxide ion resulting from deprotonation of the hydroxyl group in 13 would be expected to take part in a conjugate addition reaction to give pyran ring C. Compound 13 can be traced, in a straightforward manner, to aldehyde 14 through a *trans*-selective Wittig reaction. Compound 14 possesses a stereochemically and architecturally complex tetraoxacyclic framework consisting of two oxepane and two tetrahydropyran rings. Compound 14 could be derived from compound 15 in the synthetic direction, a region- and diastereoselective hydroboration of the enol ether moiety in 15, followed by oxidative workup, could accomplish the introduction of the adjacent C-10 and C-11 stereo centers in compound 14. A straightforward sequence of functional group manipulations would then complete the path from 15 to 14 (Scheme 2.3b). It was found that enol triflates derived from lactones can be coupled easily with aldehydes in the presence of chromium (II) chloride and a catalytic amount of nickel (II) chloride in DMF. Compound 15 can thus be traced to intermediates 16 and 17 by cleavage of the indicated C-C bond, and after a simple Barton deoxygenation sequence. Chiral building block 16 could conceivably be derived from commercially available D-mannitol (18) and enol triflate 17 could be fashioned with ease from tetracyclic lactone 19 (Scheme 2.3c). In the context of 19, ring D is in the form of a lactone

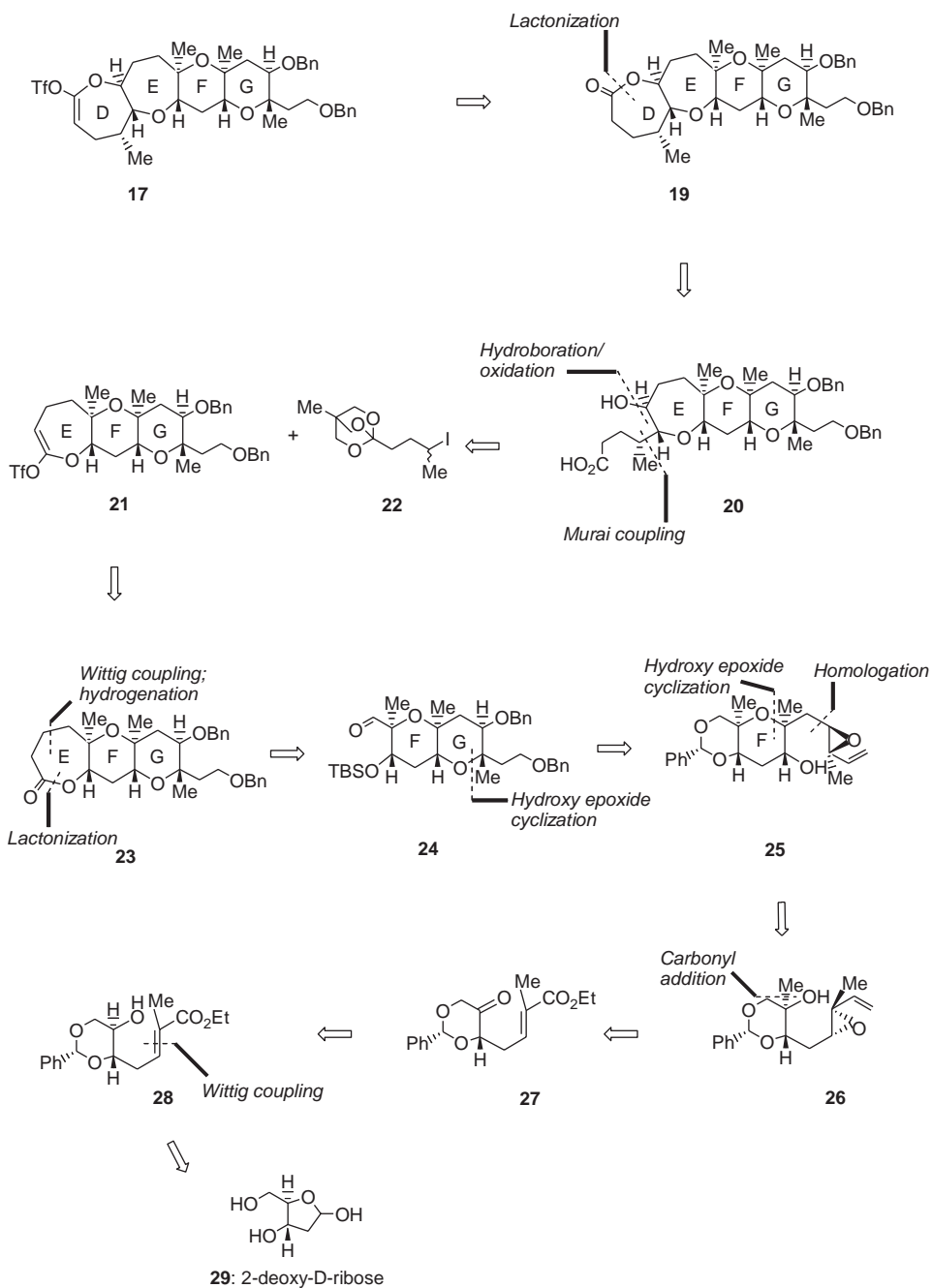


**Scheme 2.3a.** Retrosynthetic analysis of brevetoxin B (1): the third generation approach.





**Scheme 2.3b.** Retrosynthetic analysis of brevetoxin B (1): the third generation approach. (*Continued*).



**Scheme 2.3c.** Retrosynthetic analysis of brevetoxin B (1): the third generation approach.

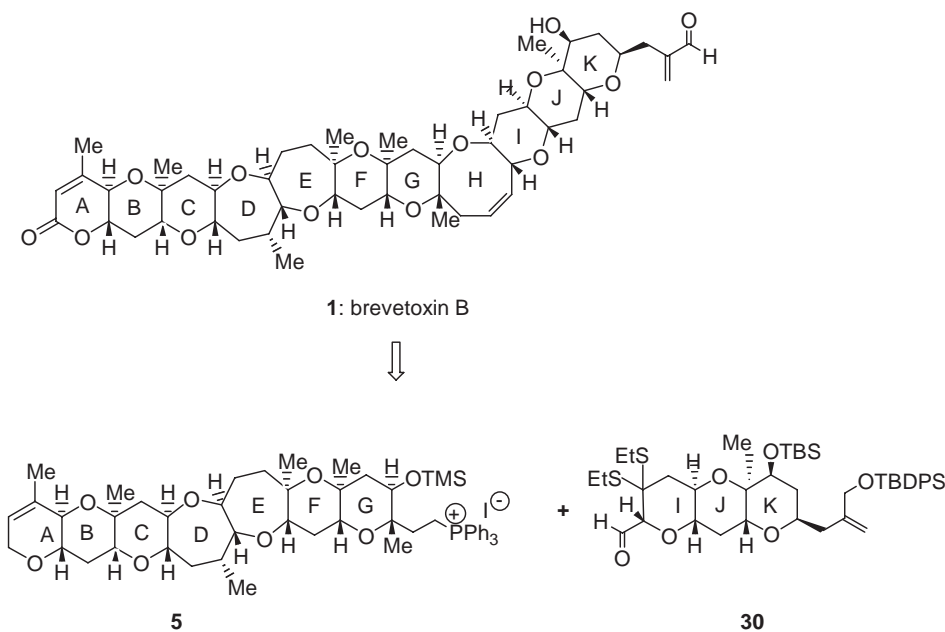
that can be conveniently dismantled retro-synthetically to give hydroxyl acid 20. The E-ring substituents in 20, which permit the annulation of ring D, can be removed retro-synthetically to give compounds 21 and 22 as potential precursors. Enol triflate 22 can be traced to the corresponding lactone (see 23). In the synthetic direction, enolization of the E-ring lactone in 23 with a strong, non-nucleophilic base, followed by trapping of the lactone enolate oxygen with *N*-phenyltrifluoromethanesulfonimide (PhNTf<sub>2</sub>), could give enol triflate 22. Compound 23 could be derived from the FG bicyclic ring system 24 with intermolecular Wittig and lactonization reactions as key synthetic operations. Retro-synthetic simplification of 24 reveals epoxy alcohol 25 as a plausible precursor. Compound 25 can be dismantled in a similar fashion, producing epoxy alcohol 26 as a viable precursor.

A chemo- and diastereoselective carbonyl addition reaction and standard manipulations could be used to fashion compound 26 from ketone 27, a substance that can ultimately be traced retro-synthetically to enantiomerically pure 2-deoxy-D-ribose (29) (Scheme 2.3c). This doubly convergent approach reduces the synthetic problem to three readily available and enantiomerically pure building blocks, D-mannose (10), D-mannitol (18), and 2-deoxy-D-ribose (29).

Nicolaou and co-workers synthesized 1 from the simple starting material 2-deoxy-D-ribose in 83 steps. The overall yield of the synthesis was 0.043%, but the average yield for each site was about 91% (Nicolaou and Sorensen 1996).

### Other Methodologies Relevant to the Synthesis of Brevetoxin B (1)

A new total synthesis of BTX B (1) was accomplished by Matsuo and co-workers in 2004 via the coupling of 5 and 30 (Scheme 2.4), each ether ring of which was stereoselectively and efficiently constructed on the basis of SmI<sub>2</sub>-induced intra-molecular Reformatsky-type reaction



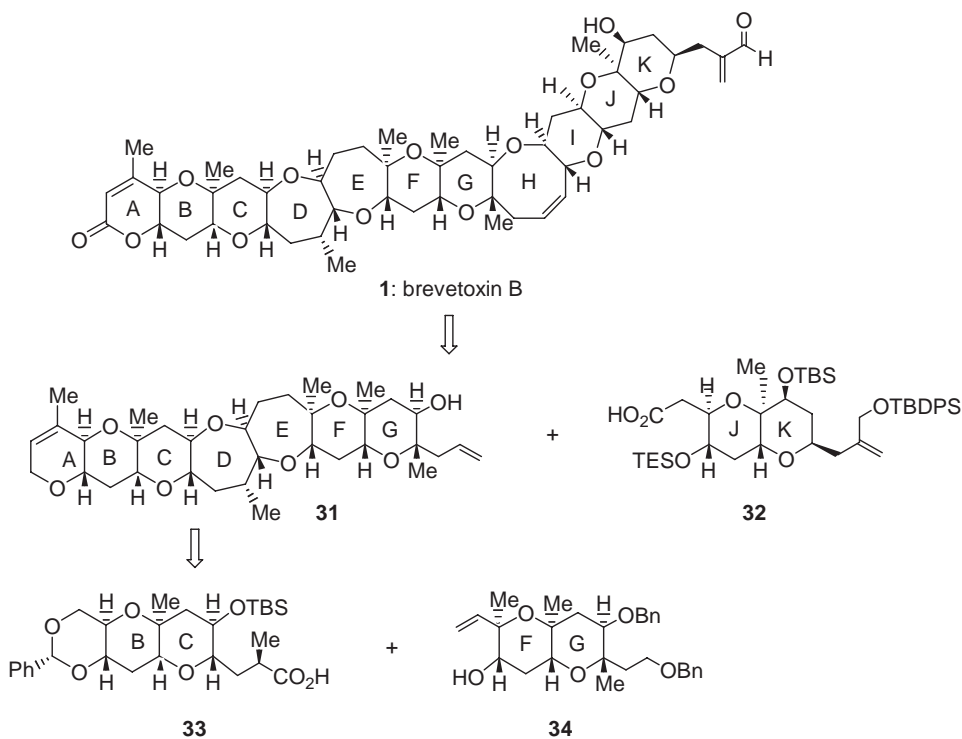
**Scheme 2.4.** Retrosynthetic plan for brevetoxin B (1).

(Matsuo et al. 2004). Several kinds of double reactions at the left and right sides were efficiently used throughout the synthesis. Thus, the total synthesis of BTX-B (1) was efficiently achieved with high stereoselectivity in 59 steps as the longest linear sequence and in total 90 steps with an average of 93% yield for each step.

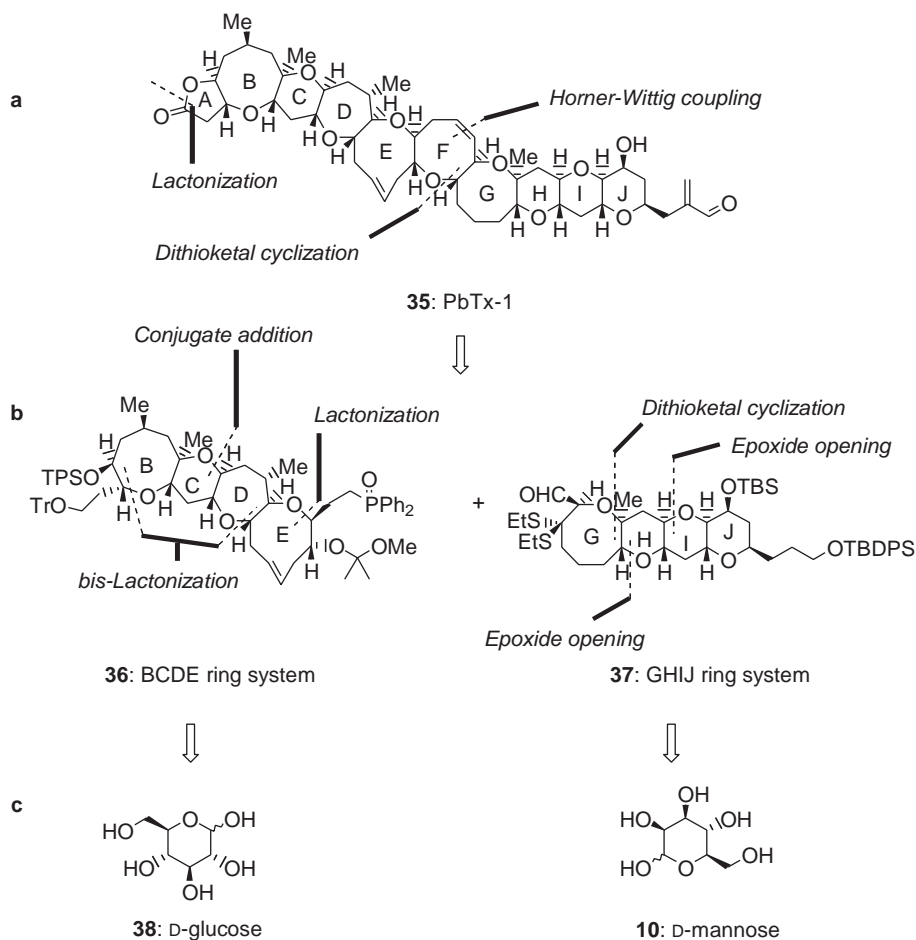
Other total synthesis of BTX B (1) was accomplished by Kadota and co-workers in 2005 in a highly convergent manner via the assembly of three fragments (Kadota et al. 2005). A brief retrosynthetic analysis of 1 is illustrated in Scheme 2.5. It is a convergent method for the synthesis of polycyclic ether frameworks via the intra-molecular allylation of  $\alpha$ -acetoxy ethers and subsequent ring-closing metathesis (Kadota et al. 2002). On the basis of this methodology, the polycyclic ether framework of 1 was retrosynthetically broken down into the A-G ring segment 31 and the J-K fragment 32. The heptacycle 31 was prepared from 33 and 34 via the same methodology. The longest linear sequence leading to 1 was 63 steps with 0.28% overall yield, and the number of total steps was 108.

### Brevetoxin A: Retrosynthetic Analysis and Strategy

Within the polluted “red tide” waters there often resides a more powerful neurotoxin, and that is BTX A (35) (Scheme 2.6). Isolated from the dinoflagellate species *K. brevis*, PbTx-1 was structurally elucidated in 1986 (Shimizu et al. 1986; Pawlak et al. 1987). With its 10 fused ring structure



**Scheme 2.5.** Retrosynthetic analysis of brevetoxin B (1).



**Scheme 2.6.** Molecular structure and strategic bond disconnections (a), and retrosynthetic analysis (b, c) of brevetoxin A (35). Abbreviations for chemical groups: Me, methyl; Ph, phenyl; Tr, trityl; TBDPS, *t*-butyldiphenylsilyl; Et, ethyl; TBS, *t*-butyldimethylsilyl.

and its 22 stereo centers, BTX A rivals BTX B in complexity, but as a synthetic target it arguably exceeds the latter in difficulty and challenge because of the presence of the 9-membered ring. Indeed, with rings ranging in size from 5- to 9-membered, all sizes in between included, BTX A can be considered as the ultimate challenge to the synthetic chemist as far as medium-sized ring construction is concerned. After a 10-year campaign, K.C. Nicolau and co-workers reported the total synthesis of PbTx-1 in 1998 (Nicolau et al. 1998, 1999a, 1999b, 1999c, 1999d).

Scheme 2.6 shows the synthetic strategy for the construction of BTX A (35) (Scheme 2.6a), in bond disconnection (Scheme 2.6b), and retro-synthetic (Scheme 2.6c) formats. This strategy led to the expectation of using D-glucose 38 (Scheme 2.6c) and D-mannose 10 (Scheme 2.6c) as starting materials for the construction of the requisite BCDE 36 (Scheme 2.6b) and GHIJ 37 (Scheme 2.6b) advanced intermediates, respectively. The union of 36 and 37 under Horner–Wittig conditions was

expected to furnish, in a highly convergent manner and after ring closure, the basic ring skeleton of the target molecule, from which BTX A could be fashioned through de-protections and functional group manipulations. At the outset of this project, it was also evident that although the 5- and 6-membered rings of the target molecule could be derived via well-developed synthetic methods (Nicolaou et al. 1989b), the three larger rings were not easily accessible through conventional techniques. Thus, to construct the 7-, 8- and 9-membered rings two important reactions were used; namely, the silver-promoted hydroxydithioacetal cyclization reaction (Nicolaou et al. 1989a) (rings F and G) and the palladium-catalysed functionalisation of lactones via coupling of their cyclic ketene acetal phosphates (Nicolaou et al. 1997) (rings B, D, and E) were specifically developed for this purpose.

As in the case of BTX B, this program was abundant in new synthetic technologies and strategies, which emerged as broadly useful spin-offs (Scheme 2.7). Among the most important synthetic technologies developed during this program was the palladium-catalyzed coupling of cyclic ketene acetal phosphates generated from lactones with appropriate appendages to afford cyclic enol ether diene systems (Nicolaou et al. 1997) suitable for a cyclo addition reaction with singlet oxygen. This method provided the crucial turning point in solving the problems associated with the 7-, 8-, and 9-membered rings of the target and facilitated the final and successful step to the production of BTX A.

The total synthesis of BTX A (35) became possible only after a long campaign which involved several unsuccessful strategies and the development of a number of new synthetic technologies. Particularly useful were the solutions found to the synthetic challenges posed by the 7-, 8- and 9-membered rings of the target molecule and the convergent strategy finally developed to reach the complex structure of BTX A.

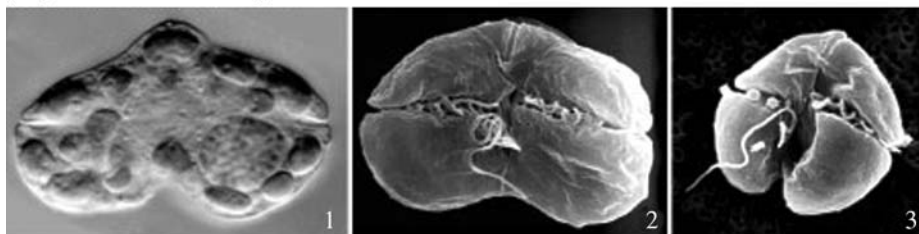
## Etiology of Brevetoxins

Toxic red tides have been observed in Florida since the 1840s and have resulted in fish kills and gastric and respiratory illness in human since then (Gray et al. 2003). More recently, prolonged red tides have forced the closure of shellfish beds from Florida to Mexico (Bossart et al. 1998; Hopkins, Heber, and Hammond 1997; Trainer and Baden 1999). The BTX as well as lesser quantities of the haemolytic toxins are produced by the motile form of *Karenia brevis* (formerly *Gymnodium breve* and *Ptychodiscus breve*) (Fig. 2.4). *K. brevis* is a non-peridinin-containing dinoflagellate that grows to around 20–40 µm in diameter. It is positively phototactic and negatively geotactic and is thought to be an obligate photoautotroph (Aldrich 1962; Geesey and Tester 1993; Kamykowski, Mulligan, and Reed 1998; Steidinger and Joyce 1973). The cell wall of *K. brevis* possess no armor and, thus, is relatively fragile; it is easily ruptured during wave action along beaches spilling its toxin into the water. However, four BTX analogues have been isolated from shellfish exclusively. These are thought to be metabolites formed by the bioconversion of some algal-borne BTX in shellfish (Ishida et al. 1995; Morohashi et al. 1995; Murata and Yasumoto 1995). *K. brevis* is identified by microscopy, pigment analysis, or culturing. Gray et al. (2003) have developed a reverse transcription-PCR method targeting the *rbcl* gene for the identification of this organism.

*Chattonella antique*, *Fibrocapsa japonica*, *Heterosigma akashiwo*, and *Chattonella marina* are four algal species of the Raphidophyceae class and produce BTX-like neurotoxins (Khan, Arakawa, and Onoue 1996a, 1996b, 1997; Khan et al. 1995).

*K. brevis* and related species inhabit the oceanic regions around the Gulf of Mexico, West Atlantic, Portugal, Spain, Greece, New-Zealand, and Japan (Smith, Chang, and MacKenzie 1993; Hallegraef 1995; Van der Vyver et al. 2000; Rademaker et al. 1997, 1995; Khan, Arakawa, and

*Karenia brevis* (Davis) G. Hansen et Moestrup  
(=*Gymnodinium breve* Davis)



1-3: Ventral view, Length: 18–40  $\mu\text{m}$ . Width: 15–70  $\mu\text{m}$   
photo: Haruyoshi Takayama

**Figure 2.4.** *K. brevis* progenitor of BTX (Daugbjerg et al. 2000).

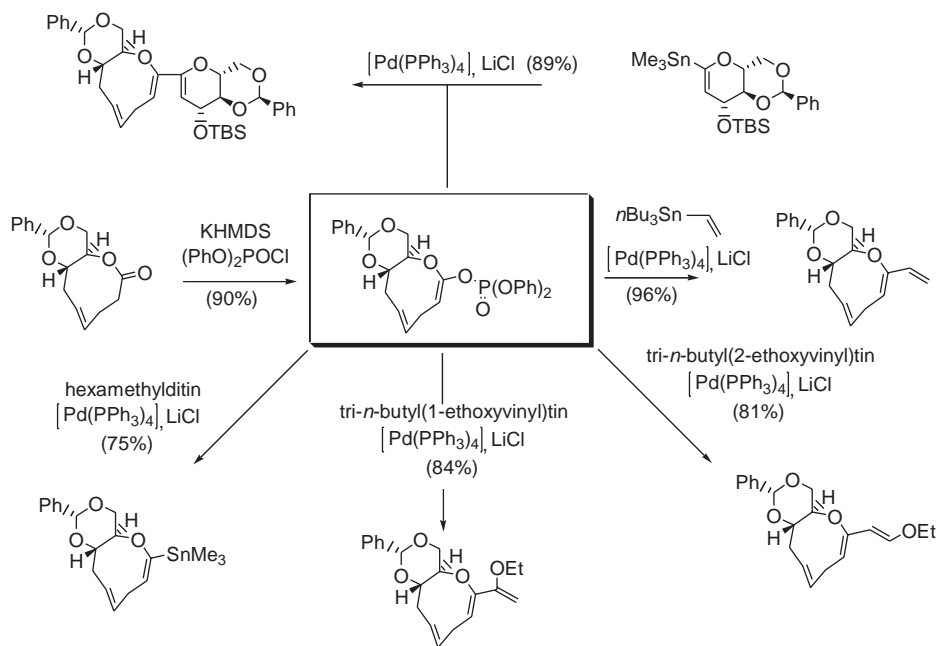
Onoue 1996a, 1996b, 1997). *K. brevis* proliferates on the west coast of Florida mostly during the autumn; the bloom begins to accumulate offshore during the summer and then is blown toward the coast when easterly winds intensify during the autumn (Stumpf et al. 1998). Man-made nutrient runoffs may be responsible for the persistence of blooms. It has also been documented that BTXs are transported from the Gulf of Mexico to Florida's east coast (Tibbets 1998).

Research conducted by Maier Brown et al. (2006) on three clones of *K. brevis* would suggest that optimum salinity for the growth of the algae ranged between low values of 20–25 psu and high values of 37.5–45 psu depending on the clone. However, many questions remain unanswered in regard to the production by dinoflagellates of BTX: Why do these organisms produce toxins? What stimulates the algae to bloom? With what degree of certainty may imminent blooms be predicted?

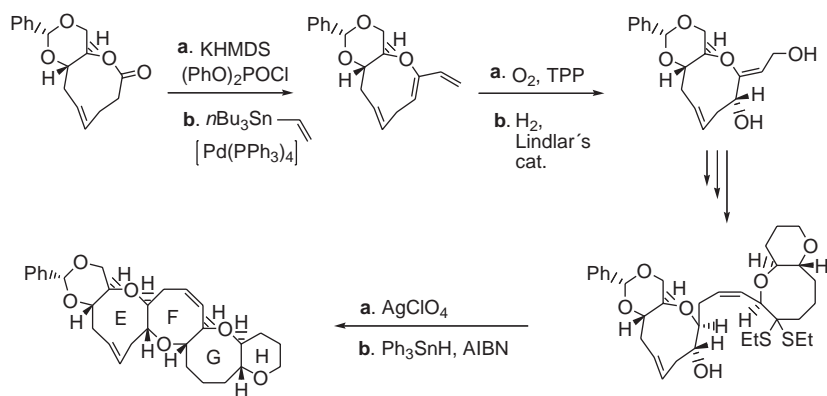
## Toxicological Studies

### *Bioactivity of Brevetoxins*

Brevetoxins exert their toxic effects by targeting a specific site of the  $\alpha$ -subunit of voltage-dependent sodium channels (VDSC). VDSC form ion-selective, voltage-gated pores through the membranes of cells. At resting membrane potential, the  $\text{Na}^+$  channels are closed, but upon membrane depolarization they change their conformation to the open state. Therefore,  $\text{Na}^+$  channels initiate the generation of action potentials in nerve, cardiac, and muscle tissues. In order to function satisfactorily, the VDSCs must be able to accomplish, in a timeframe of milliseconds, their state transitions between resting, open, and fast inactivation states. Any slight perturbation in the gating of the  $\text{Na}^+$  channel will precipitate very serious consequences for membrane excitability (Wang and Wang 2003). The series of events typically recorded in animals suffering from BTX poisoning includes hyperexcitability of excitable tissues, followed by convulsions, paralysis, and death (Baden et al. 2005). All natural polyether BTXs and synthetically prepared bioactive BTX analogues have certain structural characteristics in common: an electrophilic A-ring with a lactone group; a “spacer” region of 6 fused ether rings (B–G rings) possessing limited flexibility; a very rigid cylindrically shaped terminal (H–K rings); and a variable side chain (Fig. 2.5).



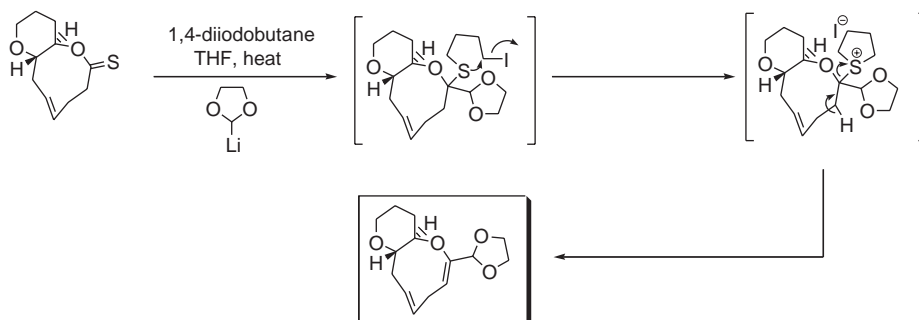
*Enol-phosphates and thioketal-mediated etherification for the construction of the EFGH ring skeleton of brevetoxin A*



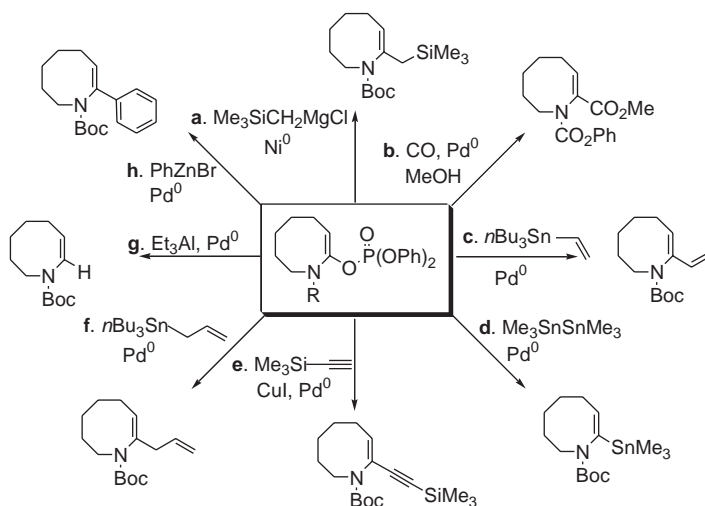
**Scheme 2.7.** Key synthetic methodologies developed in the course of the total synthesis of brevetoxin A (35).



Novel stereocontrolled synthesis of the nonacene ring system of brevetoxin A. Conformational-reactivity effects in nine-membered rings



Synthesis of *N*-heterocycles via lactam-derived ketene acinal phosphates. Asymmetric synthesis of cyclic amino acids



Scheme 2.7. (Continued)

Studies have shown that any alteration that compromises the integrity of the A-ring lactone or that reduces the rigidity of the H-K ring region will reduce or negate the toxicity of the compound (Jeglitsch et al. 1998; Purkerson, Baden, and Fieber 1999). The synthesis of a BTX analogue missing only the B-G ring spacer region shows significantly reduced bioactivity (Gawley et al. 1995).

The VDSC is comprised of three proteins: an  $\alpha$ -subunit and two  $\beta$ -subunits (Fig 2.6). The  $\alpha$ -subunit is a single polypeptide with fourfold internal homology-denoted domains I-IV. Each homologous

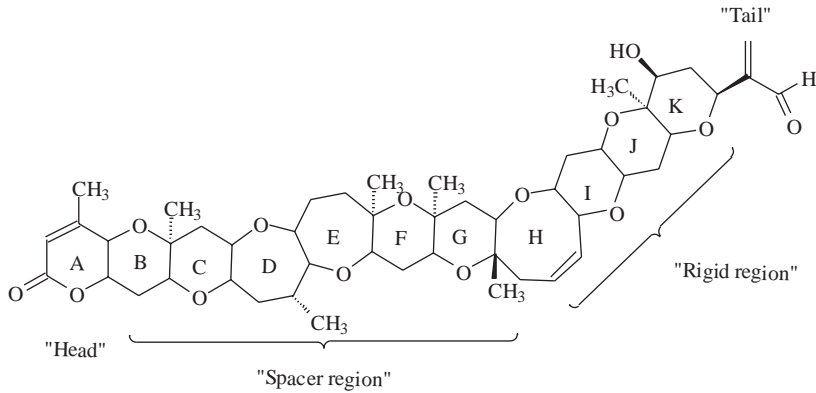


**Figure 2.5.** Key structural regions of the BTX molecule (Baden et al. 2005).

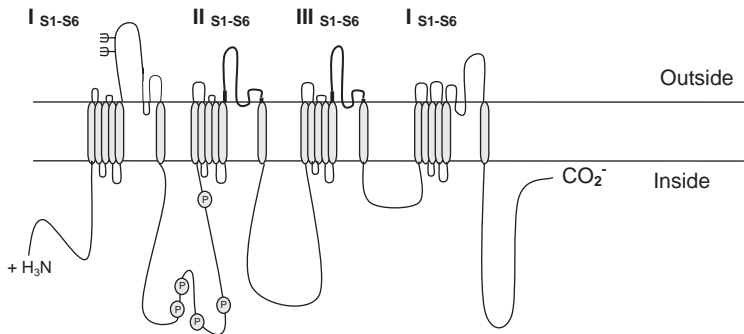


**Figure 2.6.** The alpha subunit of the voltage sensitive sodium channel (Baden et al. 2005).

domain has six transmembrane helices, S1–S6. S1–S3 have relatively neutral charges, S4 is highly positively charged, and S5 and S6 are relatively hydrophobic (Catterall 1992).

Many naturally occurring biotoxins, many of them algal toxins, are Na<sup>+</sup> channel selective toxins. To date, six toxin binding sites have been discovered on the Na<sup>+</sup> channel. Toxins that bind to site 1, found in the pore of the channel, block the conductance of Na<sup>+</sup> ions through the channel. These toxins include tetrodotoxin, STX, and the  $\mu$ -conotoxins. Strictly speaking, while TTX and STX share a common binding site, the  $\mu$ -conotoxins bind in fact to a site that is located in the pore and which overlaps the TTX/STX site. The other part of the  $\mu$ -conotoxins binding site is located on the external part of the IIS5–S6 loop. The five remaining toxin binding sites alter the voltage dependency of channel gating. These sites are located within the membrane: Sites 2 and 5 are on the extra cellular sites, 3 and 4. The toxins that bind to sites 2 and 5 are lipophilic in character and include the plant-derived alkaloids veratridine and aconite and the toxin batrachotoxin from the skin of the frog, *Phyllobates aurotaenia*. Site 3 binds toxins from some spiders, sea anemones, and scorpions. Site 5 binds the BTX and ciguatoxins (CTX).

Anderson and co-workers go so far as to suggest that algal toxins were involved in the evolution of voltage-gated Na<sup>+</sup> channels, citing examples of the resistance to Na<sup>+</sup> channel specific toxins of

many eukaryotic organisms, particularly those that are routinely exposed to such toxins (Anderson, Roberts-Misterly, and Greenberg 2005; Trainer et al. 1996).

Poli, Mende, and Baden (1986) demonstrated that the BTXs bind to a different site than do any other sodium channel specific neurotoxins. This receptor site was postulated to exist on site 5.

Trainer et al. demonstrated that BTX binds to receptor site 5 with the tail end of the molecule located near the S5-S6 extracellular loop of domain 5 of the Na<sup>+</sup> channel  $\alpha$ -subunit (Fig. 2.7) (Baden et al. 2005). The discovery that all BTX derivatives shift the voltage dependence of activation to more negative potentials implies that the oxygen rich backbone of the BTX interacts with the channel so as to stabilize the open configuration. The BTX are thus thought to act as helix mimics, disturbing the normal ion-pairing that holds S4 in a “trigger-ready” conformation awaiting depolarization. This ultimately leads to the shifting of the activation potential to more negative values (Poli, Mende, and Baden 1986; Poli et al. 2000).

The effects on the Na<sup>+</sup> channels, as a result of the co-occurrence of BTX with other toxins or xenobiotics, were also investigated. Trainer et al. (1993) demonstrated that the binding of the BTX to receptor site 5 causes allosteric enhancement of batrachotoxin benzoate binding at site 2 in concert with the pyrethroid insecticide RU39568. Inoue et al. (2003) demonstrated that gambierol, a polyether from the dinoflagellate, *Gambierdiscus toxicus*, and gambieric acid A, inhibits the binding of PBTX-3 to site 5. Le Boydron–Le Garrec et al. (2005) studied the effects of 31 plant extracts traditionally administered to treat CTX poisoning in the Pacific area and found that 27 of the plant extracts tested in vivo were found to offer a protective effect against the action of CTX and/or BTX, making them possible drug targets for the treatment of CTX and BTX poisoning.

## Symptoms of Brevetoxins Poisoning

### Human Exposure to Neurotoxic Shellfish Poisoning

In humans, depending on the route of exposure, two distinct modes of NSP are possible. First, on ingestion of raw or cooked BTX-contaminated shellfish, within 30 minutes to 3 hours the following

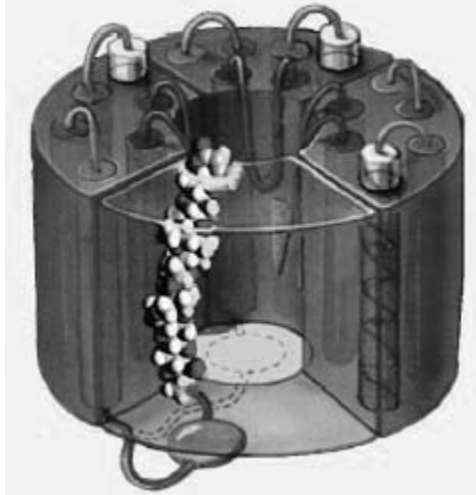


**Figure 2.7.** A model depicting the sodium-channel  $\alpha$ -subunit three-dimensional structure and hypothesised orientation of brevetoxin “head-down” between domains III and IV (Baden et al. 2005).

symptoms are typical: nausea, vomiting, diarrhoea, chills, sweats, reversal of temperature, hypotension, arrhythmias, numbness, tingling of lips, face and extremities, cramps, broncho-constriction, paralysis, seizures, and coma. These effects can persist for up to a few days (Kirkpatrick et al. 2004; van Apeldoorn, van Egmond, and Speijers 2001; Tibbets 1998; Cembrella, Milenkovic, and Doucette 1995; Novak 1998; Berman and Murray 1999). No mortalities or chronic symptoms have been reported in humans, and clinical treatment is primarily supportive (van Apeldoorn, van Egmond, and Speijers 2001). In general, NSP produces milder toxic effects than paralytic shellfish poisoning (PSP) toxins or CTX (Kirkpatrick et al. 2004).

The second route of exposure occurs from the inhalation of sea spray containing the *K. brevis* organism contaminated with BTX (aerosolised red tide blooms) (Kirkpatrick et al. 2004). The *K. brevis* dinoflagellate is relatively fragile because it does not possess a coat of armor. Therefore, particularly in wave action along beaches, the dinoflagellate is easily broken open, releasing toxins into the water and creating an onshore aerosol sea spray (Pierce et al. 2005; Kirkpatrick et al. 2004; Music, Howell, and Brumback 1973; Pierce 1986; Pierce et al. 1989, 1990, 2001, 2003; Backer et al. 2003, 2005). The toxins both in the droplets and attached to salt particles can be carried inland depending on wind and environmental conditions and can intoxicate humans by inhalation routes. Symptoms reported from the inhalation of aerosolized red tide toxins include respiratory irritation, conjunctival irritation, copious catarrhal exudates, rhinorrhea, nonproductive coughing, and broncho constriction (Music, Howell, and Brumback 1973; Asai et al. 1982, 1984; Kirkpatrick et al. 2004). On leaving the beach area or on entering an air-conditioned area symptoms are alleviated, and airborne irritation may be avoided by wearing a face mask (Steidinger and Baden 1984; Baden 1983; Watanabe, Locket, and Krzanowski 1988; Backer et al. 2003; Kirkpatrick et al. 2004). Studies carried out by Asai et al. found that asthma sufferers were highly prone to respiratory irritation following exposure to red tide aerosols, as were nonasthmatic smokers (Asai et al. 1982; Watanabe, Locket, and Krzanowski 1988).

In a pilot study of aerosolised red tide, Backer et al. (2003) measured the levels of BTX in air and water samples and conducted personal interviews and pulmonary function tests on people before and after visiting Florida beaches during *K. brevis* red tide proliferation. One hundred twenty-nine people participated in the study, which was conducted during two separate toxic red tide events in the west and east coasts of Florida. Respiratory symptoms, of varying severity depending on duration of exposure, were reported in 47% of participants.

BTX-induced broncho spasm in asthmatic sheep and other animal models exposed to aerosolized red tide toxins can be effectively blocked by the mast cell stabilizing agent cromolyn and the histamine H1 antagonist chlorpheniramine, as well as by the muscarinic blocker atropine, the beta-2-agonists, the calcium channel blocker verapamil, and the sodium channel blocker tetrodotoxin (TTX) (Baden and Mende 1982; Trainer and Baden 1991; Singer et al. 1998; Watanabe, Locket, and Krzanowski 1988). Some of these medications may be useful as prophylactics in those with compromised respiratory function. More worrying are anecdotal reports of chronic lung disease, especially in susceptible populations such as the elderly, associated with repeated exposures to BTX contaminated red tides (Fleming and Baden 1999; Watters 1995).

Kirkpatrick et al. (2005) carried out a study to determine whether there was an increase in respiratory diagnosis emergency room admissions to a Florida hospital, in Sarasota, during the period of a toxic red tide. The rates of admission were compared for a three-month time period when there was an onshore red tide in 2001 and during the same three-month period in 2002 when no red tide bloom occurred. There was no significant increase in the total number of respiratory admissions between the two time periods. However, there was a 19% increase in the rate of pneumonia cases diagnosed

during the red tide period compared with the non-red tide period. This study also revealed that the majority of admissions were patients living close to the coastline.

The drive to develop an antidote for BTX has increased following promising experimental animal studies on the development of specific monoclonal antibodies and antidotes against BTX (Templeton, Poli, and Leclaire 1988, 1989). In the meantime, regular monitoring of red tides by regulatory authorities and allocation of additional resources to hospitals serving those living near affected coastal areas may be prudent to ensure human safety.

### *Marine and Other Organisms Susceptible to NSP*

*Karina brevis* has long been associated with large fish kills and intoxication of mammalian species and aquatic species (Tester, Turner, and Shea 2000; Landsberg 2002). BTXs have been detected in tuna and other finfish, in manatees, and Muir birds (Bossart et al. 1998; Quilliam 1999). Under laboratory conditions, it has been demonstrated that BTX can persist in the food chain from dinoflagellate, through copepod grazers, to juvenile fish (Tester, Turner, and Shea 2000).

Bivalve shellfish are the main accumulators of BTXs (Viviani 1992). PbTx-2 and PbTx-3 were determined in the oyster *Crassostrea gigas* in New Zealand (Ishida et al. 1996). BTX-B1, BTX-B2, BTX-B3, and BTX-B4 have been found in cockles (*Austrovenus stutchburyi*). These analogues were found only in the shellfish, which may imply that they are metabolites formed by the mollusc in vitro (Fig. 2.8) (Ishida et al. 2004b; Plakas et al. 2002). These analogues demonstrated, in common with members of the main BTX group, bioactivity toward the Na<sup>+</sup> channels, but were not shown to be ichthyologic (Ishida et al. 1996; Morohashi 1999, 1995). In 1996, clams (*Chione cancellata* and *Mercenaria* spp.) and whelks (*Busycon contrarium*) from Sarasota Bay, Florida, were demonstrated to be positive for PbTx-2 and PbTx-3 as well as several metabolites (Poli et al. 2000). In 2004, Ishida et al. (2004a, 2004b) determined the presence of an array of brevetoxins and shellfish-formed metabolites in cockles, greenshell mussels, and Pacific oyster that had been implicated in an NSP episode in New Zealand.

Rodriguez, Escobales, and Maldonado (1994) conducted in vivo toxicity studies using murine liver slices to examine the effects of PbTx-3 on several parameters related to hepatic metabolism. The results indicated that PbTx-3 inhibited oxygen consumption and increased the intracellular Na<sup>+</sup> levels and also stimulated a K<sup>+</sup> efflux. The effect of PbTx-3 on the Na<sup>+</sup> content of liver slices was negated by the Na<sup>+</sup> blocker TTX, which also served to reduce the inhibition of oxygen consumption. TTX, however, did not alter the effects of PbTx-3 on the K<sup>+</sup> movements, indicating perhaps that two distinct ion channels were activated by PbTx-3.

In vitro studies have been conducted on laboratory animals. Oral administration of <sup>3</sup>H-labelled PbTx-3 indicated that the toxin distributed to all organs but accumulated to the greatest degree in the liver (Poli et al. 1990a, 1990b). Seven days following dosing by oral bolus, 80% of the toxin was excreted via faeces and urine (Cattet and Geraci 1993).

Poli and co-workers (Poli et al. 1990b; Cattet and Geraci 1993) demonstrated that rats, when dosed intravenously, showed a rapid clearance of the labelled PbTx-3 toxin from the system. Examination of the excrement by thin layer chromatography indicated the bioconversion of the toxin to more polar metabolites. This study corroborated the oral study, indicating that the main site of detoxification of the BTXs is the liver.

Benson et al. (1999) conducted an intratracheal study into the effects of aerosol-borne PbTx-3. Tritium-labelled PbTx-3 was administered by intratracheal instillation to rats. The results of

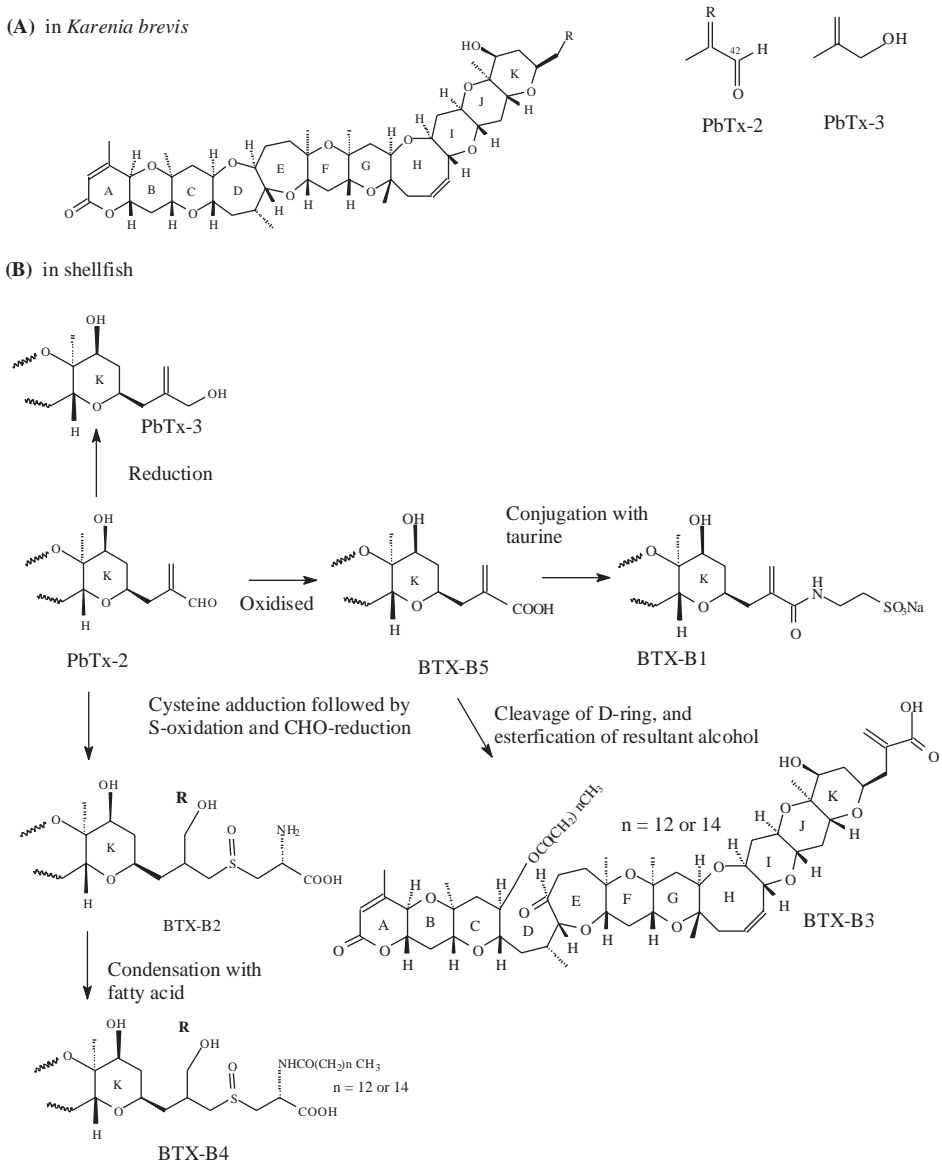


**Figure 2.8.** Shellfish metabolites of PbTx/BTX (A) and plausible metabolic pathway of PbTx-2 in shellfish (B) (Ishida et al. 2004).

investigation demonstrated that within 30 minutes most of the toxin was cleared from the lungs and distributed about the body by the blood stream. PbTx-3 was found after this interval to have accumulated to the greatest extent in the skeletal muscle (49%), intestines (32%), and liver (8%). Only negligible quantities were found in the blood, brain, and fat. After one week, about 20% of the toxin dose was retained in the tissues, the vast majority of PbTx-3 having been eliminated in the feces and

urine in the first 48 hours. Extrapolation of these results may indicate the persistence of low levels of BTXs in toxic-aerosol-exposed humans after the initial respiratory tract irritation has abated.

The application of labelled PbTx-3 in water, methanol, and dimethylsulphoxide (DMSO) to the skin of humans and guinea pigs was investigated to establish the degree of permeability of the dermis to the toxin. Results indicated that total penetration of PbTx-3 through human skin was 0.43%, 0.14%, and 1.53% of the dose administered in water, methanol, and DMSO, respectively, and that penetration through the skin of guinea pigs was faster than through human skin with methanol and DMSO as solvent vehicles (Kempainen et al. 1989). Kempainen et al. (1991) conducted another skin permeability study using pigs. In this study, the  $^3\text{H}$ -PbTx-3-carrier solvent was DMSO. Absorption of the toxin through the skin was rapid with a maximum of 9.1% of the toxin absorbed through the skin after four hours; after 24 hours the amount in the dermis had decreased to around 2%.

Rodriguez-Rodriguez and Malonado (1996) studied the effects of PbTx-3 on liver cells. Microscopy studies showed hypertrophy and increased vacuolation of cells. Also observed was swelling in the smooth endoplasmic reticulum, degranulation of the rough endoplasmic reticulum and damage to the mitochondria structure. Presence of active lysosomes was also apparent.

Rodgers et al. (1984) demonstrated that PbTx-2 was also a powerful cardiotoxin. These toxicological studies highlight the need for the implementation of a regular and reliable monitoring program in regions affected by BTX.

## Protection of Human Health

Up to the late 1980s, it was assumed that BTX was restricted to the Gulf of Mexico and the east coast of Florida. However, the appearance in different regions of *K. brevis*-like algae and the isolation of BTX-like toxins have raised fears that this is a worldwide phenomenon.

In 1993, nearly 200 people became ill after eating shellfish in New Zealand with symptoms that were consistent with NSP. The culprit dinoflagellate was very similar to *K. brevis*, and it is probable that the species was always present in the region in low concentrations, but environmental and climatic factors may have contrived to initiate a massive bloom of the algae (Smith, Chang, and MacKenzie 1993; Hallegraeff 1995). A similar species to *K. Brevis* was found in Japan in 1992. BTXs have also been determined in birds originating from the coast of California and in tuna from Australia. In 1995–1996 in False Bay, South Africa, sea aerosols caused respiratory symptoms conducive with BTX. In fact, this incident and subsequent events in the region have been linked with a species of algae similar to *K. brevis*; the incident happened during the autumn and correlated with a green discoloration of the water. The presence of the raphidophyte, *Fibrocapsa japonica*, a progenitor of BTX related compounds, has been found in certain locations of Europe, Asia, and North America (Van der Vyver et al. 2000; Hallegraeff 1995; Rademaker et al. 1995; Smith, Chang, and MacKenzie 1993; Kan, Arakawa, and Onoue 1996a, 1996b, and 1997).

Some scientists believe a major contributory factor to the spread of BTX may be the transportation of dinoflagellate cysts in ships' ballasts or due to the translocation of shellfish stocks (Viviani 1992; Quilliam 1999).

What measures have been taken worldwide to protect human health and the shellfish industry?

In the United States, a level of  $\geq 20$  MU/100 g in shellfish tissue established by mouse bioassay will initiate regulatory action by the Food and Drug Administration (FDA) (U.S. FDA 2000; Dickey et al. 1999). Florida is especially susceptible to BTX incidents, and since the 1970s the Florida Department of Natural Resources has run a general control program; a cessation of shellfish



harvesting is imposed when *K. brevis* concentrations exceed 5,000 cells per liter; 14 days after the cell counts have dropped below the action level, the mouse bioassay testing of shellfish is carried out; when levels drop below 20 MU/100 g harvesting is again permitted (Fleming and Baden 1999). In Europe, algae monitoring is conducted in Denmark and Italy (van Egmond, Speyers, and Van de Top 1992; Shumway et al. 1995; Viviani 1992). Since the intoxication incident in 1993, New Zealand has a weekly mouse bioassay-based monitoring program of all shellfish in place; the regulatory limit is set at 20 MU/100 g (Trusewich et al. 1996).

In spite of the risk posed to human health by NSP toxins, relatively few countries have regular testing programs in place. The mouse bioassay testing that is in place in the United States, Italy, and New Zealand has debatable reliability. The protection of human health would be served much better by instrumental analysis. The biggest obstacle to the instigation of reliable BTX monitoring programs is perhaps the worldwide lack of certified reference materials (James et al. 2004).

## Conclusion

*Karenia brevis* is the progenitor of several potent toxic molecules including the BTXs. While a lot is understood regarding the structure and molecular mechanism of action of BTXs, there is a dearth of literature or formal epidemiological studies on the effects to human health from these toxins. As a consequence, NSP is highly underreported and underdiagnosed. There are few existing statistics for the incidence of NSP poisonings, even in endemic areas, and little research has been conducted on the possible chronic health effects in humans or on the identification of biomarkers for diagnosis.

The existence of evidence demonstrating that BTXs can climb the food chain and pose a threat to higher organisms, including humans, emphasises the urgent need for research into the impacts of BTX and related toxins in the areas of public health, management of sustainable shellfisheries, detection of neurotoxins, and determining the impact of those toxins in marine ecosystems.

## Acknowledgements

The authors wish to acknowledge Science Foundation Ireland (SFI) Basic Research Grant Programme, 2004.

## References

- Abraham, W.M., Bourdelais, A.J., Ahmed, A., Serebriakov, I. and Baden, D.G. 2005. Effects of inhaled brevetoxins in allergic airways: toxin-allergen interactions and pharmacologic intervention. *Environmental Health Perspectives* 113, 632–637.
- Aldrich, D.V. 1962. *Science* 137, 988–990.
- Anderson, P.A.V., Roberts-Misterly, J., and Greenberg, R. M. 2005. The evolution of voltage-gated sodium channels: were algal toxins involved? *Harmful Algae* 4, 95–107.
- Asai, S., Krzanowski, J.J., Anderson, W.H., Martin, D.F., Polson, J.B., Lockey, R.F., Bukantz, S.C., Szentivanyi, A. 1982. Effects of the toxin of red tide, *Ptychodiscus brevis*, on canine tracheal smooth muscle: a possible new asthma triggering mechanism. *J Allergy Clin Immunol* 69, 418–428.
- . 1984. Site of action of *Ptychodiscus brevis* within parasymphathetic axonal sodium channel h gate in airway smooth muscle. *J Allergy Clin Immunol* 73, 824–828.
- Backer, L.C., Fleming, L.E., Rowan, A., Cheng, Y., Benson, J., Pierce, R.H., Zaias, J., Bean, J., Bossart, G.D., Johnson, D., Quimbo, R., Baden, D.G. 2003. Recreational exposure to aerosolized brevetoxins during Florida red tide events. *Harmful Algae* 2, 19–28.



- Backer, L.C., Kirkpatrick, B., Fleming, L.E., Cheng, Y.S., Pierce, R., Bean, J.A., Clark, R., Johnson, D., Wanner, A., Tamer, R., Zhou, Y., Baden, D.G. 2005. Occupational exposure to aerosolized brevetoxins during Florida red tide events: Effects on a healthy worker population. *Environmental Health Perspectives* 113, 644–649.
- Baden, D.G. 1983. Marine food-borne dinoflagellate toxins. *Int Rev Cytol* 82, 99–150.
- Baden, D.G., Bourdelais, A.J., Jacocks, H., Michelliza, S., and Naar, J. 2005. Natural and derivative brevetoxins: historical background, multiplicity, and effects. *Environmental Health Perspectives* 113, 621–625.
- Baden, D.G., and Mende, T.J. 1982. Toxicity of two strains from the Florida red tide marine dinoflagellate, *Gymnodinium breve*. *Toxicon* 20, 457–461.
- Benson, J.M., Tischler, D.L., and Baden, D.G. 1999. Uptake, tissue distribution, and excretion of brevetoxin 3 administered to rats by intratracheal instillation. *Journal of Toxicology and Environmental Health-Part A* 57, 345–355.
- Berman, F.W., and Murray, T.F. 1999. Brevetoxins cause acute excitotoxicity in primary cultures of rat cerebellar granule neurons. *Journal of Pharmacology and Experimental Therapeutics* 290, 439–444.
- Bossart, G.D., Baden, D.G., Ewing, R.Y., Roberts, B., and Wright, S.D. 1998. Brevetoxicosis in manatees (*Trichechus manatus latirostris*) from the 1996 epizootic: gross, histologic, and immunohistochemical features. *Toxicologic Pathology* 26, 276–282.
- Bourdelais, A.J., and Baden, D.G. 2004. Toxic brevetoxin complexes are in aqueous solutions. Abstract. *Toxicologist* 78(1-S), 807.
- Cane, D.E., Celmer, W.D., and Westley, J.W. 1983. *J Am Chem Soc* 105, 3594.
- Catterall, W.A. 1992. Cellular and molecular biology of voltage-gated sodium channels. *Physiol Rev* 72, 15–48.
- Cattet, M., and Geraci, J.R. 1993. Distribution and elimination of ingested brevetoxin (PbtX-3) in rats. *Toxicon* 31, 1483–1486.
- Cembella, A.D., Milenkovic, L.V., and Doucette, G.J. 1995. In *Manual on Harmful Marine Microalgae, IOC Manuals and Guides No. 33*, ed. Hallegraeff, G.M., Anderson, D.M., Cembella, A.D., and Enevoldsen, H.O. Paris: UNESCO, 181–211.
- Daugbjerg, N., Hansen, G., Larsen, J., and Moestrup, Ø. 2000. *Karenia brevis* (C.C. Davis) G. Hansen and Ø. Moestrup. *Phycologia* 39, 308.
- Dickey, R., Jester, E., Granade, R., Mowdy, D., Monereiff, C., Rebarchik, D., Robl, M., Musser, S., Poli, M. 1999. Monitoring brevetoxins during a *Gymnodinium breve* red tide: comparison of sodium channel specific cytotoxicity assay and mouse bioassay for determination of neurotoxic shellfish toxins in shellfish extracts. *Natural Toxins* 7, 157–165.
- Fleming, L.E., and Baden, D.G. 1999. <http://www.redtide.who.edu/hab/illness/floridaredtide.html>.
- Garson, M. 1993. *J Chem Rev* 93, 1600.
- Gawley, R.E., Rein, K.S., Jeglich, G., Adams, D.J., Theodorakis, E.A., Tieves, J., Nicolaou, K.C., Baden, D.G. 1995. The relationship of brevetoxin length and a-ring functionality to binding and activity in neuronal sodium channels. *Chemistry & Biology* 2, 533–541.
- Geesey, M.E., and Tester, P.A. 1993. In *Proceedings of the Fifth International Conference on Toxic Marine Phytoplankton*, ed. Smayda, T.J.S., and Shimizu, Y. New York: Elsevier Science Publishing.
- Gray, M., Wawrik, B., Paul, J., and Casper, E. 2003. Molecular detection and quantitation of the red tide dinoflagellate *Karenia brevis* in the marine environment. *Applied and Environmental Microbiology*, 5726–5730.
- Hallegraeff G.M. 1995. In *Manual on Harmful Marine Microalgae, IOC Manuals and Guides No. 33*, ed. Hallegraeff, G.M., Anderson D.M., Cembella A.D., and Enevoldsen, H.O. Paris: UNESCO, 1–22.
- Hallegraeff, G.M., and Hara, Y. 1995. In *Manual on Harmful Marine Microalgae. IOC Manuals and Guides No. 33*, ed. Hallegraeff, G.M., Anderson, D.M., Cembella, A.D., and Enevoldsen, H.O. Paris: UNESCO, 365–371.
- Hopkins, R.S., Heber, S., and Hammond, R. 1997. Water related disease in Florida: continuing threats require vigilance. *J Florida Med Assoc* 84, 441–445.
- Husain, K., Singh, R., Kaushik, M.P., and Gupta, A.K. 1996. Acute toxicity of synthetic *Gymnodinium breve* toxin metabolite and its analogues in mice. *Ecotoxicol Environ Safety* 35, 77–80.
- Inoue, M., Hiramata, M., Satake, M., Sugiyama, K., and Yasumoto, T. 2003. Inhibition of brevetoxin binding to the voltage-gated sodium channel by gambierol and gambieric acid-A. *Toxicon* 41, 469–474.
- Ishida, H., Nozawa, A., Totoribe, K., Muramatsu, N., Nukaya, H., Tsuji, K., Yamaguchi, K., Yasumoto, T., Kaspar, H., Berkett, N., Kosuge, T. 1995. Brevetoxin-B-1, a new polyether marine toxin from the New Zealand shellfish, *Austrovenus stutchburyi*. *Tetrahedron Letters* 36, 725–728.
- Ishida, H., Nozawa, A., Nukaya, H., Rhodes, L., McNabb, P., Holland, P.T., Tsuji, K. 2004a. Confirmation of brevetoxin metabolism in cockle, *Austrovenus stutchburyi*, and greenshell mussel, *Perna canaliculus*, associated with New Zealand neurotoxic shellfish poisoning, by controlled exposure to *Karenia brevis* culture. *Toxicon* 43, 701–712.
- Ishida, H., Muramatsu, N., Nukaya, H., Kosuge, T., and Tsuji, K. 1996. Study on neurotoxic shellfish poisoning involving the oyster, *Crassostrea gigas*, in New Zealand. *Toxicon* 34, 1050–1053.
- Ishida, H., Nozawa, A., Nukaya, H., and Tsuji, K. 2004b. Comparative concentrations of brevetoxins PbTx-2, PbTx-3, BTX-B1 and BTX-B5 in cockle, *Austrovenus stutchburyi*, greenshell mussel, *Perna canaliculus*, and Pacific oyster, *Crassostrea gigas*, involved neurotoxic shellfish poisoning in New Zealand. *Toxicon* 43, 779–789.

- James, K.J., Fidalgo Sáez, M.J., Furey, A., and Lehane, M. 2004. Azaspiracid poisoning, the food-borne illness associated with shellfish consumption. *Food Additives and Contaminants* 21, 879–892.
- Jeglitsch, G., Rein, K., Baden, D.G., and Adams, D.J. 1998. Brevetoxin-3 (PbTx-3) and its derivatives modulate single tetrodotoxin-sensitive sodium channels in rat sensory neurons. *Journal of Pharmacology and Experimental Therapeutics* 284, 516–525.
- Kadota, I., Ohno, A., Matsuda, K., and Yamamoto, Y. 2002. Convergent synthesis of polycyclic ethers via the intramolecular allylation of alpha-acetoxy ethers and subsequent ring-closing metathesis. *Journal of the American Chemical Society* 124, 3562–3566.
- Kadota, I., Takamura, H., Nishii, H., and Yamamoto, Y. 2005. Total synthesis of brevetoxin B. *Journal of the American Chemical Society* 127, 9246–9250.
- Kamykowski, D., Milligan, E.J., and Reed, R.E. 1998. Relationships between geotaxis/phototaxis and diel vertical migration in autotrophic dinoflagellates. *J Plankton Res* 20, 1781–1796.
- Kempainen, B.W., Mehta, M., and Clarke, C.R. 1989. Effect of vehicle on in vitro percutaneous penetration of [3H] PbTx-3 (a red tide toxin) in human and guinea-pig skin. *Toxicol* 27, 54–55.
- Kempainen, B.W., Reifenrath, W.G., Stafford, R.G., and Mehta, M. 1991. Methods for in vitro skin absorption studies of a lipophilic toxin produced by red tide. *Toxicology* 66, 1–17.
- Khan, S., Ahmed, M.S., Arakawa, O., and Onoue, Y. 1995. Properties of neurotoxins separated from a harmful red tide organism *Chattonella marina*. *Israel J Aquacult-Bamidgeh* 47, 137–141.
- Khan, S., Arakawa, O., and Onoue, Y. 1996a. Neurotoxin production by a chloromonad *Fibrocapsa japonica* (Raphidophyceae). *Journal of the World Aquaculture Society* 27, 254–263.
- . 1996b. A toxicological study of the marine phytoflagellate *Chattonella antiqua* (Raphidophyceae). *Phycologia* 35, 239–299.
- . 1997. Neurotoxins in a toxic red tide of *Heterosigma akashiwo* (Raphidophyceae) in Kagoshima Bay, Japan. *Aquaculture Research* 28, 9–14.
- Kirkpatrick, B., Fleming, L.E., Squicciarini, D., Backer, L.C., Clark, R., Abraham, W., Benson, J., Cheng, Y.S., Johnson, D., Pierce, R., Zaias, J., Bossart, G.D., Baden, D.G. 2004. Literature review of Florida red tide: implications for human health effects. *Harmful Algae* 3, 99–115.
- Kirkpatrick, B., Fleming, L.E., Backer, L.C., Bean, J.A., Tamer, R., Kirkpatrick, G., Kane, T., Wanner, A., Dalpra, D., Reich, A., Baden, D.G. 2005. Environmental exposures to Florida red tides: effects on emergency room respiratory diagnoses admissions. *Harmful Algae*, in press.
- Koley, J., Sinha, S., Basak, A.K., Das, M., Dube, A.N., Manunder, P.K. 1995. Cardiovascular and respiratory changes following exposure to a synthetic toxin of *Ptychodiscus brevis*. *Eur J Pharmacol Environ Toxicol Pharmacol*, section 293, 483–486.
- Krishna Prasad, A.V. and Shimizu, Y. 1989. *J Am Chem Soc* 111, 6476.
- Landsberg, J.H. 2002. The effects of harmful algal blooms on aquatic organisms. *Reviews in Fisheries Science* 10, 113–390.
- le Boydron-Le Garrec, R., Benoit, E., Sauriat, M.P., Lewis, R.J., Molgo, J., Laurent, D. 2005. Ability of some plant extracts, traditionally used to treat ciguatera fish poisoning, to prevent the in vitro neurotoxicity produced by sodium channel activators. *Toxicol* 46, 625–634.
- Lee, M.S., Qin, G., Nakanishi, K., and Zagorski, M.G. 1989. *J Am Chem Soc* 111, 6234.
- Lin, Y.Y., Risk, M., Ray, S.M., Vanengen, D., Clardy, J., Golik, J., James, J.C., Nakanishi, K. 1981. Isolation and structure of brevetoxin-B from the red tide dinoflagellate *Ptychodiscus brevis* (*Gymnodinium, Breve*). *Journal of the American Chemical Society* 103, 6773–6775.
- Maier Brown, A.F., Dortch, Q., Dolah, F.M., Van, Leighfield, T.A., Morrison, W., Thessen, A.E., Steidinger, K., Richardson, B., Moncreiff, C.A., Pennock, J.R. 2006. Effect of salinity on the distribution, growth and toxicity of *Karenia spp.* *Harmful Algae* 5, 199–212.
- Matsuo, G., Kawamura, K., Hori, N., Matsukura, H., and Nakata, T. 2004. Total synthesis of brevetoxin-B. *Journal of the American Chemical Society* 126, 14374–14376.
- Mazunder, P.K., Gupta, A.K., Kaushik, M.P., Dumar, D., and Dube, S.N. 1997. Cardiovascular effects of an organophosphate toxin isolated from *ptychodiscus brevis*. *Biomed Environ Sci* 10, 23–27.
- Morohashi, A., Satake, M., Naoki, H., Kasper, H.F., Oshima, Y., Yasumoto, T. 1999. Brevetoxin B4 isolated from greenshell mussels *Perna canaliculus*, the major toxin involved in neurotoxic shellfish poisoning in New Zealand. *Natural Toxins* 7, 45–48.
- Morohashi, A., Satake, M., Murata, K., Naoki, H., Kasper, H.F., Yasumoto, T. 1995. Brevetoxin B3, a new brevetoxin analog isolated from the greenshell mussel *Perna canaliculus* involved in neurotoxic shellfish poisoning in New Zealand. *Tetrahedron Letters* 36, 8995–8998.
- Murata, M., and Yasumoto, T. 1995. Structure of maitotoxin, the most toxic and largest natural non-biopolymer. *Journal of Synthetic Organic Chemistry Japan* 53, 207–217.
- Music, S.I., Howell, J.T., and Brumback, L.C. 1973. Red tide: its public health implications. *Floride Med J* 60, 27–29.
- Nakanishi, K. 1985. *Toxicol* 23, 473.

- Nicolaou, K.C., et al. 1998. Total synthesis of brevetoxin A. *Nature* 392, 264–269.
- . 1999a. Total synthesis of brevetoxin A: Part 1: First generation strategy and construction of BCD ring system. *Chemistry-a European Journal* 5, 599–617.
- . 1999b. Total synthesis of brevetoxin A: Part 2: Second generation strategy and construction of EFGH model system. *Chemistry-a European Journal* 5, 618–627.
- . 1999c. Total synthesis of brevetoxin A: Part 3: Construction of GHIJ and BCDE ring systems. *Chemistry-a European Journal* 5, 628–645.
- . 1999d. Total synthesis of brevetoxin A: Part 4: Final stages and completion. *Chemistry-a European Journal* 5, 646–658.
- . 1995a. Total synthesis of brevetoxin B (2). Completion. *Journal of the American Chemical Society* 117, 1173–1174.
- . 1995b. Total synthesis of brevetoxin B (2). 2nd Generation strategies and construction of the dioxepane region DEFG. *Journal of the American Chemical Society* 117, 10239–10251.
- Nicolaou, K.C., et al. 1995c. Total synthesis of brevetoxin B (2). Final strategy and completion. *Journal of the American Chemical Society* 117, 10252–10263.
- Nicolaou, K.C., Prasad, C.V.C., Hwang, C.-K., Duggan, M.E., and Veale, C.A. 1989a. *J Am Chem Soc* 111, 5321.
- Nicolaou, K.C., Prasad, C.V.C., Somers, P.K., and Hwang, C.-K. 1989b. *J Am Chem Soc* 111, 5330.
- Nicolaou, K.C., Shi, G.Q., Gunzner, J.L., Gartner, P., and Yang, Z. 1997. Palladium-catalyzed functionalization of lactones via their cyclic ketene acetal phosphates. Efficient new synthetic technology for the construction of medium and large cyclic ethers. *Journal of the American Chemical Society* 119, 5467–5468.
- Nicolaou, K.C., and Sorensen, E.J. 1996. *Classics in total Synthesis*. Weinheim: VCH.
- Novak, S. M. 1998. Foodborne illness: chemical fish and shellfish poisoning. *Clin Microbiol Newslett* 20, 17–21.
- Pawlak, J., Tempesta, M.S., Golik, J., Zagorski, M.G., Lee, M.S., Nakanishi, K., Iwashita, T., Gross, M.L., Tomer, K.B. 1987. Structure of Brevetoxin-A as constructed from Nmr and Ms Data. *Journal of the American Chemical Society* 109, 1144–1150.
- Pierce, R. 1986. Red tide (*Ptychodiscus brevis*) toxin aerosols: a review. *Toxicon* 24, 955–965.
- Pierce, R., Henry, M.S., Boggess, S., and Rule, A. 1989. In *The Climate and Health Implications of Bubble-Mediated Sea-Air Exchange*, ed. Monahan, E., and van Patton, P. Connecticut Sea Grant Publications.
- Pierce, R., Henry, M.S., Blum, P., and Payne, P. 2001. In *Harmful Algae Blooms 2000. Proceedings of the 9th International Conference on Harmful Algal Blooms*, ed. Hallegraff, G.M., Bolch, C.J., Blackburn, S.I., and Lewis, R.J. Paris: IOC of UNESCO, 421–424.
- Pierce, R., Henry, M.S., Proffitt, L.S., and Hasbrouck, P.A. 1990. In *Toxic Marine Phytoplankton*, ed. Graneli, E., Sundström, S., Elder, L., and Anderson, D.M. 397–402.
- Pierce, R.H., Henry, M.S., Blum, P.C., Lyons, J., Cheng, Y.S., Yazzie, D., Zhou, Y. 2003. Brevetoxin concentrations in marine aerosol: Human exposure levels during a *Karenia brevis* harmful algal bloom. *Bulletin of Environmental Contamination and Toxicology* 70, 161–165.
- Pierce, R.H., Henry, M.S., Blum, D.C., Hamel, S.L., Kirkpatrick, B., Cheng, Y.S., Zhou, Y., Irvin, C.M., Naar, J., Weidner, A., Fleming, L.E., Backer, L.C., Baden, D.G. 2005. Brevetoxin composition in water and marine aerosol along a Florida beach: Assessing potential human exposure to marine biotoxins. *Harmful Algae* 4, 965–972.
- Plakas, S.M., El Said, K.R., Jester, E.L.E., Granade, H.R., Musser, S.M., Dickey, R.W. 2002. Confirmation of brevetoxin metabolism in the Eastern oyster (*Crassostrea virginica*) by controlled exposures to pure toxins and to *Karenia brevis* cultures. *Toxicon* 40, 721–729.
- Poli, M.A., Mende, T.J., and Baden, D.G. 1986. Brevetoxins, unique activators of voltage-sensitive sodium channels, bind to specific sites in rat brain synaptosomes. *Mol Pharmacol.* 30, 129–135.
- Poli, M.A., Musser, S.M., Dickey, R.W., Eilers, P.P., and Hall, S. 2000. Neurotoxic shellfish poisoning and brevetoxin metabolites: a case study from Florida. *Toxicon* 38, 981–993.
- Poli, M.A., Templeton, C.B., Thompson, W.L., and Hewetson, J.F. 1990a. Distribution and elimination of brevetoxin Pbtx-3 in rats. *Toxicon* 28, 903–910.
- . 1990b. Detection, Metabolism and Pathophysiology of brevetoxins. In *Marine Toxins. Origin, Structure and Molecular Pharmacology*, ACS Symposium Series, ed. Hall, S., and Strichartz, G. 176–191.
- Purkerson, S.L., Baden, D.G., and Fieber, L.A. 1999. Brevetoxin modulates neuronal sodium channels in two cell lines derived from rat brain. *Neurotoxicology* 20, 909–920.
- Quilliam, M. 1999. General Referee Reports. Committee on Natural Toxins. *Phycotoxins, JAOAC Int* 82/3, 773–784.
- Rademaker, M., Reckermann, M., Tilla, U., Tillman-Mayer, A., Colijn, F., Zevenboom, W. 1997. *Fibrocapsa japonica* and *Heterosigma akashiwo* (*Raphidophyceae*) along the Dutch and German coasts: new observations. *Harmful Algae News* 17, 8–10.
- Rademaker, M., Janmaat, L., Zevenboom, W., and Jong, B.D. 1995. Potentially toxic algae along the Dutch coast in 1994. *Harmful Algae News* 10/11 (2), 2.

- Rein, K.S., Baden, D.G., and Gawley, R.E. 1994. Conformational analysis of the sodium-channel modulator brevetoxin-A, comparison with brevetoxin-B conformations, and a hypothesis about the common pharmacophore of the site-5 toxins. *Journal of Organic Chemistry* 59, 2101–2106.
- Rein, K.S., Lynn, B., Gawley, R.E., and Baden, D.G. 1994. Brevetoxin-B: chemical modifications, synaptosome binding, toxicity, and an unexpected conformational effect. *Journal of Organic Chemistry* 59, 2107–2113.
- Rodgers, R.L., Chou, H.N., Temma, K., Akera, T., and Shimizu, Y. 1984. Positive inotropic and toxic effects of brevetoxin-B on rat and guinea-pig heart. *Toxicology and Applied Pharmacology* 76, 296–305.
- Rodriguez, F.A., Escobales, N., and Maldonado, C. 1994. Brevetoxin-3 (Pbtx-3) inhibits oxygen consumption and increases Na<sup>+</sup> content in mouse-liver slices through a tetrodotoxin-sensitive pathway. *Toxicon* 32, 1385–1395.
- Rodriguez-Rodriguez, F.A., and Maldonado, C. 1996. Brevetoxin-3 (PbTx-3) on mouse liver slices: a histological study. *P R Health Sci J* 15, 261–267.
- Shimizu, Y., Chou, H.N., Bando, H., Vanduyne, G., and Clardy, J.C. 1986. Structure of brevetoxin-A (Gb-1 toxin), the most potent toxin in the Florida red tide organism *Gymnodinium breve* (*Ptychodiscus-Brevis*). *Journal of the American Chemical Society* 108, 514–515.
- Shimizu, Y., Gupta, S., and Krishna Prasad, A.V. 1990. In *Toxic Marine Phytoplankton*, ed. Graneli, E., Substrom, B., Edler, L., and Anderson, D.M. New York: Elsevier, 62–76.
- Shumway, S.E., van Egmond, H.P., Hurst, J.W., and Bean, L.L., eds. 1995. *Management of Shellfish Resources*. Paris: UNESCO.
- Singer, L.J., Lee, T., Rosen, K.A., Baden, D.G., and Abraham, W.M. 1998. Inhaled Florida red tide toxins induced bronchoconstriction (BC) and airway hyperresponsiveness (AHR) in sheep. *Am J Respir Crit Care Med* 157, A158.
- Smith, P., Chang, F.H., and MacKenzie, L. 1993. In Marine toxins and New Zealand shellfish. *Proceedings of a workshop on research issues, 10–11 June 1993*, Miscellaneous Series 24, ed. Jasperse, J.A. *The Royal Society of New Zealand*, 11–17.
- Steidinger, K.A., and Baden, D.G. 1984. In *Dinoflagellates*, ed. Spector, D.L. New York: Academy Press, 201–261.
- Steidinger, K.A., and Joyce Jr., E.A. 1973. Florida red tides. *State Fla Dep Nat Resour Educat Ser* 17, 1–26.
- Stumpf, R.P., Ransibrahmanakul, V., Steidinger, K.A., and Tester, P.A. 1998. In *Harmful Algae: Proceedings of the VIII International Conference on Harmful Algae, 1997 June 25–29*, ed. Reguera, B., Blanco, J., and Fernandez, M.L. Vigo, Spain, 145–148.
- Templeton, C.B., Poli, M.A., and Leclaire, R.D. 1988. Antibodies to prevent the effects of brevetoxin poisoning in conscious rats. Abstract. *Gov Rep Announce Index* 88, 155.
- . 1989. Cardiorespiratory effects of brevetoxin (Pbtx-2) in conscious, tethered rats. *Toxicon* 27, 1043–1049.
- Tester, P.A., Turner, J., and Shea, D. 2000. Vectorial transport of toxins from the dinoflagellate *Gymnodinium breve* through copepods to fish. *Journal of Plankton Research* 22, 47–61.
- Tibbets, J. 1998. Toxic tides. *Environ Health Perspect* 106, A326–A331.
- Townsend, C.A., and Basak, A. 1991. Experiments and speculations on the role of oxidative cyclization chemistry in natural product biosynthesis. *Tetrahedron* 47, 2591–2602.
- Trainer, V.L., and Baden, D.G. 1991. An enzyme-immunoassay for the detection of Florida red tide brevetoxins. *Toxicon* 29, 1387–1394.
- Trainer, V.L., and Baden, D.G. 1999. High affinity binding of red tide neurotoxins to marine mammal brain. *Aquatic Toxicology* 46, 139–148.
- Trainer, V.L., Brown, G.B., and Catterall, W.A. 1996. Site of covalent labeling by a photoreactive batrachotoxin derivative near transmembrane segment IS6 of the sodium channel alpha subunit. *Journal of Biological Chemistry* 271, 11261–11267.
- Trainer, V.L., Moreau, E., Guedin, D., Baden, D.G., and Catterall, W.A. 1993. Neurotoxin binding and allosteric modulation at receptor site-2 and site-5 on purified and reconstituted rat-brain sodium channels. *Journal of Biological Chemistry* 268, 17114–17119.
- Trusewich, B., Sim, J., Busby, P., and Hughes, C. 1996. In *Harmful and Toxic Algal Blooms: Proceedings of the VII International Conference on Toxic Phytoplankton, 1995, July 12–16*, ed. Yasumoto, T., Oshima, Y., and Fukuyo, Y. Sendai, Japan, 27–30.
- U.S. FDA. 2000. <http://www.agen.ufl.edu/foodsaf/sf100.html>.
- van Apeldoorn, M.E., van Egmond, H.P., and Speijers, G.J.A. 2001. In *RIVM Report 388802 023*. National Institute of Public Health and the Environment.
- Van der Vyver, I., Pitcher, G., Matthews, S., and Maneveldt, G W. 2000. <http://www.botany.uwc.ac.za/Envfacts/redtides/index.hum>. November 13, 2000.
- van Egmond, H.P., Speyers, G.J.A., and Van de Top, H.J. 1992. Current situation on worldwide regulations for marine phyco-toxins. *J Nat Toxins* 1, 67–85.
- Viviani, R. 1992. Eutrophication, marine biotoxins, human health. *Sci Total Environ Suppl*, 631–662.
- Wang, S.Y., and Wang, G.K. 2003. Voltage-gated sodium channels as primary targets of diverse lipid-soluble neurotoxins. *Cellular Signalling* 15, 151–159.
- Watanabe, T., Locket, R.F., and Krzanowski, J.J. 1988. Airway smooth muscle contraction induced by *Ptychodiscus brevis* (red tide) toxin as related to a trigger mechanism of bronchial asthma. *Immunol Allergy Pract* 10, 185–192.
- Watters, M.R. 1995. Review article. Organic neurotoxins in seafoods. *Clin Neurol Neurosurg* 97, 119–124.

## 3 Chemistry of Maitotoxin

Masayuki Satake

### Introduction

Ciguatera is the most famous seafood poisoning prevalent in circumtropical areas (Scheuer 1994). Its effects to human health and economic impacts are serious problems in those areas. The clinical symptoms are diverse. Neurological disturbances are prominent; reversal of thermal sensation, called “dry ice sensation,” is one of the most characteristic symptoms of ciguatera. Other illnesses include joint pain, miosis, erethism, cyanosis, and prostration.

Gastrointestinal disorders are nausea, vomiting, and diarrhea. Cardiovascular disturbances are low blood pressure and bradycardia. The poisoning is caused by ingestion of coral reef fish that have become toxic through diet. The principal toxins are ciguatoxin and its congeners. The other toxin is maitotoxin (MTX) (Fig. 3.1). Maitotoxin was first detected in the gut of the surgeonfish *Ctenochaetus striatus* as one of the causative toxins of ciguatera (Yasumoto, Baginis, and Vernoux 1976). MTX was named after the Tahitian fish *maito*. Both groups are produced by the epiphytic dinoflagellate *Gambierdiscus toxicus* and transfer to herbivorous fish and subsequently to carnivores through the food chain (Yasumoto et al. 1977). In French Polynesia, the poisoning cause by ingestion of herbivorous fish poses a more serious threat to public health than the carnivorous fishes.

Maitotoxin has attracted much attention for the following three reasons: First, it has a molecular weight of 3422 Da (as the disodium salt), which exceeds that of any other known natural products, except for biopolymers. Second, it presumably plays a role in diversifying ciguatera symptoms, particularly in the poisoning caused by herbivorous fish. Finally, it has extremely potent bioactivity. The lethality against mice ( $LD_{50}$  is ca. 50 ng/kg, i.p.), for example, suggests that it might be the most potent nonproteineaceous toxin. It implies that 1 mg of MTX can kill one million mice. Thus, its structural determination has been regarded as one of the most exciting challenges in natural products chemistry.

### Culture of *Gambierdiscus toxicus*

The dinoflagellate *Gambierdiscus toxicus* was collected at Gambier Islands in French Polynesia (Yasumoto et al. 1977). To accumulate enough material for structural elucidation, large-scale cultures have been continued for over 10 years. Laboratory cultures of *G. toxicus* were carried out in 3 L Fernbach flasks in a seawater medium enriched with ES-1 nutrients. After inoculated with a seed culture, cultures were kept for 38 days at 25°C under an 18/6-light/dark photocycle.

### Isolation of Maitotoxin

Maitotoxin was first isolated from *G. toxicus* in 1988 by Yasumoto's group at Tohoku University (Yokoyama et al. 1988). The harvested cells by filtration were extracted with MeOH twice and 50%

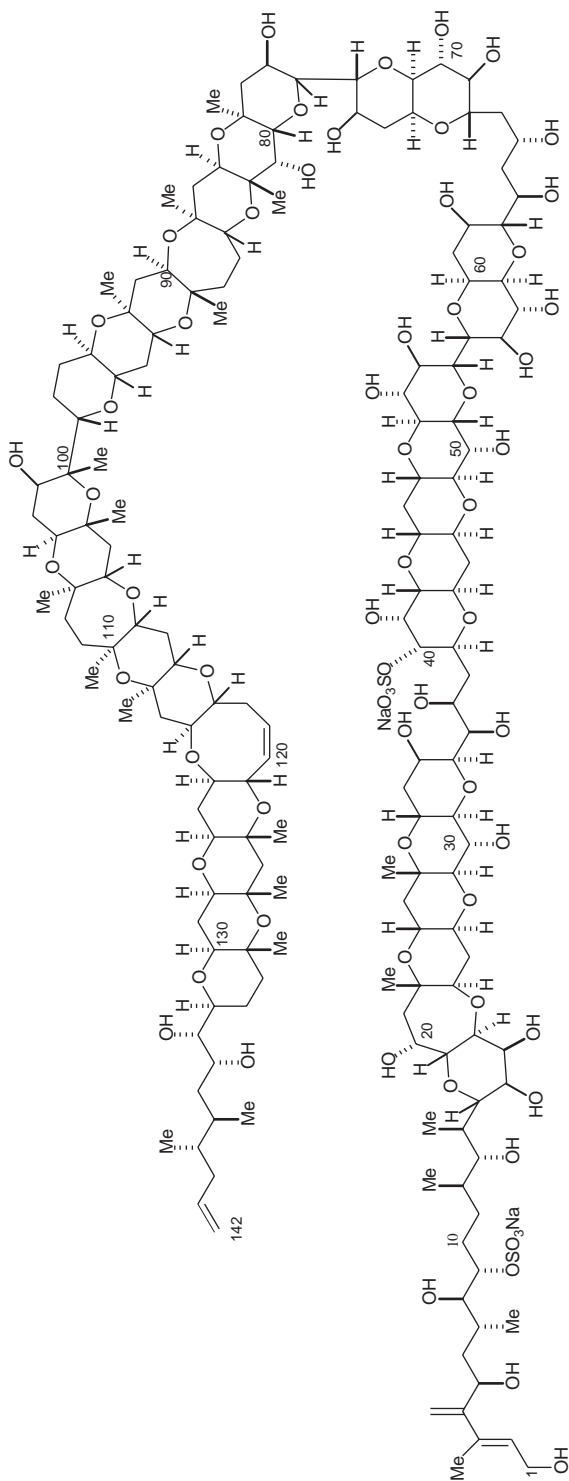


**Figure 3.1.** Structure of maitotoxin.



MeOH twice under reflux. After solvent removal, the residue was partitioned first between 40% MeOH and  $\text{CH}_2\text{Cl}_2$  and then between water and BuOH. MTX in the BuOH layer was chromatographed on a silica gel column. The MTX containing fraction was chromatographed on successive reversed phase columns. Final purification of MTX was done on a Develosil TMS column with MeCN/ $\text{H}_2\text{O}$  (35:65). MTX was eluted at around 33–35 minutes.

MTX is soluble in aqueous MeOH, aqueous MeCN, or DMSO, and relatively stable in alkaline but not acidic conditions.

Physicochemical properties of MTA are  $[\alpha]_D^{25} +16.8$  (c 0.36, MeOH- $\text{H}_2\text{O}$ , 1:1) and UV  $\lambda$ -max 230 nm ( $\epsilon$  9600).

## Structural Determination of MTX

### *FAB MS Analysis of Maitotoxin*

Molecular related ions of MTX were obtained with a thioglycerol-glycerol mixture as a matrix in a negative-ion FAB mode. In the spectrum, the ion peak losing a sulfate group ( $-\text{SO}_3\text{Na}+\text{H}$ ,  $m/z$  102) was observed, which was characteristic for compounds possessing at least one sulfate in the molecule and an additional anionic functionality where a negative charge remained after loss of sulfate, thus suggesting that MTX possesses two sulfate esters. In the spectrum, two sets of multiple ion peaks showed at round  $m/z$  3400 ( $\text{M}-\text{Na}$ ) $^-$  and at 3300 ( $\text{M}+\text{H}-\text{SO}_3\text{Na}$ ) $^-$ . On the basis of these data, the molecular weight of MTX as a disodium salt was suggested to be  $3424.5 \pm 0.5$ .

### *NMR Analysis and Chemical Degradation of MTX*

A total structure including partial stereochemistry has been proposed for MTX on the basis of extensive spectroscopic analysis (Murata et al. 1992, 1993, 1994). The 2D NMR analysis of MTX led to the structural elucidation of some partial structures such as the C1-C36 moiety. However, overlap and poor resolution of  $^1\text{H}$  and  $^{13}\text{C}$  NMR signals hampered the elucidation of the  $^1\text{H}$ - $^1\text{H}$  connectivity, particularly for the middle part of the molecule. A large number of cross peaks of the middle part overlapped each other in the 2D spectra due to recurring similar structural units. Several chemical degradations were attempted to reduce the size of the molecule. MTX gave no small fragments by ozonolysis because three double bonds reside on both side chains and the rest are present in a ring. MTX has no carbonyl carbons in the molecule, since no fragments were generated by hydrolysis. Periodate reaction of MTX resulted in C-C bond cleavage at six vicinal-diol sites and led to three degradation products (fragments A, B, and C) split at C36-C37 and C135-C-136 (Fig. 3.2). Multidimensional NMR experiments were applied to these fragments. The structure of fragment A was elucidated by the conventional 2D NMR experiments. Among them, fragment B was the largest with the molecular weight of 2328 Da (as sodium salt). The NMR spectra of fragment B was complicated by the presence of 160 protons. Structure assignments from C37 to C78 were mainly deduced by detailed analyses of interproton 2D NMR spectra. In the C79-C135 portion, 13 quaternary carbons interrupted the  $^1\text{H}$ - $^1\text{H}$  spin connectivities, and thus interproton 2D data did not provide much structural information. All of the quaternary carbons were bearing a methyl group. The connectivity around quaternary carbons could be assigned by HMBC. The configurations of the ring substituents were elucidated by NOEs between angular protons and/or angular methyls, and large  $^3J_{\text{H,H}}$  showed the transfusing of cyclic ethers. All feasible NMR spectra with 2  $\mu\text{mol}$  of the material were measured, but a few parts of the structure remained unassigned.

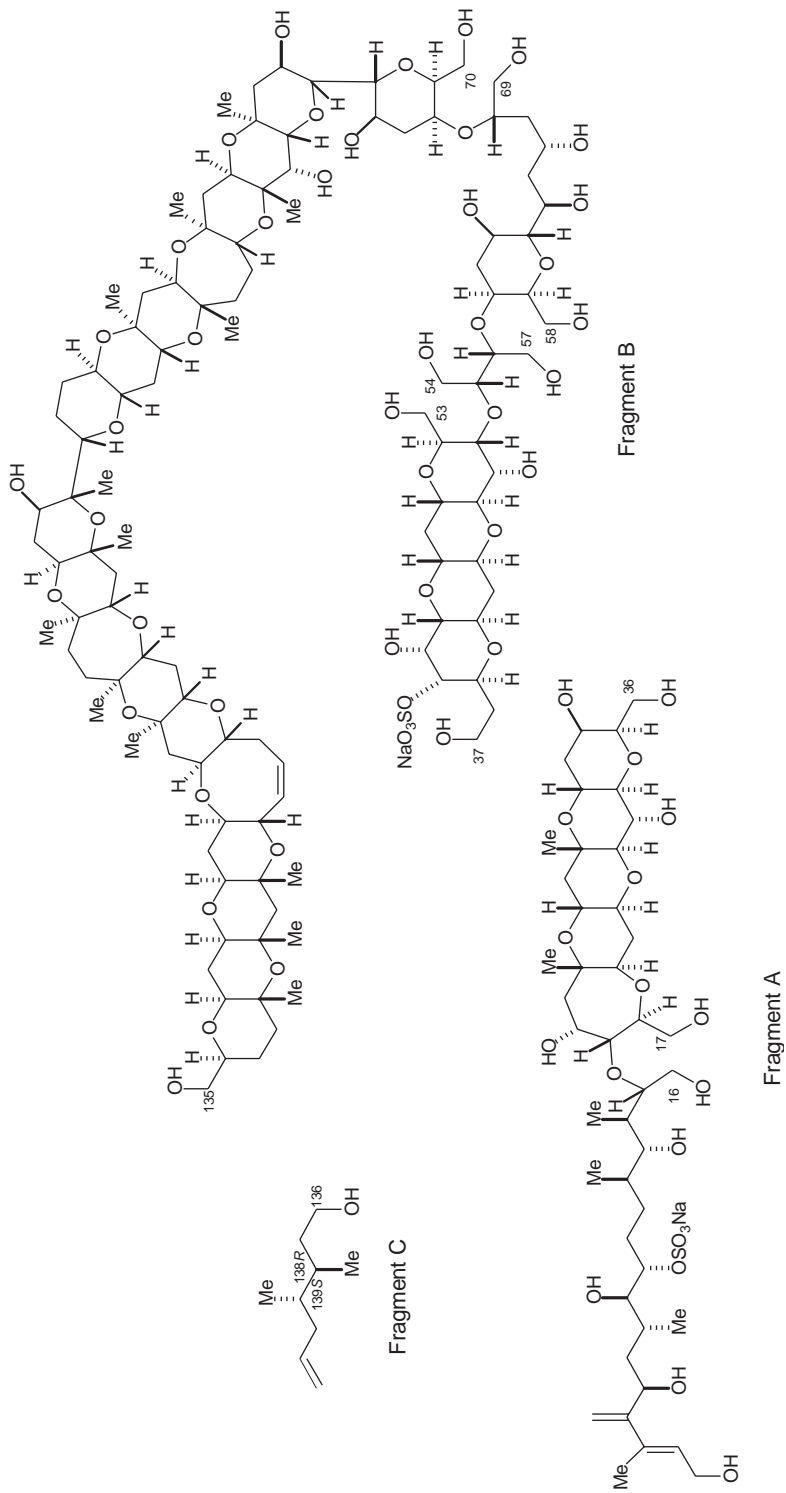


**Figure 3.2.** Structures of fragments generated by periodate degradation.



### CID MS/MS Experiments of Fragment B

Further structural conclusions on MTX were obtained with negative CID MS/MS (collision-induced dissociation tandem mass spectrometry) experiments. This provided invaluable information for assigning the sizes of the ether rings and the sequence around the acyclic ethers formed as a result of periodate degradation. The sulfate ester resides at the terminus of fragment B. Since a negative charge is located at this sulfate, bond cleavage occurred from the opposite side of the molecule. A series of product ions derived from bond cleavage at particular sites of each ether ring were observed (Fig. 3.3). The acyclic ethers generated by periodate degradation were cleaved at both sides of the ethereal linkages, which allowed the sequencing of four parts separated by the ether bonds. The MS/MS experiments supported the validity of the structures deduced by NMR studies. This exceeded the molecular size of all natural products and biomolecules that had been totally identified for gross structure by spectroscopic methods without further degradation.

### 3D NMR Experiments of Maitotoxin

Structural confirmation and complete  $^{13}\text{C}$  NMR assignments were accomplished by 3D PFG NOESY-HMQC experiments using a  $^{13}\text{C}$ -enriched sample (Satake et al. 1995). Although the 3D NMR technique has become a routine method for studies of protein and nucleotide, applications to natural products are rare. Unlike proteins, it is very difficult to enrich marine natural products with more than 90%  $^{13}\text{C}$  abundance. Moreover, the structural elucidation of most natural products can be accomplished by 2D NMR experiments. MTX needed 3D NMR experiments because more than 200 proton signals give rise to over 2000 cross peaks in the 2D NOESY spectra.

To obtain a  $^{13}\text{C}$ -enriched sample, *G. toxicus* was cultured in a medium containing 0.01% of  $\text{Na}_2^{13}\text{CO}_3$ . A modified method was applied to isolate  $^{13}\text{C}$ -enriched MTX. MTX in the BuOH layer was purified by successive chromatography on gel permeation and reversed phase columns. The final purification of MTX was accomplished on Develosil TMS-5 with 10 mM phosphate buffer in 40% MeCN. From 950 L cultured cells, 9 mg of MTX with  $^{13}\text{C}$  isotope abundance at around 4% was isolated. The 3D PFG NOESY-HMQC measurement had been run for one week, and 64 NOESY planes were obtained. In NOESY planes, no overlapping of cross peaks occurred. With these data, NOE information led to reconstruction of the bond connection that was cleaved by the periodate reaction, and the relative configuration of cyclic parts in MTX was established.

### Relative Stereochemistry of Acyclic Parts of Maitotoxin

The configuration of the acyclic moieties (C1-C15, C35-C39, C63-C68, and C135-C142) and the absolute stereochemistry remained unassigned. Relative stereochemistry of both termini was assigned using the *J*-based configuration analysis (Matsumori et al. 1996). Measurements of hetero half-filtered TOCSY (HETLOC) were effective to determine geminal and vicinal C-H coupling constants ( $^{2,3}J_{\text{C,H}}$ ). The  $^{13}\text{C}$ -enriched MTX prepared for the 3D NMR was used for measurements of *J* values. Based on the analysis method, the stereochemistry of asymmetric carbons in C5-C9 and C134-C138 was deduced. Essential  $^{2,3}J_{\text{C,H}}$  values could be determined for both side chains by these methods because relatively long  $T_2$ -relaxation times resulted in enhancement of signal intensity, while heavy overlap and broadening of cross peaks of the polyether part hampered the  $^{2,3}J_{\text{C,H}}$  measurement. In order to elucidate the configuration of the middle portion, synthetic approaches were attempted by two synthetic groups (Sasaki et al. 1994, 1995a, 1995b, 1996; Zheng et al. 1996).

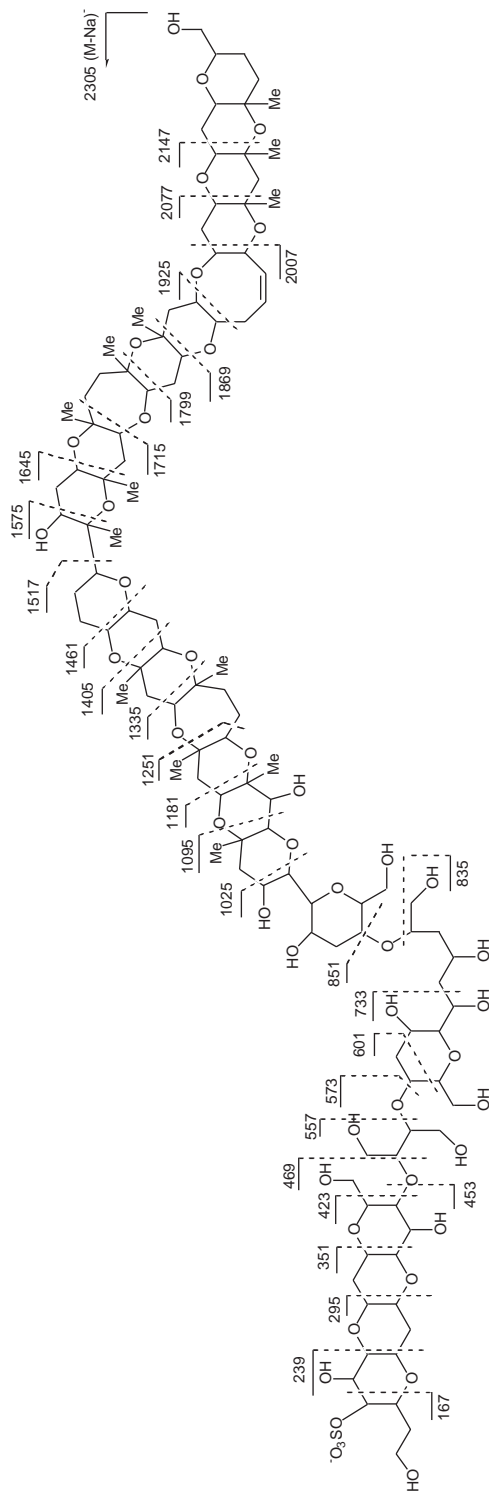


**Figure 3.3.** Fragmentation patterns of fragment B by CID MS/MS.

Possible diastereomers of MTX were synthesized, and their spectral identity was compared with that of MTX.

Stereostructures of C1-C15, C35-C39, C63-C68, and C99-C100 were determined by combining synthetic methods and NMR analyses.

### *Absolute Configuration of Maitotoxin*

The absolute configuration of MTX was determined using fragment C by Tachibana, Yasumoto, and co-workers (Nonomura et al. 1996). Enantioselective synthesis of the four possible stereoisomers of fragment C was carried out for chromatographic comparison with fragment C. Four stereoisomers were synthesized in an enantioselective manner. The 138-139 anti-isomers of fragment C were synthesized by Sharpless epoxidation, and the 138-139 syn-isomers were prepared by diastereoselective Diels-Alder reaction. All the stereoisomers were separated by chiral gas chromatography. Fragment C was prepared from MTX (50  $\mu\text{g}$ ) by treatment with  $\text{NaIO}_4$  and then with  $\text{NaBH}_4$ . Fragment C showed a single peak on the chiral gas chromatography at the retention time identical with that of the 138*R*, 139*S* isomer. This result elucidated the absolute configuration of the C135-C142 side chain. The relationship between C134-C136 could be unambiguously assigned by using the *J*-based configuration analysis. Thus, complete structural determination of MTX has been accomplished. Kishi and co-workers also elucidated the absolute stereostructure of MTX by synthesis (Zheng et al. 1996).

### References

- Matsumori, N., Nonomura, T., Sasaki, M., Murata, M., Tachibana, K., Satake, M., and Yasumoto, T. 1996. *Tetrahedron Lett* 37, 1269–1272.
- Murata, M., Iwashita, T., Yokoyama, A., Sasaki, M., and Yasumoto, T. 1992. *J Am Chem Soc* 114, 6594–6596.
- Murata, M., Naoki, H., Iwashita, T., Matusunaga, S., Sasaki, M., Yokoyama, A., and Yasumoto, T. 1993. *J Am Chem Soc* 115, 2060–2062.
- Murata, M., Naoki, H., Matsunaga, S., Satake, M., and Yasumoto, T. 1994. *J Am Chem Soc* 116, 7098–7107.
- Nonomura, T., Sasaki, M., Matsumori, N., Murata, M., Tachibana, K., and Yasumoto, T. 1996. *Angew Chem Inter Ed Engl* 35, 1675–1678.
- Satake, M., Ishida, S., Yasumoto, T., Murata, M., Utsumi, H., and Hinomoto, T. 1995. *J Am Chem Soc* 117, 7019–7020.
- Sasaki, M., Matsumori, N., Maruyama, T., Nonomura, T., Murata, M., Tachibana, T., and Yasumoto, T. 1996. *Angew Chem Inter Ed Engl* 35, 1672–1675.
- Sasaki, M., Matsumori, N., Murata, M., Tachibana, K., and Yasumoto, T. 1995. *Tetrahedron Lett* 36, 9011–9014.
- Sasaki, M., Nonomura, M., Murata, M., and Tachibana, K. 1994. *Tetrahedron Lett* 35, 5023–5026.
- . 1995. *Tetrahedron Lett* 36, 9007–9010.
- Scheuer, P.J. 1994. *Tetrahedron* 50, 3–18.
- Yasumoto, T., Baginis, R., and Vernoux J.P. 1976. *Bull Jpn Soc Sci Fish* 42, 359–365.
- Yokoyama, A., Murata, M., Oshima, Y., Iwashita, T., and Yasumoto, T. 1988. *J Biochem* 104, 184–187.
- Yasumoto, T., Nakajima, I., Baginis, R., and Adachi, R. 1977. *Bull Jpn Soc Sci Fish* 43, 1021–1026.
- Zheng, W., DeMattei, J.A., Wu, J.-P., Duan, J.J.-W., Cook, L.R., Oinuma, H., and Kishi, Y. 1996. *J Am Chem Soc* 118, 7946–7968.

## 4 Biochemistry of Maitotoxin

Laura A. de la Rosa, Emilio Alvarez-Parrilla,  
and Alejandro Martínez-Martínez

### Introduction

Maitotoxin (MTX) is the most potent ( $LD_{50} = 0.05$  mg/kg, mouse i.p. injection) and largest (3422 D) nonpeptide marine toxin described (Yasumoto 2000). MTX increases cytosolic free calcium ( $[Ca^{2+}]_i$ ) in all cell types tested by activating  $Ca^{2+}$  entrance. In contrast, MTX does not release  $Ca^{2+}$  from internal stores (Gutierrez, Diaz de León, and Vaca 1997). It is currently accepted that the first MTX action is the activation of nonselective cation channels (NSCCs) permeable mainly to  $Na^+$  and  $K^+$ , but also  $Ca^{2+}$  and other divalent cations (Table 4.1). NSCC activation induces membrane depolarization and a large increase in  $[Ca^{2+}]_i$ , which trigger numerous downstream events such as secretion (Obara et al. 1999; Verhoef et al. 2004) and activation of protein kinases (Malaguti, Yasumoto, and Paolo Rossini 1999; Takeda et al. 2004). With few exceptions, all MTX effects in all cell types tested are dependent on the presence of extracellular  $Ca^{2+}$ . Many of MTX effects are also dependent on a rise in  $[Ca^{2+}]_i$  and some require a basal  $[Ca^{2+}]_i$ ; however, not all of these effects can be mimicked by other  $[Ca^{2+}]_i$  elevating agents with ionophoretic activity, such as ionomycin. Several studies have, through different approaches, almost discarded the idea that MTX acts simply as an ionophore; on the contrary, a MTX receptor protein with an elevated affinity and highly conserved among species and tissues is suspected, although to date its identity remains a mystery.

### Evidence Against MTX Acting as an Ionophore

Classic studies showed that MTX elicited  $Ca^{2+}$  entry into a variety of cells but not to artificial phospholipids vesicles (Takahashi et al. 1983; Murata et al. 1992). Red blood cell ghosts are the simplest system responsive to MTX, although their sensitivity is lower than that of intact cells (Konoki et al. 1999). In other studies, only one or two  $Na^+$  channels were activated in cardiomyocyte membrane patches, despite a wide range of experimental conditions (Nishio, Muramatsu, and Yasumoto 1996). MTX induced opening of NSCC when applied in the outer surface of MDCK epithelial cells and insulinoma HIT cells, in contrast, when applied in the inner surface of the membrane, MTX showed no effect (Dietl and Völkl 1994; Leech and Habener 1998). Trypsin treatment of human skin fibroblasts induced a 90% inhibition of MTX-elicited  $[Ca^{2+}]_i$  increment, while having no effect on thapsigargin or ionomycin-induced  $[Ca^{2+}]_i$  increment (Gutierrez, Diaz de León, and Vaca 1997). Intracellular dialysis with trypsin and dithiothreitol (DTT) also blocked MTX-elicited cation currents in insulinoma HIT cells, arguing for a role of proteins with disulfide bond-containing domains (Leech and Habener 1998). In this cell line, MTX activation of cation currents is also apparently dependent on ATP and tyrosine phosphorylation, suggesting an upstream membrane target(s) coupled to second messenger systems that modulate cation currents (Leech and Habener 1997). Finally, channels with the same conductance as those activated by MTX, with spontaneous activity in resting

**Table 4.1.** Electrophysiological properties of maitotoxin-activated nonselective cation channels

Cell type	MTX	Reversal potential	Permeability	Ca <sup>2+</sup> sensitivity	Inhibitors	Single-channel conductance	Reference
<b>Excitable cells</b>							
Cardiac muscle (guinea pig)	90 pM	ND	Ca <sup>2+</sup> , Ba <sup>2+</sup> , not Cd <sup>2+</sup>	ND	ND	12 pS	Kobayashi, Ochi, and Ohizumi 1987
Cardiac muscle (guinea pig)	3–100 nM	Close to 0 mV	Na <sup>+</sup> , not choline <sup>+</sup>	Ca <sup>2+</sup> -independent (in and outside)	ND	16 pS	Nishio, Muramatsu, and Yasumoto 1996
β cells (mouse primary culture)	1–10 pM	–15 mV	Na <sup>+</sup> , Li <sup>+</sup> , not Ca <sup>2+</sup> , NMDG <sup>+</sup>	None [Ca <sup>2+</sup> ] <sub>o</sub> 0–10 mM	ND	ND	Worley et al. 1994
β cells (BTC cell line)	10–50 pM	–8 to –10 mV	Na <sup>+</sup> , Cs <sup>+</sup> , K <sup>+</sup> , Li <sup>+</sup> > Ca <sup>2+</sup> , Not choline <sup>+</sup> , NMDG <sup>+</sup>	Inhibited by [Ca <sup>2+</sup> ] <sub>o</sub> 100 mM 0 and [EGTA] <sub>o</sub> 5 mM	SKF96365 (50 μM), econazole (10 μM), genistein (100 μM), SKF96365 (40 μM), Na <sup>+</sup> replaced by NMG <sup>+</sup> , Tripsin, DTT, ATP-free (inside) 0 mM [Ca <sup>2+</sup> ] <sub>o</sub>	ND	Leech and Habener 1997
β cells (BTC cell line)	1–100 pM	–10 mV	Identical to Worley et al. 1994	ND	SKF96365	ND	Roe et al. 1998
β cells (HT-T15 cell line)	10 nM	0 to –2 mV	Na <sup>+</sup> , Cs <sup>+</sup> , K <sup>+</sup> > Li <sup>+</sup> , not NMDG <sup>+</sup>	Inhibited by long incubation in	Tripsin, DTT, ATP-free (inside) 0 mM [Ca <sup>2+</sup> ] <sub>o</sub>	25–30 pS	Leech and Habener 1998
<b>Nonexcitable cells</b>							
Kidney epithelial (MDCK cell line)	3–30 nM EC <sub>50</sub> = 824 pM	ND	Na <sup>+</sup> , K <sup>+</sup> , Cs <sup>+</sup>	Inhibited by 0, not by 10 mM [Ca <sup>2+</sup> ] <sub>o</sub>	La <sup>3+</sup> (100 μM), Not by SKF96365 25 μM.	40 pS	Dietl and Völkl 1994
Mouse L-fibroblasts	0.1–100 nM	Close to 0 mV	Ca <sup>2+</sup> , Na <sup>+</sup> , K <sup>+</sup>	Not inhibited by very low (micromolar) [Ca <sup>2+</sup> ] <sub>o</sub>	Flufenamic acid and dihydropyridines insensitive	28 pS	Estacion, Nguyen, and Gargus 1996
Human skin fibroblasts	1 nM	+7 mV	Na <sup>+</sup> , K <sup>+</sup> = Ca <sup>2+</sup> , not NMDG <sup>+</sup>	Dependent on extracellular Ca <sup>2+</sup> , Ba <sup>2+</sup> or Sr <sup>2+</sup>	ND	ND	Schilling, Sinkins, and Estacion 1999
Human skin fibroblasts	0.5 nM	–10 mV	Na <sup>+</sup> , K <sup>+</sup> > Ca <sup>2+</sup> , not NMDG <sup>+</sup>	Ca <sup>2+</sup> or Ba <sup>2+</sup> required for activation	ND	ND	Martinez-François, Morales-Tlalpan, and Vaca 2002

Oocytes ( <i>Xenopus laevis</i> )	50 pM–1 nM $EC_{50} = 250$ pM	ND	$NH_4^+ > K^+ > Na^+ >$ $Li^+ > Ca^{2+}$ not NMDG <sup>+</sup>	Inhibited by high $[Ca^{2+}]_o$	Benzamil, amiloride (1 mM), SKF96365 (100 $\mu$ M), $Gd^{3+}$ (100 $\mu$ M), Flufenamic acid insensitive	ND	Biefeld- Ackermann, Range, and Korbmacher 1998
Oocytes ( <i>Xenopus laevis</i> )	25 pM	-10 mV	$Na^+$ not TMA <sup>+</sup>	Inhibited by 0 and 40 mM $[Ca^{2+}]_o$	Amiloride, $Gd^{3+}$ (500 $\mu$ M), Flufenamic acid insensitive	ND	Weber et al. 2000
Oocytes ( <i>Xenopus laevis</i> )	1 nM	ND	$Cs^+ > K^+ > Na^+ >$ $Li^+ > Ca^{2+}$	$[Ca^{2+}]_i$ - independent	Amiloride 1 mM, Flufenamic acid insensitive	28 pS	Diakov et al. 2001
Rat liver hepatoma (H4-IIIE)	60 pM	+10 mV	$Na^+ > Ca^{2+}$ not TRIS <sup>+</sup> with a TRIS <sup>+</sup> permeable component	Dependent on low $[Ca^{2+}]_i$ , inhibited by 10–100 mM $[Ca^{2+}]_o$	$Gd^{3+}$ (100 $\mu$ M), TRIS <sup>+</sup> permeability insensitive to $Gd^{3+}$	ND	Brereton et al. 2001
hTRPC1- Transfected H4-IIIE	60 pM		$Na^+ = Ca^{2+}$	Not inhibited by 100 mM $[Ca^{2+}]_o$		ND	Brereton et al. 2001

ND = not determined.

conditions, were found and are likely to play an important role in setting the membrane potential of insulin-secreting  $\beta$ -cells (Leech and Habener 1998).

## MTX-Activated Nonselective Cation Channels

Evidence has accumulated in support of the notion that MTX-activated ion conductance takes place mainly through NSCCs, discarding the ionophore-like nature of MTX. NSCCs are voltage independent channels expressed in both electrically excitable and nonexcitable cells. Their physiological roles are diverse and, therefore, are not completely characterized; however, NSCCs are involved in cell proliferation, cell death, contraction, mechanical sensing, among other processes. NSCCs have received recent attention for being made up by members of the transient receptor potential (TRP) protein family (reviewed by Plant and Schaefer 2003; Nilius and Voets 2005). Electrophysiological characterization of the MTX-activated NSCCs has been carried out in several cell types and excellent reviews have been published (Escobar et al. 1998; Estacion 2000).

### *Excitable Cells*

Some of the first electrophysiological studies on the MTX-induced conductance were carried out in guinea pig cardiac muscle cells (Kobayashi, Ochi, and Ohizumi 1987) in which 0.09 nM MTX produced a voltage-independent current carried by  $\text{Ca}^{2+}$  and  $\text{Ba}^{2+}$  but not  $\text{Cd}^{2+}$ . In cell-attached patches, the single-channel conductance was 12 pS in the presence of 50 mM  $\text{Ba}^{2+}$ . Further studies showed that 10 nM MTX induced a voltage-insensitive current carried mainly by  $\text{Na}^+$ , not  $\text{choline}^+$ , with a reversal potential close to 0 mV and a single channel conductance of 16 pS in cell-attached configuration. This current was independent of the presence of  $\text{Ca}^{2+}$  at both sides of the membrane patch (Nishio, Muramatsu, and Yasumoto 1996).

In insulin-secreting  $\beta$ -cells (primary mouse  $\beta$ -cells and  $\beta$ TC cell line) MTX concentrations ranging from 1 to 100 pM stimulated a voltage independent, depolarizing current, permeable to several monovalent cations excluding  $\text{choline}^+$  and  $\text{NMDG}^+$  (N-methyl-D-glucamine), with a slightly negative reversal potential ( $-15$  to  $-8$  mV), and a very low or even undetectable  $\text{Ca}^{2+}$  permeability (Leech and Habener 1997; Worley et al. 1994; Roe et al. 1998). In these studies, the MTX-activated current also showed little sensitivity to extracellular  $\text{Ca}^{2+}$  concentrations ( $[\text{Ca}^{2+}]_o$ ); it was not inhibited by nominally  $\text{Ca}^{2+}$ -free extracellular medium but was inhibited by high  $[\text{Ca}^{2+}]_o$  and intracellular  $\text{Ca}^{2+}$  chelation with EGTA (Leech and Habener 1997). The depolarizing action of the cation conductance opened voltage-dependent, nitrendipine-sensitive  $\text{Ca}^{2+}$  channels (Worley et al. 1994). The primary MTX-activated nonselective cation conductance was inhibited by SKF 96365 (40–50  $\mu\text{M}$ ), econazole (10  $\mu\text{M}$ ), and genistein (100  $\mu\text{M}$ ), (Leech and Habener 1997; Roe et al. 1998). Single-channel conductance of MTX-activated currents in insulinoma HIT-T15 cells was 25–30 pS in cell-attached recordings and outside-out patches, with a reversal potential very close to 0 mV. These channels carried  $\text{Na}^+$   $\text{Cs}^+$  and  $\text{K}^+$  with the same selectivity, followed by  $\text{Li}^+$ , but were blocked by  $\text{NMDG}^+$  and long incubations (2 h) in  $\text{Ca}^{2+}$ -free buffer (outside solution). Currents were also inhibited by dialysis with trypsin, DTT, and ATP-free solutions (inside solution). Considering maximum current amplitudes and single-channel conductance, more than 5,000 channels were estimated within the cell membrane (Leech and Habener 1998). MTX-activated currents in  $\beta$ -cells are proposed to be carried through store-operated, nonselective cation channels whose physiological role is to respond to glucose and cAMP mobilizing agents such as glucagon-like peptide 1 (GLP-1), by

allowing ion fluxes which produce membrane depolarization and opening of voltage-sensitive  $\text{Ca}^{2+}$  channels. However,  $[\text{Ca}^{2+}]_i$  increments are induced by relatively high MTX concentrations (10 nM) in voltage-clamped cells, suggesting that  $\text{Ca}^{2+}$  entering through the NSCC may be important in mediating MTX effects (Leech and Habener 1998).

### Non-Electrically Excitable Cells

In MDCK renal epithelial cells and Mouse L-fibroblasts, MTX activated a nonselective cation current with single-channel conductance of 40 and 28 pS, respectively (Dietl and Völkl 1994; Estacion, Nguyen, and Gargus 1996). In both cell types, the current carried  $\text{Na}^+$  and  $\text{K}^+$  and required  $\text{Ca}^{2+}$  in the outside surface; however, a  $\text{Ca}^{2+}$  concentration in the low micromolar range was enough to allow for the development of the current in L-cells. A  $\text{Ca}^{2+}$ -dependent  $\text{K}^+$  conductance with a polarizing effect was also detected in these cells (Estacion, Nguyen, and Gargus 1996). In human skin fibroblasts, 1 nM MTX induced  $\text{Na}^+$  inward and  $\text{K}^+$  outward currents with reversal potential of +7 mV, and no permeability to NMDG<sup>+</sup>. These channels were predicted to have equal  $\text{Ca}^{2+}$  and  $\text{K}^+$  permeability. Approximately 4 minutes after MTX addition, a NMDG<sup>+</sup> permeable current developed as evidenced by the shift in reversal potential toward zero. The first cation conductance was suggested to occur through NSCC, while the NMDG<sup>+</sup> conductance would be taking place through a large membrane pore permeable to molecules as big as 715 Da. Both the channel activation and large pore formation depended on the presence of extracellular  $\text{Ca}^{2+}$ , although  $\text{Ba}^{2+}$  and  $\text{Sr}^{2+}$  could substitute (Schilling, Sinkins, and Estacion 1999). In another study on human skin fibroblasts, MTX induced cation currents with a reversal potential of -10 mV, and the current carried  $\text{Na}^+$ ,  $\text{K}^+$ , and  $\text{Ca}^{2+}$  but not NMDG<sup>+</sup>, with a selectivity  $\text{Na}^+ \approx \text{K}^+ > \text{Ca}^{2+}$ . Activation of this current was dependent on the presence of both extracellular and intracellular  $\text{Ca}^{2+}$ . As in the previous study,  $\text{Ba}^{2+}$  could substitute  $\text{Ca}^{2+}$ . Extracellular  $\text{Ca}^{2+}$  was only required for the activation of the current; removal of  $\text{Ca}^{2+}$  after activation did not reduce the current carried by other cations (Martínez-François, Morales-Tlalpan, and Vaca 2002).

In *Xenopus laevis* oocytes, evidence of activation of nonselective cation channels was obtained for the first time by measuring membrane currents activated by 50–1000 pM MTX ( $\text{EC}_{50} = 250$  pM). This current carried  $\text{Na}^+$  but not NMDG<sup>+</sup>; had a selectivity range of  $\text{NH}_4^+ > \text{K}^+ > \text{Na}^+ > \text{Li}^+$ ; showed a low  $\text{Ca}^{2+}$  permeability; was inhibited by high  $[\text{Ca}^{2+}]_o$  (57.5 mM), 1 mM benzamil, 1 mM amiloride, and 100  $\mu\text{M}$  SKF96365; and was reduced by  $\text{Gd}^{3+}$  concentrations as high as 100  $\mu\text{M}$ . The current was not inhibited by flufenamic acid (Bielfeld-Ackermann, Range, and Korbmacher 1998). Similar results were obtained by Weber et al. (2000). These authors also found that MTX produced an increase in membrane area (Fig. 4.1), measured as an increase in membrane capacitance ( $C_m$ ), suggesting insertion of new NSCCs from sequestered pools. MTX effects showed a considerable delay after toxin application (Weber et al. 2000). In another study, 1 nM MTX applied to the extracellular surface of outside-out patches evoked currents with single-channel conductance of 28 pS and properties virtually identical to those described earlier. The MTX-activated current also shared properties with a current elicited by exposure of oocytes to DIDS (250  $\mu\text{M}$ ) in the inside surface. The DIDS-activated current was independent of  $[\text{Ca}^{2+}]_i$ , suggesting the channel is  $\text{Ca}^{2+}$  independent from the cytosolic surface but  $\text{Ca}^{2+}$  dependent from the outer surface. These authors also found activation of a second smaller  $\text{Na}^+$  selective conductance in some cells, by both MTX and DIDS (Diakov et al. 2001).

The main nonselective cation current activated by MTX in *Xenopus* oocytes is suggested to be carried through stretch-activated NSCCs (SAC) in these cells. Though these are not very permeable to  $\text{Ca}^{2+}$ , the small  $\text{Ca}^{2+}$  amount entering the cell through the NSCCs may be sufficient to raise  $[\text{Ca}^{2+}]_i$



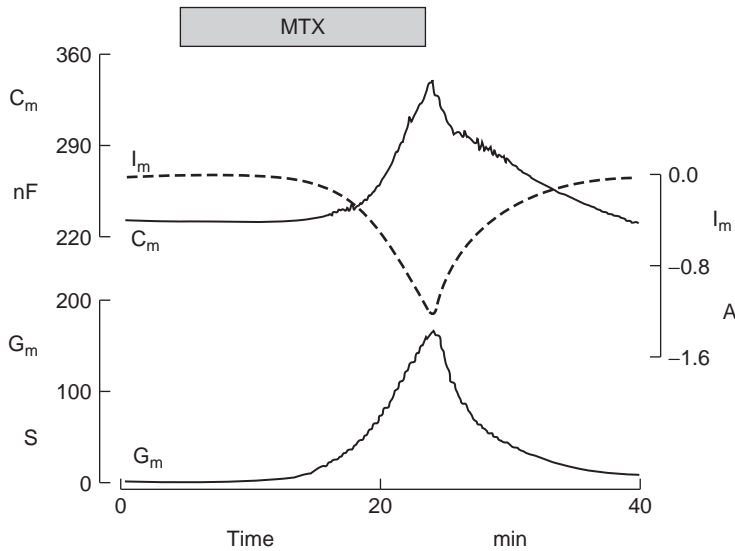


**Figure 4.1.** Maitotoxin-induced changes in membrane current ( $I_m$ ), conductance ( $G_m$ ) and capacitance ( $C_m$ ) in *Xenopus laevis* oocytes. After a short delay, a large inward current was developed, accompanied by an increase in membrane conductance and surface area (increase in  $C_m$ ). Reproduced with permission from Weber et al. 2000, © Springer Verlag.

enough to produce other intracellular events, including insertion of new channels (Bielfeld-Ackermann, Range, and Korbmacher 1998; Weber et al. 2000). At a very hyperpolarized membrane holding potential ( $-120$  mV), a low MTX concentration ( $15$  pM) exerted a  $\text{Ca}^{2+}$ -dependent  $\text{Cl}^-$  current, which was shown to be secondary to the  $[\text{Ca}^{2+}]_i$  increment and therefore is most probably secondary to the activation of the  $\text{Ca}^{2+}$ -permeable NSCC previously described (Martínez et al. 1999).

In rat liver hepatoma cells (H4-IIIE),  $60$  pM MTX induced a current carried mainly by  $\text{Na}^+$ , with a reversal potential of  $+10$  mV and low  $\text{Ca}^{2+}$  conductance. Current activation was not affected by  $\text{Cl}^-$  and showed a concentration-dependent inhibition by EGTA in the internal solution, indicating a requirement for low  $[\text{Ca}^{2+}]_i$ . The current had two components: one inhibited by  $100$   $\mu\text{M}$   $\text{Gd}^{3+}$ , which was impermeable to  $\text{Tris}^+$  and also inhibited by high  $\text{Ca}^{2+}$  ( $10$ – $100$  mM) in the external solution; and a second component (probably nonspecific leakage) that was not inhibited by  $\text{Gd}^{3+}$  and could be carried by  $\text{Tris}^+$  (Brereton et al. 2001). Moreover, in cells transfected with the human Transient Receptor Canonical form 1 gene (hTRPC1), the same MTX concentration activated a larger current that in nontransfected cells. This current did not appear to be the same as the one in control cells (nontransfected or transfected by an empty vector) since it showed the same permeability for  $\text{Ca}^{2+}$  and  $\text{Na}^+$  and was not inactivated by  $100$  mM  $\text{Ca}^{2+}$  in the external solution (Brereton et al. 2001). However, this study gave the first evidence that TRPC proteins might form  $\text{Ca}^{2+}$  permeable channels responsive to MTX. In Table 4.1, the main features of MTX-activated NSCCs in excitable and nonexcitable cells are summarized. On average, the MTX-activated NSCC has a reversal potential close to  $0$  (ranging from  $-15$  to  $+10$  mV), is mainly permeable to  $\text{Na}^+$  and  $\text{K}^+$ , has a low  $\text{Ca}^{2+}$ , and has no  $\text{TRIS}^+$ ,  $\text{choline}^+$ , or  $\text{NMDG}^+$  permeability. Current activation is blocked by high extracellular  $\text{Ca}^{2+}$  ( $40$ – $100$  mM) and by extracellular  $\text{Ca}^{2+}$ -free conditions, although a strong chelator or long preincubation may be needed for the latter effect. A basal intracellular  $\text{Ca}^{2+}$  concentration is probably also

needed. The current can be inhibited by SKF96365 (40–100  $\mu\text{M}$ ) and lanthanides (100  $\mu\text{M}$ ) and has a single-channel conductance close to 30 pS.

## MTX-Activated Calcium Influx Pathway

### *Pharmacological Characterization*

The numerous studies showing activation of NSCC as the first event elicited after MTX application in both excitable and nonexcitable cells strongly indicate that  $\text{Ca}^{2+}$  enters the cell through these channels, inducing all the subsequent  $\text{Ca}^{2+}$ -dependent intracellular processes. However, it is also clear that the NSCC is not the only  $\text{Ca}^{2+}$  entry pathway. This is more evident in electrically excitable cells and tissues, in which opening of the NSCC induces membrane depolarization and opening of voltage-gated  $\text{Ca}^{2+}$  selective channels, which carry most of the  $\text{Ca}^{2+}$  current that elevates  $[\text{Ca}^{2+}]_i$  (Leech and Habener 1998; Worley et al. 1994; Roe et al. 1998). Nevertheless, the small amount of  $\text{Ca}^{2+}$  entering through the NSCC may be sufficient to trigger some of the processes downstream of MTX binding and channel activation. In neuroendocrine cell line  $\text{GH}_4\text{C}_1$  (Xi, Dolah, and Ramsdell 1992; Xi Kurtz, and Ramsdell 1996) and in a nonexcitable cell line transfected with L-type voltage-sensitive  $\text{Ca}^{2+}$  channels (Cataldi et al. 1999), very low MTX doses (<30 pM) elicited effects on  $[\text{Ca}^{2+}]_i$  and membrane voltage, which were fully blocked by dihydropyridines (L-type channel antagonists). In contrast, the effect of higher MTX concentrations was only partially or not inhibited by these compounds in the same cells. These MTX concentrations are in the range of those used in other cells to activate NSCCs. Although these studies suggested MTX might directly activate L-type voltage-sensitive cation channels and these channels have a higher affinity for MTX than NSCC, growing evidence has shown that a nonselective cation channel is the main ion conductance stimulated by MTX in both excitable and nonexcitable cells. It seems possible that since MTX-sensitive NSCCs have a low  $\text{Ca}^{2+}$  permeability, low MTX doses might not activate  $\text{Ca}^{2+}$  entry enough to overwhelm the intracellular  $\text{Ca}^{2+}$  extrusion mechanisms and, therefore, no  $[\text{Ca}^{2+}]_i$  rise could be observed. However, this would not explain the lack of depolarization and stimulation of  $^{45}\text{Ca}^{2+}$  uptake observed in the  $\text{GH}_4\text{C}_1$  cell line when stimulated with MTX (Xi, Kurtz, and Ramsdell 1996). Therefore, it is also possible that dihydropyridines are low affinity inhibitors of MTX-activated NSCCs, and consequently, low MTX concentrations are unable to antagonize the blocking effect of dihydropyridines. In fact, it has been shown that the NSCC is probably formed at least in part by proteins members of the TRP family (Brereton et al. 2001; Chen and Barritt 2003), and cation channels formed by TRP proteins have a predicted topology similar to that of voltage-sensitive  $\text{Ca}^{2+}$  channels (reviewed by Schaefer 2005), which are targets of dihydropyridines.

Further evidence supporting  $\text{Ca}^{2+}$  entry through NSCCs in other excitable cells was obtained from neuroblastoma SH-SY5Y cells. In a study, 10 pM to 1 nM MTX induced a  $[\text{Ca}^{2+}]_i$  increase dependent on  $\text{Ca}^{2+}$  entry, inhibited by SKF96365 (50  $\mu\text{M}$ ), but not by L-type or N-type inhibitors such as nifedipine and SNX185 (Wang et al. 1996). One study in rat cerebrocortical synaptosomes found MTX (0.3 nM) to induce a  $[\text{Ca}^{2+}]_i$  increment in a nominally  $\text{Ca}^{2+}$ -free medium, suggesting  $\text{Ca}^{2+}$  release from intracellular stores. These authors also found  $\text{Ca}^{2+}$  entry; nevertheless, the pathway was not inhibited by 30  $\mu\text{M}$  SKF96365 but was inhibited by high nonspecific concentrations of verapamil (Satoh, Ishii, and Nishimura 2001).

In nonexcitable cells, electrophysiological and pharmacological evidence has shown MTX does not induce  $\text{Ca}^{2+}$  entry through the classical store-operated  $\text{Ca}^{2+}$  channels (SOCs), also named calcium-release activated calcium channels (CRAC) (reviewed by Parekh and Putney 2005).

In HL-60 cells, inhibition studies clearly demonstrated MTX-activated calcium entry is not through SOCs, despite MTX-induced  $IP_3$  formation (Daly et al. 1995). In CHO cells, MTX-induced  $Ca^{2+}$  influx (MTX 0.3 nM) was only partially reduced by high doses of SOC inhibitors SKF96365 and CAI, suggesting entrance through more than one pathway or through a channel with less sensitivity to the same inhibitors (Gusovsky et al. 1993). In the same cell line, 0.1–10 nM MTX induced an immediate  $[Ca^{2+}]_i$  and  $[Na^+]_i$  increment, with similar kinetics. Both events were completely dependent on external calcium and independent on external  $Na^+$ . In fact, low sodium accelerated the  $[Ca^{2+}]_i$  increment, suggesting competition for the same nonselective cation channel (Morales-Tlalpan and Vaca 2002). Similar results were found in C6 glioma cells (MTX 3 nM) in which  $Ca^{2+}$  was also proposed to enter through NSCCs (Obara et al. 1999).

The  $Ca^{2+}$  influx pathway activated by MTX in human skin fibroblasts ( $ED_{50} = 0.45$  pM) is also different from the store-operated  $Ca^{2+}$  entry pathway and partially inhibited by diphenoxylate up to 100  $\mu$ M (Gutierrez, Diaz de León, and Vaca 1997). In fibroblasts,  $Ca^{2+}$  enters mainly through the NSCC and MTX does not induce  $Ca^{2+}$  release from internal stores. MTX effects on this cell model are dependent on both extracellular and intracellular free calcium (Estacion, Nguyen, and Gargus 1996; Martínez-François, Morales-Tlalpan, and Vaca 2002). In a human fibroblast cell line, MTX also induced  $Ca^{2+}$  entry through a NSCC ( $ED_{50} = 0.5$  nM). Entry was insensitive to blockade by  $Gd^{3+}$  and also occurred through large pores that became evident at incubation times longer than five minutes (Shilling, Sinkins, and Estacion 1999).  $Ca^{2+}$  has also been suggested to enter through nonselective cation channels in THP-1 monocytes ( $ED_{50} = 10$  pM), HEK cells (Schilling et al. 1999), and bovine aortic endothelial cells ( $ED_{50} \sim 0.3$  nM), where MTX had no effect in the absence of extracellular  $Ca^{2+}$  (Estacion and Schilling 2001).

Further evidence to distinguish between the MTX-activated NSCCs and SOCs was provided by the use of 2-aminoethyl diphenylborate (2-APB). In primary cultures of rat hepatocytes, 2-APB inhibited  $Ca^{2+}$  entry through SOCs and endoplasmic reticulum store refilling, with no effect on MTX-sensitive NSCCs (Gregory, Rychkov, and Barritt 2001; Gregory, Sykiotis, and Barritt 2003). It is noteworthy to mention that compound U73343, inactive analogue of phospholipase-C (PLC) inhibitor U73122, blocked MTX-induced  $Ca^{2+}$  entry with high potency ( $ID_{50} = 0.66$   $\mu$ M) in bovine aortic endothelial cells. Therefore, it is suggested that this compound might be considered as a relatively specific blocker of the MTX-activated  $Ca^{2+}$  influx pathway (Estacion and Schilling 2002).

### *MTX Receptor and Mechanism of $Ca^{2+}$ Entry Activation*

Despite many efforts, neither the MTX receptor identity nor MTX binding and  $Ca^{2+}$  influx activation mechanisms have been yet clearly understood. Nevertheless, great progress has been made from the times when L-type  $Ca^{2+}$  channels were thought to be MTX targets.

Complete characterization of the MTX structure (Fig. 4.2) has led some authors to propose a two-step binding model: (1) the MTX hydrophobic tail inserts itself in the plasma membrane in a non-specific manner, while its hydrophilic part folds like a hairpin; (2) MTX moves through the lipid bilayer until it binds to its receptor. In binding, both the hydrophilic and hydrophobic parts are necessary (Konoki, Hashimoto, Nonomura et al. 1998; Konoki, Hashimoto, Murata et al. 1999). This slow binding could be in part responsible for the latency period of MTX actions observed in Fig. 4.1. MTX insertion or interaction with a receptor is suggested to be ATP dependent in insulin-secreting cell lines (Leech and Habener 1998). Calcium ions are also supposed to play a role in MTX binding, since the first detectable MTX action (NSCC activation) is  $Ca^{2+}$  sensitive. Several authors have been able to observe MTX effects when added in a  $Ca^{2+}$ -free medium followed by wash out and

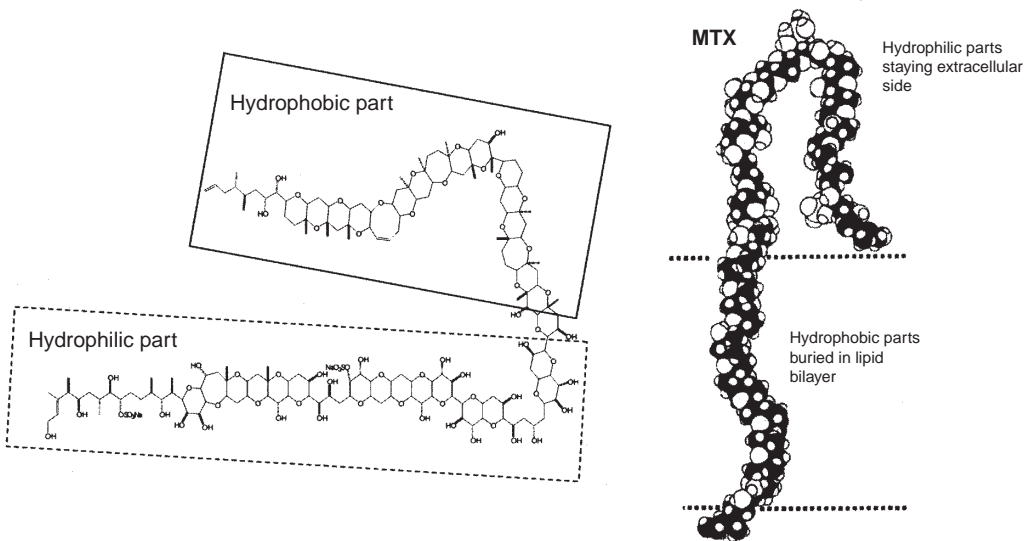


**Figure 4.2.** Structure of maitotoxin and space-filling model showing hydrophobic and hydrophilic regions. Hydrophobic region is drawn buried in the lipid bilayer and hydrophilic part folded like a hairpin. Reproduced with permission from Obara 1999, © American Chemical Society.

$\text{Ca}^{2+}$  addition, and the authors therefore concluded MTX binding is  $\text{Ca}^{2+}$  independent (Venant et al. 1995). However, considering the two step binding model, it is possible that MTX insertion into the membrane is  $\text{Ca}^{2+}$  independent, while the MTX-receptor binding is  $\text{Ca}^{2+}$  dependent. Alternatively, the putative MTX receptor or MTX-sensitive NSCC could be allosterically modulated by calcium.

In erythrocyte ghosts, intact erythrocytes, C6 glioma, and aortic endothelial cells, MTX-induced  $\text{Ca}^{2+}$  influx was inhibited by gangliosides, especially GM1 (Konoki et al. 1999; Bressler, Belloni-Olivi, and Forman 1994). The inhibitory effect of gangliosides is interpreted as their ability to aggregate and form clusters, once inserted into the plasma membrane, and then retain MTX in these clusters. Also in erythrocyte ghosts and C6 cells, molecules that mimic both the hydrophobic and hydrophilic portions of MTX were able to inhibit the MTX-induced  $\text{Ca}^{2+}$  entry and depolarization, probably by competitively binding to the MTX receptor (Konoki et al. 1998). In contrast, in human lymphocytes pretreatment with yessotoxin, a marine phycotoxin that resembles the hydrophobic portion of MTX increased the rate of the MTX-induced  $[\text{Ca}^{2+}]_i$  increment. Yessotoxin has been shown to inhibit phosphodiesterases, hence elevating cAMP levels (Alfonso et al. 2003); however, its effect on the MTX-induced  $\text{Ca}^{2+}$  entry was suggested to be independent of cAMP elevation (de la Rosa et al. 2001).

Identity of the putative MTX receptor and MTX-activated NSCC has been suggested by several authors. In THP-1 monocytes and HEK cells, MTX stimulation of  $\text{Ca}^{2+}$  entry was not temperature dependent, suggesting that the MTX receptor is also the nonselective cation channel (Schilling et al. 1999). Very rapid effects of the toxin in a number of cell types have also been reported (Gutierrez, Diaz de León, and Vaca 1997; Schilling, Sinkins, and Estacion 1999; Morales-Tlalpan and Vaca 2002; Schilling et al. 1999). In support of this notion is the fact that red blood cell ghosts, which have

been emptied of all cytosolic components, respond to MTX (Konoki, Hashimoto, Nonomura et al. 1998; Konoki, Hashimoto, Murata et al. 1999), suggesting that MTX binding and  $\text{Ca}^{2+}$  entry occur through the same pathway or at least that all events linking both pathways should be membrane bound.

Several authors have, however, detected a considerable delay between MTX addition and any detectable  $[\text{Ca}^{2+}]_i$  increment or even stimulation of  $^{45}\text{Ca}^{2+}$  influx in several cell types (Dietl and Völkl 1994; Weber et al. 2000; Brereton et al. 2001; de la Rosa et al. 2001; Watanabe et al. 1993; Woods et al. 1999). Although the slow kinetics of the  $[\text{Ca}^{2+}]_i$  rise induced by MTX could be explained in terms of a slow and irreversible activation of many NSCCs, allowing  $\text{Ca}^{2+}$  influx to reach a rate that overwhelms the cell's homeostasis mechanisms before any  $[\text{Ca}^{2+}]_i$  increment can be detected (Estacion, Nguyen, and Gargus 1996), it could also reflect activation of enzymatic steps linking MTX receptor and  $\text{Ca}^{2+}$ -permeable NSCC at least in some cell types. Insertion of new proteins (Weber et al. 2000; Brereton et al. 2001), tyrosine phosphorylation (Leech and Hebener 1997; Venant et al. 1994) and phosphatidil inositol 3-kinase activation (de la Rosa et al. 2001) have been suggested as possible steps linking MTX binding with NSCC opening. Alternatively, most of the delayed MTX response might be dependent on the opening of an unspecific large membrane pore involved in cell death (Schilling, Sinkins, and Estacion 1999; Schilling et al. 1999; Estacion and Schilling 2001), although this seems to be unlikely in liver cells (Brereton et al. 2001).

Pharmacological differentiation between MTX-activated NSCCs and the  $\text{Ca}^{2+}$  entry pathway has been observed. In C6 glioma cells, gangliosides inhibited both  $\text{Ca}^{2+}$  influx and membrane depolarization, while alkylamines inhibited only  $\text{Ca}^{2+}$  entry and not membrane depolarization, suggesting that both events may occur through different pathways (Konoki et al. 1999, 1996). In the MDCK renal cell line, the MTX-activated NSCC was insensitive to SKF96365 and instantaneous and dependent on extracellular  $\text{Ca}^{2+}$ ; in contrast, MTX-induced  $[\text{Ca}^{2+}]_i$  elevation was inhibited by more than 50% by SKF96365 and was delayed by more than one minute after MTX application. These authors concluded that although the NSCC has a low  $\text{Ca}^{2+}$  permeability and its activation is  $\text{Ca}^{2+}$  dependent, the main  $\text{Ca}^{2+}$  entry pathway in these cells is different and downstream from the NSCC (Dietl and Völkl 1994). In a more recent study,  $\text{Ca}^{2+}$  was shown to enter the MDCK cell mainly through a SKF96365-sensitive pathway, while  $\text{Cd}^{2+}$  entered through an insensitive pathway, namely the nonselective cation channel (Olivi and Bressler 2000). In summary, although more than one  $\text{Ca}^{2+}$  entry mechanism may be activated by MTX in different cell lines, the first and most important  $\text{Ca}^{2+}$  influx pathway in most cells is probably the NSCC. The identity of the NSCC and MTX receptor is not completely clear, however. Receptors for many agonists may be upstream regulators of NSCCs, but their distribution and role is different according to cell and channel type.

### *Molecular Identity*

Studies in the rat liver hepatoma cell line H4-IIIE have convincingly shown MTX-sensitive NSCCs may be composed of TRPC proteins. The  $\text{Ca}^{2+}$  influx pathway was shown to be mainly a NSCC permeable to  $\text{Ca}^{2+}$ ,  $\text{Mn}^{2+}$ , and  $\text{Na}^+$  (with a higher  $\text{Na}^+$  permeability). It was partially inhibited by  $\text{Gd}^{3+}$  ( $\text{ID}_{50} = 1 \mu\text{M}$ ), and  $[\text{Ca}^{2+}]_i$  increase showed a delay of approximately four minutes (60 pM MTX). No toxic effects were observed for as long as 15 minutes with MTX concentration as high as 300 pM. However, these authors also observed a secondary  $\text{TRIS}^+$ -permeable  $\text{Ca}^{2+}$  influx pathway that may be a nonselective pore (Brereton et al. 2001). In addition, these authors observed that the MTX effect on  $[\text{Ca}^{2+}]_i$  was greatly enhanced in cells transfected with the human TRPC-1 protein, which forms  $\text{Ca}^{2+}$ -permeable nonselective cation channels (reviewed by Clampham, Runnel, and Strübing 2001; Beech 2005).  $\text{Gd}^{3+}$  inhibited  $\text{Ca}^{2+}$  entry in transfected cells to a similar degree as control cells.

Nevertheless, patch clamp studies showed that the endogenous cation channel activated by MTX in control or nontransfected H4-IIIE cells is different from the hTRPC-1 channel formed in transfected cells. TRP proteins (including hTRPC-1) form channels by inserting themselves in the membrane probably in homo- or heterotetramers to yield a channel with properties that depend on the individual polypeptides. It is possible that the endogenous MTX-activated cation channel contains endogenous TRP1 proteins forming heteromers with other polypeptides, and therefore the resulting channel shows properties different from those of the channels formed in cells overexpressing the hTRPC-1 protein, which are likely to be homotetramers. Another possibility is that a different protein forms the endogenous channel in H4-IIIE hepatoma cells (Brereton et al. 2001). In H4-IIIE liver cells, expression of the endogenous TRPC1 protein was 50% reduced by transfection with a single-strand, small interfering RNA, and this maneuver led to a similar reduction of MTX-induced  $\text{Ca}^{2+}$  and  $\text{Mn}^{2+}$  influx (Fig. 4.3). Therefore, these authors concluded that the MTX-activated NSCC may be formed by TRPC1 and another TRPC polypeptide (probably TRPC3). This channel may be also activated by thapsigargin, although it is different from the highly  $\text{Ca}^{2+}$ -selective and store-operated CRAC or SOC channel (Chen and Barritt 2003).

### Physiological Role

MTX-activated NSCC is suggested to be involved in regulation of insulin secretion in pancreatic  $\beta$ -cells (Leech and Habener 1998). In *Xenopus* oocytes, the MTX activated nonselective cation conductance is proposed to be carried through stretch-activated channels (SACs) involved in volume regulation (Diakov et al. 2001). In other cell types, MTX-activated channels may be involved in cell proliferation (Estacion, Nguyen, and Gargus 1996). In hepatocytes, MTX-activated channels are poorly coupled to  $\text{Ca}^{2+}$  store refilling and therefore must have a different physiological role, probably volume regulation (Gregory, Sykiotis, and Barritt 2003). In sperm cells, MTX-sensitive channels are suggested to have a role in acrosome reaction (Trevino et al. 2005). It is now also clear that the MTX-sensitive NSCCs may have an important role in cell death. In fact, MTX has been recently used as tool to induce cell death and oxidative stress responses in several cell types (Malaguti, Yasumoto, and Paolo Rossini 1999; Takeda et al. 2004; Auvin et al. 2004).

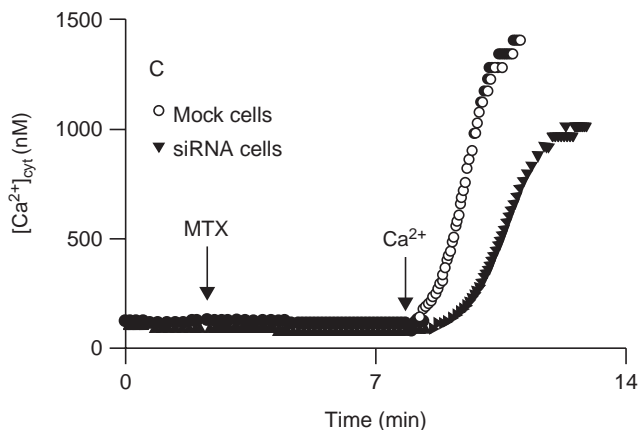


**Figure 4.3.** Treatment with single stranded RNA targeted against TRPC1 inhibits maitotoxin-induced  $[\text{Ca}^{2+}]_i$  increment in H4-IIIE hepatoma cells. (Reproduced with permission from Chen and Barritt 2003, © the Biochemical Society).



## MTX and Cell Death

A rise in  $[Ca^{2+}]_i$  is one of the earliest detectable events associated with cell death; therefore, MTX has proven to be a valuable tool in studying cell death processes. Some of the first descriptions of cell death processes activated by MTX were made in nervous cells, SH-SY5Y neuroblastoma and primary septo-hippocampal cultures. MTXs induced necrotic cell death through a pathway partially dependent on calpain activation. Identification of calpain-specific autolysis fragments and  $\alpha$ -spectrin breakdown products, in combination with use of calpain and caspase inhibitors, indicated activation of the first but not the latter enzyme by MTX (Wang et al. 1996; Zhao et al. 1999). Despite lack of caspase activation, cytochrome C was released from mitochondria in SH-SY5Y cells challenged with 0.1 nM MTX; furthermore, MTX-induced calpain activation produced caspase-3 and caspase-9 hydrolysis; however, calpain inhibition did not allow for caspase-3 activation indicating that caspase cleavage by calpain is not the reason for the nonactivation of this apoptotic enzyme. The authors suggested that ATP depletion might have a role in directing MTX-induced cell death toward necrosis instead of apoptosis (McGinnis et al. 2003). Novel drugs designed with calpain inhibitory action and antioxidant activity showed a 15%–38% inhibition of MTX-induced cell death in C6 glial cells (Auvin et al. 2004).

MTX also induces necrosis in all nonexcitable cell models tested so far. MTX-induced cell death has been studied by measuring incorporation of ionic fluorescent dyes that are excluded from healthy cells and can only cross the plasma membrane via big pores. These assays have been developed both in cell populations and on a single cell level. Nevertheless, this approach does not reflect true cell lysis but only major membrane permeability, and therefore, LDH release is the assay most used to detect final cell death. Using these techniques, MTX has been shown to produce similar progression of membrane permeability changes in several cell models: human skin fibroblasts (Schilling, Sinkins, and Estacion 1999), bovine aortic endothelial cells (Estacion and Schilling 2001, 2002; Estacion et al. 2003; Wisnoskey, Estacion, and Schilling 2004) and cell lines of diverse origins (Verhoef et al. 2004; Schilling et al. 1999).

In all these experimental models, the MTX effect could be divided in three phases: (1) a rapidly developing  $Ca^{2+}$  conductance through NSCC; (2) uptake of vital dyes (ethidium, YO-PRO and POPO-3) and Fura-2 loss via a cytolitic-oncotic pore (COP); and (3) a secondary phase of vital dye uptake and Fura loss in which membrane permeability to larger molecules like LDH enzyme occurs. Fig. 4.4 shows permeability changes in a population study of bovine aortic endothelial cells (BAECs) treated with 0.3 nM MTX. Two phases of ethidium bromide uptake may be observed (steps 2 and 3 of the death process), the second phase correlating in time with LDH release (step 3 of death process).

In BAECs, the first phase of vital dyes uptake is dependent on MTX concentration, and the uptake rate is inversely proportional to dye molecular weight, suggesting a fixed COP size. On a single cell level, the first phase of dye uptake was associated with the formation of membrane blebs with an average diameter of approximately 4  $\mu$ m, and the secondary dye uptake phase and LDH release are associated with dramatic bleb growth or dilation, suggesting a massive exocytotic event during cell lysis and oncotic cell death (Estacion and Schilling 2001).

Only minor differences were apparent in different cells: the range of MTX concentrations used in all studies was similar, although some cell lines were more sensitive (Schilling et al. 1999); delay between phases also varied slightly among cell types, and the bleb formation-dilation pattern was not identical in BAECs and a macrophage cell line (Verhoef et al. 2004).

The fact that the series of events elicited by MTXs, which ultimately led to cell death, are reminiscent of those produced by  $P2X_7$  receptor stimulation raised the possibility that MTX could be acting through that same protein.  $P2X$  receptors are ion channels that open in response to the binding of

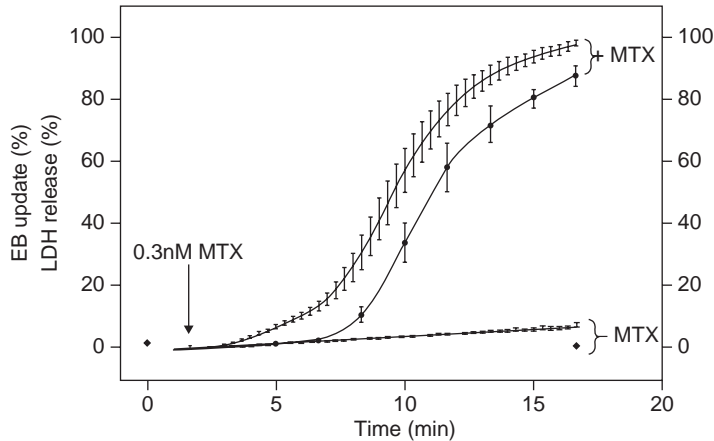


**Figure 4.4.** Changes in membrane permeability induced by maitotoxin in bovine aortic endothelial cells. Ethidium (EB) uptake shows a biphasic response where the second phase corresponds with LDH release, indicative of cell lysis. Reproduced with permission from Estacion and Schilling 2001, © BioMed Central.

extracellular ATP. P2X<sub>7</sub> channels are homomultimers with a relatively low affinity for ATP and a high affinity for 2', 3'-(benzoyl-4-benzoyl)ATP (BzATP) (reviewed by North 2002). However, further studies clearly showed that this was not the case. MTX responses on Ca<sup>2+</sup> and ethidium permeability were virtually identical in cells that do not express functional P2X<sub>7</sub> receptors and in cells overexpressing them. Bz-ATP, in contrast, induced cell death only in cells stably expressing P2X<sub>7</sub> proteins. In a cell line in which P2X<sub>7</sub> receptors are expressed but are poorly coupled to pore formation, MTX induced Ca<sup>2+</sup> but not ethidium permeability. Therefore, these authors concluded that Ca<sup>2+</sup>-permeable channels (NSCCs) activated by MTX and Bz-ATP are different, and therefore the P2X<sub>7</sub> receptor is not the MTX receptor. On the other hand, the ethidium-permeable pathway (cytolytic-oncotic pore or COP) is the same for MTX and P2X<sub>7</sub> agonists. A model is proposed in which the Ca<sup>2+</sup>-permeable MTX-activated and P2X<sub>7</sub> NSCCs compete for an endogenous pore, which ultimately produces cell death (Fig. 4.5). The opening of the pore is temperature sensitive and suggested to be inhibited by high [Ca<sup>2+</sup>]<sub>i</sub>. In contrast, NSCC gating is temperature independent, suggesting its direct activation by MTX binding (Schilling et al. 1999).

In submandibular acini cells, 1–10 nM MTX (ED<sub>50</sub> ~ 5 nM) induced ethidium uptake in a Ca<sup>2+</sup>- and temperature-dependent fashion. This effect was delayed by the β-antagonist propranolol (100–300 μM). Propranolol and its inactive optical isomer also inhibited the ethidium uptake induced by BzATP, suggesting a common entry pathway (COP) activated by both agonists (Alzola et al. 2001). Further evidence of different Ca<sup>2+</sup> entry pathways, but which still suggests a common COP activated by P2X<sub>7</sub> agonists and MTX, was obtained in CHO cells (Lundy et al. 2004). In this study, several pharmacological differences were noted between MTX- and BzATP-induced cell death: (1) MTX-induced ethidium uptake was more evident in a physiological saline buffer and was reduced in an isosmotic sucrose buffer, while the opposite was true for BzATP-induced ethidium uptake; (2) MTX effects were abolished by preincubation with the calmodulin inhibitor W7 (300 μM), while BzATP action was insensitive to the drug; (3) BzATP effects were blocked by oxidized ATP (oATP), while MTX action was unaffected; and (4) MTX- but not BzATP-induced ethidium



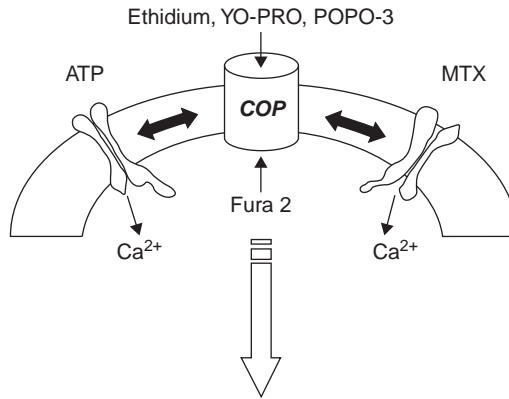


**Figure 4.5.** Maitotoxin and P2X<sub>7</sub> agonists activate different Ca<sub>v</sub> permeable nonselective cation channels but share a common cytolitic-oncotic pore (COP) for which the NSCCs compete in order to induce necrosis. Reproduced with permission from Schilling et al. 1999, © American Physiological Society.

uptake and cell lysis (LDH release) was very sensitive to extracellular [Ca<sup>2+</sup>]. Nevertheless, in the absence of added Ca<sup>2+</sup>, MTX still induced cell death after a 24-hour exposure, with a LC<sub>50</sub> = 2.4 nM (Lundy et al. 2004). Schilling et al. (1999) showed MTX- and BzATP-induced COP formation by different pathways in THP1 monocytes primed with LPS (lipopolysaccharide) and IFN $\gamma$ . Donnelly-Roberts et al. (2004) observed inhibition of BzATP-induced YO-PRO uptake (through COP) by p38 MAP kinase inhibitors, caspase 1 and 3 inhibitors, and PKC inhibitors. BzATP also induced IL-1 $\beta$  secretion and this effect was also inhibited by caspase and PKC inhibitors (Donnelly-Roberts et al. 2004). In contrast, MTX-induced pore formation was inhibited by calmidazolium and U73122, both inhibitors of MTX-induced [Ca<sup>2+</sup>]<sub>i</sub> increment (Schilling et al. 1999; Estacion and Schilling 2002) but was unaffected by the p38, caspase and PKC inhibitors (Donnelly-Roberts et al. 2004).

As previously stated, COP formation, characterized by vital dye uptake (phase 2), does not reflect true cell lysis; on the contrary, the lytic phase (phase 3) is associated with release of LDH and other cytosolic proteins such as immature IL-1 $\beta$  p38 MAP kinase (Verhoef et al. 2004) and green fluorescent protein constructs (Estacion et al. 2003). This lytic phase has been studied at the single-cell level in BAECs (Estacion et al. 2003). In this study, cell lysis and loss of LDH and green fluorescent protein constructs as big as 162 kDa occurred at the same time as dilation of blebs formed in the cell surface, and the blebs continued to grow even after proteins were leaving the cytoplasm. Glycine and L-alanine (EC<sub>50</sub> ~ 1 mM) inhibited MTX-induced cell lysis without affecting Ca<sup>2+</sup> entry, COP formation/permeability, or bleb formation/dilation. These observations suggest MTX-induced cell lysis is not due to a massive rupture of the plasma membrane but due to formation or activation of an endogenous channel of large pore size termed a lytic pore or death channel (Estacion et al. 2003). In addition, 5 mM Gly blocked cytolysis in murine macrophages without inhibiting other MTX effects (Verhoef et al. 2004). Gly-protected cells from MTX induced cell death for at least 48 hours, indicating long-lasting cytoprotection by this amino acid.

The MTX-activated death cascade is exquisitely dependent on extracellular calcium. In BAECs treated with MTX in the absence of extracellular Ca<sup>2+</sup>, no effect was detected; however, on Ca<sup>2+</sup> re-addition, cells showed a response virtually identical to that of cells treated with MTX in the presence

of extracellular  $\text{Ca}^{2+}$  (Estacion and Schilling 2001). Intracellular  $\text{Ca}^{2+}$  loading with ionomycin mimicked MTX effect, and intracellular BAPTA delayed both phases of cell death, indicating a  $[\text{Ca}^{2+}]_i$  rise is both necessary and sufficient to trigger the MTX-induced necrotic death cascade. Ion substitution experiments showed  $\text{Sr}^{2+}$  and  $\text{Ba}^{2+}$  are permeable through the MTX-activated NSCC and do not seem to interfere with channel activation by the toxin; however, formation/activation of the COP and death channel were delayed by  $\text{Ba}^{2+}$ , which is a poor surrogate for  $\text{Ca}^{2+}$ , in a number of cellular reactions that involve high affinity  $\text{Ca}^{2+}$  binding proteins. The fact that  $\text{Ca}^{2+}$ -binding proteins are probably required for MTX-induced necrosis and that, during  $\text{Ca}^{2+}$  overload conditions,  $\text{Ca}^{2+}$  pumps (SERCA and PMCA) are expected to work at near-maximum level, exhausting the cell ATP pool, suggests a role for these  $\text{Ca}^{2+}$  transporters in MTX-induced necrosis (Wisnoskey, Estacion, and Schilling 2004). U73343 and to a lesser extent U73122 (inactive analogue and PLC inhibitor, respectively) inhibited MTX-induced  $\text{Ca}^{2+}$  entry and ethidium uptake into BAECs, inhibiting therefore necrotic cell death. However, in the presence of an inhibitory concentration of U73343 (10  $\mu\text{M}$ ), MTX induced another pattern of membrane blebbing, denominated zeiosis, which ultimately leads to apoptotic cell death. No COP formation, membrane blebbing, or cell lysis was observed in the majority of these cells. In contrast, caspase-3 activity was found elevated after 48 hours of MTX + U73343 treatment, indicating apoptosis. Therefore, the authors concluded that a rise in  $[\text{Ca}^{2+}]_i$  is required for MTX-induced necrosis but not for MTX-induced apoptosis (Estacion and Schilling 2002). Cell death was also observed after long MTX treatment of CHO cells in nominally  $\text{Ca}^{2+}$ -free medium (Lundy et al. 2004). In human fibroblasts, extracellular cations were required to detect MTX effects on membrane permeability; however, a  $[\text{Ca}^{2+}]_i$  increase was neither sufficient or evidently necessary to induce the progressive changes characteristic of MTX (Schilling, Sinkins, and Estacion 1999). Therefore, as for other MTX-dependent processes, the role for  $\text{Ca}^{2+}$  ions in MTX-induced necrosis is still not resolved.

## Other Effects of MTX

### *Phospholipid Metabolism*

MTX activates phospholipase-A and -C (PLA, PLC) and downstream processes in a number of cells (Gusovsky et al. 1993, 1990; Venant et al. 1994; Bernard et al. 1988; Nakahata et al. 1999; Nakahata, Yaginuma, and Ohizumi 1999). In all cases, MTX effects required extracellular  $\text{Ca}^{2+}$ , but a  $[\text{Ca}^{2+}]_i$  rise was not always necessary (Venant et al. 1994; Bernard et al. 1988; Gusovsky et al. 1990; Nakahata, Naginuma, and Ohizumi 1999). Tyrosine kinase activation has been described as downstream  $\text{Ca}^{2+}$  entry and upstream PLC activation (Gusovsky et al. 1993; Nakahata et al. 1999) but also as upstream  $\text{Ca}^{2+}$  entry (Leech and Habener 1997; Venant et al. 1994). Nevertheless, no more recent studies address this issue at this time, and therefore the exact mechanism by which MTX stimulates PLA or PLC has not been elucidated. Direct activation of PLC by MTX has been discarded (Gusovsky et al. 1990), so it is most probable that the MTX receptor/NSCC somehow interacts, in a  $\text{Ca}^{2+}$ -sensitive manner, with phospholipases.

### *Activation of Ser/Thr Protein Kinases*

Phosphorylation and activation of extracellular signal-regulated MAP kinases (ERK1 and ERK2) were observed in MCF-7 breast cancer cells after 15 minutes of exposure to MTX (0.5 nM). Longer

incubation times triggered loss of both proteins and cell-cell adhesion molecule E-cadherin, followed by cell death. MTX effects were extracellular calcium dependent (Malaguti, Yasumoto, and Paolo Rossini 1999). In mouse fibroblasts and He-La cells, MTX stimulated the apoptosis-linked enzymes ASK1 (apoptosis signal-regulating kinase) and p38. Activation of ASK1 by MTX is dependent on extracellular  $\text{Ca}^{2+}$  and apparently also on a  $[\text{Ca}^{2+}]_i$  rise and activation of  $\text{Ca}^{2+}$ /calmodulin-dependent protein kinase type II (CaMKII). These authors concluded that the CaMKII-ASK1-p38 kinase cascade constitutes a novel  $\text{Ca}^{2+}$  signal involved in cytokine and stress-induced apoptosis (Takeda et al. 2004). No cell death was induced by MTX under the conditions of this study.

### *Activation of Tissue Transglutaminase (tTG)*

Tissue transglutaminase is a  $\text{Ca}^{2+}$ -activated enzyme and a signal-transducing, GTP-binding protein involved in apoptotic cell death, cell cycle progression, axonal growth and regeneration, and cell adhesion, among other processes. The tTG is activated by MTX in SH-SY5Y neuroblastoma cells (1–5 nM MTX) and 3T3 fibroblasts (0.5 nM MTX). In neuroblastoma cells, MTX treatment induced activation of nuclear and cytosolic tTG (Lesort et al. 1998) without loss of cell viability (LDH release) under the conditions employed (Zhang et al. 1998). In 3T3 fibroblasts, MTX stimulated tTG 7.5- and 3.7-fold in BAPTA-free and BAPTA-loaded cells, respectively (Lee et al. 2003). Reduction of cytosolic GTP levels reduced the MTX-induced activation of tTG, in a calpain-dependent manner. Therefore, tTG is likely to be a substrate for calpain (also activated by MTX), and GTP presence is likely to protect the enzyme from calpain-dependent degradation. However, elevating  $[\text{GTP}]_i$  by microinjection of GTP $\gamma$ S also reduced MTX-dependent tTG activation. LPA also induced activation of tTGase through a reactive oxygen species (ROS)-mediated mechanism (Lee et al. 2003). Both tissue transglutaminase and ASK1-p38 are also activated by oxidative stress.

### *Secretion and Other Cellular Responses*

MTX induced extracellular  $\text{Ca}^{2+}$ -dependent secretion of nerve growth factor in a glioma cell line (Obara et al. 1999). In murine macrophages from the BAC1 cell line, MTX induced cytokine processing and secretion of the mature form of IL-1b (17 kDa), a process generally assumed to be dependent on caspase-1 activation. P38 MAPK kinase was also seen to be secreted together with mature IL-1b. Higher MTX concentrations also induced cell death as judged from membrane permeability to vital dyes and release of nonprocessed IL-1b. Both effects, regulated secretion and cytotoxicity, were dependent on the presence of extracellular  $\text{Ca}^{2+}$  (Verhoef et al. 2004). Activation of the  $\text{P2X}_7$  receptor with BzATP also leads to both IL-1b secretion and COP formation in a monocytic cell line (THP1) differentiated with LPS and IFN $\gamma$  (Donnelly-Roberts et al. 2004). However, as mentioned before, the intracellular cascades activated by MTX and BzATP are different.

Other cellular responses elicited by MTX, among many, are platelet aggregation (Watanabe et al. 1993; Nakahata et al. 1999), ciliary beating of tracheal epithelium (Venant, Dazy, and Diogène 1995; Venant et al. 1994), inhibition of sea urchin eggs fertilization and development (Girard et al. 1996), and prostaglandin release from bovine endometrial tissue (Burns, Hayes, and Silvia 1998). In addition, more recently it was described to induce acrosome reaction in murine sperm cells (Trevino et al. 2005). All events are dependent on extracellular  $\text{Ca}^{2+}$ . Finally, in cell-free extracts, MTX directly inhibited GTP/GDP exchange and GTP binding to G $\alpha$  subunits of Gs, Go, and Gi proteins (Khan et al. 2001).

## References

- Alfonso A., de la Rosa, L.A., Vieytes, M.R., Yasumoto, T., and Botana, L.M. 2003. Yessotoxin, a novel phycotoxin, activates phosphodiesterase activity. Effect of yessotoxin on cAMP levels in human lymphocytes. *Biochem Pharmacol* 65, 193–208.
- Alzola, E., Chab, N., Pochet, S., Kabre, E., Marino, A., and Dehaye, J.-P. 2001. Modulation by propranolol of the uptake of ethidium bromide by rat submandibular acinar cells exposed to a P2X7 agonist or to maitotoxin. *Cellular Signalling* 13, 465–473.
- Auvin, S., Pignol, B., Navet, E., Pons, D., Marin, J.-G., Bigg, D., Chabrier, P.-E. 2004. Novel dual inhibitors of calpain and lipid peroxidation. *Bioorganic and Medicinal Chemistry Letters* 14, 3825–3828.
- Beech, D.J. 2005. TRPC1: store-operated channel and more. *Pflugers Arch* 451, 53–60.
- Bernard, V., Laurent, A., Derancourt, J., Clement-Durand, M., Picard, A., Le Peuch, C., Berta, P., and Doree, M. 1988. Maitotoxin triggers the cortical reaction and phosphatidylinositol-4,5- biphosphate breakdown in amphibian oocytes. *Eur J Biochem* 174, 655–662.
- Bielfeld-Ackermann, A., Range, C., and Korbmacher, C. 1998. Maitotoxin (MTX) activates a nonselective cation channel in *Xenopus laevis* oocytes. *Pflugers Arch* 436, 329–337.
- Brereton, H.M., Chen, J., Rychkov, G., Harland, M.L., and Barritt, G.J. 2001. Maitotoxin activates an endogenous non-selective cation channel and is an effective initiator of the activation of the heterologously expressed hTRPC-1 (transient receptor potential) non-selective cation channel in H4-IIIE liver cells. *Biochem Biophys Acta* 1540, 107–126.
- Bressler, J.P., Belloni-Olivi, L., and Forman, S. 1994. Effect of ganglioside GM1 on arachidonic acid release in bovine aortic endothelial cells. *Life Sci* 54, 49–60.
- Burns, P.D., Hayes, S.H., and Silvia, W.J. 1998. Cellular mechanisms by which oxytocin mediates uterine prostaglandin F2a synthesis in bovine endometrium: role of calcium. *Domestic Animal Endocrinology* 15, 477–487.
- Cataldi, M., Secondo, A., D'Alessio, A., Tagliatela, M., Hofmann, F., Klugbauer, N., Renzo, G.D., and Annunziato, L. 1999. Studies on maitotoxin-induced intracellular Ca(2+) elevation in Chinese hamster ovary cells stably transfected with cDNAs encoding for L-type Ca2+ channel subunits. *J Pharmacol Exp Ther* 290, 725–730.
- Chen, J., and Barritt, G.J. 2003. Evidence that TRPC1 (transient receptor potential canonical 1) forms a Ca(2+)-permeable channel linked to the regulation of cell volume in liver cells obtained using small interfering RNA targeted against TRPC1. *Biochem J* 373, 327–336.
- Clapham, D.E., Runnels, L.W., Strübing, C. 2001. The TRP ion channel family. *Nat Rev Neurosci* 2, 387–396.
- Daly, J.W., Lueders, J., Padgett, W.L., Shin, Y., and Gusovsky, F. 1995. Maitotoxin-elicited calcium influx in cultured cells. Effect of calcium-channel blockers. *Biochem Pharmacol* 50, 1187–1197.
- de la Rosa, L.A., Alfonso, A., Vilarino, N., Vieytes, M.R., Yasumoto, T., and Botana, L.M. 2001. Maitotoxin-induced calcium entry in human lymphocytes - Modulation by yessotoxin, Ca2+ channel blockers and kinases. *Cellular Signalling* 13, 711–716.
- Diakov, A., Koch, J.P., Ducoudret, O., Müller-Berger, S., and Frömter, E. 2001). The disulfonic stilbene DIDS and the marine poison maitotoxin activate the same two types of endogenous cation conductance in the cell membrane of *Xenopus laevis* oocytes. *Pflugers Arch* 442, 700–708.
- Dietl, P., and Völkl, H. 1994. Maitotoxin activates a nonselective cation channel and stimulates Ca<sup>2+</sup> entry in MDCK renal epithelial cells. *Mol Pharmacol* 45, 300–305.
- Donnelly-Roberts, D.L., Namovic, M.T., Faltynek, C.R., and Jarvis, M.F. 2004. Mitogen-activated protein kinase and caspase signaling pathways are required for P2X7 receptor (P2X7R)-induced pore formation in human THP-1 cells. *J Pharmacol Exp Ther* 308, 1053–1061.
- Estacion, M. 2000. In *Ciguatera Toxins: Mechanism of Action and Pharmacology of Maitotoxin*, ed. L.M. Botana, pp. 473–503.
- Estacion, M., Nguyen, H.B., and Gargus, J.J. 1996. Calcium is permeable through a maitotoxin-activated nonselective cation channel in mouse L cells. *Am J Physiol* 270, C1145–C1152.
- Escobar, L.I., Salvador, C., Martínez, M., and Vaca, L. 1998. Maitotoxin, a cationic channel activator. *Neurobiology (Bp)* 6, 59–74.
- Estacion, M., and Schilling, W. 2001. Maitotoxin-induced membrane blebbing and cell death in bovine aortic endothelial cells. *BMC Physiology* 1, 2.
- Estacion, M., and Schilling, W.P. 2002. Blockade of maitotoxin-induced oncotic cell death reveals zeiosis. *BMC Physiology* 2, 2.A
- Estacion, M., Weinberg, J.S., Sinkins, W.G., and Schilling, W.P. 2003. Blockade of maitotoxin-induced endothelial cell lysis by glycine and L-alanine. *Am J Physiol Cell Physiol* 284, C1006–C1020.

- Girard, J.-P., Graillet, C., Pesando, D., and Payan, P. 1996. Calcium homeostasis and early embryotoxicity in marine invertebrates. *Comparative Biochemistry and Physiology—Part C: Pharmacology, Toxicology and Endocrinology* 113, 169–175.
- Gregory, R.B., Rychkov, G., and Barritt, G.J. 2001. Evidence that 2-aminoethyl diphenylborate is a novel inhibitor of store-operated  $\text{Ca}^{2+}$  channels in liver cells, and acts through a mechanism which does not involve inositol triphosphate receptors. *Biochem J* 354, 285–290.
- Gregory, R.B., Sykiotis, D., and Barritt, G.J. 2003. Evidence that store-operated  $\text{Ca}^{2+}$  channels are more effective than intracellular messenger-activated non-selective cation channels in refilling rat hepatocyte intracellular  $\text{Ca}^{2+}$  stores. *Cell Calcium* 34, 241–251.
- Gusovsky, F., Bitran, J.A., Yasumoto, T., and Daly, J.W. 1990. Mechanism of maitotoxin-stimulated phosphoinositide breakdown in HL-60 cells. *J Pharmacol Exp Ther* 252, 466–473.
- Gusovsky, F., Lueders, J.E., Kohn, E.C., and Felder, C.C. 1993. Muscarinic receptor-mediated tyrosine phosphorylation of phospholipase C-gamma. *J Biol Chem* 268, 7768–7772.
- Gutierrez, D., Diaz de León, L., and Vaca, L. 1997. Characterization of the maitotoxin-induced calcium influx pathway from human skin fibroblasts. *Cell Calcium* 22, 31–38.
- Khan, R.N., Tall, E.G., Rebecchi, M., Ramsdell, J.S., and Pentylala, S. 2001. Effect of maitotoxin on guanine nucleotide interaction with G-protein alpha subunits. *Int J Toxicol* 20, 39–44.
- Kobayashi, M., Ochi, R., and Ohizumi, Y. 1987. Maitotoxin-activated single calcium channels in guinea-pig cardiac cells. *Br J Pharmacol* 92, 665–671.
- Konoki, K., Hashimoto, M., Murata, M., and Tachibana, K. 1996. Blockade of MTX-induced  $\text{Ca}^{2+}$  influx in rat glioma C6 cells by alkylamines. *J Nat Toxins* 2, 209–217.
- . 1999. Maitotoxin-induced calcium influx in erythrocyte ghosts and rat glioma C6 cells, and blockade by gangliosides and other membrane lipids. *Chem Res Toxicol* 12, 993–1001.
- Konoki, K., Hashimoto, M., Nonomura, T., Sasaki, M., Murata, M., and Tachibana, K. 1998. Inhibition of maitotoxin-induced  $\text{Ca}^{2+}$  influx in rat glioma C6 cells by brevetoxins and synthetic fragments of maitotoxin. *J Neurochem* 70, 409–416.
- Lee, Z.-W., Kwon, S.-M., Kim, S.-W., Yi, S.-J., Kim, Y.-M., and Ha, K.-S. 2003. Activation of in situ tissue transglutaminase by intracellular reactive oxygen species. *Biochem Biophys Res Commun* 305, 633–640.
- Leech, C.A., and Habener, J.F. 1997. Insulinotropic glucagon-like peptide-1-mediated activation of non-selective cation currents in insulinoma cells is mimicked by maitotoxin. *J Biol Chem* 272, 17987–17993.
- . 1998. A role for  $\text{Ca}^{2+}$ -sensitive nonselective cation channels in regulating the membrane potential of pancreatic beta-cells. *Diabetes* 47, 1066–1073.
- Lesort, M., Attanavanich, K., Zhang, J., and Johnson, G.V. 1998. Distinct nuclear localization and activity of tissue transglutaminase. *J Biol Chem* 273, 11991–11994.
- Lundy, P.M., Nelson, P., Mi, L., Frew, R., Minaker, S., Vair, C., and Sawyer, T.W. 2004. Pharmacological differentiation of the P2X7 receptor and the maitotoxin-activated cationic channel. *European Journal of Pharmacology* 487, 17–28.
- Malaguti, C., Yasumoto, T., and Paolo Rossini, G. 1999. Transient  $\text{Ca}^{2+}$ -dependent activation of ERK1 and ERK2 in cytotoxic responses induced by maitotoxin in breast cancer cells. *FEBS Letters* 458, 137–140.
- Martínez, M., Salvador, C., Farias, J.M., Vaca, L., and Escobar, L.I. 1999. Modulation of a calcium-activated chloride current by Maitotoxin. *Toxicon* 37, 359–370.
- Martínez-François, J.R., Morales-Tlalpan, V., and Vaca, L. 2002. Characterization of the maitotoxin-activated cationic current from human skin fibroblasts. *I* 538, 79–86.
- McGinnis, K.M., Gnegy, M.E., Falk, N., Nath, R., and Wang, K.K.W. 2003. Cytochrome c translocation does not lead to caspase activation in maitotoxin-treated SH-SY5Y neuroblastoma cells. *Neurochemistry International* 42, 517–523.
- Morales-Tlalpan, V., and Vaca, L. 2002. Modulation of the maitotoxin response by intracellular and extracellular cations. *Toxicon* 40, 493–500.
- Murata, M., Gusovsky, F., Yasumoto, T., and Daly, J.W. 1992. Selective stimulation of  $\text{Ca}^{2+}$  flux in cells by maitotoxin. *Eur J Pharmacol* 227, 43–49.
- Nakahata, N., Ohkubo, S., Ito, E., Nakano, M., Terao, K., and Ohizumi, Y. 1999. Comparison of maitotoxin with thromboxane A2 in rabbit platelet activation. *Toxicon* 37, 1375–1389.
- Nakahata, N., Yaginuma, T., and Ohizumi, Y. 1999. Maitotoxin-induced phosphoinositide hydrolysis is dependent on extracellular but not intracellular  $\text{Ca}^{2+}$  in human astrocytoma cells. *Jpn J Pharmacol* 81, 240–243.
- Nilius, B., and Voets, T. 2005. TRP channels a tr(i)p through a world of multifunctional cation channels. *Pflugers Arch* 451, 1–10.
- Nishio, M., Muramatsu, I., and Yasumoto, T. 1996.  $\text{Na}^{+}$ -permeable channels induced by maitotoxin in guinea-pig single ventricular cells. *European Journal of Pharmacology* 297, 293–298.

- North, R.A. 2002. Molecular physiology of P2X receptors. *Physiol Rev* 82, 1013–1067.
- Obara, Y. *Chem Res Toxicol* 12, 995.
- Obara Y, Takahashi M, Nakahata N, Ohizumi Y. (1999) Maitotoxin-induced nerve growth factor production accompanied by the activation of a voltage-insensitive Ca<sup>2+</sup> channel in C6-BU-1 glioma cells. *Br J Pharmacol* 127, 1577–1582.
- Olivi, L., and Bressler, J. 2000. Maitotoxin stimulates Cd influx in Madin-Darby kidney cells by activating Ca-permeable cation channels. *Cell Calcium* 27, 187–193.
- Parekh, A.B., and Putney, J.W.J. 2005. Store-operated calcium channels. *Physiol Rev* 85, 757–810.
- Plant, T.D., and Schaefer, M. 2003. TRPC4 and TRPC5: receptor-operated Ca<sup>2+</sup>-permeable nonselective cation channels. *Cell Calcium* 33, 441–450.
- Roe, M.W., Worley, J.F., Qian, F., Tamarina, N., Mittal, A.A., Dralyuk, F., Blair, N.T., Mertz, R.J., Philipson, L.H., and Dukes, I.D. 1998. Characterization of a Ca<sup>2+</sup> release-activated nonselective cation current regulating membrane potential and [Ca<sup>2+</sup>]<sub>i</sub> oscillations in transgenically derived b-cells. *J Biol Chem* 273, 10402–10410.
- Satoh, E., Ishii, T., and Nishimura, M. 2001. The mechanism of maitotoxin-induced elevation of the cytosolic free calcium level in rat cerebrocortical synaptosomes. *Jpn J Pharmacol* 85, 98–100.
- Schaefer, M. 2005. Homo- and heteromeric assembly of TRP channel subunits. *Pflugers Arch* 451, 35–42.
- Schilling, W.P., Sinkins, W.G., and Estacion, M. 1999. Maitotoxin activates a nonselective cation channel and a P2Z/P2X(7)-like cytolitic pore in human skin fibroblasts. *Am J Physiol* 277, C755–C765.
- Schilling, W.P., Wasylina, T., Dubyak, G.R., Humphreys, B.D., and Sinkins, W.G. 1999. Maitotoxin and P2Z/P2X(7) purinergic receptor stimulation activate a common cytolitic pore. *Am J Physiol* 277, C766–C776.
- Takahashi, M., Tatsumi, M., Ohizumi, Y., and Yasumoto, T. 1983. Ca<sup>2+</sup> channel activating function of maitotoxin, the most potent marine toxin known, in clonal rat pheochromocytoma cells. *J Biol Chem* 258, 10944–10949.
- Takeda, K., Matsuzawa, A., Nishitoh, H., Tobiume, K., Kishida, S., Ninomiya-Tsuji, J., Matsumoto, K., and Ichijo, H. 2004. Involvement of ASK1 in Ca<sup>2+</sup>-induced p38 MAP kinase activation. *EMBO Reports* 5, 161–166.
- Trevino, C.L., De la Vega-Beltran, J.L., Nishigaki, T., Felix, R., and Darszon, A. 2005. Maitotoxin potently promotes Ca(2+) influx in mouse spermatogenic cells and sperm, and induces the acrosome reaction. *J Cell Physiol*, Epub.
- Venant, A., Dazy, A.C., Diogène, G., and Marano, F. 1995. Differential effects of maitotoxin on calcium entry and ciliary beating in the rabbit ciliated tracheal epithelium. *Biol Cell* 85, 197–205.
- Venant, A., Dazy, A.C., Diogene, G., Metezeau, P., and Marano F. 1994. Effects of maitotoxin on calcium entry and phosphoinositide breakdown in the rabbit ciliated tracheal epithelium. *Biol Cell* 82, 195–202.
- Verhoef, P.A., Kertesy, S.B., Estacion, M., Schilling, W.P., and Dubyak, G.R. 2004. Maitotoxin induces biphasic interleukin-1beta secretion and membrane blebbing in murine macrophages. *Mol Pharmacol* 66, 909–920.
- Wang, K.K.W., Nath, R., Raser, K.J., and Hajimohammadreza, I. 1996. Maitotoxin induces calpain activation in SH-SY5Y neuroblastoma cells and cerebrocortical cultures. *Archives of Biochemistry and Biophysics* 331, 208–214.
- Watanabe, A., Ishida, Y., Honda, H., Kobayashi, M., and Ohizumi, Y. 1993. Ca(2+)-dependent aggregation of rabbit platelets induced by maitotoxin, a potent marine toxin, isolated from a dinoflagellate. *Br J Pharmacol* 109, 29–36.
- Weber, W.M., Popp, C., Clauss, W., and Driessche, W.V. 2000. Maitotoxin induces insertion of different ion channels into the *Xenopus* oocyte plasma membrane via Ca(2+)-stimulated exocytosis. *Pflugers Arch* 439, 363–369.
- Wisnoskey, B.J., Estacion, M., and Schilling, W.P. 2004. Maitotoxin-induced cell death cascade in bovine aortic endothelial cells: divalent cation specificity and selectivity. *Am J Physiol Cell Physiol* 287, C345–C356.
- Woods, N.M., Dixon, C.J., Yasumoto, T., Cuthbertson, K.S., and Cobbold, P.H. 1999. Maitotoxin-induced free Ca changes in single rat hepatocytes. *Cell Signal* 11, 805–811.
- Worley, J.F., McIntyre, M.S., Spencer, B., and Dukes, I.D. 1994. Depletion of intracellular Ca<sup>2+</sup> stores activates a maitotoxin-sensitive nonselective cationic current in beta-cells. *J Biol Chem* 269, 32055–32058.
- Xi, D., Dolah, F.M.V., and Ramsdell, J.S. 1992. Maitotoxin induces a calcium-dependent membrane depolarization in GH4C1 pituitary cells via activation of type L voltage-dependent calcium channels. *J Biol Chem* 267, 25025–25031.
- Xi, D., Kurtz, D.T., and Ramsdell, J.S. 1996. Maitotoxin-elevated cytosolic free calcium in GH4C1 rat pituitary cells nimodipine-sensitive and -insensitive mechanisms. *Biochemical Pharmacology* 51, 759–769.
- Yasumoto, T. 2000. In *Historic Considerations Regarding Seafood Safety*, ed. L.M. Botana, pp. 1–17.
- Zhang, J., Lesort, M., Guttman, R.P., and Johnson, G.V. 1998. Modulation of the in situ activity of tissue transglutaminase by calcium and GTP. *J Biol Chem* 273, 2288–2295.
- Zhao, X., Pike, B.R., Newcomb, J.K., Wang, K.K., Posmantur, R.M., and Hayes, R.L. 1999. Maitotoxin induces calpain but not caspase-3 activation and necrotic cell death in primary septo-hippocampal cultures. *Neurochem Res* 24, 371–382.



## 5 Chemistry of Palytoxins and Ostreocins

Panagiota Katikou

### Introduction

Palytoxin, a toxic compound initially isolated in 1971 from marine soft corals of the genus *Palythoa* (Moore and Scheuer 1971), is the most poisonous nonprotein substance known to date. The gross structure of palytoxin was elucidated almost 10 years later, in 1981, by two groups independently, one led by Professor Hirata at Nagoya in Japan (Uemura et al. 1981b) and the other by Professor Moore at Honolulu in the United States (Moore and Bartolini 1981). Palytoxin is a large, very complex molecule with both lipophilic and hydrophilic areas, and has the longest chain of continuous carbon atoms known to exist in a natural product. Its chemical formula is  $C_{129}H_{223}N_3O_{54}$  with 115 of the 129 carbons being in a continuous chain. Another unusual structural feature of palytoxin is that it contains 64 stereogenic centers, which means that palytoxin can have  $2^{64}$  stereogenic isomers. Moreover, there are eight double bonds able to exhibit cis/trans-isomerism, which means that palytoxin can have more than  $10^{21}$  (one sextillion) stereoisomers (Patockaa and Stredab 2002). Despite this huge amount of isomers, in 1989 a group led by Professor Kishi at Harvard University achieved the monumental task of complete chemical synthesis of the correct isomer of palytoxin in its carboxylic acid form (Armstrong et al. 1989a).

The present chapter will highlight the most important points regarding the chemistry of this fascinating molecule, palytoxin, together with those of certain naturally occurring palytoxin analogues, the ostreocins.

### Palytoxin

#### *Palytoxin Origin, Biogenesis, and Sequestration*

The origin of palytoxin in the *Palythoa* zoanthids has long been a matter of speculation because its contents markedly fluctuate both seasonally and regionally. For this reason, a bacterial origin has been suggested, but this has never been experimentally confirmed (Moore et al. 1982b). In this context, Uemura et al. (1985), after isolation and structural elucidation of at least four minor toxins coexisting with palytoxin in *Palythoa tuberculosa*, supported the theory of palytoxin biosynthesis by symbiotic microorganisms. This was attributed to the location of the structural difference between palytoxin, homo-palytoxin and bishomo-palytoxin being in the  $\omega$ -aminoalcohol moiety, which is often observed in natural products produced by microorganisms. Recently, Frolova et al. (2000) reported that species of the bacterial genera *Aeromonas* and *Vibrio* were capable of producing compounds antigenically related to palytoxin.

Other potential producers such as symbiotic algae, which are able to synthesize secondary products similar to palytoxin (Nakamura et al. 1993) and which live in large masses in the mesogloea of the Zoantharia, have also been considered. In this context, Maeda et al. (1985; cited from Halstead 2002) reported the detection of palytoxin or a closely related compound in the red alga *Chondria crispus*. However, the lack of correlation between algae (as expressed by chlorophyll *a* content) and

palytoxin content appears to contradict their involvement in toxin synthesis (Gleibs et al. 1995). Kimura et al. (1972) reported a correlation between the presence of eggs in *Palythoa* polyps from the Pacific and their palytoxin content. However, this was not confirmed in *Palythoa* species from the Caribbean Sea. Considerable concentrations of palytoxin were measured even in sterile polyps; on the other hand, some egg-bearing polyps were entirely free from palytoxin (Gleibs et al. 1995).

Dinoflagellates belonging to the genus *Ostreopsis* have been proposed as possible biogenetic origins of palytoxin (Usami et al. 1995; Taniyama et al. 2003). This theory is further supported because of the implication of *Ostreopsis siamensis* in a case of clupeotoxism where the causative agent was found to be palytoxin or one of its analogues (Onuma et al. 1999).

Palytoxin is one of the most potent natural nonprotein compounds exhibiting extreme toxicity in mammals (i.v. LD<sub>50</sub> 10–100 ng/kg; Wiles et al. 1974). Its toxic dose in humans has obviously not been experimentally determined; however, extrapolation of the available animal toxicity data will give a toxic dose in humans of about 4 µg (Taniyama et al. 2002). Despite its high lethality in terrestrial animals, palytoxin has also been detected in crabs (Yasumoto et al. 1986; Lau et al. 1995), in various fish (Hashimoto et al. 1969; Fukui et al. 1987, 1988; Kodama et al. 1989), and in a sea anemone (Mahnir et al. 1992) without causing any deleterious effects. This resistance of marine animals to palytoxin enables its sequestration and accumulation in the food chain (Gleibs and Mebs 1999), as these have been repeatedly implicated in numerous cases of human poisoning and lethality (Gonzalez and Alcala 1977; Alcala 1983; Alcala et al. 1988; Noguchi et al. 1988).

### Properties

Palytoxin is a white, amorphous, hygroscopic solid that has not yet been crystallized. It is insoluble in nonpolar solvents such as chloroform, ether, and acetone; sparingly soluble in methanol and ethanol; and soluble in pyridine, dimethyl sulfoxide, and water. The partition coefficient for the distribution of palytoxin between 1-butanol and water is 0.21 at 25°C based on comparison of the absorbance at 263 nm for the two layers. In aqueous solutions, palytoxin foams on agitation, like a steroidal saponin, probably because of its amphipathic nature. The toxin shows no definite melting point and is resistant to heat but chars at 300°C. It is an optically active compound, having a specific rotation of +26°±2° in water. The optical rotatory dispersion curve of palytoxin exhibits a positive Cotton effect with  $[\alpha]_{250}$  being +700° and  $[\alpha]_{215}$  being +600° (Moore and Scheuer 1971; Tan and Lau 2000).

### Structure

Palytoxin is one of the most complicated and largest molecules except for the naturally occurring polymers. The basic molecule consists of a long, partially unsaturated (with eight double bonds) aliphatic backbone with spaced cyclic ethers, 64 chiral centers, and 40–42 hydroxyl and 2 amide groups (Uemura et al. 1985; Tan and Lau 2000). The third nitrogen present as a primary amino group at the C-115 end of the molecule accounts for the basicity of palytoxin (Moore et al. 1980). Moore and Bartolini (1981) reported that both molecular weight and molecular formula of palytoxins differ depending on the species from which they are obtained and that certain species contain mixtures of different isomers. These subtle differences are attributed to structural differences in the hemiketal ring. Fragmentation by sodium periodate oxidation and ozonolysis and subsequent ordering of the fragments, together with the use of mass spectrometry and nuclear magnetic resonance, have been employed during the determination of the gross structures of palytoxins (Moore et al. 1980; Uemura et al. 1980a, b, 1981a, b; Moore and Bartolini 1981).



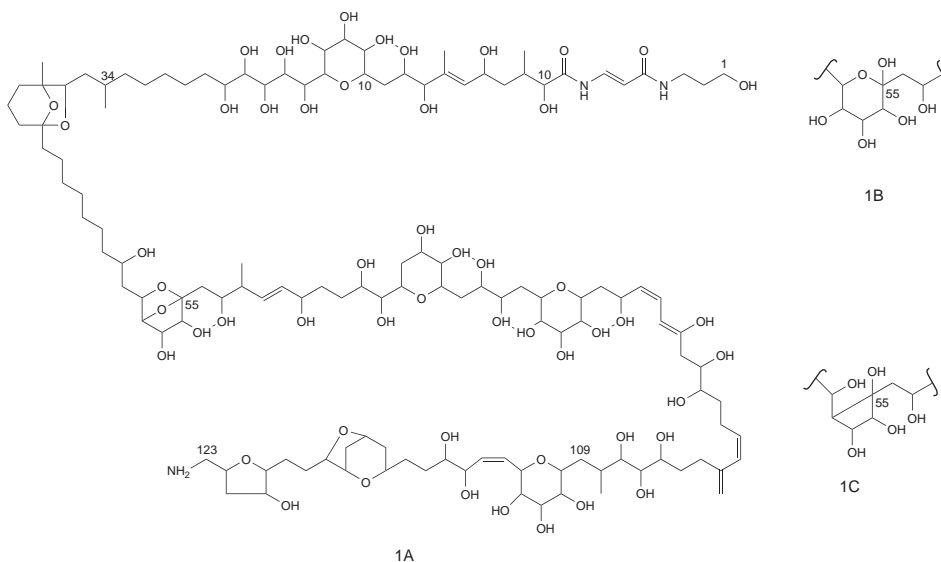


**Figure 5.1.** Proposed structure of palytoxin from a Tahitian *Palythoa* sp. (1A). The two palytoxins from Hawaiian *P. toxica* are the related C-55 hemiketals (partial structures 1B and 1C). Reproduced with permission from Moore and Bartolini 1981, © American Chemical Society.

Palytoxin from the Tahitian *Palythoa* has a molecular form of  $C_{129}H_{221}N_3O_{54}$  ( $M_r$  2659). On the other hand, palytoxin from *P. toxica* has a molecular form of  $C_{129}H_{223}N_3O_{54}$  ( $M_r$  2677), with two possible structures (Fig. 5.1) that differ from the former in the C-55 hemiketal ring. Palytoxin from the Hawaiian *P. tuberculosa* is a mixture of the three palytoxins from the Tahitian *Palythoa* and *P. toxica* (Moore and Bartolini 1981). The two components in palytoxin from the Okinawan *P. tuberculosa* ( $M_r$  2681; Macfarlane et al. 1980) may be the related C-54 ketal and hemiketal (Moore and Bartolini 1981). The palytoxin from *P. caribaoreum* has a molecular mass of 2680, while the palytoxin-like substance isolated from *Lophozozymus pictor* crab, which showed a very similar positive ion MS profile, was estimated to possess a molecular mass of 2681.0 Da (Lau et al. 1995).

Four other minor toxins have been found to co-occur with palytoxin in *P. tuberculosa*, namely homopalytoxin, bishomopalytoxin, neopalytoxin, and deoxypalytoxin. These have been structurally characterized as palytoxin analogues, having minor differences from the major palytoxin. For instance, the structural difference between homo-, bishomo-, and palytoxin is in the proximity of the C-a proton (Fig. 5.2), while the molecular weight is larger than palytoxin by 14 and 28 mass units for homo- and bishomopalytoxin, respectively. The same major and minor toxins have been isolated from another unclassified *Palythoa* species in Ishigaki Island, but the contents of homo-, bishomo-, and deoxypalytoxins were higher than that in *P. tuberculosa* (Uemura et al. 1985).

The absolute stereochemistry of palytoxins from both *P. toxica* and *P. tuberculosa* (Fig. 5.2) has been assigned to all 64 chiral centers (Cha et al. 1982; Moore et al. 1982) by a long series of degradation experiments involving the use of X-ray crystallography, nuclear magnetic resonance (NMR), and circular dichroic spectroscopy together with organic synthesis (Klein et al. 1982; Ko et al. 1982; Fujioka et al. 1982).

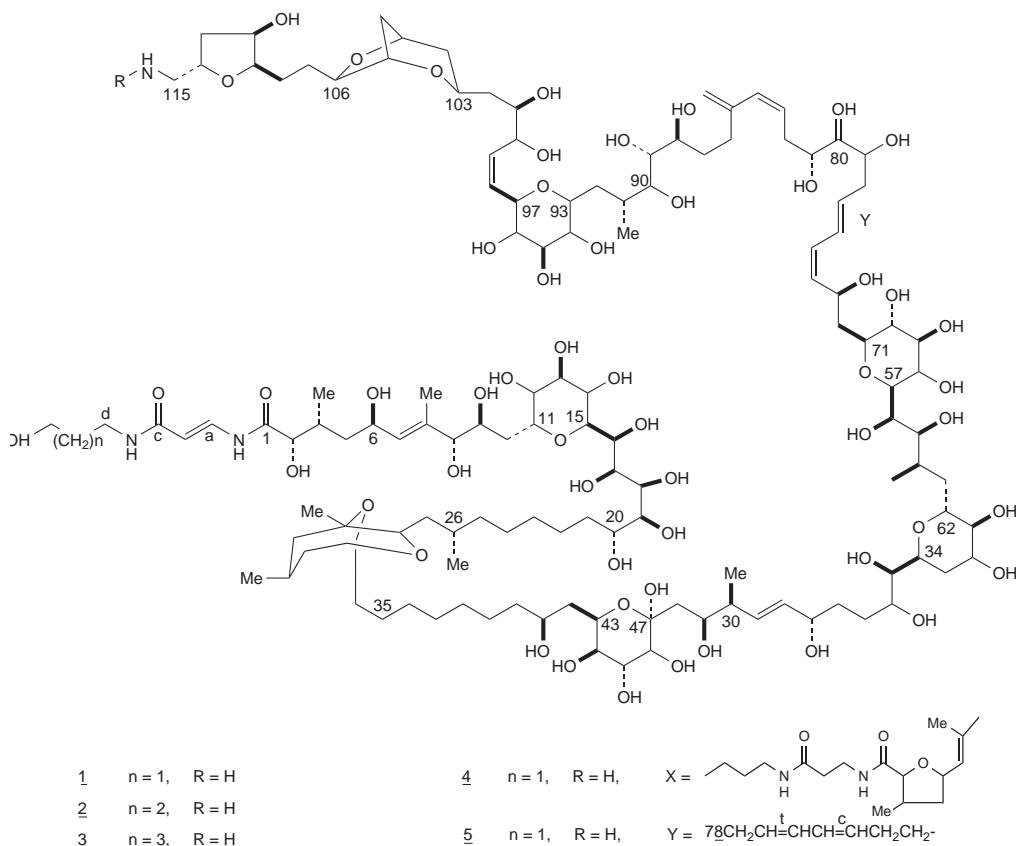


**Figure 5.2.** Complete structure of the major palytoxin from *P. tuberculosis* (1) and of minor palytoxins: (2) homopalytoxin, (3) bishomopalytoxin, (4) neopalytoxin, and (5) deoxypalytoxin. Reproduced with permission from Uemura et al. 1985, © Elsevier.

### Mass Spectrometry

Mass spectrometry (MS) data have been very useful for detection of palytoxin's presence, as well as determination of molecular weights and elucidation of the structural differences between palytoxins from various origins. For example, loss of numerous water molecules during MS analysis indicated that palytoxins possess a large number of hydroxyl and/or ether moieties (Lau et al. 1995; Lenoir et al. 2004). On the other hand, the presence of a fragment ion at or near  $m/z = 327$  in the bi-valent and tri-valent positive ion MS/MS spectra is indicative of palytoxin-like substances. This fragment ion could arise from cleavage between carbons 8 and 9 of palytoxin (Fig. 5.3) and the additional loss of one water molecule (Uemura et al. 1985; Lenoir et al. 2004). Presence of the  $m/z = 327$  fragment ion has been confirmed in the palytoxin from *P. tuberculosis* (Uemura et al. 1985; Penna et al. 2005), *P. caribaoreum* (Lau et al. 1995), and *P. toxica* (Lenoir et al. 2004). The absence of this fragment ion, however, does not necessarily exclude the possibility of a palytoxin-like compound but could be attributed to structural differences at this end of the molecule, as in the case of *L. pictor* toxin or minor *P. tuberculosis* toxins (Uemura et al. 1985; Lau et al. 1995).

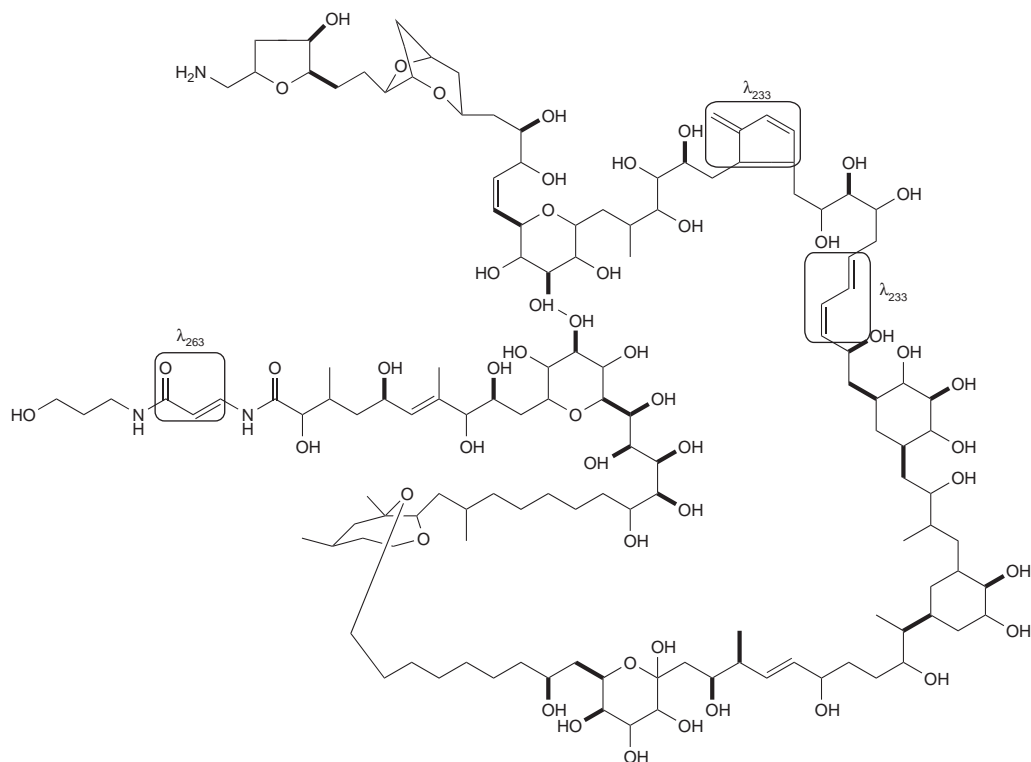


**Figure 5.3.** Planar structure of reference Pacific palytoxin (P-PTX) showing the UV chromophores. Asterisk denotes carbon eight. Reproduced with permission from Lenoir et al. 2004, © Blackwell Publishing.

### Ultraviolet Spectrum

Palytoxin exhibits an ultraviolet (UV) absorption spectrum with  $\lambda_{\text{max}}$  at 233 ( $\epsilon$  47000) and 263 nm ( $\epsilon$  28000) (Hirata et al. 1979), attributed to the presence of respective chromophores (Figs. 5.3 and 5.4). The ratio of UV absorbance between 233 and 263 nm is 1.71 (Moore and Scheuer 1971).

This spectrum is similar for all palytoxins, regardless of subtle differences present in their proton magnetic resonance (PMR;  $^1\text{H-NMR}$ ) and carbon magnetic resonance (CMR;  $^{13}\text{C-NMR}$ ) spectra, as in the case of palytoxins from *P. toxica* from Hawaii, *P. mammilosa* from Jamaica, and *Palythoa* sp. from Tahiti (Moore et al. 1975; Béress et al. 1983). This characteristic UV absorption profile of palytoxin is another parameter that could verify the presence of this toxin and its analogues (Tan and Lau 2000).

The 233-nm absorption maximum is reported to occur because of the presence of two chromophores, a conclusion deduced from the respective value of the extinction coefficient (Uemura et al. 1980a).  $^1\text{H NMR}$  studies suggest that both these chromophores are conjugated dienes (Moore et al. 1978).

The  $\lambda$  263 chromophore is a *N*-(3'-hydroxypropyl)-*trans*-3-amidoacrylamide moiety (Moore et al. 1975). This moiety accounts for the positive response of palytoxin to the ninhydrin test, while its destruction is connected to loss of toxicity, accompanied by a negative ninhydrin test (Uemura et al. 1980a). The 263-nm chromophore is sensitive to methanolic 0.05 M HCl or aqueous 0.05 M NaOH, disappearing with a half-life of 85 and 55 minutes, respectively. However, neutralization within 2 minutes regenerates palytoxin with no apparent loss in toxicity (Moore and Scheuer 1971).

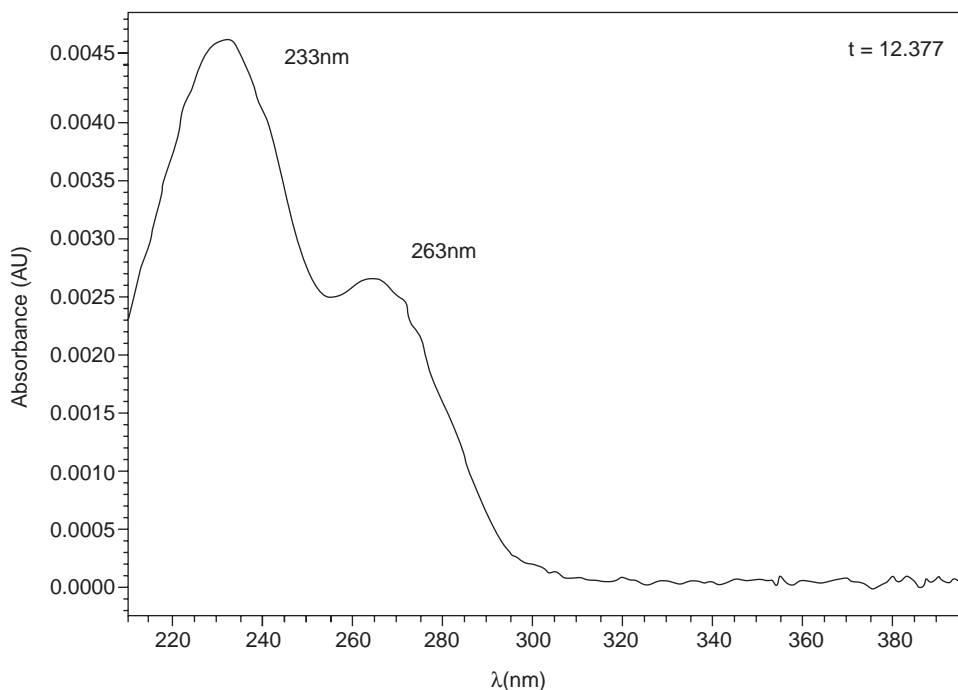


**Figure 5.4.** Ultraviolet spectrum of reference palytoxin from *Palythoa tuberculosa* at 25 µg/ml in water.

Exposure of palytoxin to both visible and UV light results in structural changes in both the 263 and 233 chromophores and can reduce its toxicity at least twentyfold in only 5 minutes in UV and 30 minutes in visible light (Hewetson et al. 1990).

### *Infrared Spectrum*

The infrared (IR) spectrum of purified palytoxin or its congener shows a band at  $1670\text{ cm}^{-1}$  due to the presence of an  $\alpha$ ,  $\beta$ -unsaturated amide carbonyl group (Moore and Scheuer 1971). Similar IR data have also been obtained for purified palytoxin both from *P. caribaeorum* (Béress et al. 1983) and from the xanthid crab *Lophozozymus pictor* (Tan and Lau 2000).

### *Nuclear Magnetic Resonance Spectra*

Many studies aimed at structural elucidation of palytoxin have included data derived from NMR determinations on various degradation products from periodate oxidation or ozonolysis (Moore and Bartolini 1981; Cha et al. 1982; Moore et al. 1982a). The complete chemical shift assignment of  $^1\text{H}$  and  $^{13}\text{C}$  NMR signals of the whole *P. tuberculosa* palytoxin molecule was reported by Kan et al. (2001; Table 5.1). A detailed description of NMR spectra is beyond the purpose of this chapter. However, it is interesting to note that deuterated methanol ( $\text{CD}_3\text{OD}$  or  $\text{CD}_3\text{OH}$ ) gave much sharper

**Table 5.1.**  $^1\text{H}$  and  $^{13}\text{C}$  NMR chemical shift data of *P. tuberculosis* palytoxin in  $\text{CD}_3\text{OD}$  or  $\text{CD}_3\text{OH}$  with one drop of deuterium oxide

No.	$^{13}\text{C}$ ( $\delta$ )	Mult.	$^1\text{H}$ ( $\delta$ )	$^1\text{H}$ ( $\delta$ )	No.	$^{13}\text{C}$ ( $\delta$ )	Mult.	$^1\text{H}$ ( $\delta$ )	$^1\text{H}$ ( $\delta$ )
1	175.92	s	—		60	70.18	d	3.85	
2	75.70	d	4.09		61	76.57	d	3.15	
3	34.73	d	2.17		62	73.11	d	3.74	
3-Me	13.99	q	0.88		63	36.77	t	1.96	1.70
4	41.73	t	1.77	1.40	64	71.77	d	3.68	
5	66.62	d	4.50		65	72.20	d	3.76	
6	131.85	d	5.49		66	37.01	t	2.04	1.53
7	138.28	s	—		67	77.22	d	3.44	
7-Me	13.17	q	1.72		68	76.04	d	3.12	
8	80.91	d	3.92		69	79.74	d	3.36	
9	72.34	d	3.81		70	75.85	d	3.09	
10	29.23	t	2.12	1.73	71	77.08	d	3.44	
11	76.19	d	4.18		72	41.51	t	2.04	1.43
12	73.88	d	3.64		73	64.99	d	4.84	
13	75.17	d	3.54		74	133.47	d	5.37	
14	71.68	d	3.60		75	130.04	d	6.00	
15	72.91	d	3.62		76	128.87	d	6.46	
16	71.28	d	4.03		77	133.88	d	5.78	
17	71.68	d	4.04		78	38.64	t	2.42	
18	73.27	d	3.54		79	71.20	d	3.93	
19	71.35	d	3.79		80	76.29	d	3.27	
20	71.11	d	3.87		81	73.04	d	3.63	
21	27.38	t	1.48	1.39	82	34.35	t	2.75	2.39
22	26.93	t	1.47	1.35	83	130.18	d	5.69	
23	35.03	t	1.64	1.55	84	132.64	d	5.95	
24	28.44	t	1.36		85	146.73	s	—	
25	39.72	t	1.26		85'	114.86	t	5.07	4.94
26	29.70	d	1.67		86	34.30	t	2.34	2.25
26-Me	19.30	q	0.92		87	33.13	t	1.72	1.59
27	40.78	t	1.47	0.91	88	74.19	d	3.71	
28	80.17	d	3.97		89	74.02	d	3.50	
29	82.31	s	—		90	77.82	d	3.35	
29-Me	21.01	q	1.18		91	33.00	d	1.89	
30	45.74	t	1.70	1.14	91-Me	15.65	q	0.91	
31	25.55	d	2.04		92	27.86	t	2.21	1.30
31-Me	21.89	q	0.91		93	74.83	d	4.03	
32	43.74	t	1.67	1.09	94	73.04	d	3.65	
33	109.23	s	—		95	74.73	d	3.61	
34	38.64	t	1.60		96	76.01	d	3.15	
35	23.98	t	1.41		97	69.71	d	4.32	
36	30.98	t	1.31		98	132.43	d	5.55	
37	30.93	t	1.31		99	135.28	d	5.71	
38	30.81	t	1.31		100	71.90	d	4.36	
39	31.29	t	1.36		101	71.77	d	3.68	
40	39.20	t	1.48		102	40.21	t	1.58	
41	69.26	d	3.80		103	68.39	d	4.22	
42	39.37	t	1.86	1.44	104	40.53	t	1.74	1.38
43	64.86	d	4.39		105	76.14	d	4.51	
44	73.88	d	3.65		106	36.83	t	1.84	1.78
45	74.28	d	3.95		107	79.62	d	4.21	

**Table 5.1.** (Continued)

No.	<sup>13</sup> C (d)	Mult.	<sup>1</sup> H (d)	<sup>1</sup> H (d)	No.	<sup>13</sup> C (d)	Mult.	<sup>1</sup> H (d)	<sup>1</sup> H (d)
46	68.25	d	3.67		108	82.74	d	4.35	
47	101.24	s	—		109	26.59	t	1.78	1.67
48	41.95	d(t)	1.83		110	32.30	t	1.47	
49	72.40	d	3.94		111	83.81	d	3.89	
50	44.07	d	2.26		112	73.27	d	4.27	
50-Me	16.58	q	1.03		113	39.78	t	2.10	1.86
51	134.46	d	5.62		114	75.31	d	4.36	
52	134.74	d	5.51		115	45.13	t	2.99	2.87
53	74.06	d	4.05		a	134.82	d	7.79	
54	34.93	t	1.77	1.61	b	106.82	d	5.95	
55	27.79	t	1.69	1.46	c	169.66	s	—	
56	73.11	d	3.74		d	37.42	t	3.33	
57	72.81	d	3.85		e	33.28	t	1.74	
58	74.19	d	3.87		f	60.40	t	3.60	
59	33.05	t	2.27	1.66					

Source: Reproduced with permission from Kan et al. 2001, © Elsevier

Note: TMS was used as an internal or external chemical shift reference of 0 ppm in proton NMR spectra. The solvent peak was used as an internal chemical shift reference of 49.00 ppm in carbon-13 NMR spectra. The “mult.” column shows a number of proton attached to the carbon as a multiplicity of peak (s = singlet, d = doublet, t = triplet, q = quartet). Row nos. 16 and 17 and 36–38 show groups of carbons that are exchangeable with each other.

signals in the <sup>1</sup>H NMR spectrum than deuterated water (D<sub>2</sub>O), probably due to a fast averaged conformation or a monomer (Kan et al. 2001).

### Chemical Synthesis

Despite the huge number of possible stereoisomers, in 1989 Kishi's group managed to achieve the total chemical synthesis of a fully protected palytoxin carboxylic acid (Armstrong et al. 1989a), which subsequently was converted to palytoxin carboxylic acid and palytoxin amide without the use of protecting groups (Armstrong et al. 1989b). On comparison of biological activity, chromatographic behavior, and spectroscopic data (MS, 1D and 2D <sup>1</sup>H NMR, <sup>13</sup>C NMR), the synthetic products were found identical to their naturally occurring counterparts (Armstrong et al. 1989b; Kishi 1989). A few years later this work was completed by conversion of palytoxin carboxylic acid to palytoxin identical to the natural product from *Palythoa tuberculosa* (Suh and Kishi 1994), with a yield of 100%. However, the chemical synthesis of palytoxin involves approximately 65 steps (Li 2005), which makes it unlikely to be of practical use.

### Palytoxin Analogues from *Ostreopsis* spp. (Ostreocins)

The term “ostreocins” generally describes toxins produced from dinoflagellates belonging to the genus *Ostreopsis* (Dinophyceae), although frequently some of the produced toxins are named after the producing species. Usami and co-workers were the first to establish the palytoxin-like character

of the major ostreocin from *O. siamensis* and indicate this species as one of the biogenetic sources of palytoxin (Usami et al. 1995).

*Ostreopsis* species are distributed worldwide and are mainly benthic and epiphytic dinoflagellates. They are important components of subtropical and tropical marine coral reef-lagoonal environments and are thought to be potential pregenitors of toxins associated with ciguatera fish poisoning (Nakajima et al. 1981; Tindall et al. 1990; Quod 1994). During the past decade, however, *Ostreopsis* sp. have been also isolated, mostly during summertime, in temperate areas of the world. Presence of potentially toxic *Ostreopsis* sp. has been reported in the Mediterranean countries Spain, Italy, Greece, and Tunisia (Vila et al. 2001; Sansoni et al. 2003; Aligizaki et al. 2005; Penna et al. 2005; Turki 2005). In the south of Spain and certain areas of Greece, their presence was accompanied by the incidence of relevant toxicity in shellfish (L.M. Botana, personal communication; NRLMB Greece, unpublished data). Until today, nine different *Ostreopsis* species have been described; five of them—namely, *Ostreopsis siamensis*, *O. ovata*, *O. mascarenensis*, *O. lenticularis*, and *O. heptagona*—are reported as producers of toxic substances (Table 5.2). On the other hand, no data is available to date with regard to the toxin production ability of the remaining four species—*O. labens*, *O. marinus*, *O. belizeanus* and *O. caribbeanus* (Faust et al. 1996; Faust 1999).

This section will focus on the available chemical data concerning only toxic substances produced by *Ostreopsis* sp., shown to possess palytoxin characteristics. For reasons of convenience, toxins will be presented according to producing species. Palytoxin-like compounds have been reported for *O. siamensis*, *O. ovata*, and *O. mascarenensis*. The neurotoxins ostreotoxin-1 and -3 produced by *O. lenticularis* have not been to date characterised by use of analytical methods as palytoxin analogues, despite their reported mouse lethality and possible connection to ciguatera (Tindall et al. 1990; Mercado et al. 1994; Meunier et al. 1997). With regard to the last of the toxic species, the only

**Table 5.2.** Toxic *Ostreopsis* species and summary of reported data on properties of respective toxins produced

Producing species	Toxin	Considered Palytoxin analogue?	Molecular weight	Chemical formula	Mouse lethality (LD <sub>50</sub> i.p.)	Reference
<i>O. siamensis</i>	Unnamed Ostreocin-D	Yes	~2635	C <sub>127</sub> H <sub>219</sub> N <sub>3</sub> O <sub>53</sub>	0.75 µg/kg	Nakajima et al. (1981) Usami et al. (1995); Ukena et al. (2001, 2002)
<i>O. mascarenensis</i>	Unnamed					Quod (1994)
	Mascarenotoxin-A	Yes	~2500–2535	n.d.	0.9 mg/kg	Turquet et al. (2002)
	Mascarenotoxin-B					Lenoir et al. (2004)
<i>O. ovata</i>	Unnamed	Yes	n.d.	n.d.	n.d.	Nakajima et al. (1981) Penna et al. (2005)
<i>O. lenticularis</i>	Ostreotoxin Ostreotoxin 1 Ostreotoxin 3	Not known	n.d.	n.d.	32.1 mg/kg	Tindall et al. (1990) Mercado et al. (1994) Meunier et al. (1997)
<i>O. heptagona</i>	Unnamed	Not known	n.d.	n.d.	n.d.	Norris et al. (1988)

Note: n.d. = not determined

available information is that methanol extracts of clonal cultures of *O. heptagona* isolated from Knight Key, Florida, were weakly toxic to mice (Norris et al. 1985).

### *Ostreopsis siamensis* (*Ostreocins*)

#### *Origin, Distribution, and Toxin Production*

*Ostreopsis siamensis* was first isolated by Schmidt in the Gulf of Siam, Thailand, in 1901 (Schmidt 1901). This dinoflagellate occurs in many tropical and subtropical areas of the world, mainly as epiphytic and less frequently as planktonic, and also in temperate areas during summertime. Until today, the presence of *O. siamensis* has been reported in the coastal waters of Japan (Yasumoto et al. 1987), New Zealand (Chang et al. 2000; Rhodes et al. 2000), Tasmania (Pearce et al. 2000), Spain, Italy (Vila et al. 2001; Penna et al. 2005), Greece (Aligizaki et al. 2005), and Tunisia (Turki 2005).

*O. siamensis* was first characterized as a toxin producer by Nakajima et al. (1981). Some years later, Yasumoto et al. (1987) and Holmes et al. (1988) reported the lethality and haemolytic activity of the *O. siamensis* toxins. Usami et al. (1995) were the first to elucidate the structure of the major ostreocin produced by *O. siamensis* (strain SOA 1 from Aka island, Okinawa, Japan) and point out its structural and chemical properties' resemblance to palytoxin. This major constituent was named ostreocin-D and accounted for 90% of total toxicity of extracts. None of the other (more than 10) minor ostreocins present in the *O. siamensis* extracts were identical to palytoxin, as initially indicated by ESI-MS (Ukena et al. 2001, 2002). New Zealand *O. siamensis* isolates have also been reported to produce toxins exhibiting strong haemolytic activity and mouse lethality (Rhodes et al. 2000, 2002). Recently, Penna et al. (2005) have reported the presence of toxins with strong delayed haemolytic activity in *Ostreopsis* cf. *siamensis* from the NW Mediterranean Sea. This haemolytic activity was inhibited by the palytoxin antagonist ouabain, indicating the palytoxin-like nature of these toxins.

Detailed studies regarding the chemistry of *O. siamensis* toxins have been reported only for ostreocin-D to date.

#### *Ostreocin-D: Properties and Structure*

Ostreocin-D is a colorless, amorphous solid, positive to ninhydrin. It is an optically active compound, having a specific rotation of +16.6 in water ( $c$  0.12,  $T = 23^\circ\text{C}$ ). Its UV absorption spectrum exhibits two maxima, at 234 ( $\epsilon$  35000) and 263 nm ( $\epsilon$  22000). The UV absorptions together with NMR spectra indicate that ostreocin-D has conjugated diene and ketone functionality analogous with palytoxin (Usami et al. 1995).

Mass spectrometry and NMR spectra (Table 5.3) were employed for ostreocin-D structure elucidation. In the high mass range of the fast-atom bombardment mass spectrometry (FABMS), ostreocin-D displayed cluster ions having a centroid at  $m/z$  2636.51. The ion distribution pointed to a composition of  $\text{C}_{127}\text{H}_{219}\text{N}_3\text{O}_{53}$ , with the  $\text{MH}^+$  calculated to be 2636.47. This difference in composition ( $\text{C}_2\text{H}_4\text{O}$ ) between palytoxin and ostreocin-D was initially attributed to the substitution of two methyls and one hydroxyl of the former with protons in the latter. The substitution of methyls is located at C3 and C26 (Fig. 5.5). Partial structures around methyls and double bonds were identified by comparison of NMR spectra of palytoxin and ostreocin-D in 0.2%  $\text{CD}_3\text{COOD}/\text{D}_2\text{O}$ . However, severe congestion of the NMR signals required reduction of the molecule size. Degradation of the molecule by ozonolysis proved useful for dissolving the NMR signals and for clarification of the entire structure. Finally it was discovered that in ostreocin-D, compared to palytoxin, two hydroxyls



**Table 5.3.** NMR Assignments of Ostreocin-D in 0.2% CD<sub>3</sub>COOD/D<sub>2</sub>O

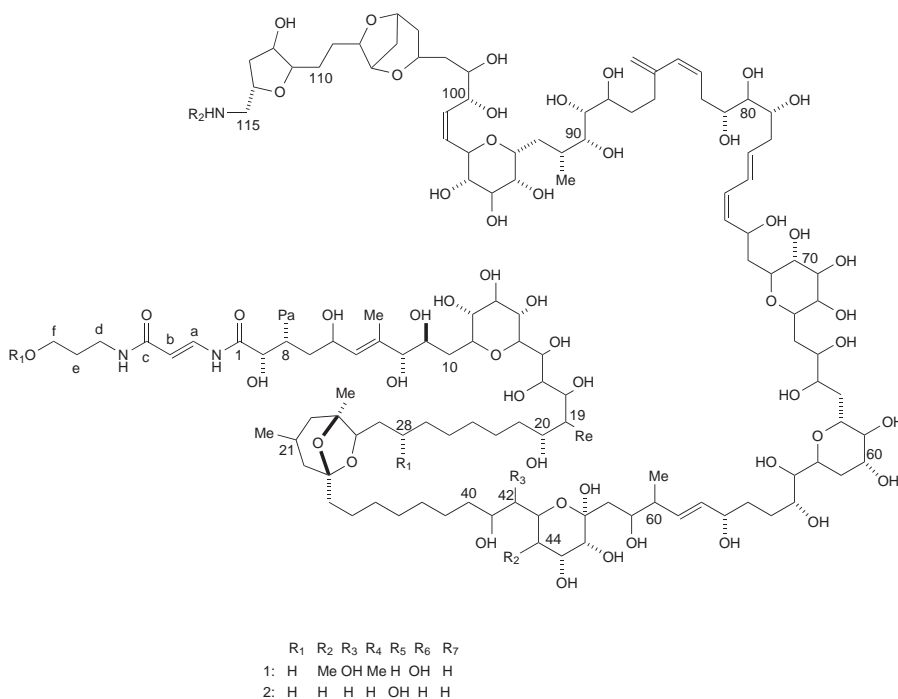
No.	<sup>1</sup> H (δ)	<sup>1</sup> H (δ)	<sup>13</sup> C (δ)	No.	<sup>1</sup> H (δ)	<sup>1</sup> H (δ)	<sup>13</sup> C (δ)
1	—		175.5	47	—		100.00
2	4.31		71.2	48	1.85	1.92	40.5
3	1.69	1.88	29.8	49	3.94		71.0
3-Me	—		—	50	2.34		42.3
4	1.59	1.75	31.8	50-Me	1.04		15.4
5	4.51		67.3	51	5.62		134.5
6	5.46		129.9	52	5.56		132.6
7	—		137.9	53	4.14		72.8
7-Me	1.71		12.1	54	1.62	1.77	33.1
8	3.96		79.7	55	1.44	1.74	32.4
9	3.86		70.5	56	3.83		71.0
10	1.72	2.13	27.9	57	4.04		71.7
11	4.23		74.5	58	3.84		71.9
12	3.72		71.2	59	1.72	2.30	31.8
13	3.64		73.2	60	3.93		68.5
14	3.62		70.1	61	3.21		75.1
15	3.67		72.6	62	3.68		71.4
16	3.62		74.9	63	1.56	2.09	35.5
17	4.02		68.7	64	3.65		70.3
18	4.01		67.3	65	3.77		70.4
19	1.50	1.80	40.6	66	1.49	2.09	35.6
20	3.85		68.2	67	3.48		75.9
21	1.52		24.9	68	3.51		75.7
22	1.35		29.0	69	3.21		74.0
23	1.35		29.0	70	3.22		74.1
24	1.35		29.0	71	3.49		77.4
25	1.35		29.0	72	1.55	2.12	39.2
26	1.35		29.0	73	4.86		63.8
26-Me	—		—	74	5.43		131.2
27	1.34		31.8	75	6.14		130.1
28	3.95		81.6	76	6.49		127.7
29	—		81.9	77	5.86		133.4
29-Me	1.24		19.9	78	2.42		36.9
30	1.19	1.77	43.8	79	3.94		69.9
31	2.00		23.9	80	3.41		75.2
31-Me	0.92		20.8	81	3.79		71.5
32	1.16	1.74	41.9	82	2.48	2.66	32.1
33	—		108.5	83	5.69		128.8
34	1.66		36.8	84	6.04		132.1
35	1.40		22.3	85	—		145.1
36	1.35		29.0	CH <sub>2</sub> =	5.00	5.14	114.4
37	1.35		29.0	86	2.27	2.32	32.7
38	1.35		29.0	87	1.61	1.75	31.3
39	1.35		29.0	88	3.76		72.6
40	1.50		37.4	89	3.60		72.9
41	3.72		71.1	90	3.47		76.1
42	3.40		75.1	91	1.84		31.7
43	4.39		63.4	91-Me	0.92		14.3
44	1.78	2.05	33.5	92	1.34	2.16	25.9
45	4.25		68.9	93	4.17		73.6
46	3.51		69.7	94	3.78		71.2

**Table 5.3.** (Continued)

No.	<sup>1</sup> H (δ)	<sup>1</sup> H (δ)	<sup>13</sup> C (δ)	No.	<sup>1</sup> H (δ)	<sup>1</sup> H (δ)	<sup>13</sup> C (δ)
95	3.70		72.6	109	1.52		30.4
96	3.32		74.3	110	1.66	1.76	24.8
97	4.29		68.2	111	3.94		82.3
98	5.62		130.9	112	4.37		71.9
99	5.78		134.8	113	1.98	2.21	37.9
100	4.35		70.9	114	4.45		73.4
101	3.66		70.3	115	3.05	3.16	43.2
102	1.58	1.62	38.5	a	7.71		133.4
103	4.21		67.4	b	5.95		106.5
104	1.48	1.79	38.5	c	—		168.9
105	4.64		75.1	d	3.34		36.4
106	1.83	1.93	35.3	e	1.79		31.2
107	4.33		78.4	f	3.68		59.3
108	4.42		81.6				

Source: Reproduced with permission from Ukena et al. 2001, © Japan Society for Bioscience Biotechnology and Agrochemistry

Note: CH<sub>3</sub>COOD was used as an internal reference at 2.06 ppm for <sup>1</sup>H and at 21.0 ppm for <sup>13</sup>C

**Figure 5.5.** Structures of palytoxin (1) and ostreocin-D (2). Reproduced with permission from Ukena et al. 2002, © John Wiley & Sons Limited.

(positions C19 and C44) are substituted by protons, while an extra hydroxyl is present at C42. Ostreocin-D was therefore deduced to be 42-hydroxy-3,26-didemethyl-19,44-dideoxypalytoxin (Usami et al. 1995; Ukena et al. 2001), a structure that was also confirmed by using negative ion FAB/MS (Ukena et al. 2002). It is noteworthy that the small structural differences between ostreocin-D and palytoxin barely have an effect on the mouse lethality of the former [ $LD_{50}$  (i.p.): 0.75 and 0.50  $\mu\text{g}/\text{kg}$ , respectively], but cause significant reduction in cytotoxicity and haemolytic potency (Usami et al. 1995; Ukena et al. 2001).

## *Ostreopsis ovata*

### *Origin, Distribution, and Toxin Production*

*Ostreopsis ovata* is the smallest species in the genus *Ostreopsis*. Its presence has been reported in numerous areas of the world such as the Pacific Ocean (Fukuyo 1981; Yasumoto et al. 1987), the Caribbean Sea (Tindall et al. 1990), the Brazilian coasts in the Atlantic Ocean (Granéli et al. 2002), and the Mediterranean Sea (Tognetto et al. 1995; Sansoni et al. 2003, Aligizaki et al. 2005; Penna et al. 2005).

*O. ovata* from Okinawa, Japan, produced a butanol-soluble compound which was lethal to mice (Nakajima et al. 1981); this was later confirmed by Yasumoto et al. (1987), who also detected slight haemolytic activity in the *O. ovata* cell extracts. On the other hand, crude methanol extracts of *O. ovata* from the Virgin Islands were found to be nontoxic to mice (Tindall et al. 1990). Summer blooms of *O. ovata* in the Italian coasts have been connected to respiratory problems in swimmers and sunbathers, most probably through inhalation of toxic aerosols (Sansoni et al. 2003; Simoni et al. 2003, 2004); such problems could possibly arise from inhalation of a palytoxin-like substance (Paddle 2003). Finally, extracts of *O. ovata* from Brazil and the Mediterranean Sea contained substances exhibiting strong delayed haemolysis, inhibited by ouabain, and mouse lethality with symptoms typical of palytoxin (Granéli et al. 2002; Riobó et al. 2004; Penna et al. 2005).

### *Properties and Structure of O. ovata toxins*

Availability of data regarding the chemistry of *O. ovata* toxins is rather limited. The extracts from all tested strains of *Ostreopsis ovata* from Brazil and the Mediterranean Sea (Italy and Spain) exhibited strong delayed hemolytic activity, which was neutralized by ouabain (Riobó et al. 2004; Penna et al. 2005). Subsequent HPLC-UV analysis of the extract from one of the strains (*O. ovata* OS06BR) showed a peak at the same retention time (at minute 9) as the standard palytoxin from *Palythoa tuberculosa*. UV spectrum of this peak exhibited two absorbance maxima, at 230 and 263 nm, indicating the palytoxin-like character of the contained compound (Fig. 5.6a). MS spectrum of this characteristic peak from the *O. ovata* extract was identical to that of the palytoxin standard showing a positive ion spray with bi-charged ions with  $m/z$  1346.7 and a fragment at  $m/z$  327 from a thermic fragmentation process (Fig. 5.6b). This  $m/z$  327 fragment is characteristic of thermally fragmented palytoxin (Uemura et al. 1985) and, combined with the  $m/z$  1346.7 of the molecule, is evidence of compounds structurally similar to palytoxin (Turquet et al. 2002).

## *Ostreopsis mascarenensis (Mascarenotoxin-1 and 2)*

### *Origin, Distribution, and Toxin Production*

*Ostreopsis mascarenensis* was first identified in shallow (2–5 m) barrier reef environments and coral reefs in the Southwest Indian Ocean and is the largest species of the genus (Quod 1994;

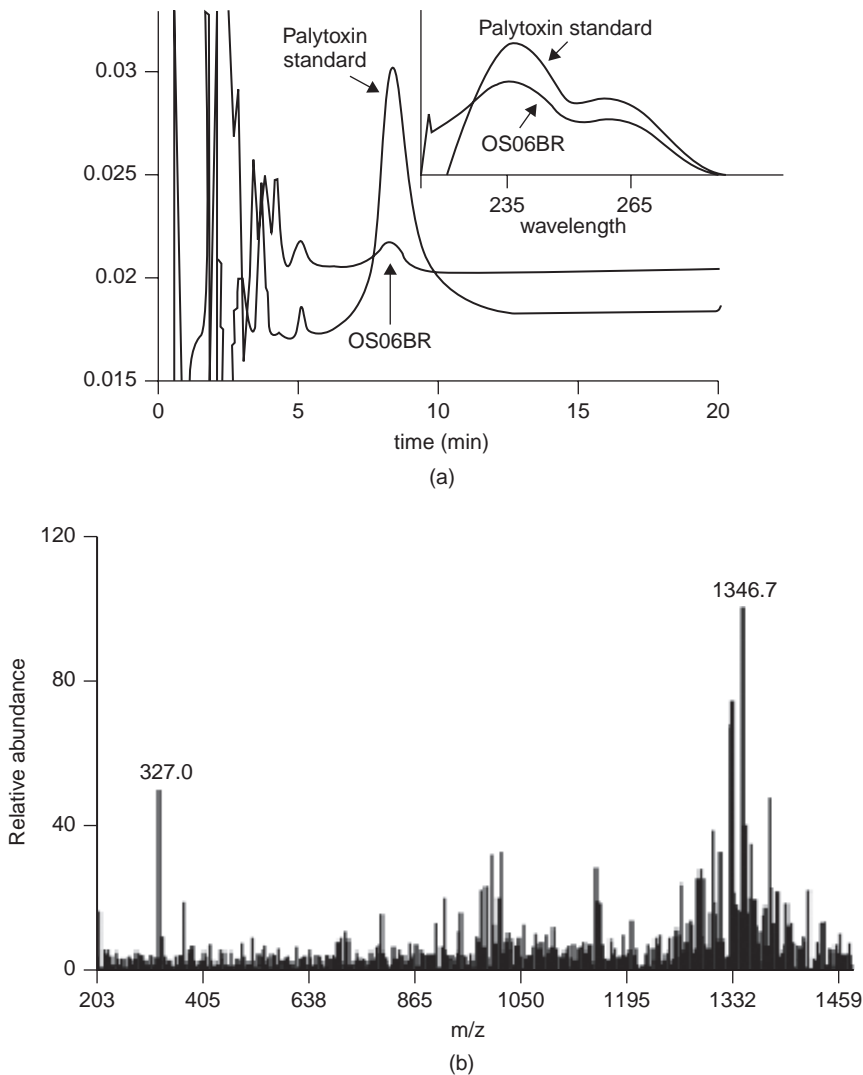


**Figure 5.6.** (a) Overlapped UV-photodiode array detector chromatograms of palytoxin standard and an extract of *Ostreopsis ovata* IEO-OS06BR showing peaks at the same retention time (minute 9) with a similar UV spectrum shown in the upper right window. (b) MS spectrum of palytoxin and an extract of *O. ovata* IEO-OS06BR showing bi-charged ion  $m/z$  1346.7 and characteristic fragment  $m/z$  327. Reproduced with permission from Penna et al. 2005, © Blackwell Publishing.

Hansen et al. 2001). This species was found in low numbers as an epiphyte on macroalgae (*Turbina-ria* sp., *Galaxaura* sp.) and dead corals and sediments at Mayotte and Reunion Islands and in high numbers at Rodrigues Island (Turquet et al. 1998). Crude methanol extracts of this species were toxic to mice (Quod 1994; Turquet et al. 2002). During a monospecific bloom of *O. mascarensis* in 1996 in Rodrigues Island (Mascareignes Archipelago, Southwest Indian Ocean), both crude methanol extracts (CME) and their polar n-butanol soluble fractions (BSF) were lethal to mice ( $LD_{50} \sim 0.9$  mg/kg) with symptoms similar to those induced by palytoxin but without diarrhea. Both

CME and BSF also exhibited the typical of palytoxin delayed haemolytic activity. Most of the mouse toxicity and haemolytic potency were found in the BSF and subsequent analyses were carried out to identify the nature of the toxic compounds (Turquet et al. 2002; Lenoir et al. 2004).

### *Mascarenotoxin-A and -B: Properties and Structure*

The BSF was further analysed with HPLC-DAD and compared to reference palytoxin from *P. toxica*, by using a mobile phase of water acidified to pH 2.5 with trifluoroacetic acid (solvent A) and pure acetonitrile (solvent B). A linear gradient was applied from 30% to 70% of solvent B over 45 minutes. The BSF HPLC screening revealed two distinct peaks, which were eluted at approximately 38% acetonitrile with retention times very close to that of reference palytoxin. Both peaks also showed two UV absorption maxima, at 233 and 263 nm, while the ratio between their absorbance (233 versus 263 nm) was identical to that calculated for reference palytoxin. The peaks were collected separately and the toxic compounds purified from the BSF were called mascarenotoxin-A (McTx-A) and mascarenotoxin-B (McTx-B) (Lenoir et al. 2004).

Further analyses of both McTx-A and McTx-B in comparison to reference palytoxin were carried out by nano-electrospray ionization quadrupole time-of-flight (nano-ESI-Q-TOF) and LC-ESI MS/MS. McTx-A and McTx-B fragmentation patterns showed a serial dehydration process, indicating the presence of numerous hydroxyls. Furthermore, the fragment ion  $m/z = 327.2$  was obtained abundantly for both McTx-A and McTx-B by selecting the bi- and tri-charged ions. The same typical fragment ion  $m/z = 327.2$  was also detected in reference palytoxin (Lenoir et al. 2004), as described before for Caribbean palytoxin (Uemura et al. 1985; Lau et al. 1995).

The MS profiles of McTx-A and McTx-B were both very similar to the respective profile of reference palytoxin, but the estimated molecular masses (between 2500–2535 Da) were lower than that of reference palytoxin (2680 Da) or other palytoxins and ostreocin-D. Nevertheless, the MS profile and fragmentation patterns of McTx-A and McTx-B together with mouse bioassay symptomatology and delayed haemolytic activity confirm the palytoxin-like character of these compounds. Quantitative differences in the hemolytic action and mouse lethality, as well as minor deviations in the MS spectra and retention times, could be attributed to structural variations between mascarenotoxins and the reference palytoxin (Lenoir et al. 2004). This is also supported by Usami et al. (1995), who showed that small changes in the structure of palytoxin analogues can have an impact on mouse toxicity, haemolytic potency, and cytotoxicity.

*Ostreopsis* sp. have been suspected to be a source of palytoxin in cases of clupeotoxism (Yasumoto 1998; Onuma et al. 1999), and the Southwest Indian Ocean is a known clupeotoxism endemic zone (Hansen et al. 2001). It is therefore highly possible that *O. mascarenensis*, which is largely distributed in the western Indian Ocean, is involved in regional clupeotoxism incidents.

## Conclusion

Palytoxin is one of the most potent marine natural products known, and there is evidence that potential production sources are species of the genus *Ostreopsis*. The relation between toxic *Ostreopsis* sp. presence and palytoxin seafood poisoning is suspected but has not to date been established for certain. Further studies will be needed to elucidate the possibility of the *Ostreopsis*-derived palytoxin analogues to enter the human food chain. Nevertheless, until this situation is clarified, vigilance is required regarding this dinoflagellate species. Taking into consideration the fact that toxic *Ostreopsis* sp. are gradually

starting to appear in large abundances in temperate waters all over the world, possibly due to the global warming effect, it should be realized that both routine monitoring of these species and regulatory limits for palytoxin and palytoxin-analogues will be required in susceptible areas.

## References

- Alcala, A.C. 1983. Recent cases of crab, cone shell and fish intoxication on southern Negros island, Philippines. *Toxicon Supplement* 3:1–3.
- Alcala, A.C., Alcala, L.C., Garth, J.S., Yasumura, D., and Yasumoto, T. 1988. Human fatality due to ingestion of the crab *Demania reynaudii* that contained a palytoxin-like toxin. *Toxicon* 28(1):105–107.
- Aligizaki, K., Koukaras, K., and Nikolaidis, G. 2005. The genus *Ostreopsis* in Greek coastal waters. *International Workshop: Ostreopsis: Is It a Problem in the Mediterranean Sea? Genova, Italy*.
- Armstrong, R.W., Beau, J.-M., Cheon, S.H., Christ, W.J., Fujioka, H., Ham, W.H., Hawkins, L.D., Jin, H., Kang, S.H., Kishi, Y., Martinelli, M.J., McWhorter Jr., W.W., Mizuno, M., Nakata, M., Stutz, A.E., Talamas, F.X., Taniguchi, M., Tino, J.A., Ueda, K., Uenishi, J.I., White, J.B., and Yonaga, M. 1989a. Total synthesis of a fully protected palytoxin carboxylic acid. *Journal of the American Chemical Society* 111(19):7525–7530.
- . 1989b. Total synthesis of palytoxin carboxylic acid and palytoxin amide. *Journal of the American Chemical Society* 111(19):7530–7533.
- Béres, L., Zwick, J., Kolkenbrock, H.J., Kaul, P.N., and Wassermann, O. 1983. A method for the isolation of the Caribbean palytoxin (C-PTX) from the coelentrates (Zoanthid) *Palythoa caribaeorum*. *Toxicon* 21(2):285–290.
- Cha, J.K., Christ, W.J., Finan, J.M., Fujioka, H., Kishi, Y., Klein, L.L., Ko, S.S., Leder, J., McWhorter Jr., W.W., Pfaff, K.-P., Yonaga, M., Uemura, D., and Hirata, Y. 1982. Stereochemistry of palytoxin. 4. Complete structure. *Journal of the American Chemical Society* 104(25):7369–7371.
- Chang, F.H., Shimizu, Y., Hay, B., Stewart, R., Mackay, G., and Tasker, R. 2000. Three recently recorded *Ostreopsis* spp. (Dinophyceae) in New Zealand: temporal and regional distribution in the upper North Island from 1995 to 1997. *New Zealand Journal of Marine and Freshwater Research* 34:29–39.
- Faust, M.A. 1999. Three new *Ostreopsis* species (Dinophyceae): *O. marinus* sp. nov., *O. belizeanus* sp. nov., and *O. caribbeanus* sp. nov. *Phycologia* 38(2):92–99.
- Faust, M.A., Morton, S.L., and Quod, J.P. 1996. Further SEM study of marine dinoflagellates: the genus *Ostreopsis* (Dinophyceae). *Journal of Phycology* 32(6):1053–1065.
- Frolova, G.M., Kuznetsova, T.A., Michailov V.V., and Eliakov, G.B. 2000. Immunoenzyme method for detecting bacterial producers of palytoxin (in Russian). *Bioorganicheskaya Khimiya* 26(4):315–320.
- Fujioka, H., Christ, W.J., Cha, J.K., Leder, J., and Kishi, Y. 1982. Stereochemistry of palytoxin. 3. C7–C51 segment. *Journal of the American Chemical Society* 104(25):7367–7369.
- Fukui, M., Murata, M., Inoue, A., Gawel, M., and Yasumoto, T. 1987. Occurrence of palytoxin in the trigger fish *Melichthys vidua*. *Toxicon* 25(10):1121–1124.
- Fukui, M., Yasumura, D., Murata, M., Alcala, A.C., and Yasumoto, T. 1988. The occurrence of palytoxin in crabs and fish. *Toxicon* 26(1):20–21.
- Fukuyo, Y. 1981. Taxonomical study on benthic dinoflagellates collected in coral reefs. *Bulletin of Japanese Society of Science and Fisheries* 47(8):967–978.
- Gleibs, S., and Mebs, D. 1999. Distribution and sequestration of palytoxin in coral reef animals. *Toxicon* 37(11):1521–1527.
- Gleibs, S., Mebs, D., and Werding, B. 1995. Studies on the origin and distribution of palytoxin in a Caribbean coral reef. *Toxicon* 33(11):1531–1537.
- Gonzales, R.B., and Alcala, A.C. 1977. Fatalities from crab poisoning on Negros island, Philippines. *Toxicon* 15(2):169–170.
- Granéli, E., Ferreira, C.E.L., Yasumoto, T., Rodrigues, E., Maria, H., and Neves, B. 2002. Sea urchins poisoning by the benthic dinoflagellate *Ostreopsis ovata* on the Brazilian Coast. *Book of Abstracts, 10th International Conference on Harmful Algae, Florida, USA*, p. 113.
- Halstead, B.W. 2002. The microbial biogenesis of aquatic biotoxins. *Toxicology Mechanisms and Methods* 12(2):135–153.
- Hansen, G., Turquet, J., Quod, J.P., Ten-Hage, L., Lugomela, C., Kyewalyanga, M., Hurbungs, M., Wawiye, P., Ogongo, B., Tunje, S., and Rakotoarinjanahary, H. 2001. Potentially harmful Microalgae of the western Indian Ocean: a guide based on a preliminary survey. In *Intergovernmental Oceanographic Commission Manuals and Guides No. 41*. Paris: UNESCO, p. 105.

- Hashimoto, Y., Fusetani, N., and Kimura, S. 1969. Aluterin: a toxin of filefish, *Alutera scripta*, probably originating from a zoantharian *Palythoa tuberculosa*. *Bulletin of the Japanese Society of Scientific Fisheries* 35:1086–1093.
- Hewetson, J.F., Rivera, V.F., Poli, M.A., and Hines, H.B. 1990. Modification of palytoxin activity and structure by visible and ultraviolet light. *Toxicon* 28(6):612.
- Hirata, Y., Uemura, D., Ueda, K. and Takano, S. 1979. Several compounds from *Palythoa tuberculosa* (coelentrata). *Pure and Applied Chemistry* 51(9):1875–1883.
- Holmes, M.J., Gillespie, N.C., and Lewis, R.J. 1988. Toxicity and morphology of *Ostreopsis* cf. *siamensis* cultured from a ciguatera endemic region of Queensland, Australia. *Proceedings of the 6th International Coral Reef Symposium* 3:49–54.
- Kan, Y., Uemura, D., Hirata, Y., Ishiguro, M., and Iwashita, T. 2001. Complete NMR signal assignment of palytoxin and N-acetylpalytoxin. *Tetrahedron Letters* 42(18):3197–3202.
- Kimura, S., Hashimoto, Y., and Yamazato, K. 1972. Toxicity of the zoanthid *Palythoa tuberculosa*. *Toxicon* 10(6):611–617.
- Kishi, Y. 1989. Natural products synthesis: palytoxin. *Pure and Applied Chemistry* 61(3):313–324.
- Klein, L.L., McWhorter Jr., W.W., Ko, S.S., Pfaff, K.-P., and Kishi, Y. 1982. Stereochemistry of palytoxin. 2. C1–C6, C47–C74 and C77–C83 segments. *Journal of the American Chemical Society* 104(25):7364–7367.
- Ko, S.S., Finan, J.M., Yonaga, M., and Kishi, Y. 1982. Stereochemistry of palytoxin. 1. C85–C115 segment. *Journal of the American Chemical Society* 104(25):7362–7364.
- Kodama, A.M., Hokama, Y., Yasumoto, T., Fukui, M., Manea, S.J., and Sutherland, N. 1989. Clinical and laboratory findings implicating palytoxin as cause of ciguatera poisoning due to *Decapterus macروسoma* (mackerel). *Toxicon* 27(9):1051–1053.
- Lau, C.O., Tan, C.H., Khoo, H.E., Yuen, R., Lewis, R.J., Corpuz, G.P., and Bignami, G.S. 1995. *Lophozozymus pictor* toxin: a fluorescent structural isomer of palytoxin. *Toxicon* 33(10):1373–1377.
- Lenoir, S., Ten-Hage, L., Turquet, J., Quod, J.-P., Bernard, C., and Hennion, M.C. 2004. First evidence of palytoxin analogues from an *Ostreopsis marseillensis* (Dinophyceae) benthic bloom in southwestern Indian Ocean. *Journal of Phycology* 40(6):1042–1051.
- Li, C.J. 2005. Challenges and opportunities of Green Chemistry. Green Chemistry round table, Chemistry Division Conference, Special Libraries Association, Toronto, Canada. <http://www.sla.org/division/dche/2005/li.pdf>.
- Macfarlane, R.D., Uemura, D., Ueda, K., and Hirata, Y. 1980. <sup>252</sup>Cf plasma desorption mass spectrometry of palytoxin. *Journal of the American Chemical Society* 102(2):875–876.
- Maeda, M., Kodama, T., Tanaka, T., Yoshizumi, H., Nomoto, K., and Takemoto, K. 1985. Structure of an insecticidal substance from a red alga, *Chondria armata*. *Tennen Yuki Kagobutsu Toronkai Koen Yoshishu* 27:616–623.
- Mahnir, V.M., Kozlovskaya, E.P., and Kalinovsky, A.I. 1992. Sea anemone *Radianthus macrodactylus*—a new source of palytoxin. *Toxicon* 30(11):1449–1456.
- Mercado, J.A., Viera, M., Escalona de Motta, G., Tosteson, T.R., González, I., and Silva, W. 1994. An extraction procedure modification changes the toxicity, chromatographic profile and pharmacologic action of *Ostreopsis lenticularis* extracts. *Toxicon* 32(3):256.
- Meunier, F.A., Mercado, J.A., Molgó, J., Tosteson, T.R., and Escalona de Motta, G. 1997. Selective depolarization of the muscle membrane in frog nerve-muscle preparations by a chromatographically purified extract of the dinoflagellate *Ostreopsis lenticularis*. *British Journal of Pharmacology* 121(6):1224–1230.
- Moore, R.E., and Bartolini, G. 1981. Structure of palytoxin. *Journal of the American Chemical Society* 103(9):2491–2494.
- Moore, R.E., Bartolini, G., and Barchi, J. 1982a. Absolute stereochemistry of palytoxin. *Journal of the American Chemical Society* 104(13):3776–3779.
- Moore, R.E., Dietrich, R.F., Hatton, B., Higa, T., and Scheuer, P.J. 1975. The nature of the  $\lambda$  263 chromophore in the palytoxins. *Journal of Organic Chemistry* 40(4):540–542.
- Moore, R.E., Helfrich, P., and Patterson, G.M.L. 1982b. The deadly seaweed of Hana. *Oceanus* 25:54–63.
- Moore, R.E., and Scheuer, P.J. 1971. Palytoxin: a new marine toxin from a coelenterate. *Science* 172(3982):495–498.
- Moore, R.E., Woolard, F.X., and Bartolini, G. 1980. Periodate oxidation of N-(p-Bromobenzoyl)palytoxin. *Journal of the American Chemical Society* 102(24):7370–7372.
- Moore, R.E., Woolard, F.X., Sheikh, M.Y., and Scheuer, P.J. 1978. Ultraviolet chromophores of palytoxins. *Journal of the American Chemical Society* 100(24):7758–7759.
- Nakajima, L., Oshima, Y., and Yasumoto, T. 1981. Toxicity of benthic dinoflagellates found in coral-reef. 2. Toxicity of the benthic dinoflagellates in Okinawa. *Bulletin of the Japanese Society of Scientific Fisheries* 47(8):1029–1033.
- Nakamura, K., Asari, T., Ohizumi, Y., Kobayashi, J., Yamasu, T., and Murai, A. 1993. Isolation of zooxanthellatoxins, novel vasoconstrictive substances from zooxanthella *Symbiodinium* sp. *Toxicon* 31(4):371–376.
- Noguchi, T., Hwang, D.F., Arakawa, G., Daigo, K., Sato, S., Ozaki, H., Kawai, N., Ito, M., and Hashimoto, K. 1988. Palytoxin as the causative agent in parrotfish poisoning. *Toxicon* 26(1):34.



- Norris, D.R., Bomber, J.W., and Balech, E. 1985. Benthic dinoflagellates associated with ciguatera from the Florida Keys. I. *Ostreopsis heptagona* sp. nov. In *Toxic Dinoflagellates*, ed. Anderson, D.M., White, A.W., and Baden, D.G. New York: Elsevier Scientific, 39–44.
- Onuma, Y., Satake, M., Ukena, T., Roux, J., Chanteau, S., Rasolofonirina, N., Ratsimaloto, M., Naoki, H., and Yasumoto, T. 1999. Identification of putative palytoxin as the cause of clupeotoxism. *Toxicon* 37(1):55–65.
- Paddle, B.M. 2003. Therapy and prophylaxis of inhaled biological toxins. *Journal of Applied Toxicology* 23(3):139–170.
- Patockaa, J., and Stredab, L. 2002. Brief overview of natural non-protein neurotoxins. *The ASA Newsletter* 89:16–23.
- Pearce, I., Marshall, J., and Hallegraef, G.M. 2001. Toxic epiphytic dinoflagellates from East Coast Tasmania, Australia. In *Harmful Algal Blooms 2000*, ed. Hallegraef, G., Blackburn, S.I., Bolch, C.J., and Lewis, R.J. Hobart: Intergovernmental Oceanographic Commission of UNESCO, 54–57.
- Penna, A., Vila, M., Fraga, S., Giacobbe, M.G., Andreoni, F., Riobó, P., and Vernesi, C. 2005. Characterization of *Ostreopsis* and *Coolia* (Dinophyceae) isolates in the western Mediterranean sea based on morphology, toxicity and internal transcribed spacer 5.8S rDNA sequences. *Journal of Phycology* 41(1):212–225.
- Quod, J.P. 1994. *Ostreopsis mascarenensis* sp. nov. (Dinophyceae), dinoflagelle toxique associé à la ciguatera dans l’Ocean Indien. *Cryptogamie Algologie* 15(4):243–251.
- Rhodes, L., Adamson, J., Suzuki, T., Briggs, L., and Garthwaite, I. 2000. Toxic marine epiphytic dinoflagellates, *Ostreopsis siamensis* and *Coolia monotis* (Dinophyceae), in New Zealand. *New Zealand Journal of Marine and Freshwater Research* 34:371–383.
- Rhodes, L., Towers, N., Briggs, L., Munday, R., and Adamson, J. 2002. Uptake of palytoxin-like compounds by shellfish fed *Ostreopsis siamensis* (Dinophyceae). *New Zealand Journal of Marine and Freshwater Research* 36(3):631–636.
- Riobó, P., Paz, B., Fernandez, M.L., Fraga, S., and Franco, J.M. 2004. Lipophilic toxins of different strains of *Ostrepsidaceae* and *Gonyaulaceae*. In *Harmful Algae 2002*, ed. Steidinger, K.A., Landsberg, J.H., Thomas, C.R., and Vargo, G.A. Proceedings of the Xth International Conference on Harmful Algae, Florida Fish and Wildlife Conservation Commission, Florida Institute of Oceanography, and Intergovernmental Oceanographic Commission of UNESCO, Florida, USA, pp. 119–121.
- Sansoni, G., Borghini, B., Camici, G., Casotti, M., Righini, P., and Rustighi, C. 2003. Fioriture algali di *Ostreopsis ovata* (Gonyaulacales: Dinophyceae): un problema emergente. *Biologia Ambientale* 17(1):17–23.
- Schmidt, J. 1901. Peridiniales. *Botanisk Tidsskrift* 24:212–221.
- Simoni, F., Gaddi, A., Di Paolo, C., and Lepri, L. 2003. Harmful epiphytic dinoflagellate on Tyrrhenian Sea reefs. *Harmful Algae News* 24:13–14.
- Simoni, F., Gaddi, A., Di Paolo, C., Lepri, L., Mancino, A., and Falaschi, A. 2004. Further investigation on blooms of *Ostreopsis ovata*, *Coolia monotis*, *Prorocentrum lima* on the macroalgae of artificial and natural reefs in the Northern Tyrrhenian Sea. *Harmful Algae News* 26:5–7.
- Suh, E.M., and Kishi, Y. 1994. Synthesis of palytoxin from palytoxin carboxylic acid. *Journal of the American Chemical Society* 116(24):11205–11206.
- Tan, C.H., and Lau, C.O. 2000. Palytoxin: Chemistry and Detection. In *Seafood and Freshwater Toxins: Pharmacology, Physiology and Detection*, ed. Botana, L.M. New York: Marcel Dekker Inc., 533–548.
- Taniyama, S., Arakawa, O., Terada, M., Nishio, S., Takatani, T., Mahmud, Y., and Noguchi, T. 2003. *Ostreopsis* sp., a possible origin of palytoxin in parrotfish *Scarus oivifrons*. *Toxicon* 42(1):29–33.
- Taniyama, S., Mahmud, Y., Terada, M., Takatani, T., Arakawa, O., and Noguchi, T. 2002. Occurrence of a food poisoning incident by palytoxin from a serranid *Epinephelus* sp. in Japan. *Journal of Natural Toxins* 11(4):277–282.
- Tindall, D.R., Miller, D.M., and Tindall, P.M. 1990. Toxicity of *Ostreopsis lenticularis* from the British and United States Virgin Islands. In *Toxic Marine Phytoplankton*, ed. Granéli, E., Sundström, B., Edler, L., and Anderson, D.M. New York: Elsevier, pp. 424 – 429.
- Tognetto, L., Bellato, S., Moro, I., and Andreoli, C. 1995. Occurrence of *Ostreopsis ovata* (Dinophyceae) in the Tyrrhenian Sea during summer 1994. *Botanica Marina* 38(4):291–295.
- Turki, S. 2005. Distribution of toxic dinoflagellates along the leaves of seagrass *Posidonia oceanica* and *Cymodocea nodosa* from the Gulf of Tunis. *Cahiers de Biologie Marine* 46(1):29–34.
- Turquet, J., Lenoir, S., Quod, J.P., Ten-Hage, L., and Hennion, M.C. 2002. Toxicity and toxin profiles of a bloom of *Ostreopsis mascarenensis*, Dinophyceae, from the SW Indian Ocean. *Book of Abstracts, 10th International Conference on Harmful Algae, Florida, USA*, 286.
- Turquet, J., Quod, J.P., Couté, A., and Faust, M. 1998. Assemblage of benthic dinoflagellates and monitoring of harmful species in Réunion island (SW Indian Ocean) during the 1993–1996 period. In *Harmful Algae*, ed. Reguera, B., Blanco, J., Fernandez, M.L., and Wyatt, T. Vigo: Xunta de Galicia and Intergovernmental Oceanographic Commission of UNESCO, 44 – 47.



- Uemura, D., Ueda, K., Hirata, Y., Katayama, C., and Tanaka, J. 1980a. Structural studies on palytoxin, a potent coelenterate toxin. *Tetrahedron Letters* 21(50):4857–4860.
- . 1980b. Structures of two oxidation products obtained from palytoxin. *Tetrahedron Letters* 21(50):4861–4864.
- Uemura, D., Ueda, K., Hirata, Y., Naoki, H., and Iwashita, T. 1981a. Further studies on palytoxin. I. *Tetrahedron Letters* 22(20):1909–1912.
- . 1981b. Further studies on palytoxin. II. Structure of palytoxin. *Tetrahedron Letters* 22(29):2781–2784.
- Uemura, D., Hirata, Y., Iwashita, T., and Naoki, H. 1985. Studies on palytoxins. *Tetrahedron* 41(6):1007–1017.
- Ukena, T., Satake, M., Usami, M., Oshima, Y., Fujita, T., Kan, Y., and Yasumoto, T. 2001. Structure elucidation of ostreocin-D, a palytoxin analog isolated from the dinoflagellate *Ostreopsis siamensis*. *Bioscience, Biotechnology and Biochemistry* 65(11):2585–2588.
- Ukena, T., Satake, M., Usami, M., Oshima, Y., Fujita, T., Naoki, H., and Yasumoto, T. 2002. Structural confirmation of ostreocin-D by application of negative-ion fast-atom bombardment collision-induced dissociation tandem mass spectrometric methods. *Rapid Communications in Mass Spectrometry* 16(24):2387–2393.
- Usami, M., Satake, M., Ishida, S., Inoue, A., Kan, Y., and Yasumoto, T. 1995. Palytoxin analogues from the dinoflagellate *Ostreopsis siamensis*. *Journal of the American Chemical Society* 117(19):5389–5390.
- Vila, M., Garcés, E., and Masó, M. 2001. Potentially toxic epiphytic dinoflagellate assemblages on macroalgae in the NW Mediterranean. *Aquatic Microbial Ecology* 26:51–60.
- Wiles, J.S., Vick, J.A., and Christensen, M.K. 1974. Toxicological evaluation of palytoxin in several animal species. *Toxicon* 12(4):427–433.
- Yasumoto, T. 1998. Fish poisoning due to toxins of microalgal origins in the Pacific. *Toxicon* 36:1515–1518.
- Yasumoto, T., Seino, N., Murakami, Y., and Murata, M. 1987. Toxins produced by benthic dinoflagellates. *Biological Bulletin* 172(1):128–131.
- Yasumoto, T., Yasumura, D., Ohizumi, Y., Takahashi, M., Alcalá, A.C., and Alcalá, L.C. 1986. Palytoxin in two species of xanthid crab from the Philippines. *Agricultural and Biological Chemistry* 50(1):163–167.

## 6 Biochemistry of Palytoxins and Ostreocins

Carmen Vale and Isabel R. Ares

### Palytoxin Origin

According to an ancient Hawaiian legend, in the Hana district on Maui lived a man who always seemed to be busy planting and harvesting. Whenever the people in the neighborhood went fishing, one of the group was missing upon their return. This went on for some time without the people having any explanation about the disappearances. At last, the fishermen became suspicious of the man who tended his humble patch. They grabbed him, tore off his clothes and discovered on his back the mouth of a shark. They killed and burned him and threw the ashes into the sea. At the spot where this happened, the limu (seaweed) became toxic. The tide pool containing the poisonous limu subsequently became kapu (sacred) to the Hawaiians. They would cover the limu with stones and were very secretive about its location, believing that disaster would occur if anyone attempted to gather the toxic limu (later identified as a soft coral, *Palythoa toxica*). This toxic moss was known as “limu make o Hana” (deadly seaweed of Hana) and from this material, Professors Moore and Scheuer, at the University of Hawaii, extracted by ethanol a new substance they named palytoxin (Patockaa and Stredab 2002).

Moore and colleagues identified the organism producer of palytoxin as an animal of the *Zoanthidae* family and assigned to the genus *Palythoa* (Moore and Scheuer 1971). In coral reefs of the Caribbean Sea (Colombia), palytoxin has also been detected in *zoanthid* species of the genus *Zoanthus*, space competitors of *Palythoa* in the coral reefs (Gleibs et al. 1995). However, the origin of palytoxin is still a matter of controversy. First, a bacterial origin was suggested by Moore et al. (1982), however this has not yet been corroborated experimentally. Other suggested potential producers were symbiotic algae (Nakamura et al. 1993). Recently, the dinoflagellate *Ostreopsis* sp has been proposed as one of the biogenetic origins of palytoxin (Usami et al. 1995; Taniyama et al. 2003). Sequestration of palytoxin has been observed in crustaceans (*Platypodiella* sp.) living in close association with *Palythoa* colonies and in polychaete worms (*Hermodice carunculata*) feeding on the zoanthids. Resistance of marine animals to the toxin may enable it to enter food chains.

### Pharmacological Targets of Palytoxin

The postulated mechanism of action of palytoxin is to bind to the mammalian Na-K-ATPase (or sodium pump) and convert this enzyme into an open channel. However, the ubiquity of pumps and channels in the living tissues and the high diversity of preparations used to study the mechanism of action of palytoxin make it difficult to rule out the possibility that another site may be involved. In this sense, recent evidences indicate that the Na-K-ATPase may not be the only target of the toxin. It must be pointed out that the vast majority of work performed to test the mechanism of action of palytoxin had relied on the initial experiments indicating palytoxin binding to Na-K-ATPase (Bottinger and Habermann 1984; Bottinger et al. 1986).

This section will start with a short review of the functioning of the sodium pump and then examine the main evidence supporting an action of the toxin in the sodium pump or in other cellular targets.

### *Mammalian Sodium Pump*

The Na-K-ATPase or sodium pump is a transmembrane protein that transports three Na<sup>+</sup> out of the cell and two K<sup>+</sup> in, using ATP hydrolysis as the driving force. The electrochemical gradient, established by the Na-K-ATPase, is essential for the maintenance of cell homeostasis. This gradient also drives many plasma membrane transport processes. The Na-K-ATPase is composed of two subunits: the catalytic  $\alpha$  subunit, which binds translocating cations and ATP; and the  $\beta$  subunit, which modulates cation affinity and is necessary for the proper folding and translocation of the sodium pump to the plasma membrane (Lingrel and Kuntzweiler 1994). To date, four  $\alpha$  and three  $\beta$  isoforms have been identified that exhibit 85% and 45% of sequence identity, respectively, and that show a tissue-specific distribution and a developmentally regulated pattern of expression.

Biochemical evidence and transfection studies suggest that  $\alpha$  and  $\beta$  isoforms can assemble in different combinations and potentially form functional pumps. The sodium pump is specifically inhibited by a series of naturally occurring steroids, such as ouabain (Hansen 1984). Based on their clinical use, these substances are also referred to as cardiac glycosides or cardioactive steroids. Cardiac glycoside sensitivity is conferred by the  $\alpha$  subunit of the Na-K-ATPase, and this class of drugs is used to treat congestive heart failure (Scheiner-Bobis and Schneider 1997).

Inhibition of the Na-K-ATPase activity alters the cation homeostasis of the cell. Failure of the Na-K-ATPase raises intracellular Na<sup>+</sup>, which in turn increases the intracellular Ca<sup>2+</sup> concentration. Recent advances in the understanding of the functioning of the Na-K-ATPase demonstrated that, in this type of pump, transported ions approach their binding sites from one membrane surface, become occluded within conformations in which the sites are inaccessible from either side of the membrane, and are then deoccluded and released to the opposite membrane surface. This describes an alternating-gate transport mechanism, in which the pump acts like an ion channel with two gates that open and close alternately. The occluded states ensure that one gate closes before the other can open, thus preventing ion fluxes that would undo the pump's electrochemical work (Artigas and Gadsby 2003).

The ion transport processes by the sodium pump comprise the following steps: In the presence of ATP and Na<sup>+</sup>, the enzyme occludes Na<sup>+</sup> ions. When Na<sup>+</sup> is released to the extracellular space, K<sup>+</sup> binds to extracellular sites. After this step, the enzyme becomes dephosphorylated and K<sup>+</sup> occluded within the protein. Finally, high concentrations of ATP lead to deocclusion and release of K<sup>+</sup> into the cytosol.

### *Palytoxin and the Mammalian Sodium Pump*

In 1977, Weidmann exposed rabbit and dog muscles to an extract of partially purified palytoxin. He found a decrease of the membrane potential and an increase of the rise time of the action potential, while repolarization was shortened. These effects were reversible in a concentration-dependent manner (Weidmann 1977). In 1982, Habermann and Chhatwall described that very low concentrations of palytoxin (1 pM) raised the potassium permeability of rat, human, and sheep erythrocytes and the sodium permeability of human erythrocytes. These effects of palytoxin in red blood cells were antagonized in a specific manner by the Na-K-ATPase inhibitor ouabain (Habermann and Chhatwall 1982). That the Na-K-ATPase is the target for palytoxin action was initially suggested from antagonism of

palytoxin action by cardiotoxic steroids such as ouabain and by  $K^+$  ions (Habermann 1989). Several experimental approaches have since confirmed that proposal. The first direct evidence indicating that the Na-K-ATPase could be necessary for palytoxin action came from the work of Anner and Moosmayer (1994), who showed that when the enzyme is incorporated into liposomes, ouabain prevented the palytoxin induced  $K^+$  efflux when the enzyme was ouabain sensitive (rabbit kidney) but not when the enzyme was ouabain resistant (rat kidney).

The second approach exploited the fact that yeast cells do not express endogenous Na-K-ATPases and by expressing both  $\alpha$  and  $\beta$  subunits of the mammalian Na-K-ATPase in yeast palytoxin could elicit ouabain-sensitive cation fluxes; however, palytoxin did not have this effect if the yeast expressed either subunit alone (Scheiner-Bobis et al. 1994) nor if the 44 aminoacid residues of the carboxy-terminal of the alpha subunit were deleted (Redondo et al. 1996). Moreover, because binding of  $^3H$ -ouabain to intact yeast cells was inhibited by palytoxin, it was postulated that the truncated Na-K-ATPase was expressed at the cell surface and could interact with either ligand, and it seemed that palytoxin opened a cation pathway within or in the vicinity of the Na-K-ATPase. But the catalytical activity of the sodium pump was not essential since palytoxin still elicited ouabain-sensitive cation fluxes in yeast expressing mutant sodium pumps in which the phosphate accepting residue Asp369 of the  $\alpha$  subunit was replaced by Ala (Scheiner-Bobis and Schneider 1997) and palytoxin also caused  $K^+$  efflux in yeast cells expressing a chimera in which the catalytic subunit of the sodium-pump was replaced by that of the endoplasmic reticulum  $Ca^{2+}$ -ATPase (Artigas and Gadsby 2003).

The third approach used mammalian sodium pumps expressing the  $\alpha 3$  and  $\beta 1$  subunits synthesized by *in vitro* translation in a cell-free expression system and then incorporated into a planar phospholipid bilayer, where exposure to palytoxin elicited single-channel currents that had a conductance of about 10 pS (Hirsh and Wu 1997).

In spite of the experimental evidence, the role of the Na-K-ATPase in the formation of the palytoxin channel has not been clarified in detail. The recent advances in the understanding of the Na-K-ATPase function have recently allowed Artigas and Gadsby (2003) to postulate that palytoxin could disrupt the strict coupling between the pump's inner and outer gates, allowing them to both be open. Thus, it is not clear whether the palytoxin-sensitive channel is located within the enzyme and the step(s) in the normal functioning of the pump(s) that are affected by palytoxin remain to be elucidated.

### *Possible Interaction of Palytoxin with Other Molecular Targets*

Very few molecular targets other than the sodium pump have been evaluated to test palytoxin action, although different studies indicate that the sodium pump may not be the only target of palytoxin. A series of alternative sites of action for the toxin were also proposed. At least in excitable cells, palytoxin induces the activity of a small conductance (9–25 pS), nonselective cationic channel that then triggers secondary activations of voltage dependent  $Ca^{2+}$  channels and of  $Na^+/Ca^{2+}$  exchange. This results in neurotransmitter release by nerve terminals and contractions of striated and smooth muscle cells. Palytoxin-induced channels are blocked by amiloride derivatives such as 3,4 dichlorobenzamil. They are also blocked by ouabain but at concentrations higher than those required to inhibit the Na-K-ATPase. A second and independent action of palytoxin is to open a membrane conductive pathway for  $H^+$  that causes  $H^+$  influx inside the cells and secondarily activates  $Na^+/H^+$  exchange activity. A third action of palytoxin in chick cardiomyocytes is to raise  $[Ca^{2+}]_i$  in a manner independent of its depolarizing action or of its action on intracellular pH.

All these observations led Frelin and Van Renterghem to suggest that palytoxin probably has more than one site of action in excitable cells and that it may act as an agonist for a family of

low-conductance channels that conduct  $\text{Na}^+/\text{K}^+$ ,  $\text{H}^+$  and  $\text{Ca}^{2+}$  ions (Frelin and Van Renterghem 1995). The possibility of palytoxin acting as a channel forming cytotoxin in mouse neuroblastoma cells was also taken into consideration. In this preparation, palytoxin-induced channels were permeable to sodium and potassium and slightly permeable to calcium, choline, and tetramethylammonium. They did not seem to be highly permeable to chloride or protons. The effect of palytoxin was decreased when either external sodium was replaced by potassium or in the absence of calcium in external and/or internal media. These observations led the authors to suggest that palytoxin appeared to bind to a receptor molecule in the cell surface and the complexes between palytoxin and its receptor could be internalized (Rouzaire-Dubois and Dubois 1990).

Among the other mechanism of action tested it was recently found that palytoxin caused  $\text{K}^+$  efflux in an hybrid between the Na-K-ATPase and the H-K-ATPase, converting this enzyme into an open channel (Farley et al. 2001). Furthermore, palytoxin stimulated a cation-dependent current in rat distal and proximal colon in a concentration-dependent manner when applied to the mucosal surface of the tissue whose apical membrane does not express Na-K-ATPase. The observation that the palytoxin-induced current was blocked by vanadate but was resistant to ouabain supported the suggestion that the toxin was able to convert a vanadate-sensitive H-K-ATPase into an electrogenic cation transporter and, consequently, that the pore-forming action of palytoxin was not restricted to Na-K-ATPase since it was also observed with the colonic H-K-ATPase (Scheiner-Bobis et al. 2002). The toxin was also found to interfere with the sarcolemmal  $\text{Ca}^{2+}$  pump in cardiac myocytes (Kockskamper et al. 2004).

Recent studies also found differences between the action of palytoxin and ouabain. Thus, the toxin was able to produce  $\text{K}^+$  loss in ouabain resistant cells, whereas ouabain inhibited the effect of palytoxin in ouabain-sensitive cells but not in ouabain resistant cells (Artigas and Gadsby 2003). In a very recent report, Artigas and Gadsby have described that palytoxin and ouabain can simultaneously occupy the same sodium pump, each destabilizing the binding of the other (Artigas and Gadsby 2004), indicating that palytoxin and ouabain binding sites cannot be identical, but probably these sites share some structural determinants for binding. Supporting this view and using a resonant mirror optical biosensor, we have recently found a concentration-dependent binding of ouabain but not binding of palytoxin to immobilized Na-K-ATPase isolated from porcine cerebral cortex and dog kidney (Vale et al. 2006).

In conclusion, what seems clear to the moment is that normally low concentrations of palytoxin are sufficient to produce a massive increase in the permeability of cells to cations. On the basis of experimental evidence, palytoxin appears to bind to the Na-K-ATPase at the cell membrane, open up a yet unidentified pathway for cations, and inhibit the sodium pump. Experiments with a truncated  $\alpha$  subunit of the sodium pump that can still bind palytoxin without allowing the formation of a channel, indicating that the palytoxin-induced channel is not formed between the palytoxin molecule and the enzyme but rather within the protein of the sodium pump (Redondo et al. 1996). Whether the high cytotoxicity of palytoxin is merely a consequence of its disruption of the ionic environment of the cell remains to be elucidated.

### *Effects of Palytoxin in Primary Neuronal Cultures*

The vast majority of work to study the action of palytoxin and its interaction with ouabain and other inhibitors and agonists comes from work on red cells from diverse species. Red cells have been used to study the action of palytoxin on cationic permeability since they have a lower number of  $\text{Na}^+/\text{H}^+$  and  $\text{Na}^+/\text{Ca}^{2+}$  exchangers and of  $\text{Ca}^{2+}$  activated  $\text{K}^+$  channels. We have recently started to investigate

the effects of palytoxin on primary cultures of cerebellar granule cells (CGCs). Primary cultures of CGCs contain mainly glutamatergic neurons and a small proportion of GABAergic neurons that express functional ionotropic glutamate receptors and constitute one of the most reliable neuronal models for the study of neural function and pathology (Schousboe et al. 1985; Sonnewald et al. 2004). Cell calcium is thought to play a key role in mediating neuronal damage. Cytosolic  $\text{Ca}^{2+}$  is elevated during brain insults such as ischemia and exposure to neurotoxins (Nakamura et al. 1999; Berman et al. 2002). In glutamatergic neurons, the  $[\text{Ca}^{2+}]_c$  is controlled by various transport mechanisms, which include voltage-dependent calcium channels,  $\text{Ca}^{2+}$  pumps, and  $\text{Na}^+$ - $\text{Ca}^{2+}$  exchanger and calcium influx through glutamate receptors. Although much is known about the cellular mechanisms of action of palytoxin in several cell types, relatively little is known about how palytoxin affects the central nervous system. The results presented in this section, using cultured cerebellar granule cells, were designated to understand more fully the mechanisms by which palytoxin can alter cultured neurons.

In primary cultures of cerebellar granule cells palytoxin produced a concentration-dependent depolarization of the cell membrane, as assessed with the membrane potential sensitive probe bis-oxonol (Fig. 6.1). Significant differences between control and palytoxin-treated cells were found at palytoxin concentrations equal or higher than 5 nM.

A primary action of palytoxin in excitable cells is to induce the activity of a small conductance, nonselective cationic channel, which then triggers secondary activations of voltage dependent  $\text{Ca}^{2+}$  channels and of  $\text{Na}^+$ / $\text{Ca}^{2+}$  exchange (Frelin and Van Renterghem 1995). In primary cultures of CGC, palytoxin induced a dose-dependent increase on  $[\text{Ca}^{2+}]_c$ . Fig. 6.2 shows the effect of 0.1, 1, 10, 25, and 50 nM palytoxin on cytosolic calcium concentration in primary cultures of CGC. At 0.1 nM,

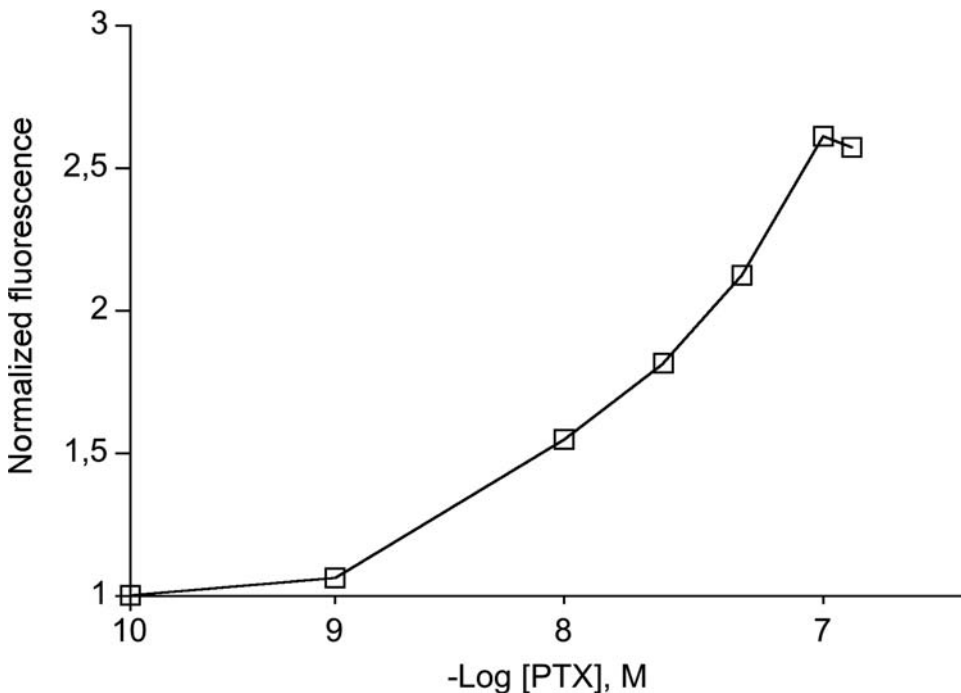


**Figure 6.1.** Palytoxin-depolarized cerebellar granule neurons as assessed with the membrane potential probe bis-oxonol.

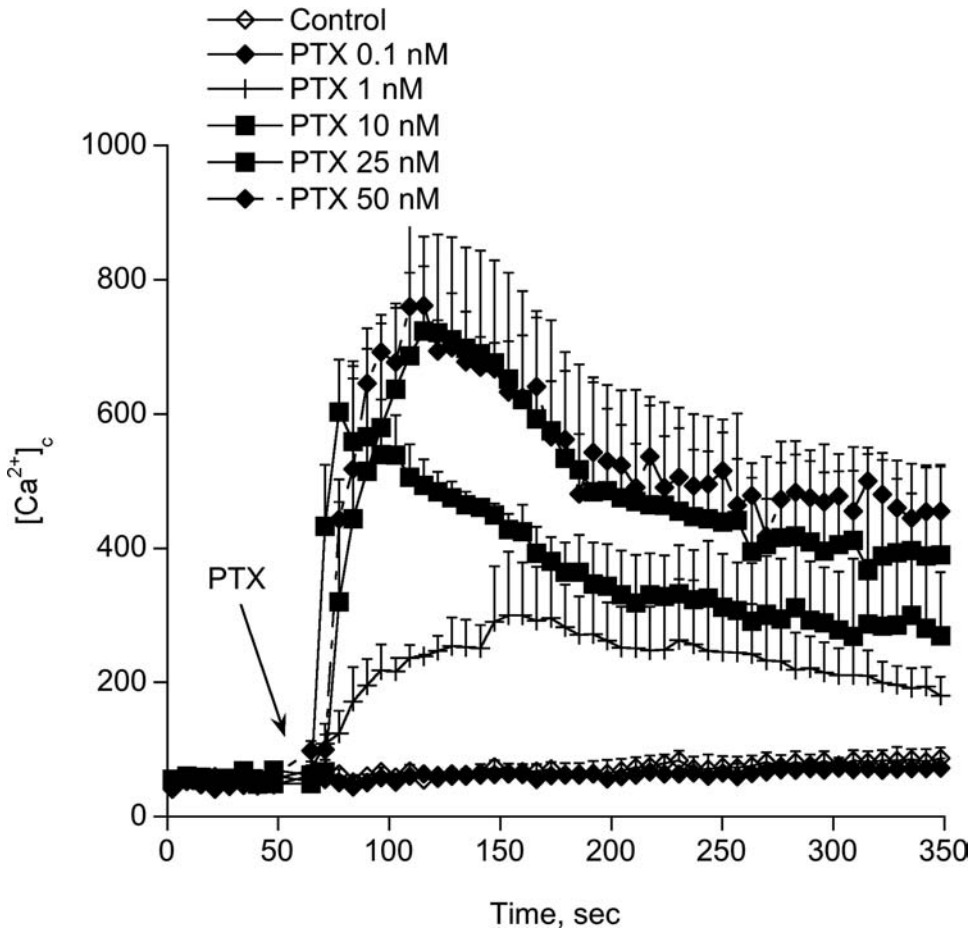


**Figure 6.2.** Effect of palytoxin on the cytosolic calcium concentration in cultured cerebellar neurons loaded with the fluorescent calcium dye Fura 2-AM.

palytoxin did not modify  $[Ca^{2+}]_c$ ; however, a significant increase on  $[Ca^{2+}]_c$  was observed at palytoxin concentrations of 1 nM ( $p < 0.01$  versus control), and this effect was maximal for palytoxin concentrations of 10, 25, and 50 nM ( $p < 0.001$  versus control). The effect of palytoxin on  $[Ca^{2+}]_c$  was immediate after addition of the toxin; palytoxin-induced calcium increase showed a typical pattern characterized by an initial and fast calcium rise followed by a plateau phase. In the initial calcium rise, palytoxin increased  $[Ca^{2+}]_c$  from 50 to 700 nM, reaching a value of about 400 nM  $[Ca^{2+}]_c$  in the plateau phase.

Under depolarization, cerebellar neurons release glutamate that can activate calcium-permeable glutamate receptor. The palytoxin-induced exocytotic synaptic vesicle release was measured in cultured cerebellar granule cells by loading the cells with the fluorescent dye FM1-43 and monitoring the fluorescence with total internal reflection fluorescence microscopy (TIRFM) imaging. This dye stains membranes of recycled synaptic vesicles, and it is released during exocytosis increasing the



fluorescence when synaptic vesicles fuse to the plasma membrane. Figs. 6.3A and 6.3B show TIRFM images of FM1-43 fluorescence in control cells and in CGC exposed to 10 nM palytoxin. Each neuronal cell body and neurite had several FM1-43 positive bouton-like spots near the plasma membrane, which correspond to synaptic vesicles. While in control cells (Fig. 6.3A) the number of the near-membrane fluorescent spots was constant during the recording, palytoxin increased the number and fluorescence intensity of the spots near the plasma membrane immediately after its addition to the cell culture (Fig. 6.3B). The bar graph in Fig. 6.3 shows the mean average fluorescence intensities of FM1-43 loaded cells in control and palytoxin-treated CGC. At 10 nM, palytoxin significantly ( $p < 0.05$ ) increased the membrane fluorescence intensities of FM1-43 loaded spots very rapidly after its addition, indicating a strong effect of the toxin on the exocytotic release of neurotransmitter. Released glutamate can exacerbate the cytotoxic effects of the toxin in cultured glutamatergic neurons.

In our experimental system, the calcium increase caused by palytoxin involved at least three pathways:  $\text{Na}^+$ -dependent activation of voltage-dependent sodium channels and voltage-dependent calcium channels, reverse operation of the  $\text{Na}^+/\text{Ca}^{2+}$  exchanger and indirect activation of excitatory amino acid receptors through glutamate release. The neuronal injury produced by the toxin could be partly mediated by the palytoxin-induced overactivation of glutamate receptors, voltage-dependent sodium and calcium channels, and the glutamate efflux into the extracellular space (Vale-González et al. 2006).

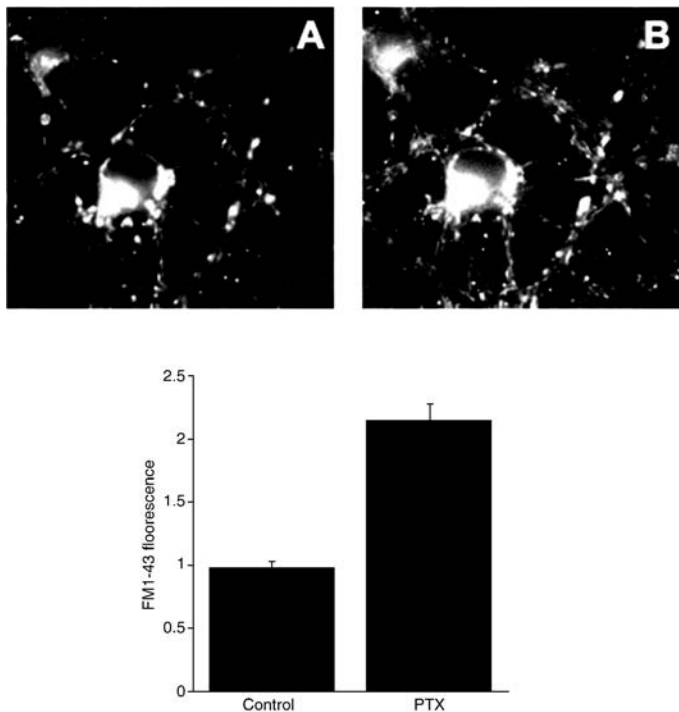


**Figure 6.3.** Palytoxin increases glutamate release in cultured cerebellar neurons loaded with FM1-43. Fluorescence was monitored with TIRFM imaging.

During the investigation of the calcium entry pathways activated by palytoxin in cultured neurons, we observed that the toxin caused a rapid intracellular acidification. Since pH plays a pivotal role in signal transduction in several cell models, we have examined the effect of palytoxin on intracellular pH. Previous studies have shown that palytoxin induces cell acidification in embryonic chick ventricular cells (Frelin et al. 1990) and osteoblasts (Monroe and Tashjian 1995). In primary cultures of CGC, palytoxin from 0.1 to 50 nM induced a dose-dependent intracellular acidification (Fig. 6.4). As in the case of calcium increase induced by palytoxin, the  $\text{pH}_i$  decrease was significant at palytoxin concentrations as low as 1 nM ( $p < 0.01$ ). Maximum intracellular acidification was observed for palytoxin concentrations of 10, 25, and 50 nM ( $p < 0.001$ ). At these concentrations, palytoxin decreased  $\text{pH}_i$  by 0.6 units. The effect of palytoxin on  $\text{pH}_i$  was immediate after addition of the toxin.

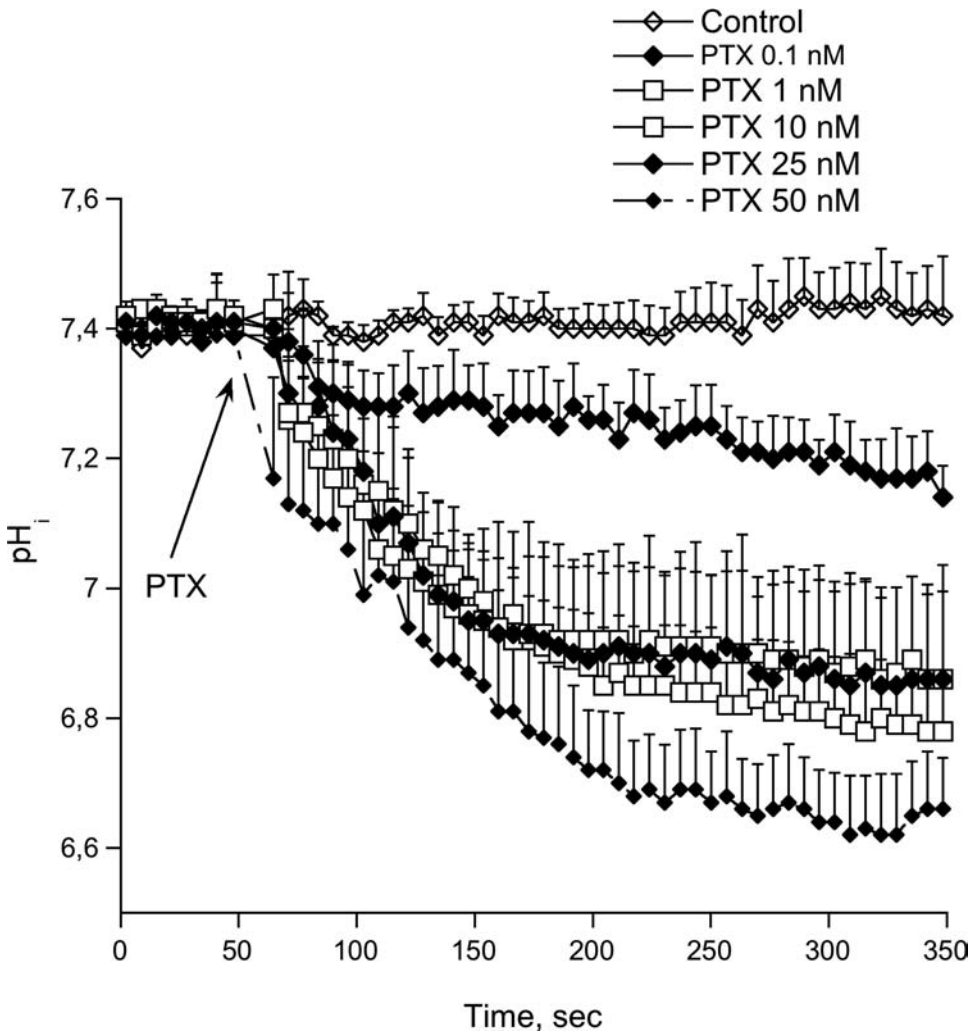


**Figure 6.4.** Intracellular acidification produced by palytoxin in cultured cerebellar neurons.

In our experimental model, the palytoxin-induced cellular acidification was completely prevented by inhibitors of the plasma-membrane calcium ATPase, including orthovanadate, lanthanum and an extracellular pH of 8.5. Our results therefore indicate that the plasma-membrane calcium ATPase is involved in the palytoxin-induced intracellular acidification in primary cultures of cerebellar granule cells. We suggest that the increase in intracellular calcium evoked by palytoxin will activate the calcium extrusion mechanisms through the calcium pump, which, in turn, will decrease intracellular pH through countertransport of H<sup>+</sup> ions (Vale-González et al. 2007).

## Mitogenic Action of Palytoxin

Palytoxin is a potent tumor promoter in the mouse skin carcinogenesis model (Wattenberg et al. 1989). The biochemical mechanism of action of palytoxin as a tumor promoter differs significantly from that of the prototypical phorbol esters tumor promoters. In contrast to the skin tumor promoter 12-O-tetradecanoylphorbol-13-acetate (TPA), palytoxin does not activate protein kinase C or increase ornithine decarboxylase activity in mouse skin (Fujiki et al. 1986). The biochemical mechanisms by which palytoxin-stimulated signaling contributes to tumor promotion have not been established in detail and it seems that they could depend on the experimental cellular model. The activation of signal transduction pathways by palytoxin, at doses as low as 5–80 ng/kg in mice, may be a consequence of the primary action of palytoxin altering the cation composition of the cells.

Mitogen-activated protein kinases (MAPKs) could play an important role in mediating the distinct signal transduction pathways stimulated by palytoxin (Kuroki et al. 1996; Li and Wattenberg 1998). MAPKs are a family of serine/threonine kinases that coordinate the transmission of various types of signals to the nucleus (Schaeffer and Weber 1999). Once activated, MAPKs translocate from the cytoplasm to the nucleus, phosphorylate specific transcription factors, and thereby modulate gene expression (Karin et al. 1997). Extracellular signal-regulated kinase (ERK), c-Jun N-terminal kinase (JNK), and p38 represent three major members of the MAPK family. Palytoxin predominantly stimulates the activation of the stress-activated MAPKs, JNK and p38, in cell types commonly used to study signal transduction, including Swiss 3T3, COS7 and HeLa (Kuroki et al. 1996; Li and Wattenberg 1998). Treatment of Swiss 3T3 fibroblasts with palytoxin at doses as low as 0.1 nM results in significant activation of JNK; this effect was dependent on extracellular sodium and mimicked by the sodium ionophore gramicidin, suggesting that the sodium influx may play a key role in the activation of JNK by palytoxin (Kuroki et al. 1996). Palytoxin potently inhibits protein synthesis in the concentration range (0.1–0.3 nM) that leads to activation of the MAPKs. This fact places palytoxin among the most potent translational inhibitors and may account for its potent toxicity. The inhibition of translation by palytoxin does not result from its direct binding to the translational apparatus. Moreover, the substitution of Na<sup>+</sup> by K<sup>+</sup> in the extracellular media strongly inhibited the ability of palytoxin both to inhibit protein translation and to activate SAPK/JNK1, whereas the substitution of Na<sup>+</sup> by choline<sup>+</sup> did not. These results led the authors to suggest that palytoxin-induced efflux of cellular K<sup>+</sup> mimics ribotoxic stress by provoking both translational inhibition and activation of protein kinases associated with cellular defense against stress (Iordanov and Magun 1998).

## Palytoxin Toxicity

In the first attempts to determine palytoxin toxicity, the crude ethanol extracts of the *Palythoa toxica* proved to be so toxic that an accurate LD<sub>50</sub> was difficult to determine. More recently, the toxicity

has been determined to be about 50–100 ng/kg i.p. in mice (Patoockaa and Stredab 2002). In dogs, palytoxin at doses below 0.05 µg/kg i.v. caused a sustained rise in arterial pressure; at doses above 0.06 µg/kg i.v. it produced a transient rise in arterial pressure followed by rapid hypotension and death within five minutes, suggesting that palytoxin exerts its toxic action through intense vasoconstriction in the whole body, particularly in the coronary and renal vascular beds, and through depression of the cardiac function (Ito, Urakawa, and Koike 1982). The toxin was equally cytotoxic for normal human bronchial epithelial cells, a human lung tumor cell line, and human bronchial epithelial cells immortalized by infection with adenovirus 12-SV40 hybrid virus (BEAS-2B cells). Palytoxin did not induce a change in the free cytosolic Ca<sup>2+</sup> concentration of BEAS-2B cells. At doses as low as 1 pM, palytoxin increased the steady-state level of c-myc mRNA in BEAS-2B cells as well as the uptake of [<sup>3</sup>H]thymidine. The cytotoxic effects of palytoxin were also observed in an ouabain-resistant cell line (Bonnard et al. 1988). Palytoxin toxicity to cultured human epidermal cells was observed at very low concentrations of palytoxin, with 50% loss of colony-forming efficiency observed at approximately  $3 \times 10^{-13}$  M (Gabrielson et al. 1992).

In agreement with previous reports on palytoxin cytotoxicity, we have recently found that in cultured cerebellar granule neurons palytoxin at 10 and 50 nM killed about 40% of cells after five minutes exposure of cultured neurons to the toxin as assessed with the MTT assay, while four hours exposure of neuroblastoma cells to 1 nM palytoxin decreased cell viability by about 100% (Fig. 6.5).

Between October 30 and November 4, 2000, 11 persons were intoxicated due to ingestion of a serranid fish *Epinephelus* sp. in Kochi Prefecture, Japan. Their symptoms included severe muscle pain, low back pain, and discharge of black urine. The causative agent was identified as palytoxin on the basis of delayed haemolytic activity, which was inhibited by an anti-palytoxin antibody and ouabain (Taniyama et al. 2002). Although the toxic dose of palytoxin in humans could not be determined, extrapolation of the data available in animals will give a toxic dose in a human of about 4 µg. This fact places palytoxin among the most toxic nonproteinic animal toxins known to date (Taniyama et al. 2002); however, its mechanisms of toxicity remain to be elucidated.

## Palytoxin Analogues from *Ostreopsis* spp.

### Introduction

Marine dinoflagellates from *Ostreopsis* spp. are one of the biogenetic sources of palytoxin and its potent analogues. These species are known to be widespread around the world and have consistently been recorded in the tropical and subtropical areas through the Pacific, Atlantic, and Indian Oceans (Fukuyo 1981; Bagnis et al. 1985; Carlson and Tindall 1985; Ballantine et al. 1988; Tindall et al. 1990; Quod 1994; Faust 1995; Quod et al. 1995; Faust et al. 1996; Usup et al. 1997; Holmes et al. 1998). This section provides an overview about origin, distribution, toxicity and pharmacological targets of the palytoxin analogues produced by marine dinoflagellates belonging to the genus *Ostreopsis*.

### *Ostreocins*

#### Origin and Distribution

*Ostreopsis siamensis* (Schmidt 1901), originally discovered in the Gulf of Siam (Thailand), was the first species described within the genus *Ostreopsis*. This group includes mainly benthic and epiphytic dinoflagellates (Steidinger and Tangen 1996), which were identified a few years ago as

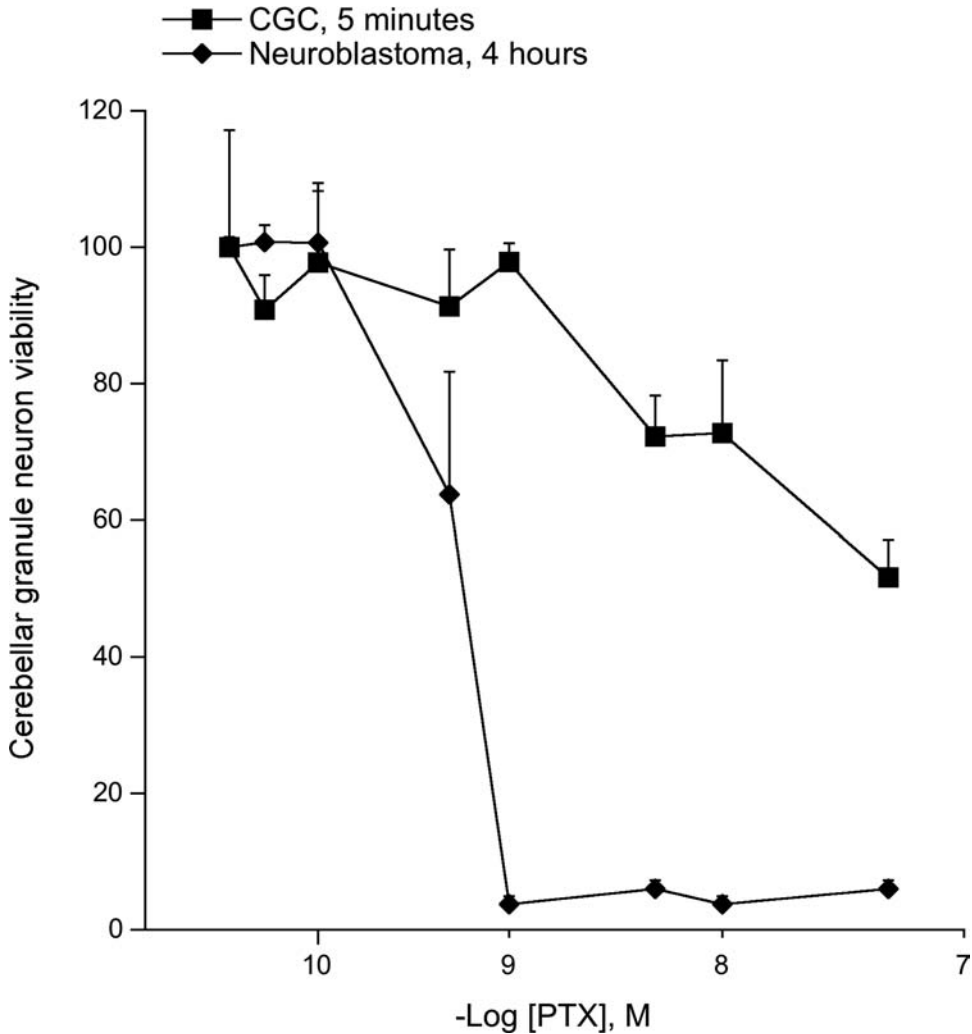


**Figure 6.5.** Cytotoxicity of palytoxin in cultured cerebellar mouse neurons and human neuroblastoma cells as assessed with the MTT test.

producers of highly toxic palytoxin analogues, the ostreocins. In 1995, Usami et al. (1995) isolated ostreocins from cultures of *Ostreopsis siamensis* (SOA1 strain) collected at Aka Island, Okinawa, Japan. The most important compound purified from these cultures was ostreocin-D which exhibited an extremely high toxicity in mice when administered intraperitoneally ( $\text{LD}_{50}$  0.75  $\mu\text{g}/\text{kg}$ ). Other insignificant ostreocins, different from palytoxin, were also detected in the chemical analysis. Further work using the same strain of *Ostreopsis siamensis* allowed researchers to clarify the entire structure of ostreocin-D (Ukena et al. 2001, 2002).

In New Zealand's subtropical coastal waters *Ostreopsis siamensis* is frequently present as epiphytic on seaweeds and planktonic in some occasions as well (Chang et al. 2000; Rhodes et al. 2000). Since 1994, restrictions on the harvesting of oyster in Rangaunu Harbour, Northland,

New Zealand, were imposed for considerable periods due to common occurrence of low levels of unidentified lipid-soluble toxins. These toxins were detected by biotoxin regulatory tests in shellfish collected in this very important commercial shellfish harvesting area. Studies on marine microflora conducted over the period from November 1995 to April 1997 revealed that *Ostreopsis* spp. (*O. siamensis*, *O. lenticularis*, and *O. ovata*) were the most common and widely distributed epiphytic dinoflagellate species in northern New Zealand, being clearly *Ostreopsis siamensis* the dominant species in summer (Chang et al. 2000). However, the link between the lipid-soluble toxins detected in shellfish from Rangaunu Harbour and the presence of *Ostreopsis siamensis* could not be established. Further, low levels of a palytoxin-like material have been reported in extracts of oysters from this area. This *Ostreopsis siamensis* toxin showed a higher toxicity to mice by intraperitoneal injection than by oral administration without evident accumulative effect after repetitive sublethal doses (Briggs et al. 1998). It was also observed that acid treatment (PH 3) at 100°C can decrease the toxicity (unpublished observation by Rhodes et al. 2000). Therefore, a reduction in the hazard of intoxication could be possible by cooking the shellfish before consumption.

### Toxicity

Toxicity tests (summarized in Table 6.1) on cultures of *Ostreopsis siamensis* isolates (Rhodes et al. 2000), collected from Northland in New Zealand, showed that they were toxic to brine shrimps (*Artemia salina*) and killed mice by intraperitoneal injection. Likewise, cytotoxicity to neuroblastoma cells and irreversible suppression of cell firing in hippocampal rat brain slices was also detected. It has reported that delayed hemolytic activity against mammalian erythrocytes in vitro is characteristic of palytoxin and its analogues (Habermann et al. 1981; Beress et al. 1983; Mahnir et al. 1992; Onuma et al. 1999; Lenoir et al. 2004). A sensitive palytoxin-selective assay using hemolysis of erythrocytes with neutralization of hemolysis by the anti-palytoxin monoclonal antibody (method of Bignami 1993) revealed the presence of a biotoxin similar to palytoxin, although neither this one nor ostreocin could be finally confirmed by high-performance liquid chromatography. Based on the fact that this uncharacterized compound binds to the anti-palytoxin monoclonal antibody, which is thought to react only with palytoxin or closely related compounds (Bignami et al. 1992), this toxin must be another derivative of palytoxin (Rhodes et al. 2000).

It has been reported that the palytoxin group may cause fatal human intoxications from the ingestion of contaminated fish (Onuma et al. 1999; Taniyama et al. 2003). However, only few data are known about the potential risks for human health through consumption of shellfish contaminated by *Ostreopsis* spp. toxins. In 1998, a suspected case of human shellfish poisoning was associated with

**Table 6.1.** Evaluation of toxicity and toxin analyses conducted on *Ostreopsis siamensis* cells isolated from Northland, New Zealand

Type of study	<i>Ostreopsis siamensis</i>
Artemia salina assays	50% dead in 24 hours
Mouse bioassay	Death 22 minutes ( $\approx 2.0 \times 10^6$ cells)
Neuroblastoma assay	Cytotoxic ( $\approx 4.5 \times 10^6$ cells)
Hippocampal brain slice assay	Suppression of cell firing
Palytoxin hemolysis neutralization assay	0.3 pg cell <sup>-1</sup> palytoxin equivalents (isolated from Rangiputa)
HPLC palytoxin/ostreocin	Negative

Source: Summarized from Rhodes et al. 2000



wild mussels collected from Anson's Bay, Tasmania. The incident led to further investigations showing that *Ostreopsis siamensis* (which produced  $\leq 0.1$  pg palytoxin equivalents cell<sup>-1</sup>) were usually taken up by wild mussels (*Mytilus edulis planulatus*) from this place (Pearce et al. 2001). Recently, it has been observed that Pacific oyster (*Crassostrea gigas*) and scallops (*Pecten novaezealandiae*) fed under laboratory conditions with  $8.6 \times 10^6$  *Ostreopsis siamensis* cells from Northland (Rangiputa), New Zealand, containing 0.3 pg palytoxin equivalents cell<sup>-1</sup>, accumulated palytoxin-like material in a different manner (Rhodes et al. 2002). In fact, oysters (from Rabbit Island, Nelson) contained some amounts of toxin in hepatopancreas, muscle, and roe, while higher concentrations, only in the hepatopancreas, were present in scallops (from Tasmania Bay). The presence of palytoxin-like compounds in the hepatopancreas of scallops has suggested the extraction of this organ in seafood for human consumption. It could be a risk that considerable amounts of *Ostreopsis siamensis* toxins were accumulated in the hepatopancreas during blooms of this dinoflagellate. Interestingly, the same study carried out with mussels (*Perna canaliculus* from farms in Marlborough Sounds) did not reveal the presence of toxins in any of tested parts (muscle, roe, and hepatopancreas). Two explanations have been suggested for this finding: (1) The shellfish did not incorporate the toxin, or (2) the toxin was taken up and transformed further in an undetectable compound with or without toxicity.

Although *Ostreopsis siamensis* is typical of tropical and subtropical environments, its distribution is not restricted to these areas. It is present in temperate water as well. In this sense, several works have reported its occurrence in the Mediterranean Sea (Taylor 1979; Mamán et al. 2000; Vila et al. 2001a, 2001b). The palytoxin-like activity in *Ostreopsis siamensis* Mediterranean extracts was reported for first time by Riobó et al. (2004). Recent characterization of isolates belonging to the genus *Ostreopsis* from the western Mediterranean Sea have identified *Ostreopsis siamensis* as one of the major clades in this area (Penna et al. 2005). Toxicity tests on several Mediterranean algal extracts (from Italy and Spain) based on checking the delayed hemolysis of human erythrocytes with inhibition by ouabain (Habermann and Chhatwal 1982) resulted positive, indicating the presence of palytoxin-like material in these isolates. Other studies using also Mediterranean strains of *Ostreopsis siamensis* showed toxicity in mouse bioassays, delayed hemolytic activity, and chromatographic properties with similar characteristics to palytoxin (Riobó et al. 2003). More information is necessary on incidence of *Ostreopsis siamensis* toxins in the waters of the Mediterranean Sea and on its magnitude for damaging the human health through seafood.

### Pharmacological Targets

Recently, Botana's group has published the first data about the biological activity of ostreocin-D (Ares et al. 2005). The effect of ostreocin-D and palytoxin to the cytoskeleton was investigated on isolated rabbit intestinal cells where the filamentous actin was specifically labeled with a fluorescent marker. Fluorescence quantification was obtained through laser-scanning cytometry, while confocal microscopy was using for recording images. Interestingly, using the same concentration in two cases (75 nM), ostreocin-D showed a behavior very similar to palytoxin. Both toxins decreased the filamentous actin of enterocytes in a way that did not affect the shape of cells (Fig. 6.6). In eukaryotic cells, the cytoskeleton is closely associated with signal transduction and other regulatory systems (Smith et al. 1991; Zigmond 1996; Schmidt and Hall 1998; Salmon and Way 1999; Sotiropoulos et al. 1999; Kamal and Goldstein 2000; Gourlay and Ayscough 2005), which makes this structure an important target for many toxic agents (Richard et al. 1999; Spector et al. 1999; Leira et al. 2001). Taking into account the relation reported between Ca<sup>2+</sup> and the modifications on cytoskeleton (Fifkova 1985; Yin 1987; Furukawa and Mattson 1995), the role of this second messenger in these effects was also



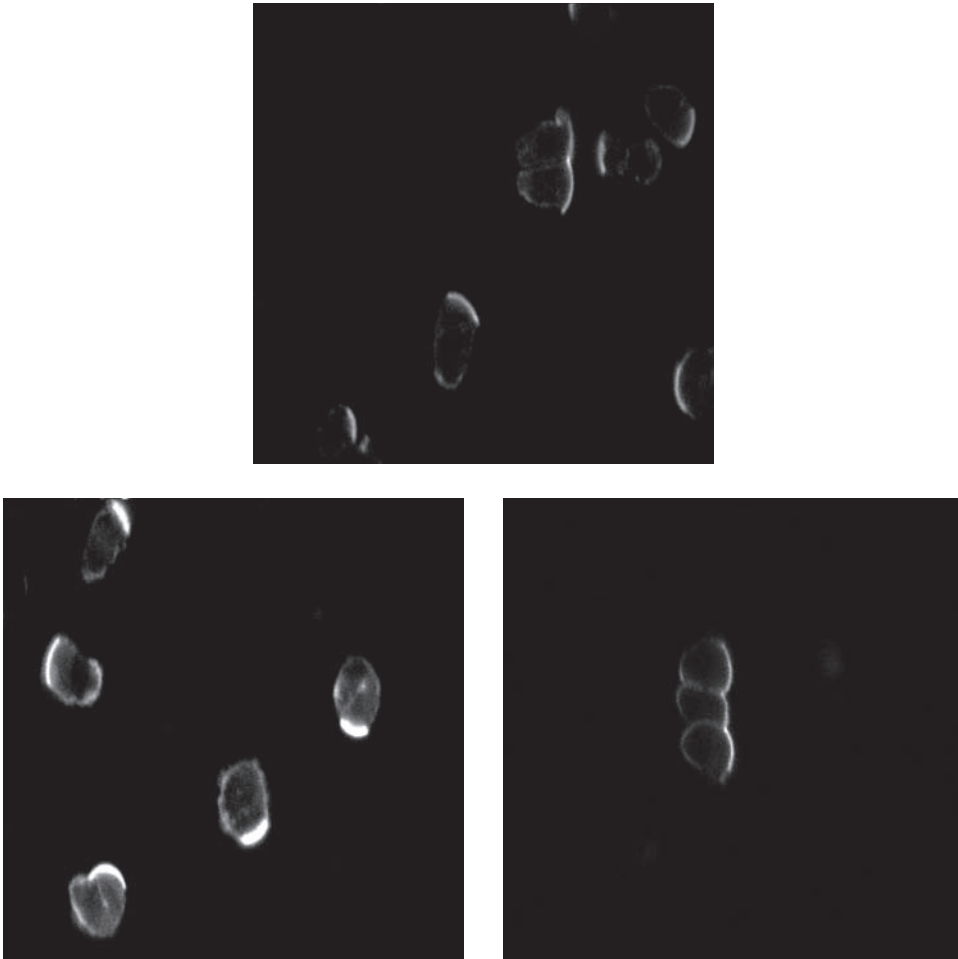


**Figure 6.6.** Visualization with confocal microscopy of actin filaments of rabbit intestinal cells loaded with Oregon Green Phalloidin. Images show control (left position) and enterocytes incubated for 4 hours with palytoxin (central position) or osteoreocin-D (right position). Reproduced with permission from Ares et al. 2005.

evaluated (Ares et al. 2005). In this sense, the effect of osteoreocin-D and palytoxin on actin cytoskeleton was partially dependent of  $\text{Ca}^{2+}$  influx (it was almost half reduced when this cation was not present in extracellular medium) (Table 6.2). The comparable outcome of these toxins on actin filaments has led us to think that osteoreocin-D and palytoxin have similar targets in intestinal cells.

Botana and collaborators also evaluated the effect of osteoreocin-D and palytoxin in an excitable cellular model (human neuroblastoma cells). Both toxins caused an important loss of filamentous actin associated to morphological alterations (Fig. 6.7). In neuroblastoma cells, the variation of ion fluxes caused by osteoreocin-D and palytoxin was studied by using the membrane potential sensitive probe bis-oxonol and the  $\text{Ca}^{2+}$  sensitive dyes fluo-3 and fura red. Osteoreocin-D modifies the membrane potential, causing depolarization, although more slight than that produced by palytoxin (Fig. 6.8a).

**Table 6.2.** Percentage of reduction of filamentous actin evoked by ostreocin-D and palytoxin following 4 hours of incubation

Condition	Ostreocin-D	Palytoxin
Ca <sup>+2</sup> -containing medium	47% ± 6.8%	52% ± 4.4%
Ca <sup>+2</sup> -free medium	25% ± 3.2%	26% ± 6.3%

Source: Data extracted from Ares et al. 2005

Note: Cellular model was intestinal cells. The actin filaments specific fluorescent marker, Oregon green phalloidin, detected with laser-scanning cytometry allowed to quantify the microfilaments in rabbit intestinal cells

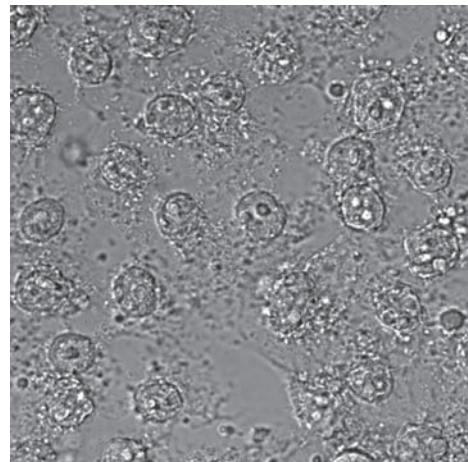
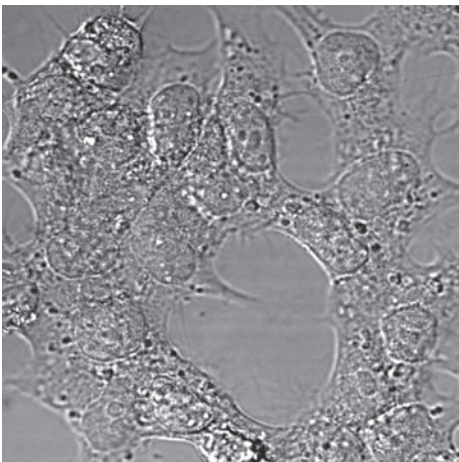
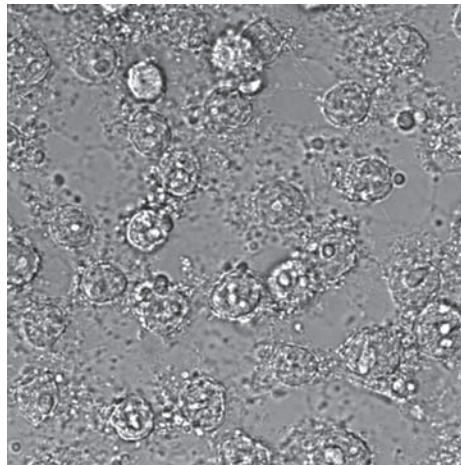


**Figure 6.7.** Transmission images of human neuroblastoma cells obtained with confocal microscopy showing the morphological alterations induced by palytoxin (center) and ostreocin-D (right) after 4 hours incubation. Normal cells are at left.

In addition, it triggered the increasing of cytosolic  $\text{Ca}^{2+}$  level (Fig. 6.8b) in a not very different way to palytoxin. Therefore, these data together to those obtained in intestinal cells could indicate that both toxins share the same targets.

## Mascarenotoxins

### Origin and Distribution

Two new palytoxin analogues from another species of *Ostreopsis*, *Ostreopsis mascarenensis* (Quod 1994), have been identified in the Indian Ocean. The dinoflagellate producer was originally discovered in the Mascareignes Archipelago (Southwest Indian Ocean), where it is widely spread (Quod 1994; Turquet et al. 1998; Hansen et al. 2001). It is commonly associated with shallow barrier reef environments and coral reefs or as epiphytes on macroalgae. The toxins produced by this species have been already reported (Quod 1994; Turquet et al. 2002); however, these compounds had not been well characterized so far.

### Toxicity

High quantities of *Ostreopsis mascarenensis* cells from a monospecific outbreak occurred in Rodrigues Island (Mascareignes Archipelago, March 1996) were collected and their extracts checked for detecting potential toxic activity (Turquet et al. 2002; Lenoir et al. 2004). Evaluation of toxicity *in vivo* using the mouse bioassay indicated the presence of neurotoxic compounds in the polar n-butanol-soluble fraction extracted from *Ostreopsis mascarenensis*. Symptoms such as prostration,

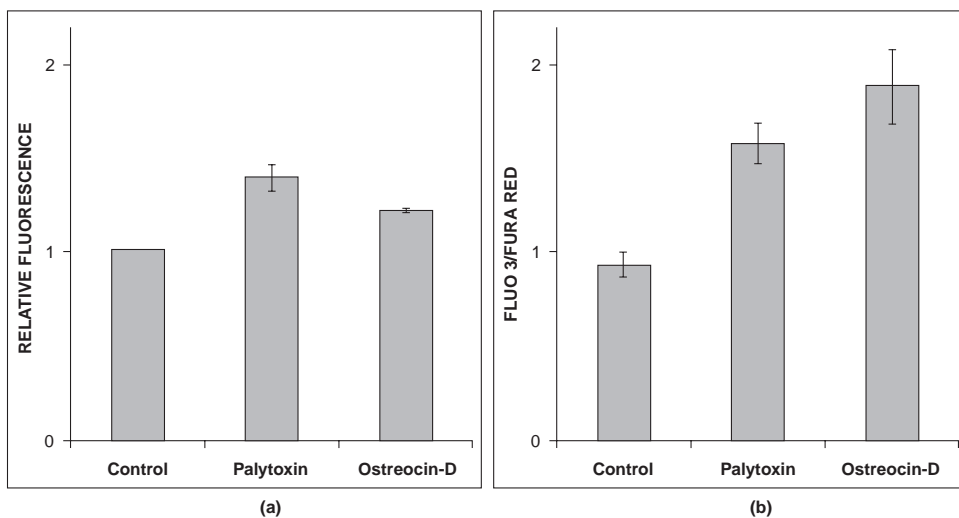


**Figure 6.8.** (a) Depolarization registered in neuroblastoma cells loaded with bis-oxonol after 350 seconds of exposition to palytoxin or ostreocin-D. (b) Comparative cytosolic calcium increase induced by palytoxin or ostreocin-D in neuroblastoma cells at 350 seconds of exposition to the toxins. Ratio of fluorescent dyes Fluo 3 and Fura red, which bind to  $\text{Ca}^{2+}$  free, was measured through confocal microscopy.

paralysis, or dyspnea between others and finally death in a short time (20 minutes) were observed after intraperitoneal injection in mice. However, this study did not find the diarrhoeic effect associated to palytoxin, although the most of symptoms were comparable to those reported in previous investigations (Moore and Scheuer 1971; Vick and Wiles 1975; Habermann et al. 1981).

The toxic compounds purified from the polar n-butanol-soluble fraction were called mascarenotoxin-A (McTx-A) and mascarenotoxin-B (McTx-B), and the estimation of their masses (around 2500–2535 daltons) showed to be lower than palytoxin isolated from *Palythoa toxica* or ostreocin-D from *Ostreopsis siamensis*, although the implication of this fact is unknown. On the other hand, the hemolytic potency of McTx-B in the assays for delayed hemolysis (typical of palytoxin and its analogues; Habermann et al. 1981) on mouse erythrocytes was higher than McTx-A. However, both activities were lower than that for the Pacific palytoxin (obtained from *Palythoa toxica*) used as the reference for these assays (Lenoir et al. 2004). Authors suggested that these differences in the hemolytic action could be attributed to small variations in the structure existing between mascarenotoxins and the reference palytoxin. In any case, further investigations leading to elucidate the molecular structure of these palytoxin analogues are required. Likewise, information on its capacity for entry in the food chain as well as on biological targets of mascarenotoxins has not been available.

It is known that clupeotoxism is a form of highly fatal human poisoning associated with clupeoid fishes contaminated with palytoxin (Onuma et al. 1999). In recent years, palytoxin analogues were implicated in mortalities associated with ingestion of this type of fishes occurred in southwestern Indian Ocean (Yasumoto 1998, Hansen et al. 2001), a clupeotoxism endemic area where *Ostreopsis mascarenensis* is highly distributed. This fact associated with confirmation of palytoxin analogues production by this species has suggested to *Ostreopsis mascarenensis* as a possible origin of palytoxin poisoning in this region.

## Another Potential Palytoxin Analogues from *Ostreopsis ovata*

### Origin and Distribution

Populations of *Ostreopsis ovata* (Fukuyo 1981), the smaller of members within of genus *Ostreopsis*, are usually found in protected, inshore regions from the tropical Pacific Ocean (Fukuyo 1981; Yasumoto et al. 1987; Quod 1994), the Caribbean Sea (Carlson and Tindall 1985), and the Tyrrhenian Sea (Tognetto et al. 1995). Unfortunately, only little information was available until now about the toxic compounds produced by this species, but they are suspected to be related with palytoxins. Likewise, its poisonous potential for health human is also unknown.

### Toxicity

In 1998, alterations on exoskeleton accompanied by high mortality in the marine invertebrate *Equinometra lucunter* were registered in southeastern Brazil (coastline of Cabo Frio), coinciding with an outbreak of a benthic dinoflagellate, which was reported as belonging to *Prorocentrum* sp. (Odebrecht 2002). However, in a study on a further bloom in the same area (2001–2002) the dinoflagellate responsible was confirmed to be *Ostreopsis ovata*. Toxicological studies of algal extracts from this occurrence revealed the existence of molecules with a slow hemolytic activity and that were fatal to *Artemia salina* and mice (Table 6.3). Moreover, chemical analyses on chromatographic properties and UV absorption maxima of a partially purified sample of this dinoflagellate displayed characteristics that resemble those attributed to the palytoxin group. In sum, all the observations

**Table 6.3.** Toxicity test carried out on *Ostreopsis ovata* extracts collected in southern east Brazil coast

Toxicity	Quantity of <i>Ostreopsis ovata</i> cells
Fatal to mouse (80 minutes)	5000
Hemolytic action on rabbit blood cells after 4 hours	100
Death in <i>Artemia salina</i> (100%)	125

Source: From Granéli et al. 2002.

have suggested that toxins produced by *Ostreopsis ovata* could be ostreocin or palytoxin analogues, although their structure remains to be determined (Granéli et al. 2002).

During the last few years, blooms of the dinoflagellate *Ostreopsis ovata* have become a growing problem in the Mediterranean region. Studies on the reefs of the Tuscany coast (Massa and Livorno), Italy, have showed that this dinoflagellate rapidly colonizes the macroalgae of the natural and artificial reefs in late spring and in summer (when temperature rises 20°C–25°C) (Simoni et al. 2003, 2004). In fact, it has been observed that *Ostreopsis ovata* density increases enormously fast in summer; however, its reduction and apparent absence in autumn-winter is gradual. This dinoflagellate could produce resistant forms at lower temperatures, which would activate in summer as occurs with *Ostreopsis siamensis* (Pearce et al. 2001). With regard to toxicological analysis, tests conducted on *Artemia salina* displayed an important association between mortality occurring in crustaceans after 24 hours and the number of *Ostreopsis ovata* in extracts of macroalgae from reefs (65%–100% death in ranges of 542 to 906 of dinoflagellate cells mL<sup>-1</sup>) (Simoni et al. 2004). *Ostreopsis ovata* have also been found on the islands of the Tuscany archipelago such as Elba and Sicily; however, this species seems to be absent in the northern Adriatic Sea (Simoni et al. 2003).

Within of genus *Ostreopsis*, *Ostreopsis ovata* together with *Ostreopsis siamensis*, constitute the principal clades in the western Mediterranean Sea. Comparative phylogenetic analyses between *Ostreopsis ovata* cells from different localities (Mediterranean Sea, West Atlantic, and Asia) have showed a high genetic diversity between the western Mediterranean and Asian isolates, which has led us to think both types developed independently over time. In this study, the existence of palytoxins in the Mediterranean (from Italy and Spain) *Ostreopsis ovata* algal extracts was detected through assays for delayed hemolytic action with neutralization by ouabain, two criteria associated with the presence of palytoxin (Penna et al. 2005). *Ostreopsis ovata* isolates from the western Atlantic (Brazil) tested in the same investigation were affirmatives in the hemolysis assays; in addition, mouse bioassay and the liquid chromatography analysis together with mass spectrometry give strong evidence of palytoxin-like compounds (Riobó et al., 2003, Riobó et al., 2004, Penna et al., 2005). Likewise, more work carried out with isolates also from the Mediterranean revealed an effect in mice (by intraperitoneal injection) as well as chromatographic profiles comparable to those obtained with palytoxin (Riobó et al. 2003).

From 1998 to 2001, summer blooms of *Ostreopsis ovata* that occurred on the shoreline of Massa-Carrara (Tuscany, Italy) led to major consequences in the common biocenosis, causing massive mortalities between marine invertebrates and macroalgae populations. Likewise, these algal outbreaks have been also related to human malaises. In 1998, in the region inland from the bloom-affected zone, a hundred people reported symptoms such as irritation of the upper respiratory tract, coughing, muscular and articular pains, and even fever in some cases. The symptoms were evident at 2–3 hours following exposure to the marine aerosol and apparently disappeared in 12 hours, coming back as a product of new inhalations. The number of cases was lower in blooms of *Ostreopsis ovata* that occurred

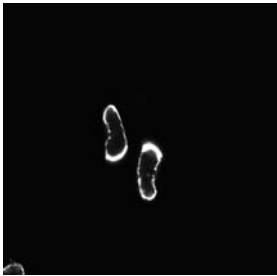
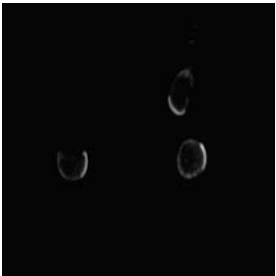
in 2000–2001. This symptomatology was associated with the breathing of sea spray aerosol, given that a great percentage of the people affected had not dipped in these waters (Sansoni et al. 2003). Interestingly, human disturbances caused by inhalation of toxic agents through marine aerosols had been only reported for *Gymnodinium breve* (Hemmert 1975; Pierce 1986; Pierce et al. 1990; Backer et al. 2005). Related to this, a study carried out on further blooms of toxic dinoflagellates of genus *Ostreopsis* that occurred in the Bari coast (2003–2004, Italy) indicated a high relationship between this phenomenon and the human malaises observed (Gallitelli et al. 2005).

In July 2005, the Regional Environmental Protection Agency of Liguria, Italy, detected a new outbreak of *Ostreopsis ovata* on the coast of Genoa, which has been linked to human disturbances. Several kilometers of beach in this area were closed for a time because around 150 people presented symptoms including nausea and diarrhea, breathing difficulties, and fever. This phenomenon was evident in both swimmers and sunbathers who did not swim, which has suggested once again that the poison could be carried in the air.

### Pharmacological Data

A sample purified of an *Ostreopsis ovata* extract was lately assayed on actin cytoskeleton of isolated rabbit intestinal cells by Botana's group. The measure of a fluorescent dye bound specifically to actin filaments (Oregon green 514-phalloidin) showed that *Ostreopsis ovata* toxin also interfered the cytoskeleton as occurred in the two previous cases (Table 6.4). In addition, activity on membrane potential of neuroblastoma cells was studied through the fluorescent probe bis-oxonol. The purified extract displayed a depolarizing effect (the value of relative fluorescence obtained at 350 seconds for cells exposed to the sample was  $1.49 \pm 0.12$  versus control) also similar to palytoxin and ostreocin-D. Therefore, although these studies only shed very preliminary information about the toxic compound produced by *Ostreopsis ovata*, they appear to point out some link between its cellular targets and those identified for palytoxin and ostreocin-D in these studies.

**Table 6.4.** Biological activity of a sample purified of *Ostreopsis ovata* on actin cytoskeleton of rabbit enterocytes

Parameter	Control	Sample
% Filamentous actin	100%	Reduction of $53\% \pm 3.1\%$
Fluorescence images of filamentous actin		

Note: Cellular model was intestinal cells. The techniques employed for actin studies were laser-scanning cytometry and confocal microscopy



## References

- Anner, B.M., and Moosmayer, M. 1994. Na,K-ATPase characterized in artificial membranes. 2. Successive measurement of ATP-driven Rb-accumulation, ouabain-blocked Rb-flux and palytoxin-induced Rb-efflux. *Mol Membr Biol* 11, 247–254.
- Ares, I.R., Louzao, M.C., Vieytes, M.R., Yasumoto, T., and Botana, L.M. 2005. Actin cytoskeleton of rabbit intestinal cells is a target for potent marine phycotoxins. *J Exp Biol* 208, 4345–4354.
- Artigas, P., and Gadsby, D.C. 2003. Ion occlusion/deocclusion partial reactions in individual palytoxin-modified Na/K pumps. *Ann NY Acad Sci* 986, 116–126.
- Artigas, P., and Gadsby, D.C. 2004. Large diameter of palytoxin-induced Na/K pump channels and modulation of palytoxin interaction by Na/K pump ligands. *J Gen Physiol* 123, 357–376.
- Backer, L.C., Kirkpatrick, B., Fleming, L.E., Cheng, Y.S., Pierce, R., Bean, J., Clark, R., Johnson, D., Wanner, A., Tamer, R., Zhou, Y., and Baden, D.G. 2005. Occupational Exposure to Aerosolized Brevetoxins during Florida Red Tide Events: Effects on a Healthy Worker Population. *Environ Health Perspect* 113, 644–649.
- Bagnis, R., Bennet, J., Prieur, C., and Legrand, A.M. 1985. The dynamics of three toxic benthic dinoflagellates and the toxicity of ciguateric surgeonfish in French Polynesia. In *Toxic Dinoflagellates*, ed. Anderson, D.M., White, A.W., and Baden, D.G. New York: Elsevier, 177–182.
- Ballantine, D.L., Tosteson, T.R., and Bardales, A.T. 1988. Population dynamics and toxicity of natural populations of benthic dinoflagellates in southwestern Puerto Rico. *J Exp Mar Biol Ecol* 119, 201–212.
- Beress, L., Zwick, J., Kolkenbrock, H.J., Kaul, P.N., and Wassermann, O. 1983. A method for the isolation of the caribbean palytoxin (C-PTX) from the coelenterate (zoanthid) *Palythoa caribaeorum*. *Toxicon* 21, 285–290.
- Berman, F.W., LePage, K.T., and Murray, T.F. 2002. Domoic acid neurotoxicity in cultured cerebellar granule neurons is controlled preferentially by the NMDA receptor Ca(2+) influx pathway. *Brain Res* 924, 20–29.
- Bignami, G.S. 1993. A rapid and sensitive hemolysis neutralization assay for palytoxin. *Toxicon* 31, 817–820.
- Bignami, G.S., Raybould, T.J., Sachinvala, N.D., Grothaus, P.G., Simpson, S.B., Lazo, C.B., Byrnes, J.B., Moore, R.E., and Vann, D.C. 1992. Monoclonal antibody-based enzyme-linked immunoassays for the measurement of palytoxin in biological samples. *Toxicon* 30, 687–700.
- Bonnard, C., Lechner, J.F., Gerwin, B.I., Fujiki, H., and Harris, C.C. 1988. Effects of palytoxin or ouabain on growth and squamous differentiation of human bronchial epithelial cells in vitro. *Carcinogenesis* 9, 2245–2249.
- Bottinger, H., Beress, L., and Habermann, E. 1986. Involvement of (Na+ + K+)-ATPase in binding and actions of palytoxin on human erythrocytes. *Biochim Biophys Acta* 861, 165–176.
- Bottinger, H., and Habermann, E. 1984. Palytoxin binds to and inhibits kidney and erythrocyte Na+, K+-ATPase. *Naunyn Schmiedeberg's Arch Pharmacol* 325, 85–87.
- Briggs, L., Rhodes, L., Munday, R., and Towers, N. 1998. Detection of palytoxin using a haemolysis neutralisation assay. *Proceedings of the NZMAF Marine Biotxin Workshop* 10, 91–97.
- Carlson, R.D., and Tindall, D.R. 1985. Distribution and periodicity of toxic dinoflagellates in the Virgin Islands. In *Toxic Dinoflagellates*, ed. Anderson, D.M., White, A.W., and Baden, D.G. New York: Elsevier, 171–176.
- Chang, F.H., Shimizu, Y., Hay, B., Stewart, R., Mackay, G., and Tasker, R. 2000. Three recently recorded *Ostreopsis* spp. (Dinophyceae) in New Zealand: temporal and regional distribution in the upper North Island from 1995 to 1997. *NZ J Mar Freshwater Res* 34, 29–39.
- Farley, R.A., Schreiber, S., Wang, S.G., and Scheiner-Bobis, G. 2001. A hybrid between Na+,K+-ATPase and H+,K+-ATPase is sensitive to palytoxin, ouabain, and SCH 28080. *J Biol Chem* 276, 2608–2615.
- Faust, M.A. 1995. Benthic, toxic dinoflagellates: an overview. In *Harmful Marine Algal Blooms*, ed. Lassus, P., Arzul, G., Erard, E., Gentien, P., and Marcaillou-LeBaut, C. Paris: Lavoisier, 847–854.
- Faust, M.A., Morton, S.L., and Quod, J.P. 1996. Further SEM study of marine dinoflagellates: the genus *Ostreopsis* (Dinophyceae). *J Phycol* 32, 1053–1065.
- Fifkova, E. 1985. Actin in the nervous system. *Brain Res* 356, 187–215.
- Frelin, C., and Van Renterghem, C. 1995. Palytoxin. Recent electrophysiological and pharmacological evidence for several mechanisms of action. *Gen Pharmacol* 26, 33–37.
- Frelin, C., Vigne, P., and Breittmayer, J.P. 1990. Palytoxin acidifies chick cardiac cells and activates the Na+/H+ antiporter. *FEBS Lett* 264, 63–66.
- Fujiki, H., Suganuma, M., Nakayasu, M., Hakii, H., Horiuchi, T., Takayama, S., and Sugimura, T. 1986. Palytoxin is a non-12-O-tetradecanoylphorbol-13-acetate type tumor promoter in two-stage mouse skin carcinogenesis. *Carcinogenesis* 7, 707–710.
- Fukuyo, Y. 1981. Taxonomic study on benthic dinoflagellates collected in coral reefs. *Bull Jap Soc Sci Fish* 41, 967–978.
- Furukawa, K., and Mattson, M.P. 1995. Cytochalasins protect hippocampal neurons against amyloid beta-peptide toxicity: evidence that actin depolymerization suppresses Ca2+ influx. *J Neurochem* 65, 1061–1068.



- Gabrielson, E.W., Kuppasamy, P., Povey, A.C., Zweier, J.L., and Harris, C.C. 1992. Measurement of neutrophil activation and epidermal cell toxicity by palytoxin and 12-O-tetradecanoylphorbol-13-acetate. *Carcinogenesis* 13, 1671–1674.
- Gallitelli, M., Ungaro, N., Addante, L. M., Procacci, V., Silveri, N.G., and Sabba, C. 2005. Respiratory illness as a reaction to tropical algal blooms occurring in a temperate climate. *JAMA* 293, 2599–2600.
- Gleibs, S., Mebs, D., and Werding, B. 1995. Studies on the origin and distribution of palytoxin in a Caribbean coral reef. *Toxicon* 33, 1531–1537.
- Gourlay, C.W., and Ayscough, K.R. 2005. A role for actin in aging and apoptosis. *Biochem Soc Trans* 33, 1260–1264.
- Granéli, E., Ferreira, C.E.L., Yasumoto, T., Rodrigues, E., and Neves, M.H.B. 2002. Sea urchins poisoning by the benthic dinoflagellate *Ostreopsis ovata* on the Brazilian Coast. In *Tenth International Conference on Harmful Algae, Florida, USA*, 113.
- Habermann, E. 1989. Palytoxin acts through Na<sup>+</sup>,K<sup>+</sup>-ATPase. *Toxicon* 27, 1171–1187.
- Habermann, E., Ahnert-Hilger, G., Chhatwal, G.S., and Beress, L. 1981. Delayed haemolytic action of palytoxin. General characteristics. *Biochim Biophys Acta* 649, 481–486.
- Habermann, E., and Chhatwal, G.S. 1982. Ouabain inhibits the increase due to palytoxin of cation permeability of erythrocytes. *Naunyn Schmiedebergs Arch Pharmacol* 319, 101–107.
- Hansen, G., Turquet, J., Quod, J.P., Ten-Hage, L., Lugomela, C., Kyewalyanga, M., Hurbungs, M., Wawiye, P., Ogongo, B., Tunje, S., and Rakotoarinjanahary, H. 2001. *Potentially Harmful Microalgae of the Western Indian Ocean: A Guide Based on a Preliminary Survey*. Intergovernmental Oceanographic Commission Manuals and Guides No. 41. Paris: UNESCO, 105.
- Hansen, O. 1984. Interaction of cardiac glycosides with (Na<sup>+</sup> + K<sup>+</sup>)-activated ATPase. A biochemical link to digitalis-induced inotropy. *Pharmacol Rev* 36, 143–163.
- Hemmert, W.H. 1975. The public health implications of *Gymnodinium breve* red tides, a review of the literature and recent events. In *Toxic Dinoflagellate Blooms*, ed. LoCicero, V.R. Wakefield, MA: Massachusetts Science and Technology Foundation, 489–497.
- Hirsh, J.K., and Wu, C.H. 1997. Palytoxin-induced single-channel currents from the sodium pump synthesized by in vitro expression. *Toxicon* 35, 169–176.
- Holmes, M.J., Lee, F.C., Teo, S.L.M., and Khoo, H.W. 1998. A survey of benthic dinoflagellates on Singapore Reefs. In *Harmful Algae*, ed. Reguera, B., Blanco, J., Fernandez, M.L., and Wyatt, T. Vigo: Xunta de Galicia and Intergovernmental Oceanographic Commission of UNESCO, 50–51.
- Iordanov, M.S., and Magun, B.E. 1998. Loss of cellular K<sup>+</sup> mimics ribotoxic stress. Inhibition of protein synthesis and activation of the stress kinases SEK1/MKK4, stress-activated protein kinase/c-Jun NH2-terminal kinase 1, and p38/HOG1 by palytoxin. *J Biol Chem* 273.
- Ito K., Urakawa, N., and Koike, H. 1982. Cardiovascular toxicity of palytoxin in anesthetized dogs. *Arch Int Pharmacodyn Ther* 258, 146–154.
- Kamal, A., and Goldstein, L.S. 2000. Connecting vesicle transport to the cytoskeleton. *Curr Opin Cell Biol* 12, 503–538.
- Karin, M., Liu, Z., and Zandi, E. 1997. AP-1 function and regulation. *Curr Opin Cell Biol* 9, 240–246.
- Kockskamper, J., Ahmmed, G.U., Zima, A.V., Sheehan, K.A., Glitsch, H.G., and Blatter, L.A. 2004. Palytoxin disrupts cardiac excitation-contraction coupling through interactions with P-type ion pumps. *Am J Physiol Cell Physiol* 287, C527–538.
- Kuroki, D.W., Bignami, G.S., and Wattenberg, E.V. 1996. Activation of stress-activator protein kinase/c-Jun N-terminal kinase by the non-TPA-type tumor promoter palytoxin. *Cancer Res* 56, 637–644.
- Leira, F., Alvarez, C., Vieites, J.M., Vieytes, M.R., and Botana, L.M. 2001. Study of cytoskeletal changes induced by okadaic acid in BE(2)-M17 cells by means of a quantitative fluorimetric microplate assay. *Toxicol in Vitro* 15, 277–282.
- Lenoir, S., Ten-Hage, L., Turquet, J., Quod, J.P., Bernard, C., and Hennion, M.C. 2004. First evidence of palytoxin analogues from an *ostreopsis mascarenensis* (Dinophyceae) benthic bloom in Southwestern Indian Ocean. *J Phycol* 40, 1042–1051.
- Li, S., and Wattenberg, E.V. 1998. Differential activation of mitogen-activated protein kinases by palytoxin and ouabain, two ligands for the Na<sup>+</sup>,K<sup>+</sup>-ATPase. *Toxicol Appl Pharmacol* 151, 377–384.
- Lingrel, J.B., and Kuntzweiler, T. 1994. Na<sup>+</sup>,K<sup>(+)</sup>-ATPase. *J Biol Chem* 269, 19659–19662.
- Mahnir, V.M., Kozlovskaya, E.P., and Kalinovsky, A.I. 1992. Sea anemone *Radianthus macrodactylus*—a new source of palytoxin. *Toxicon* 30, 1449–1456.
- Mamán, L., Fernández, L., Ocaña, A., Marco, J.J., Morales, J., Caballos, M., Márquez, I., and Aguilar, M. 2000. Seguimiento de fitoplancton tóxico en la costa de Andalucía. Incidencias durante los años 1997 y 1998. In *Actas de la VI Reunión Ibérica de Fitoplancton Tóxico y Biotoxinas*, ed. Márquez, I. Sevilla, Spain: Consejería de Agricultura y Pesca, Junta de Andalucía, 41–49.
- Monroe, J.J., and Tashjian, A.H., Jr. 1995. Actions of palytoxin on Na<sup>+</sup> and Ca<sup>2+</sup> homeostasis in human osteoblast-like Saos-2 cells. *Am J Physiol* 269, C582–589.

- Moore, R. E., Helfrich, P., and Patterson, G.M.L. 1982. The deadly seaweed of Hana. *Oceanus* 25, 54–63.
- Moore, R.E., and Scheuer, P.J. 1971. Palytoxin: a new marine toxin from a coelenterate. *Science* 172, 495–498.
- Nakamura, K., Asari, T., Ohizumi, Y., Kobayashi, J., Yamasu, T., and Murai, A. 1993. Isolation of zooxanthellatoxins, novel vasoconstrictive substances from zooxanthella *Symbiodinium* sp. *Toxicon* 31, 371–376.
- Nakamura, T., Minamisawa, H., Katayama, Y., Ueda, M., Terashi, A., Nakamura, K., and Kudo, Y. 1999. Increased intracellular  $Ca^{2+}$  concentration in the hippocampal CA1 area during global ischemia and reperfusion in the rat: a possible cause of delayed neuronal death. *Neuroscience* 88, 57–67.
- Odebrecht, C. 2002. Floraciones de microalgas nocivas en Brasil: estado del arte y proyectos en curso. In *Floraciones Algas Nocivas en el Cono Sur Americano*, ed. Sar, E.A., Ferrario, M.E., and Reguera, B. Vigo: Instituto Español de Oceanografía, 217–233.
- Onuma, Y., Satake, M., Ukena, T., Roux, J., Chanteau, S., Rasolofonirina, N., Ratsimaloto, M., Naoki, H., and Yasumoto, T. 1999. Identification of putative palytoxin as the cause of clupeotoxism. *Toxicon* 37, 55–65.
- Patockaa, J., and Stredab, L. 2002. Brief review of natural nonprotein neurotoxins. *ASA newsletter*.
- Pearce, I., Marshall, J., and Hallegraeff, G.M. 2001. Toxic epiphytic dinoflagellates from East Coast Tasmania, Australia. In *Harmful Algal Blooms 2000*, ed. Hallegraeff, G., Blackburn, S.I., Bolch, C.J., and Lewis, R.J. Hobart: Intergovernmental Oceanographic Commission of UNESCO, 54–57.
- Penna, A., Vila, M., Fraga, S., Giacobbe, M.G., Andreoni, F., Riobo, P., and Vernesi, C. 2005. Characterization of *Ostreopsis* and *Coolia* (Dinophyceae) isolates in the western Mediterranean sea based on morphology, toxicity and internal transcribed spacer 5.8S rDNA sequences. *J Phycol* 41, 212–225.
- Pierce, R., Henry, M.S., Proffitt, L.S., and Hasbrouck, P.A. 1990. Red tide toxin (brevetoxin) enrichment in marine aerosol. In *Toxic Marine Phytoplankton*, ed. Graneli, E., Sundstrom, B., Elder, L., and Anderson, D.M. New York: Elsevier, 397–402.
- Pierce, R.H. 1986. Red tide (*Gymnodinium breve*) toxin aerosols: a review. *Toxicon* 24, 955–965.
- Quod, J.P. 1994. *Ostreopsis mascarenensis* sp. nov. (Dinophyceae), dinoflagellates toxiques associes a la ciguatera dans l’Ocean Indien. *Cryptogam Algol* 15, 243–251.
- Quod, J.P., Turquet, J., Diogene, G., and Fessard, V. 1995. Screening of extracts of dinoflagellates from coral reefs (Reunion Island, Indian Ocean), and their biological activities. In *Harmful Marine Algal Blooms*, ed. Lassus, P., Arzul, G., Erard, E., Gentien, P., and Marcaillou-LeBaut, C. Paris: Lavoisier, 815–820.
- Redondo, J., Fiedler, B., and Scheiner-Bobis, G. 1996. Palytoxin-induced  $Na^{+}$  influx into yeast cells expressing the mammalian sodium pump is due to the formation of a channel within the enzyme. *Mol Pharmacol* 49, 49–57.
- Rhodes, L., Adamson, J., Suzuki, T., Briggs, L., and Garthwaite, I. 2000. Toxic marine epiphytic dinoflagellates, *Ostreopsis siamensis* and *Coolia monotis* (Dinophyceae), in New Zealand. *NZ J Mar Freshwater Res* 34, 371–383.
- Rhodes, L., Towers, N., Briggs, L., Munday, R., and Adamson, J. 2002. Uptake of palytoxin-like compounds by shellfish fed *Ostreopsis siamensis* (Dinophyceae). *NZ J Mar Freshwater Res* 36, 631–636.
- Richard, J.F., Petit, L., Gibert, M., Marvaud, J.C., Bouchaud, C., and Popoff, M.R. 1999. Bacterial toxins modifying the actin cytoskeleton. *Int Microbiol* 2, 185–194.
- Riobó, P., Paz, B., Fernandez, M. L., Fraga, S., and Franco, J.M. 2004. Lipophilic Toxins of Different Strains of *Ostrepsidaceae* and *Gonyaulacaceae*. In *Harmful Algae 2002*, ed. Steidinger, K.A., Landsberg, J.H., Thomas, C.R., and Vargo, G.A. Florida: Florida Fish and Wildlife Conservation Commission, Florida Institute of Oceanography, and Intergovernmental Oceanographic Commission of UNESCO, 119–121.
- Riobó, P., Paz, B., Fraga, S., and Franco Soler, J.M. 2003. *Palitoxinas en Ostreopsis spp., VIII Reunión Ibérica sobre Fito-plancton Tóxico y Biotoxinas, La Laguna, Tenerife*, 149–157.
- Rouzairre-Dubois, B. and Dubois, J. M., 1990. Characterization of palytoxin-induced channels in mouse neuroblastoma cells. *Toxicon* 28, 1147–1158.
- Salmon, E.D., and Way, M. 1999. Cytoskeleton. *Curr Opin Cell Biol* 11, 15–17.
- Sansoni, G., Borghini, B., Camici, G., Casotti, M., Righini, P., and Rustighi, C. 2003. Fioriture algali di *Ostreopsis ovata* (Gonyaulacales: Dinophyceae): un problema emergente. *Biologia Ambientale* 17, 17–23.
- Schaeffer, H.J., and Weber, M.J. 1999. Mitogen-activated protein kinases: Specific messages from ubiquitous messengers. *Mol Cell Biol* 19, 2435–2444.
- Scheiner-Bobis, G., Hubschle, T., and Diener, M. 2002. Action of palytoxin on apical  $H^{+}/K^{+}$ -ATPase in rat colon. *Eur J Biochem* 269, 3905–3911.
- Scheiner-Bobis, G., Meyer zu Heringdorf, D., Christ, M., and Habermann, E. 1994. Palytoxin induces  $K^{+}$  efflux from yeast cells expressing the mammalian sodium pump. *Mol Pharmacol* 45, 1132–1136.
- Scheiner-Bobis, G., and Schneider, H. 1997. Palytoxin-induced channel formation within the  $Na^{+}/K^{+}$ -ATPase does not require a catalytically active enzyme. *Eur J Biochem* 248, 717–723.

- Schmidt, A., and Hall, M.N. 1998. Signaling to the actin cytoskeleton. *Annu Rev Cell Dev Biol* 14, 305–338.
- Schmidt, J. 1901. Preliminary report of the biological results of the Danish Expedition to Siam (1899–1900). IV. Peridinales. *Bot Tidss* 24, 212–221.
- Schousboe, A., Drejer, J., Hansen, G.H., and Meier, E. 1985. Cultured neurons as model systems for biochemical and pharmacological studies on receptors for neurotransmitter amino acids. *Dev Neurosci* 7, 252–262.
- Simoni, F., Gaddi, A., Di Paolo, C., and Lepri, L. 2003. Harmful epiphytic dinoflagellate on Tyrrhenian Sea reefs. *Harmful Algae News* 24, 13–14.
- Simoni, F., Gaddi, A., Di Paolo, C., Lepri, L., Mancino, A., and Falaschi, A. 2004. Further investigation on blooms of *Ostreopsis ovata* Coolia monotis, Prorocentrum lima on the macroalgae of artificial and natural reefs in the Northern Tyrrhenian Sea. *Harmful Algae News* 26, 5–7.
- Smith, P.R., Saccomani, G., Joe, E.H., Angelides, K.J., and Benos, D.J. 1991. Amiloride-sensitive sodium channel is linked to the cytoskeleton in renal epithelial cells. *Proc Natl Acad Sci USA* 88, 6971–6975.
- Sonneward, U., Olstad, E., Qu, H., Babot, Z., Cristofol, R., Sunol, C., Schousboe, A., and Waagepetersen, H. 2004. First direct demonstration of extensive GABA synthesis in mouse cerebellar neuronal cultures. *J Neurochem* 91, 796–803.
- Sotiropoulos, A., Gineitis, D., Copeland, J., and Treisman, R. 1999. Signal-regulated activation of serum response factor is mediated by changes in actin dynamics. *Cell* 98, 159–169.
- Spector, I., Braet, F., Shochet, N.R., and Bubb, M.R. 1999. New anti-actin drugs in the study of the organization and function of the actin cytoskeleton. *Microsc Res Tech* 47, 18–37.
- Steidinger, K.A., and Tangen, K. 1996. Dinoflagellates. In *Identifying Marine Diatoms and Dinoflagellates*, ed. Tomas, C.R. New York: Academic Press, 387–598.
- Taniyama, S., Arakawa, O., Terada, M., Nishio, S., Takatani, T., Mahmud, Y., and Noguchi, T. 2003. *Ostreopsis* sp., a possible origin of palytoxin in parrotfish *Scarus oivifrons*. *Toxicon* 42, 29–33.
- Taniyama, S., Mahmud, Y., Terada, M., Takatani, T., Arakawa, O., and Noguchi, T. 2002. Occurrence of a food poisoning incident by palytoxin from a serranid *Epinephelus* sp. in Japan. *J Nat Toxins* 11, 277–282.
- Taylor, F.J.R. 1979. A description of the benthic dinoflagellate associated with maitotoxin and ciguatoxin, including observations on Hawaiian material. In *Toxic Dinoflagellate Blooms*, ed. Taylor, D.L., and Seliger, H.H. New York: Elsevier, 71–76.
- Tindall, D.R., Miller, D.M., and Tindall, P.M. 1990. Toxicity of *Ostreopsis lenticularis* from the British and United States Virgin Islands. In *Toxic Marine Phytoplankton*, Graneli, E., Sundstrom, B., Edler, L., and Anderson, D.M. New York: Elsevier, 424–429.
- Tognetto, L., Bellato, S., Moro, I., and Andreoli, C. 1995. Occurrence of *Ostreopsis ovata* (Dinophyceae) in the Tyrrhenian Sea during summer 1994. *Bot Mar* 38, 291–295.
- Turquet, J., Lenoir, S., Quod, J. P., Ten-Hage, L., and Hennion, M. C. 2002. Toxicity and toxin profiles of a bloom of *Ostreopsis mascarenensis* (Dinophyceae) from the SW Indian Ocean. *Tenth International Conference on Harmful Algae, Florida, USA*, 286.
- Turquet, J., Quod, J. P., Couté, A., and Faust, M. 1998. Assemblage of benthic dinoflagellates and monitoring of harmful species in Réunion island (SW Indian Ocean) during the 1993–1996 period. In *Harmful Algae*, ed. Reguera, B., Blanco, J., Fernandez, M. L., Wyatt, T. Vigo: Xunta de Galicia and Intergovernmental Oceanographic Commission of UNESCO, 44–47.
- Ukena, T., Satake, M., Usami, M., Oshima, Y., Fujita, T., Naoki, H., and Yasumoto, T. 2002. Structural confirmation of ostreocin-D by application of negative-ion fast-atom bombardment collision-induced dissociation tandem mass spectrometric methods. *Rapid Commun Mass Spectrom* 16, 2387–2393.
- Ukena, T., Satake, M., Usami, M., Oshima, Y., Naoki, H., Fujita, T., Kan, Y., and Yasumoto, T. 2001. Structure elucidation of ostreocin D, a palytoxin analog isolated from the dinoflagellate *Ostreopsis siamensis*. *Biosci Biotechnol Biochem* 65, 2585–2588.
- Usami, M., Satake, M., Ishida, S., Inoue, A., Kan, Y., and Yasumoto, T. 1995. Palytoxin analogs from the dinoflagellates *Ostreopsis siamensis*. *J Am Chem Soc* 117.
- Usup, G., Lim, P.T., Lew, C.P., and Ahmad, A. 1997. The physiology and toxicity of epiphytic dinoflagellates from the Strait of Malacca, Malaysia. *Eighth International Conference on Harmful Algae, Vigo, Spain*, 206.
- Vale, C., Alfonso, A., Suñol, C., Vieytes, M.R., and Botana, L.M. 2006. Modulation of calcium entry and glutamate release in cultured cerebellar granule cells by palytoxin. *Journal of Neuroscience Research* 83, 1393–1406.
- Vale-González, C., Gumez-Limia, B., Vieytes, M.R., and Botana, L.M. 2007. Effects of the marine phycotoxin palytoxin on neuronal pH in primary cultures of cerebellar granule cells. *Journal of Neuroscience Research* 85, 90–98.
- Vick, J.A., and Wiles, J.S. 1975. The mechanism of action and treatment of palytoxin poisoning. *Toxicol Appl Pharmacol* 34, 214–223.

- Vila, M., Camp, J., Garcés, E., Masó, M., and Delgado, M. 2001a. High resolution spatio-temporal detection of HABs in confined waters of the NW Mediterranean. *J Plankton Res* 23, 497–514.
- Vila, M., Garcés, E., and Masó, M. 2001b. Potentially toxic epiphytic dinoflagellate assemblages on macroalgae in the NW Mediterranean. *Aquat Microb Ecol* 26, 51–60.
- Wattenberg, E.V., McNeil, P.L., Fujiki, H., and Rosner, M.R. 1989. Palytoxin down-modulates the epidermal growth factor receptor through a sodium-dependent pathway. *J Biol Chem* 264, 213–219.
- Weidmann, S. 1977. Effects of palytoxin on the electrical activity of dog and rabbit heart. *Experientia* 33, 1487–1489.
- Yasumoto, T. 1998. Fish poisoning due to toxins of microalgal origins in the Pacific. *Toxicon* 36, 1515–1518.
- Yasumoto, T., Seino, N., Murakami, Y., and Murata, M. 1987. Toxins produced by benthic dinoflagellates. *Biol Bull* 172, 128–131.
- Yin, H.L. 1987. Gelsolin: calcium- and polyphosphoinositide-regulated actin-modulating protein. *Bioessays* 7, 176–179.
- Zigmond, S. H. 1996. Signal transduction and actin filament organization. *Curr Opin Cell Biol* 8, 66–73.

## 7 Chemistry of Cyanobacterial Neurotoxins—Anatoxin-a: Synthetic Approaches

Nuria Armesto Arbella, Keith O'Callaghan,  
Ambrose Furey, and Kevin J. James

### Introduction

Anatoxin-a is a naturally occurring neurotoxic alkaloid, produced by several strains of cyanobacteria. Originally, the species, *Anabaena flos aquae*, was the source of the toxin, which was consequently named anatoxin-a. Since its isolation (Devlin et al. 1977) and characterisation as a (1*R*,6*R*)-2-acetyl-9-azabicyclo[4.2.1]nonane (Huber et al. 1972; Koskinen and Rapoport 1985) in the 1970s, anatoxin-a (**1**; Fig. 7.1A) has stimulated the scientific community worldwide. While synthetic chemists devised methods for the construction of the novel 9-azabicyclo[4.2.1]nonane ring system, medicinal chemists were intrigued by its powerful biological activity.

Anatoxin-a mimics the neurotransmitter acetylcholine (Fig. 7.1B), but owing to its resistance to degradation by the enzyme acetylcholine esterase (Carmichael et al. 1975; Spivak et al. 1980), anatoxin-a remains available in the organism to overstimulate muscle tissue, resulting in respiratory paralysis and ultimately death. (+)-Anatoxin-a is approximately 50 times more potent than (–)-nicotine (Fig. 7.1C) and about 20 times more potent than acetylcholine. This makes it one of the most potent agonist of nicotinic acetylcholine receptors (nAChRs) (Devlin et al. 1977; Thomas et al. 1993). However, despite its poisonous nature, anatoxin-a has become a useful pharmacological probe, providing information for elucidating the mechanism of acetylcholine-mediated neurotransmission and the disease states associated with abnormalities in this important signalling pathway. As acetylcholine deficiency is implicated in disease states such as Alzheimer's, muscular dystrophy, Myasthenia gravis, and Parkinson's, it is hoped that analogues of anatoxin-a, possessing lower levels of toxicity, may be used as acetylcholine replacements in the treatment of brain disorders (Breining 2004).

Until recently, anatoxin-a was the only naturally occurring alkaloid possessing the 9-azabicyclo[4.2.1]nonane ring skeleton, in contrast with the many examples of the similar 8-azabicyclo[3.2.1]octane ring systems found in the diverse and widely distributed atropine alkaloids (i.e., ferruginine and cocaine). As a result of the combination of its biological potency and its rare structure,

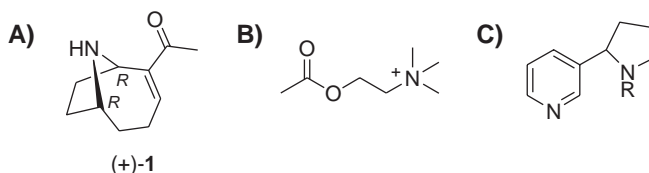


**Figure 7.1.** Structure and stereochemistry of (A) (+)-anatoxin-a, (B) acetylcholine, (C) nicotine (R = CH<sub>3</sub>) and nornicotine (R = H).

it is an attractive synthetic target, leading to numerous racemic and chiral syntheses (Mansell 1996). Construction of the aforementioned ring system and introduction of the methyl ketone at the correct oxidation level has proved to be the major challenges in this regard. There are many different approaches to anatoxin-a synthesis, and most of these can be classified into the synthetic strategies, named according to the methodology used in a crucial step as outlined below. Other isolated strategies were developed as well by the Parson (Parson et al. 1995, 1996, 2000; Forró et al. 2001), Tufariello (Tufariello et al. 1984, 1985), and Gallagher (Vernon and Gallagher, 1987; Huby et al. 1991) groups. A brief explanation of each synthetic approach is presented in approximately chronological order of development:

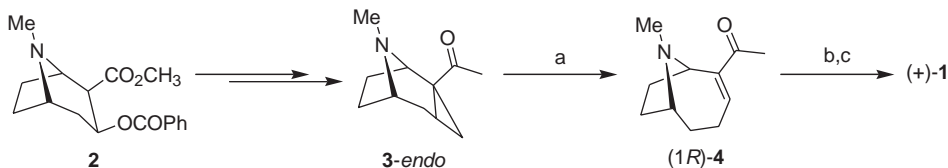
- Cyclic expansion of tropanes
- Cyclization of cyclooctenes
- Enantioselective enolisation strategy
- Intramolecular cyclization of iminium ions
- Enyne metathesis
- Other synthetic approaches to anatoxin-a and analogues

### Synthesis of Anatoxin-a via Cyclic Expansion of Tropanes

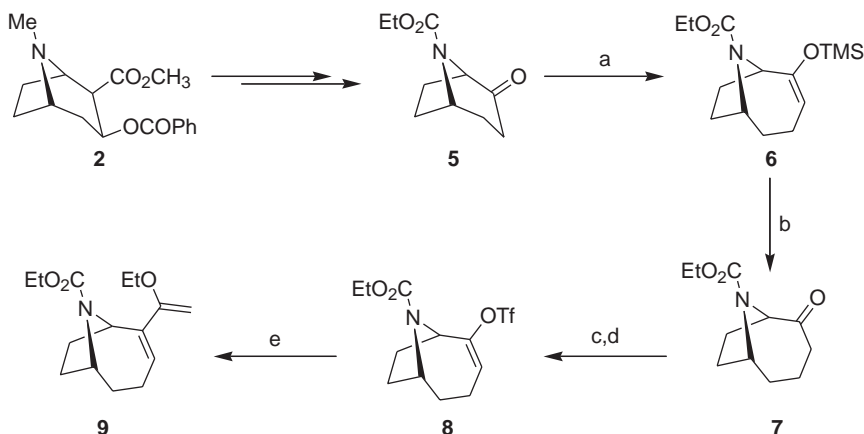
One synthetic approach to prepare an optically pure molecule is to use a starting material from the “chiral pool,” a compound that is easily accessible, normally a natural product, with the same stereochemical configuration as the target product.

The first synthesis of anatoxin-a was achieved using (–)-cocaine (**2**; Scheme 7.1) as the starting material (Campbell et al. 1977). Cocaine was selected since its absolute configuration is coincident with anatoxin-a stereochemistry (Hardegger and Ott 1955). To achieve the basic homotropane structure of anatoxin-a, cocaine was converted into the cyclopropane **3**, which was obtained as a mixture of *endo/exo* isomers in proportion 65:35, respectively (Zirkle et al. 1962; Corey and Chaykovky, 1962). The ring expansion of the *endo*-cyclopropane isomer constituted the crucial step of this synthesis (Scheme 7.1) and was achieved by photolytic cleavage to give the  $\alpha,\beta$ -unsaturated ketone **4** in 46% yield (Pitts and Norman 1954; Winter and Lindauer 1967; Dauben et al. 1969). After *N*-demethylation of this ketone using diethyl azodicarboxylate (DEAD) (Smismann and Makriyannis 1973), (+)-anatoxin-a was obtained, but the overall yield was rather low.

A recent improvement in the synthesis starting from (–)-cocaine was reported by Seitz and co-workers (Wegge et al. 2000) (Scheme 7.2). Initially, cocaine was transformed into the (+)-2-tropinone in two high-yielding steps (Zhang et al. 1997); this was treated with ethyl chloroformate, affording the *N*-protected bicyclic ketone **7** in 57% overall yield. A ring enlargement with the incorporation of the methylene group exclusively at the less hindered side was achieved using trimethylsilyldiazomethane



**Scheme 7.1.** Ring expansion of (–)-cocaine. (a)  $h\nu$ ,  $H_2O$ , 46%. (b) DEAD, Benzene,  $\Delta$ . (c) dil. HCl,  $\Delta$ .



**Scheme 7.2.** Ring expansion of (–)-cocaine. (a)  $\text{TMSCHN}_2$ ,  $\text{Al}(\text{CH}_3)_3$ , 94%. (b)  $\text{CF}_3\text{CO}_2/\text{H}_2\text{O}$ , 94%. (c)  $\text{KHMDS}$ , toluene,  $-78^\circ\text{C}$ . (d) 2- $N(\text{Tf}_2)$ -5-chloro-pyridine, 67%. (e)  $\text{CH}_2 = \text{CH-OEt}$ ,  $\text{Pd}(\text{OAc})_2$ ,  $\text{Et}_3\text{N}$ ,  $\text{DMSO}$ .

( $\text{TMSCHN}_2$ ) and an organoaluminium Lewis acid (Podlech 1998; Yang et al. 1998). The ring expansion of the tropane **7** gave the trimethylsilyl enol ether **8** in 94% yield (overall yield 53%), the first key step in this synthesis.

To get the methyl ketone side chain, **6** was transformed into the triflate **8** (Comins and Deghani 1992; Luker et al. 1997), which under Heck conditions (Andersson and Hallberg 1989) gave the 2-ethoxydiene **9**. The hydrolysis of **9** afforded the  $\alpha,\beta$ -unsaturated ketone moiety, establishing the second key step in this synthesis. *N*-deprotection with iodotrimethylsilane ( $\text{Me}_3\text{SiI}$ ) in chloroform generated the natural (+)-anatoxin-a as the free base after treatment with sodium methoxide in methanol (26% overall yield starting from cocaine).

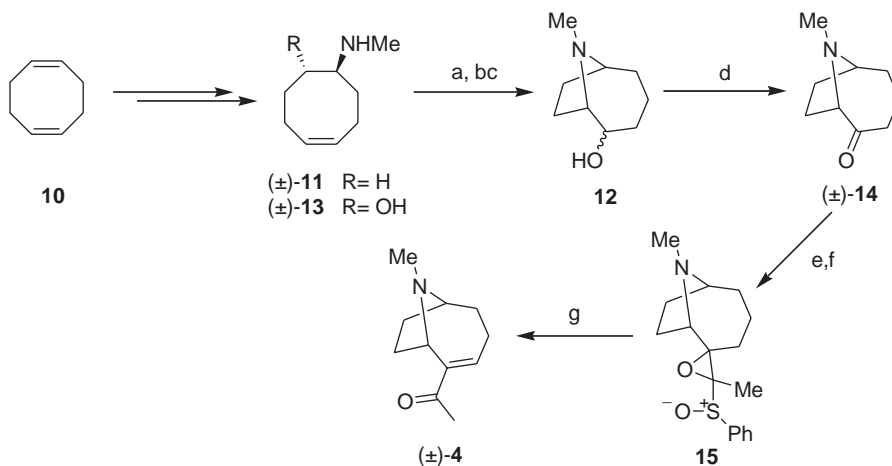
An important advantage of this approach is that it provides the versatile intermediates ketone **7** and enol triflate **8**, which should allow access to various anatoxin analogues (Wright et al. 1997). This group applied their methodology using confiscated grade (–)-cocaine hydrochloride as the starting material.

## Synthesis of Anatoxin via Cyclization of Cyclooctenes

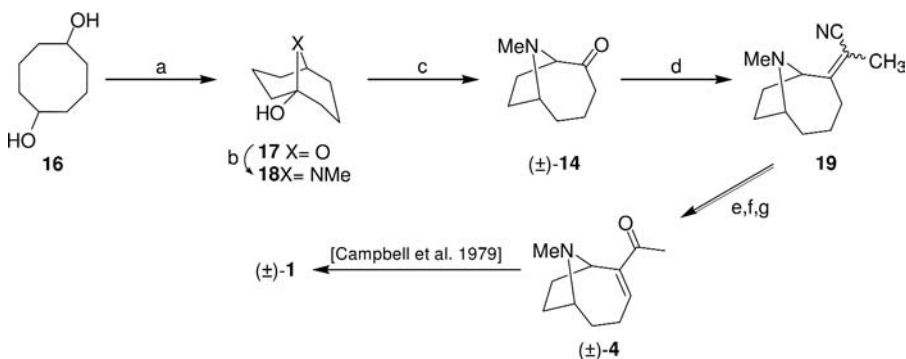
One of the most popular methods for creating the anatoxin-a skeleton is by transannular cyclization of a suitably substituted cyclooctene. This approach was used in the first synthesis of racemic anatoxin-a (Campbell et al. 1979). They carried out two different methodologies in order to reach the 9-azabicyclo[4.2.1]nonane structure (Scheme 7.3). The 1,5-cyclooctadiene (**10**) starting compound was transformed into the methyl amine **11** which was treated with hypobromous acid to produce the desired bicycle **12** as a mixture of diastereoisomers in 29% overall yield, with some amount of the azabicyclo[3.2.1] analogue (Bastable et al. 1972).

The aminoalcohol **13** was also used to generate the anatoxin-a skeleton. The cyclization step was achieved using mercuric (II) acetate (Barrelle and Appar, 1976, 1977), followed by reduction with sodium borohydride in basic media giving the desired bicycle **12** with some traces of the azabicyclo[3.2.1]nonane (33% overall yield). The common intermediate **12** was oxidised to the racemic





**Scheme 7.3.** Cyclisation of aminocyclooctenes. (a) **11**, NBS, HClO<sub>4</sub>, dimethylether, H<sub>2</sub>O, 82%. (b) **13**, Hg(OAc)<sub>2</sub>, THF. (c) NaBH<sub>4</sub>, NaOH, H<sub>2</sub>O, quant. (d) CrO<sub>3</sub>, H<sub>2</sub>SO<sub>4</sub>, acetone, AcOH, 52%. (e) chloroethyl phenyl sulfoxide, LDA, THF, -78°C, 90%. (f) KO<sup>t</sup>Bu, THF, -20°C, 69%. (g) Benzene, Δ, 41%.



**Scheme 7.4.** (a) CrO<sub>3</sub>, H<sub>2</sub>SO<sub>4</sub>, acetone, 49%. (b) aq. MeNH<sub>2</sub>, TsOH, 100°C, 82%. (c) HBr·Py·Br<sub>2</sub>, AcOH, 115°C, 56%. (d) NaNH<sub>2</sub>, (EtO)<sub>2</sub>P(O)CH(CH<sub>2</sub>)CN, THF, 20°C, 64%. (e) LDA, THF/HMPA, O<sub>2</sub>. (f) Na<sub>2</sub>SO<sub>3</sub>, H<sub>2</sub>O. (g) NaOH, H<sub>2</sub>O, 43% (Overall the last three steps)

ketone **14**. This ketone was transformed into the epoxysulfoxide **15** (Jończyk et al. 1975) and by thermal rearrangement (Reutrakul and Kanghae 1977) afforded the α,β-ketone **4** as a predominant product. Eventually, the deprotection of the *N*-methyl group using oxidation by ethyl azodicarboxylate (DEAD) followed by acid hydrolysis provided the (±)-anatoxin-a as its hydrochloride salt in 35% yield (last two steps).

Wiseman and Lee (1986) also reached the ketone **14** by a route involving the cyclization of 1,5-cyclooctanediol (**16**; Scheme 7.4). This transformation involved the Jones oxidation of **16** to give the hemiketal **17**, which was transformed into the 9-methyl-9-azabicyclo[3.3.1]nonan-1-ol **18** by treatment with methylamine, followed by addition of sulphuric acid (Quinn et al. 1973). This skeleton was reconverted into the 9-azabicyclo[4.2.1]nonane by bromination-reorganisation with pyridinium bromide perbromide in hot acetic acid in one direct step (Stjernlöf et al. 1989). This constitutes the key step of this synthesis, affording the ketone **14** in 56% yield.

The conversion of amino ketone **14** into *N*-methyl anatoxin (**4**) was accomplished through the intermediate enonitrile **19** (D'Incan and Seyden-Penne 1975; Wroble and Watt 1976). *N*-Demethylation was achieved before with diethyl azodicarboxylate (Campbell et al. 1979); thus, this completed the synthesis of racemic anatoxin-a.

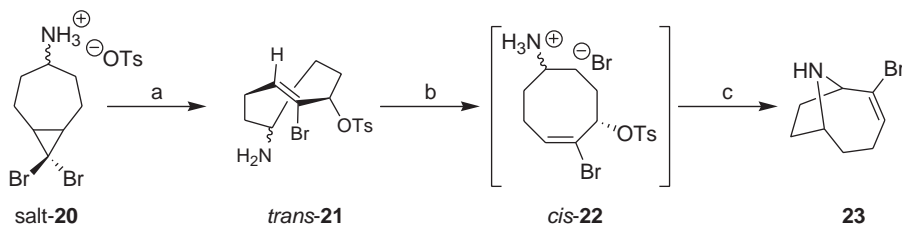
Subsequently, alternative methods were developed by Stjernlöf and co-workers for introducing the acyl moiety and different sidechains in the ketone intermediate **14** (Lindgren et al. 1987; Stjernlöf et al. 1989; Ferguson et al. 1995), which was achieved using the Campbell synthesis (Campbell et al. 1979). The resolution of **14** was performed by traditional diastereomeric crystallisation of its (+)- and (–)-dibenzoyltartaric acid salts from ethanol (Stjernlöf et al. 1989). This allowed the syntheses of both (–)- and (+)-anatoxin-a in 96% *ee*, respectively, as they could prove later in a different conversion of **14** into anatoxin-a (Ferguson et al. 1995).

Another different approach to derive the anatoxin-a skeleton involved the disrotatory electrocyclic dibromocyclopropane cleavage as the key step (Danheiser et al. 1985) (**20**; Scheme 7.5). The *gem*-dibromocyclopropanes are usually implicated in thermal- or silver (I)-promoted electrocyclic ring-cleavage to give  $\pi$ -allyl cations (Marvell 1980), which can be trapped in an inter- or intra-molecular fashion (Banwell and Reum, 1991), by different nucleophiles. The intramolecular trapping processes generate new polycyclic compounds that possess a cycloalkenylbromide moiety (**23**).

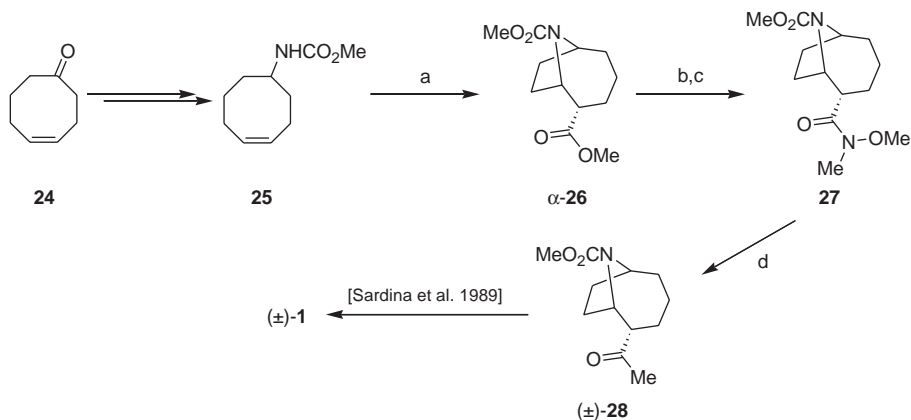
The *gem*-dibromocyclopropanes are generally readily prepared via addition of dibromocarbene to the corresponding cycloalkene (Seyferth 1972). In this case, 4-cycloheptenone gave the key intermediate, dibromobicyclo[5.2.1]octane **20**, in 67% yield (Stork and Ladesman 1956; Borch and Ho 1977). The required azabicyclic structure was achieved in a two-step process. The amine **20** was transformed into its tosylate salt prior to initiating the electrophilic cleavage with silver tosylate to produce the *trans*-cyclooctenes **21**. Photoisomerisation of the *trans*-double bond to *cis*-conformation (**22**) and transannular cyclization in a single operation gave the azabicyclononene **23**. The strategy of the last stage was to reprotect **23** with 'Boc and to generate the organolithium derivative with *tert*-butyl lithium (interchange bromide-lithium), which reacted with *N*-methoxy-*N*-methylamide (Nahm and Weinreb 1981), as an acylating agent, to furnish the *N*-Boc anatoxin-a. Finally, deprotection with trifluoroacetic acid and treatment with chlorhydric acid afforded the ( $\pm$ )-anatoxin-a as its hydrochloride salt. This racemic synthesis of anatoxin-a was achieved in seven steps (17% overall yield) and could be carried out in a gram scale.

Intramolecular aminocarbonylation (Chiou et al. 2005) was used in the synthesis of anatoxin-a by the Ham group. The key step involved an intramolecular palladium catalyzed aminocarbonylation reaction to reach the bicyclic ring skeleton characteristic of anatoxin-a (Oh et al. 1998) (Scheme 7.6).

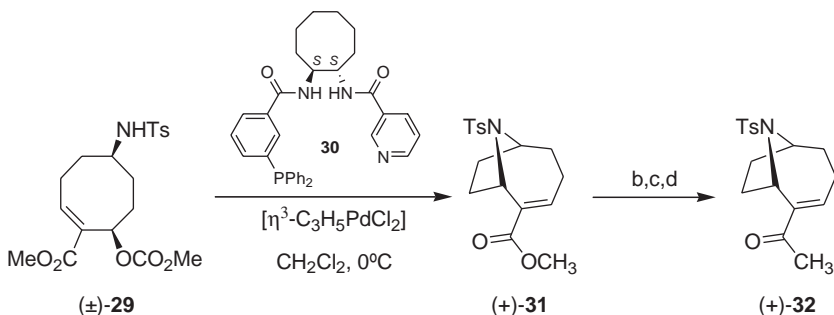
The key intermediate **25** for the cyclization step was obtained from the ketone **24** in 27% overall yield (Bastable et al. 1972). The regiochemistry toward azabicyclo[4.2.1]nonane or azabicyclo



**Scheme 7.5.** Electrocyclic aperture of cyclopropane affording the 9-azabicyclo[4.2.1]nonane structure. (a) excess AgOTs, CH<sub>3</sub>CN,  $\Delta$ , 60%. (b) HBr, Benzene, hv. (c) Et<sub>3</sub>N, CH<sub>3</sub>CN,  $\Delta$ , 32%.



**Scheme 7.6.** Cyclization via intramolecular aminocarbonylation. (a)  $\text{PdCl}_2$ ,  $\text{CuCl}_2$ , press. CO, MeOH, rt, 61%. (b) KOH, MeOH, reflux, 98%. (c)  $\text{HNCH}_3(\text{OCH}_3)$ , EDCl, HOBT,  $\text{CH}_2\text{Cl}_2$ , 87%. (d)  $\text{MeMgBr}$ , THF,  $0^\circ\text{C}$ , 85%.



**Scheme 7.7.** Catalytic asymmetric allylic alkylation using the phosphine ligand **30**. (a)  $[\text{Pd}(\text{dba})_3]$ , (*S,S*)-**30**,  $\text{CHCl}_3$ ,  $0^\circ\text{C}$ , 94%, 88% ee. (b) LiOH,  $\text{H}_2\text{O}$ , MeOH. (c)  $(\text{COCl})_2$ ,  $\text{CH}_2\text{Cl}_2$ . (d)  $\text{Me}_3\text{Al}$ ,  $\text{AlCl}_3$ , 85%. (e) Na(Hg),  $\text{Na}_2\text{HPO}_4$ , 71%.

[3.2.1]nonane of the transannular cyclization was dependent on the nature of *N*-substituent. The best way to achieve the required bicyclo[4.2.1]nonane as the main product was with the carbamate **25**. Thus, palladium (II) chloride catalyzed the intramolecular aminocarbonylation of **25**, giving mainly the azabicyclo  $\alpha$ -**26** (Ham et al. 1997). Treatment of this azabicyclo with potassium hydroxide to furnish the acid and subsequent reaction with the *N,O*-dimethylhydroxylamine gave the amide **27** (Nahm and Weinreb 1981). Reaction with methylmagnesium bromide afforded the known ketone **28**, *N*-acetyl dihydroanatoxin-a, in 72% yield, which was converted into ( $\pm$ )-anatoxin-a following the Rapoport methodology (Sardina et al. 1989; explained in detail later, Scheme 7.11).

Continuing with palladium chemistry, Trost proposed a new asymmetric synthesis of anatoxin-a (Trost and Oslob, 1999) and the crucial step was the introduction of chirality by a catalytic process involving an intramolecular asymmetric allylic alkylation (Trost 2004) of the intermediate ( $\pm$ )-**29** affording (+)-**31** (Scheme 7.7). This step was catalyzed by palladium in presence of a chiral phosphine ligand.

The *N*-tosyl group was chosen as a result of preliminary studies. Eventually, the cyclization product was reached with  $[\text{Pd}(\text{dba})_3]$  catalyst in the presence of the chiral ligand (*S,S*)-**30**, giving the bicycle

(+)-**31**. Transformation of the ester moiety into the ketone **32** (Arisawa et al. 1997) and reductive desulphonylation (Trost et al. 1976; Somfai and Åhman 1992) generated (–)-anatoxin-a in 88% *ee*. The natural (+)-enantiomer would be equally accessible simply by switching the chirality of the ligand.

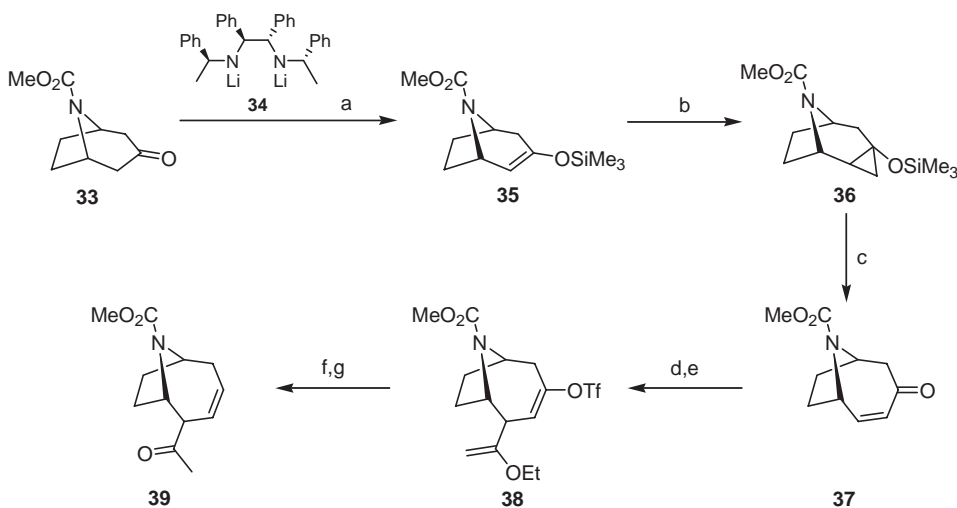
The *de novo* asymmetric syntheses prior to this were the Simpkins (Newcombe and Simpkins 1995) and the Aggarwal (Aggarwal et al. 1999) approaches, but in those cases stoichiometric amounts of the chiral base were employed in the enantioselective step.

## Synthesis of Anatoxin-a via Enantioselective Enolization Strategy

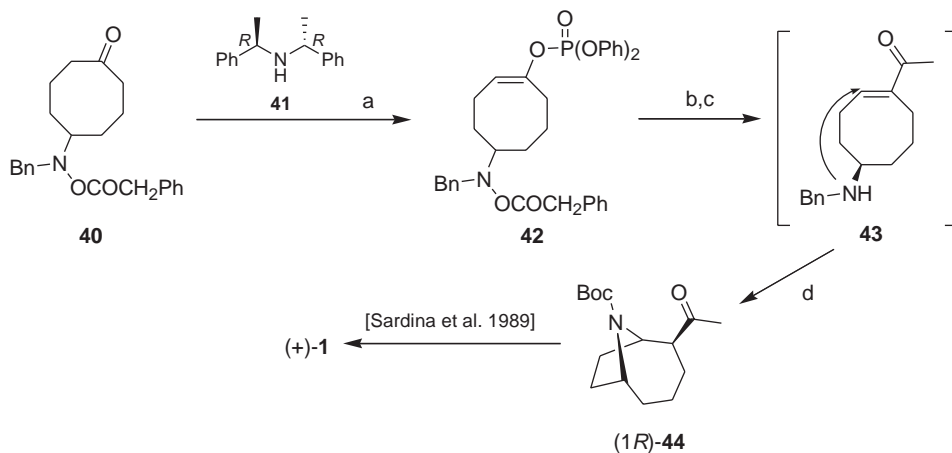
Simpkins and co-workers were the first to use an asymmetric catalytic process in (–)-anatoxin-a synthesis (Newcombe and Simpkins, 1995) instead of resorting to the “chiral pool” strategy. Their total synthesis of (–)-anatoxin-a relied on an enantioselective enolisation reaction of a readily available ( $\pm$ )-3-tropinone (**33**), by a chiral lithium amide base (**34**) (Bunn et al. 1993a, 1993b) and subsequent cyclopropanation/ring expansion reaction giving the ketone **37** (Scheme 7.8).

The enantioselective enolisation of the tropinone **33** with the chiral base **34** and quenching the reaction mixture with  $\text{Me}_3\text{SiCl}$  resulted in the formation of the desired enol silane **35** in 84% yield and 78% *ee*. The effective ring expansion of the tropane ring was achieved via cyclopropanation reaction with chloriodomethane and diethylzinc (**36**) (Denmark and Edwards 1991). Subsequent reaction with  $\text{FeCl}_3$  and mild basic conditions (Ito et al. 1976) afforded the homotropane ketone **37** in 71% yield. The purity (% *ee*) of the enantiomerically enriched ketone **37** was improved to greater than 99% by induced crystallization using cold storage.

The 1,4-addition of an organocuprate to the  $\alpha,\beta$ -unsaturated ketone **37**, followed by a triflimide reagent, gave the enol triflate derivative **38**. Hydrogenolysis of the enol triflate function, and successive treatment of the crude reaction in acidic conditions in order to hydrolyze the vinyl ether side chain, afforded the deconjugated system **39**. The effective isomerization to the  $\alpha,\beta$ -unsaturated



**Scheme 7.8.** (a) **34**, THF,  $\text{Me}_3\text{SiCl}$ ,  $-100^\circ\text{C}$ , 84%, 78% *ee*; (b)  $\text{Et}_2\text{Zn}$ ,  $\text{ICH}_2\text{Cl}$ ,  $\text{ClCH}_2\text{CH}_2\text{Cl}$ , 99%. (c)  $\text{FeCl}_3$ , DMF,  $\text{NaOAc}$ ,  $\text{MeOH}$ , 71%. (d)  $[\text{CH}_2=\text{C}(\text{OEt})_2\text{Cu}(\text{CN})\text{Li}]_2$ , THF,  $\text{Et}_2\text{O}$ . (e) 2-triflimido-5-chloropyridine, 65%. (f)  $\text{Pd}(\text{OAc})_2(\text{PPh}_3)_2$ ,  $\text{Bu}_3\text{N}$ ,  $\text{HCO}_2\text{H}$ , DMF. (g)  $\text{HCl}$ ,  $\text{MeOH}$ , 64%.



**Scheme 7.9.** (a) (*R,R*)-**41**,  $n\text{BuLi}$ ,  $(\text{PhO})_2\text{POCl}$ , THF,  $-100^\circ\text{C}$ , 89%, 89% ee. (b)  $[\text{Pd}(\text{PPh}_3)_4]$ ,  $\text{CH}_2=\text{CH}(\text{OEt})\text{SnBu}_3$ , LiCl, THF,  $\Delta$ , 84%. (c) HBr/AcOH, 95%. (d) Pd/C,  $\text{H}_2$ , MeOH,  $(\text{Boc})_2\text{O}$ , 89%.

ketone in 80% yield was achieved using  $\text{RhCl}_3$  (Grieco et al. 1976). The total synthesis of unnatural (–)-anatoxin-a was accomplished by deprotection with  $\text{Me}_3\text{SiI}$  (Jung and Lyster 1978). The natural (+)-anatoxin-a could be available by using the antipode of chiral base **34**. They also achieved the racemic synthesis of anatoxin-a using the simple LDA base with the same procedure.

Aggarwal and co-workers used the same key strategy but with a different Simpkins base (*R,R*)-**41** (Cain et al. 1990) to achieve the rare enantioselective deprotonation of an eight-membered ring ketone (**40**, Scheme 7.9) at the low temperature of  $-100^\circ\text{C}$  to ensure the presence of only one cyclooctanone conformer and consequently increase the enantioselectivity of the process (Aggarwal et al. 1999).

Under these conditions they achieved the enantiomerically enriched lithium enolate intermediate, which was trapped with diphenyl chlorophosphate, affording the enol phosphate **42** in 89% ee and 89% yield. The Stille coupling reaction of **42** (Nicolaou et al. 1997) with ethoxyvinyltributyltin ( $\text{CH}_2=\text{CH}(\text{OEt})\text{SnBu}_3$ ) gave a vinyl ether, which was hydrolyzed in acidic conditions, giving the masked ketone moiety (intermediate **43**). This intermediate undergoes simultaneous deprotection of the amine group and intramolecular conjugated addition, affording directly in one step the required azabicyclic structure, and constituting another key step in the synthesis. The change of the benzyl group for *tert*-butoxycarbonyl in one step under Rapoport conditions gave the ketone (*1R*)-**44**, which was converted into the (+)-anatoxin-a, using the Rapoport procedure (Sardina et al. 1989), explained in detail later (Scheme 7.11). Eventually, they obtained the enantiomerically enriched (+)-anatoxin-a in a 34% overall yield.

## Synthesis of Anatoxin-a via Intramolecular Cyclization of Iminium Ions

The asymmetric approaches leading to the construction of enantiomerically pure 9-azabicyclo[4.2.1]nonane skeleton are mostly concerned with the intramolecular cyclization of a pyrrolidine iminium ion (**46**). They differ significantly in the preparation of *cis*-substituted pyrrolidine (**45**) precursors and in overall yield for the construction of this basic skeleton. See Fig. 7.2.

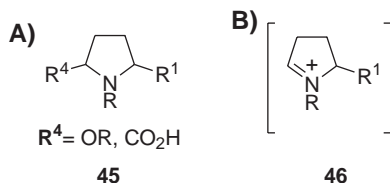
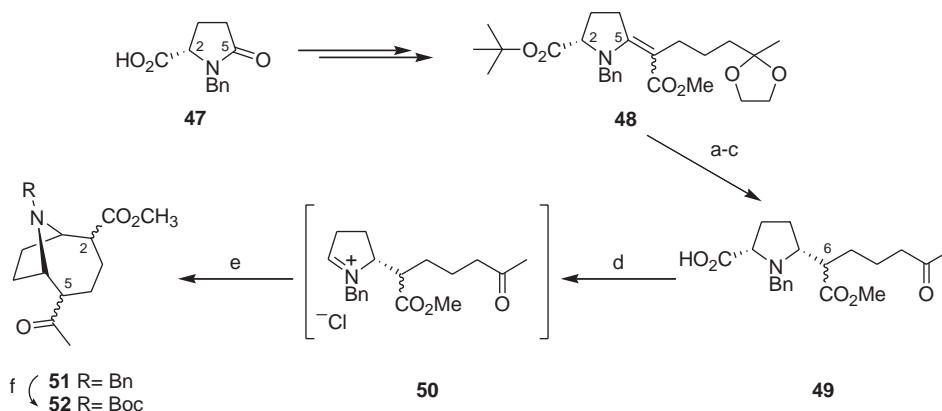


**Figure 7.2.** Structures of generic pyrrolidine iminium ion (46) and its pyrrolidine precursor (45).



**Scheme 7.10.** Synthesis of the common intermediate 2,5-difunctionalized homotropane 52. (a) 10% Pd/C, H<sub>2</sub>, MeOH. (b) BnBr, K<sub>2</sub>CO<sub>3</sub>, CH<sub>3</sub>CN, 93%. (c) AcOH/ *i*-PrOH/ H<sub>2</sub>O 1:5.5, 100°C, 89%. (d) Oxalyl chloride, CH<sub>2</sub>Cl<sub>2</sub>, -15°C–3°C. (e) Heating 60°C, Toluene, 91%. (f) (tBoc)<sub>2</sub>O, Pd/C, H<sub>2</sub>, MeOH, 98%.

### Via Alkyl Iminium Salts

The Rapoport group, using this concept, has made the most significant contributions to the asymmetric synthesis and generation of structure-activity information on anatoxin-a and its analogues (Hernandez and Rapoport, 1994; Swanson et al. 1986, 1989, 1991; Wonnacott et al. 1991). After previous approaches to the racemic anatoxin-a synthesis using this methodology (Bates and Rapoport 1979; Petersen, Töterberg-Kaulen, and Rapoport 1984), Rapoport reported a total synthesis of optically active (+)-anatoxin-a and its enantiomer starting from D- and L-glutamic acid, respectively (Petersen, Fels, and Rapoport 1984). Improvements in this synthesis were later published (Koskinen and Rapoport 1985; Sardina et al. 1989), establishing the basis for an enantiodivergent synthesis of both enantiomers of anatoxin-a starting from a single chiral material, L-glutamic acid (Sardina et al. 1990). Many of the developed methodologies and synthetic strategies employed by this group have been used extensively by others in various syntheses of anatoxin-a.

The L-glutamic acid was transformed into the L-benzyl pyroglutamate (**47**; Scheme 7.10) in two steps as described (Quitt et al. 1963; Stadler 1978). The alkyl chain introduction on C-5 pyrrolidine position using a sulphide contraction reaction (Fischli and Eschenmoser 1967; Shiosaki and Rapoport 1985; Sakurai et al. 1994) was one of the crucial steps in this synthesis, giving the enantiomerically pure vinylogous carbamate **48** as a mixture of diastereomers (Petersen, Fels, and Rapoport 1984; Koskinen and Rapoport 1985). Highly *cis*-diastereoselective reduction of the carbamate double bond was carried out over Pd/C affording exclusively the 2,5-*cis*-disubstituted pyrrolidine (Petersen, Fels, and Rapoport 1984; Sardina et al. 1989). Rebenzylation of the *N*-debenzylated

material and subsequent hydrolysis of the *tert*-butyl ester gave the *N*-benzyl amino acid **49** as a 4:1 mixture of epimers at C-6. This is the key product for the cyclization step.

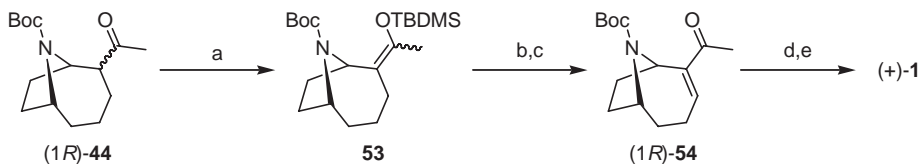
The iminium ion **50** was generated by a decarbonylative cyclization procedure, based on the known instability of tertiary amino acid chlorides toward decarbonylation (Dean et al. 1976; Weinstein and Craig 1976) and the well-established electrophilic character of iminium ions (Tramontini 1973; Koskinen and Lousnasmaa 1983). Thus, treatment of the amino acid **49** with oxalyl chloride gave acyl chloride, which directly generated the iminium intermediate **50**, and after heating furnished the product **51**, 2,5-difunctionalised homotropane, as a mixture of diastereomers at C-2 and C-5 (Sardina et al. 1989). Conversion of the *N*-benzyl group to *N-tert*-butyl carbamate, was reached directly in one step under neutral hydrogenolysis conditions of the mixture of **51** in methanol and in presence of di-*tert*-butyl dicarbonate. This afforded **52** in an overall yield of 43% (all stereoisomers) (Sardina et al. 1989).

The product **52** is the common intermediate for the synthesis of both enantiomers of anatoxin-a. Because of the formation of all stereoisomers at C-2 and C-5, their synthetic strategy required transforming all four diastereomers into the desired products. With the aim of obtaining the (+)-anatoxin-a, deoxygenation of the ketone group (C-5) in the common intermediate **52** and a one carbon side-chain extension (C-2) formed the pathway to initially reach the *t*Boc-dihydroanatoxin-a (**44**; Scheme 7.11) (Petersen, Fels, and Rapoport 1984; Sardina et al. 1989). Conversion of the *t*Boc-dihydroanatoxin-a into *t*Boc-anatoxin-a **54** was another important transformation in this synthesis (Petersen, Fels, and Rapoport 1984; Koskinen and Rapoport 1985). The reaction of *tert*-butyldimethylsilyl enol ether **53** with phenylselenenyl chloride (PhSeCl), followed by oxidation with *m*-chloroperoxybenzoic acid (MCPBA) afforded (1*R*)-*t*Boc-anatoxin-a (**54**) in 84% yield (Sardina et al. 1989). Cleavage of the *t*Boc protecting group with trifluoroacetic acid proceeded quantitatively, providing the (+)-anatoxin-a as its hydrochloride salt in 18% overall yield.

Unnatural (–)-anatoxin-a has previously been prepared from L-glutamic acid using the same sequence reactions used for the synthesis of (+)-anatoxin from D-glutamic acid (Petersen, Fels, and Rapoport 1984; Sardina et al. 1989). However, the intermediate **52** might also serve as a precursor to (–)-anatoxin-a by removing the C-2 group. The ester moiety was transformed into its chloride acid and via a reductive radical decarboxylation (Barton et al. 1984, 1987) furnished the (1*S*)-*t*Boc-dihydroanatoxin-a in 82% yield. Double-bond introduction, as shown in the previous Scheme, followed by nitrogen deprotection, gave the (–)-anatoxin-a in 30% overall yield (hydrochloride salt).

### Via Acyl Iminium and Tosyl Iminium Salts

Speckamp and Hiemstra (1985) proposed a similar approach to anatoxin-a synthesis by applying their previous work on *N*-acyliminium chemistry. The use of a carbomethoxy group on the nitrogen, inside an alkyl group, would enhance the electrophilicity of the iminium ion owing to the electron-attracting



**Scheme 7.11.** Transformation of the *t*Boc-dihydroanatoxin-a **44** into anatoxin-a. (a) NaH, THF; TBMSCl, Et<sub>3</sub>N, THF, 98%. (b) PhSeCl, THF, –78°C. (c) MCPBA, THF, 0°C, 84%. (d) TFA, CH<sub>2</sub>Cl<sub>2</sub>. (e) HCl, EtOH, 97%.



properties of the carbonyl group on nitrogen (Maryanoff et al. 2004; Speckamp and Moolenaar 2000). This could be advantageous in the cyclization step and reduce the number of protection-deprotection steps of nitrogen. In their first published synthesis (Melching et al. 1986), they used an  $\alpha,\beta$ -unsaturated ketone as a nucleophile in the lateral chain of the pyrrolidine **56** (Scheme 7.12), which was synthesized starting from the succinimide **55**, leading in a more direct way to the desired unsaturated bicyclic system.

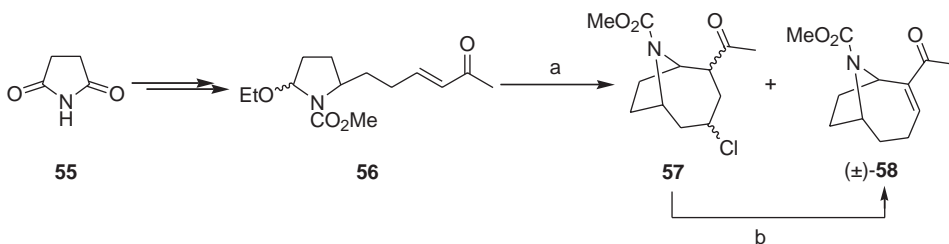
In this cyclization the  $\alpha$ -carbon of this  $\alpha,\beta$ -unsaturated ketone formally reacts as the nucleophilic centre with the *N*-acyliminium ion, bringing the corresponding *N*-acyl anatoxin-a (**58**). To achieve this cyclization, the compound **56** was treated with HCl in MeOH at  $-50^\circ\text{C}$ , affording a mixture of **58** and the chloride **57** (11% and 47%, respectively) (Wijnberg and Speckamp 1981). The chlorides were converted into **58** by refluxing in toluene in the presence of DBN to give the pure enone in 60% yield. The synthesis of ( $\pm$ )-anatoxin-a was completed through *N*-deprotection using iodotrimethylsilane in refluxing acetonitrile (55% yield). The overall unoptimized yield from succinimide was between 3% and 4%.

The second proposal by Speckamp and co-workers used an allylsilane as an excellent nucleophile for an *N*-acyliminium cyclization reaction (Esch et al. 1987) (Scheme 7.13). The  $\beta$ -effect of the silicon atom is a powerful determinant of the regiochemistry of allylsilane reactions with electrophiles, so the new carbon-carbon bond is formed at the vinyl carbon distal to silicon, that is, at the  $\gamma$ -position (Hiemstra et al. 1984, 1985).

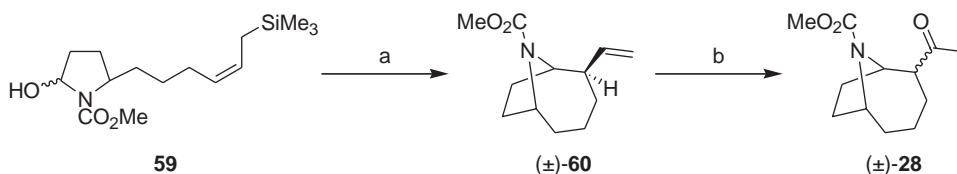
Allylsilane **59** was obtained by initial reaction of the succinimide **55** with the corresponding Grignard alkylsilane and a subsequent simple sequence of reactions. This allylsilane was readily cyclized in formic acid at room temperature to **60**, which was subjected to a Wacker oxidation (Tsuji 1984) to afford the dihydroanatoxin-a derivative **28**. The nitrogen deprotection step with iodotrimethylsilane (Melching et al. 1986) furnished the ( $\pm$ )-dihydroanatoxin-a, which was reprotected with 'Boc according to the previously discussed Rapoport methodology (Sardina et al. 1989) to furnish the racemic ( $\pm$ )-anatoxin-a. The overall yield of this synthesis was 7% from the succinimide.

Somfai et al. demonstrated that it is also possible to use *N*-sulphonyl groups (Somfai and Åhman 1992; Åhman and Somfai 1992; Weinreb 1997) using the same concept for the cyclization step developed by Speckamp with the allylsilanes (Esch et al. 1987). In this case, the starting product was the L-pyroglutamic acid, inside the succinimide (Esch et al. 1987), allowing the enantioselective synthesis of the (+)-anatoxin-a. The key step consisted of an intramolecular cyclization of an *N*-tosyl iminium ion, catalysed by a Lewis acid,  $\text{TiCl}_4$ , to set up the desired bicyclic ring system (Somfai and Åhman 1992).

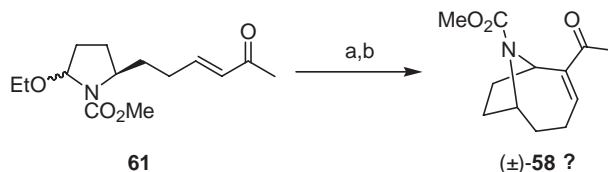
Somfai et al. also carried out the cyclization involving an  $\alpha,\beta$ -unsaturated ketone and the *N*-tosyl iminium ion (Somfai and Åhman 1992) under the same cyclization conditions that were developed



**Scheme 7.12.** Cyclization of an *N*-acyliminium ion with an  $\alpha,\beta$ -unsaturated ketone. (a) HCl, MeOH,  $-50^\circ\text{C}$ – $-20^\circ\text{C}$ . (b) DBN, toluene, reflux, 60%.



**Scheme 7.13.** Cyclization of an *N*-acyliminium ion with an allylsilane. (a) Formic acid, rt 73% (exo:endo, 19:1). (b) PdCl<sub>2</sub>, CuCl, O<sub>2</sub>, DMF/H<sub>2</sub>O, 64%.



**Scheme 7.14.** Cyclization of an *N*-Acyliminium ion with an  $\alpha,\beta$ -unsaturated ketone. (a) HCl, MeOH,  $-50^{\circ}\text{C}$  to rt. (b) DBU, toluene, reflux, 51% overall yield.

previously by Hiemstra and Speckamp (Melching et al. 1986), yielding the *N*-tosylanatoxin-a and the corresponding saturated  $\beta$ -chloroketone (see Scheme 7.12). Finally, removal of the *N*-tosyl group with sodium amalgam afforded (+)-anatoxin-a. Nonetheless, both Somfai group approaches have low overall yields (4–8%) due to the long sequence for achieving the key intermediate in the cyclization step.

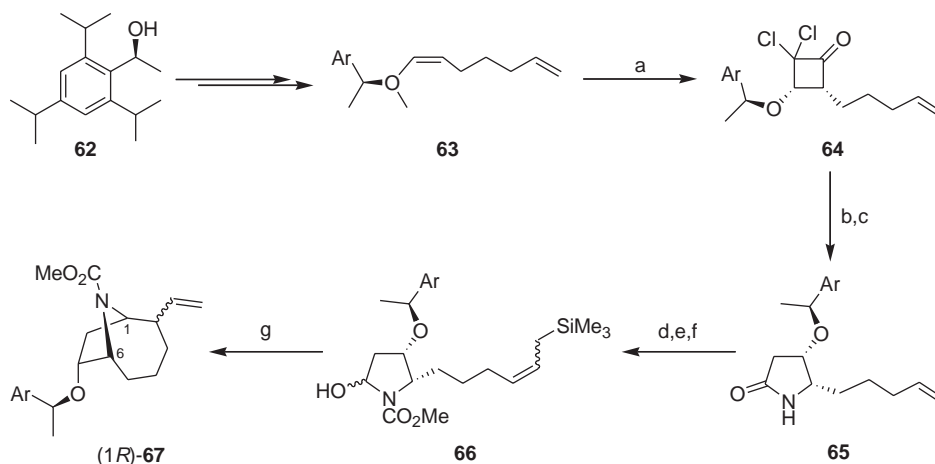
Two other approaches using acyl iminium ion intermediates were developed by the Shono (Shono et al. 1987) and Skrinjar (Skrinjar et al. 1992) groups in a synthesis of racemic and (+)-anatoxin-a, respectively.

Recently, a new attempt to synthesise (+)-anatoxin-a was published by Tanner and co-workers (Hjelmgaard et al. 2005). They transformed the L-pyrroglutamic acid into the intermediate **61** (Scheme 7.14), performing some improvements for achieving the lateral chain with the  $\alpha,\beta$ -unsaturated ketone compared with the Speckamp (Melching et al. 1986) and Somfai (Somfai and Åhman 1992) approaches. They carried out the cyclization of **61** under Speckamp and Hiemstra conditions, also used by Somfai.

The desired bicycle **58** was obtained, but oddly the enantiopurity of the previous intermediate was lost, and the bicycle was a completely racemic mixture. It was an unexpected result in view of the previous work by Somfai describing the same reaction leading to enantiopure product from the *N*-tosyl analogue (with a methoxy instead ethoxy group in the  $\alpha$ -position) (Skrinjar et al. 1992; Somfai and Åhman 1992). Although there was no logical explanation for these discrepancies, they proposed that the racemization could go via hydride abstraction by the iminium ion. As a result, a different ( $\pm$ )-anatoxin-a synthesis was completed by deprotection (TMSI) (Manfré et al. 1992) in 65% yield (9% overall for nine steps).

The most recent formal asymmetric synthesis of (+)-anatoxin-a was achieved through a highly diastereoselective [2+2] cycloaddition of dichloroketene with a chiral enol ether (**63**; Scheme 7.15) in order to reach the general structure of 2,5-disubstituted pyrrolidine (**66**) for generating the acyliminium ion and getting the required bicycle skeleton (**67**) (Muniz et al. 2005).

The [2+2] cycloaddition of this chiral enol ether **63** with *in situ* generated dichloroketene proceeded with a high level of facial discrimination (95:5) to afford dichlorocyclobutanone **64** (Greene



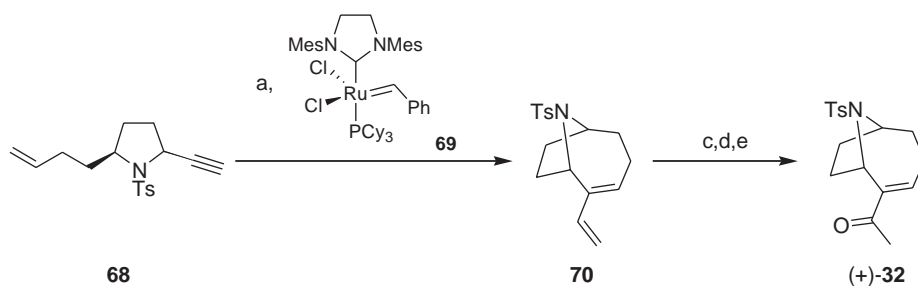
**Scheme 7.15.** (a) Zn-Cu,  $\text{Cl}_3\text{CCOCl}$ , diethylether. (b)  $\text{NH}_2\text{OSO}_2\text{C}_6\text{H}_2(\text{CH}_3)_3$ ,  $\text{CH}_2\text{Cl}_2$ ;  $\text{Al}_2\text{O}_3$ , MeOH. (c) Zn-Cu,  $\text{NH}_4\text{Cl}$ , MeOH, (36% from 62). (d)  $n\text{-C}_4\text{H}_9\text{Li}$ , THF;  $\text{NCCO}_2\text{CH}_3$ , 91%. (e)  $\text{LiB}(\text{C}_2\text{H}_5)_3\text{H}$ , THF, 92%. (f)  $\text{CH}_2=\text{CHCH}_2\text{Si}(\text{CH}_3)_3$ , second generation Grubbs' catalyst,  $\text{CH}_2\text{Cl}_2$ , 74%. (g) Formic acid,  $\text{CH}_2\text{Cl}_2$ , 77%. Ar = 2,4,6-triisopropylphenyl.

and Charbonier 1985). This adduct was submitted to Beckmann ring expansion (Tamura et al. 1977) and subsequent dechlorination (Johnston et al. 1985) of the resultant  $\alpha,\alpha$ -dichlorolactam gave the lactam **65**. This lactam was *N*-protected, and the formation of the allylsilane was achieved through cross metathesis using second generation Grubbs' catalyst (Scholl et al. 1999), obtaining the key intermediate **66**, equivalent to the Speckamp **59** (see Scheme 7.13). The cyclization reaction was performed under the same Speckamp conditions using formic acid to reach the desired bicycle **67** (Esch et al. 1987). The ether group (C-7) was transformed into the alcohol and removed through its transformation into the iodide and posterior reduction affording the compound (1*R*)-**60**, previously obtained as a racemic mixture. Conversion into the (+)-anatoxin-a was performed using the methodology previously developed by Speckamp (Esch et al. 1987).

## Synthesis of Anatoxin-a via Enyne Metathesis

Although much emphasis has been placed on the importance of alkene metathesis in organic synthesis (Didier 2005), alkyne metathesis is also significant. Metathesis reactions of alkynes with alkenes and metathesis reactions of alkynes with alkynes have both been carried out efficiently (Storm and Madsen 2005). Among the various metathesis reactions, the most commonly used is the ring-closing metathesis (RCM). The large number of cyclic natural products that have been obtained using RCM as one of the key steps is evidence of the synthetic efficiency of this methodology (Deiters et al. 2004). The utility of the process for the synthesis of functionalized, bridged nitrogen heterocycles had been established in many cases (Deiters et al. 2004; Randl and Blechert 2003; Martin 2005) since the seminal discovery by Grubbs and Fu in 1992 that RCM could be applied to the formation of heterocycles (Grubbs and Fu 1992a, 1992b).

In fact, the enantiospecific syntheses of the two potent anti-Alzheimer's agents like (+)-ferruginine (Aggarwal et al. 2004), a tropane ring system, and two enantiospecific syntheses of the anatoxin-a, were submitted essentially simultaneously at the beginning of 2004 (Mori et al. 2004; Brenneman and



**Scheme 7.16.** Ring closing metathesis reaction to obtain *N*-tosylanatoxin-a. (a) BuLi, TMSCl, 95%. (b) second generation Grubbs' catalyst **69**, CH<sub>2</sub>Cl<sub>2</sub>, 85%. (c) Hg(OAc)<sub>2</sub>. (d) NaBH<sub>4</sub>, 42%. (e) Dess-Martin oxidation, 86%.

Martin 2004; Brenneman, Machauer, and Martin 2004). In each case, the starting material used was the inexpensive pyroglutamic acid, and additionally the synthesis depended on Ru-catalyzed alkyne-alkene metathesis (Grubbs' catalysts). The first report applying this methodology to anatoxin-a synthesis belongs to the Mori group (Mori et al. 2004). They developed the synthesis of *N*-tosyl anatoxin-a by metathesis of an enyne in the substituent on a 2,5-*cis*-pyrrolidine derivative (**68**; Scheme 7.16) synthesized from L-pyroglutamic acid.

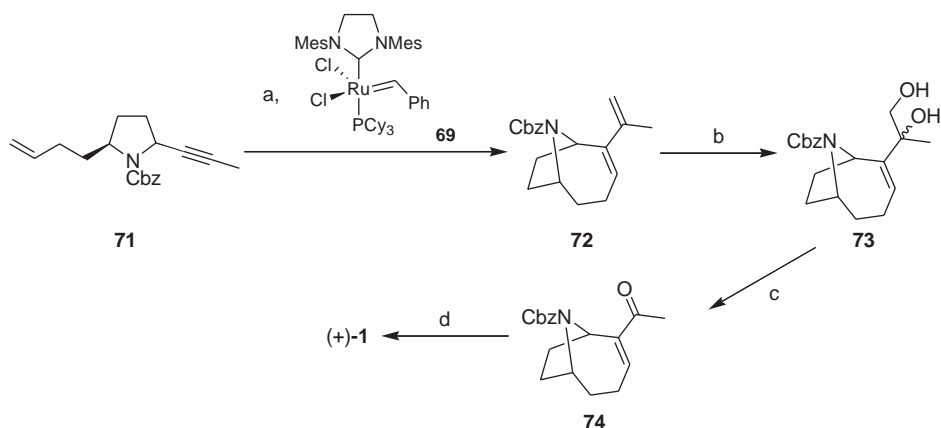
With this key compound, the metathesis reaction was carried out with the second generation Grubbs' catalyst **69** (Scholl et al. 1999), following protection on the alkyne with silyl group. Thus, they obtained the desired bicycle **70** in 85% yield. The desilylation process occurred during the reaction. In order to achieve the  $\alpha,\beta$ -unsaturated ketone moiety, the oxymercuration of **70** followed by treatment with NaBH<sub>4</sub>, was carried out and then the resultant alcohol was subjected to Dess-Martin oxidation to afford *N*-tosylanatoxin-a (**32**), whose spectral data and  $[\alpha]_D^{20}$  value agreed with those reported in the literature (Somfai and Åhman 1992). Since the transformation into anatoxin-a could be performed with the same procedure developed previously (Somfai and Åhman 1992), they achieved the total synthesis of (+)-anatoxin-a.

The second reported synthesis was by Martin and co-workers (Brenneman and Martin 2004; Brenneman, Machauer, and Martin 2004; Martin 2005). Fundamentally, this synthesis differs with respect to the previous one in the strategy for achieving the synthesis of the *cis*-2,5-disubstituted pyrrolidine **71** (Scheme 7.17). The starting product in this case was the D-methyl pyroglutamate.

The reaction of ring closing metathesis was performed with the second generation Grubbs' catalyst, like in the previous case. The bicyclic compound **72** was obtained with 87% yield. The terminal alkene in **72** was dihydroxylated affording the diol **73**. The diol moiety was cleaved with periodate to deliver the *N*-protected anatoxin-a **74**, which was deprotected with TMSI affording (+)-1 in near quantitative yield. They completed the (+)-anatoxin-a in 9-step synthesis with an overall yield of 27% from commercially available D-methyl pyroglutamate.

## Other Synthetic Approaches to Anatoxin and Analogues

Many natural azabicyclo derivatives have been reported to exhibit agonist activity for nicotinic receptors, such as (-)-epibatidine (Fig. 7.3A) and (+)-ferruginine (Fig. 7.3B), both less potent than (+)-anatoxin-a. The biological activity of these compounds emerges from their structural similarity with nicotine. It therefore appeared interesting to design a general access to azabicyclo[*n*.2.1]alkanes (Fig. 7.3C) that could also be valuable for the synthesis of these alkaloids and some of their analogues.



**Scheme 7.17.** Ring closing metathesis reaction to obtain (+)-anatoxin-a. (a) second generation Grubbs catalyst 69, CH<sub>2</sub>Cl<sub>2</sub>, 87%. (b) OsO<sub>4</sub>, EtN<sub>3</sub>, THF, -78°C to rt, then aq. NaHSO<sub>3</sub>, Δ, 76%. (c) NaIO<sub>4</sub>, THF/H<sub>2</sub>O, rt, 95%. (d) TMSI, CH<sub>3</sub>CN, -10°C, 99%.

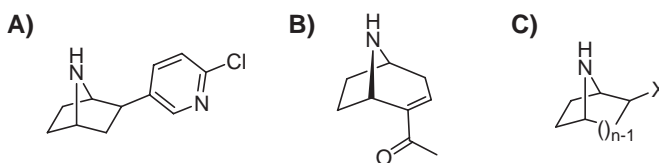


**Figure 7.3.** Similar alkaloids to anatoxin-a with agonist activity for nicotinic receptors: (A) (-)-epibatidine, (B) (+)-ferruginine, and (C) azabicyclo[*n*.2.1]alkanes.

Recently, some different methodologies were devised in order to synthesise these systems in a general way. Thus, Pandey studied the [3+2] cycloaddition of cyclic azomethine ylides with suitable dipolarophiles (Pandey et al. 2002), Royer applied the CN(*R,S*) strategy (Gillaizeau-Gauthier et al. 2002), and Ateeq and Simpkins explored higher order cycloaddition reactions [6+2] mediated by chromium (Ateeq 1994; Beckwith et al. 2002). Although they generated some of the azabicycles, none of them reached anatoxin-a.

Taking into account the potent agonist character of anatoxin-a toward the acetylcholine receptors and its chiral and semi-rigid skeleton renders anatoxin-a as the perfect substrate for making structural modifications in order to study the structure-activity relationships. Relevant contributions to the synthesis of anatoxin-a analogues were by Rapoport (Sardina et al. 1989, 1990; Hernandez and Rapoport 1994) and Gallagher (Huby et al. 1991; Brough et al. 1992; Wonnacott et al. 1992; Magnus et al. 1997) groups, as well as structure-activity relationship studies (Swanson et al. 1986, 1989, 1991; Wonnacott et al. 1991; Thomas et al. 1994).

The simple alkyl derivatives such homo-, propyl-, and *iso*-propylanatoxin-a (Fig. 7.4A) are all potent nicotinic ligands (Wonnacott et al. 1992). Most of the efforts to determine the precise structural requirements of the receptor have resulted in the synthesis of conformationally restricted derivatives (Hernandez and Rapoport 1994; Brough et al. 1992). The first bioisosteric and conformationally constrained variation of (+)-anatoxin-a found to retain much of the potency of the natural compound was racemic (±)-pyrido[3,4-*b*]homotropane (PHT) (Fig. 7.4B), representing the

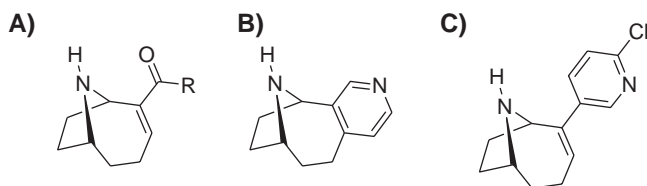


**Figure 7.4.** The most active anatoxin-a analogues: (A) homoanatoxin-a ( $R = C_2H_5$ ), propylanatoxin-a ( $R = C_3H_7$ ), isopropylanatoxin-a ( $R = CH(CH_3)_2$ ); (B) ( $\pm$ )-pyrido[3,4-b]homotropine (PHT); (C) UB-165.

conceptual combination of anatoxin-a and nornicotine (Kanne and Abood 1988). Novel analogues of PHT have also been developed (Gündisch et al. 2002).

Another hybrid anatoxin-a/epibatidine, UB-165 (Fig. 7.4C), was synthesized by the Gallagher group (Wright et al. 1997). It was identified as a potent nicotinic ligand and showed a potency that was intermediate between anatoxin-a and epibatidine. Different derivatives of this compound have been synthesized lately (Gohlke et al. 2002; Sutherland et al. 2003; Karig et al. 2003).

Anatoxin-a is a useful core structure for nicotinic drug design. For this reason, synthetic approaches to anatoxin-a are still active research areas, open to new proposals, and the search for new analogues that would act like drugs in the treatment of brain disease is still an important task in medicinal chemistry (Breining 2004).

## References

- Aggarwal, V.K., Astle, C.J., and Rogers-Evans, M. A. 2004. Concise asymmetric route to the bridged bicyclic tropane alkaloid ferruginine using enyne ring-closing metathesis. *Org Lett* 6, 1469–1471.
- Aggarwal, V.K., Humphries, P.S., and Fenwick, A. 1999. A formal asymmetric synthesis of (+)-anatoxin-a using an enantioselective deprotonation strategy on an eight-membered ring. *Angew Chem Int Ed* 38, 1985–1986.
- Åhman, J., and Somfai, P. 1992. Carbon-carbon bond formation via *N*-tosyliminium ions. *Tetrahedron* 48, 9537–9544.
- Andersson, C.-M., and Hallberg, A. 1989. Palladium-catalyzed vinylation of alkyl vinyl ethers with enol triflates. A convenient synthesis of 2-alkoxy 1,3-dienes. *J Org Chem* 54, 1502–1505.
- Arisawa, M., Torisawa, Y., Kawahara, M., Yamanaka, M., Nishida, A., and Nakagawa, M. 1997. Lewis acid-promoted coupling reactions of acid chlorides with organoaluminum and organozinc reagents. *J Org Chem* 62, 4327–4329.
- Ateeq, H.S. 1994. Higher order cycloaddition reactions in natural products synthesis. *Pure and Appl Chem* 66, 2029–2032.
- Banwell, M.G., and Reum, M.E. 1991. *Advances in Strain in Organic Chemistry*, vol. 1, ed. Halton, B. Greenwich, CT: JAI Press, 19–64.
- Barrelle, M., and Appar, M. 1976. Obtention de derives azabicyclononaniques *N*-phenyles par aminomercuration intramoléculaire. *Tetrahedron Lett* 30, 2611–2614.
- . 1977. Aminomercuration intramoléculaire d'aziridines cycloocténiques et de leurs aminoalcools précurseurs. *Tetrahedron* 33, 1309–1319.
- Barton, D.H.R., Bridon, D., Fernandez-Picot, I., and Zard, S.Z. 1987. The invention of radical reactions: Part XV. Some mechanistic aspects of the decarboxylative rearrangement of thiohydroxamic esters. *Tetrahedron* 43, 2733–2740.
- Barton, D.H.R., Herve, Y., Potier, P., and Thiery, J. 1984. Reductive radical decarboxylation of amino-acids and peptides. *J Chem Soc Chem Commun* 1298–1299.
- Bastable, J.W., Hobson, J.D., and Ridell, W.D. 1972. Transannular cyclization of cyclo-olefinic *N*-chloro-amines. Synthesis of azabicyclic compounds. *J Chem Soc Perkin Trans 1*, 2205–2213.
- Bates, H.A., and Rapoport, H. 1979. Synthesis of anatoxin-a via intramolecular cyclization of iminium salts. *J Am Chem Soc* 101, 1259–1265.
- Beckwith, R.E.J., Gravestock, M.B., and Simpkins, N.S. 2002. Nucleophilic addition reactions of bridged triene  $h^6$ -chromiumtricarboxyl complexes. *J Chem Soc Perkin Trans 1*, 2352–2359.
- Borch, R.F., and Ho, B.C. 1977. A new synthesis of the pyrrolizidine alkaloids ( $\pm$ )-isoretronecanol and ( $\pm$ )-trachelanthamidine. *J Org Chem* 32, 1225–1227.

- Breining, S.R. 2004. Recent developments in the synthesis of nicotinic acetylcholine receptor ligands. *Curr Top Med Chem* 4, 609–629.
- Brenneman, J.B., Machauer, R., and Martin, S.F. 2004. Enantioselective synthesis of (+)-anatoxin-a via enyne metathesis. *Tetrahedron* 60, 7301–7314.
- Brenneman, J.B., and Martin, S.F. 2004. Application of intramolecular enyne metathesis to the synthesis of aza[4.2.1]bicyclics: Enantiospecific total synthesis of (+)-anatoxin-a. *Org Lett* 6, 1329–1331.
- Brough, P.A., Gallagher, T., Thomas, P., Wonnacott, S., Baker, R., Abdul Malik, K.M., and Hursthouse, M.B. 1992. Synthesis and X-Ray crystal structure of 2-acetyl-9-azabicyclo[4.2.1]nonan-3-one. A conformationally locked *s-cis* analogue of anatoxin-a. *J Chem Soc Chem Commun* 1087–1089.
- Bunn, B.J., Cox, P.J., and Simpkins, N.S. 1993a. Enantioselective deprotonation of 8-oxabicyclo[3.2.1]octan-3-one systems using homochiral lithium amide bases. *Tetrahedron* 49, 207–218.
- Bunn, B.J., Simpkins, N.S., Spavold, Z., and Crimmin, M.J. 1993b. The effect of added salts on enantioselective transformations of cyclic ketones by chiral lithium amide bases. *J Chem Soc Perkin Trans* 1, 3113–3116.
- Cain, C.M., Cousins, R.P.C., Coubarides, G., and Simpkins, N.S. 1990. Asymmetric deprotonation of prochiral ketones using chiral lithium amide bases. *Tetrahedron* 46, 523–544.
- Campbell, H.F., Edwards, O.E., Elder, J.W., and Kolt, R.J. 1979. Total Synthesis of DL-anatoxin-a and DL-isoanatoxin-a. *Pol J Chem* 53, 27–37.
- Campbell, H.F., Edwards, O.E., and Kolt, R. 1977. Synthesis of *nor*-anatoxin-a and anatoxin-a. *Can J Chem* 55, 1372–1379.
- Carmichael, W.W., Biggs, D.F., and Gorham P.R. 1975. Toxicology and pharmacological action of *Anabaena flos-aquae* toxin. *Science* 187, 542–544.
- Chiou, W.H., Lee, S.Y., and Ojima, I. 2005. Recent advances in cyclohydrocarbonylation reactions. *Can. J. Chem* 83, 681–692.
- Comins, D.L., and Deghani, A. 1992. Pyridine-derived triflating reagents: An improved preparation of vinyl triflates from metallo enolates. *Tetrahedron Lett* 33, 6299–6302.
- Corey, E.J., and Chaykovsky, M. 1962. Dimethylsulfoxonium methylide. *J Am Chem Soc* 84, 867–868.
- Danheiser, R.L., Morin, J.M., Jr., and Salaski, E.J. 1985. Efficient total synthesis of ( $\pm$ )-anatoxin-a. *J Am Chem Soc* 107, 8066–8073.
- Dauben, W.G., Schutte, L., and Wolf, R.E. 1969. Solution photolysis of *cis*- and *trans*-2-methylcyclopropyl methyl ketone. *J Org Chem* 34, 1849–1851.
- Dean, R.T., Padgett, H.C., and Rapoport, H. 1976. A high yield regiospecific preparation of iminium salts. *J Am Chem Soc* 98, 7448–7449.
- Deiters, A., and Martin, S.F. 2004. Synthesis of oxygen- and nitrogen-containing heterocycles by Ring-Closing Metathesis (a review of RCM reactions). *Chem Rev* 104, 2199–2238.
- Denmark, S.E., and Edwards, J.P. 1991. A comparison of (chloromethyl)- and (iodomethyl)zinc cyclopropanation reagents. *J Org Chem* 56, 6974–6981.
- Devlin, J.P., Edwards, O.E., Gorham, P.R., Hunter, N.R., and Stavric, B. 1977. Anatoxin-a, a toxic alkaloid from *anabaena-flos-aquae* NRC-44H. *Can J Chem* 55, 1367–1371.
- Didier, A. 2005. The metathesis reactions: from a historical perspective to recent developments. *New J Chem* 29, 42–56.
- D'Incan, E., and Seyden-Penne, J. 1975. Ion Pair Extraction: Alkylation of phosphonates and the Wittig/Horner Reaction. *Synthesis* 516–517.
- Esch, P.M., Hiemstra, H., Klaver, W.J., and Speckamp, W.N. 1987. An *N*-acyliminium route to the 8-azabicyclo[3.2.1]octane (tropane) and the 9-azabicyclo[4.2.1]nonane ring system. Synthesis of ( $\pm$ )-anatoxin-a. *Heterocycles* 26, 75–79.
- Ferguson, J.R., Lumbard, K.W., Scheinmann, F., Stachulski, A.V., Stjernlöf, P., and Sundell, S. 1995. Efficient new syntheses of (+)- and (–)-anatoxin-a. Revised configuration of resolved 9-methyl-9-azabicyclo[4.2.1]nonan-2-one. *Tetrahedron Lett* 36, 8867–8870.
- Fischli, A., and Eschenmoser, A. 1967. A synthetic route to metal-free corrins. *Angew Chem Int Ed* 6, 866–868.
- Forró, E., Árva, J. and Fülöp, F., 2001. Preparation of (1*R*,8*S*)- and (1*S*,8*R*)-9-azabicyclo[6.2.1]dec-4-en-10-one: potential starting compounds for the synthesis of anatoxin-a. *Tetrahedron Asymmetry* 12, 643–649.
- Gillaizeau-Gauthier, I., Royer, J., and Husson, H.-P. 2002. Toward an asymmetric general access to azabicyclo[*n*.2.1]alkanes according to the CN(*R,S*) method. *Eur J Org Chem* 1484–1489.
- Gohlke, H., Gündisch, D., Schwarz, S., Seitz, G., Tilotta, M.C., and Wegge, T. 2002. Synthesis and nicotinic binding studies on enantiopure diazine analogues of the novel (2-chloro-5-pyridyl)-9-azabicyclo[4.2.1]non-2-ene UB-165. *J Med Chem* 45, 1064–1072.
- Greene, A.E., and Charbonier, F. 1985. Asymmetric induction in the cyclo-addition reaction of dichloroketene with chiral enol ethers. A versatile approach to optically-active cyclopentenone derivatives. *Tetrahedron Lett* 26, 5525–5528.



- Grieco, P.A., Nishizawa, M., and Marisovic, N. 1976. Remote double bond migration via rhodium catalysis: A novel enone transposition. *J Am Chem Soc* 98, 7102–7104.
- Grubbs, R.H., and Fu, G.C. 1992a. The application of catalytic ring-closing olefin metathesis to the synthesis of unsaturated oxygen heterocycles. *J Am Chem Soc* 114, 5426–5427.
- . 1992b. The synthesis of nitrogen heterocycles via catalytic ring-closing metathesis of dienes. *J Am Chem Soc* 114, 7324–7325.
- Gündisch, D., Kämpchen, T., Schwarz, S., Seitz, G., Siegl, J., and Wegge, T. 2002. Syntheses and evaluation of pyridazine and pyrimidine containing bioisosteres of ( $\pm$ )-pyrido[3.4-b]homotropane and pyrido-[3.4-b]tropene as novel nAChR ligands. *Bioorg Med Chem* 10, 1–9.
- Ham, W.-H., Jung, Y.H., Lee, K., Oh, C.-Y., and Lee, K.-Y. 1997. A formal total synthesis of ( $\pm$ )-ferruginine by Pd-catalyzed intramolecular aminocarbonylation. *Tetrahedron Lett* 38, 3247–3248.
- Hardegger, E., and Ott, H. 1955. Konfiguration des cocains und derivate der ecgoninsäure. *Helv Chim Acta* 38, 312–320.
- Hernandez, A., and Rapoport, H. 1994. Conformationally constrained analogues of anatoxin. chiroselective synthesis of *s-trans* carbonyl ring-fused analogues. *J Org Chem* 59, 1058–1066.
- Hiemstra, H., Klaver, W.J., and Speckamp, W.N. 1984. W-Alkoxy lactams as dipolar synthons. Silicon-assisted synthesis of azabicycles and a  $\beta$ -amino acid. *J Org Chem* 49, 1149–1151.
- Hiemstra, H., Sno, M.H.A.N., Vijn, R.J., and Speckamp, W.N. 1985. Silicon directed *n*-acyliminium ion cyclizations. highly selective syntheses of ( $\pm$ )-isoretroecanone and ( $\pm$ )-epilupinine. *J Org Chem* 50, 4014–4020.
- Hjelmgaard, T., Sjøtofte, I., and Tanner, D. 2005. Total synthesis of pinnamine and anatoxin-a via a common intermediate. A caveat on the anatoxin-a endgame. *J Org Chem* 70, 5688–5697.
- Huber, C.S. 1972. The crystal structure and absolute configuration of 2,9-diacetyl-9-azabicyclo[4.2.1]non-2,3-ene. *Acta Cryst B* 28, 2577–2582.
- Huby, N.J.S., Kinsman, R.G., Lathbury, D., Vernon, P.G., and Gallagher, T. 1991. Synthetic and stereochemical studies directed towards anatoxin-a. *J Chem Soc Perkin Trans 1*, 145–155.
- Huby, N.J.S., Thompson, P., Wonnacott, S., and Gallagher, T. 1991. Structural modification of anatoxin-a: synthesis of model affinity ligands for the nicotinic acetylcholine receptor. *J Chem Soc Chem Commun* 243–245.
- Ito, Y., Fujii, S., and Saegusa, T. 1976. Reaction of 1-silyloxybicyclo[*n*.1.0]alkanes with Fe<sup>III</sup>Cl<sub>3</sub>. A facile synthesis of 2-cycloalkenones via ring enlargement of cyclic ketones. *J Org Chem* 41, 2073–2074.
- Johnston, B.D., Slessor, K.N., and Oehlschlager, A.C. 1985. Synthesis of ( $\pm$ )-lineatin by 2+2 cycloaddition of dichloroketene with a cyclic allyl ether. *J Org Chem* 50, 114–117.
- Jończyk, A., Bańko, K., and Makosza, M. 1975. Some carbanionic reactions of halomethyl aryl sulfones. *J Org Chem* 40, 266–267.
- Jung, M.E., and Lyster, M.A. 1978. Conversion of alkyl carbamates into amines via treatment with trimethylsilyliodide. *J Chem Soc Chem Commun* 315–316.
- Kanne, D.B., and Abood, L.G. 1988. Synthesis and biological characterization of pyridohomotropanes. structure-activity relationships of conformationally restricted nicotinoids. *J Med Chem* 31, 506–509.
- Karig, G., Large, J.M., Sharples, C.G.V., Sutherland, A., Gallagher, T., and Wonnacott, S. 2003. Synthesis and nicotinic binding of novel phenyl derivatives of UB-165. identifying factors associated with  $\alpha 7$  selectivity. *Bioorg Med Chem Lett* 13, 2825–2828.
- Koskinen, A., and Lousnasmaa, M. 1983. Novel applications of the modified polonovski reaction. 6. Mild general-synthesis of 4-substituted piperidines. *J Chem Soc Chem Commun* 821–822, and references therein.
- Koskinen, A.M.P., and Rapoport, H. 1985. Synthetic and conformational studies on anatoxin-a: a potent acetylcholine agonist. *J Med Chem* 28, 1301–1309.
- Lindgren, B., Stjernöf, P., and Trogen, L. 1987. Synthesis of anatoxin-a. a constituent of blue-green freshwater algae. *Acta Chem Scand B* 41, 180–183.
- Luker, T., Hiemstra, H., and Speckamp, W.N. 1997. Total synthesis of desoxopropoxyphylline: application of a lactam-derived enol triflate to natural product synthesis. *J Org Chem* 62, 3592–3596.
- Magnus, N.A., Ducry, L., Rolland, V., Wonnacott, S., and Gallagher, T. 1997. Direct C-11 functionalisation of anatoxin-a. Application to the synthesis of new ligand-based structural probes. *J Chem Soc Perkin Trans 1*, 2313–2318.
- Majewski, M., Lazny, R., and Nowak, P. 1995. Effect of lithium salts on enantioselective deprotonation of cyclic ketones. *Tetrahedron Lett* 36, 5465–5468.
- Manfré, F., Kern, J.-M., and Biellman, J.-F. 1992. Syntheses of proline analogs as potential mechanism-based inhibitors of proline dehydrogenase: 4-methylene-1-, (*e*)- and (*z*)-4-(fluoromethylene)-1-, *cis*- and *trans*-5-ethynyl-( $\pm$ )-, and *cis*- and *trans*-5-vinyl-1-proline. *J Org Chem* 57, 2060–2065.
- Mansell, H.L. 1996. Synthetic approaches to anatoxin-a. *Tetrahedron* 52, 6025–6061.

- Martin, S.F. 2005. Ring-Closing metathesis: A facile construct for alkaloid synthesis. *Pure and Appl. Chem* 77, 1207–1212.
- Marvell, E.N. 1980. *Thermal Electrocyclic Reactions*. New York: Academic Press, 23–53.
- Maryanoff, B.E., Zhang, H.-C., Cohen, J.H., Turchi, I.J., and Maryanoff, C. 2004. Cyclizations of *N*-acyliminium ions. *Chem Rev* 104, 1431–1628.
- Melching, K.H., Hiemstra, H., Klaver, W.J., and Speckamp, W.N. 1986. Total synthesis of ( $\pm$ )-anatoxin-a via *N*-acyliminium intermediates. *Tetrahedron Lett* 27, 4799–4802.
- Mori, M., Tomita, T., Kita, Y., and Kitamura, T. 2004. Synthesis of (+)-anatoxin-a using enyne metathesis. *Tetrahedron Lett* 45, 4397–4399.
- Muniz, M.N., Kanazawa, A., and Greene, A.E. 2005. Formal synthesis of (+)-anatoxin-a by asymmetric [2+2] cycloaddition. *Synlett* 1328–1330.
- Nahm, S., and Weinreb, S.M. 1981. *N*-methoxy-*N*-methylamides as effective acylating agents. *Tetrahedron Lett* 22, 3815–3818.
- Newcombe, N.J., and Simpkins, N.S. 1995. A concise asymmetric synthesis of (–)-anatoxin-a using an enantioselective enolisation strategy. *J Chem Soc Chem Commun* 831–832.
- Nicolaou, K.C., Shi, G.-Q., Gunzer, J.L., Gärtner, P., and Yang, Z. 1997. Palladium-catalyzed functionalization of lactones via their cyclic ketene acetal phosphates. efficient new synthetic technology for the construction of medium and large cyclic ethers. *J Am Chem Soc.* 119, 5467–5468.
- Oh, C.-Y., Kim, K.-S., and Ham, W.-H. 1998. A formal total synthesis of ( $\pm$ )-anatoxin-a by an intramolecular Pd-catalyzed aminocarbonylation reaction. *Tetrahedron Lett* 39, 2133–2136.
- Pandey, G., Laha, J.K., and Lakshmaiah, G. 2002. Stereoselective construction of X-azabicyclo[*m*.2.1]alkanes by [3+2]-cycloaddition of non-stabilized cyclic azomethine ylides: synthesis of enantiopure constrained amino acids and formal total synthesis of optically active epibatidine. *Tetrahedron* 58, 3525–3534.
- Parsons, P.J., Camp, N.P., Edwards, N., and Sumoreeah, L.R. 2000. Synthesis of ( $\pm$ )-anatoxin-a and analogues. *Tetrahedron* 56, 309–315.
- Parsons, P.J., Camp, N.P., Underwood, J.M., and Harvey, D.M. 1995. A short and efficient route to ( $\pm$ )-anatoxin-a. *J Chem Soc Chem Commun* 1461–1462.
- . 1996. Tandem reactions of anions: a short and efficient route to ( $\pm$ )-anatoxin-a. *Tetrahedron* 52, 11637–11642.
- Petersen, J.S., Fels, G., and Rapoport, H. 1984. Chiroselective syntheses of (+)- and (–)-anatoxin-a. *J Am Chem Soc* 106, 4539–4547.
- Petersen, J.S., Töterberg-Kaulen, S., and Rapoport, H. 1984. Synthesis of ( $\pm$ )-w-aza[x.y.1]bicycloalkanes by an intramolecular Mannich reaction. *J Org Chem* 49, 2948–2953.
- Pitts, J.N., Jr., and Norman, I. 1954. Structure and reactivity in the vapor-phase photolysis of ketones. i. methyl cyclopropyl ketone. *J Am Chem Soc* 76, 4815–4819.
- Podlech, J. 1998. Trimethylsilyldiazomethane (TMS-CHN<sub>2</sub>) and lithiated trimethylsilyldiazomethane—versatile substitutes for diazomethane. *J Prakt Chem.* 340, 679–682.
- Quinn, C.B., and Wiseman, J.R. 1973. Bredt's rule. VI. 9-Oxabicyclo[3.3.1]non-1-ene. *J Am Chem Soc* 95, 1342–1343.
- Quitt, P., Hellerbach, J., and Vogler, K. 1963. Die synthese optisch aktiver *N*-monomethyl-aminosäuren. *Helv Chim Acta* 46, 327–333.
- Randl, S., and Blechert, S. 2003. In *Handbook of Metathesis: Applications in Organic Synthesis*, vol. 2, ed. Grubbs, R.H. Morlenbach: Wiley-VCH.
- Reutrakul, V., and Kanghae, W. 1977. The synthesis of  $\alpha,\beta$ -unsaturated aldehydes by one-carbon homologation of carbonyl compounds. *Tetrahedron Lett* 18, 1377–1380.
- Sakurai, O., Ogiku, T., Takahashi, M., Horikawa, H., and Iwasaki, T. 1994. A new synthetic method of 1b-methylcarbapenems utilizing the eschenmoser sulfide contraction. *Tetrahedron Lett* 35, 2187–2190.
- Sardina, F.J., Howard, M.H., Koskinen, A.M.P., and Rapoport, H. 1989. Chiroselective synthesis of nitrogen and side chain modified analogues of (+)-anatoxin. *J Org Chem* 54, 4654–4660.
- Sardina, F.J., Howard, M.H., Morningstar, M., and Rapoport, H. 1990. enantiodivergent synthesis of (+)- and (–)-anatoxin from l-glutamic acid. *J Org Chem* 55, 5025–5033.
- Scholl, M., Ding, S., Lee, C.W., and Grubbs, R.H. 1999. Synthesis and activity of a new generation of ruthenium-based olefin metathesis catalysts coordinated with 1,3-dimesityl-4,5-dihydroimidazol-2-ylidene ligands. *Org Lett* 1, 953–956.
- Seyferth, D. 1972. Phenyl(trihalomethyl)mercury compounds. Exceptionally versatile dihalocarbene precursors. *Acc Chem Res* 5, 65–74.
- Shiosaki, K., and Rapoport, H. 1985.  $\alpha$ -Amino acids as chiral educts for asymmetric products. chiroselective syntheses of the 5-butyl-2-heptylpyrrolidines from glutamic acid. *J Org Chem* 50, 1229–1239.

- Shono, T., Matsumura, Y., Uchida, K., and Tagami, K. 1987. A new method of formation of 9-azabicyclo-[4.2.1]nonane skeleton and its application to synthesis of ( $\pm$ )-anatoxin-a. *Chem Lett* 919–922.
- Skrinjar, M., Nilsson, C., and Wistrand, L.-G. 1992. An efficient synthesis of (+)-anatoxin-a. *Tetrahedron Asymmetry* 3, 1263–1270.
- Smissman, E.E., and Makriyannis, A. 1973. Azodicarboxylic acid esters as dealkylating agents. *J Org Chem* 38, 1652–1657.
- Somfai, P., and Åhman, J. 1992. A short and enantioselective synthesis of (+)-anatoxin-a. *Tetrahedron Lett* 33, 3791–3794.
- Speckamp, W.N., and Hiemstra, H. 1985. Intramolecular reactions of *N*-acyliminium intermediates. *Tetrahedron* 41, 4367–4416.
- Speckamp, W.N., and Moolenaar, M.J. 2000. New developments in the chemistry of *n*-acyliminium ions and related intermediates. *Tetrahedron* 56, 3817–3856.
- Spivak, C.E., Witkop, B., and Alburquerque, E.X. 1980. Anatoxin-a: a novel, potent agonist at the nicotinic receptor. *Mol Pharmacol* 18, 384–394.
- Stadler, P.A. 1978. Eine einfache veresterungsmethode im eintopf-verfahren. *Helv Chim Acta* 61, 1675–1681.
- Stjernlöf, P., Trogen, L., and Andersson, Å. 1989. Synthesis of (+)- and (–)-anatoxin-a via classical diastereomeric salt resolution. *Acta Chem Scand* 43, 917–918.
- Stork, G., and Ladesman, H.K. 1956. A new ring enlargement sequence. *J Am Chem Soc* 78, 5129–5130.
- Storm, C., and Madsen, R. 2003. Enyne metathesis catalyzed by ruthenium carbene complexes (review of alkyne metathesis reactions). *Synthesis* 1–19.
- Sutherland, A., Gallagher, T., Sharples, C.G.V., and Wonnacott, S. 2003. Synthesis of two fluoro analogues of the nicotinic acetylcholine receptor agonist UB-165. *J Org Chem* 68, 2475–2478.
- Swanson, K.L., Allen, C.N., Aronstam, R.S., Rapoport, H., and Albuquerque, E.X. 1986. Molecular mechanisms of the potent and stereospecific nicotinic receptor agonist (+)-anatoxin-a. *Mol Pharmacol* 29, 250–257.
- Swanson, K.L., Aracava, Y., Sardina, F.J., Rapoport, H., Aronstam, R. S., and Albuquerque, E.X. 1989. *N*-Methylanatoxinol isomers. derivatives of the agonist (+)-anatoxin-a block the nicotinic acetylcholine-receptor ion channel. *Mol Pharmacol* 35, 223–231.
- Swanson, K.L., Aronstam, R.S., Wonnacott, S., Rapoport, H., and Albuquerque, E.X. 1991. Nicotinic pharmacology of anatoxin analogues. 1. side-chain structure-activity-relationships at peripheral agonist and noncompetitive antagonist sites. *J Pharmacol Exp Ther* 259, 377–386.
- Tamura, Y., Minamikawa, J., and Ikeda, M. 1977. *O*-Mesitylenesulfonylhydroxylamine and related compounds. Powerful aminating reagents. *Synthesis* 1–17.
- Thomas, P., Stephens, M., Wilkie, G., Amar, M., Lunt, G.G., Whiting, P., Gallagher, T., Pereira, E., Alkondon, M., Albuquerque, E.X., and Wonnacott, S. 1993. (+)-Anatoxin-a is a potent agonist at neuronal nicotinic acetylcholine receptors. *J Neurochem* 60, 2308–2311.
- Thomas, P., Brough, P.A., Gallagher, T., and Wonnacott, S. 1994. Alkyl-modified side-chain variants of anatoxin-a. series of potent nicotinic agonists. *Drug Dev Res* 31, 147–156.
- Tramontini, M. 1973. Advances in the chemistry of Mannich bases. *Synthesis* 703–775.
- Trost, B.M., Arndt, H.C., Strege, P.E., and Verhoeven, T.R. 1976. Desulfonylation of aryl alkyl sulfones. *Tetrahedron Lett* 17, 3477–3478.
- Trost, B.M., and Oslob, J.D. 1999. Asymmetric Synthesis of (–)-Anatoxin-a via an asymmetric cyclization using a new ligand for Pd-catalyzed alkylations. *J Am Chem Soc* 121, 3057–3064.
- Trost, B.M. 2004. Asymmetric allylic alkylation, an enabling methodology. *J Org Chem* 69, 5813–5837.
- Tsuji, J. 1984. Synthetic applications of the palladium-catalyzed oxidation of olefins to ketones. *Synthesis* 369–383.
- Tufariello, J.J., Meckler, H., and Senaratne, K.P.A. 1984. Synthesis of anatoxin-a: very fast death factor. *J Am Chem Soc* 106, 7979–7980.
- . 1985. The use of nitrones in the synthesis of anatoxin-a, very fast death factor. *Tetrahedron* 41, 3447–3453, and references therein about the regioselectivity of nitron cyclization.
- Vernon, P., and Gallagher, T. 1987. Neurotoxic Alkaloids: Synthesis of ( $\pm$ )-anatoxin-a. *J Chem Soc Chem Commun* 245–246.
- Wegge, T., Schwarz, S., and Seitz G. 2000. A new and efficient synthetic route to enantiopure (+)-anatoxin-a from (–)-cocaine hydrochloride. *Tetrahedron Asymmetry* 11, 1405–1410.
- Weinreb, S.M. 1997. Review of the chemistry of tosyl iminium ions. In *Topics in Current Chemistry*, vol. 190. Berlin: Springer, 132–184.
- Weinstein, B., and Craig, A.R. 1976. Synthetic approach to the cephalotaxine skeleton. *J Org Chem* 41, 875–878.
- Wijnberg, B.P., and Speckamp, W.N. 1981. *a*-acyliminium ion synthesis of elaeokanine B. *Tetrahedron Lett* 22, 5079–5082.
- Winter, R.E.K., and Lindauer, R.J. 1967. The photochemical isomerization of 1-acetylbicyclo[4.1.0]heptane an intramolecular rearrangement. *Tetrahedron Lett* 8, 2345–2348.

- Wiseman, J.R., and Lee, S.Y. 1986. Synthesis of anatoxin-a. *J Org Chem* 51, 2485–2487.
- Wonnacott, S., Jackman, S., Swanson, K.L., Rapoport, H., and Albuquerque, E.X. 1991. Nicotinic pharmacology of anatoxin analogues. 2. side-chain structure-activity-relationships at neuronal nicotinic ligand-binding sites. *J Pharmacol Exp Ther* 259, 387–391.
- Wonnacott, S., Swanson, K.L., Albuquerque, E.X., Huby, N.J.S., Thompson, P., and Gallagher, T. 1992. Homoanatoxin: a potent analogue of anatoxin-a. *Biochem Pharmacol* 43, 419–423.
- Wright, E., Gallagher, T., Sharpless, C.G.V., and Wonnacott, S. 1997. Synthesis of UB-165: A novel nicotinic ligand and anatoxin-a/epibatidine hybrid. *Bioorg Med Chem Lett* 7, 2867–2870.
- Wroble, R.R., and Watt, D.S. 1976. A synthesis of  $\alpha,\beta$ -unsaturated ketones from  $\alpha,\beta$ -unsaturated nitriles. *J Org Chem* 41, 2939–2940.
- Yang, S., Hungerhoff, B., and Metz, P. 1998. A short conversion of cyclohexanones to cycloheptenones. *Tetrahedron Lett* 39, 2097–2098.
- Zhang, G., Lomenzo, S.A., Ballay II, C.J., and Trudell, M.L. 1997. An improved synthesis of (+)-2-tropinone. *J Org Chem* 62, 7888–7889.
- Zirkle, C.L., Geissman, T.A., Bloom, M., Craig, P.N., Gerns, F.R., Indik, Z.K., and Pavloff, A.M. 1962. 3-Substituted tropane derivatives. I. The synthesis and stereochemistry of the tropane-3-carboxylic acids and their esters. A comparison of positional isomers in the tropane series. *J Org Chem* 27, 1269–1279.

## 8 Anatoxin-a and Analogues: Discovery, Distribution, and Toxicology

Kevin J. James, Janet Crowley, Justine Duphard, Mary Lehane, and Ambrose Furey

### Introduction

The synthetic aspects of anatoxin-a (AN) and analogues are discussed in a separate chapter of this text, and the analytical methods for anatoxins are the subject of a separate review to be published elsewhere. A number of reviews have demonstrated the importance of understanding toxic cyanobacteria as potential environmental and health hazards as well as a resource of bioactive molecules (Harada 1999; Skulberg 2000; Briand et al. 2003). AN was one of the first cyanobacterial toxins to be chemically and functionally characterized and its high neurotoxicity has attracted extensive research activity.

### Discovery of Anatoxins

#### *Anatoxin-a*

Anatoxin-a (AN) is produced by various species of cyanobacteria including *Anabaena*, *Planktothrix* (formerly *Oscillatoria*), *Aphanizomenon*, *Cylindrospermum*, and *Microcystis* spp. This toxin was first detected in Canada from a bloom of *Anabaena flos-aquae* in the 1960s (Gorham et al. 1964; Gorham 1964) and due to its potency was originally called very fast death factor (VFDF). Initial studies indicated that the toxin was a low molecular weight amine. Subsequently, the toxin, anatoxin-a, was isolated and determined to be a bicyclic secondary amine, 2-acetyl-9-azabicyclo[4.2.1]non-2-ene (Fig. 8.1; R = CH<sub>3</sub>), incorporating an  $\alpha,\beta$ -unsaturated ketone moiety (Devlin et al. 1977). The structure was later confirmed by X-ray crystallography (Huber 1972).

#### *Homoanatoxin-a*

In 1992, a methylene analogue of AN, named homoanatoxin-a (HMAN), was isolated from *Planktothrix* (*Oscillatoria*) *formosa* in Norway (Skulberg et al. 1992). Interestingly, HMAN

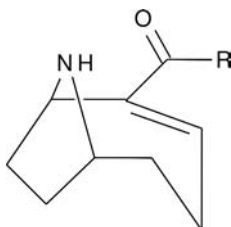


**Figure 8.1.** Structures of anatoxin-a (R = CH<sub>3</sub>) and homoanatoxin-a (R = C<sub>2</sub>H<sub>5</sub>).

(Fig. 8.1; R = C<sub>2</sub>H<sub>5</sub>) had been synthesized around this time as part of a program to investigate the structure-activity relationships of AN analogues (Wonnacott et al. 1992). Symptoms of HMAN poisoning in mice were similar to those observed with AN, such as paralysis, convulsions, and death due to respiratory arrest. Like AN, HMAN is a potent neuromuscular blocking agent with an LD<sub>50</sub> of 250 µg/kg (i.p.). Both of these toxins enhance the release of acetylcholine (ACh) from peripheral cholinergic nerves (Aas et al. 1996; Lilleheil et al. 1997). Reports of HMAN have been less common than AN, but this toxin has been found in recent years in Ireland and Japan and co-occurs with AN in *Planktothrix* (*Oscillatoria*) and *Raphidiopsis* cultures (Furey et al. 2003; Namikoshi et al. 2003; Araoz et al. 2005).

### Anatoxin-a(s)

Cyanobacterial blooms, sampled from western Canada in the 1970s, led to the discovery of other neurotoxins in strains of *Anabaena flos-aquae*. The toxins were characterized according to signs of poisoning, survival times and LD<sub>90</sub> (i.p.) produced by lyophilized axenic clones (Carmichael and Gorham 1980). One of these toxins demonstrated similar signs of poisoning as AN but also produced severe salivation and lachrymation in mice, rats, and chicks and in rats there was also chromodacryorrhea (bloody tears). This new toxin was named anatoxin-a(s), abbreviated AN-a(s), due to the observed salivation and was structurally elucidated as a unique N-hydroxyguanidine methyl phosphate ester (Fig. 8.2) (Matsunaga et al. 1989). Although AN and AN-a(s) have some similar toxicological symptoms, they are not only chemically unrelated but also have different physiological modes of action (Mahmood and Carmichael 1986, 1987; Hyde and Carmichael 1991). AN-a(s) is an acetylcholinesterase inhibitor with an LD<sub>50</sub> of approximately 50 µg/kg (i.p. mouse). By impeding acetylcholinesterase from breaking down ACh, it ensures that this remains continuously available to overstimulate muscle cells (Cook et al. 1988, 1989). Unfortunately, the similarity in the names of these different anatoxins has led to some confusion in the literature and great care should be exercised in interpreting reports regarding these neurotoxins.

Reports of AN-a(s) are much less common when compared with the extensive worldwide distribution of AN (Table 8.1). AN-a(s) has been identified in cyanobacteria from lakes in Denmark and in the stomach contents of poisoned birds (Henriksen et al. 1997). Among the factors that may have contributed to the low incidence of AN-a(s) reports are the instability of the toxin and difficulties in detection due to a lack of commercially available analytical standard. AN-a(s) readily loses the methyl phosphate moiety to produce a nontoxic product, and investigations of suspected AN(s) poisonings should also involve a search for the degradation product.

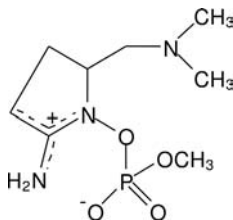


**Figure 8.2.** Structures of (A) anatoxin-a(s) and (B) its main degradation product.

**Table 8.1.** Distribution of anatoxin-a and analogues and toxic incidents

Country	Predominant species	Toxin identified	Affected animals	Reference
Canada	<i>Anabaena flos-aquae</i>	AN	Cattle, dogs	Gorham 1964; Carmichael et al. 1975
USA	<i>Anabaena flos-aquae</i>	AN	Cattle, dogs	Juday et al. 1981
Scotland	<i>Microcystis, Anabaena</i>	—	—	Richard et al. 1983
USA	<i>Anabaena</i>	AN	Cattle, dogs	Stevens and Krieger 1988
Finland	<i>Anabaena</i> sp.	AN	Cattle	Sivonen et al. 1989, 1990
Norway	<i>Planktothrix formosa</i>	HMAN	—	Skulberg et al. 1992
Scotland	<i>Planktothrix</i>	AN	Dogs	Edwards et al. 1992
USA	<i>Anabaena, Planktothrix</i>	AN	—	Kangatharalingam and Priscu 1993
Japan	<i>Anabaena, Planktothrix</i>	AN, epoxy-AN	—	Park et al. 1993
Italy	<i>Anabaena planctonica</i>	AN	—	Bruno et al. 1994
Norway	<i>Anabaena, Planktothrix</i>	AN	—	Skulberg et al. 1994
Sweden	—	AN	—	Willen and Mattsson 1997
Ireland	<i>Anabaena, Planktothrix</i>	AN	Dogs	James et al. 1997
Korea	<i>Anabaena, Planktothrix</i>	AN	—	Park et al. 1998
Germany	<i>Anabaena, Aphanizomenon</i>	AN	—	Bumke-Vogt et al. 1999
New Zealand	<i>Planktothrix</i>	Dihydro-AN?	Dogs	Hamill 2001
Ireland	<i>Anabaena, Planktothrix</i>	HMAN	—	Furey et al. 2003
Kenya	Benthic species	AN	Birds	Krienitz et al. 2003
Japan	<i>Raphidiopsis mediterranea</i>	AN, HMAN	—	Namikoshi et al. 2003; Watanabe et al. 2003
Poland	—	AN	—	Mazur and Plinski 2003
China	—	AN	—	Zhang et al. 2003
Poland	<i>Anabaena</i>	AN	—	Pawlik-Skowronska et al. 2004
Kenya	<i>Anabaena fusiformis</i>	AN	Birds	Ballot et al. 2004, 2005
Italy	<i>Planktothrix rubescens</i>	AN	—	Viaggiu et al. 2004
USA	<i>Aaabaena</i> sp.	AN	Dogs	Hill 2005
Japan	<i>Raphidiopsis mediterranea</i>	AN, HMAN epoxy-HMAN, hydroxy-HMAN	—	Namikoshi et al. 2004
France	<i>Phormidium favosum</i>	AN	Dogs	Gugger et al. 2005
Ireland	<i>Planktothrix</i> sp.	AN, dihydro-AN	Dogs	James et al. 2005

### Isolation of Anatoxins

Anatoxin-a was first isolated from *Anabaena flos-aquae* in 1976 (Devlin et al. 1977). The isolation and enrichment of AN from cultured material involved adjustment of the algae suspension to pH 5 prior to lyophilization. The residual material was then extracted with methanol containing dilute hydrochloric acid. After evaporation the resulting syrup was neutralized and extracted with benzene



and chloroform and finally purified by thin layer chromatography (TLC). Other methods for the isolation of AN involved a combination of reversed phase liquid chromatography (LC) and TLC (Astrachan and Archer 1981; Al-Layl et al. 1988; Himberg 1989). The reversed phase stages were carried out in basic media (pH 10–11), but this may lead to toxin degradation if not carried out rapidly. Harada and co-workers explored a number of methods for the isolation of AN, and the most efficient was the use of a weak cation exchange (WCX) column. This is also used for sample clean-up using solid phase extraction (SPE) in analytical methods for the determination of AN (Harada et al. 1989; James et al. 1997).

A single semipreparative reversed phase LC has been employed for the isolation of AN, and also a similar approach has been used for the analytical separation of AN and HMAN hydrochloride salts, at pH 3 (Zotou et al. 1993). HMAN was isolated, based on the methods previously developed for the purification of AN (Harada et al. 1989; Skulberg et al. 1992). Lyophilized cells were extracted with acidified ethanol, followed by a mixture of butanol, methanol, and acidified water. The combined supernatant volume was reduced and the aqueous extract was applied to reversed phase silica SPE cartridge. Elution was performed sequentially with acidified water, methanol/water, and methanol. HMAN was isolated from a culture of *Planktothrix (Oscillatoria) formosa* using a combination of WCX and reversed phase SPE steps (Furey et al. 2003). The final purification was completed on C<sub>18</sub> LC using an elution medium of water/acetonitrile (95:5, 0.5 ml/minute), containing trifluoroacetic acid (TFA, 0.05%). A similar approach was used to isolate AN, HMAN, and degradation products from a culture of the cyanobacterium, *Raphidiopsis mediterranea* Skuja, obtained from a Japanese lake (Namikoshi et al. 2003). This procedure included (1) extraction of dried cells with methanol/water (4:1), (2) evaporation of methanol and application of the aqueous residue to a reversed phase SPE cartridge, (3) washing with water and methanol/water (1:1), (4) elution of the anatoxins using methanol/water (1:4) containing 0.1% TFA, and (5) LC on a C<sub>18</sub> column with elution using methanol/water containing 0.05% TFA.

## Toxin Distribution and Toxic Incidents

In Canada, between 1961 and 1975, suspected AN poisoning of cattle and dogs occurred in six locations. While *Anabaena flos-aquae* was found to be the predominant bloom in each case, other toxins were reported to be present in addition to AN, including anatoxin-a(s) (Gorham 1964; Carmichael et al. 1975; Carmichael and Gorham 1978; Juday et al. 1981). While the earliest confirmation that AN was implicated in animal poisonings was reported in Canada (Carmichael and Gorham 1978), the majority of locations where AN was detected, or toxic incidents have occurred, have been in Europe (Codd et al. 2005).

### *Anatoxins in Europe*

In Scotland, during 1981–1982, cyanobacteria from several lakes were found to be toxic by mouse bioassay (i.p.) (Richard et al. 1983), but the first case of AN intoxication due to benthic cyanobacteria was reported 10 years later (Edwards et al. 1992). The neurotoxic bloom consisted mainly of *Planktothrix* species and was associated with three canine fatalities; AN was identified in the stomach contents of one of the dogs (Gunn et al. 1992). In Finland, the first survey of cyanobacterial blooms during 1985–1987 revealed that 13 out of 30 bloom samples contained AN (Sivonen et al. 1989). Toxin content was in the range 12–4360 µg AN/g lyophilized material. During this

study, a number of cattle poisonings associated with *Anabanea* blooms occurred (Sivonen et al. 1990). The first identification of HMAN was made from a *Planktothrix formosa* strain from an eutrophic lake (Skulberg et al. 1992). During 1989–1991, a widespread survey of lakes in Norway showed that 6 out of 64 samples tested positive for AN (Skulberg et al. 1994).

In Italy, AN was identified in *Anabaena planctonica* found in three lakes connected to a reservoir that supplied drinking water in Sardinia during 1987–1990 (Bruno et al. 1994). AN was also found in a fishing pond in the north of Italy, with an estimated concentration of 12 µg AN/g (Viaggiu et al. 2004). The first identification of AN in Ireland was confirmed following incidents of fatal canine neurotoxicosis in Caragh Lake, County Kerry. AN was found in *Anabaena* and a *Planktothrix* species in concentrations of 2–444 µg AN/g of dried cells (James et al. 1997). HMAN was also later reported in Ireland, and this toxin was identified in 4 out of 20 lakes studied, at concentration levels 1.4–34 µg HMAN/L (Furey et al. 2003). Recently, AN associated with the rapid deaths of dogs was also reported in France, in a benthic species, *Phormidium favosum*. However, due to the presence of phenylalanine in the stomach contents of the dogs, quantitation of AN was not possible (Gugger 2005).

A screening program, carried out in Germany (1995–1997), tested 80 water bodies, and 22% were positive for AN with the highest level of 13 µg AN/L (Bumke-Vogt et al. 1999). In Poland, nodularin, microcystins, and AN were detected in the coastal waters of the Gulf of Gdansk (Mazur and Plinski 2003). In 2001–2003, mass occurrence of *Anabaena* strains producing AN was observed for the first time in Poland. AN concentration in the reservoir water was positively correlated with total abundance of three taxa of *Anabaena* (Pawlik-Skowronska et al. 2004).

### *Anatoxins in Non-European Countries*

Outside Europe, most reports of anatoxins have been in North America. In October 1981, a toxic *Anabaena* bloom from Black Lake, Idaho, USA, containing 2500 µg AN/g, resulted in the deaths of 11 cows and 2 dogs (Stevens and Krieger 1988). *Anabaena flos-aquae* collected in 1991 from Hebgen Lake in Montana, USA, was found to contain AN producing clones in 2 out of 23 samples (Kangatharalingam and Priscu 1993). While no intoxications were reported during this study, there have been previous accounts of cattle and wildlife deaths in the area. Recent investigations of a series of dog fatalities in northern California led to the identification of AN in the stomach contents of two dogs (Hill 2005).

In Japan, the first detection of AN and its degradation product, epoxy-AN, have been reported (Park et al. 1993). This was also the first study to show that *Microcystis* could produce both AN and microcystins. The predominant species were *Anabanea* and *Planktothrix* with toxin concentrations in the range 0.4–16 µg AN/g. In addition, AN, HMAN, and a new compound, hydroxy-HMAN, were isolated from *Raphidiopsis mediterranea* in Japan (Namikoshi et al. 2003; Watanabe et al. 2003). AN was also found in four of 26 samples from Korean lakes, collected during 1992–1995 (Park et al. 1998).

It has been suggested that cyanobacterial mats at hot springs on the shore of an alkaline lake in Kenya contributed to the death of Lesser Flamingos (Krienitz et al. 2003; Ballot 2004). AN was present in the algae samples (10–18 AN µg/g) and stomach contents of the birds. AN was also identified in two alkaline crater lakes in Kenya. This was the first study to show that *Arthrospira fusiformis* was a producer of both AN and microcystins (Ballot et al. 2005). Although cyanobacterial blooms frequently occur in Australia and New Zealand, AN has not been reported. The first report of suspected AN poisoning in 1998 when dihydro-AN was tentatively identified in New Zealand in

a benthic *Planktothrix* sample that was linked to a number of dog deaths (Hamill 2001). Table 8.1 provides a summary of the reported worldwide occurrences of AN and its analogues.

## Toxicological Studies

### Mechanisms of Toxicity

Anatoxin-a and homoanatoxin-a mimic the neurotransmitter acetylcholine (ACh) by binding to the nicotinic acetylcholine receptor (NACHR) at the axon terminal at the neuromuscular interface; unlike ACh, the binding of anatoxin-a to NACHR is irreversible (Carmichael et al. 1975, 1979; Aronstam and Witkop 1981; Thomas et al. 1993; Aas et al. 1996; Lilleheil et al. 1997). Normal neuromuscular action is achieved by the release of acetylcholine which binds to NACHR, activating the opening of a related sodium channel. The resultant movement of the sodium ion creates a potential difference across the nerve synapse, causing muscle contraction. Acetylcholine esterase then cleaves the neurotransmitter, causing the sodium channel to return to the resting state and muscle relaxation. The anatoxin-NACHR complex cannot be cleaved by the enzyme: the sodium channel is locked open, becomes overstimulated, fatigued, and eventually paralyzed. The interaction of AN with NACHR in the respiratory system results in a lack of oxygen to the brain, subsequent convulsions, and death by suffocation. It has been shown that AN is about 20 times more potent a nicotinic agonist than acetylcholine (Astrachan et al. 1980; Aronstam and Witkop 1981; Feuerstein and Siren 1988; Gordon et al. 1992; Fawell et al. 1999).

AN fits geometric models of nicotinic agonists; existing primarily with the seven-membered ring in the twist-chair conformation, the *s-cis* enone conformation is favored 3:1 over the *s-trans* conformation because of less steric crowding (Fig. 8.3). The *s-cis* conformer is considered to be the preferred agonist conformation since the distance between the nitrogen and the carbonyl oxygen is 6.0 Å, which compares well with acetylcholine (ACh) where the distance from the nitrogen to the carbonyl oxygen is 5.9 Å (Spivak et al. 1980; Koskinen and Rapoport 1985; Swanson et al. 1986; Swanson et al. 1990; Thompson et al. 1992).

Since AN binds the nicotinic acetylcholine receptor irreversibly, this toxin is useful for studying this receptor as well as the mechanisms of neuromuscular action. Analogues of AN have been used to study the receptor subtypes, and important research goals are the development of new drug

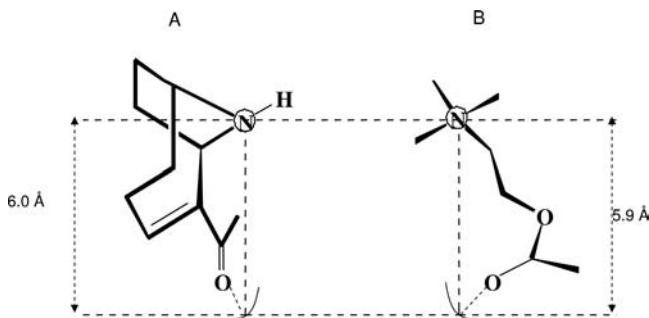


**Figure 8.3.** Conformations of (A) anatoxin-a and (B) acetylcholine, showing spatial similarities for competitive receptor binding. Adapted from Swanson et al. 1986.

targets that have potential in increasing acetylcholine levels to be used for the treatment of neurodegenerative disorders (Swanson et al. 1990; Nicolotti et al. 2002). Early structure-activity relationship studies showed that N-methylation of AN destroyed potency, whereas side-chain modifications retained potency (Kofuji et al. 1990; Stevens and Krieger 1990; Wonnacott et al. 1991, 1992). This research into analogues of AN continues to be a major driving force in the development of new synthetic pathways to AN and analogues (Wonnacott et al. 1992; Swanson et al. 1990; Brough et al. 1994; Breining 2004) and this is discussed in more detail in chapter 7.

### *In Vivo Toxicity*

Clinical signs of toxicosis in mice, rats, birds, dogs, and calves follow a sequence of muscle fasciculations, decreased movement, collapse, exaggerated abdominal breathing, cyanosis, convulsions, and death. The LD<sub>50</sub> mouse (i.p.) is 200–250 µg/kg body weight, with a survival time that is usually less than 30 minutes. The oral toxicity of AN is such that animals can receive a lethal amount of toxin by ingesting anything from a few milliliters to several liters of surface. Autopsy examinations have revealed that there are no specific internal lesions evident in animals poisoned by AN, although edema of the brain, spinal cord, and meninges may be apparent as well as fluid congestion of the lungs (Beasley et al. 1989b). There is no chemical antidote for AN intoxication, and the only support measure that can be taken is water (Carmichael et al. 1977; Carmichael and Gorham 1978). Cardio-respiratory changes in rats were examined using (+)-AN and a racemic mixture (Siren and Feuerstein 1990; Adeyemo and Siren 1992). Studies of the sub-acute effects of AN on rats did not reveal significant biological effects and no changes were observed in food consumption and in body weight (Jarema and MacPhail 2003). The subacute toxicity and the teratogenicity of AN were also studied in the mouse. The results confirmed the potent nicotinic agonist action of AN, which can produce neuromuscular blockade and death by respiratory arrest. Additionally, there was no biologically significant tolerance to acute AN exposure (Stevens and Krieger 1991a; Stolerman et al. 1992). Repeated sublethal oral administration over 28 days in the mouse did not produce treatment-related toxicity, and AN did not appear to be a developmental toxicant in the mouse. It was further concluded that a guideline value for AN in drinking water of 1 µg/l would provide an adequate margin of safety (Fawell et al. 1999). In another study, time-pregnant mice received 125 or 200 µg kg<sup>-1</sup> anatoxin-a by intraperitoneal injection on gestation days (GD) 8–12 or 13–17. Although maternal toxicity (decreased motor activity) was observed at 200 µg kg<sup>-1</sup> in both treatment periods, there were no significant treatment-related effects on pup viability, and overall no significant postnatal neurotoxicity was observed (Rogers et al. 2005).

The effect of nicotine on the motor activity of adult mice that had been exposed prenatally to AN was also examined. This study showed that nicotine decreased both horizontal and vertical activity in all mice, regardless of prenatal AN treatment and that there were no enduring effects of prenatal AN in adult mice following nicotine challenge (MacPhail et al. 2005).

A report suggests that the intravenous administration of a “cell-free extract of *Anabaena flos-aquae* (containing anatoxin-a)” produced a transient vasodepressor response followed by a sustained rise in blood pressure in rats. Prolonged apnoea with attendant bronchoconstriction was observed, which remained unaltered by atropine. However, the statement by these authors that AN should be considered as a weapon of mass destruction, mainly due to its lethal anticholinesterase activity (Dube et al. 1996), raises the possibility of confusion with anatoxin-a(s) since AN is a nicotinic agonist and not a cholinesterase inhibitor.

### *In Vitro Toxicity*

The usefulness of AN for the study of nicotinic receptors has been demonstrated, and AN has been shown to interact with  $\alpha$ -4  $\beta$ -2 nicotinic acetylcholine receptors in the human cortex (Durany et al. 1999). AN evoked [H-3] dopamine release from rat striatal synaptosomes, and this is modulated by protein kinase C (Soliakov et al. 1995; Soliakov and Wonnacott 2001). A water extract of the alga *Anabaena flos-aquae* enhanced substantially the release of [H-3]acetylcholine from cholinergic nerves of rat bronchi; this was attributed to the presence of AN (Holte et al. 1998). The effect of different nicotinic agonists on the [H-3] norepinephrine release from rat hippocampal slices has also been examined (Kiss et al. 2001). Using isolated bovine adrenal chromaffin cells, the secretion of catecholamines stimulated by AN was completely inhibited in a noncompetitive manner by the nicotinic antagonist mecamylamine. It was concluded that AN acts as a potent and selective nicotinic agonist, capable of evoking secretion of endogenous catecholamines from chromaffin cells via their neuronal-type nicotinic receptor (Molloy et al. 1995; Dar and Zinder 1998).

AN was also used to show that endothelial cells that line blood vessels express functional nAChRs. Thus, cultured human endothelial cells expressed ion channels that were opened by AN and blocked by dihydro-beta-erythroidine. These are specific agonist and antagonist, respectively, of neuronal AChRs of the  $\alpha$ -3 subtype. It is also suggested that the toxic effects of nicotine on the vascular system could be related to this phenomenon (Macklin et al. 1998). It has recently been shown that AN induced apoptosis in non-neuronal cells, cultured rat thymocytes, and African green monkey kidney cells. Evidence of AN-induced apoptosis included plasma membrane blebbing, condensed chromatin, and nuclear fragmentation. It was suggested that AN-induced apoptosis could possibly be mediated by the generation of reactive oxygen species and caspase activation (Rao et al. 2002a, 2002b).

AN was also shown to have cytotoxic effects on mouse B- and T-lymphocyte subpopulations in vitro, but these effects were driven by mechanisms different from apoptosis (Teneva et al. 2005). Cellular systems have also been used to study the comparative potency of nicotinic agonists and the expression of homomeric nicotinic AchRs  $\alpha$ -7, achieved in GH3 rat pituitary cells. This system was used to show that AN was second only to epibatidine in potency as a nicotinic agonist (Feuerbach et al. 2005).

### *Environmental Toxicology*

One of the interesting aspects of the production of potent toxins by cyanobacteria is the possibility that it is carried out in order to gain a competitive edge against other organisms in the environment. The effects of toxic cyanobacteria, or the purified toxins, on a variety of species have been studied in recent years. Neonate *Daphnia pulex* were exposed to toxic strains of *Anabaena*, and to pure AN, at 12°C–25°C. The fecundity and survival of individual animals were assessed under different temperature conditions. The sensitivity of *D. pulex* to the cyanobacteria and AN, at various temperatures, was measured by determining the finite population growth rate of *D. pulex*, and this showed that there was a statistically significant pattern of increased sensitivity at higher temperatures. The presence of cyanobacteria affected brood size, brood number, the time to first reproduction, and the inter-clutch interval (Claska and Gilbert 1998).

The effects of cyanobacterial hepatotoxins and neurotoxins were examined on the embryos of fish and amphibians up to advanced stages of embryonic development. No acute toxic effects were observed after exposure to microcystins, but at the highest applied concentration of microcystin-LR (10 mg/L), morphological effects were detected. AN (400  $\mu$ g/L) altered the heart rate in zebrafish, but no chronic effects were observed (Oberemm et al. 1999). The effects of cyanobacterial toxins on

the survival and egg hatching of estuarine calanoid copepods was studied and this showed that, although the egg hatching was unaffected, survival was marginally influenced by high concentrations of AN and nodularin (Reinikainen et al. 2002).

The effect of AN was studied on the neurones of two snail species, and it was concluded that AN affects the neuronal membrane of neurones acting on ACh receptors (Kiss et al. 2002).

Studies have also been conducted to investigate whether toxin production by cyanobacteria may provide a competitive advantage against algae and aquatic plants. Thus, both AN and microcystin-LR paralyze the motile green alga *Chlamydomonas reinhardtii*, representing a novel mechanism for phytoplankton settling, which may allow the toxin-producing species to flourish (Kearns and Hunter 2001). AN adversely influences some aquatic plants by stimulating an increase in peroxidase and glutathione S-transferase activity. The free floating aquatic plant *Lemna minor* and the filamentous macroalga *Chladophora fracta* were used as representative organisms. A significant depletion in photosynthetic oxygen production by *L. minor* was also observed at concentrations in the range 5–20 µg AN/mL (Mitrovic et al. 2004).

## Anatoxin Poisoning: Investigation and Control

### Degradation of Anatoxins

Cyanobacterial culture studies and reported observations of natural blooms have shown that differences in cyanobacterial composition and toxicity are dependent on a number of environmental factors including, light, temperature, pH, and nutrients and physical factors such as buoyancy of the algae, prevailing weather conditions, and water currents (Rapala et al. 1993; Gupta et al. 2002). These variables, along with the age of the cells, their tendency to lyse and release toxins, decomposition and detoxification mechanisms (Rapala et al. 1994), help to explain why poisonous cyanobacterial blooms tend to occur in such an erratic and unpredictable fashion (Carmichael and Gorham 1980).

The stable nontoxic degradation product of AN, dihydro-AN, was first identified from a mature bloom of *Anabaena flos-aquae* (Smith and Lewis 1987). A sample analysed shortly after a toxic incident tested positive for the presence of AN, while a sample that had been frozen and analyzed later was found to contain only trace amounts of AN and significant quantities of dihydro-AN. Dihydro-AN was found to be nontoxic by mouse bioassay. This investigation concluded that AN tends to disappear along with the toxicity within a few days of the event to a nontoxic degradation product, thus complicating diagnosis (Smith and Lewis 1987). Epoxy-AN, another nontoxic metabolite of AN, has also been identified from various blooms (Harada et al. 1993). A laboratory study showed that AN degrades readily, especially in sunlight and at high pH, to nontoxic degradation products (Fig. 8.4). Light and alkaline pH caused rapid degradation of AN, with a half-life of only 1–2 hours (Stevens and Krieger 1991b), and in natural blooms in eutrophic lakes, the AN half-life is typically less than 24 hours. Copper sulphate addition to cyanobacterial blooms has been frequently used, resulting in temporary high surface copper concentrations in the water, lysing of cells and releasing of toxins (Carmichael and Mahamood 1984; Beasley et al. 1989a). The Stevens study also compared the detoxification of AN using copper and iron and found that the rate of AN loss was greatest with  $\text{Cu}^{2+}$  solutions (Stevens and Krieger 1991b). Rapala et al. (1994) investigated the biodegradability of microcystins and AN, and concluded that micro-organisms, sediments, light, pH, and high copper levels played a significant role in the degradation of cyanobacterial toxins in nature. Studies using a culture of the cyanobacterium *Raphidiopsis mediterranea* Skuja (Namikoshi et al. 2004) showed



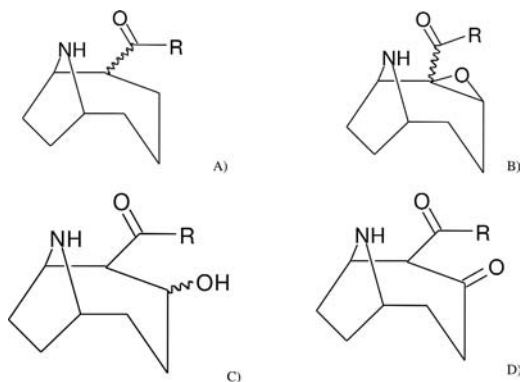


**Figure 8.4.** Anatoxin degradation products: (A) dihydro-AN ( $R = \text{CH}_3$ ), dihydro-HMAN ( $R = \text{C}_2\text{H}_5$ ); (B) epoxy-AN ( $R = \text{CH}_3$ ), epoxy-HMAN ( $R = \text{C}_2\text{H}_5$ ); (C) 4-hydroxy-HMAN ( $R = \text{C}_2\text{H}_5$ ); (D) 4-keto-HMAN ( $R = \text{C}_2\text{H}_5$ ).

that HMAN was readily transformed into two hydroxy-HMAN isomers (Fig. 8.4C,  $R = \text{C}_2\text{H}_5$ ), epoxy-HMAN (Fig. 8.4B,  $R = \text{C}_2\text{H}_5$ ), and 4-keto-HMAN (Fig. 8.4D,  $R = \text{C}_2\text{H}_5$ ).

Despite the ease with which AN and HMAN can rapidly degrade, it is surprising that there have been few reports of the presence of these degradation products, and this may be a consequence of both the lack of commercially available standards and the fact that most studies of anatoxins relied on the use of LC with UV detection for analysis. The degradation products are not detectable using this method as they do not possess the unsaturated ketone chromophore.

### *Forensic Investigations of Anatoxin-a Poisoning*

In many ways, AN is an intriguing poison: it acts quickly with fatal consequences and leaves no sign of organ damage; residual toxin is rapidly degraded; and the toxin mimics a harmless natural product in some assays. The reliable determination of anatoxins in environmental and forensic samples presents an array of difficulties. As discussed previously, AN and HMAN degrade quickly to nontoxic degradation products, usually dihydro and epoxy analogues, and the degradation is accelerated in sunlight and at elevated pH (Stevens and Krieger 1991b). Both the mouse bioassay (Skulberg et al. 1994; Bruno et al. 1994) and LC with UV detection (Astrachan and Archer 1981; Zotou et al. 1993) fail to detect these degradation products. The mouse bioassay fails because the degradation products are nontoxic and UV detection fails to detect the dihydro- and epoxy-degradation products (James et al. 1997). In addition, only AN is commercially available and standard dihydro, and epoxy degradation products must be prepared by synthesis from the parent toxins (James et al. 1997). In view of the above problems, it is apparent that samples are frequently stored incorrectly, and ideally they should be protected from light and acidified prior to storage at  $-20^\circ\text{C}$ , in order to limit degradation of the anatoxins.

In some cases AN has been discounted as the causative agent of suspected animal poisoning because of the low amount of AN present, a conclusion that is unreliable due to the lability of this toxin. For example, cyanobacteria have been investigated as a possible cause of the high rate of alligator mortality in Lake Griffin, Florida, USA. Although AN was found in liver and muscle



samples, it was concluded that AN could not be responsible due to the low levels detected (Richey et al. 2001), but this study failed to investigate the degradation products of AN.

Two recent incidents have highlighted the possible confusion that can occur in forensic investigations of suspected AN poisonings due to the presence of Phe. The death of a young adult in the USA in July 2002, following exposure to lake water, was ascribed to AN poisoning in the coroner's report. This conclusion was based mainly on evidence obtained by using LC-MS with a single quadrupole MS instrument. This identification has since been shown to be incorrect and was due to confusion between Phe and AN, which have the same nominal mass and similar chromatographic retention times (Carmichael and Yuan 2004). In 2003, an investigation into the fatal intoxication of two dogs in a lake in eastern France identified AN in benthic cyanobacteria, collected along the shoreline. However, confirmation and quantification of AN in the stomach and intestine contents of these dogs was not possible because of the large quantity of Phe present (Gugger et al. 2005). Not only is the single quadrupole MS insufficient to confirm AN, but multiple tandem MS methods must be used with care as the spectra of AN and Phe reveal a number of similar product ions (Fig. 8.5). A number of strategies have been proposed to limit the confusion between AN and Phe. These include (1) multiple tandem MS ( $MS^n$ ), (2) accurate mass measurements using time-of-flight (TOF) MS, (3) methylation of Phe in samples prior to analysis of AN, and (4) derivatisation of AN prior to analysis (Furey et al. 2005). The high mass accuracy of TOF MS is such that the isobaric precursor ions are partially resolved because of the small differences in their accurate masses,  $[M+H]^+$ , AN ( $m/z$  166.1232) and Phe ( $m/z$  166.0868).

### *Health Implications and Risk Management*

Confirmations of human deaths from cyanotoxins are limited to exposure to microcystins through renal dialysis in Caruaru, Brazil, in 1996. Issues of human health, safe water practices, management, prevention, and remediation have been published by the World Health Organization (WHO 1998) and the potential risk of cyanobacterial toxins to human health has been reviewed (Carmichael 2001). A preliminary 28-day repeat sublethal oral dosing study with mice suggests that a guideline value of 1  $\mu\text{g}$  AN/L in drinking water would provide a safety margin of about three orders of magnitude (Fawell et al. 1999). Key procedures in the risk management of cyanobacterial toxins and cells have also been reviewed, including derivations of tolerable daily intakes and guideline values with reference to the toxins in drinking water and guideline levels for toxigenic cyanobacteria in bathing waters (Codd et al. 2005). A toxicity assessment of cyanobacterial toxin mixtures, based on the derivation of toxicity equivalent factors for these toxins and on the use of a toxicity equivalent method similar to that used for dioxins, has been proposed. However, it was concluded that more data on acute and chronic toxicity were required to establish toxicologically validated exposure limit values for cyanobacterial toxins (Wolf and Frank 2002; Rao et al. 2002a). Since the main risks associated with anatoxin poisoning involve farm and domestic animals, public information is important to warn users of potentially toxic water bodies (Fig. 8.6).

The effectiveness of various drinking water treatment processes for the removal of microcystins and AN has been examined in several studies involving laboratory and pilot-scale experiments using cyanobacterial blooms and laboratory-grown algal cultures as test materials. Substantial reduction of toxins, including AN, was achieved by granulated activated carbon filtration and by ozonization (Keijola et al. 1988; Bruchet et al. 1998; Hitzfeld et al. 2000; Hoeger et al. 2002). The stability and

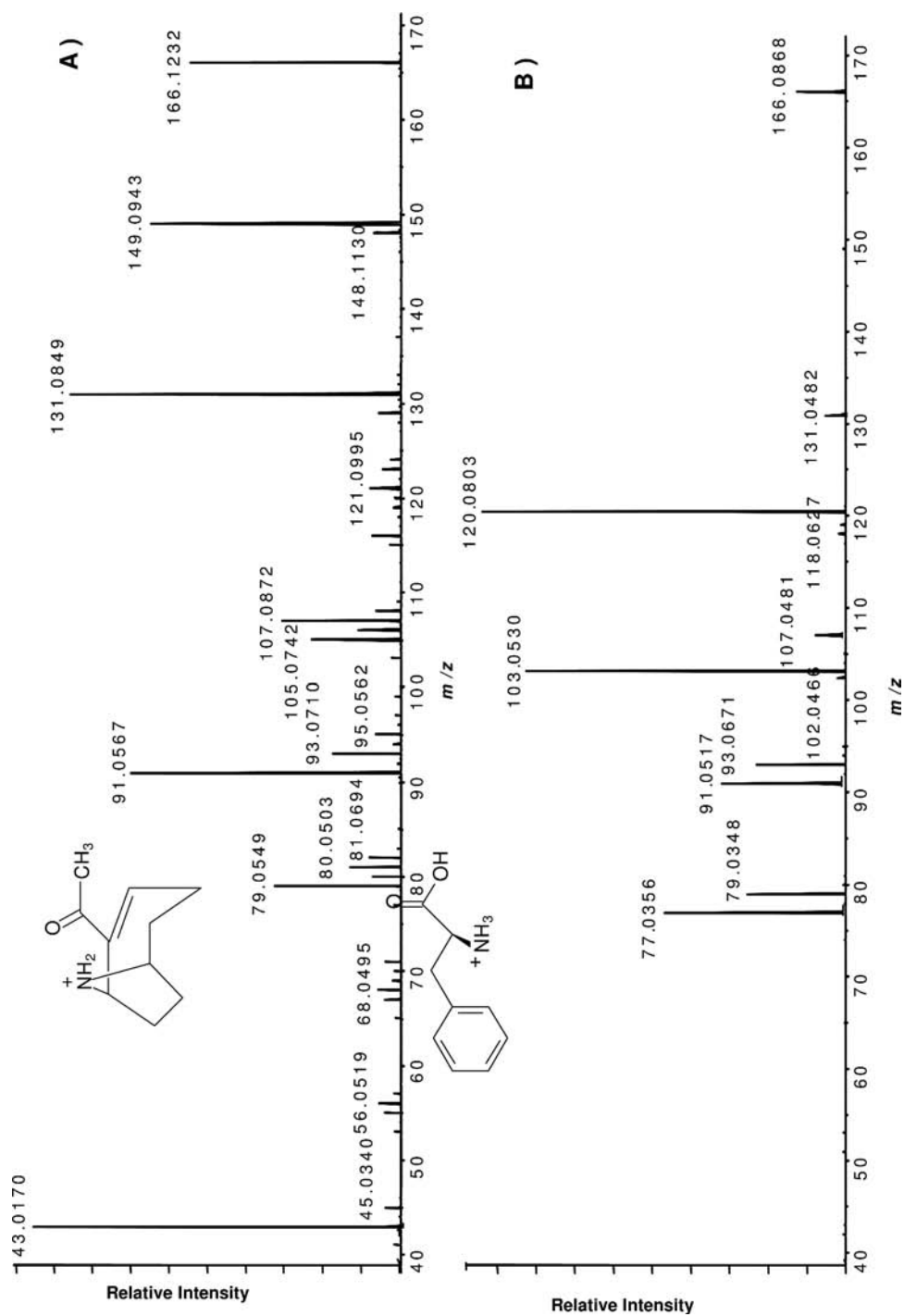


**Figure 8.5.** Quadrupole TOF mass spectra, in positive mode, (A) anatoxin-a, (B) phenylalanine, showing the similarity in the masses of the precursor ions,  $[M+H]^+$ , and several main product ions. Adapted from Furey et al. 2005.

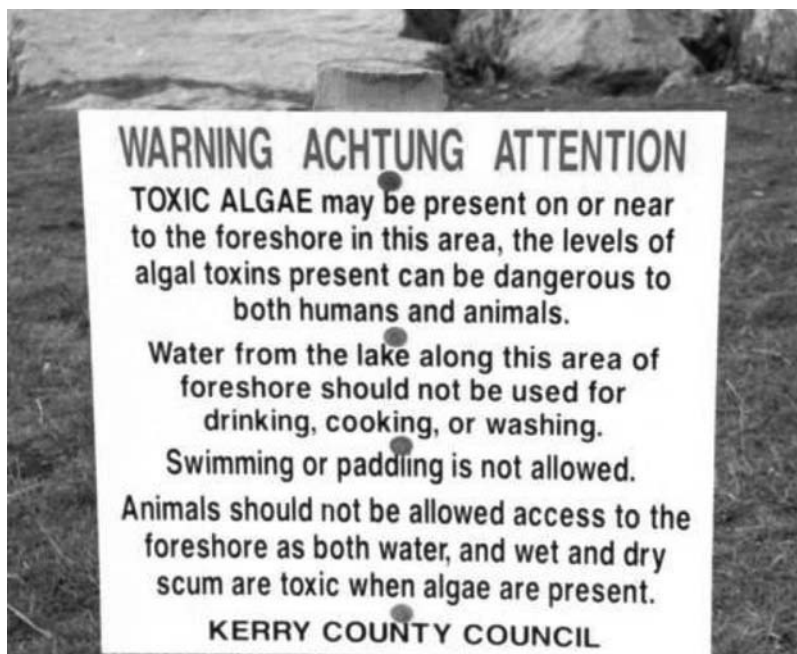


**Figure 8.6.** Warning sign of toxic algae erected near Caragh Lake, County Kerry, Ireland, following incidents of fatal canine neurotoxicosis.

persistence of microcystins, when compared with the lability of anatoxins, suggests that the latter toxins should present a reduced human health hazard.

## References

- Aas, P., Eriksen, S., Kolderup, J., Lundy, P., Haugen, J.-E., Skulberg, O.M., and Fonnum, F. 1996. Enhancement of acetylcholine release by homoanatoxin-a from *Oscillatoria formosa*. *Environ Toxicol Pharm* 2, 223–232.
- Adeyemo, O.M., and Siren, A.L. 1992. Cardio-respiratory changes and mortality in the conscious rat induced by (+)– and (+/–)-anatoxin-a. *Toxicon* 30, 899–905.
- Al-Layl, K., Poon, G., and Codd, G. 1988. Isolation and purification of peptide and alkaloid toxins from *Anabaena flos-aquae* using high performance thin-layer chromatography. *J Microbiol Meth* 7, 251–258.
- Araoz, R., Nghiem, H.O., Rippka, R., Palibroda, N., de Marsac, N.T., and Herdman, M. 2005. Neurotoxins in axenic oscillatory cyanobacteria: coexistence of anatoxin-a and homoanatoxin-a determined by ligand-binding assay and GC/MS. *Microbiol* 151, 1263–1273.
- Aronstam, R.S., and Witkop, B. 1981. Anatoxin-a interactions with cholinergic synaptic molecules. *Proc Natl Acad Sci* 78, 4639.
- Astrachan, N.B., and Archer, B.G. 1981. Simplified monitoring of anatoxin-a by reverse phase high performance liquid chromatography and sub-acute effects of anatoxin-a in rats. In *The Water Environment: Algal Toxins and Health*, ed. Carmichael, W.W. New York: Plenum Press, 437–446.
- Astrachan, N.B., Archer, B.G., and Hilbelink, D.R. 1980. Evaluation of the sub-acute toxicity and teratogenicity of anatoxin-a. *Toxicon* 18, 684–688.
- Ballot, A., Krienitz, L., Kotut, K., Wiegand, C., and Pflugmacher, S. 2005. Cyanobacteria and cyanobacterial toxins in the alkaline crater Lakes Sonachi and Simbi, Kenya. *Harmful Algae* 4, 139–150.
- Beasley, V.R., Cook, W.O., Dahlem, A.M., Hooser, S.B., Lovell, R.A., and Valentine, W.M. 1989a. Algae intoxication in livestock and water fowl. *Clin Toxicol* 5, 345–361.

- Beasley, V.R., Dahlem, A.M., Cook, W.O., Valentine, W.M., Lovell, R.A., Hooser, S.B., Harada, K., Suzuki, M., and Carmichael, W.W. 1989b. Diagnostic and clinical important aspects of cyanobacterial (blue-green) toxicoses. *J Vet Diagn Invest* 1, 359–365.
- Breining, S.R. 2004. Recent developments in the synthesis of nicotinic acetylcholine receptor ligands. *Curr Top Med Chem* 4, 609–629.
- Briand, J.F., Jacquet, S., Bernard, C., and Humbert, J.F. 2003. Health hazards for terrestrial vertebrates from toxic cyanobacteria in surface water ecosystems. *Vet Res* 34, 361–377.
- Brough, P., Thomas, P., Gallagher, T., and Wonnacott, S. 1994. Anatoxin structure-activity studies. *Synth Chem* 246–248.
- Bruchet, A., Bernazeau, F., Baudin, I., and Pieronne, P. 1998. Algal toxins in surface waters: analysis and treatment. *Water Supply* 16, 619–624.
- Bruno, M., Barbani, D., Pierdominici, E., Serse, A., and Ioppolo, A. 1994. Anatoxin-a and a previously unknown toxin in *Anabaena Planctonica* blooms found in lake Mulargia (Italy). *Toxicon* 32, 369–373.
- Bumke-Vogt, C., Mailahn, W., and Chorus, I. 1999. Anatoxin-a and neurotoxic cyanobacteria in German lakes and reservoirs. *Environ Toxicol* 14, 117–125.
- Carmichael, W., and Mahamood, N. 1984. Toxins from freshwater cyanobacteria. In *Seafood Toxins: ACS Symposium Series* 262. Washington, DC: American Chemical Society, 377.
- Carmichael, W.W. 2001. Health effects of toxin-producing cyanobacteria: “The CyanoHABs.” *Hum Ecol Risk Assess* 7, 1393–1407.
- Carmichael, W.W., Biggs, D.F., and Gorham, P.R. 1975. Toxicological and pharmacological action of *Anabaena flos-aquae* toxin. *Science* 187, 542–544.
- Carmichael, W.W., Biggs, D.F., and Peterson, M.A. 1979. Pharmacology of anatoxin-a, produced by freshwater cyanophyte *Anabaena flos-aquae* NRC-44-1. *Toxicon* 17, 229–236.
- Carmichael, W.W., and Gorham, P.R. 1978. Anatoxins from clones of *Anabaena flos-aquae* isolated from lakes in western Canada. *Mitt Int Verein Theor Angew Limon* 21, 285–295.
- . 1980. Freshwater cyanophyte toxins: types and their effects on the use of micro algae biomass. In *Algae Biomass: Production and Use* (G. Shelef and C. J. Soeder, eds.), pp. 437–438. Elsevier/North Holland Biomedical Press, Amsterdam.
- Carmichael, W.W., Gorham, P.R., and Biggs, D.F. 1977. Two laboratory case studies on the oral toxicity to calves of the freshwater cyanocytes (blue green algae) *Anabaena flos-aquae* NRC-44-1. *Can Vet J* 18, 71–75.
- Carmichael, W.W., and Yuan, M.C.F. 2004. Human mortality from accidental ingestion of toxic cyanobacteria – A case re-examined. In Sixth international conference on toxic cyanobacteria, p. 61 (abstract), Bergen, Norway.
- Claska, M.E., and Gilbert, J.J. 1998. The effect of temperature on the response of *Daphnia* to toxic cyanobacteria. *Freshwat Biol* 39, 221–232.
- Codd, G.A., Morrison, L.F., and Metcalf, J.S. 2005. Cyanobacterial toxins: risk management for health protection. *Toxicol Appl Pharmacol* 203, 264–272.
- Cook, W., Beasley, V., Dahlem, A., Dellinger, J., Harlin, K., and Carmichael, W. 1988. Comparison of effects of anatoxin-a(s) and paraoxon, physostigmine and pyridostigmine on mouse-brain cholinesterase activity. *Toxicon* 26, 750–753.
- Cook, W.O., Dellinger, J.A., Singh, S.S., Dahlem, A.M., Carmichael, W.W., and Beasley, V.R. 1989. Regional brain cholinesterase activity in rats injected intraperitoneally with anatoxin-a(s) or paraoxon. *Toxicol Letts.* 29–34.
- Dar, D.E., and Zinder, O. 1998. Catecholamine secretion from bovine adrenal chromaffin cells induced by the dextrorotatory isomer of anatoxin-a. *Gen Pharmacol* 31, 737–740.
- Devlin, J.P., Edwards, O.E., Gorham, P.R., Hunter, N.R., Pike, R.K., and Stavric, B. 1977. Anatoxin-a, a toxic alkaloid from *Anabaena flos-aquae* NRC-44h. *Can J Chem* 55, 1367–1371.
- Dube, S.N., Mazumder, P.K., Kumar, D., Rao, P.V.L., and Bhaskar, A.S.B. 1996. Cardiorespiratory and neuromuscular effects of freshwater cyanophyte *Anabena flos-aquae* in rats. *Defence Sci J* 46, 135–141.
- Durany, N., Riederer, P., and Deckert, J. 1999. The CNS toxin anatoxin-A interacts with alpha 4 beta 2-nicotinic acetylcholine receptors in human cortex. *Alzheimers Reports* 2, 263–266.
- Edwards, C., Beattie, K.A., Scrimgeour, C.M., and Codd, G.A. 1992. Identification of anatoxin-a in benthic cyanobacteria (blue-green algae) and in associated dog poisonings at Loch Insh, Scotland. *Toxicon* 30, 1165–1175.
- Fawell, J.K., Mitchell, R.E., Hill, R.E., and Everett, D.J. 1999. The toxicity of cyanobacterial toxins in the mouse: II anatoxin-a. *Hum Exp Toxicol* 18, 168–173.
- Feuerbach, D., Lingenhohl, K., Dobbins, P., Mosbacher, J., Corbett, N., Nozulak, J., and Hoyer, D. 2005. Coupling of human nicotinic acetylcholine receptors alpha 7 to calcium channels in GH3 cells. *Neuropharmacol* 48, 215–227.
- Feuerstein, G., and Siren, A.L. 1988. Mechanisms of anatoxin a induced shock. *Circulatory Shock* 24, 278–278.

- Furey, A., Crowley, J., Hamilton, B., Lehane, M., and James, K.J. 2005. Strategies to avoid the mis-identification of anatoxin-a using mass spectrometry in the forensic investigation of acute neurotoxic poisoning. *J Chromatogr A* 1082, 91–97.
- Furey, A., Crowley, J., Shuilleabhain, A.N., Skulberg, A. M., and James, K.J. 2003. The first identification of the rare cyanobacterial toxin, homoanatoxin-a, in Ireland. *Toxicon* 41, 297–303.
- Gordon, R.K., Gray, R.R., Reaves, C.B., Butler, D.L., and Chiang, P.K. 1992. Induced release of acetylcholine from guinea pig ileum longitudinal muscle-myenteric plexus by anatoxin-a. *J Pharmacol Exp Ther* 263, 997–1002.
- Gorham, P.R. 1964. Toxic algae. In *Algae and Man*, ed. Jackson, D. New York: Plenum Press, 307–336.
- Gorham, P.R., McLachlan, J., Hammer, U.T., and Kim, W.K. 1964. Isolation and culture of toxic strains of *Anabaena flos-aquae* (Lyngb.) de Breb. *Mitt internat Verein Limnol* 15, 796–804.
- Gugger, M., Lenoir, S., Berger, C., Ledreux, A., Druart, J.C., Humbert, J.F., Guette, C., and Bernard, C. 2005. First report in a river in France of the benthic cyanobacterium *Phormidium favosum* producing anatoxin-a associated with dog neurotoxicosis. *Toxicon* 45, 919–928.
- Gunn, G.J., Rafferty, A.G., Rafferty, G.C., Cockburn, N., Edwards, C., Beattie, K.A., and Codd, G.A. 1992. Fatal canine neurotoxicosis attributed to blue-green algae (cyanobacteria). *Vet Rec* 130, 301–302.
- Gupta, N., Bhaskar, A.S.B., and Rao, P.V.L. 2002. Growth characteristics and toxin production in batch cultures of *Anabaena flos-aquae*: effects of culture media and duration. *World J Microbiol Biotechnol* 18, 29–35.
- Hamill, K.D. 2001. Toxicity in benthic freshwater cyanobacteria (blue-green algae): first observations in New Zealand. *New Zealand J Mar Freshwat Res* 35, 1057–1059.
- Harada, K. 1999. Recent advances of toxic cyanobacteria researches. *J Health Sci* 45, 150–165.
- Harada, K., Kimura, I., Ogawa, K., Suzuki, M., Dahlem, A.M., Beasley, V.R., and Carmichael, W.W. 1989. A new procedure for the analysis and purification of naturally occurring anatoxin-a from the blue-green alga *Anabaena flos-aquae*. *Toxicon* 27, 1289–1296.
- Harada, K.-I., Nagai, H., Kimura, Y., Suzuki, M., Park, H.-D., Watanabe, M., Kuukkainen, R., Sivonen, K., and Carmichael, W.W. 1993. Liquid chromatography/mass spectrometric detection of anatoxin-a, a neurotoxin from cyanobacteria. *Tetrahedron* 49, 9251–9260.
- Henriksen, P., Carmichael, W.W., An, J., and Moestrup, O. 1997. Detection of an anatoxin-a(s)-like anticholinesterase in natural blooms and cultures of cyanobacteria/blue-green algae from Danish lakes and in the stomach contents of poisoned birds. *Toxicon* 35, 901–913.
- Hill, H. 2005. Dog deaths in Humboldt and Mendocino County water bodies possibly related to cyanobacterial toxicity. California Animal Health and Food Safety Laboratory. <http://www.waterboards.ca.gov/docs/bluegreenalgae/harriethill.pdf>
- Himberg, K. 1989. Determination of anatoxin-a, the neurotoxin of *Anabaena flos-aquae* cyanobacterium, in algae and water by gas chromatography-mass spectrometry. *J Chromatogr* 481, 358–362.
- Hitzfeld, B.C., Hoeger, S.J., and Dietrich, D.R. 2000. Cyanobacterial toxins: Removal during drinking water treatment, and human risk assessment. *Environ Health Perspect* 108, 113–122.
- Holte, H.R., Eriksen, S., Skulberg, O., and Aas, P. 1998. The effect of water soluble cyanotoxin(s) produced by two species of *Anabaena* on the release of acetylcholine from the peripheral cholinergic nervous system of the rat airway. *Environ Toxicol Pharmacol* 5, 51–59.
- Huber, C.S. 1972. The crystal structure and absolute configuration of 2,9-diacetyl-9-azabicyclo(4,2,1)non-2,3-ene. *Acta Cryst B* 28, 2577–2582.
- Hyde, E.G., and Carmichael, W.W. 1991. Anatoxin-a(s), a naturally occurring organophosphate, is an irreversible active site directed inhibitor of acetylcholinesterase (EC 3.1.1.7). *J Biochem Toxicol* 6, 195–201.
- James, K.J., Sherlock, I.R., and Stack, M.A. 1997. Anatoxin-a in Irish freshwaters and cyanobacteria, determined using a new fluorimetric liquid chromatographic method. *Toxicon* 35, 963–971.
- Jarema, K.A., and MacPhail, R.C. 2003. Comparative effects of weekly exposures to anatoxin-a and nicotine on the operant performance of rats. *Toxicol Sci* 72, 359.
- Juday, R.E., Keller, E.J., Horpestad, A., Bahls, L.L., and Glasser, S. 1981. A toxic bloom of *Anabaena flos-aquae* in Hebgen reservoir Montana in 1977. In *The water environment: Algal toxins and health* (W.W. Carmichael, ed.), pp. 103–112. Plenum Press, New York.
- Kangatharalingam, N., and Priscu, J. 1993. Isolation and verification of anatoxin-a producing clones of *Anabaena flos-aquae* (lyngb.) de Breb. from a eutrophic lake. *FEMS Microbiol Ecol* 12, 127–130.
- Kearns, K.D., and Hunter, M.D. 2001. Toxin-producing *Anabaena flos-aquae* induces settling of *Chlamydomonas reinhardtii*, a competing motile alga. *Microbiol Ecol* 42, 80–86.
- Keijola, A.M., Himberg, K., Esala, A. L., Sivonen, K., and Hiisvirta, L. 1988. Removal of cyanobacterial toxins in water treatment processes: laboratory and pilot-scale experiments. *Tox Assess* 3, 643–656.



- Kiss, J.P., Windisch, K., De Oliveira, K., Hennings, E.C.P., Mike, A., and Szasz, B.K. 2001. Differential effect of nicotinic agonists on the H-3 Norepinephrine release from rat hippocampal slices. *Neurochem Res* 26, 943–950.
- Kiss, T., Vehovszky, A., Hiripi, L., Kovacs, A., and Voros, L. 2002. Membrane effects of toxins isolated from a cyanobacterium, *Cylindrospermopsis raciborskii*, on identified molluscan neurones. *Comp Biochem Physiol C-Toxicol Pharmacol* 131, 167–176.
- Kofuji, P., Aracava, Y., Swanson, K., Aronstam, R., Rapoport, H., and Albuquerque, E. 1990. Activation and blockade of the acetylcholine receptor-ion channel by the agonists (+)-anatoxin-a, the N-methyl derivative and the enantiomer. *J Pharmacol Expt Therapeut* 252, 517–525.
- Koskinen, A.M.P., and Rapoport, H. 1985. Synthetic and conformational studies on anatoxin-a: a potent acetylcholine agonist. *J Med Chem* 28, 1301–1309.
- Krienitz, L., Ballot, A., Kotut, K., Wiegand, C., Putz, S., Metcalf, J.S., Codd, G.A., and Pflugmacher, S. 2003. Contribution of hot spring cyanobacteria to the mysterious deaths of Lesser Flamingos at Lake Bogoria, Kenya. *FEMS Microbiol Ecol* 43, 141–148.
- Lilleheil, G., Andersen, R.A., Skulberg, O.M., and Alexander, J. 1997. Effects of a homoanatoxin-a-containing extract from *Oscillatoria formosa* (Cyanophyceae/cyanobacteria) on neuromuscular transmission. *Toxicon* 35, 1275–1289.
- Macklin, K.D., Maus, A.D.J., Pereira, E.F.R., Albuquerque, E.X., and Conti-Fine, B.M. 1998. Human vascular endothelial cells express functional nicotinic acetylcholine receptors. *J Pharmacol Expt Therapeut* 287, 435–439.
- MacPhail, R.C., Farmer, J.D., Jarema, K.A., and Chernoff, N. 2005. Nicotine effects on the activity of mice exposed prenatally to the nicotinic agonist anatoxin-a. *Neurotoxicol Teratol* 27, 593–598.
- Mahmood, N.A., and Carmichael, W.W. 1986. The pharmacology of anatoxin-a(s), a neurotoxin produced by the freshwater cyanobacterium *Anabaena flos-aquae* NRC 525–17. *Toxicon* 24, 425–434.
- . 1987. Anatoxin-A (S), an anticholinesterase from the cyanobacterium *Anabaena flos-aquae* NRC-525-17. *Toxicon* 25, 1221–1227.
- Matsunaga, S., Moore, R., Niemczura, W., and Carmichael, W. 1989. Anatoxin-a (s), a potent anticholinesterase from *Anabaena flos-aquae*. *J Am Chem Soc* 111, 8021–8023.
- Mazur, H., and Plinski, M. 2003. Nodularia spumigena blooms and the occurrence of hepatotoxin in the Gulf of Gdansk. *Oceanologia* 45, 305–316.
- Mitrovic, S.M., Pflugmacher, S., James, K.J., and Furey, A. 2004. Anatoxin-a elicits an increase in peroxidase and glutathione S-transferase activity in aquatic plants. *Aquatic Toxicol* 68, 185–192.
- Molloy, L., Wonnacott, S., Gallagher, T., Brough, P.A., and Livett, B.G. 1995. Anatoxin-a is a potent agonist of the nicotinic acetylcholine receptor of bovine adrenal chromaffin cells. *Eur J Pharmacol* 289, 447–453.
- Namikoshi, M., Murakami, T., Fujiwara, T., Nagai, H., Niki, T., Harigaya, E., Watanabe, M. F., Oda, T., Yamada, J., and Tsujimura, S. 2004. Biosynthesis and transformation of homoanatoxin-a in the cyanobacterium *Raphidiopsis mediterranea* Skuja and structures of three new homologues. *Chem Res Toxicol* 17, 1692–1696.
- Namikoshi, M., Murakami, T., Watanabe, M.F., Oda, T., Yamada, J., Tsujimura, S., Nagai, H., and Oishi, S. 2003. Simultaneous production of homoanatoxin-a, anatoxin-a, and a new non-toxic 4-hydroxyhomoanatoxin-a by the cyanobacterium *Raphidiopsis mediterranea* Skuja. *Toxicon* 42, 533–538.
- Nicolotti, O., Pellegrini-Calace, M., Altomare, C., Carotti, A., Carrieri, A., and Sanz, F. 2002. Ligands of neuronal nicotinic acetylcholine receptor (nAChR): Inferences from the Hansch and 3-D quantitative structure-activity relationship (QSAR) models. *Curr Med Chem* 9, 1–29.
- Oberemm, A., Becker, J., Codd, G.A., and Steinberg, C. 1999. Effects of cyanobacterial toxins and aqueous crude extracts of cyanobacteria on the development of fish and amphibians. *Environ Toxicol* 14, 77–88.
- Park, H., Watanabe, M., Harada, K., Nagai, H., Suzuki, M., Watanabe, M.F., and Hayashi, H. 1993. Hepatotoxin (microcystin) and neurotoxin (anatoxin-a) contained in natural blooms and strains of cyanobacteria from Japanese freshwaters. *Nat Toxins* 1, 353–360.
- Park, H.-D., Kim, B., Kim, E., and Okino, T. 1998. Hepatotoxic microcystins and neurotoxic anatoxin-a in cyanobacterial blooms from Korean lakes. *Environ Toxicol Water Qual* 13, 225–234.
- Pawlik-Skowronska, B., Skowronski, T., Pirszel, J., and Adamczyk, A. 2004. Relationship between cyanobacterial bloom composition and anatoxin-a and microcystin occurrence in the eutrophic dam reservoir (SE Poland). *Polish J Ecol* 52, 479–490.
- Rao, P.V., Gupta, N., Bhaskar, A.S., and Jayaraj, R. 2002a. Toxins and bioactive compounds from cyanobacteria and their implications on human health. *J Environ Biol* 23, 215–224.
- Rao, P.V.L., Bhattacharya, R., Gupta, N., Parida, M.M., Bhaskar, A.S.B., and Dubey, R. 2002b. Involvement of caspase and reactive oxygen species in cyanobacterial toxin anatoxin-a-induced cytotoxicity and apoptosis in rat thymocytes and Vero cells. *Archiv Toxicol* 76, 227–235.

- Rapala, J., Lahiti, K., Sivonen, K., and Niemelae, S.I. 1994. Biodegradability and adsorption on lake sediments of cyanobacterial hepatotoxins and anatoxin-a. *Lett Appl Microbiol* 19, 423–428.
- Rapala, J., Sivonen, K., Luukkainen, R., and Niemela, S. 1993. Anatoxin-a concentration in *Anabaena* and *Aphanizomenon* under different environmental conditions and comparison of growth by toxic and non-toxic *Anabaena*-strains – a laboratory study. *J Appl Phycol* 5, 581.
- Reinikainen, M., Lindvall, F., Meriluoto, J.A.O., Repka, S., Sivonen, K., Spoof, L., and Wahlsten, M. 2002. Effects of dissolved cyanobacterial toxins on the survival and egg hatching of estuarine calanoid copepods. *Mar Biol* 140, 577–583.
- Richard, D.S., Beattie, K.A., and Codd, G.A. 1983. Toxicity of cyanobacterial blooms from Scottish freshwater. *Environ Technol Lett* 4, 377–382.
- Richey, L.J., Carbonneau, D.A., Schoeb, T.R., Taylor, S.K., Woodward, A.R., and Clemmons, R. 2001. Potential toxicity of cyanobacteria to American alligators (*Alligator mississippiensis*). Florida Fish and Wildlife Conservation Commission. <http://myfwc.com/gators/research/griffin.htm>.
- Siren, A.L., and Feuerstein, G. 1990. Cardiovascular effects of anatoxin-a in the conscious rat. *Toxicol Appl Pharmacol* 102, 91–100.
- Sivonen, K., Himberg, K., Luukkainen, R., Niemela, S.I., Poon, G.K., and Codd, G.A. 1989. Preliminary characterization of neurotoxic cyanobacteria blooms and strains from Finland. *Toxic Ass* 4, 339–352.
- Sivonen, K., Niemela, S., Niemi, R., Lepisto, L., Luoma, H., and Rasanen, L. 1990. Toxic cyanobacteria (blue-green algae) in Finnish fresh and coastal waters. *Hydrobiologia* 190, 267–275.
- Skulberg, O.M. 2000. Microalgae as a source of bioactive molecules—experience from cyanophyte research. *J Appl Phycol* 12, 341–348.
- Skulberg, O.M., Carmichael, W.W., Anderson, R.A., Matsunaga, S., Moore, R.E., and Skulberg, R. 1992. Investigations of a neurotoxic oscillatorial strain (Cyanophyceae) and its toxin. Isolation and characterisation of homoanatoxin-a. *Environ Toxic Chem* 11, 321–329.
- Skulberg, O.M., Underdal, B., and Utkilen, H. 1994. Toxic waterblooms with cyanophytes in Norway—current knowledge. *Algological Studies* 75, 279–289.
- Smith, R.A., and Lewis, D. 1987. A rapid analysis of water for anatoxin-a, the unstable toxic alkaloid from *Anabaena flos-aquae*, the stable non-toxic alkaloids left after bioreduction and a related amine which may be nature's precursor to anatoxin-a. *Vet Hum Toxicol* 29, 153–154.
- Soliakov, L., Gallagher, T., and Wonnacott, S. 1995. Anatoxin-a evoked [H-3] dopamine release from rat striatal synaptosomes. *Neropharmacol* 34, 1535–1541.
- Soliakov, L., and Wonnacott, S. 2001. Involvement of protein kinase C in the presynaptic nicotinic modulation of [H-3] – dopamine release from rat striatal synaptosomes. *British J. Pharmacol.* 132, 785–791.
- Spivak, C.E., Witkop, B., and Albuquerque, E.X. 1980. Anatoxin-a: a novel, potent agonist at the nicotinic receptor. *Mol Pharmacol* 18, 384–394.
- Stevens, D.K., and Krieger, R.I. 1988. Analysis of Anatoxin-a by GC/ECD. *J Anal Toxicol* 12, 126–131.
- Stevens, D.K., and Krieger, R.I. 1990. N-Methylation of anatoxin-a abolishes nicotinic cholinergic activity. *Toxicon* 28, 133–134.
- . 1991a. Effect of route of exposure and repeated doses on the acute toxicity in mice of the cyanobacterial nicotinic alkaloid anatoxin-A. *Toxicon* 29, 134–138.
- . 1991b. Stability studies on the cyanobacterial nicotinic alkaloid anatoxin-a. *Toxicon* 29, 167–179.
- Stolerman, I.P., Albuquerque, E.X., and Garcha, H.S. 1992. Behavioural effects of anatoxin, a potent nicotinic agonist, in rats. *Neuropharmacol* 31, 311–314.
- Swanson, K.L., Allen, C.N., Aronstam, R.S., Rapoport, H., and Albuquerque, E.X. 1986. Molecular mechanisms of the potent and stereospecific nicotinic receptor agonist (+)-anatoxin-a. *Molec Pharmacol* 29, 250–257.
- Swanson, K.L., Rapoport, H., Aronstam, R.S., and Albuquerque, E.X. 1990. Nicotinic acetylcholine receptor function studied with synthetic (+)-anatoxin-a and derivatives. In *ACS Symposium Series: Marine Toxins*, vol. 418, ed. Hall, S., and Strichartz, G. Washington, DC: American Chemical Society, 107–118.
- Teneva, I., Mladenov, R., Popov, N., and Dzhambazov, B. 2005. Cytotoxicity and apoptotic effects of microcystin-LR and anatoxin-a in mouse lymphocytes. *Folia Biologica* 51, 62–67.
- Thomas, P., Stephens, M., Wilkie, G., Amar, M., Lunt, G. G., Whiting, P., Gallagher, T., Pereira, E., Alkondon, M., and Albuquerque, E.X. 1993. (+)-Anatoxin-a is a potent agonist at neuronal nicotinic acetylcholine receptors. *J Neurochem* 60, 2308–2311.
- Thompson, P.E., Manallack, D.T., Blaney, F.E., and Gallagher, T. 1992. Conformational studies on (+)-anatoxin-a and derivatives. *J Computer-Aided Molec Design* 6, 287–298.



- Viaggiu, E., Melchiorre, S., Volpi, F., Di Corcia, A., Mancini, R., Garibaldi, L., Crichigno, G., and Bruno, M. 2004. Anatoxin-A toxin in the cyanobacterium *Planktothrix rubescens* from a fishing pond in northern Italy. *Environ Toxicol* 19, 191–197.
- Watanabe, M.F., Tsujimura, S., Oishi, S., Niki, T., and Namikoshi, M. 2003. Isolation and identification of homoanatoxin-a from a toxic strain of the cyanobacterium *Raphidiopsis mediterranea* Skuja isolated from Lake Biwa, Japan. 42. *Phycologia* 42, 364–369.
- WHO. 1998. Health criteria and other supporting information, addendum to volume 2. *Guidelines for Drinking Water Quality*, 2nd ed. Geneva: World Health Organization.
- Wolf, H.U., and Frank, C. 2002. Toxicity assessment of cyanobacterial toxin mixtures. *Environ Toxicol* 17, 395–399.
- Wonnacott, S., Jackman, S., Swanson, K. L., Rapoport, H., and Albuquerque, E.X. 1991. Nicotinic pharmacology of anatoxin analogs. 2. Side-chain structure-activity-relationships at neuronal nicotinic ligand-binding sites. *J Pharmacol Expt Therapeut* 259, 387–391.
- Wonnacott, S., Swanson, K.L., Albuquerque, E.X., Huby, N. J.S., Thomson, P., and Gallaghers, T. 1992. Homoanatoxin: a potent analogue of anatoxin-a. *Biochem Pharmacol* 43, 419–423.
- Zotou, A., Jefferies, T.M., Brough, P.A., and Gallagher, T. 1993. Determination of anatoxin-a and homoanatoxin in blue-green algal extracts by high-performance liquid chromatography and gas chromatography-mass spectrometry. *Analyst* 118, 753–758.

## 9 Pectenotoxins

Christopher O. Miles

### Introduction

Pectenotoxins (PTXs) are lipophilic macrocyclic polyethers (Fig. 9.1), the first examples of which were isolated from the Japanese scallop (*Patinopecten yessoensis*) from which the name pectenotoxin is derived (Yasumoto et al. 1984, 1985). Since the isolation of the first pectenotoxin, pectenotoxin-1 (PTX-1), a number of other PTXs have been isolated or identified in a range of source organisms. Many of these PTXs are products of metabolism, produced after ingestion of PTX-containing algae. The co-extractability of PTXs with diarrhetic toxins such as okadaic acid and dinophysistoxins from shellfish, together with their toxicity to mice in the traditional i.p. mouse bioassay for lipophilic toxins, led to PTXs being included together with okadaic acid analogues (and yessotoxins) in the diarrhetic shellfish poisoning (DSP) toxin group. However, this is inappropriate from a toxicological perspective because PTXs are not strongly diarrhetic and, unlike okadaic acid, some PTXs are hepatotoxic when administered intraperitoneally (Aune 1997). A reclassification of the shellfish toxin groups has recently been suggested, and it has been recommended that PTXs be classified together in their own group on the basis of their chemical and toxicological properties (FAO/IOC/WHO 2004). Because PTXs were toxic in the traditional mouse bioassay for DSP toxins, their levels have been regulated in shellfish in some countries. However, recent evidence suggests that PTXs may be much less of a threat to public health than was originally supposed based on the mouse bioassay results. PTXs have been reviewed previously, often as part of a wider review of DSP toxins or of shellfish and algal toxins in general (Aune 1997; Bhakuni 1995; Yasumoto 2001; Yasumoto and Murata 1993, 1990). More focused reviews have been published recently (Draisici, Lucentini, and Mascioni 2000; Burgess and Shaw 2001), but knowledge about PTXs has advanced at a rapid rate. Historical aspects and recent findings related to pectenotoxins are reviewed here, including their occurrence, chemistry, synthesis, and metabolism. Biological activities of PTXs are also summarized but are not critically evaluated. Analytical methods for PTXs are not covered, but are mentioned where relevant to discussions of other aspects.

### Occurrence

Although PTXs were first isolated from filter-feeding shellfish, it quickly became apparent that PTXs originated from microalgae in the diet of the shellfish. Thus far, only the genus *Dinophysis* has been implicated in contamination of shellfish with PTXs. This genus appears to be widespread, and to be widely associated with a variety of toxins in many regions including Europe (Zingone et al. 2006; Bravo et al. 1995; Della Loggia et al. 1993), Japan (Sato, Koike, and Kodama 1996), the Americas (Cembella 1989; Norris and Berner 1970), and Australasia (Hallegraeff and Lucas 1988).

## Algae

PTX-1 and -2 were originally isolated from *P. yessoensis*, but it appeared likely that the PTX-2 in these shellfish was of algal origin. *Dinophysis fortii*, which was already known as a source of okadaic acid analogues, and possibly *Dinophysis acuminata*, were proposed as the sources of the PTXs in Japan (Yasumoto et al. 1985). A study of PTXs in *Dinophysis* spp. using HPLC-UV analysis revealed PTX-2 in picked cells of Japanese *D. fortii*, and although PTX-2 was apparently not detected in *D. acuta* (Norway and Spain), *D. acuminata* (France and Japan), *D. rotundata* (Japan), *D. mitra* (Japan), *D. tripos* (Japan), or *D. norvegica* (Japan) (Lee et al. 1989), this may have been due to lack of sufficient sensitivity of the method combined with low abundance of the toxin in these algal samples. PTX-2 was subsequently detected together with okadaic acid in European *D. fortii* by LC-MS (Draisci et al. 1996). The advent of LC-MS methods has greatly facilitated the identification and quantitation of PTXs in algae and shellfish, and there is now evidence that PTXs are present in many *Dinophysis* spp. throughout the world (Tables 9.1 and 9.2). Furthermore, the even more widely documented presence of PTXs in shellfish (Table 9.3) is indicative of very broad distribution of PTX-producing algae. Although it often stated that *Dinophysis* spp. produce PTXs (and okadaic acid analogues), there is as yet no direct experimental evidence for this. It is clear that numerous species of *Dinophysis* contain PTXs, particularly when picked and washed cells have been analyzed for their toxin content. However, as *Dinophysis* are heterotrophic or mixotrophic, and may consume prey species in their natural environment, it is possible that the PTXs in *Dinophysis* samples harvested from Nature originate from prey species. This possibility is not unrealistic, given that PTXs have recently been detected in *Protoperidinium* spp. that had been observed preying on *Dinophysis* spp. (Miles et al. 2004b). It is also possible that bacteria or other micro-organisms may be involved PTX biosynthesis. The current inability to maintain *Dinophysis* in culture means that such possibilities cannot be excluded, and also precludes studies of PTX biosynthesis. However, the ubiquity of PTXs in *Dinophysis* spp. from around the world (Tables 9.1 and 9.2) suggests that PTX biosynthesis is probably a constitutive trait for many species in this genus.

Until recently, it has not been possible to study the occurrence of toxins in small numbers of picked cells. Many studies of PTXs in algae have therefore relied on relatively large samples of algae fractionated from mixed blooms, or on analysis of extracts from blooms containing essentially one species of *Dinophysis* (Draisci et al. 1996; Daiguji et al. 1998; Suzuki et al. 1998). However, advances in analytical methods mean that analysis of toxins in picked cells is now possible, sometimes even in single cells. An ELISA method for analyzing both shellfish and plankton samples has recently been developed (Briggs et al. 2000) and gave similar results to LC-MS analysis for extracts of plankton from Norway (Briggs et al. 2000) and New Zealand (MacKenzie et al. 2004). ELISA analysis of picked cells indicated that *D. norvegica* from Sognefjord, Norway, contained an average of 11.6 pg/cell PTXs (with a standard deviation for 6 replicates of 20 cells of 3 pg/cell) and that *D. acuminata* from Akaroa Harbour, New Zealand, contained 28 pg/cell PTXs (sub-aliquot from 10 cells) (Samdal et al. 2002). With modern LC-MS technology and sample preparation methods it is now possible to determine both the toxin content and profile of very small numbers of picked algal cells (Quilliam et al. 2003; Puente et al. 2004a, 2004b). This approach has been used to analyze PTXs in *Dinophysis* cells (Miles et al. 2004b; Quilliam et al. 2003; Puente et al. 2004a, 2004b; Fernández and Reguera 2002); their power is well illustrated by the study of PTXs and okadaic acid analogues in four *Dinophysis* species picked from a mixed bloom and in *Protoperidinium* spp. observed preying on the *Dinophysis* (Miles et al. 2004b). Such methods should help advance our understanding of toxin production and biosynthesis, even in unculturable genera.

**Table 9.1.** Worldwide occurrence of pectenotoxins in identified algal species

Species	PTX-2 <sup>a</sup>	PTX-11	PTX-12	PTX-13	PTX-2 SA
<i>D. acuminata</i>	Australia (Eaglesham et al. 2000a) Canada (Quilliam et al. 2003) Ireland (Puente et al. 2004) New Zealand (MacKenzie et al. 2005) Norway (Miles et al. 2004b) Portugal (Vale and Sampayo 2002b)	New Zealand (MacKenzie et al. 2005)	Norway (Miles et al. 2004b)		Canada (Quilliam et al. 2003) Croatia (Pavela-Vrančić et al. 2001) <sup>b</sup> New Zealand (MacKenzie et al. 2005)
<i>D. acuta</i>	Portugal (Vale and Sampayo 2002b) Ireland (Puente et al. 2004a, 2004b; Nogueiras et al. 2003) New Zealand (MacKenzie et al. 2005, 2002; Miles et al. 2004a; Suzuki et al. 2003, 2006) Norway (Miles et al. 2004b) Portugal (Vale and Sampayo 2002b; Vale 2004)	New Zealand (MacKenzie et al. 2002, 2005; Miles et al. 2004a; Suzuki et al. 2003, 2006)	Norway (Miles et al. 2004b)	New Zealand (Suzuki et al. 2003, 2006; Miles et al. 2006b)	Ireland (Puente et al. 2004a, 2004b; Nogueiras et al. 2003; Daiguji et al. 1998; James et al. 1999) New Zealand (MacKenzie et al. 2002, 2005; Miles et al. 2004a)
<i>D. caudata</i>	Italy (Burgess et al. 2003) <sup>c</sup>				
<i>D. fortii</i>	Italy (Draisci et al. 1996) Japan (Lee et al. 1989; Sasaki et al. 1999; Suzuki et al. 1998)				
<i>D. norvegica</i>	Norway (Miles et al. 2004b)		Norway (Miles et al. 2004b) Norway (Miles et al. 2004b)		Australia (Burgess et al. 2003)
<i>D. rotundata</i>	Norway (Miles et al. 2004b)		Norway (Miles et al. 2004b)		
<i>P. crassipes</i>	Norway (Miles et al. 2004b)		Norway (Miles et al. 2004b)		
<i>P. depressum</i>	Norway (Miles et al. 2004b)		Norway (Miles et al. 2004b)		
<i>P. divergens</i>	Norway (Miles et al. 2004b)		Norway (Miles et al. 2004b)		

<sup>a</sup>No PTX-2 was detected initially in *D. acuta*, *D. acuminata*, *D. rotundata*, *D. mitra*, *D. tripos*, or *D. norvegica* by HPLC-UV (Lee et al. 1989).

<sup>b</sup>Possibly *D. sacculus*

<sup>c</sup>Possible occurrence, but *D. caudata* was also present

Estimates of the amount of PTXs per cell have been made for a range of species. The most common method has been to analyze extracts of sea water or net-haul concentrates after determining the cell density of algal species by microscopy. The alternative approach, analyzing relatively small numbers of hand-picked cells, is used less often because it requires sensitive analytical methods and tedious picking and washing of the cells. The published results are summarized in Table 9.2. A significant amount of PTXs can be present in cell-free sea water from *Dinophysis* blooms (Briggs et al. 2000; MacKenzie et al. 2004) due to leakage from cells. This dissolved toxin would be measured in the bloom-extract procedures, but not in the picked-cell methods, and may account for some of the variability and higher values determined by the former method. While PTX-2 seco acids (PTX-2 SAs) were detected in *Dinophysis* in some studies (Pavela-Vranj et al. 2001; Puente et al. 2004a; Daiguji et al. 1998; James et al. 1999; Draisci et al. 1999; Fernández et al. 2002), it now appears that seco acids are not present in significant amounts in healthy intact *Dinophysis* cells (Puente et al. 2004b; MacKenzie et al. 2005; Vale and Sampayo 2002b; MacKenzie et al. 2002; Miles et al. 2004c). The presence of PTX SAs in algal extracts is thought to result from hydrolysis of PTXs by enzymes released from damaged cells (MacKenzie et al. 2002; Fernández et al. 2002).

### Shellfish

PTXs have been found in shellfish from most regions of the world, reflecting the world-wide distribution of *Dinophysis* spp. There is relatively little information on concentrations of PTXs in shellfish due to the previous scarcity of analytical standards and because monitoring for PTXs by instrumental methods has until recently not been widespread, but the bulk of the published information is summarized in Table 9.3. A certified reference material (CRM) for PTX-2 became available from the Certified Reference Materials Program (CRMP) of the National Research Council of Canada (Institute for Marine Biosciences, Halifax; [http://imb-ibm.nrc-cnrc.gc.ca/crmp/shellfish/index\\_e.php](http://imb-ibm.nrc-cnrc.gc.ca/crmp/shellfish/index_e.php)) in 2003 (Quilliam 2004), and a CRM for PTX-11 is expected in 2006 (M.A. Quilliam, personal communication). The availability of such standards should result in an increasing amount of reliable information on the type and concentration of PTXs present in natural samples.

PTXs appear to be concentrated primarily in the hepatopancreas in mussels (MacKenzie et al. 2002), and when PTX-6 was injected into the adductor muscle of the scallop *P. yessoensis* the toxin was rapidly transported to the hepatopancreas (Suzuki et al. 2005a). Levels of PTX seco acids in shellfish can be quite high, with concentrations reportedly as much as 2 mg/kg in Australian and 4.1 mg/kg in New Zealand shellfish (Burgess 2003), and levels of up to 17 mg/kg of seco acids of PTX-2 and PTX-12 were measured in Norwegian *M. edulis* (Miles et al. 2004b). Several studies have shown positive correlations between concentrations of PTXs in shellfish and *Dinophysis* cells in sea water from which the shellfish were collected (Eaglesham et al. 2000a; Vale and Sampayo 2002b; Vale 2004; MacKenzie et al. 2004; Fernández et al. 2002; Aune et al. 2002; Holland et al. 2003). The data from the study of MacKenzie et al. (MacKenzie et al. 2004), using the so-called SPATT method, are particularly convincing because the authors were able to correlate the toxin content of the mussels, the toxin concentration in the sea water, and the concentration of the various species of *Dinophysis* in the water.

### Japan

PTXs were originally identified in the Japanese scallop *P. yessoensis*, and PTX-1–7 were isolated or identified from this source (PTX-8 and PTX-9 are artifactual, and details of PTX-10 have yet to be published). Published information on PTX concentrations in Japanese shellfish are limited, although

**Table 9.2.** Levels of pectenotoxins (pg/cell) in *Dinophysis* spp. determined by analysis of extracts from *Dinophysis* blooms or by analysis of picked *Dinophysis* cells

Species	Country	Method	PTX-2 SAs	PTX-11 SAs	PTX-12 SAs	PTX-12 SAs	Reference
<i>D. acuminata</i> + <i>D. acuta</i> + <i>D. caudata</i> + <i>D. fortii</i>	Spain	Extract	0–2,5				(Fernández et al. 2002)
<i>D. acuminata</i>	New Zealand	Extract	2–26	0.4–2			(MacKenzie et al. 2005)
	Norway	Picked cells	1–12	n.d.	0.4–5	n.d.	(Miles et al. 2004b)
	New Zealand	Extract	81–82	22–47			(MacKenzie et al. 2002)
	New Zealand	Extract	33–108	5–65			(MacKenzie et al. 2005)
	Portugal	Extract	48				(Vale 2004)
	Norway	Picked cells	0.7–4	n.d.	9–26	n.d.	(Miles et al. 2004b)
	Ireland	Picked cells	14	13			(Puente et al. 2004)
	Ireland	Picked cells	7	n.d.			(Puente et al. 2004)
	Spain	Picked cells	≅30				(Fernández et al. 2002)
<i>D. acuta</i> or <i>D. caudata</i>	Japan	Extract	182				(Suzuki et al. 1998)
<i>D. fortii</i>	Japan	Extract	10				(Burgess et al. 2003)
	Japan	Picked cells	43				(Lee et al. 1989)
	Japan	235					(Burgess et al. 2003)
<i>D. fortii</i> + <i>D. caudata</i>	Norway	Picked cells	0.3–2	nd	0.1–24	nd	(Miles et al. 2004b)
<i>D. norvegica</i>	Norway	Picked cells	1	nd	0.6–2	nd	(Miles et al. 2004b)
<i>D. rotundata</i>	Italy	Extract	192	nd			(Burgess et al. 2003)

Note: n.d. = not determined

**Table 9.3.** Maximum levels ( $\mu\text{g}/\text{kg}$ ) of PTXs reported for whole bivalve shellfish from various countries

Pectenotoxin	Shellfish Species	NZ	Australia	Norway	Croatia	Ireland	Japan	Portugal	UK	Chile	Russia
PTX-1	<i>M. edulis</i>			486 (48) <sup>a</sup>							
PTX-2	<i>P. yessoensis</i>						260 <sup>bc</sup>				20 <sup>d</sup>
	<i>A. purpuratus</i>		110 (Madigan et al. 2006)								
	<i>C. gigas</i>			5 (Miles et al. 2004b)				550 (Vale 2004)			
	<i>C. edule</i>										
	<i>D. deltooides</i>		9 (Eaglesham et al. 2000b)								
	<i>M. edulis</i>			929 (Miles et al. 2004b)		14 <sup>b</sup> (Puente et al. 2004)			70 (Morris et al. 2003)		0.2 <sup>b</sup> (Vershinin et al. 2006)
	<i>M. galloprovincialis</i>							950 (Vale 2004)			
	<i>P. bicolor</i>										
	<i>P. canaliculus</i>	105 (MacKenzie et al. 2002)	13 (Madigan et al. 2006)								
	<i>P. fumatus</i>		23 (Madigan et al. 2006)								
	<i>P. maximus</i>								85 (Stobo et al. 2004)		
PTX-2 SA <sup>e</sup>	<i>P. yessoensis</i>										
	<i>A. purpuratus</i>		790 (Madigan et al. 2006)				41 <sup>bc</sup>				
	<i>C. gigas</i>									150 <sup>d</sup>	
	<i>C. edule</i>			190 (Miles et al. 2004b)							
	<i>D. deltooides</i>		298 (Eaglesham et al. 2000b)								
	<i>D. trunculus</i>										1020 (Vale and Sampayo 2002b)



	<i>M. edulis</i>		15875 (Miles et al. 2004b)	130 <sup>b</sup> (Puento et al. 2004)	2.2 <sup>b</sup> (Vershinin et al. 2006)
	<i>M. galloprovincialis</i>	140 (MacKenzie et al. 2004)		228 <sup>b</sup> (Pavela-Vrančić et al. 2002)	8900 (Vale 2004)
	<i>P. bicolor</i>		150 (Madigan et al. 2006)		
	<i>P. canaliculus</i>	1560 (MacKenzie et al. 2002)			
	<i>P. fumatus</i>		510 (Madigan et al. 2006)		
	<i>V. antiqua</i>				48 <sup>d</sup>
	<i>P. yessoensis</i>				
PTX-6					1310 <sup>bf</sup> (Suzuki et al. 1998)
PTX-11					
PTX-11 SA <sup>e</sup>					
PTX-12					
	<i>C. edule</i>				
	<i>M. edulis</i>		92 (Miles et al. 2004b)		
			2306 (Miles et al. 2004b)		
			2070 (Miles et al. 2004b)		
PTX-12 SA <sup>e</sup>					

<sup>a</sup>May include a hydroxylated PTX other than PTX-1

<sup>b</sup>Value estimated for whole shellfish by dividing the reported value for digestive glands by a factor of 5 for mussels (Aasen et al. 2004) and 10 for scallops (T. Suzuki, personal communication)

<sup>c</sup>T. Suzuki, personal communication (data from Suzuki et al. 2005)

<sup>d</sup>A. López and B.A. Suárez-Isla, personal communication

<sup>e</sup>Sum of seco acid isomers, where data is reported

<sup>f</sup>PTX-6 was not detected in *M. galloprovincialis* from the same site at the same time

high levels of PTX-6 were found in *P. yessoensis* by HPLC fluorescence (Suzuki et al. 1998) and LC-MS (Suzuki and Yasumoto 2000), and no PTX-6 was detected in the mussel *Mytilus galloprovincialis* (Suzuki and Yasumoto 2000). PTX seco acids have not been reported in *P. yessoensis*, reflecting the differential metabolism of PTX-2 found in this species. PTX-6 was the dominant PTX in a recent survey of *P. yessoensis*, with relatively modest levels of PTX-1 and only low levels of PTX-2 (Suzuki et al. 2005b), but absolute concentrations were not reported. PTX-3–5 are reported to be very rare, even in *P. yessoensis* from Mutsu Bay (Yasumoto et al. 1989). No PTX-6 and only traces of PTX-1 and PTX-2 (up to 4 µg/kg whole shellfish, T. Suzuki, personal communication of data from Suzuki et al. 2005b) were occasionally detected in a survey Japanese mussels (*M. galloprovincialis* and *Mytilus coruscus*), although unspecified amounts of PTX-2 seco acid (PTX-2 SA) were detected in *M. galloprovincialis* (Suzuki et al. 2005b).

### Europe

PTXs appear to be common in European shellfish, although the first reports are relatively recent (Daiguji et al. 1998; James et al. 1999; Draisci et al. 1999). In Norway, PTXs are regularly found in blue mussels (*Mytilus edulis*) and cockles (*Cerastoderma edule*). Among the analogues detected are “PTX-1” (Aune et al. 2004) (possibly misidentified, see below), PTX-2, PTX-12, PTX-2 SAs, and what appear to be seco acids of PTX-12 (Miles et al. 2004b). PTX-2 and PTX-12 have also been detected in mixed *Dinophysis* blooms in Sweden (Miles et al. 2004c), so the presence of these PTXs and their metabolites in shellfish from elsewhere in Scandinavia is to be expected. PTX-2 SA and 7-*epi*-PTX-2 SA were found in shellfish on the Adriatic coast of Croatia (Pavela-Vrančić et al. 2001, 2002) by HPLC-fluorescence after blooms of *Dinophysis*. *M. galloprovincialis* from Italy’s Adriatic coast have also been shown to contain PTX-2 SA isomers (Draisci et al. 1999). Modest levels of PTX-2 SAs have been detected in a wide range of Portuguese shellfish including *Donax trunculus*, *M. galloprovincialis*, and *C. edule* (Vale and Sampayo 2002a, 2002b; Vale 2004; 2006). PTX-2 SA was also detected at up to 120 µg/kg in edible parts of the crab *Carcinus maenas* from Portugal and was present at the same time in the shellfish the crabs were presumed to be feeding on (Vale and Sampayo 2002a, 2002b). In Ireland, PTX-2 SA isomers have been reported in *M. edulis* during *D. acuta* blooms (Puente et al. 2004b; Draisci et al. 1999). Low levels of PTX-2 were measured in *M. edulis* in England (Morris et al. 2003) and *M. galloprovincialis* in Spain (Fernández et al. 2002), and although PTX-2 SA and 7-*epi*-PTX-2 SA were also present, concentrations were not reported. In Scotland, LC-MS analysis revealed PTX-2 and PTX-2 SA in scallops (*Pecten maximus*) (Stobo et al. 2004, 2005), PTX-2 in mussels (*M. edulis*) (Stobo et al. 2004; 64), and PTX-1 in *M. edulis* (Stobo et al. 2004). Very recently, PTX-2 and PTX-2 SAs were detected at low levels in mussels from the White Sea, Russia (Vershinin et al. 2006).

### Australasia

In New Zealand, PTX-2, PTX-11, PTX-13, PTX-2 SA, and a putative PTX-11 seco acid were found in green-lipped mussels (MacKenzie et al. 2002; Holland et al. 2003) during a *D. acuta* bloom. MacKenzie et al. also reported PTX-2 in *M. edulis* and *P. canaliculus* during minor blooms of *D. acuminata* (MacKenzie et al. 2004) in New Zealand. Low levels of PTX-2 and modest levels of PTX-2 SAs were found in a range of Australian shellfish species including pipis (*Donax deltooides*) implicated in a human poisoning event (Eaglesham et al. 2000a, 2000b; Takahashi et al. 2003), although higher levels (2000 µg/kg) have been mentioned (Burgess 2003) in Australian shellfish.

Very recently, PTX-2 and PTX-2 SA were identified in scallops (*Pecten fumatus*), oysters (*Crassostrea gigas*) and razor fish (*Pinna bicolor*) from South Australia (Madigan et al. 2006).

### The Americas

PTXs have been observed in shellfish from both coasts of North America (M.A. Quilliam, personal communication), and one of the sources on the east coast has been identified as *D. acuminata* (Quilliam et al. 2003). PTX-2 and its seco acids have recently been detected in scallops (*Argopecten purpuratus*) and clams (*Venus antiqua*) from Chile (A. López and B.A. Suárez-Isla, personal communication).

### Other Sources

PTX-2 was isolated from extracts of a two-sponge association (a *Poecillastra* sp. and a *Jaspis* sp.) by brine-shrimp-lethality bioassay guided fractionation (Jung et al. 1995). Okadaic acid analogues have similarly been isolated from marine sponges (Britton et al. 2003; Tachibana et al. 1981; Schmitz et al. 1981; Sakai and Rinehart 1995). It seems likely that the PTXs and okadaic analogues, which co-occur in *Dinophysis* spp., originate in the sponges either through algae living in association with the sponges, or through filter feeding of the sponges on toxin-containing algae. Copepods feeding on *Dinophysis* spp. contained low levels of okadaic acid (Kozlowsky-Suzuki et al. 2006), and it would not be surprising if PTXs were eventually identified in Copepods.

## Structure and Chemistry

### Structures

The structures of known PTXs are presented in Fig. 9.1. There are no structures reported for PTX-5 or PTX-10. The structures of pectenotoxins were initially defined through X-ray crystallography of PTX-1 (Yasumoto et al. 1985). The X-ray crystal structure defined the solid-phase conformation of PTX-1 and revealed the relative configurations of all its chiral centers. The absolute configuration of PTX-6 was later determined by NMR studies of chiral amide derivatives (Sasaki, Satake, and Yasumoto 1997), thereby establishing the structures of the natural 7*R*-PTXs (PTX-1, -2, -3, -6, -11, -12, and -13, and PTX-2 SA) as depicted in Fig. 9.1. The correctness of the assigned absolute stereochemistry (Sasaki, Satake, and Yasumoto 1997) was confirmed by total synthesis of PTX-4 and comparison of its optical rotation with that reported for PTX-4 from a natural source (Evans et al. 2002). It should be noted that the absolute configuration established for PTXs by Sasaki et al. (Sasaki, Satake, and Yasumoto 1997) is the antipode of that tentatively depicted in the earlier reports. Therefore, because of the delay between identifying the structures of PTXs and the establishment of their absolute configurations, much of the older literature depicts the incorrect enantiomers of PTX analogues. The chemical properties of PTXs are summarized in Table 9.4. PTXs-1–7 were isolated by mouse-bioassay- and TLC-guided fractionation of shellfish extracts (Yasumoto et al. 1984, 1985; Yasumoto et al. 1989; Sasaki, Satake, and Yasumoto 1997; Murata et al. 1986; Sasaki, Wright, and Yasumoto 1998), while PTX-8 and PTX-9 were obtained by chemical transformations (Sasaki, Wright, and Yasumoto 1998). Subsequent isolations of PTXs from shellfish and algae have relied on assessment of fractions by HPLC-UV, HPLC-fluorescence, and more recently, LC-MS analytical methods developed primarily for analysis of shellfish (Miles et al. 2004a, 2004b, 2006b; Suzuki et al. 2006; Daiguji et al. 1998).

A good outline of the methods and strategy for purification of PTXs from shellfish have been presented (Yasumoto et al. 1989; Goto et al. 1997), and the citations in Table 9.4 contain information on the purification methods used for isolation of individual PTXs as well as information about structurally informative mass-spectral fragmentations and NMR data. Efficient methods for isolating sufficient quantities of high-purity toxin are essential for chemical identification, production of analytical standards, and toxicological evaluations of PTXs. Recent work has shown that it is relatively easy to purify PTXs from algal concentrates harvested from natural blooms (Miles et al. 2004a, 2004b, 2006b; Suzuki et al. 2006) or by *in vitro* enzymatic conversion of isolated PTX-2 (Miles et al. 2004ab, 2006). Unfortunately, some PTX metabolites are currently only obtainable via shellfish (PTX-1, PTX-3–9), and blooms of appropriate *Dinophysis* spp. can be difficult to find and harvest and this genus cannot yet be grown on a large scale in the laboratory.

PTX-1 and PTX-2 were originally isolated from hepatopancreas of *P. yessoensis*, and their structures determined by X-ray crystallography, mass spectrometry and NMR spectroscopy (Yasumoto et al. 1984, 1985). Formally, PTX-1 is 43-hydroxyPTX-2. As part of the same study, three other analogues (PTX-3–5) were also isolated and partially identified from UV spectra and mass spectrometry, but their structures were not established (Yasumoto et al. 1984, 1985). Continuation of this work led to the isolation and identification of PTX-3, a C-43-aldehyde analogue of PTX-1 (Murata et al. 1986). PTX-6 was the next analogue to be identified, and its structure was determined by mass spectrometry and comparison of its NMR spectra with those of PTX-3 (Yasumoto et al. 1989). Although mentioned in passing in earlier reports (Yasumoto et al. 1989; Yasumoto 1988), the structure of PTX-4 was only reported much later (Sasaki, Wright, and Yasumoto 1998), together with that of PTX-7. As part of this study, Sasaki et al. (Sasaki, Wright, and Yasumoto 1998) also identified PTX-8 and PTX-9 as artifactual isomers produced via acid-catalyzed isomerization of PTX-1/4 and PTX-6/7, respectively. The isomerization chemistry of PTXs is discussed in more detail below. An unidentified analogue, PTX-10, was also mentioned as being present in acidic fractions from *P. yessoensis* (Sasaki, Wright, and Yasumoto 1998), but no details appear to have been published.

Two new PTXs were identified in *D. acuta* from Ireland and mussels (*P. canaliculus*) from New Zealand. Isolation of these compounds from the mussels afforded PTX-2 SA and 7-*epi*-PTX-2 SA (Daiguji et al. 1998), analogues of PTX-2 in which the lactone ring had been hydrolyzed. It appears that PTX-2 SA is produced by enzymatic hydrolysis of PTX-2, and that 7-*epi*-PTX-2 SA is produced by nonenzymatic isomerization of the 7-ketal moiety in PTX-2 SA (see discussion of chemistry and metabolism below).

A compound tentatively characterised as a new PTX with the same molecular weight as PTX-1 was detected by LC-MS analyses of *P. canaliculus* and *D. acuta* from New Zealand and temporarily designated as “PTX-1i” (MacKenzie et al. 2002). After further studies this compound was named PTX-11 (Suzuki et al. 2003), and was isolated from *D. acuta* and identified by NMR and mass spectrometry as 34*S*-hydroxyPTX-2 (Suzuki et al. 2006) (Fig. 9.1). The same sample of *D. acuta* also showed the presence of another compound temporarily designated PTX-11x on the basis of LC-MS/MS spectra (Suzuki et al. 2003). This was isolated from algal concentrates to afford PTX-13, identified as 32*R*-hydroxyPTX-2 (Suzuki et al. 2006; Miles et al. 2006b). A second compound, PTX-14, was identified as the cyclized 32,36-dehydration product of PTX-13 and may be artifactual in origin (Miles et al. 2006b).

A pair of peaks attributable to PTXs with a molecular weight of two less than that of PTX-2 were observed during LC-MS analyses of extracts obtained by solid-phase extraction of a *Dinophysis* bloom from the east coast of Norway. The compounds were isolated from a bloom of *D. acuta* from the west coast of Norway and identified as PTX-12 (38,47-dehydroPTX-2) as a pair of equilibrating 36-epimers (Miles et al. 2004b).

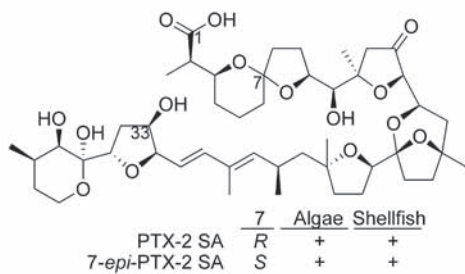
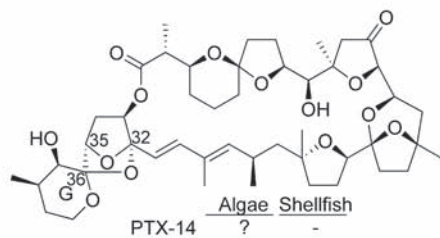
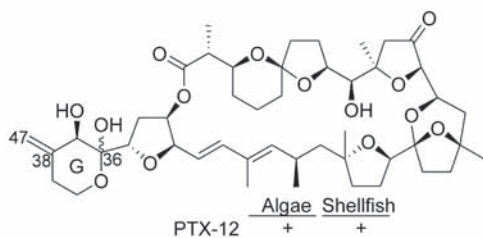
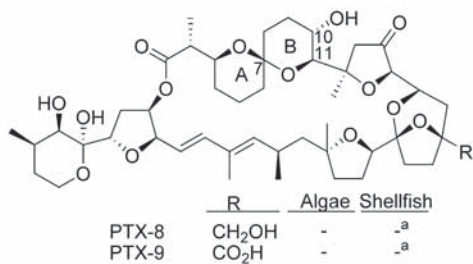
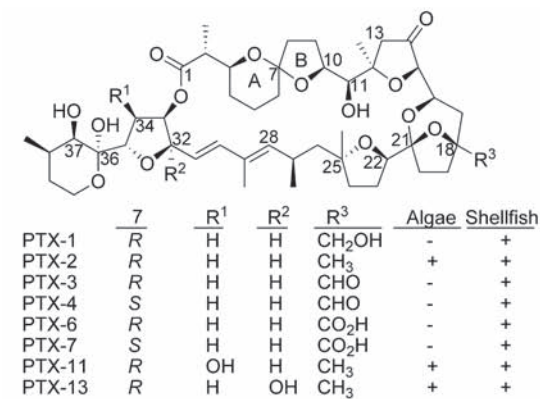


**Figure 9.1.** Pectenotoxins whose structures have been definitively identified. Key: +, reported; -, not reported; ?, possible artifact; <sup>a</sup>, found only as an acid-induced artifact (see Figure 9.2).

Several PTXs have been tentatively identified on the basis of LC-MS or chemical studies. A compound proposed as PTX-12 SA was observed as a mixture of four equilibrating isomers (7- and 36-epimers) during LC-MS analysis of Norwegian shellfish (Miles et al. 2004b). Similarly, a putative PTX-11 SA was observed by LC-MS in New Zealand shellfish by LC-MS (MacKenzie et al. 2002). The evidence for these identifications is only circumstantial. In the case of PTX-12 SA, PTX-12 was present in the shellfish and in the algae present in the water, the putative seco acids were demonstrated to be carboxylic acids by derivatization with diazomethane, and no other compounds were observed with the correct molecular weights in shellfish or algae by LC-MS (Miles et al. 2004). The case for PTX-11 SA is less certain, as there were other PTXs in the algae with the same molecular weight as PTX-11 (Suzuki et al. 2003; Miles et al. 2006). No enzymatic hydrolysis of PTX-11 was observed in vitro with homogenised mussel hepatopancreas (Suzuki et al. 2006), and that it is possible that mussels could oxidize PTX-2 SA in much the same way as *P. yessoensis* oxidizes PTX-2 (see discussion below). An apparent isomer of PTX-2 SA was detected by HPLC-UV (James et al. 1999), HPLC-fluorescence (Nogueiras et al. 2003; James et al. 1999) and LC-MS (Puente et al. 2004a, 2004b; James et al. 1999) in Irish shellfish and phytoplankton. This compound may be an isomerization product of PTX-2 SA or 7-*epi*-PTX-2 SA (see discussion of chemistry below) and does not yet appear to have been identified in other sources.

## Chemistry

All PTXs absorb UV light at ca 235 nm due to the presence of a 1,3-dienyl moiety at C-28–C-31 (Table 9.4), allowing these compounds to be easily detected by HPLC-UV and TLC. During HPLC-UV monitoring of preparative enzymatic conversions of PTX-2 into PTX-2 SA the UV absorbance maximum of PTX-2 SA and its 7-*epimer* consistently occurred at 2 nm longer wavelength than that of PTX-2, presumably due to release of conformational strain in the dienyl moiety after opening of the lactone ring (Miles et al. 2004a). It should be noted that while PTX-2 was stable for more than 24 hr between pH 4.5–pH 9.1 (Suzuki et al. 2001b), treatment with strong base destroyed PTXs in shellfish extracts (Vale and Sampayo 2002b), and attempts to prepare PTX-2 SA by controlled basic hydrolysis of the lactone moiety of PTX-2 resulted only in degradation (Miles et al. 2004).

The presence of a hemiketal (C-36) and several ketal centres (C-7 and C-21), along with a ketone  $\alpha$ - to an ether linkage mean that PTXs are susceptible to isomerization, especially by acids (Suzuki et al. 2003; Evans et al. 2002; Sasaki, Wright, and Yasumoto 1998). The ketal at C-7 is especially sensitive to epimerisation, particularly when carboxylic acid moieties are present in the structure (Sasaki, Wright, and Yasumoto 1998). So although PTXs isolated from algae appear to be almost exclusively 7*R*-isomers like PTX-2, PTXs isolated from shellfish sometimes also contain a small amount of the corresponding 7*S*-isomers (PTX-4 and PTX-7) (Sasaki, Wright, and Yasumoto 1998). Treatment of 7*R*- or 7*S*-PTXs with weak acid leads to an equilibrium mixture of the 7*R*-, 7*S*-, and six-membered-B-ring-isomers (Suzuki et al. 2003; Evans et al. 2002; Sasaki, Wright, and Yasumoto 1998) as illustrated in Fig. 9.2. PTX-1, PTX-4, and PTX-8 are therefore isomeric forms of each other in the A–B ring system, as are PTX-6, PTX-7, and PTX-9. Extended treatment of any one member any trio of compounds with weak acid leads to an equilibrium mixture of it and its two corresponding isomers. The reaction seems to be quite general, as similar treatment of PTX-2 and PTX-11 also led to a mixture of three isomers presumed to correspond to those depicted in Fig. 9.2 (Suzuki et al. 2003). Although it is possible that the 7*S*-isomers (PTX-4 and PTX-7) in shellfish are produced by isomerization from their corresponding 7*R*-isomers during isolation procedures, it is also possible that these compounds originate from the algae, as supported by evidence, presented by Suzuki et al. (2003), of low levels of 7*S*-PTX-2

**Table 9.4.** Chemical and physical properties and locations of spectral and structural data for PTXs depicted in Figure 9.1

Compound	Mwt	UV $\lambda_{\text{max}}$ (nm) <sup>a</sup>	<sup>1</sup> H NMR	<sup>13</sup> C NMR	MS/MS	TLC	Structure
PTX-1	874	235 $\epsilon$ 12400 (Yasumoto et al. 1984, 1985)	(CD <sub>3</sub> ) <sub>2</sub> CO (Yasumoto et al. 1984, 1985) C <sub>3</sub> D <sub>5</sub> N (Sasaki, Wright, and Yasumoto 1998) (CD <sub>3</sub> ) <sub>2</sub> CO (Yasumoto et al. 1984, 1985; Jung et al. 1995) CD <sub>3</sub> OD (Miles et al. 2004a)	CDCl <sub>3</sub> -CD <sub>3</sub> OD (Yasumoto et al. 1984, 1985) C <sub>3</sub> D <sub>5</sub> N (Sasaki, Wright, and Yasumoto 1998) CDCl <sub>3</sub> -CD <sub>3</sub> OD (Yasumoto et al. 1984, 1985) (CD <sub>3</sub> ) <sub>2</sub> CO (Jung et al. 1995) CD <sub>3</sub> OD (Miles et al. 2004a)	(Suzuki et al. 2003, 2006)	(Yasumoto et al. 1984, 1985)	(Yasumoto et al. 1984, 1985)
PTX-2	858	235 $\epsilon$ 16000 (Yasumoto et al. 1984, 1985) 235 <sup>b</sup> (Draisci et al. 1996; Miles et al. 2004a; Suzuki et al. 2001b) 238 <sup>b</sup> (James et al. 1999)	(CD <sub>3</sub> ) <sub>2</sub> CO (Yasumoto et al. 1984, 1985; Jung et al. 1995) CD <sub>3</sub> OD (Miles et al. 2004a)	CDCl <sub>3</sub> -CD <sub>3</sub> OD (Yasumoto et al. 1984, 1985) (CD <sub>3</sub> ) <sub>2</sub> CO (Jung et al. 1995) CD <sub>3</sub> OD (Miles et al. 2004a)	(Suzuki et al. 2003; James et al. 1999)	(Yasumoto et al. 1984, 1985)	(Yasumoto et al. 1984, 1985)
PTX-3	872	235 $\epsilon$ 11000 (Yasumoto et al. 1985; Murata et al. 1986)	CDCl <sub>3</sub> (Murata et al. 1986)	CDCl <sub>3</sub> -CD <sub>3</sub> OD (Murata et al. 1986)		(Yasumoto et al. 1984, 1985)	(Murata et al. 1986)
PTX-4	874	235 $\epsilon$ 12280 (Yasumoto et al. 1985) 235 $\epsilon$ 12000 (Sasaki, Wright, and Yasumoto 1998)	C <sub>3</sub> D <sub>5</sub> N (Sasaki, Wright, and Yasumoto 1998)	C <sub>3</sub> D <sub>5</sub> N (Sasaki, Wright, and Yasumoto 1998)		(Yasumoto et al. 1984, 1985)	(Sasaki, Wright, and Yasumoto 1998)
PTX-5	876	235 (Yasumoto et al. 1985)				(Yasumoto et al. 1984, 1985)	Unknown (Sasaki, Wright, and Yasumoto 1998)
PTX-6	888	237 $\epsilon$ 37000 (Sasaki, Wright, and Yasumoto 1998) <sup>c</sup> 235 <sup>b</sup> (Yasumoto et al. 1989)	C <sub>3</sub> D <sub>5</sub> N (Sasaki, Satake, and Yasumoto 1997) <sup>d</sup> ; (Sasaki, Wright, and Yasumoto 1998) <sup>e</sup>	C <sub>3</sub> D <sub>5</sub> N (Sasaki, Wright, and Yasumoto 1998) <sup>c</sup>	(Suzuki et al. 2003)	(Yasumoto et al. 1989; Sasaki, Satake, and Yasumoto 1997)	(Yasumoto et al. 1989; Sasaki, Satake, and Yasumoto 1997)
PTX-7	888	237 $\epsilon$ 37000 (Sasaki, Wright, and Yasumoto 1998) <sup>c</sup>	C <sub>3</sub> D <sub>5</sub> N (Sasaki, Wright, and Yasumoto 1998) <sup>c</sup>	C <sub>3</sub> D <sub>5</sub> N (Sasaki, Wright, and Yasumoto 1998) <sup>c</sup>			(Sasaki, Wright, and Yasumoto 1998)
PTX-8 <sup>e</sup>	874	237 $\epsilon$ 12000 (Sasaki, Wright, and Yasumoto 1998)	C <sub>3</sub> D <sub>5</sub> N (Sasaki, Wright, and Yasumoto 1998)	C <sub>3</sub> D <sub>5</sub> N (Sasaki, Wright, and Yasumoto 1998)			(Sasaki, Wright, and Yasumoto 1998)
PTX-9 <sup>e</sup>	888	239 $\epsilon$ 37000 (Sasaki, Wright, and Yasumoto 1998) <sup>c</sup>	C <sub>3</sub> D <sub>5</sub> N (Sasaki, Wright, and Yasumoto 1998) <sup>c</sup>	C <sub>3</sub> D <sub>5</sub> N (Sasaki, Wright, and Yasumoto 1998) <sup>c</sup>			(Sasaki, Wright, and Yasumoto 1998)
PTX-10							Unknown (Sasaki, Wright, and Yasumoto 1998)

(Continued)



**Table 9.4.** (Continued)

Compound	Mwt	UV $\lambda_{\text{max}}$ (nm) <sup>a</sup>	<sup>1</sup> H NMR	<sup>13</sup> C NMR	MS/MS	TLC	Structure
PTX-11	874	235 <sup>b</sup> (Miles et al. 2004a; Suzuki et al. 2006)	(CD <sub>3</sub> ) <sub>2</sub> CO (Suzuki et al. 2006) CD <sub>3</sub> OD (Suzuki et al. 2006)	(CD <sub>3</sub> ) <sub>2</sub> CO (Suzuki et al. 2006) CD <sub>3</sub> OD (Suzuki et al. 2006)	(Suzuki et al. 2003, 2006)	(Suzuki et al. 2006)	(Suzuki et al. 2006)
PTX-12	856	235 <sup>b</sup> (Miles et al. 2004b)	CD <sub>3</sub> OD (Miles et al. 2004b)	CD <sub>3</sub> OD (Miles et al. 2004b)	(Miles et al. 2004b)		(Miles et al. 2004b)
PTX-13	874	235 <sup>b</sup> (Miles et al. 2006b)	CD <sub>3</sub> OD (Miles et al. 2006b)	CD <sub>3</sub> OD (Miles et al. 2006b)	(Miles et al. 2006b)		(Miles et al. 2006b)
PTX-14	856	235 <sup>b</sup> (Miles et al. 2006b)	CD <sub>3</sub> OD (Miles et al. 2006b)	CD <sub>3</sub> OD (Miles et al. 2006b)	(Miles et al. 2006b)		(Miles et al. 2006b)
PTX-2 SA	876	235 $\epsilon$ 17000 (Daiguji et al. 1998)	CD <sub>3</sub> OD (Miles et al. 2004a; Daiguji et al. 1989)	CD <sub>3</sub> OD (Miles et al. 2004a)	(Daiguji et al. 1989; Miles et al. 2006a)		(Daiguji et al. 1998)
7- <i>epi</i> -PTX-2 SA	876	237 <sup>b</sup> (Miles et al. 2004a) 238 <sup>b</sup> (James et al. 1999)	CD <sub>3</sub> OD (Daiguji et al. 1989; Miles et al. 2006a)	CD <sub>3</sub> OD (Miles et al. 2006a)	(Daiguji et al. 1989; James et al. 1999)		(Daiguji et al. 1998)

<sup>a</sup>In MeOH, unless specified

<sup>b</sup>Solvent unspecified, or from diode array detection during HPLC analysis

<sup>c</sup>Phenacyl ester derivative

<sup>d</sup>pGME amide derivative

<sup>e</sup>These analogues are artifactual and have not been detected in shellfish or algae

(“PTX-2b”) and 7*S*-PTX-11 (“PTX-11b”) in extracts of New Zealand *D. acuta*. PTX-2 SA is particularly labile and has been observed to isomerize to 7-*epi*-PTX-2 SA in buffers (Miles et al. 2004a) and during attempted purification (James et al. 1999; Miles et al. 2006). PTX-2 SA is the initial product of enzymatic hydrolysis of PTX-2 (Miles et al. 2004a; Suzuki et al. 2001a, 2001b), but it steadily isomerises in aqueous solution to the thermodynamically more stable 7-*epi*-PTX-2 SA (Miles et al. 2004a, 2006a; Suzuki et al. 2001b) (although it appears to be relatively stable in methanolic solution (Miles et al. 2004)). Presumably it is this abiotic isomerization that is responsible for the presence of 7-*epi*-PTX-2 SA and for the variable ratios of seco acid epimers in shellfish and algal extracts. A third isomer of PTX-2 SA has been observed by some workers in extracts of shellfish (Puente et al. 2004a, 2004b; Nogueiras et al. 2003; James et al. 1999) which appeared to isomerise during attempted purification (James et al. 1999). These characteristics would be consistent with isomerization of PTX-2 SA in a manner analogous to that depicted in Fig. 9.2, but isomerization in other parts of the structure is also feasible. PTX-12 was isolated as a rapidly equilibrating pair of 36*R,S*-isomers, and it was proposed that this results from strain induced in the terminal G-ring by the 38,47-ene group (Miles et al. 2004b). The putative PTX-12 seco acids present in shellfish contaminated with PTX-12 appeared to partially isomerise on-column during LC-MS, although methylation of the carboxylic acid group with diazomethane greatly reduced this effect (Miles et al. 2004b). During alumina chromatography, much of the PTX-12 unexpectedly eluted in the acidic fraction (Miles et al. 2004b), possibly due to interactions of the *cis*-36,37-dihydroxy moiety of 36*R*-isomer with the stationary phase.

PTXs slowly exchange deuterium in the 13 $\beta$ -position during extended or delayed NMR analysis over a period of months if CD<sub>3</sub>OD is used as solvent (Miles et al. 2004b, 2006b). More prolonged treatment exchanges deuterium into other positions, but this occurs more slowly (Miles et al. 2006b). Different samples appeared to exchange at different rates (A.L. Wilkins, personal communication), suggesting that the reaction may be promoted by traces of acid or base in the samples. While specifically deuterated derivatives provide a means to test proposed mass spectral fragmentation pathways (Miles et al. 2006b), exchange of tritium into PTXs in the same manner could prove a valuable source of radiolabelled PTXs for radio-tracer-based assays and for metabolism studies.

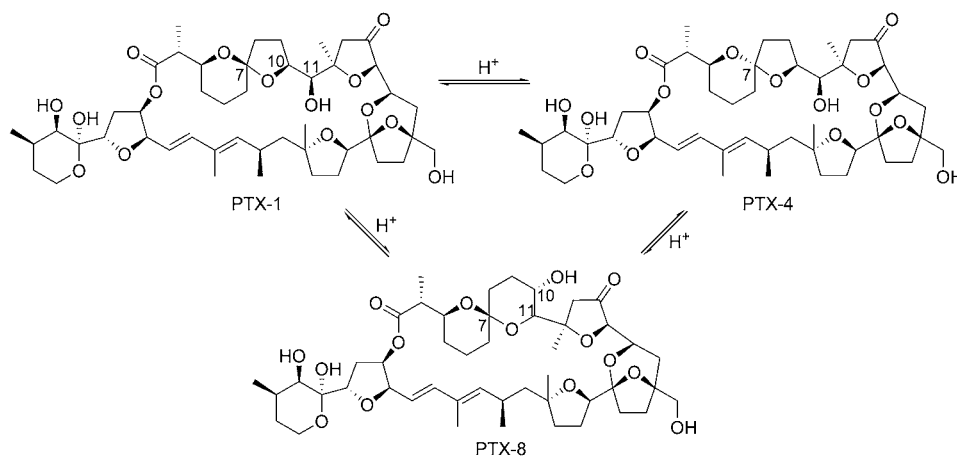


**Figure 9.2.** Acid-catalyzed isomerization of PTX-1 to PTX-4 and PTX-8 (Sasaki, Wright, and Yasumoto 1998). Analogous isomerizations have been observed for PTX-6 (Sasaki, Wright, and Yasumoto 1998), PTX-2, and PTX-11 (Suzuki et al. 2003).

Pectenotoxins undergo a number of reactions related to the functional groups they contain. PTX-3 forms a methoxy hemiacetal of the aldehyde moiety when dissolved in MeOH (Murata et al. 1986). The reactivity of the carboxylic acid group in PTX-6 has been utilised to make amide derivatives for determination of absolute stereochemistry (Sasaki, Satake, and Yasumoto 1997) and fluorescent ester derivatives for HPLC analysis (Suzuki et al. 1998) and for coupling to PTX-6 to protein for immunoassay development (Briggs et al. 2000; Sasaki 1993). Pectenotoxins contain a 28,30-dienyl moiety that reacts with dienophiles via the Diels-Alder reaction. This reaction has been used to derivatise PTXs with the fluorescent dienophile DMEQ-TAD to afford four diastereoisomeric derivatives (although two of these predominate) for HPLC analysis (Burgess et al. 2003). The carboxylic acid group in PTX seco acids reacts rapidly with diazomethane to form the methyl esters (Miles et al. 2004a, 2004b), and with 9-anthryldiazomethane (Daiguji et al. 1998; James et al. 1999), 1-bromoacetylpyrene (James et al. 1999), 3-bromomethyl-6,7-dimethoxy-1-methyl-2(1H)-quinoxalinone, and 9-chloromethylanthracene (Nogueiras et al. 2003) to form fluorescent derivatives. These reactions are useful for structural confirmation as well as for HPLC analysis.

## Synthesis

Because of their novel biological activities, as well as the complexity of the challenge of constructing the PTX structure, PTXs have in recent years become a target for synthetic chemists. The first report of the synthesis of a PTX-fragment was of the C-31–C-40 portion (Amano, Fujiwara, and Murai 1997). At the time, this unit was common to all known pectenotoxins (PTX-1–3), although several PTXs have since been identified that contain variations in this fragment (PTX-11–14). This fragment is the antipode of the natural toxins, as the work (Amano, Fujiwara, and Murai 1997) was undertaken prior to the determination of the absolute stereochemistry of PTX-6 (Sasaki, Satake, and Yasumoto 1997). The same group reported the synthesis of the C-8–C-18 unit that is common to all known PTXs (Awakura et al. 2000). Another group subsequently synthesised of a more extensive fragment (rings C–E, i.e. C-11–C-26) of PTX-2 (Micalizio and Roush 2001). The AB ring system (C-1–C-11) of the natural *7R*-PTXs (PTX-1, -2, -3, -6, -11–14) has recently been synthesised, as well as the corresponding *7S*-epimer, by a kinetic spiroketalization (Pihko and Aho 2004). The synthesis of PTX-2 is being tackled, and to date the ring A–C and D–E (C-1–C-26) (Bondar et al. 2005) and F–G (C-29–C-40) (Paquette, Peng, and Bondar 2002; Peng, Bondar, and Paquette 2004) backbone substructures have been completed but the units have yet to be correctly joined to complete the structure. Evans's group recently reported synthesis of the C-1–C-19 subunit (Evans, Rajapakse, and Stenkamp 2002) and of the C-20–C-30 and C-31–C-40 subunits, and their assembly to form PTX-4 (Evans et al. 2002). Acid-catalyzed isomerization of the material afforded primarily PTX-8, which was identical with an authentic specimen, along with a much lower amount of PTX-1 (Evans et al. 2002). This is currently the only reported total synthesis of a PTX, although it should be noted that PTX-4 is not a major natural metabolite and that PTX-8 is an artifact produced by acid-catalyzed isomerization of PTX-1. The left-hand half of the PTXs (rings A+E–F, i.e. C-1–C-7 + C-31–C-40) has been synthesized (Fujiwara et al. 2005). This unit is common to all PTXs with the exception of the seco acids and PTX-11–14. Very recently, synthesis of the ring A–C fragment (C-1–C-16) of PTX-7 has been achieved with a view to producing the major naturally occurring (and thermodynamically less stable) *7S*-epimer (PTX-6) (Halim, Brimble, and Merten 2005) by acid-catalyzed epimerization in a similar manner to that used by Evans et al. (2002). For the time being, there is no real prospect of synthetic methods replacing natural PTXs as a source for biochemical and other studies. However, synthetic fragments of PTXs and synthesized non-natural PTXs could provide

a rich resource for studying the structure–activity relationships within the PTXs. Other potential uses for synthetic analogues include internal standards for analytical methods and labelled analogues for metabolic studies.

## Metabolism

### Shellfish

PTXs ingested by shellfish are metabolized by two processes (Fig. 9.3). In the Japanese scallop, *P. yessoensis*, PTX-2 absorbed from algae undergoes apparently step-wise oxidation of the methyl group attached to C-18 (Suzuki et al. 1998; Yasumoto et al. 1989). Thus, this methyl group in PTX-2 is oxidised to an alcohol (PTX-1), aldehyde (PTX-3), and finally a carboxylic acid (PTX-6) group. In the New Zealand scallop, *Pecten novaezelandiae* (Suzuki et al. 2001a), and mussels *P. canaliculus* and *M. galloprovincialis* from New Zealand (Suzuki et al. 2001b) and *M. edulis* from Norway (Miles et al. 2004a), a different process has been demonstrated whereby the lactone moiety of PTX-2 undergoes rapid enzymatic hydrolysis to afford PTX-2 SA. In vitro, the hydrolysis can be extremely rapid, with a half-life of as little as 7 minutes (Miles et al. 2004a). Examination of the metabolite profiles reported for PTX-contaminated shellfish (Table 9.3) suggests that this is the major metabolic pathway in all shellfish species tested, apart from *P. yessoensis*. Although 7-*epi*-PTX-2 SA is also often found in shellfish contaminated with PTXs, it appears that this is formed by nonenzymatic isomerization processes from PTX-2 SA (Miles et al. 2006a). Some PTXs are more resistant to enzymatic hydrolysis than PTX-2. PTX-11 was not detectably hydrolyzed in vitro overnight, even though the half-life for PTX-2 hydrolysis in the same preparation was ca 15 minutes (Suzuki et al. 2006). This phenomenon was paralleled in vivo, as the ratio of PTX-2 SA:PTX-2 in *P. canaliculus* was very much higher than the ratio of the putative PTX-11 SA:PTX-11 (MacKenzie et al. 2002). Analysis of contaminated mussels similarly suggests that PTX-12 is more resistant to hydrolysis than PTX-2, although not to the same extent as PTX-11 (Miles et al. 2004b). Presumably, in mussels the rapid hydrolytic reaction intervenes before oxidation processes can occur to a significant extent. These esterases must be absent or inoperative in *P. yessoensis* because, if they were present, some of the PTX-1–3 and PTX-6 would be expected to be rapidly converted to the corresponding seco acids. Identification of PTX-1 by LC-MS was recently reported in *M. edulis* from Norway (Aune et al. 2004), which would constitute the first identification by of PTX-1 in a species other than *P. yessoensis* and would be surprising given the presence of PTX-hydrolysing enzymes in Norwegian *M. edulis* (Miles et al. 2004a). However, a subsequent study using different chromatographic conditions showed that the compound in the mussels did not co-elute with either PTX-1 or PTX-11, suggesting it is a novel hydroxylated PTX (T. Rundberget, J.A.B. Aasen, and C.O. Miles, unpublished observations). When PTX-6 was injected into the adductor muscle of *P. yessoensis* it was rapidly transported to the hepatopancreas (Suzuki et al. 2005a). Metabolism of other toxins similarly injected appeared to begin immediately and to occur primarily in the hepatopancreas, although no metabolism of PTX-6 was observed and PTX-2 was not included in the study (Suzuki et al. 2005a).

Algal toxins taken up by shellfish are eliminated over time by a combination of metabolism and excretion. There is only limited data on depuration of PTXs from shellfish. Elimination of PTX-2 SAs from the mussel *P. canaliculus* in New Zealand occurred with a half-lives of 26 days (MacKenzie et al. 2002) (although the estimated rate was based on limited data) on the west coast of South Island, and of 15 days in Akaroa Harbour (McNabb and Holland 2002). Depuration of PTX-2 SA and 7-*epi*-PTX-2 SA from *M. galloprovincialis* in Portugal has also been reported (Vale 2004, 2006).

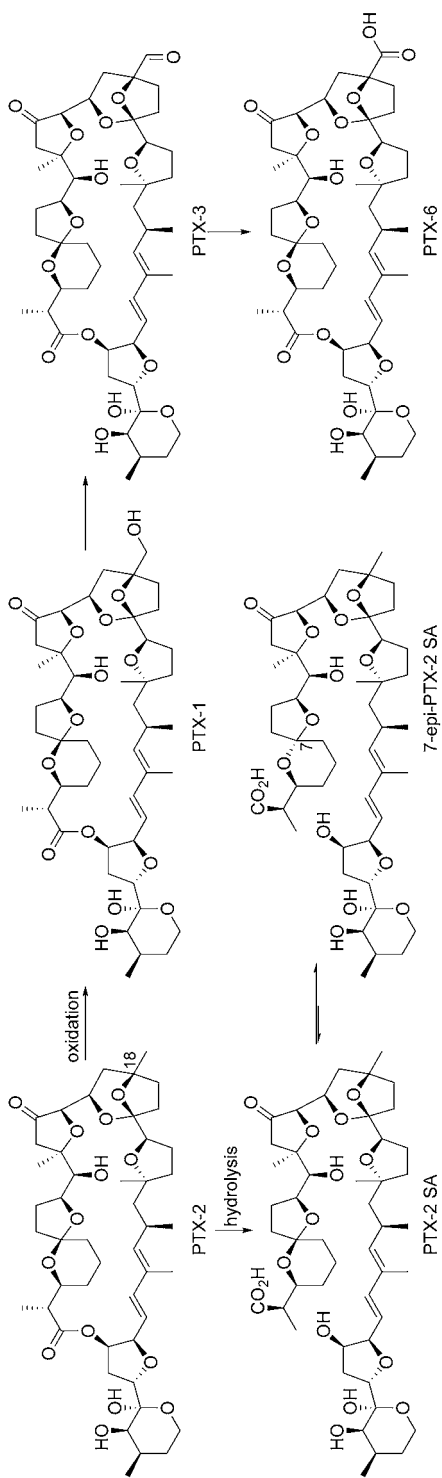


**Figure 9.3.** The two main pathways for metabolism of PTX-2 in shellfish. The oxidative pathway has so far been confirmed only in *P. yessoensis*. The hydrolytic pathway appears to occur in all other shellfish species studied, including mussels, clams, and other species of scallop.

## Mammalian

PTX-2 was rapidly metabolised by rat hepatocytes, with a half-life of 15–30 min (Sandvik et al. 2004). No PTX-2 SA or its isomers was detected by LC-MS as products. Rather, an array of mono- and di-oxygenated derivatives was formed in the C-18–C-25 moiety, none of which corresponded to PTX-1. Thus, the metabolic pathway for PTX-2 in mammalian hepatocytes appears to be quite different from those in shellfish. It is possible that rapid metabolism of PTXs contributes to the low toxicity of PTXs when administered orally to mice.

## Biological Activity

### Human Intoxication

There are only two reports implicating PTXs in poisoning of human or animal consumers via shellfish Burgess and Shaw 2001. One incident in Australia, in 1997, involved hospitalization of 56 people in New South Wales after consumption of pipis. Symptoms included nausea, vomiting, and diarrhoea, and the shellfish held to be responsible were found to contain PTX-2 SA and low levels of PTX-2 (Eaglesham et al. 2000, cited in Burgess and Shaw 2001). In the other incident, an elderly woman became ill after consuming cooked pipis (*Donax delatoides*) in Queensland, Australia. Again, the shellfish contained high levels of PTX-2 SA (Burgess and Shaw 2001; Eaglesham et al. 2000b). The implication of PTX-2 SA in human illness prompted study of the toxicological effects of PTX-2 SA in vitro and in vivo (below). In view of the maximum levels of seco acids so far reported in shellfish (Miles et al. 2004b) and the lack of detectable toxicity of pure PTX-2 SAs to mice by either oral or i.p. administration at doses up to 5000 µg/kg (Miles et al. 2004ab 30, 2006), it has been concluded that acute toxic effects from PTX-2 SAs on humans is most unlikely (Miles et al. 2006a). It now seems likely that the symptoms observed in the human intoxications were due to toxins other than PTXs, possibly the acyl esters of okadaic acid that were subsequently detected in the pipis (Burgess et al. 2003; Burgess 2003).

### Mouse Toxicity

Mice are the only mammals for which there are any reports of administration of PTXs, reflecting the scarcity of the toxins and also, perhaps, an influence from the historical importance of the mouse bioassay for DSP toxins. PTXs were first isolated from toxic mussels by mouse-bioassay- and TLC-guided fractionation (Yasumoto et al. 1984, 1985; Murata et al. 1986; Sasaki, Wright, and Yasumoto 1998), although some of the analogues were not measurably toxic (Table 9.5). Results from these chemical studies provided the initial indications as to the biological activities of the PTXs. The minimum lethal dose to mice by i.p. injection ranges (Table 9.5) from 192–770 µg/kg for the toxic analogues (PTX-1–4, PTX-6, PTX-7, PTX-11), or greater than 5000 µg/kg for the less toxic analogues (PTX-8, PTX-9, PTX-2 SA, and 7-*epi*-PTX-2 SA). Many PTXs therefore possess potent biological activity in vivo, and there is a strong link between structure and this activity. For example, analogues isomerised so as to contain a 6-membered ring-B (PTX-8 and PTX-9) were more than an order of magnitude less toxic, and the 7*R*-epimers (PTX-4 and PTX-7) were significantly less toxic, than their corresponding 7*S*-epimers (PTX-1 and PTX-6). Another trend is that oxidation at C-43 leads to reduced toxicity in the mouse bioassay so that, for example, PTX-6 is half as toxic as PTX-2. PTXs isolated in recent studies (PTX-2 SA, 7-*epi*-PTX-2 SA, PTX-11, PTX-12, PTX-13, and PTX-14)

have relied on instrumental methods to monitor isolations from shellfish and algal samples (Miles et al. 2004b, 2006a, 2006b; Suzuki et al. 2006; Daiguji et al. 1998), so only limited toxicological data was initially available for some of these compounds. However, PTX-11 had essentially the same LD<sub>50</sub> to mice as PTX-2, indicating that oxidation at C-34 did not significantly affect i.p. toxicity (Suzuki et al. 2006).

Hamano et al. (Hamano, Kinoshita, and Yasumoto 1986) found no diarrhetic activity when 0.4 “mouse units” (a mouse unit is the amount of toxin killing two of three mice in the standard i.p. mouse bioassay; a dose of 0.4 MU of PTX-1 would probably correspond to ca 200–250 µg/kg) of PTX-1 was administered orally to suckling mice. The authors concluded that PTX-1 was probably not a diarrhetic toxin (Hamano, Kinoshita, and Yasumoto 1986), although the dose rate used in the study was probably too low to draw a definitive conclusion on this point. In contrast, a subsequent study involving oral administration of PTX-2 isolated from shellfish at doses of 250–2500 µg/kg indicated that this compound was not only diarrhetic, but also induced damage to the gastrointestinal tract and to the liver at higher doses (Ishige, Satoh, and Yasumoto 1988). However, histopathological examination of suckling mice after i.p. administration revealed that PTX-1 at up to 1000 µg/kg did

**Table 9.5.** Lethality of pectenotoxins to the mouse by the intraperitoneal (i.p.) and oral routes

	i.p. LD50	i.p. MLD	i.p. symptoms <sup>a</sup>	Oral LD50	Reference
PTX-1		250	Not reported		(Yasumoto et al. 1984, 1985, 1989)
		260	Not reported		(Yasumoto et al. 1984, 1985)
	ca 200				(Yoon and Kim 1997)
PTX-2		230	Not reported		(Yasumoto et al. 1989)
	411	400	Ataxia, cyanosis, reduced temperature, liver damage		(Yoon and Kim 1997a)
	219	192	Lethargy, depressed respiration	>5000	(Miles et al. 2004a)
				ND <sup>b</sup>	(Ogino, Kumagai, and Yasumoto 1997)
PTX-3		350	Not reported		(Yasumoto et al. 1989; Murata et al. 1986)
PTX-4		770	Not reported		(Yasumoto et al. 1989)
PTX-6		500	Not reported		(Yasumoto et al. 1989)
PTX-7		500	Not reported		(Yasumoto et al. 1989)
PTX-8 <sup>c</sup>		>5000	None detected		(Sasaki, Wright, and Yasumoto 1998)
PTX-9 <sup>c</sup>		>5000	None detected		(Sasaki, Wright, and Yasumoto 1998)
PTX-11	244	250	Lethargy, depressed respiration	>5000	(Suzuki et al. 2006)
PTX-2 SA		>5000	None detected	>5000	(Miles et al. 2004a)
7- <i>epi</i> -PTX-2 SA		>5000	None detected	>5000	(Miles et al. 2006a)

<sup>a</sup>Hepatotoxicity was observed for PTX-1 and PTX-2 in some studies in which lethalties were not determined

<sup>b</sup>Not Determined (due to lack of dose-response curve). No symptoms reported

<sup>c</sup>These analogues are artifactual and have not been detected in shellfish or algae



not cause observable intestinal abnormalities, but at greater than 500 µg/kg characteristic liver damage was observed (Terao et al. 1986). Administration of PTX-2 i.p. to mice was lethal (Table 9.5), causing ataxia, hypothermia, cyanosis, and liver damage (Yoon and Kim 1997a). The activities of serum alanine aminotransferase (ALT), aspartate aminotransferase (AST), and sorbitol dehydrogenase (SDH) were elevated by PTX-2 but that of glucose-6-phosphatase was not. The treatment with PTX-2 also caused a reduction in hepatic microsomal protein content, and a range of hepatic drug metabolising enzymes were not induced (Yoon and Kim 1997a). Repeated i.p. administration of sub-lethal doses of PTX-2 (100 µg/kg/day) to mice for two weeks caused increased granularity in the liver, but no changes in ALT, AST, SDH, blood urea nitrogen, or measured drug metabolising enzymes (Yoon and Kim 1997). Nevertheless, significant alterations to the i.p. toxicity of PTX-2 were found when mice were treated with a range of metabolic inducers and inhibitors (Yoon and Kim 1997). In another study, when PTX-2 was administered orally to mice a proportion of the animals died at dose rates similar to that of the i.p. LD<sub>50</sub> (Ogino, Kumagai, and Yasumoto 1997). However, the death rates and death times were not dose related, so the proposition that the oral toxicity of PTX-2 is similar to that of its i.p. toxicity (Ogino, Kumagai, and Yasumoto 1997) should be treated with caution (Miles et al. 2004a).

In contrast to the findings of Ishige, Satoh, and Yasumoto (1988) and Ogino, Kumagai, and Yasumoto (1997) with PTX-2, recent studies involving oral administration of much higher doses (5000 µg/kg) of PTX-2 (Miles et al. 2004a) and PTX-11 (Suzuki et al. 2006) to mice failed to elicit diarrhetic or other toxic effects, and demonstrate that PTXs are much less toxic and diarrhetic by the oral route than DSP toxins such as okadaic acid and its analogues. Nevertheless, both PTX-2 and PTX-11 were highly toxic (Table 9.5) when administered i.p. to mice (Miles et al. 2004a; Suzuki et al. 2006) in the same manner as many of the PTXs in Table 9.5. Symptoms of i.p. injection of toxic PTXs into mice include hepatotoxicity (Yoon and Kim 1997a; Terao et al. 1986), ataxia, cyanosis, reduced temperature (Yoon and Kim 1997a), lethargy, and depressed respiration (Miles et al. 2004a; Suzuki et al. 2006). At lethal doses, death usually occurred within 4–15 hours (Miles et al. 2004a; Suzuki et al. 2006). These findings, together with the lack of inhibition of protein phosphatase exhibited by PTXs (below), indicate that PTXs should not be regarded as DSP toxins.

The suspected involvement of PTX-2 SAs in human intoxications (see above) led to investigation of their *in vitro* and *in vivo* toxicology. Preliminary *in vivo* studies included oral dosing of a 35:65 mixture of PTX-2 SA and 7-*epi*-PTX-2 SA at up to 875 µg/kg (Burgess et al. 2002) and showed a range of toxicological and pathological effects in the mice including necrosis and haemorrhage in the duodenum and stomach at higher dose levels, although no diarrhoea was observed. Subsequent batches of toxin did not show these effects, and it was suggested that other toxic contaminants from shellfish were responsible for the earlier observations (Burgess 2003). PTX-2 SAs were found in the liver and GI tract after oral or i.p. dosing, with as much as 34% excreted via the faeces, and there were changes to the basal lamina of cells in the villi of the duodenum (Burgess 2003). In contrast, recent studies with highly purified PTX-2 SA (Miles et al. 2004a, 2006a) and 7-*epi*-PTX-2 SA (Miles et al. 2006a) isolated from algae showed these compounds to be non-toxic to mice by the oral and i.p. routes at 5000 µg/kg, with no observable diarrhoea, behavioural or pathological changes.

Although there can be no doubt that some PTXs are toxic to mice by i.p. administration, the question of whether these compounds are orally toxic, or cause diarrhoea when administered orally, is more controversial. There have been relatively few oral dosing studies, due to the scarcity of high-purity PTXs, and the results have not been consistent. However, recent evidence suggests that PTXs are weakly diarrhetic at most and are of relatively low oral toxicity. Based on their toxicity by the i.p. route in the mouse bioassay, PTX-1 and PTX-2 are currently regulated in shellfish together with okadaic acid

and dinophysistoxins by the European Union at a level of 160 µg/kg of “okadaic acid equivalents” (European Union 2002). The data reviewed here clearly show that PTXs are chemically and toxicologically different to okadaic acid and dinophysistoxins, and do not act via inhibition of protein phosphatases, so the regulation of PTXs in terms of “okadaic acid equivalents” is not appropriate.

### *In Vitro Studies*

It should be pointed out that *in vitro* studies involving incubations of PTXs with cells and cell extracts need to be interpreted with caution because of the rapid metabolism of PTX-2 observed in rat hepatocytes (Sandvik et al. 2004) and in cell-free extracts of shellfish tissue (Miles et al. 2004a, 2006a; Suzuki et al. 2001a, 2001b).

Because many PTXs are hepatotoxic to mice by *i.p.* injection, several studies have focussed on the *in vitro* effects of PTXs on liver cells. When rat hepatocytes were incubated for 2 hours with PTX-1 at 7.5–50 µg/mL, cells retained their spherical shape and did not display blebs, in contrast to cells treated with okadaic acid, but dose-dependent vacuolisation was observed and the cells were devoid of microvilli at doses above 5 µg/mL (Aune, Yasumoto, and Engeland 1991). Apparent holes were observed in the cells, but lack of enzyme leakage suggested that these were associated with invagination rather than disrupted membranes. Zhou et al. (1994) found that treatment of chick liver cells with PTX-1 at 0.05–50 µg/mL caused time- and dose-dependent loss and rearrangement of microtubules, disruption of stress fibres, accumulation of actin at the cellular periphery, and cell shrinkage. Cells transferred to a PTX-free culture medium after 4 hours recovered relatively normal morphology within 24 hours (Zhou et al. 1994). The effects of several apoptogenic algal toxins, including PTX-1, were compared in suspension cultures of rat and salmon hepatocytes (Fladmark et al. 1998). PTX-1 induced rapid apoptosis, detectable by microscopy, which could be counteracted by caspase and kinase inhibitors, and cell shrinkage. In addition, PTX-1 did not inhibit PP2A (Fladmark et al. 1998). The rat and salmon hepatocytes were equally sensitive to PTX-1 but not to most of the other toxins in the study, and it was suggested that a test for apoptogenic toxins in food could be based on a hepatocyte bioassay.

PTX-2 SA was not toxic to KB cells even at 1.8 µg/mL, whereas PTX-2 was cytotoxic at 0.05 µg/mL, suggesting that an intact lactone ring is necessary for cytotoxicity (Daiguji et al. 1998). In a cytotoxicity assay with a human liver cell line (HepG<sub>2</sub>), the LC<sub>30</sub> for PTX-2 SAs was 2.2 µg/mL at 24 hours and 0.92 µg/mL at 96 hours (Burgess 2003). There was an effect on cell-cycle distribution, but no apoptosis was seen (Burgess et al. 2003). Up- and down-regulation of a number of genes was observed in these cells by cDNA microarray, including down-regulation of genes involved in lipid metabolism (Burgess 2003).

Studies have been conducted to elucidate the mechanism of the *in vitro* biochemical effects of PTXs. PTX-2 inhibited actin polymerization in a concentration-dependent manner (IC<sub>50</sub> 0.3 µg/mL), inhibited contractions induced by KCl or phenylephrine in the isolated rat aorta (IC<sub>50</sub> 0.3 µg/mL), and formed a 1:4 complex with G-actin (Hori et al. 1999; Karaki et al. 1999). PTX-2 sequestered purified actin with a K<sub>d</sub> of 17 µg/mL without causing severing or endcapping, and disrupted the organisation of actin in several cell types in a time- and concentration-dependent manner and details of the microscopic cellular changes have been described (Spector et al. 1999). PTX-6 caused time- and dose-dependent depolymerization of F-actin in neuroblastoma cells, with a 24-hour EC<sub>50</sub> of 0.7 µg/mL (Leira et al. 2002). No other major effects were seen in any cell signal transduction pathways or in cell survival, and PTX-6 did not affect cytosolic calcium levels in human lymphocytes. However, when capacitative calcium influx was activated before toxin addition, PTX-6 reduced calcium

influx but only modified cAMP levels under calcium-free conditions. No effects on cell attachment or apoptosis were observed, leading the authors to propose F-actin cytoskeletal disruption as a key mechanism for PTX-6 toxicity to eukaryotic cells (Leira et al. 2002). Incubation of enterocytes from rabbit duodenum–jejunum with PTX-6 (0.9 µg/mL) for 4 hr damaged the F-actin microfilament network, but did not alter the cellular morphology (Ares et al. 2005). This result suggests the cytoskeleton of intestinal cells as a potential target for ingested PTXs. An assay for okadaic acid based on F-actin polymerisation has recently been demonstrated (Leira et al. 2003) and might be useful for studying PTXs.

PTX-2 inhibited cytokinesis in mammalian ovulated oocytes and induced apoptosis in p53-deficient tumours both in vivo and in vitro (Chae et al. 2005). The authors found that treatment with PTX-2 influenced proteins involved in apoptosis in p53-deficient cells. PTX-2 displayed potent cytotoxicity, with LC<sub>50</sub> values as low as 6.7 µg/mL, to a wide range of human cancer cell lines in vitro (Jung et al. 1995). The authors also presented evidence that PTX-2 did not block oxidation–reduction processes in the membrane or block DNA synthesis in vitro.

### Nonmammalian Species

PTX-1 did not show any activity against the fungi *Aspergillus niger*, *Candida rugosa* or *Penicillium funiculosum*, or the bacterium *Bacillus megaterium* (Nagai, Satake, and Yasumoto 1990). PTX-2 was lethal to brine shrimps (LC<sub>50</sub> < 0.1 µg/mL) during a search for bioactive natural products in sponges (Jung et al. 1995). Injection of PTX-6 into the scallop *P. yessoensis* caused some mortalities but no other visible symptoms, and was markedly less toxic than okadaic acid and yessotoxin (Suzuki et al. 2005a).

### Summary

PTXs are widely distributed in shellfish from most parts of the world, and are closely associated with the presence of *Dinophysis* spp. in the water. Some PTXs are rapidly metabolised in shellfish, so that metabolites are the major components present. There are no documented cases of human poisonings reliably attributable to PTXs, even though many PTXs are toxic by i.p. injection into mice and are regulated in some countries because of this. However, there is growing evidence that PTXs are much less toxic to mice orally than they are by the i.p. route, and PTXs may therefore be of less concern to human health than was previously supposed. Because the chemistry and toxicology of the PTXs are distinctly different from those of okadaic acid analogues, PTXs should not be considered to be members of the DSP toxin group. PTXs also display a range of interesting biological activities in vitro that could make them useful tools in the biosciences. More research is required to understand the toxicology, mechanism of action, and metabolism in shellfish and mammals, of PTXs. Studies of PTX biosynthesis are currently hindered by the difficulty of holding *Dinophysis* spp. in culture.

### References

- Aasen, J., Samdal, I.A., Miles, C. O., Dahl, E., Briggs, L.R., and Aune, T. 2004. Yessotoxins in Norwegian blue mussels (*Mytilus edulis*): uptake from *Protoceratium reticulatum*, metabolism and depuration. *Toxicon* 45, 265–272.
- Ares, I.R., Louzao, M. C., Vieytes, M.R., Yasumoto, T., and Botana, L.M. 2005. Actin cytoskeleton of rabbit intestinal cells is a target for potent marine phycotoxins. *J Exp Biol* 208, 4345–4354.

- Amano, S., Fujiwara, K., and Murai, A. 1997. The synthesis of the common C31–C40 fragment of pectenotoxins. *Synlett* 1997, 1300–1302.
- Aune, T. 1997. Health effects associated with algal toxins from seafood. *Arch Toxicol Suppl* 19, 389–97.
- Aune, T., Torgersen, T., Arff, J., and Tangen, K. 2004. Detection of pectenotoxin in Norwegian blue mussels (*Mytilus edulis*). In *Harmful Algae 2002*, ed. Steidinger, K.A., Landsberg, J.H., Tomas, C.R., and Vargo, G.A. St. Petersburg, Florida, USA: Florida Fish and Wildlife Conservation Commission, Florida Institute of Oceanography, and International Oceanographic Commission of UNESCO, 306–308.
- Aune, T., Yasumoto, T., and Engeland, E. 1991. Light and scanning electron microscopic studies on effects of marine algal toxins toward freshly prepared hepatocytes. *J Toxicol Environ Health* 34, 1–9.
- Awakura, D., Fujiwara, K., and Murai, A. 2000. Synthetic studies on pectenotoxins: synthesis of the common C8–C18 THF fragment. *Synlett* 1733–1736.
- Bhakuni, D.S. 1995. The toxic metabolites of marine organisms. *J Sci Ind Res* 54, 702–716.
- Bondar, D., Liu, J., Müller, T., and Paquette, L.A. 2005. Pectenotoxin-2 synthetic studies. 2. Construction and conjoining of ABC and DE eastern hemisphere subtargets. *Org Lett* 7, 1813–1816.
- Bravo, I., Delgado, M., Fraga, S., Honsell, G., Lassus, P., Montresor, M., and Sampayo, M.A. 1995. The *Dinophysis* genus: toxicity and species definition in Europe. In *Harmful Marine Algal Blooms*, ed. Lassus, P., Arzul, G., Erard, E., Gentien, P., and Marcaillou, C. Paris: Lavoisier Intercept Ltd., 843–845.
- Briggs, L.R., Garthwaite, L.L., Miles, C. O., Garthwaite, I., Ross, K.M., Towers, N.R., and Quilliam, M.A. 2000. The newest ELISA—pectenotoxin, Marine Biotoxin Science Workshop No. 14, Wellington, New Zealand: MAF, 71–75.
- Britton, R., Roberge, M., Brown, C., van Soest, R., and Andersen, R. J. 2003. New okadaic acid analogues from the marine sponge *Merriamum oxeato* and their effect on mitosis. *J Nat Prod* 66, 838–843.
- Burgess, V.A. 2003. *Toxicology Investigations with the Pectenotoxin-2 Seco Acids*. Ph.D. dissertation. Brisbane, Australia: Griffith University.
- Burgess, V.A., Seawright, A., Eaglesham, G., Shaw, G., and Moore, M. 2002. The acute oral toxicity of the shellfish toxins pectenotoxin-2 seco acid and 7-epi-pectenotoxin-2 seco acid in mice. Poster presented at the 4th International Conference on Molluscan Shellfish Safety, Santiago de Compostela, Spain, June 4–8, 2002.
- Burgess, V., Shaw, G. 2001. Pectenotoxins—an issue for public health. A review of their comparative toxicology and metabolism. *Environ Internat* 27, 275–283.
- Burgess, V., Zhang, Y., Eaglesham, G., Tzang, C.H., Yang, Z., Shaw, G., Lam, P. K. S., Mengsu, Y., and Moore, M.R. 2003. Investigation of changes in cell cycle distribution in cultured HepG<sub>2</sub> cells with pectenotoxin-2 seco acids. In *Proceedings of the 4th International Conference on Molluscan Shellfish Safety, Santiago de Compostella, Spain, June 4–8, 2003*, ed. Villalba, A., Reguera, B., Romalde, J.L., and Beiras, R. Xunta de Galicia and IOC of UNESCO, 97–105.
- Cembella, A.D. 1989. Occurrence of okadaic acid, a major diarrhetic shellfish toxin, in natural populations of *Dinophysis* spp. from the eastern coast of North America. *J Appl Phycol* 1, 307–310.
- Chae, H.D., Choi, T.-S., Kim, B.-M., Jung, J.H., Bang, Y.-J., and Shin, D.Y. 2005. Oocyte-based screening of cytokinesis inhibitors and identification of pectenotoxin-2 that induces Bim/Bax-mediated apoptosis in p53-deficient tumors. *Oncogene* 24, 4813–4819.
- Daiguji, M., Satake, M., James, K.J., Bishop, A., MacKenzie, L., Naoki, H., and Yasumoto, T. 1998. Structures of new pectenotoxin analogs, pectenotoxin-2 seco acid and 7-epi-pectenotoxin-2 seco acid, isolated from a dinoflagellate and greenshell mussels. *Chem Lett* 653–654.
- Della Loggia, R., Cabrini, M., Del Negro, P., Honsell, G., and Tubaro, A. 1993. Relationship between *Dinophysis* spp. in seawater and DSP toxins in mussels in the northern Adriatic Sea. In *Toxic Phytoplankton Blooms in the Sea*, ed. Smayda, T.J., and Shimizu, Y. Amsterdam: Elsevier, 483–488.
- Draisci, R., Lucentini, L., Giannetti, L., Boria, P., and Poletti, R. 1996. First report of pectenotoxin-2 (PTX-2) in algae (*Dinophysis fortii*) related to seafood poisoning in Europe. *Toxicon* 34, 923–935.
- Draisci, R., Lucentini, L., and Mascioni, A. 2000. Pectenotoxins and yessotoxins: chemistry, toxicology, pharmacology, and analysis. In *Seafood and Freshwater Toxins: Pharmacology, Physiology, and Detection*, ed. Botana, L.M. New York: Marcel Dekker, Inc., 289–324.
- Draisci, R., Palleschi, L., Giannetti, L., Lucentini, L., James, K.J., Bishop, A.G., Satake, M., and Yasumoto, T. 1999. New approach to the direct detection of known and new diarrhetic shellfish toxins in mussels and phytoplankton by liquid chromatography–mass spectrometry. *J Chromatogr A* 847, 213–221.
- Eaglesham, G.K., Brett, S.J., Davis, B.C., and Holling, N. 2000a. Detection of pectenotoxin 2 and pectenotoxin 2 seco acids in phytoplankton and shellfish from the Ballina region of New South Wales, Australia. *X International IUPAC Symposium on Mycotoxins and Phycotoxins, Guarujá, Brazil, Official Program and Abstract Book*, ed. Sabino, M., Rodriguez-Amaya, D., and Corrêa, B.

- Eaglesham, G.K., Shaw, G.R., Smith, M.R., Burgess, V., and Moore, M.R. 2000b. Human diarrhoeic shellfish poisoning incident involving dinoflagellate toxins in south-east Queensland, Australia. Abstract. *Toxicol Lett* 116, 49.
- European Union. 2002. Commission decision of 15 March 2002 laying down detailed rules for the implementation of Council Directive 91/492/EEC as regards the maximum permitted levels and the methods for analysis of certain marine biotoxins in bivalve molluscs, echinoderms, tunicates and marine gastropods (2002/225/EC). *Off J Eur Communities, L* 75/62.
- Evans, D.A., Rajapakse, H.A., Chiu, A., and Stenkamp, D. 2002. Asymmetric syntheses of pectenotoxins-4 and -8, part II: synthesis of the C20–C30 and C31–C40 subunits and fragment assembly. *Angew Chem, Int Ed Engl* 41, 4573–4576.
- Evans, D.A., Rajapakse, H.A., and Stenkamp, D. 2002. Asymmetric syntheses of pectenotoxins-4 and -8, part I: synthesis of the C1–C19 subunit. *Angew Chem Int Ed Engl* 41, 4569–4573.
- FAO/IOC/WHO. 2004. *Report of the Joint FAO/IOC/WHO ad hoc Expert Consultation on Biotoxins in Bivalve Molluscs (Advance Prepublication Copy)*. [http://www.fao.org/es/ESN/food/risk\\_biotoxin\\_en.stm](http://www.fao.org/es/ESN/food/risk_biotoxin_en.stm). September 26–30, 2004. Oslo, Norway: FAO/IOC/WHO.
- Fernández, M. L., Míguez, A., Martínez, A., Moroiño, Á., Arévalo, F., Pazos, Y., Salgado, C., Correa, J., Blanco, J., González-Gil, S., and Reguera, B. 2002. First report of pectenotoxin-2 in phytoplankton net-hauls and mussels from the Galician Rías Baixas (NW Spain) during proliferations of *Dinophysis acuta* and *Dinophysis caudata*. In *Proceedings of the 4th International Conference on Molluscan Shellfish Safety, Santiago de Compostella, Spain, June 4–8, 2002*, ed. Villalba, A., Reguera, B., Romalde, J. L., and Beiras, R. Xunta de Galicia and IOC of UNESCO, 75–83.
- Fernández, M.L., and Reguera, B. 2002. First report of pectenotoxin-2 in isolated *Dinophysis caudata* cells determined by liquid chromatography-mass spectrometry. In *X International Conference on Harmful Algae, St. Pete Beach, Florida, USA, October 21–25, 2002, Book of Abstracts*, p. 91.
- Fladmark, K.E., Serres, M.H., Larsen, N.L., Yasumoto, T., Aune, T., and Döskeland, S.O. 1998. Sensitive detection of apoptogenic toxins in suspension cultures of rat and salmon hepatocytes. *Toxicon* 36, 1101–1114.
- Fujiwara, K., Kobayashi, M., Yamamoto, F., Aki, Y.-I., Kawamura, M., Awakura, D., Amano, S., Okano, A., Murai, A., Kawai, H., and Suzuki, T. 2005. Synthesis of the common left-half part of pectenotoxins. *Tetrahedron Lett* 46, 5067–5069.
- Goto, H., Igarashi, T., Sekiguchi, R., Tanno, K., Satake, M., Oshima, Y., and Yasumoto, T. 1997. A Japanese project for production and distribution of shellfish toxins as calibrants for HPLC analysis. In *Proceedings of the VIII International Conference on Harmful Algae, Vigo, Spain, 25–29 June, 1997*, ed. Reguera, B., Blanco, J., Fernández, M.L., and Wyatt, T. Xunta de Galicia and Intergovernmental Oceanographic Commission of UNESCO, 216–219.
- Halim, M., Brimble, M.A., and Merten, J. 2005. Synthesis of the ABC fragment of the pectenotoxins. *Org Lett* 7, 2659–2662.
- Hallegraef, G.M., and Lucas, I A.N. 1988. The marine dinoflagellate genus *Dinophysis* (Dinophyceae): photosynthetic, neritic, and non-photosynthetic, oceanic species. *Phycologia* 27, 25–42.16.
- Norris, D.R., and Berner, L.D., Jr. 1970. The cal morphology of selected species of *Dinophysis* (Dinoflagellata) from the Gulf of Mexico. *Contrib Mar Sci* 15, 145–192.
- Hamano, Y., Kinoshita, Y., and Yasumoto, T. 1986. Enteropathogenicity of diarrhetic shellfish toxins in intestinal models. *J Food Hyg Soc Jpn* 27, 375–379.
- Holland, P.T., McNabb, P., Selwood, A.L., MacKenzie, L., and Beuzenberg, V. 2003. LC-MS methods for marine biotoxins and their introduction into the New Zealand shellfish regulatory programme. In *HABTech 2003*, Cawthron Report No. 906, ed. Holland, P., Rhodes, L., and Brown, L. Nelson, New Zealand: Cawthron Institute, 10–17.
- Hori, M., Matsuura, Y., Yoshimoto, R., Ozaki, H., Yasumoto, T., and Karaki, H. 1999. Actin depolymerizing action by marine toxin, pectenotoxin-2. *Nippon Yakurigaku Zasshi* 114, 225P–229P (in Japanese).
- Ishige, M., Satoh, N., and Yasumoto, T. 1988. Pathological studies on mice administered with the causative agent of diarrhetic shellfish poisoning (okadaic acid and pectenotoxin-2). *Hokkaidoritsu Eisei Kenkyushoho* 15–18.
- James, K.J., Bishop, A.G., Draisci, R., Palleschi, L., Marchiafava, C., Ferretti, E., Satake, M., and Yasumoto, T. 1999. Liquid chromatographic methods for the isolation and identification of new pectenotoxin-2 analogues from marine phytoplankton and shellfish. *J Chromatogr A* 844, 53–65.
- Jung, J. H., Sim, C. J., and Lee, C.-O. 1995. Cytotoxic compounds from a two-sponge association. *J Nat Prod* 58, 1722–1726.
- Karaki, H., Matsuura, Y., Hori, M., Yoshimoto, R., Ozaki, H., and Yasumoto, T. 1999. Pectenotoxin-2, a new actin depolymerizing compound isolated from scallop *Patinopecten yessoensis*. *Jpn J Pharmacol* 79, 268P.
- Kozlowsky-Suzuki, B., Carlsson, P., Rühl, A., and Granéli, E. 2006. Food selectivity and grazing impact on toxic *Dinophysis* spp. by copepods feeding on natural plankton assemblages. *Harmful Algae* 5, 57–68.
- Lee, J.-S., Igarashi, T., Fraga, S., Dahl, E., Hovgaard, P., and Yasumoto, T. 1989. Determination of diarrhetic shellfish toxins in various dinoflagellate species. *J Appl Phycol* 1, 147–152.
- Leira, F., Alvarez, C., Cabado, A.G., Vieites, J.M., Vieytes, M.R., and Botana, L.M. 2003. Development of a F actin-based live-cell fluorimetric microplate assay for diarrhetic shellfish toxins. *Anal Biochem* 317, 129–135.



- Leira, F., Cabado, A.G., Vieytes, M.R., Roman, Y., Alfonso, A., Botana, L.M., Yasumoto, T., Malaguti, C., and Rossini, G.P. 2002. Characterization of F-actin depolymerization as a major toxic event induced by pectenotoxin-6 in neuroblastoma cells. *Biochem Pharmacol* 63, 1979–1988.
- MacKenzie, L., Beuzenberg, V., Holland, P., McNabb, P., Suzuki, T., and Selwood, A. 2005. Pectenotoxin and okadaic acid-based toxin profiles in *Dinophysis acuta* and *Dinophysis acuminata* from New Zealand. *Harmful Algae* 4, 75–85.
- MacKenzie, L., Beuzenberg, V., Holland, P., McNabb, P., and Selwood, A. 2004. Solid phase adsorption toxin tracking (SPATT): a new monitoring tool that simulates the biotoxin contamination of filter feeding bivalves. *Toxicon* 44, 901–918.
- MacKenzie, L., Holland, P., McNabb, P., Beuzenberg, V., Selwood, A., and Suzuki, T. 2002. Complex toxin profiles in phytoplankton and Greenshell mussels (*Perna canaliculus*), revealed by LC-MS/MS analysis. *Toxicon* 40, 1321–1330.
- Madigan, T.L., Lee, K.G., Padula, D.J., McNabb, P., and Pointon, A.M. 2006. Diarrhetic shellfish poisoning (DSP) toxins in South Australian shellfish. *Harmful Algae*, in press.
- McNabb, P., and Holland, P.T. 2002. Using liquid chromatography mass spectrometry to manage shellfish harvesting and protect public health. In *Proceedings of the 4th International Conference on Molluscan Shellfish Safety, Santiago de Compostella, Spain, June 4–8, 2002*, ed. Villalba, A., Reguera, B., Romalde, J.L., and Beiras, R. Xunta de Galicia and IOC of UNESCO, 179–186.
- Micalizio, G.C., and Roush, W.R. 2001. Studies on the synthesis of pectenotoxin II: synthesis of a C(Zingone et al. 2006)–C(Pavela-Vrančić et al. 2001) fragment precursor via [3 + 2]-annulation reactions of chiral allylsilanes. *Org Lett* 3, 1949–1952.
- Miles, C.O., Wilkins, A.L., Munday, R., Dines, M.H., Hawkes, A.D., Briggs, L.R., Sandvik, M., Jensen, D.J., Cooney, J.M., Holland, P.T., Quilliam, M.A., MacKenzie, A.L., Beuzenberg, V., and Towers, N.R. 2004a. Isolation of pectenotoxin-2 from *Dinophysis acuta* and its conversion to pectenotoxin-2 seco acid, and preliminary assessment of their acute toxicities. *Toxicon* 43, 1–9.
- Miles, C.O., Wilkins, A.L., Munday, J.S., Munday, R., Hawkes, A.D., Jensen, D.J., Cooney, J.M., and Beuzenberg, V. 2006a. Production of 7-*epi*-pectenotoxin-2 seco acid and assessment of its acute toxicity to mice. *J Agric Food Chem*, in press.
- Miles, C.O., Wilkins, A.L., Hawkes, A.D., Jensen, D.J., Cooney, J.M., Beuzenberg, V., Mackenzie, A.L., Selwood, A.I., and Holland, P.T. 2006b. Isolation and Identification of Pectenotoxins-13 and -14 from *Dinophysis acuta* in New Zealand. *Toxicon*, submitted.
- Miles, C.O., Wilkins, A.L., Samdal, I.A., Sandvik, M., Petersen, D., Quilliam, M.A., Naustvoll, L.J., Rundberget, T., Torgersen, T., Hovgaard, P., Jensen, D.J., and Cooney, J.M. 2004b. A novel pectenotoxin, PTX-12, in *Dinophysis* spp. and shellfish from Norway. *Chem Res Toxicol* 17, 1423–1433.
- Miles, C.O., Wilkins, A.L., Samdal, I.A., Sandvik, M., Petersen, D., Quilliam, M.A., Naustvoll, L.J., Rundberget, T., Torgersen, T., Hovgaard, P., Jensen, D.J., Lundve, B., and Lindahl, O. 2004c. PTX-12, a new pectenotoxin from *Dinophysis* species and mussels in Scandinavia. In *5th International Conference on Molluscan Shellfish Safety, Galway, Ireland, June 14–18, Book of Abstracts*, p. 17.
- Morris, S., Stubbs, B., Cook, A., Milligan, S., and Quilliam, M.A. 2003. The first report of the co-occurrence of pectenotoxins, okadaic acid and dinophysistoxin-2 in shellfish from England. In *HABTech 2003*, Cawthron Report No. 906, ed. Holland, P., Rhodes, L., and Brown, L. Nelson, New Zealand: Cawthron Institute, 83–89.
- Murata, M., Sano, M., Iwashita, T., Naoki, H., and Yasumoto, T. 1986. The structure of pectenotoxin-3, a new constituent of diarrhetic shellfish toxins. *Agric Biol Chem* 50, 2693–2695.
- Nagai, H., Satake, M., and Yasumoto, T. 1990. Antimicrobial activities of polyether compounds of dinoflagellate origins. *J Appl Phycol* 2, 305–308.
- Nogueiras, M.J., Gago-Martínez, A., Paniello, A.I., Twohig, M., James, K.J., and Lawrence, J.F. 2003. Comparison of different fluorimetric HPLC methods for analysis of acidic polyether toxins in marine phytoplankton. *Anal Bioanal Chem* 377, 1202–1206.
- Ogino, H., Kumagai, M., and Yasumoto, T. 1997. Toxicologic evaluation of yessotoxin. *Nat Toxins* 5, 255–259.
- Paquette, L.A., Peng, X.W., and Bondar, D. 2002. Pectenotoxin-2 synthetic studies. 1. Alkoxide precoordination to [Rh(NBD)(DIPHOS-4)]BF<sub>4</sub> allows directed hydrogenation of a 2,3-dihydrofuran-3-ol without competing furan production. *Org Lett* 4, 937–940.
- Pavela-Vrančić, M., Mestrovčić, V., Marasović, I., Gillman, M., Furey, A., and James, K.K. 2001. The occurrence of 7-*epi*-pectenotoxin-2 seco acid in the coastal waters of the central Adriatic (Kaštela Bay). *Toxicon* 39, 771–779.
- . 2002. DSP toxin profile in the coastal waters of the central Adriatic Sea. *Toxicon* 40, 1601–1607.
- Peng, X., Bondar, D., and Paquette, L.A. 2004. Alkoxide precoordination to rhodium enables stereodirected catalytic hydrogenation of a dihydrofuranol precursor of the C29–40 F/G sector of pectenotoxin-2. *Tetrahedron* 60, 9589–9598.

- Pihko, P.M., and Aho, J.E. 2004. Access to both anomers of pectenotoxin spiroketals by kinetic spiroketalization. *Org Lett* 6, 3849–3852.
- Puente, P.F., Sáez, M.J.F., Hamilton, B., Furey, A., and James, K.J. 2004a. Studies of polyether toxins in the marine phytoplankton, *Dinophysis acuta*, in Ireland using multiple tandem mass spectrometry. *Toxicon* 44, 919–926.
- Puente, P.F., Sáez, M.J.F., Hamilton, B., Lehane, M., Ramstad, H., Furey, A., and James, K.J. 2004b. Rapid determination of polyether marine toxins using liquid chromatography–multiple tandem mass spectrometry. *J Chromatogr A* 1056, 77–82.
- Quilliam, M.A. 2004. Certified reference materials for marine toxins. In *5th International Conference on Molluscan Shellfish Safety, Galway, Ireland, June 14–18, 2004*.
- Quilliam, M.A., Aasen, J., Hardstaff, W.R., and Lewis, N. 2003. Analysis of phycotoxins in handpicked plankton cells by micro-column liquid chromatography–tandem mass spectrometry. In *HABTech 2003*, Cawthron Report No. 906, ed. Holland, P., Rhodes, L., and Brown, L. Nelson, New Zealand: Cawthron Institute, 107–112.
- Sakai, R., and Rinehart, K.L. 1995. A new polyether acid from a cold water marine sponge, a *Phakellia* species. *J Nat Prod* 58, 773–777.
- Samdal, I.A., Naustvoll, L.J., Miles, C.O., Olseng, C.D., Briggs, L.R., Rhodes, L.L., and Mackenzie, L. 2002. Analysis of picked algal cells using ELISA, Poster presented at X International Conference on Harmful Algal Blooms, St Pete Beach, Florida, USA, October 21–25, 2002.
- Sandvik, M., Fæste, C., Rundberget, T., Flåøyen, A., Miles, C.O., and Petersen, D. 2004. *In vitro* biotransformations of algal toxins, In *5th International Conference on Molluscan Shellfish Safety, Galway, Ireland, June 14–18, Book of Abstracts*, p. 162.
- Sasaki, K. 1993. *Structural Elucidation and Preparation of Useful Derivatives of Diarrhetic Shellfish Toxins*. MSc thesis. Tohoku University, Japan.
- Sasaki, K., Satake, M., and Yasumoto, T. 1997. Identification of the absolute configuration of pectenotoxin-6, a polyether macrolide compound, by NMR spectroscopic method using a chiral anisotropic reagent, phenylglycine methyl ester. *Biosci Biotech Biochem* 61, 1783–1785.
- Sasaki, K., Takizawa, A., Tubaro, A., Sidari, L., Loggia, R.D., and Yasumoto, T. 1999. Fluorometric analysis of pectenotoxin-2 in microalgal samples by high performance liquid chromatography. *Nat Toxins* 7, 241–246.
- Sasaki, K., Wright, J.L., and Yasumoto, T. 1998. Identification and characterization of pectenotoxin (PTX) 4 and PTX7 as spiroketal stereoisomers of two previously reported pectenotoxins. *J Org Chem* 63, 2475–2480.
- Sato, S., Koike, K., and Kodama, M. 1996. Seasonal variation of okadaic acid and dinophysistoxin-1 in *Dinophysis* spp. in association with the toxicity of scallop. In *Harmful and Toxic Algal Blooms*, ed. Yasumoto, T., Oshima, Y., and Fukuyo, Y. Intergovernmental Oceanographic Commission of UNESCO, 285–288.
- Schmitz, F.J., Prasad, R.S., Gopichand, Y., Hossain, M.B., van der Helm, D., and Schmidt, P. 1981. Acanthifolicin, a new episulfide-containing polyether carboxylic acid from extracts of the marine sponge *Pandaros acanthifolium*. *J Am Chem Soc* 103, 2467–2469.
- Spector, I., Braet, F., Shochet, N.R., and Bubb, M.R. 1999. New anti-actin drugs in the study of the organization and function of the actin cytoskeleton. *Microscop Res Tech* 47, 18–37.
- Stobo, L.A., Lacaze, J.-P.C.L., Scott, A.C., Gallacher, S., Smith, E.A., and Quilliam, M.A. 2005. Liquid chromatography with mass spectrometry: detection of lipophilic shellfish toxins. *J Assoc Off Anal Chem Int* 88, 1371–1382.
- Stobo, L.A., Lacaze, J.-P., Scott, A.C., and Smith, E. A. 2004. An investigation into the occurrence of pectenotoxins (PTXs) in shellfish from Scottish waters, Poster presented at the 11th International Conference on Harmful Algae, Cape Town, South Africa, November 15–19, 2004.
- Suzuki, T., Beuzenberg, V., Mackenzie, L., and Quilliam, M.A. 2003. Liquid chromatography–mass spectrometry of spiroketal stereoisomers of pectenotoxins and the analysis of novel pectenotoxin isomers in the toxic dinoflagellate *Dinophysis acuta* from New Zealand. *J Chromatogr A* 992, 141–150.
- Suzuki, T., Igarashi, T., Ichimi, K., Watai, M., Suzuki, M., Ogiso, E., and Yasumoto, T. 2005a. Kinetics of diarrhetic shellfish poisoning toxins, okadaic acid, dinophysistoxin-1, pectenotoxin-6 and yessotoxin in scallops *Patinopecten yessoensis*. *Fish Sci* 71, 948–955.
- Suzuki, T., Jin, T., Shirota, Y., Mitsuya, T., Okumura, Y., and Kamiyama, T. 2005b. Quantification of lipophilic toxins associated with diarrhetic shellfish poisoning (DSP) in Japanese bivalves by liquid chromatography–mass spectrometry (LC-MS) and comparison with mouse bioassay (MBA) as the official testing method in Japan. *Fish Sci* 71, 1370–1378.
- Suzuki, T., MacKenzie, L., Stirling, D., and Adamson, J. 2001a. Conversion of pectenotoxin-2 to pectenotoxin-2 seco acid in the New Zealand scallop, *Pecten novaezelandiae*. *Fish Sci* 67, 506–510.
- . 2001b. Pectenotoxin-2 seco acid: a toxin converted from pectenotoxin-2 by the New Zealand Greenshell mussel, *Perna canaliculus*. *Toxicon* 39, 507–514.



- Suzuki, T., Mitsuya, T., Matsubara, H., and Yamasaki, M. 1998. Determination of pectenotoxin-2 after solid-phase extraction from seawater and from the dinoflagellate *Dinophysis fortii* by liquid chromatography with electrospray mass spectrometry and ultraviolet detection. Evidence of oxidation of pectenotoxin-2 to pectenotoxin-6 in scallops. *J Chromatogr A* 815, 155–160.
- Suzuki, T., Walter, J. A., LeBlanc, P., Mackinnon, S., Miles, C.O., Wilkins, A.L., Munday, R., Beuzenberg, V., Mackenzie, A.L., Jensen, D.J., Cooney, J.M., and Quilliam, M.A. 2006. Identification of pectenotoxin-11 as 34S-hydroxypectenotoxin-2, a new pectenotoxin analogue in the toxic dinoflagellate *Dinophysis acuta* from New Zealand. *Chem Res Toxicol*, in press.
- Suzuki, T., and Yasumoto, T. 2000. Liquid chromatography–electrospray ionization mass spectrometry of the diarrhetic shellfish-poisoning toxins okadaic acid, dinophysistoxin-1 and pectenotoxin-6 in bivalves. *J Chromatogr A* 874, 199–206.
- Tachibana, K., Scheuer, P.J., Tsukitani, Y., Kikuchi, H., Van Engen, D., Clardy, J., Gopichand, Y., and Schmitz, F.J. 1981. Okadaic acid, a cytotoxic polyether from two marine sponges of the genus *Halichondria*. *J Am Chem Soc* 103, 2469–2471.
- Takahashi, E., Eaglesham, G., Shaw, G., Yu, Q., and Connell, D. 2003. Detection of marine algal toxins in shellfish from North Stradbroke Island, Queensland, Australia. In *HABTech 2003*, Cawthron Report No. 906, ed. Holland, P., Rhodes, L., and Brown, L. Nelson, New Zealand: Cawthron Institute: Cawthron Institute, 131–136.
- Terao, K., Ito, E., Yanagi, T., and Yasumoto, T. 1986. Histopathological studies on experimental marine toxin poisoning. I. Ultrastructural changes in the small intestine and liver of suckling mice induced by dinophysistoxin-1 and pectenotoxin-1. *Toxicon* 24, 1141–1151.
- Vale, P. 2004. Differential dynamics of dinophysistoxins and pectenotoxins between blue mussel and common cockle: a phenomenon originating from the complex toxin profile of *Dinophysis acuta*. *Toxicon* 44, 123–134.
- Vale, P. 2006. Differential dynamics of dinophysistoxins and pectenotoxins, part II: offshore bivalve species. *Toxicon*, in press.
- Vale, P., and Sampayo, M.A.M. 2002a. First confirmation of human diarrhoeic poisonings by okadaic acid esters after ingestion of razor clams (*Solen marginatus*) and green crabs (*Carcinus maenas*) in Aveiro lagoon, Portugal and detection of okadaic acid esters in phytoplankton. *Toxicon* 40, 989–996.
- Vale, P., and Sampayo, M.A.M. 2002b. Pectenotoxin-2 seco acid, 7-epi-pectenotoxin-2 seco acid and pectenotoxin-2 in shellfish and plankton from Portugal. *Toxicon* 40, 979–987.
- Vershinin, A., Moruchkov, A., Morton, S.L., Leighfield, T.A., Quilliam, M.A., and Ramsdell, J.S. 2006. Phytoplankton composition of the Kandalaksha Gulf, Russian White Sea: *Dinophysis* and lipophilic toxins in the blue mussel (*Mytilus edulis*). *Harmful Algae*, in press.
- Yasumoto, T. 1988. Recent progress in the chemistry of dinoflagellate and related toxins. Abstract. *Toxicon* 26, 50.
- . 2001. The chemistry and biological function of natural marine toxins. *Chem Rec* 1, 228–242.
- Yasumoto, T., and Murata, M. 1990. Polyether toxins involved in seafood poisoning. In *Marine Toxins: Origin, Structure and Molecular Physiology*, vol. 418, ed. Hall, S., and Strichartz, G. ACS: Washington, DC: ACS, 120–132.
- Yasumoto, T., and Murata, M. 1993. Marine Toxins. *Chem Rev* 93, 1897–1909.
- Yasumoto, T., Murata, M., Lee, J.-S., and Torigoe, K. 1989. Polyether toxins produced by dinoflagellates. In *Mycotoxins and Phycotoxins '88*, ed. Natori, S., Hashimoto, K., and Ueno, Y. Amsterdam: Elsevier, 375–382.
- Yasumoto, T., Murata, M., Oshima, Y., Matsumoto, G. K., and Clardy, J. 1984. Diarrhetic shellfish poisoning. In *ACS Symposium Series* 262, 207–214.
- Yasumoto, T., Murata, M., Oshima, Y., Sano, M., Matsumoto, G.K., and Clardy, J. 1985. Diarrhetic shellfish toxins. *Tetrahedron* 41, 1019–1025.
- Yoon, M.Y., and Kim, Y.C. 1997a. [Acute toxicity of pectenotoxin-2 and its effects on hepatic metabolising enzyme system in mice]. *Korean J Toxicol* 13, 183–186 (in Korean).
- Yoon, M.Y., and Kim, Y.C. 1997b. Toxicity and changes in hepatic metabolizing enzyme system induced by repeated administration of pectenotoxin 2 isolated from marine sponges. *Korean J Pharmacogn* 28, 280–285 (in Korean).
- Zhou, Z.-H., Komiyama, M., Terao, K., and Shimada, Y. 1994. Effects of pectenotoxin-1 on liver cells in vitro. *Nat Toxins* 2, 132–135.
- Zingone, A., Siano, R., D'Alelio, D., and Sarno, D. 2006. Potentially toxic and harmful microalgae from coastal waters of the Campania region (Tyrrhenian Sea, Mediterranean Sea). *Harmful Algae*, in press.

## 10 Chemistry, Origins, and Distribution of Yessotoxin and Its Analogues

Philipp Hess and John A. B. Aasen

### Introduction

Yessotoxin (YTX) is a ladder shaped disulphated polycyclic ether toxin that was first isolated from the digestive glands of scallops *Patinopecten yessoensis* in Japan (Murata et al. 1987). Because of its discovery through the mouse bioassay (MBA) originally developed by Yasumoto et al. (1978), for the detection of diarrhetic shellfish toxins, and due to its frequent co-occurrence with truly diarrhetic toxins, YTX was initially misclassified as one of the diarrhetic shellfish poisoning (DSP) toxins. Later it was shown that YTX causes no diarrhetic effects when administered orally to mice (Aune et al. 2002, Tubaro et al. 2003 and 2004). Yessotoxin and its analogues are produced by the dinoflagellate algae *Protoceratium reticulatum* (Ciminiello et al. 2003; Samdal et al. 2004b; Satake et al. 1997a; Satake et al. 1999), *Lingulodinium polyedrum* (Draisci et al. 1999) and recently reported to also be produced in *Gonyaulax spinifera* (Rhodes et al. 2006). Since the initial discovery of YTX, several more analogues of YTXs have been discovered in many parts of the world including Japan, Norway, Italy, Scotland, and Chile (Draisci et al. 2000). Over the last years, this toxin group has been shown to contain a large number of analogues including 45-hydroxyYTX, carboxyYTX, 1-desulfoYTX, homoYTX, 45-hydroxyhomoYTX, carboxyhomoYTX, heptanor-41-oxoYTX, heptanor-41-oxohomoYTX, trinorYTX, adriatoxin, (44-R,S)-44,55-dihydroxyYTX. 9-methylYTXs (Finch et al. 2005). In a paper by Miles et al. (2005a), numerous analogues of YTX in *P. reticulatum* are described.

Updating previous reviews by Draisci et al. (2000) and FAO (2004), this chapter describes the biogenetic origin of YTX, the structures and physicochemical properties of 32 analogues, the distribution, profiles and levels found, as well as recent findings in the synthesis of the base structure of YTX. The different approaches in determining the comparative bioactivities of different YTX analogues are reviewed and difficulties for analytical methodology outlined.

### Biogenetic Origin of Yessotoxins

From the initial discovery of YTX as a bioactive compound accumulated in the Japanese scallop *Patinopecten yessoensis* (Murata et al. 1987), it had taken another 10 years before *P. reticulatum* was identified unequivocally as one of the causative organisms of YTXs (Satake et al. 1997a). The authors showed production of YTX in cultured *P. reticulatum* (3 pg/cell), isolated from a bloom in New Zealand in 1996.

Even though YTX was discovered in blue mussels in 1988 in Norway (Lee et al. 1988), for many years the biogenetic origin of YTX in Norway remained a mystery due to low cell numbers of *P. reticulatum* in seawater. However, a recent study (Samdal et al. 2004a) showed that the content of YTX per cell from Norwegian strains (18–79 pg/cell) can be much larger than the originally

reported content (3 pg/cell). The authors analyzed both picked cells from net hauls and picked cells from non-axenic uni-algal cultures of *P. reticulatum*. Additionally, *P. reticulatum* cells in culture tend to excrete YTX and its analogues into the culture medium (Konishi et al. 2004; Samdal et al. 2004a). The fact that YTX and its analogues are exotoxins together with the comparatively high water solubility of the compounds, contributing to substantial losses of toxin in harsher filtration regimes (C. Miles, personal communication), resulted probably in an underestimation of the toxin content per cell in the initial studies. These high toxin contents per cell, also confirmed in cultured *P. reticulatum* from Norway, in combination with a close relationship observed between *P. reticulatum* cells in seawater and YTX in shellfish (Aasen et al. 2005), result in wide acceptance of *P. reticulatum* as the main biogenetic origin of YTXs in Norway.

The occurrence of YTX in Italy was first observed in 1996 for shellfish harvested on the Adriatic coast (Ciminiello et al. 1997; Satake et al. 1997b). At the same time, a bloom of *Lingulodinium polyedrum* (formerly *Gonyaulax polyedra*) had been observed (> 16,000,000 cells/L) in the same area, suggesting that this organism produced the YTX and its analogues observed in shellfish and phytoplankton (Tubaro et al. 1998). In addition, complex YTX profiles have also been reported from *P. reticulatum* isolated and cultured from the Adriatic Sea (Ciminiello et al. 2003), thereby confirming that at least two causative organisms are associated with the production of YTX and its analogues in these waters.

Similarly, the study by Konishi et al. 2004, on the YTX production of a number of *P. reticulatum* strains from Japan, leaves very little doubt that this alga is the main causative organism of YTXs in Japan.

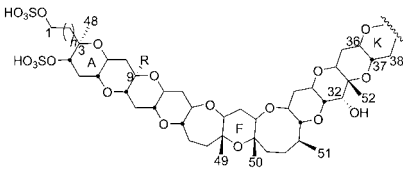
*P. reticulatum* from the East coast of the United Kingdom (North Sea) and Canada have been isolated, cultured and shown to produce YTXs, although relatively low concentrations of 0.3 pg/cell (Stobo et al. 2002). This study also showed a very low toxin production of *L. polyedrum* compared to *P. reticulatum*, thus possibly explaining the relatively low concentrations of YTXs found in U.K. and Canadian shellfish to date (Stobo et al. 2004 and 2005, van de Riet et al. 2004).

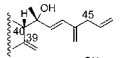
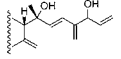
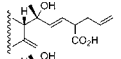
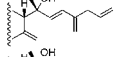
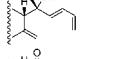
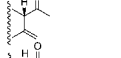
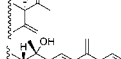
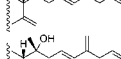
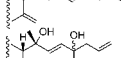
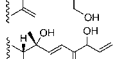
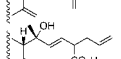
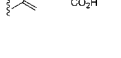
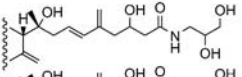
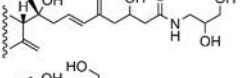
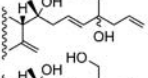
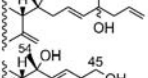
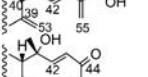
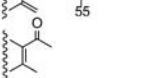
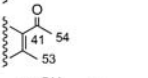
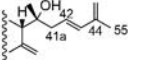
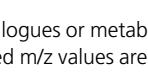
More recently, Rhodes et al. 2006, reported that YTXs had been found in shellfish from the Marlborough Sounds (New Zealand) without any *P. reticulatum* present in the surrounding seawater, even though a monitoring programme including this species had been implemented. *Gonyaulax spinifera* may have been the causative organism in this event, since cultures of this species produced YTX as detected by ELISA. However, further confirmation may be required since the same alga isolated from the North Sea did not produce YTXs in culture (Stobo et al. 2002).

It is likely that the above-mentioned algae are producing YTXs relatively independently of their bacterial flora, since a study by Seamer (2001) found that apparently axenic cultures of *P. reticulatum* also produced YTXs. However, *P. reticulatum* has been reported to produce significantly different profiles of YTXs in different countries (Ciminiello et al. 2003; Konishi et al. 2004; Miles et al. 2005a and b, Souto et al. 2005), and further studies are required to clarify whether these differences in profiles are due to environmental conditions, subspecies differences in the genome of the algae, associated bacterial contamination or a combination of these factors. In summary, we can conclude that *Protoceratium reticulatum*, *Lingulodinium polyedrum* and *Gonyaulax spinifera* have been very strongly linked with the production of YTX or its analogues in Japan, Europe, North and South America, and New Zealand.

## Chemical Structures of Yessotoxin and Its Analogues

YTXs (Figs. 10.1 and 10.2) are disulphated polyethers and the structure of YTX is related to those of brevetoxins (BTXs) and ciguatoxins as YTXs have 10 or 11 contiguously transfused ether



		R	n	m/z	
<b>1</b>	YTX		H	1	1141
<b>2</b>	45-hydroxyYTX		H	1	1157
<b>3</b>	carboxyYTX		H	1	1173
<b>4</b>	1a-homoYTX		H	2	1155
<b>5</b>	45,46,47-trinorYTX		H	1	1101
<b>6</b>	ketoYTX		H	1	1047
<b>7</b>	40-epi-ketoYTX		H	1	1047
<b>8</b>	41a-homoYTX		H	1	1155
<b>9</b>	9-Me-41a-homoYTX		CH <sub>3</sub>	1	1169
<b>10</b>	44,55-dihydroxyYTX		H	1	1175
<b>11</b>	45-hydroxy-1a-homoYTX		H	2	1171
<b>12</b>	carboxy-1a-homoYTX		H	2	1187
		R	n	m/z	
<b>13</b>	41a-homoYTX amide		H	1	1290
<b>14</b>	9-Me-41a-homoYTX amide		CH <sub>3</sub>	1	1304
<b>15</b>	44,55-dihydroxy 8		H	1	1189
<b>16</b>	44,55-dihydroxy 9		CH <sub>3</sub>	1	1203
<b>17</b>	45-hydroxydinorYTX		H	1	1131
<b>18</b>	44-oxotrinorYTX		H	1	1117
<b>19</b>	YTX enone		H	1	1047
<b>20</b>	9-MeYTX enone		CH <sub>3</sub>	1	1061
<b>21</b>	41a-homo-44-oxotrinorYTX		H	1	1131

**Figure 10.1.** Structures of YTX and known analogues or metabolites with the A to K ring system. The structures are depicted in their sulfonic acid forms, and observed m/z values are for the mono-anions.

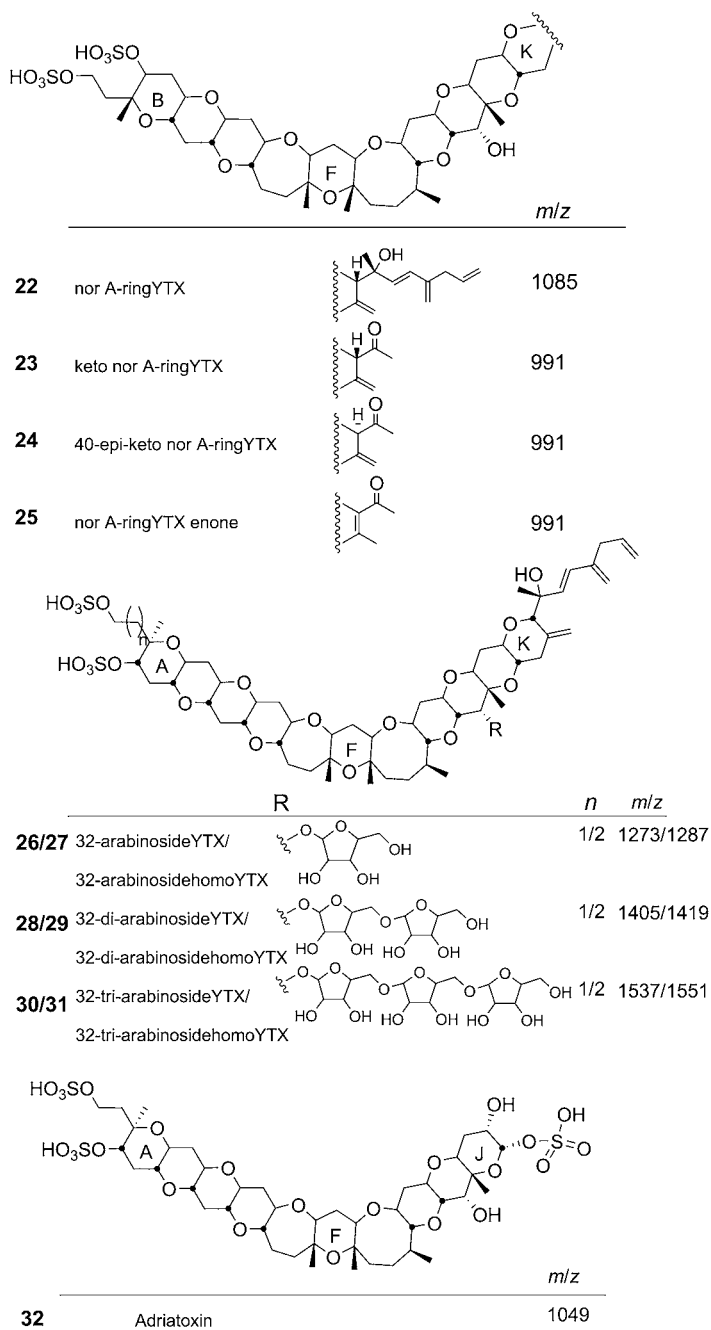


**Figure 10.2.** Structures of YTX analogues or metabolites without A or K ring, and arabinosides of YTX. The structures are depicted in their sulfonic acid forms, and observed *m/z* values are for the mono-anions.

rings and an unsaturated side chain. Compared to brevetoxin, YTX has a longer backbone of 47 carbons.

YTX was first isolated by Murata et al. (1987), and its planar structure was determined using NMR techniques. The structure was also confirmed using FAB-MS (Naoki et al. 1993). The relative configuration was later reported by Satake et al. (1996), while the absolute configuration was provided by Takahashi et al. (1996). Desulphated YTX (dsYTX) was then produced by solvolysis of the precursor YTX, for the determination of the sulphate ester positions by comparison between the NMR spectra. Morohashi et al. (2000) reported the absolute configuration at C45 in 45-hydroxy YTX. To this point, a number of YTXs have been identified in shellfish and algae, more than 90 analogues have been postulated by LC-MS<sup>3</sup> and neutral loss LC-MS/MS, although structures for most of them have not yet been confirmed (Miles et al. 2005a).

Some of the analogues described for YTX are 1a-homo-YTX (previously homoYTX) with an extra methylene in the chain in 1 position, 41a-homoYTX with an extra methylene group in the side chain and 9-Methyl-41a-homoYTX with an additional methyl group at 9 position (Miles et al. 2004b). Adriatoxin lacks the K ring and has an additional sulphonic acid group (Ciminiello et al. 1998), the norring-A-YTX, and ketone analogues of this compound lack the A ring (Miles et al. 2004b). Heptanor-41-oxoYTX (Ciminiello et al. 2002) and heptanor-41-oxohomoYTX (Ciminiello et al. 2001) both are missing the side chain at the K ring. The 1,3enone isomer of heptanor-41-oxoYTX has been isolated by Miles et al. (2004b), while 45,46,47-trinorYTX was found by Satake et al. (1996), and 1-desulfoYTX by Daiguji et al. (1998).

Polyhydroxylated amide analogues of YTX were reported very recently by Miles et al. (2005b), and 44,55-dihydroxyYTX by Finch et al. (2005). Mono-, di- and tri-arabinosides of YTX and 1a-homoYTX have also been identified (Konishi et al. 2004; Miles et al. 2006b; Satake et al. 2002)

Metabolites found in shellfish include YTX and 1a-homoYTX oxidised to 45-hydroxy derivatives (Satake et al. 1997b), other compounds are 55-carboxylated derivatives of YTX and 1a-homoYTX (Ciminiello et al. 2000a and b), and a 55-carboxylated derivative of 45-hydroxyYTX has been tentatively shown with LC-MS/MS data (Aasen et al. 2005).

## Physico-Chemical Properties of Yessotoxin and Analogues

Following the first isolation of YTX by Murata et al. (1987), characterization was carried out by NMR as well as other techniques, and the purified toxin was found as an amorphous solid,  $[\alpha]_D^{20} +3.01^\circ$  (c 0.45, CH<sub>3</sub>OH), maximum absorption in UV spectra was found to be 230 nm (in CH<sub>3</sub>OH) ( $\epsilon$  10600). The same authors found absorption bands in IR (KBr) at 3400, 1240, 1220, 1070 and 820 cm<sup>-1</sup>, and this is the only YTX this has been reported for. Later additions to the YTX family have mainly been characterised by NMR and (LC-)MS/MS, UV absorption data being reported for some.

Until now, most of the recently reported analogues have only been characterized using LC-MS/MS, where scanning of neutral losses during collision-induced fragmentation can be used to identify tentative YTXs in algae (Miles et al. 2005a). The theoretical fragmentation pattern of YTX is shown in Fig. 10.3, and has been confirmed by acquiring a mass spectrum of YTX from a contaminated shellfish sample (Norway 2002; Fig. 10.4). This pattern of fragmentation of the main ring is common for YTXs, and the change in mass of fragments can be used to identify substituents in different positions on the base frame of YTXs. In Table 10.1, all YTXs have been reported giving their molecular formulae and weights, structure and reference to first publication (also for NMR). YTXs have traditionally been reported as the sodium salt of the sulphonic acid but in Table 10.1 and Figs. 10.1 and 10.2 we chose to

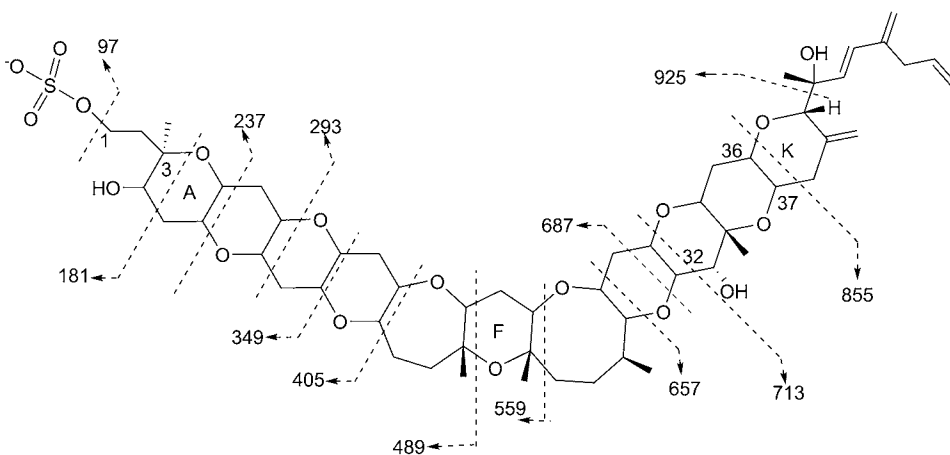


**Figure 10.3.** Fragmentation of the  $[M-SO_3]^-$  of YTX with the  $m/z$  values and the fragmentation shown.

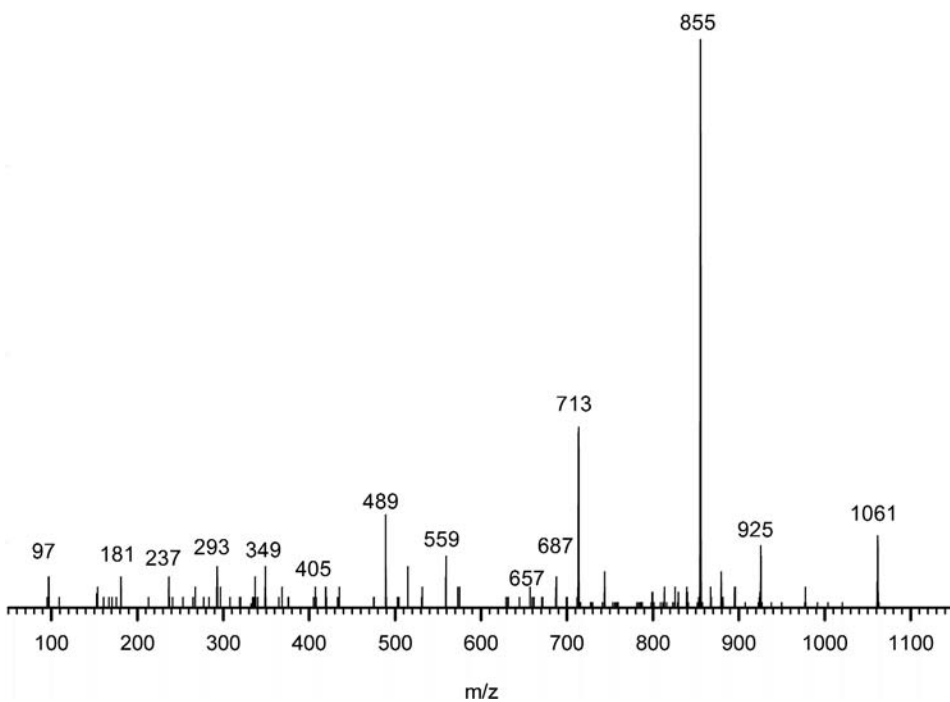


**Figure 10.4.** Spectra of YTX obtained by LC-MS/MS (QqQ) from a contaminated blue mussel sample from Norway (2002).



**Table 10.1.** Chemical properties of characterized YTXs

Fig. No.	Name	Molecular formula	MW	UV $\lambda_{max}$ (nm)	References	NMR references
1	YTX	$C_{55}H_{82}O_{21}S_2$	1142	230	Murata et al. 1987	Murata et al. 1987
2	45-hydroxy YTX	$C_{55}H_{82}O_{22}S_2$	1158	230	Satake et al. 1996	Satake et al. 1996; Morohashi et al. 2000 Ciminiello et al. 2000b
3	carboxy YTX	$C_{55}H_{82}O_{23}S_2$	1174	—	Ciminiello et al. 2000b	Ciminiello et al. 2000b
5	45,46,47-trinor YTX	$C_{52}H_{78}O_{21}S_2$	1102	226	Satake et al. 1996	Satake et al. 1996
8	41a-homo YTX	$C_{56}H_{84}O_{21}S_2$	1156	239*	Miles et al. 2004a	Miles et al. 2004a
4	1a-homo YTX	$C_{56}H_{84}O_{21}S_2$	1156	231	Satake et al. 1997,	Satake et al. 1997; Konishi et al. 2004
9	1-desulfo YTX	$C_{55}H_{82}O_{18}S$	1062	—	Daiguji et al. 1998	Daiguji et al. 1998
9	9-Me-41a-homo YTX	$C_{57}H_{86}O_{21}S_2$	1170	239*	Miles et al. 2004a	Miles et al. 2004a
10	44,55-dihydroxy YTX	$C_{55}H_{84}O_{23}S_2$	1176	205*	Finch et al. 2005	Finch et al. 2005
11	45-hydroxy-1a-homo YTX	$C_{56}H_{84}O_{22}S_2$	1172	—	Satake et al. 1997	Satake et al. 1997
12	carboxy-1a-homo YTX	$C_{56}H_{84}O_{23}S_2$	1188	—	Ciminiello et al. 2000a	Ciminiello et al. 2000a
32	adriatoxin	$C_{42}H_{66}O_{14}S_3$	1050	—	Ciminiello et al. 1998	Ciminiello et al. 1998
26	32-arabinoside YTX	$C_{60}H_{90}O_{25}S_2$	1274	—	Suoto et al. 2005	Suoto et al. 2005; Miles et al. 2006b
27	32-arabinoside 1a-homo YTX	$C_{61}H_{92}O_{25}S_2$	1288	—	Konishi et al. 2004	Konishi et al. 2004
28	32-di-arabinoside YTX	$C_{65}H_{98}O_{29}S_2$	1406	—	Cooney et al. 2003	Miles et al. 2006b
29	32-di-arabinoside 1a-homo YTX	$C_{66}H_{100}O_{29}S_2$	1420	230	Konishi et al. 2004	Konishi et al. 2004
30	32-tri-arabinoside YTX**	$C_{70}H_{106}O_{33}S_2$	1538	—	Miles et al. 2005b	Miles et al. 2004
31	32-tri-arabinoside 1a-homo YTX	$C_{71}H_{108}O_{33}S_2$	1552	—	Konishi et al. 2004	Konishi et al. 2004
22	nor A-ring YTX	$C_{52}H_{78}O_{20}S_2$	1086	239*	Miles et al. 2004a	Miles et al. 2004a
6	keto YTX (heptanor-41-oxo YTX)	$C_{48}H_{72}O_{19}S_2$	1048	—	Ciminiello et al. 2002	Ciminiello et al. 2002
7	40-epi-keto YTX	$C_{48}H_{72}O_{21}S_2$	1048	—	Miles et al. 2004b	Miles et al. 2004b
19	YTX enone	$C_{48}H_{72}O_{21}S_2$	1048	273*	Miles et al. 2004b	Miles et al. 2004b
	keto 1a-homo YTX (heptanor-41-oxohomo YTX)	$C_{49}H_{74}O_{21}S_2$	1062	—	Ciminiello et al. 2001	Ciminiello et al. 2001
13	41a-homo YTX amide	$C_{60}H_{93}O_{25}NS_2$	1291	233*	Miles et al. 2005a	Miles et al. 2005a
14	9-Me-41a-homo YTX amide	$C_{61}H_{95}O_{25}NS_2$	1305	233*	Miles et al. 2005a	Miles et al. 2005a
15	44,55-dihydroxy-41a-homo YTX**	$C_{56}H_{86}O_{23}S_2$	1190	205*	Finch et al. 2005	Finch et al. 2005
16	44,55-dihydroxy-9-methyl-41a-homo YTX**	$C_{57}H_{88}O_{23}S_2$	1204	205*	Finch et al. 2005	Finch et al. 2005

(Continued)

**Table 10.1.** Chemical properties of characterized YTXs. (Cont.)

17	45-hydroxy-dinorYTX	$C_{33}H_{80}O_{22}S_2$	1132	230*	Miles et al. 2006a	Miles et al. 2006a
18	44-oxotrinorYTX	$C_{32}H_{78}O_{22}S_2$	1118	230*	Miles et al. 2006a	Miles et al. 2006a
20	9-Me-YTX enone	$C_{39}H_{74}O_{21}S_2$	1062	275*	Miles et al. 2006a	Miles et al. 2006a
21	41a-homo-44-oxotrinorYTX**	$C_{33}H_{80}O_{22}S_2$	1132	—	Miles et al. 2006a	Miles et al. 2006a
23	keto-nor A-ringYTX**	$C_{45}H_{68}O_{20}S_2$	992	—	Miles et al. 2004a	Miles et al. 2004a
24	40-epi-keto-nor A-ringYTX**	$C_{45}H_{68}O_{20}S_2$	992	—	Miles et al. 2004a	Miles et al. 2004a
25	nor A-ringYTX enone**	$C_{45}H_{68}O_{20}S_2$	992	—	Miles et al. 2004a	Miles et al. 2004a
	45-hydroxycarboxyYTX**	$C_{35}H_{82}O_{24}S_2$	1190	—	Aasen et al. 2005	

\*  $\lambda$  (nm) given as reported by PDA scanning in LC. \*\*tentative based on MS data

report the molecular mass of the protonated form (e.g., 1142 amu for YTX) to facilitate reference to mass spectral identification.

The persistence of YTX under light and dark conditions has been reported by Mitrovic et al. (2005). The report shows that YTX concentrations in a culture of *Protoceratium reticulatum* killed by cooling decreased to 10% of the initial concentration within 3 days, and depleted to near zero within a week in light treatment (14-hour light, 10-hour dark routine), while for the same sample in a dark environment, the concentration decreased at a slower rate, and was reduced to approximately 10% of the initial concentration only after 18 days.

YTXs are relatively persistent in shellfish tissue (Ramstad et al. 2001; Mackenzie et al. 2002; Aasen et al. 2005; Samdal et al. 2005) and are, at least initially, concentrated in the digestive gland (Yasumoto and Takizawa 1997). Most of the compounds found in algae have also been found in contaminated shellfish tissue (Murata et al. 1987; Lee et al. 1988; Satake et al. 1997a; Draisci et al. 1999; Ciminiello et al. 1997, 1998, 2000a, 2000b, 2001, 2002, 2003; Finch et al. 2005; Aasen et al. 2005; and Samdal et al. 2005). Although 45-hydroxy YTX and carboxy YTX have been reported in algae by Ciminiello et al. 2003, it is also suggested to be metabolised from YTX in shellfish: Aasen et al. (2005) report significant amounts of 45-hydroxy and carboxy YTX in the mussels with YTX only appearing as the dominating toxin at the peak of the algal bloom, then decreasing rapidly.

YTX appears more water-soluble than the other lipophilic toxins as it predominantly extracts to the aqueous methanolic phase in partitioning with dichloromethane or to the aqueous phase when partitioned with ethyl acetate (T. Yasumoto 2001 and authors' observations), which may be explained by the sulphate groups giving YTXs a more polar behavior. This behaviour in partitioning has also posed a problem for the extraction of shellfish samples for determination by MBA where YTX has shown irreproducible recovery in the partitioning with diethyl ether. A revised protocol was proposed by Yasumoto in 2001, allowing for separation of YTXs from other, more lipophilic toxins such as okadaic acid or azaspiracids.

## Global Distribution, Levels, and Profiles of Yessotoxin Analogues

Yessotoxins have been reported initially in Japan in 1987 (Murata et al. 1987), rapidly followed by their discovery in Norway (Lee et al. 1988) and a few years later in New Zealand (Satake et al. 1997b) and Italy (Ciminiello et al. 1997; Satake et al. 1997c; Tubaro et al. 1998). Since then, YTXs have also been reported to occur in shellfish from Chile (Yasumoto and Tazikawa, 1997), U.K. (Stobo et al. 2005), and Canada (Finch et al. 2005, van de Riet 2006), while the production of yessotoxin or its analogues was reported from phytoplankton organisms originating from a number of countries, including Spain and the USA (Paz et al. 2004). Therefore, we can assume a global distribution of the causative organism and the toxin. However, locally the distribution of the organism can vary greatly; e.g., in Japan YTXs have mainly been found in the north of the main island, whereas Norway and Italy have been more affected than other parts of Europe. Some analogues have only been reported in very localized areas, such as adriatoxin from the Adriatic Sea, Italy (Ciminiello et al. 1998). However, this may well be related to the lack of widely available specific analytical methods, in particular LC-MS (Draisci et al. 2000).

Accurate quantitation of YTXs has proven rather difficult due to the lack of calibration standards and the application of different methods, each of which measures different parameters. Ciminiello et al. (1997) and Draisci et al. (1998) reported levels of 0.3 mg/kg whole flesh and 0.15 mg/kg whole

flesh equivalent for Italian samples of *M. galloprovincialis* sampled in 1995 and 1997, respectively. Higher levels of ca. 1.5 mg/kg whole flesh equivalent were reported by Draisci et al. (1999), using LC-MS. Up to ca. 3 mg/kg whole flesh equivalent were measured in Italian mussels, applying a functional assay based on the effect of YTX on E-cadherin (Pierroti et al. 2003). In New Zealand (*P. caniculus*), levels of YTX have been found up to 2 mg/kg (McKenzie et al. 2002, 2004). Aasen et al. (2005) and Samdal et al. (2005) reported levels up to 3 mg/kg whole flesh found in *M. edulis* from Norway when using LC-MS for the analysis of the sum of YTX, 45-hydroxy YTX, carboxy YTX and hydroxycarboxy YTX, while they found a four-fold value of 12 mg/kg when using the ELISA assay. The antibody used in this ELISA, initially developed by Briggs et al. (2004), shows different cross-reactivity to different analogues, some of which are unfortunately opposite to the relative toxicity of the compound as determined by intraperitoneal injection into mice.

As outlined under the section on structures, most analogues of YTX have been identified in cultured algae, mainly *P. reticulatum*, which seems to produce higher levels than *L. polyedrum* (Stobo et al. 2002; Paz et al. 2004). However, the formation of a number of analogues appears specifically accelerated in shellfish, in particular the oxidation of YTX and homo-YTX to the hydroxylated and carboxylated analogues (Fig. 10.5).

## Chemical Synthesis of Yessotoxins and Analogues

Synthesis of marine polycyclic ethers has attracted attention of numerous synthetic organic chemists during the last years, and Matsuo et al. (2000) reported the efficient convergent synthesis of a transfused 6-6-6-6-membered tetracyclic ether ring system with Brevetoxin as example. This transfused ether ring system is also part of the base structure of YTX. Synthesis of partial structures of YTX has since been developed by several groups in parallel, and Mori and Hayashi (2002) reported a convergent synthetic route to the BCDE system, where the key features were the alkylation of acetylene with the B and E units. Later, Suzuki and Nakata (2002) reported the convergent synthesis of the ABCDEF-ring system of YTX and adriatoxin, performed on the basis of the coupling of the acetylide of the A-ring and the triflate of the DEF-ring, oxidation of the alkyne to diketone, intramolecular diacetalization, and stereoselective reduction of the diacetal with  $\text{Et}_3\text{SiH-TMSOTf}$ . The same ABCDEF-ring system was also reported as an iterative synthesis in a stereo controlled linear synthesis by Mori et al. (2003). Another approach was taken by Kadota et al. 2003, who performed a convergent synthesis of the ring segment via intramolecular allylation of an  $\alpha$ -chloroacetoxy ether and subsequent ring-closing metathesis. An overview of synthetic strategies of marine polycyclic ethers via intramolecular allylations with respect to linear and convergent approaches is given by Kadota and Yamamoto (2005). This group also report the further application of this technology to the synthesis of the FGHI ring segment of YTX (Kadota et al. 2006), and that further studies towards the total synthesis of YTX are in progress in their laboratories. No total synthesis of adriatoxin or YTX has yet been reported.

## Structure-Activity Relationships

Usually, structure-activity relationships rely heavily on synthetic chemistry producing large amounts of numerous structurally different but related analogues. Since complete synthesis of YTX or its analogues has not been achieved yet, progress in the area of toxicology of YTX has mostly been based on the limited amounts produced from isolation of YTX from naturally contaminated shellfish or algal cultures. Nevertheless, some basic structure-activity relationships can be derived from studies on

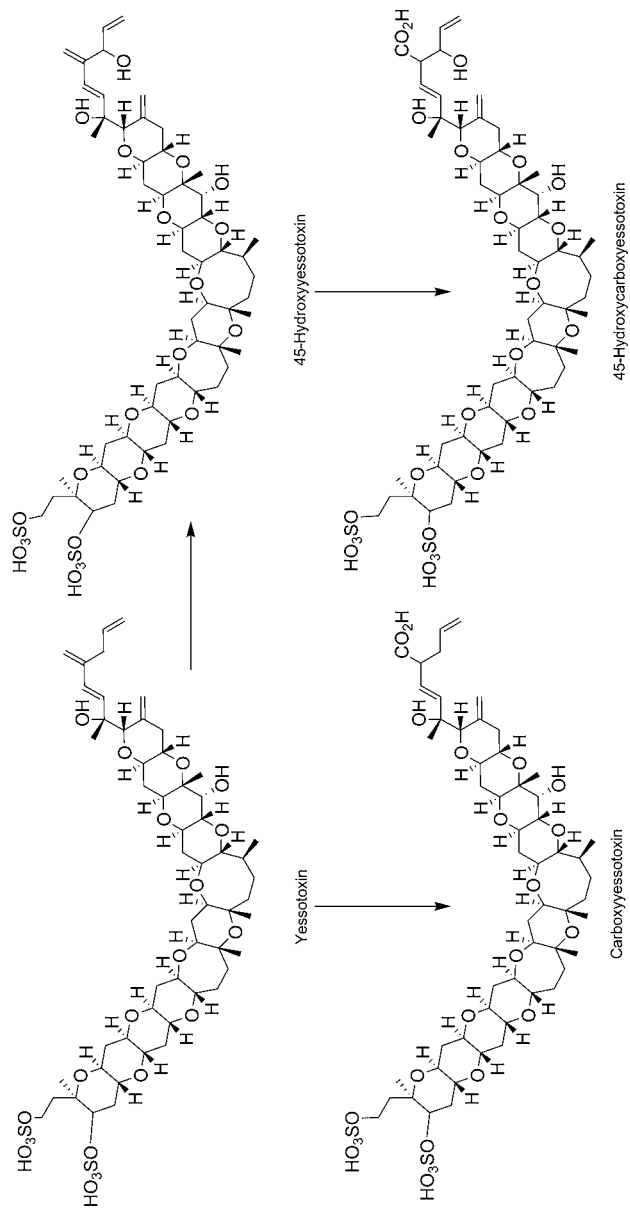


**Figure 10.5.** Metabolites of YTX found in blue mussels in Norway, including the tentative 45-hydroxycarboxyYTX, with minor modifications from Aasen et al. (2005).

the toxicity of individual analogues when injected intraperitoneally into mice (Satake et al. 1996; Miles et al. 2004a, 2005b; and Ciminiello et al. 2000a, 2000b; Tubaro et al. 2003). Although different toxicities have been reported for YTX itself when using different mouse strains (e.g. Murata et al. 1987, and Aune et al. 2002), crude estimates of relative toxicities can be obtained when using the same strain of mice for comparison of analogues, preferably in parallel. In this way, it is clear that YTX and homo-YTX have approximately the same toxicity (Satake et al. 1997), and that all other analogues have lesser toxicity than YTX, with hydroxyl and carboxy derivatives being approximately 5 times less toxic than the parent compounds. Some derivatives such as the trihydroxylated amides of 41-a-homo YTX and 1,3-enone isomer of heptanor-41-oxo YTX have not shown any toxicity by intraperitoneal injection into mice at levels greater than 5000 µg/kg bodyweight (Miles et al. 2004a, 2005b).

Another major pharmacological phenomenon directly related to the chemical structure is the large difference observed between toxicity of YTX in mice injected intraperitoneally and those orally exposed to YTX (Aune et al. 2002). This study showed that two out of three mice died when injected with a dose of 0.75 mg YTX/kg bodyweight and three of three mice injected with a dose of 1 mg YTX/kg bodyweight, while all mice survived when exposed orally to a dose of 10 mg/kg. Similar observations were made by Munday and co-workers (FAO/IOC/WHO 2006). It is highly likely that this difference is at least partly related to the comparatively high solubility of YTX in water. The large differences in toxicity between YTX, and its oxidized analogues 45-hydroxy-YTX and carboxy-YTX are likely to be related to the further increase in water solubility. A different approach on determining the relationship between structure and activity was taken by Ferrari et al. (2004), where different YTX analogues were dosed onto cultured cells. The authors obtained different toxic equivalence factors with the 45-hydroxy and the 55-carboxy analogues being ca. 20–50 times less toxic. These differences could be related to the more complex toxicology in live animals or to differences in the standards used.

## Consequences for Methods of Analysis and Regulation of YTXs

The chemical diversity and complexity described above poses particular challenges for any method of detection, be it for specific methods such as HPLC-FLD or –MS, ELISAs, functional or live animal assays. The challenge for compound-specific, analytical methods is twofold: first, the poor availability of purified calibration standards for analogues renders accurate quantification next to impossible, and second, the lack of data on the toxicity of some analogues makes it difficult to judge the relevance of compounds necessary to determine quantitatively. This situation has been slightly improved for regulatory purposes through the acceptance of the structure activity relationships described above, and the lack of calibration standards is currently being addressed in a number of European Union (EU) and internationally funded projects. Antibody-based assays face the challenge of the poor correlation between antibody binding capacity and relative toxicity of individual analogues, thereby leaving the assay with a multitude of unknowns. However, one ELISA has been extensively validated and is commercially available in kit-format, has a very good sensitivity and can be used for screening purposes. Functional assays lack the understanding of the interactivity of the various analogues and require significant efforts in terms of standardization before they can be used in a routine context. Animal assays are difficult to interpret due to their totally unspecific response, which does neither allow for identification of toxin groups nor quantification of the overall toxicity as soon as several groups of toxins are present. This means that any method applied to the determination of yessotoxins in the context of food safety needs to be empirically benchmarked

against observed effects in humans. However, the lack of data on any toxicity of yessotoxin and its analogues to humans renders this approach difficult, and the relevance of studies on this compound is questionable for public health. Current EU regulations for YTX are under review and should take into account the more recent findings on toxicology of YTXs.

The interest in this compound group over the last 20 years can only be understood from the discovery of the strong bioactivity of YTX displayed in the DSP mouse bioassay. Although the pharmacology of YTX in humans has never been studied, due to the high intraperitoneal toxicity observed in mice, the potential uptake through the intestinal barrier should be studied in the presence of other toxins interfering with this barrier, such as okadaic acid and azaspiracids. Also, due to the low oral toxicity, this compound may have desirable medicinal characteristics that should be investigated. Finally, the abundance of analogues identified in combination with the cultivability of the causative organism may allow for investigating the distinction of primary and secondary metabolites for this toxin group, which, in turn, could help clarifying the biosynthetic pathway and thus the genes implicated in the production of ladder-shaped polyether compounds, some of which have clearly shown human health implications.

## References

- Aasen, J., Samdal, I. A., Miles, C. O., Dahl, E., Briggs, L. R., and Aune, T. 2005. Yessotoxins in Norwegian blue mussels (*Mytilus edulis*): uptake from *Protoceratium reticulatum*, metabolism and depuration. *Toxicon* 45, 265–272.
- Aune, T., Sorby, R., Yasumoto, T., Ramstad, H., and Landsverk, T. 2002. Comparison of oral and intraperitoneal toxicity of yessotoxin towards mice. *Toxicon* 40, 77–82.
- Briggs L.R., Miles C.O., Fitzgerald J.M., Ross K.M., Garthwaite I., and Towers N.R. 2004. An ELISA for the detection of yessotoxin and its analogues. *J Agric Food Chem* 52, 5836–5842.
- Ciminiello, P., Dell'Aversano, C., Fattorusso, E., Forino, M., Magno, S., Guerrini, F., Pistocchi, R., and Boni, L. 2003. Complex yessotoxins profile in *Protoceratium reticulatum* from north-western Adriatic sea revealed by LC-MS analysis. *Toxicon* 42, 7–14.
- Ciminiello, P., Dell'Aversano, C., Fattorusso, E., Forino, M., Magno, S., and Poletti, R. 2002. The detection and identification of 42,43,44,45,46,47,55-heptanor-41-oxoyessotoxin, a new marine toxin from Adriatic shellfish, by liquid chromatography-mass spectrometry. *Chem Res Toxicol* 15, 979–984.
- Ciminiello, P., Fattorusso, E., Forino, M., Magno, S., Poletti, R., Satake, M., Viviani, R., and Yasumoto, T. 1997. Yessotoxin in mussels of the northern Adriatic Sea. *Toxicon* 35, 177–183.
- Ciminiello, P., Fattorusso, E., Forino, M., Magno, S., Poletti, R., and Viviani, R. 1998. Isolation of adriatoxin, a new analogue of yessotoxin from mussels of the Adriatic sea. *Tetrahedron Letters* 39, 8897–8900.
- . 1999. Isolation of 45-hydroxyessotoxin from mussels of the Adriatic Sea. *Toxicon* 37: 689–693.
- Ciminiello, P., Fattorusso, E., Forino, M., and Poletti, R. 2001. 42,43,44,45,46,47,55-Heptanor-41-oxohomoyessotoxin, a new biotoxin from mussels of the northern Adriatic sea. *Chem Res Toxicol* 14, 596–599.
- Ciminiello, P., Fattorusso, E., Forino, M., Poletti, R., and Viviani, R. 2000a. Structure determination of carboxyhomoyessotoxin, a new yessotoxin analogue isolated from adriatic mussels. *Chem Res Toxicol* 13, 770–774.
- . 2000b. A new analogue of yessotoxin, carboxy yessotoxin, isolated from Adriatic Sea mussels. *Europ. J Org Chem* 291–295.
- Cooney, J.M., Jensen, D.J., and Miles, C.O. 2003. Ion-trap LC-MS as a tool for structural characterisation of marine algal toxins. Holland, P., Rhodes, L. L., and Brown, L. pp. 59–64. 2003. In *HABTech 2003, Cawthron Report 906*. Nelson, New Zealand: Cawthron Institute.
- Daiguji, M., Satake, M., Ramstad, H., Aune, T., Naoki, H., and Yasumoto, T. 1998. Structure and fluorometric HPLC determination of 1-desulfoyessotoxin, a new yessotoxin analog isolated from mussels from Norway. *Nat Toxins* 6, 235–239.
- Draisci, R., Ferretti, E., Palleschi, L., Marchiafava, C., Poletti, R., Milandri, A., Ceredi, A., and Pompei, M. 1999. High levels of yessotoxin in mussels and presence of yessotoxin and homoyessotoxin in dinoflagellates of the Adriatic Sea. *Toxicon* 37, 1187–1193.
- Draisci, R., Giannetti, L., Lucentini, L., Ferretti, E., Palleschi, L., and Marchiafava, C. 1998. Direct identification of yessotoxin in shellfish by liquid chromatography coupled with mass spectrometry and tandem mass spectrometry. *Rapid Commun Mass Spectrom* 12, 1291–1296.



- Draisci, R., Lucentini, L., and Mascioni, A. 2000. Pectenotoxins and yessotoxins: chemistry, toxicology, pharmacology, and analysis. In *Seafood and Freshwater Toxins: Pharmacology, Physiology, and Detection*, ed. Botana, L.M. New York: Marcel Dekker, Inc., 289–324.
- FAO Food and Nutrition Paper 80. 2004. Marine Biotoxins. *Food and Agricultural Organization*, Rome.
- FAO/IOC/WHO. 2006. Advanced draft of expert consultation, Oslo. [http://www.fao.org/ag/agn/food/risk\\_biotoxin\\_en.stm](http://www.fao.org/ag/agn/food/risk_biotoxin_en.stm). Accessed February 12, 2006.
- FAO/IOC/WHO Expert Consultation on Biotoxins in Bivalve Molluscs. 2005. Background document, in preparation since 2004; version 13, October 2005.
- Ferrari, S., Ciminiello, P., Dell'Aversano, C., Forino, M., Malaguti, C., Tubaro, A., Poletti, R., Yasumato, T., Fattorusso, E., and Rossini, G.P. 2004. Structure-activity relationships of yessotoxins in cultured cells. *Chem Res Toxicol* 17, 1251–1257.
- Finch, S.C., Wilkins, A.L., Hawkes, A.D., Jensen, D.J., Mackenzie, A.L., Beuzenberg, V., Quilliam, M.A., Olseng, C.D., Samdal, I.A., Aasen, J., Selwood, A., Cooney, J.M., Sandvik, M., and Miles, C.O. 2005. Isolation and Identification of (44-*RS*)-44,55-Dihydroxyessotoxin from *Protoceratium reticulatum*, and its occurrence in extracts of shellfish from New Zealand, Norway and Canada. *Toxicon* 46, 160–170.
- Kadota, I., and Yamamoto, Y. 2005. Synthetic Strategies of Marine Polycyclic Ethers via Intramolecular Allylations: Linear and Convergent Approaches. *Acc Chem Res* 38, 423–432.
- Kadota, I., Ueno, H., Sato, Y., and Yamamoto, Y. 2006. Convergent synthesis of the FGHI ring segment of yessotoxin. *Tetrahedron Letters* 47, 89–92.
- Kadota, I., Ueno, H., and Yamamoto, Y. 2003. Convergent synthesis of the A-F ring segment of yessotoxin and adriatoxin. *Tetrahedron Letters* 44, 8935–8938.
- Konishi, M., Yang, X.M., Li, B., Fairchild, C.R., and Shimizu, Y. 2004. Highly cytotoxic metabolites from the culture supernatant of the temperate dinoflagellate *Protoceratium cf. reticulatum*. *J Nat Prod* 67, 1309–1313.
- Lee, J. ., Tangen, K., Dahl, E., Hovgaard, P., and Yasumoto, T. 1988. Diarrhetic Shellfish Toxins in Norwegian mussels. *Nippon Suisan Gakkaishi* 54, 1953–1957.
- MacKenzie, L., Holland, P., McNabb, P., Beuzenberg, V., Selwood, A., and Suzuki, T. 2002. Complex toxin profiles in phytoplankton and Greenshell mussels (*Perna canaliculus*), revealed by LC-MS/MS analysis. *Toxicon* 40, 1321–1330.
- MacKenzie, A.L., Beuzenberg, V., Holland, P.T., McNabb, P., and Selwood, A.R. 2004. Solid-phase adsorption toxin tracking (SPATT): a new monitoring tool that simulates the biotoxin contamination of filter-feeding bivalves. *Toxicon* 44: 901–918.
- Matsuo, G., Hinou, H., Koshino, H., Suenaga, T., and Nakata, T. 2000. Efficient convergent synthesis of a transfused 6-6-6-6-membered tetracyclic ether ring system. *Tetrahedron Letters* 41, 903–906.
- Miles, C.O., Samdal, I.A., Aasen, J.A.G., Jensen, D.J., Quilliam, M.A., Petersen, D., Briggs, L.M., Wilkins, A.L., Rise, F., Cooney, J.M., and MacKenzie, A.L. 2005a. Evidence for numerous analogs of yessotoxin in *Protoceratium reticulatum*. *Harmful Algae* 4, 1075–1091.
- Miles, C.O., Wilkins, A.L., Hawkes, A.D., Selwood, A., Jensen, D.J., Aasen, J., Munday, R., Samdal, I.A., Briggs, L.R., Beuzenberg, V., and MacKenzie, A.L. 2004b. Isolation of a 1,3-enone isomer of heptanor-41-oxoyessotoxin from *Protoceratium reticulatum* cultures. *Toxicon* 44, 325–336.
- Miles, C.O., Wilkins, A.L., Hawkes, A.D., Selwood, A.I., Jensen, D.J., Cooney, J.M., Beuzenberg, V., and MacKenzie, A.L. 2006a. Identification of 45-hydroxy-46,47-dinoryessotoxin, 44-oxo-45,46,47-trinoryessotoxin, and 9-methyl-42,43,44,45,46,47,55-heptanor-38-en-41-oxoyessotoxin, and partial characterization of some minor yessotoxins, from *Protoceratium reticulatum*. *Toxicon* 47, 229–240.
- Miles, C.O., Wilkins, A.L., Hawkes, A.D., Selwood, A.I., Jensen, D.J., Munday, R., Cooney, J.M., and Beuzenberg, V. 2005b. Polyhydroxylated amide analogs of yessotoxin from *Protoceratium reticulatum*. *Toxicon* 45, 61–71.
- Miles, C.O., Wilkins, A.L., Jensen, D.J., Cooney, J.M., Quilliam, M.A., Aasen, J., and MacKenzie, A.L. 2004a. Isolation of 41a-homoyessotoxin and the identification of 9-methyl-41a-homoyessotoxin and nor-ring A-yessotoxin from *Protoceratium reticulatum*. *Chem Res Toxicol* 17, 1414–1422.
- Miles, C.O., Wilkins, A.L., Selwood, A.I., Hawkes, A.D., Jensen, D.J., Cooney, J.M., Beuzenberg, V., and MacKenzie, A.L. 2006b. Isolation of Yessotoxin 32-*O*-[ $\beta$ -L-arabinofuranosyl-(5'→1'')-  $\beta$ -L-arabinofuranoside] from *Protoceratium reticulatum*. *Toxicon*, 47, 510–516.
- Mitrovic S.M., Hamilton B., McKenzie L., Furey A., and James, K.J. 2005. Persistence of yessotoxin under light and dark conditions. *Mar Environ Res* 60, 397–401.
- Mori, Y., and Hayashi, H. 2002. Synthetic studies of yessotoxin, a polycyclic ether implicated in diarrhetic shellfish poisoning: convergent synthesis of the BCDE ring system via an alkyne intermediate. *Tetrahedron* 58, 1789–1797.
- Mori, Y., Takase, T., and Noyori, R. 2003. Iterative synthesis of the ABCDEF-ring system of yessotoxin and adriatoxin. *Tetrahedron Letters* 44, 2319–2322.

- Morohashi, A., Satake, M., Oshima, Y., and Yasumoto, T. 2000. Absolute configuration at C45 in 45-hydroxyessotoxin, a marine polyether toxin isolated from shellfish. *Biosc Biotech Biochem* 64, 1761–1763.
- Murata, M., Kumagai, M., Lee, J. S., and Yasumoto, T. 1987. Isolation and structure of yessotoxin, a novel polyether compound implicated in diarrhetic shellfish poisoning. *Tetrahedron Letters* 28, 5869–5872.
- Naoki, H., Murata, M., and Yasumoto, T. 1993. Negative-ion fast-atom bombardment tandem mass spectrometry for the structural study of polyether compounds: structural verification of yessotoxin. *Rapid Commun. Mass Spectrom* 7, 179–182.
- Paz B., Riobo P., Fernandez M.L., Fraga S., and Franco J.M. 2004. Production and release of yessotoxins by the dinoflagellates *Protoceratium reticulatum* and *Lingulodinium polyedrum* in culture. *Toxicon* 44, 251–258.
- Pierotti, S., Malaguti, C., Milandri, A., Poletti, R., and Rossini, G.P. 2003. Functional assay to measure yessotoxins in contaminated mussel samples. *Anal Biochem* 312: 208–216.
- Ramstad, H., Hovgaard, P., Yasumoto, T., Larsen, S., and Aune, T. 2001. Monthly variations in diarrhetic toxins and yessotoxin in shellfish from coast to the inner part of the Sognefjord, Norway. *Toxicon* 39, 1035–1043.
- Rhodes, L., McNabb, P., de Salas, M., Briggs, L., Beuzenberg, V., and Gladstone, M. 2006. Yessotoxin production by *Gonyaulax spinifera*. *Harmful Algae* 5, 148–155.
- Samdal, I.A., Aasen, J.A.B., Briggs, L.R., Dahl, E., and Miles, C.O. 2005. Comparison of ELISA and LC-MS analyses for yessotoxins in blue mussels (*Mytilus edulis*). *Toxicon* 46, 7–15.
- Samdal, I. A., Naustvoll, L. J., Olseng, c. D., Briggs, L. R., and Miles, C.O. 2004a. Use of ELISA to identify *Protoceratium reticulatum* as a source of yessotoxin in Norway. *Toxicon* 44, 75–82.
- Samdal, I.A., Olseng, c.D., Sandvik, M., Miles, C.O., Briggs, L.R., Torgersen, T., and Jensen, D.J. 2006. Profile of yessotoxin analogues in a Norwegian strain of *Protoceratium reticulatum*. Pp. 242–247 in *Proc. 5th, Intl. Conf. Mollusc. Shellf. Safety, June 14–18, 2004, Galway, Ireland*. Published by Marine Institute.
- Satake, M., Eiki K., Oshima Y., Mitsuya T., Sekiguchi K., Koike K., and Ogata T. 2002. Yessotoxin production by *Protoceratium reticulatum* in Japan and structures of its new analogues. In *10th Intl. Conf. Harmf. Algae, St. Pete Beach, FL, USA*.
- Satake, M., Ichimura, T., Sekiguchi, K., Yoshimatsu, S., and Oshima, Y. 1999. Confirmation of yessotoxin and 45,46,47-trinoryessotoxin production by *Protoceratium reticulatum* collected in Japan. *Nat Toxins* 7, 147–150.
- Satake, M., MacKenzie, L., and Yasumoto, T., 1997a. Identification of *Protoceratium reticulatum* as the biogenetic origin of yessotoxin. *Nat Toxins* 5, 164–167.
- Satake, M., Terasawa, K., Kadowaki, Y., and Yasumoto, T. 1996. Relative configuration of yessotoxin and isolation of two new analogs from toxic scallops. *Tetrahedron Letters* 37, 5955–5958.
- Satake, M., Tubaro, A., Lee, J. S., and Yasumoto, T. 1997b. Two new analogs of yessotoxin, homoyessotoxin and 45-hydroxy-homoyessotoxin, isolated from mussels of the Adriatic Sea. *Nat Toxins* 5, 107–110.
- Seamer C. 2001. The production of yessotoxins by *Protoceratium reticulatum*. MSc dissertation. Wellington, New Zealand: Victoria University.
- Souto M.L., Fernandez J.J., Franco J.M., Paz B., Gil L.V., and Norte M. 2005. Glycoyessotoxin A, a new yessotoxin derivative from cultures of *Protoceratium reticulatum*. *J Nat Prod* 68, 420–422.
- Stobo L. 2004. Validation of a LC-MS method for the determination of toxins included in Commission Decision 2002/225/EC. Oral presentation at the 5th Intl. Conf. Molluscan Shellfish Safety, 14–18 June 2004, Galway, Ireland.
- Stobo, L.A., Lacaze, J.-P. C.L., Scott, A.C., Gallacher, S., Smith, E.A., and Quilliam, M.A. 2005. Liquid chromatography with mass spectrometry—detection of lipophilic shellfish toxins. *J Assoc Off Anal Chem Intl* 88, 1371–1382.
- Stobo, L.A., Lewis, J., Quilliam, M.A., Gallacher, S., Webster, L., and Smith, E.A. 2002. Optimisation and validation of LC-MS detection of yessotoxin in UK and Canadian isolates of phytoplankton. Abstract in *10th Intl. Conference on Harmful Algal Blooms, October 21–25, 2002, St. Pete Beach, Florida, USA*.
- Suzuki, K., and Nakata, T. 2002. Convergent synthesis of the ABCDEF-ring system of yessotoxin and adriatoxin. *Organic Letters* 4, 3943–3946.
- Takahashi, H., Kusumi, T., Kan, Y., Satake, M., and Yasumoto, T. 1996. Determination of the absolute configuration of yessotoxin, a polyether compound implicated in diarrhetic shellfish poisoning, by NMR spectroscopic method using a chiral anisotropic reagent, methoxy-(2-naphthyl)acetic acid. *Tetrahedron Letters* 37, 7087–7090.
- Tubaro, A., Sidari, L., Della Loggia, R., and Yasumoto, T. 1998. Occurrence of yessotoxin-like toxins in phytoplankton and mussels from Northern Adriatic Sea. In *Harmful Algae*, ed. Reguera B., Blanco J., Fernandez M.L., and Wyatt T. Xunta De Galicia and Intergovernmental Oceanographic Commission of UNESCO, 470–472.
- Tubaro, A., Sosa, S., Altinier, G., Soranzo, M.R., Satake, M., Della Loggia, R., and Yasumoto, T. 2004. Short-term oral toxicity of homoyessotoxins, yessotoxin and okadaic acid in mice. *Toxicon* 43, 439–445.
- Tubaro, A., Sosa, S., Carbonatto, M., Altinier, G., Vita, F., Melato, M., Satake, M., and Yasumoto, T. 2003. Oral and intraperitoneal acute toxicity studies of yessotoxin and homoyessotoxins in mice. *Toxicon* 41, 783–792.

- Van de Riet, J. 2006. The evolution of shellfish monitoring activities in a Canadian regulatory laboratory; an overview. Pp. 495–501 in *Proc. 5th. Intl. Conf. Mollusc. Shellf. Safety, June 14–18, 2004, Galway, Ireland*. Published by Marine Institute.
- Yasumoto, T. 2001. Suitability of two mouse assay methods to quantify marine toxins in bivalve molluscs. Submission to EU Reference Laboratory, Vigo, Spain.
- Yasumoto T., Oshima Y., and Yamaguchi M. 1978. Occurrence of a New Type of Shellfish Poisoning in the Tokohu District. *Bull Jap Soc Sci Fish* 44, 1249–1255.
- Yasumoto, T., and Takizawa, A. 1997. Fluorometric measurement of yessotoxins in shellfish by high-pressure liquid chromatography. *Biosci Biotechnol Biochem* 61, 1775–1777.

## 11 Pharmacology of Yessotoxin

Amparo Alfonso and Carmen Alfonso

### Mechanism of Action and Toxicity

Yessotoxin (YTX) was first postulated as a causative agent of severe clinical signs and symptoms of diarrhetic shellfish poisoning (DSP) (Terao et al. 1990). However, no diarrhogenic properties of this toxin have been reported (Draisci et al. 2000). The mechanism of action of YTX is not completely clarified even though several studies in this sense have been done.

Since YTX was first considered as DSP toxin, and this group inhibits protein phosphatases, this was the first intracellular target checked to study its mechanism of action. Okadaic acid (OA), the main DSP toxin, is a potent and specific inhibitor of serine/threonine protein phosphatases PP1 and PP2A (Bialojan and Takai 1988), which play a critical role in the phosphorylation/dephosphorylation process within eukaryotic cells. The concentration of YTX required to reduce PP2A activity was by 4 orders of magnitude higher than OA (Ogino et al. 1997); therefore, it was concluded that YTX's effect is not due to PP2A inhibition.

Intracellular calcium and the cyclic nucleotides adenosine 3',5'-cyclic monophosphate (cAMP) and guanosine 3',5'-cyclic monophosphate (cGMP) are three second messengers related with early activation pathways in cellular signaling. Several toxins, like maitotoxin, saxitoxin and azaspiracids, and some with similar structure of YTX, like brevetoxins and ciguatoxin, modify ion currents in different cellular models. YTX has slightly activated noncapacitative calcium influx and inhibited capacitative calcium entry in human lymphocytes (De la Rosa et al. 2001b). The increase in calcium influx was not affected by OA, and it was inhibited by nifedipine, which blocks L-type voltage-gated calcium channels in excitable cells, and by SKF 96365, an imidazole-based compound that inhibits different calcium currents (De la Rosa et al. 2001b). In addition, calcium influx induced by maitotoxin in human lymphocytes was increased in the presence of YTX by a mechanism different from calcium entry through a SKF-sensitive pathway (De la Rosa et al. 2001a). From these results YTX can be considered as a modulator of calcium fluxes. On the other hand, since YTX has some structural similarities with ciguatoxins and brevetoxins, the effect over site 5 of sodium channel was checked and no result was reported (Inoue et al. 2003).

Cellular cyclic nucleotide levels are regulated by a balance between adenylyl or guanylyl cyclases, synthesis, and phosphodiesterases (PDEs), hydrolysis. The cAMP is a signal often modulated by lipophilic marine toxins and therefore a good candidate to study YTX mechanism of action. In human lymphocytes cAMP levels were decreased in the presence of YTX. This effect is calcium dependent. The toxin also increased interleukin-2 production in the same cellular model, which indirectly confirms cAMP decrease (Alfonso et al. 2003). By checking toxin effect over cAMP levels in the presence of several drugs that modulate different steps in this pathway, YTX has been postulated as a PDEs activator by a calcium dependent mechanism (Alfonso et al. 2003). Later on the effect of YTX over cGMP levels was also checked in human lymphocytes, since PDEs hydrolyze either cAMP and/or cGMP. In these cells, an important decrease in cGMP levels was observed after YTX addition, more than 50% in conditions where the second messenger levels were increased (unpublished results).

By using a resonant mirror biosensor, the binding between YTX and PDEs from bovine brain was studied. The enzymes were immobilized over an aminosilane surface and the association curves after the addition of several YTX concentrations were checked. These curves follow a typical association profile that fit a pseudo-first-order kinetic equation. From these results the kinetic equilibrium dissociation constant ( $K_D$ ) for the PDE-YTX association was calculated. This value is 3.74  $\mu\text{M}$  YTX (Pazos et al. 2004).  $K_D$  is dependent on YTX structure since it increases when 44 or 45 carbons (at C9 chain) group. A higher  $K_D$  value, 7  $\mu\text{M}$  OH-YTX or 23  $\mu\text{M}$  carboxy-YTX, indicates a lower affinity of YTXs analogues by PDEs.

In addition to biosensor experiments, the interaction YTXs-PDEs was also confirmed by checking the variations in the fluorescence polarization (FP) of PDEs labeled with carboxy-fluorescein. FP units change when the molecule is bound to the toxin. With this technique, a good relationship of toxin concentration to FP units can be observed (Alfonso et al. 2005), which again confirms PDEs-YTXs binding.

Either biosensor or FP experiments were done with cyclic PDEs and with exonucleases, enzymes that catalyze the hydrolysis of phosphodiester bonds. The affinity of YTX by cyclic PDEs and exonuclease I was the same; both hydrolyze 3'-5' phosphodiester bonds in cyclic molecules, and it was lower in the case of exonuclease II, which does not act over cyclic molecules. These results are very important since they point to a big enzymes family as the YTX target.

The cAMP, calcium, and YTX cross-talks were also studied in mussel immunocytes. But only some indirect evidence of a relationship between these three parameters can be pointed to since direct levels of calcium or cAMP were not measured. In addition, it is necessary to bear in mind, in order to know YTX mechanism of action, that these are not mammalian cells (Malagoli et al. 2003, Malagoli and Ottaviani 2004).

YTX's effect was also checked studying different biochemical markers of apoptosis in neuroblastoma cells. After 12 or 48 hours of BE(2)-M17 cell incubation in the presence of YTX, low changes in mitochondrial membrane potential were observed at concentrations between 10 and 1000 nM. In these conditions, a decrease in nucleic acids content was observed after 12 hours incubation with 1000 nM toxin, or after 48 hours incubation with 10 nM YTX (Leira et al. 2002). The caspase-3 activity was increased in the presence of YTX. This effect was delayed when compared with OA effect, since 1000 nM and 48 hours incubation are necessary to induce the same effect than 1 nM OA for 12 hours. From these results, some apoptotic effect of YTX was suggested (Leira et al. 2002). The effect of YTX over caspase activity was also reported in He-La cells, even though in this case the effective concentration was 0.25 nM YTX (Malaguti et al. 2002). Therefore, when the effect is compared with OA, YTX is more potent but needs more time; it seems that the caspase pathway is not as important in case of YTX or it is more extensively affected in case of OA. OA has a powerful tumor promoting activity (Fujiki et al. 1990); it seems to induce apoptosis through the caspase activation. In this sense, no effect as tumor promoter is described in case of YTX; on the contrary, an important inhibition of cellular growth (80%) was observed in the presence of 10  $\mu\text{M}$  YTX in several tumor cellular lines, like the human cervix carcinoma cell line (HeLa-229), the human ovarian adenocarcinoma cell line A2780 and the human hepatocellular carcinoma cell line (Hep-G2). In these cases ED50 for YTX was also in the nanomolar range. In addition YTX shows a higher potency than cisplatin, a known cytostatic agent, even in cisplatin-resistant cells (unpublished results). That is, YTX is a powerful cytotoxic agent and since the caspases pathway is slightly activated in the presence of the toxin, maybe this effect is not only due to apoptosis and also to other kind of cellular death that can be PDEs mediated. In this sense, exonucleases that hydrolyze phosphodiester bonds are involved in DNA repair.

YTX induces accumulation of a 100 kDa fragment of E-cadherin (Pierotti et al. 2003); while it does not modify intact E-cadherin on the first day (Ferrari et al. 2004), even after 2–5 days a collapse of the E-cadherin system was detected (Ronzitti et al. 2004). E-cadherin is a glycoprotein related with adherent junctions in epithelial cells. This protein also mediates intracellular signaling and plays an important role in cell survival in some models of tumor cells. The effect over the 100 kDa fragment of E-cadherin depends on YTX structure; in particular, it is essential to the presence of C9 chain (Ferrari et al. 2004). This structure-activity relationship was also described after studying the kinetic constants of PDEs-YTX binding in the presence of different YTX analogues (Pazos et al. 2005). In both cases, the activity of YTX was higher than the activity of analogues with different groups in the C9 chain. This coincidence can point to different steps of the same cellular pathway. In addition, lower toxicity was showed when the polarity of the side chain was increased (Satake et al. 1996).

One important question about YTX is if the toxin enters the cellular cytosol. This matter is important to clarify where the toxin induce the effect. In a set of experiments done with YTX labeled with 9-anthryldiazomethane (ADAM), the entry of YTX either in lymphocytes and enterocytes has been studied. The toxin is going inside both cellular models even the kinetic uptake was higher and faster in enterocytes (unpublished results).

An effect of YTX as activator of the permeability transition pores of the inner mitochondrial membrane has been described. These experiments were done over isolated mitochondria in the presence of high calcium concentrations, also in hepatoma cells. These mitochondrial pores are related with caspases and apoptosis (Bianchi et al. 2004). An interaction between YTX and some hydrophobic derivatives and the glycopolin A, a membrane-integral  $\alpha$ -helix peptide, has been described (Mori et al. 2005).

Finally, a relationship between intraperitoneal (i.p.) administration and the damages in Purkinje cells through intracellular calcium-binding proteins was recently reported (Franchinia et al. 2005). However, it is not easy to establish a direct relationship between mechanism of action and i.p. administration, since no data about YTX bioavailability is reported and the route has high variability in the doses administrated and in the effect reported (see below).

On the other hand, YTX and desulfated YTX have an important antifungal activity (Nagai et al. 1990). In this sense, a decrease in cAMP levels is related with the antifungal activity of several drugs, which again confirms the effect of YTX over cyclic nucleotides pathway.

## Conclusion

In summary, the mechanism of action of YTX is a cross-talk between several intracellular pathways. It is necessary to bear in mind that YTX is effective in a range of concentrations from  $10^{-10}$  to  $10^{-5}$  M. The effects reported at high concentrations are from early steps in the transduction pathways, and probably these high concentrations are necessary to have a fast response, since it is reported after less than 10 minutes. The effects observed at low concentrations are checked after at least 12 hours of incubation. This time difference could also imply a different pathway or receptor as has been proposed (Ferrari et al. 2004). However, the same YTX target can be activated both at low or high toxin concentrations. The target activation at low concentrations can imply no evident or measurable effects, while after some hours the final effect is shown. The hypothesis here proposed is an early activation related to PDEs and calcium and the final step probably apoptosis, cytotoxicity, or maybe changes in E-cadherin pathway. To explain the different range of concentrations, in addition to different incubation time, is also important to know the origin of the YTX used, algal cultures, or



mussel meat and also the purity of samples since phthalates, lipids, and fatty acids are also extracted with the toxin. This also can explain the variability of results found when YTX toxicity is studied.

No toxic episodes attributable to YTX have been reported in humans; only toxicity in animals has been studied. After mice oral administration of YTX, the lowest observable effect level (LOEL) is 2.5 mg/kg body weight (b.w.), and no observable effect level (NOEL) is 1 mg/kg b.w. (Aune et al. 2002). YTX does not kill mice by oral administration even at high concentration (10 times the i.p. lethal dose). In this case, no sign of intoxication was observed. In cases of dinophysistoxin 1 (DTX1) or pectenotoxin 2 (PTX2), oral toxicities were comparable with their i.p. toxicities (Ogino et al. 1997). However, after i.p. administration YTX has showed high mouse lethality at doses of 80–100  $\mu\text{g}/\text{kg}$  b.w. (Murata et al. 1987; Ogino et al. 1997)]. After YTX-injection, for the first hours, mice show normal behavior and then die after sudden dyspnea (Terao et al. 1990). In this way, YTX can be distinguished from OA and DTX1, which even at low doses cause death after 24 hours, and from the fast-acting imine toxins found in shellfish such as gymnodimine and spirolides because the survival times for these toxins are reported shorter than 20 minutes. In addition, YTX does not induce fluid accumulation (Ogino et al. 1997), one effect of DSP toxins.

The target organ for YTX, after 3 hours i.p. injection, was the heart and those of the latter were the liver and pancreas. In contrast, desulfated yessotoxin at the same dose (300  $\mu\text{g}/\text{kg}$  b.w.) caused within 24 hours of i.p. injection severe fatty degeneration and intracellular necrosis in the liver and pancreas but not in the heart (Terao et al. 1990). Alterations in the inflammatory system and thymus were observed after i.p. administration of 420  $\mu\text{g}$  YTX/kg b.w. (Franchini et al. 2004b). The same concentration also induced damage to the Purkinje cells with some changes in intracellular calcium dependent proteins (Franchini et al. 2004a). However, no toxic effect in these organs was found in another study where a dose of 1000  $\mu\text{g}$  YTX/kg b.w. was used (Aune et al. 2002). Some toxic effect in these organs was also reported after oral administration of YTX combined with OA to Swiss mice (Franchinia et al. 2005).

In an extensive study (Aune et al. 2002), oral and i.p. effects of YTX were compared, by mice administration of 1–10 mg of YTX/kg b. w. in the first case and 0.1–1 mg of YTX/kg b.w. in the second case. YTX was more than 10 times less toxic to mice via oral route. Death of mice occurred at 750  $\mu\text{g}$  YTX per kg and higher after i.p. administration, while no death was observed after oral administration. Subtle changes were found in the myocardium after i.p. injections of high YTX concentrations. By oral route, only the highest YTX concentrations showed some toxic effects in cardiac cells (Ogino et al. 1997, Aune et al. 2002). But even at doses as high as 54 mg/kg b.w., YTX was not lethal (Tubaro et al. 2004).

When acute toxicity of YTX, homoYTX and 45-OH-homoYTX was checked, some differences were observed. After i.p. administration LD50 for YTX was 0.5 mg/kg and 0.4 mg/Kg for homoYTX, while 0.75 mg 45-OH-homoYTX/kg did not cause death. After oral administration either 1 or 2 mg/kg of YTX or 1 mg/kg of derivatives did not induce any symptom, except some ultrastructural myocardiocyte alterations. After these studies, the conclusion was that YTX and derivatives are less toxic than OA after acute oral and i.p. treatments (Tubaro et al. 2003).

From all these data, YTX is not toxic after oral administration even at high doses; however, it could induce cumulative toxic effects after chronic administration. In this sense, YTX toxicity after seven days treatment was also checked. The study included 2 mg YTX/kg b.w./day, 1 mg homoYTX/kg b.w./day, and 1 mg 45-OH-homoYTX /kg b.w./day, administrated by oral route. No signs of cumulative effects were found; only some structural changes in cardiac cells were reported (Tubaro et al. 2004).

In summary, after i.p. administration YTXs can cause death at doses between 100 and 1000  $\mu\text{g}/\text{kg}$ , while after oral administration of any YTX analogue, no death was observed even at very high



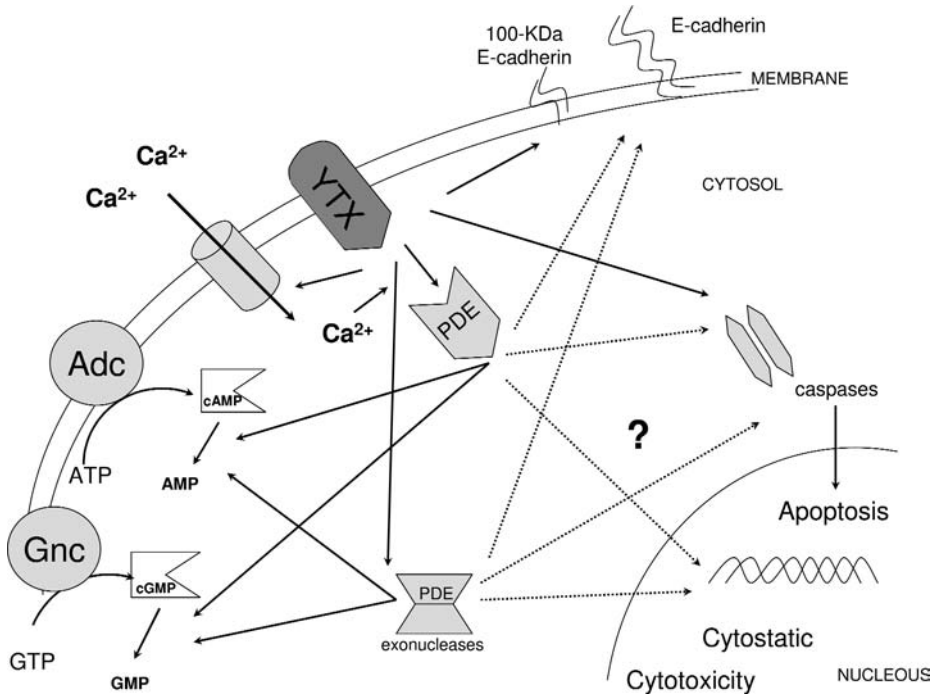


**Figure 11.1.** Summary of YTX effects. Dotted arrows indicate possible YTX effects. Adc = adenylyl cyclase; Gnc = guanylyl cyclase.

concentrations or after several days exposure. The variations in the toxic dose after i.p. injection are probably due to mice sex or age, but the origin and purity of YTX used are also important.

After i.p. administration, modifications in Purkinje cells suggest that YTX may be involved in neurological disorders. In this sense, convulsions and jumping before dying are symptoms induced by YTX that resemble those typical of neurotoxins (Franchini et al. 2004a).

In summary, YTX is not toxic either for humans or for mice after oral administration, while it is toxic in mice after i.p. injection. The question is which of the symptoms reported after i.p. administration induce death. In this sense, further experiments need to be done to know the relationship between the effects reported after i.p. administration and the mechanism of action here proposed. See Fig. 11.1 for a summary of YTX effects.

## References

- Alfonso, C., Alfonso, A., Vieytes, M.R., Yasumoto, T., and Botana, L.M. 2005. Quantification of yessotoxin using the fluorescence polarization technique and study of the adequate extraction procedure. *Anal Biochem* 344, 266–274.
- Alfonso, A., de la Rosa, L.A., Vieytes, M.R., Yasumoto, T., and Botana, L.M. 2003. Yessotoxin a novel phycotoxin, activates phosphodiesterase activity. Effect of yessotoxin on cAMP levels in human lymphocytes. *Biochem Pharmacol* 65, 193–208.
- Aune, T., Sorby, R., Yasumoto, T., Ramstad, H., and Landsverk, T. 2002. Comparison of oral and intraperitoneal toxicity of yessotoxin towards mice. *Toxicol* 40, 77–82.

- Bialojan, C., and Takai, A. 1988. Inhibitory effect of a marine-sponge toxin, okadaic acid, on protein phosphatases. Specificity and kinetics. *Biochem J* 256, 283–290.
- Bianchi, C., Fato, R., Angelin, A., Trombetti, F., Ventrella, V., Borgatti, A. R., Fattorusso, E., Ciminiello, P., Bernardi, P., Lenaz, G., and Parenti Castelli, G. 2004. Yessotoxin, a shellfish biotoxin, is a potent inducer of the permeability transition in isolated mitochondria and intact cells. *Biochim Biophys Acta* 1656, 139–147.
- De la Rosa, L. A., Alfonso, A., Vilariño, N., Vieytes, M.R., Yasumoto, T., and Botana, L.M. 2001a. Maitotoxin-induced calcium entry in human lymphocytes – Modulation by yessotoxin, Ca<sup>2+</sup> channel blockers and kinases. *Cell Signal* 13, 711–716.
- De la Rosa, L.A., Vilariño, N., Vieytes, M.R., and Botana, L.M. 2001b. Modulation of thapsigargin-induced calcium mobilisation by cyclic AMP-elevating agents in human lymphocytes is insensitive to the action of the protein kinase A inhibitor H-89. *Cell Signal* 13, 441–449.
- Draisci, R., Lucentini, L., and Mascioni, A. 2000. Enteric toxic episodes. Pectenotoxins and yessotoxins: chemistry, toxicology, pharmacology and analysis. In *Seafood and Freshwater Toxins: Pharmacology, Physiology and Detection*, ed. Botana, L.M. New York: Marcel Dekker, 289–324.
- Ferrari, S., Ciminiello, P., Dell’Aversano, C., Forino, M., Malaguti, C., Tubaro, A., Poletti, R., Yasumoto, T., Fattorusso, E., and Rossini, G.P. 2004. Structure-activity relationships of yessotoxins in cultured cells. *Chem Res Toxicol* 17, 1251–1257.
- Franchini, A., Marchesini, E., Poletti, R., and Ottaviani, E. 2004a. Acute toxic effect of the algal yessotoxin on Purkinje cells from the cerebellum of Swiss CD1 mice. *Toxicol* 43, 347–352.
- . 2004b. Lethal and sub-lethal yessotoxin dose-induced morpho-functional alterations in intraperitoneal injected Swiss CD1 mice. *Toxicol* 44, 83–90.
- . 2005. Swiss mice CD1 fed on mussels contaminated by okadaic acid and yessotoxins: effects on thymus and spleen. *Eur J Histochem* 49, 179–188.
- Fujiki, H., Suganuma, M., Nishiwaki, S., Yoshizawa, S., Winyar, B., Sugimura, T., and Schmitz, F.J. 1990. A new pathway of tumor promotion by the okadaic acid class compounds. *Adv Second Messenger Phosphoprotein Res* 24, 340–344.
- Inoue, M., Hiram, M., Satake, M., Sugiyama, K., and Yasumoto, T. 2003. Inhibition of brevetoxins binding to the voltage-gated sodium channel by gambierol and gambieric acid-A. *Toxicol* 41, 469–474.
- Leira, F., Alvarez, C., Vieites, J.M., Vieytes, M.R., and Botana, L.M. 2002. Characterization of distinct apoptotic changes induced by okadaic acid and yessotoxin in the BE(2)-M17 neuroblastoma cell line. *Toxicol in Vitro* 16, 23–31.
- Malagoli, D., Gobba, F., and Ottaviani, E. 2003. Effects of 50-Hz magnetic fields on the signalling pathways of fMLP-induced shape changes in invertebrate immunocytes: the activation of an alternative “stress pathway.” *Biochim Biophys Acta* 1620, 185–190.
- Malagoli, D., and Ottaviani, E. 2004. Yessotoxin affects fMLP-induced cell shape changes in *Mytilus galloprovincialis* immunocytes. *Cell Biol Int* 28, 57–61.
- Malaguti, C., Ciminello, P., Fattorusso, E., and Rossini, G.P. 2002. Caspase activation and death induced by yessotoxin in HeLa cells. *Toxicol in Vitro* 16, 357–363.
- Mori, M., Oishi, T., Matsuoka, S., Ujihara, S., Matsumori, N., Murata, M., Satake, M., Oshima, Y., Matsushita, N., and Aimoto, S. 2005. Ladder-shaped polyether compound, desulfated yessotoxin, interacts with membrane-integral alpha-helix peptides. *Bioorg Med Chem* 13, 5099–5103.
- Murata, M., Kumagai, M., Lee, J.S., and Yasumoto, T. 1987. Isolation and structure of Yessotoxin, a novel polyether compound implicated in diarrhetic shellfish poisoning. *Tetrahedron Letters* 28, 5869–5872.
- Nagai, H., Satake, M., and Yasumoto, T. 1990. Antimicrobial activities of polyether compounds of dinoflagellate origins. *J Appl Phycol* 2, 305–308.
- Ogino, H., Kumagai, M., and Yasumoto, T. 1997. Toxicological evaluation of yessotoxin. *Natural Toxins* 5, 255–259.
- Pazos, M.J., Alfonso, A., Vieytes, M., Yasumoto, T., and Botana, L. 2004. Resonant mirror biosensor detection method based on yessotoxin-phosphodiesterase interactions. *Analytical Biochemistry* 335, 112–118.
- . 2005. Kinetic analysis of the interaction between yessotoxin and analogues and immobilized phosphodiesterases using a resonant mirror optical biosensor. *Chem Res Toxicol* 18, 1155–1160.
- Pierotti, S., Malaguti, C., Milandri, A., Poletti, R., and Paolo Rossini, G. 2003. Functional assay to measure yessotoxins in contaminated mussel samples. *Anal Biochem* 312, 208–216.
- Ronzitti, G., Callegari, F., Malaguti, C., and Rossini, G. P. 2004. Selective disruption of the E-cadherin-catenin system by an algal toxin. *Br J Cancer* 90, 1100–1107.
- Satake, M., Terasawa, K., Kadowaki, Y., and Yasumoto, T. 1996. Relative configuration of yessotoxin and isolation of two new analogs from toxic scallops. *Tetrahedron Lett* 37, 5955–5958.

- Terao, K., Ito, E., Oarada, M., Murata, M., and Yasumoto, T. 1990. Histopathological studies on experimental marine toxin poisoning—5. The effects in mice of yessotoxin isolated from *Patinopecten yessoensis* and of a desulfated derivative. *Toxicon* 28, 1095–1104.
- Tubaro, A., Sosa, S., Altinier, G., Soranzo, M.R., Satake, M., Della Loggia, R., and Yasumoto, T. 2004. Short-term oral toxicity of homoyessotoxins, yessotoxin and okadaic acid in mice. *Toxicon* 43, 439–445.
- Tubaro, A., Sosa, S., Carbonatto, M., Altinier, G., Vita, F., Melato, M., Satake, M., and Yasumoto, T. 2003. Oral and intraperitoneal acute toxicity studies of yessotoxin and homoyessotoxins in mice. *Toxicon* 41, 783–792.

## 12 Chemistry of Diarrhetic Shellfish Poisoning Toxins

Paulo Vale

### Parent DSP Toxins

The syndrome diarrhetic shellfish poisoning (DSP) was first recognized following food poisonings resulting from eating mussels and scallops harvested in northern Japan in 1976 and 1977. The symptoms of the victims were mainly gastrointestinal disorders such as diarrhea, nausea, vomiting, and abdominal pain. The onset of symptoms after consumption of the shellfish ranged from 30 minutes to a few hours. No pathogenic bacteria could be detected in the excreta of victims or leftover meals. The victims recovered after three days irrespective of medical treatment (Yasumoto et al. 1978). Extracts obtained by hot methanol extraction and separated into the diethyl ether, 1-butanol, and water-soluble fractions were tested by intraperitoneal (i.p.) injection into mice. As the toxin was found to be fat-soluble, extraction with acetone proved as efficient as hot methanol, with the advantage of extraction at room temperature. The anatomical distribution of the toxin in the mussels indicated that the hepatopancreas was the most toxic organ (Yasumoto et al. 1978). The acetone extraction of the hepatopancreas was later to be employed worldwide to monitor for the presence of DSP toxins (van Egmond et al. 1992).

The periodic occurrence of the phenomena in the summer pointed to the presence of toxic plankton in the shellfish diet, but no red tides or fish kills were recorded (Yasumoto et al. 1978). In 1979, plankton samples were sieved with various mesh sizes and toxicity was detected only in the 40–95  $\mu\text{m}$  fraction. The dinoflagellate *Dinophysis fortii*, not only was concentrated exclusively in this fraction, but its abundance was proportional to the toxicity levels of different plankton samples. Regular phytoplankton monitoring also revealed the occurrence of this microalgae was parallel in time and quantity with mussel toxicity. The plankton toxin showed the same elution pattern both in gel permeation chromatography and partition chromatography (Yasumoto et al. 1980). The major toxin involved in DSP was named dinophysistoxin-1 (DTX1) (Fig. 12.1). It is a polyether derivative of a  $\text{C}_{38}$  fatty acid with the composition  $\text{C}_{45}\text{H}_{70}\text{O}_{13}$  (Murata et al. 1982). Separate groups searching for antitumor agents in marine organisms had previously discovered compounds with a similar structure: okadaic acid (OA) (Fig. 12.1) was isolated from a Japanese black sponge, *Halichondria okadaic*, and from *H. melanodocia*, collected in the Florida Keys (Tachibana et al. 1981), and acanthifolicin, an episulfide derivative of OA, was isolated from the sponge *Pandaros acanthifolium* from the U.S. Virgin Islands (Schmitz et al. 1981). Simultaneously, OA was found to be one of the toxic components from the benthic dinoflagellate *Prorocentrum lima*, as a possible secondary toxin involved in ciguatera fish poisoning (Murakami et al. 1982). Dinophysistoxin-1 was confirmed to be 35(S)-methyl okadaic acid (Murata et al. 1982).

The severity of illness was related to the number of mussels eaten. It was concluded that ingestion of 12 mouse-units (the minimum dose of toxin to kill a mouse in 48 hours) of this toxin was sufficient to cause a mild form of illness to an adult. With the discovery of DTX1, this level translates to just 32  $\mu\text{g}$  of toxin per person (Yasumoto et al. 1985). The lack of a proper method for detecting toxins in the

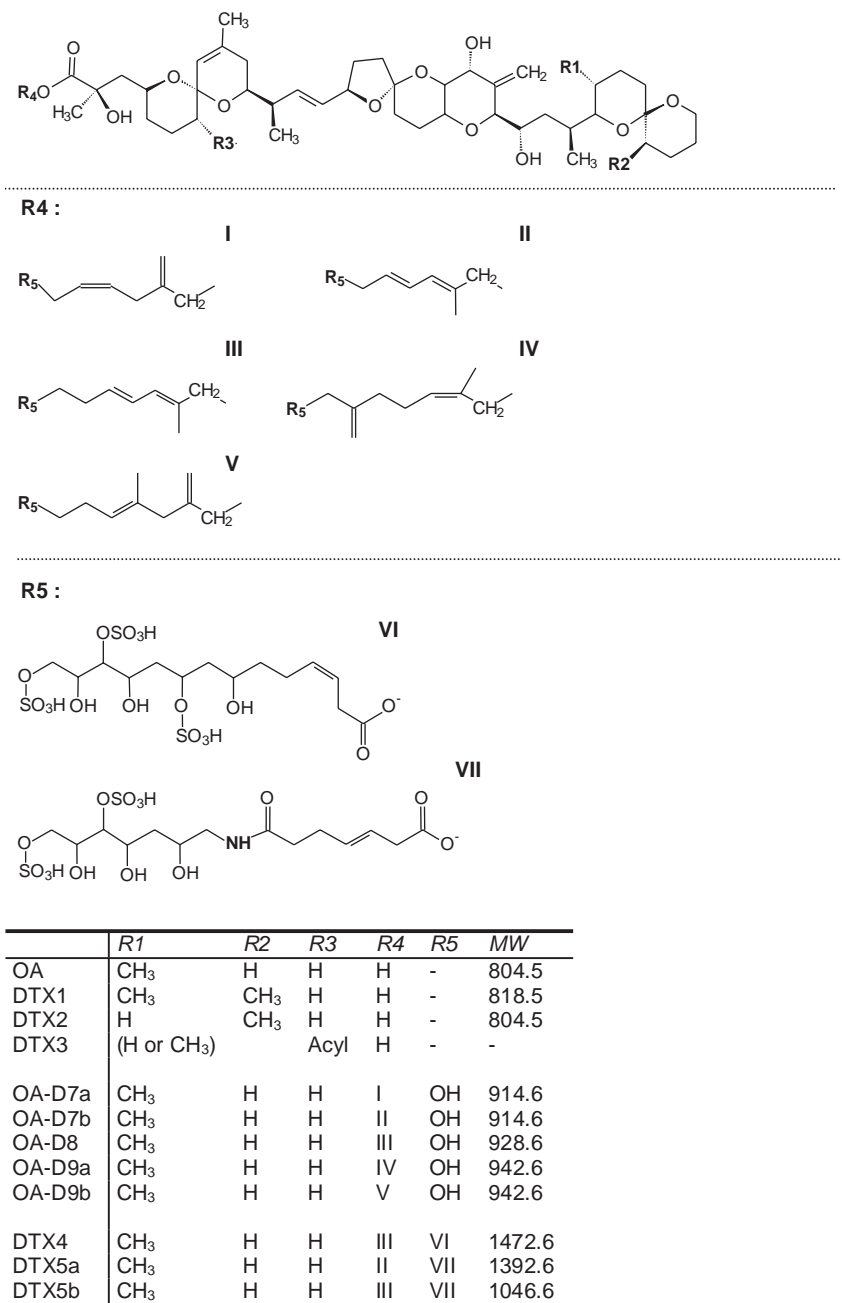


**Figure 12.1.** Structures of known okadaic acid analogues (Hu et al. 1992, 1995b). MW = molecular weight.

past, made it difficult to diagnose the suspected gastroenteritis. However, legends of a poisoning season for mussels already existed in Japanese folklore (Yasumoto et al. 1978). In Europe, a similar type of mussel poisoning not attributable to the presence of pathogenic bacteria, and also distinguishable from PSP poisoning, had already been described in the precedent decades. However, the first suspected microalgae were *Prorocentrum* spp. (Kat 1979). As scientists became aware of DSP, the number of reported cases in Japan and Europe increased rapidly to several thousand cases (Yasumoto et al. 1985), leading to the gradual introduction of monitoring programs.

The development of a fluorescent HPLC method (HPLC-FLU) based on esterification with 9-anthryl-diazomethane (ADAM) allowed the vulgarization of analysis of toxin profiles in plankton and shellfish (Lee et al. 1987). The inability to cultivate *Dinophysis* spp. under laboratory conditions and their low population densities in the sea make confirmations of their toxigenicity relatively difficult. Recurring to unialgal samples purified under a microscope, it was possible to confirm the presence of either OA or DTX1, or both, in *D. fortii*, *D. mitra*, *D. rotundata*, *D. tripos*, *D. acuta*, *D. norvegica* and *D. acuminata*, collected in Japan and in some European countries (Lee et al. 1989) (Fig. 12.2). Shellfish in many European countries were contaminated mainly by OA, while some Norwegian shellfish samples resembled Japanese shellfish, due to the predominance of DTX1 (Kumagai et al. 1986; Lee et al. 1988).

Analysis of Irish mussels by the method of Lee et al. (1987) revealed the presence of a compound eluting between OA and DTX1. A newly developed ion spray liquid chromatography coupled to mass spectrometry (LC-MS) method for DSP toxins (Pleasence et al. 1990) also indicated this compound to be an isomer of OA. Upon NMR spectroscopic analysis of the isolated compound, its structure corresponded to 31-demethyl-35-methyl OA, or dinophysistoxin-2 (DTX2) (Fig. 12.3) (Hu et al. 1992). The minor presence of isomers of DTX2 has also been reported (James et al. 1997b; Draisci et al. 1998; Vale 2004). While OA and/or DTX1 have been reported, as the main parent toxins found worldwide, DTX2 has been reported to be a major parent toxin only in Ireland, Spain, and Portugal (Carmody et al. 1996; Gago-Martinez et al. 1996; Vale and Sampayo, 1999), and limited data show its presence in Morocco and Norway (Taleb 2005; Miles et al. 2004). The unavailability of a commercial

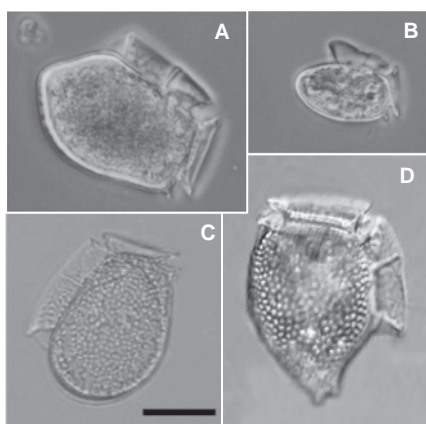


**Figure 12.2.** *Dinophysis* spp. specimens from (A) *D. acuta* and (B) *D. acuminata* from Portugal (photos courtesy of M.A. Sampayo); (C) *D. fortii* from Japan (photo courtesy of T. Kamiyama); and (D) *D. norvegica* from Norway (photo courtesy of E. Dahl).

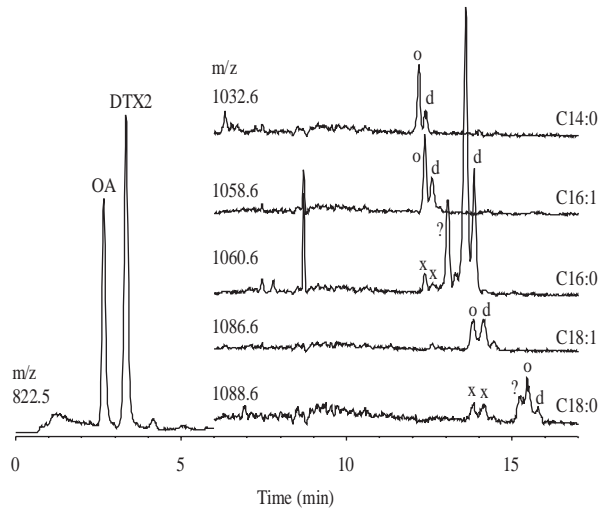


**Figure 12.3.** LC-MS chromatogram for OA group toxins in mussel hepatopancreas. o = acyl-OA; d = acyl-CTX2; x = interfering signal from isotope peak of lower molecular weight compound; ? = unknown compound. (Source: Quilliam et al. 2003.)

standard for DTX2 does not allow easily its confirmation in other parts of the world, and probably its dissemination might be wider than currently known. The only microalgae associated so far with DTX2 production has been *D. acuta* (James *et al.* 1997a). In most world areas, contamination by DSP toxins has been associated only with *Dinophysis* spp. Rarely contamination has been associated to *Prorocentrum* spp. In the Atlantic coast of Canada, the contamination of mussels that caused an outbreak of gastroenteritis was explained by isolating a strain of *P. lima* that produced toxins in culture. Being a benthic algae, it does not appear in high numbers during phytoplankton counting's, but has been found on the byssal fibers and shells of contaminated mussels (Jackson *et al.* 1993).

### Esters of DSP in Shellfish

Since the early Japanese studies on DSP, the toxins in mussels and scallops were suspected to be different. The main diarrhetic toxin found in scallops was found to be a mixture of 7-*O*-acyl derivatives of dinophysistoxin-1 (DTX-1), ranging from tetradecanoic acid (C14:0) to docosahexaenoic acid (C22:6 $\omega$ 3), and designated as dinophysistoxin-3 (DTX-3) (Yasumoto *et al.* 1985). These acylated forms have never been found in marine microalgae, and so it was presumed that they originated in the bivalve by acylation (Lee *et al.* 1989). Direct evidence of this biotransformation by shellfish was obtained by artificially feeding scallops with *D. fortii* collected from the sea (Suzuki *et al.* 1999).

When analyzing Irish mussels, it was demonstrated that also OA and DTX2 may be acylated to produce "DTX-3" (Marr *et al.* 1992). The presence of esters of OA and DTX2 was later reported in Spanish and Portuguese mussels (Férrandez *et al.* 1996; Vale and Sampayo, 1999).

The fact that DTX1, and not its acyl esters, was reported to be the main toxin in mussels, and due to the large importance of mussels for aquaculture, might explain why the main attention worldwide



has been mostly focused on OA, DTX1 and DTX2, but not on their respective acyl esters. The presence of acyl esters makes toxicity assays more complicated for scallops than for mussels, requiring an extra step of hydrolyzing these to DTX1 prior to HPLC assays. Because of their high molecular weight and lipophilicity, acyl esters cannot be directly detected by the fluorometric procedure of Lee et al. (1987), but a hot alkaline hydrolysis reaction with sodium hydroxide releases fatty acids from the parent toxins and can give an indirect estimation of their abundance (Yasumoto et al. 1989). Their direct detection by LC-LC after fluorescence labeling has been proposed by Akasaka et al. (1996) but involves a more complicated LC system and needs standards for all of the toxins involved. A recent multi-toxin LC-MS method, allowing simultaneous detection of several lipophilic marine toxins (Quilliam et al. 2001), can separate several acyl derivatives, but also does not allow their quantification due to the unavailability of commercial standards (Quilliam et al. 2003).

Aside Japanese scallops, the dominance of DSP esters was first recognized in Portuguese clams (*Donax trunculus*) implicated in human poisonings, by using ADAM derivatization after hydrolysis (Vale and Sampayo 1999). These data was further extended to other species of clams, razor clams, common cockles and oysters, by using LC-MS analysis (Vale and Sampayo 2002; Vale 2004). In highly contaminated Portuguese shellfish, it was demonstrated that acylated OA might account for 98–99% of the total OA recovered after hydrolysis. Other studies are also demonstrating esters have quite a high relevance to total DSP toxicity worldwide (Table 12.1). In the blue mussel, the percentage of esters found is quite variable. Other shellfish species from the same geographical area may contain higher percentages of esters than the blue mussel. An outbreak of human poisonings in Australia with pipis was initially attributed to the newly discovered seco acids of pectenotoxin-2 (currently no oral toxicity is known in these compounds); these were later confirmed to contain DSP esters in sufficient amount to justify the poisonings (Eaglesham, unpublished).

When feeding *Dinophysis fortii*, containing DTX1 but no DTX3, to non-toxic blue mussels, Suzuki et al. (2001) found after 5 days only 25% of the total DTX1 accumulated in mussels was DTX3. The same experiment performed with scallops showed after 5 days, 80%–100% of the total DTX1 accumulated in scallops was DTX3 (Suzuki et al. 2001). The ratio at which shellfish transform the parent DSP toxins into esters might be species-specific and toxin-specific. In bivalve mollusks, at least these two distinct metabolism types have been found concerning the biotransformation of DSP. The first one seems to be characteristic of blue mussel, which may contain an extremely wide range of ester contents, either of OA or of DTX2. (Figs. 12.4A and 12.4B exemplify the range found in the Portuguese blue mussel.) When contamination increases, OA esters typically range between 20% and 90% of total toxin recovered after hydrolysis, while DTX2 ranges only between 0 and 40%. The second metabolism type is illustrated in Figs. 12.4E and 12.4F by the common cockle from Portugal, and might also be commonplace among many other bivalves such as razor clams, clams, and oysters: either OA or DTX2 are only found esterified, the parent toxins are always at trace levels (Vale and Sampayo 2002a, 2002b). The first type of metabolism has also been demonstrated in the blue mussel from Denmark and Norway, and the second one in surf clams from Denmark and cockles from Norway (Jorgensen et al. 2005; Miles et al. 2004). An additional third type of metabolism has been recognized in Portuguese shellfish, in *Donax trunculus*, where a wide range of esters is found for lower levels of contamination. When contamination surpasses a certain baseline level, the great majority of both naturally occurring parent toxins (OA and DTX2) are found esterified, being OA commonly more easily esterified to higher ratios than DTX2 (Figs. 12.4C and 12.4D).

Some lipophilic toxins, such as NSP, present a great challenge for analysis, because several analogues are generated in different shellfish species. In the case of DSP, although one or two complex mixtures of 7-*O*-acyl derivatives are formed (typically depending on simultaneous contamination by

**Table 12.1** Percentage of esterified toxins from the total of toxins recovered after alkaline hydrolysis in selected shellfish species from different continents

Country	Species	Latin designation	OA	DTX2	DTX1	References
Europe						
Denmark	Blue mussel	<i>Mytilus edulis</i>	21–86	n.d.	n.d.	Jørgensen et al. 2005
	Surf clam	<i>Spisula spp</i>	83–98	n.d.	n.d.	Jørgensen et al. 2005
Ireland	Blue mussel	<i>M. edulis</i> (n = 321)	<LOQ–100	<LOQ–100	n.d.	Marine Institute, unpublished
	Pacific Oyster	<i>C. gigas</i> (n = 40)	<LOQ–100	n.d. <LOQ	n.d.	May 22, 2005 to September, 12, 2005
	King scallops	<i>P. maximus</i> (n = 118)	<LOD–100	<LOD–100	n.d.	Marine Institute, unpublished
Norway	Blue mussel	<i>Mytilus edulis</i>	30–70	n.d.	0–100	May 22, 2005 to September, 12, 2005
	Cockle	<i>Cerastoderma edule</i>	100	n.d.	n.a.	Miles et al. 2004
	Brown crab	<i>Cancer pagurus</i>	>93	n.a.	na	Torgersen et al. 2005
Portugal	Blue mussel	<i>Mytilus galloprovincialis</i>	20–95	0–35	n.d.	Vale 2004; Vale, unpublished
	Donax clams	<i>Donax trunculus</i>	15–95	0–50	n.d.	Vale 2004; Vale, unpublished
	Cockles, clams, razor clams	<i>Cerastoderma edule</i> , <i>Ruditapes decussatus</i> , <i>Venerupis senegalensis</i> , <i>Solen marginatus</i> , <i>Spisula solida</i>	>94	>94	n.d.	Vale and Sampayo 2002
Spain	Green crab	<i>Carcinus maenas</i>	>90	>90	n.d.	Vale and Sampayo 2002
Africa	Blue mussel	<i>Mytilus galloprovincialis</i>	3–39 <sup>b</sup>	n.a.	n.d.	Fernández et al. 1996
Morocco	Blue mussel	<i>Mytilus galloprovincialis</i>	40–60	n.a.	n.d.	CRL, unpublished
Asia	Blue mussel	<i>Mytilus galloprovincialis</i>	10–80	0–55	n.d.	Taleb and Vale, unpublished
Japan	Blue mussel	<i>Mytilus galloprovincialis</i>	na	n.d.	17–34 <sup>b</sup>	Suzuki and Mitsuya 2001
	Scallops	<i>Patinopecten yessoensis</i>	na	n.d.	>91–94 <sup>b</sup>	Suzuki and Mitsuya 2001
Oceania						
Australia	Pipis	<i>Donax deltoides</i>	> 95%	n.d.	n.d.	G. Eaglesham, unpublished
	Oysters	<i>Saccostrea commercialis</i>	30–70	n.d.	n.d.	G. Eaglesham, unpublished
	Razorfish		64	n.d.	n.d.	Madigan et al. 2005
New Zealand	Blue mussels	<i>Mytilus sp.</i>	20–80	20–80	n.d.	G. Eaglesham, unpublished
	Blue mussel	<i>Mytilus galloprovincialis</i>	50*	n.d.	25*	Mackenzie et al. 2004
	Greenshell mussel	<i>Perna canaliculus</i>	81*	n.d.	72*	Mackenzie et al. 2004
South America						
Chile	Blue mussel	<i>Mytilus chilensis</i>	n.d.	n.d.	100	Garcia et al. 2004
	Ribbed mussel, razor clams	<i>Aulacomya ater</i> , <i>Tangelus dombeyi</i>	n.d.	n.d.	100	Garcia et al. 2004

Note: In cases where a significant amount of data is available, only values most common are reported; extreme values are excluded

<sup>b</sup> = only hexane fraction tested; \* = mean values; n.d. = commonly not detected; n.a. = data not available; LOQ = limit of quantification; LOD = limit of detection

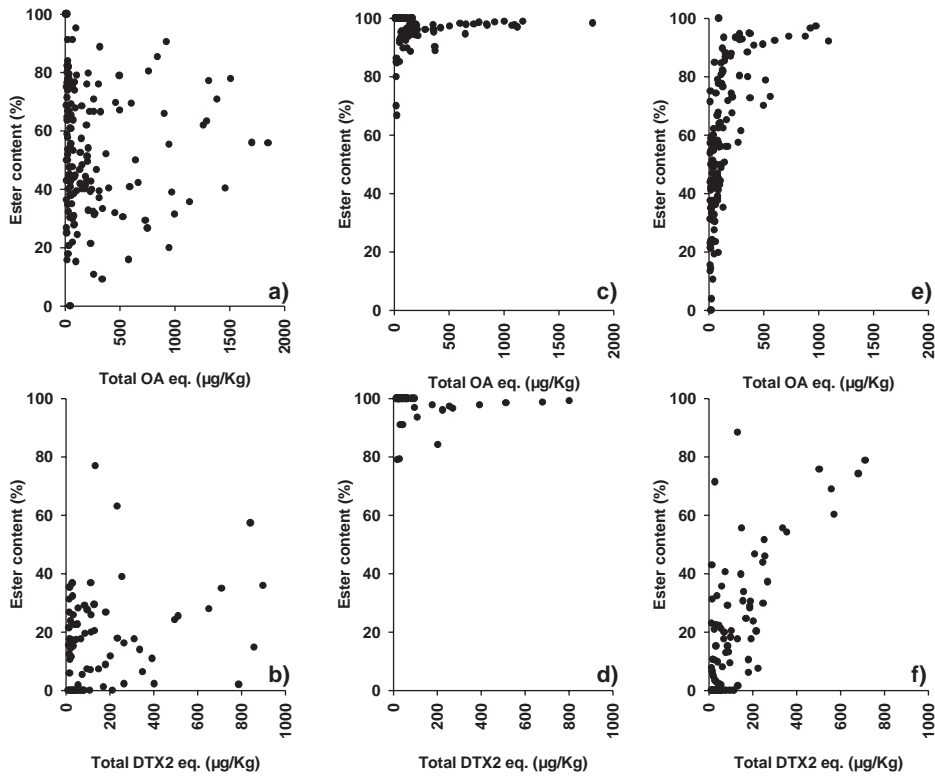


**Figure 12.4.** Percentages of esters found in Portuguese shellfish shown as a function of the total content of DSP equivalents: (a) and (b) *Mytilus galloprovincialis*; (c) and (d) *Cerastoderma edule*; (e) and (f) *Donax trunculus*. Data were reported in Vale (2004) and Vale (unpublished) and cover the years 2002–2005 for mussel and cockles and 2003–2005 for donax clams. For OA, the scale was truncated at 2000, and for DTX2 at 1000 μg/kg, in order to show details at lower concentrations. Only data where total DSP was found above the limit of qualification are presented.

one or two parent toxins), these derivatives can be turned back to the major parent toxins after a simple alkaline hydrolysis step, which in turn can be detected by common methods such as HPLC-FLU, LC-MS, phosphatase inhibition assays or immunoassays (ELISA).

The esters are eliminated faster than nonesterified OA or DTX2. In the blue mussel and donax clams that contain nonesterified OA and DTX2, these forms reside longer than the respective esters, rendering the retention of DSP longer than in clams, razor clams, or cockles that contain only traces of nonesterified toxins (Vale 2004, 2006).

Human episodes of gastroenteritis have been linked only to bivalve mollusks. So far, only one major outbreak, comprising more than 200 persons, has been linked to brown crabs in the summer of 2002 in Norway (Torgersen et al. 2005). When fed artificially with toxic mussels, the DSP toxins accumulated in the digestive organs in the crabs (Castberg et al. 2004). DSP toxins have also been detected in green crabs harvested in Portugal after being suspected of causing one single episode of gastroenteritis (Vale and Sampayo 2002). In both cases, the toxins found in crabs were comprised mainly of DSP esters (Table 12.1).

## Esters of DSP in Plankton

While the conditions for growing *in vitro* the planktonic *Dinophysis* spp. are not yet understood, the benthic *Prorocentrum* spp. are easily grown *in vitro*. *P. lima* was discovered to contain a different type of esters, where the esterification occurs at the carboxylic group (C1) to form allylic diol esters (Yasumoto et al. 1989). Variants with different unsaturated C7 to C9 diols were found in *P. maculosum* from the Caribbean sea and in *P. lima* from east Canada (Hu et al. 1992) and others in *P. lima* from Spain (Norte et al. 1994). More complex water-soluble esters with a trisulfated chain were later isolated from *P. lima* and designated as DTX4 (Hu et al. 1995b). Two similar water-soluble variants containing nitrogen were isolated from *P. maculosum* and designated as DTX5a and DTX5b (Hu et al. 1995a). By boiling the microalgae previous to toxin extraction, it was discovered the cells store most of the toxins as DTX4 (Quilliam et al. 1996a, 1996b). When cells are ruptured, DTX4 is quickly enzymatically hydrolyzed to the diol ester, and slowly the diol ester is hydrolyzed to OA (Fig. 12.5) (Quilliam and Ross 1996). More recently, the diol family was extended to C10 diols after cultures of *P. belizeanum* (Suárez-Gómez et al. 2005).

In plankton samples reach in *Dinophysis acuta*, the presence of a diol ester with a C8 chain was demonstrated in a sample from New Zealand (Suzuki et al. 2004). However, the alkaline hydrolysis methodology, which had led previously to suspecting the presence of esters in the New Zealand samples, did not show the presence of esters in *D. fortii* samples from Japan (Suzuki et al. 1999). In boiled samples of *D. acuminata* and *D. acuta* harvested in Portugal, and *D. acuminata* harvested in

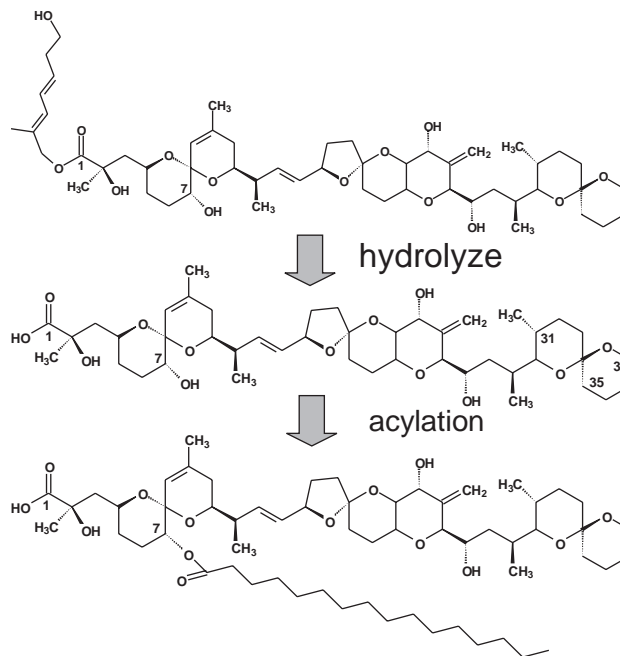


**Figure 12.5.** Biotransformation of DSP toxins: diol esters from *Dinophysis* are enzymatically hydrolyzed by the algae esterase and later acylated in shellfish digestive glands.

Spain, the presence of esters was also suspected following the alkaline hydrolysis's treatment (Vale and Sampayo 2002; Vale 2004; Moróño et al. 2003).

## Structure-Affinity Relationship between DSP Analogues

The effects of OA on smooth muscle contractility led Takai et al. (1987) to deduce that it was an inhibitor of protein phosphatase-1 (PP1) and protein phosphatase-2A (PP2A), two of the major protein phosphatases in the cytosol of mammalian cells that dephosphorylate serine and threonine residues (Cohen 1989). Because of the strong and specific inhibitor effect on PP1 and PP2A, the relationship between the structure of OA and its affinity toward these enzymes arouse a lot of interest. The activities of several OA derivatives obtained from natural sources or by chemical processes were assessed (Takai et al. 1992). Derivatives with minor modifications such as DTX1, with an extra methyl group, or acanthifolicin with an episulfide bridge at C9-C10, presented dissociation constants of the same magnitude; whereas major modifications such as the presence of an acyl group at C7 increased the dissociation constants by three orders of magnitude. The esterification of the carboxyl group at C1, as in methyl okadaate, essentially abolished the affinity for protein phosphatases. The removal of the carboxyl group (2-Oxo-decarboxyl OA), or the C15-C38 OA fragment that did not contain the carboxyl moiety, also did not possess affinity for protein phosphatases (Takai et al. 1992). Diol esters also do not inhibit *in vitro* PP1 or PP2A (Hu et al. 1992), as well as sulphate esters (DTX4) (Hu et al. 1995b). It has been shown by NMR spectroscopy and X-ray analysis that one end (C1–C24) of the OA molecule assumes a circular conformation (Tachibana et al. 1981; Schmitz et al. 1981). The enzyme inhibition assays with different OA derivatives suggest this conformation is extremely important for its activity and is only possible with the carboxylic group non esterified.

## References

- Akasaka, K., Ohru, H., Meguro, H., and Yasumoto, T. 1996. Determination of dinophysistoxin-3 by the LC-LC method with fluorometric detection. *Analytical Sciences*, 12, 557–560.
- Carmody, E.P., James, K.J., and Kelly, S.S. 1996. Dinophysistoxin-2: the predominant diarrhetic shellfish toxin in Ireland. *Toxicon*, 34 (3), 351–359.
- Castberg, T., Torgersen, T., Aasen, J., Aune, T., and Naustvoll, L.-J. 2004. Diarrhetic shellfish poisoning toxins in *Cancer pagurus* Linnaeus, 1758 (Brachyura, Cancridae) in Norwegian waters. *Sarsia*, 89(5), 311–317.
- Cohen, P. 1989. The structure and regulation of protein phosphatases. *Ann. Rev. Biochem.*, 58, 453–508.
- Draisci, R., Giannetti, L., Lucentini, L., Marchiafava, C., James, K.J., Bishop, A.G., Healy, B.M., and Kelly, S.S. 1998. Isolation of a new okadaic acid analogue from phytoplankton implicated in diarrhetic shellfish poisoning. *J. Chromatogr. A*, 798, 137–145.
- Fernández, M.L., Míguez, A., Cacho, E., and Martínez, A. 1996. Detection of okadaic acid esters in the hexane extracts of Spanish mussels. *Toxicon*, 34 (3), 381–387.
- Gago-Martinez, A., Rodriguez-Vazquez, J.A., and Thibault, P., and Quilliam, M.A. 1996. Simultaneous occurrence of diarrhetic and paralytic shellfish poisoning toxins in Spanish mussels in 1993. *Nat Toxins*, 4(2), 72–79.
- García, C., Gonzalez, V., Cornejo, C., Palma-Fleming, H., and Lagos N., 2004. First evidence of dinophysistoxin-1 ester and carcinogenic polycyclic aromatic hydrocarbons in smoked bivalves collected in the Patagonia fjords. *Toxicon*, 43(2), 121–131.
- Hu, T., Curtis, J.M., Walter, J.A., McLachlan, J.L., and Wright, J.L.C. 1995a. Two new water-soluble DSP toxin derivatives from the dinoflagellate *Prorocentrum maculosum*: possible storage and excretion products. *Tet Letts* 36, 9273–9276.
- Hu, T., Curtis, J.M., Walter, J.A., and Wright, J.L.C. 1995b. Identification of DTX4, a new water-soluble phosphatase inhibitor from the toxic dinoflagellate *Prorocentrum lima*. *J Chem Soc Chem Commun* 1995, 597–599.
- Hu, T., Marr, J., Defreitas, A.S.W., Quilliam, M.A., Walter, J.A., Wright, J.L.C., and Pleasance, S. 1992. New diol esters isolated from cultures of the dinoflagellates *Prorocentrum lima* and *Prorocentrum concavum*. *J Nat Products* 55(11), 1631–1637.

- Jackson, A.E., Marr, J.C., and McLachlan, J.L., 1993. The production of diarrhetic shellfish toxins by an isolate of *Prorocentrum lima* from Nova Scotia, Canada. In *Toxic Phytoplankton Blooms in the Sea*, ed. Smayda, T.J., and Shimizu, Y. New York: Elsevier, 513–518.
- James, K.J., Bishop, A.G., Gillman, M., Gillman, M., Kelly, S.S., Roden, C., Draisci, R., Lucentini, L., Giannetti, L., and Boria, P. 1997a. Liquid chromatography with fluorimetric, mass spectrometric and tandem mass spectrometric detection for the investigation of the seafood-toxin producing phytoplankton, *Dinophysis acuta*. *J Chromatogr A* 777, 213–221.
- James, K.J., Carmody, E.P., Gillman, M., Kelly, S.S., Draisci, R., Lucentini, L., and Giannetti, L. 1997b. Identification of a new diarrhetic toxin in shellfish using liquid chromatography with fluorimetric and mass spectrometric detection. *Toxicon* 35(6), 973–978.
- Jørgensen, K., Scanlon, S., and Jensen, L.B. 2005. Diarrhetic shellfish poisoning toxin esters in Danish blue mussels and surf clams. *Food Add Contam* 22(8), 743–751.
- Kat, M. 1979. The occurrence of *Prorocentrum* species and coincidental gastrointestinal illness of mussel consumers. In *Toxic Dinoflagellate Blooms*, ed. Taylor, D., and Seliger, H. New York: Elsevier, 215–220.
- Kumagai, M., Yanagi, T., Murata, M., Yasumoto, T., Kat, M., Lassus, P., and Rodríguez-Vázquez, A., 1986. Identification of okadaic acid as the causative toxin of diarrhetic shellfish poisoning in Europe. *Agric Biol Chem* 50, 2853–2857.
- Lee, J.S., Igarashi, T., Fraga, S., Dahl, E., Hovgaard, P., and Yasumoto, T. 1989. Determination of diarrhetic shellfish toxins in various dinoflagellate species. *J Appl Phycol* 1, 147–152.
- Lee, J.S., Tangen, K., Dahl, E., Hovgaard, P., and Yasumoto, T. 1988. Diarrhetic shellfish toxins in Norwegian mussels. *Nippon Suisan Gakkaishi* 54(11), 1953–1957.
- Lee, J.S., Yanagi, T., Kenma, R., and Yasumoto, T. 1987. Fluorometric determination of diarrhetic shellfish toxins by high performance liquid chromatography. *Agric Biol Chem* 51(3), 877–881.
- MacKenzie, L., Beuzenberg, V., Holland, P., McNabb, P., and Selwood, A. 2004. Solid phase adsorption toxin tracking (SPATT): a new monitoring tool that simulates the biotoxin contamination of filter feeding bivalves. *Toxicon* 44, 901–918.
- Madigan, T.L., Lee, K.G., Padula, D.J., McNabb, P., and Pointon, A.M. 2005. Diarrhetic shellfish poisoning (DSP) toxins in South Australian shellfish. *Harmful Algae*, in press.
- Marr, J.C., Hu, T., Pleasence, S., Quilliam, M.A., and Wright, J.L.C. 1992. Detection of new 7-O-acyl derivatives of diarrhetic shellfish poisoning toxins by liquid chromatography-mass spectrometry. *Toxicon* 30(12), 1621–1630.
- Miles, C.O., Wilkins, A.L., Samdal, I.A., Sandvik, M., Petersen, D., Quilliam, M.A., Naustvoll, L.J., Rundberget, T., Torgersen, T., Hovgaard, P., Jensen, D.J., and Cooney, J.M. 2004. A novel pectenotoxin, PTX-12, in *Dinophysis* spp. and shellfish from Norway. *Chem Res Toxicol* 17, 1426–1433.
- Moroño, A., Arévalo, F., Fernández, M.L., Maneiro, J., Pazos, Y., Salgado, C., and Blanco, J. 2003. Accumulation and transformation of DSP toxins in mussels *Mytilus galloprovincialis* during a toxic episode caused by *Dinophysis acuminata*. *Aquatic Toxicology* 62(4), 269–280.
- Murakami, Y., Oshima, Y., and Yasumoto, T. 1982. Identification of okadaic acid as a toxic component of a marine dinoflagellate *Prorocentrum lima*. *Bull Japan Soc Sci Fish* 48(1), 69–72.
- Murata, M., Shimatani, M., Sugitani, H., Oshima, Y., and Yasumoto, T. 1982. Isolation and structural elucidation of the causative toxin of the diarrhetic shellfish poisoning. *Bull Japan Soc Sci Fish* 48(4), 549–552.
- Norte, M., Padilla, A., Fernández, J.J., and Souto, M.L. 1994. Structural determination and biosynthetic origin of two ester derivatives of okadaic acid isolated from *Prorocentrum lima*. *Tetrahedron* 50(30), 9175–9180.
- Pleasence, S., Quilliam, M.A., DE Freitas, A.S.W., Marr, J.C., and Cembella, A.D. 1990. Ion-spray mass spectrometry of marine toxins. II. Analysis of diarrhetic shellfish toxins in plankton by liquid chromatography/mass spectrometry. *Rap Commun Mass Spectrom* 4, 206–213.
- Quilliam, M.A., Hardstaff, W.R., Ishida, N., McLachlan, J.L., Reeves, A.R., Ross, N.W., and Windust, A.J. 1996a. Production of diarrhetic shellfish poisoning (DSP) toxins by *Prorocentrum lima* in culture and development of analytical methods. In *Harmful and Toxic Algal Blooms*, ed. Yasumoto, T., Oshima, Y., and Fukuyo, Y.I.O.C. of UNESCO, 289–292.
- Quilliam, M.A., Hess, P., and Dell'Aversano, C. 2001. Recent developments in the analysis of phycotoxins by liquid chromatography-mass spectrometry. In (eds.) *Mycotoxins and Phycotoxins in Perspective at the turn of the Millennium*, ed. de Koe, W.J., Samson, R.A., van Egmond, H.P., Gilbert, J., and Sabino, M. Wageningen, the Netherlands: WJ de Koe, 383–391.
- Quilliam, M.A., Ishida, N., McLachlan, J.L., Ross, N.W., and Windust, A.J. 1996b. Analytical methods for diarrhetic shellfish poisoning (DSP) toxins and a study of toxin production by *Prorocentrum lima* in culture. In *Interactions between Cultured Species and Naturally Occurring Species in the Environment*, ed. Keller, B.J., Park, P.K., McVey, J.P., Takayanagi, K., and Hosoya, H., 101–106.
- Quilliam, M.A., and Ross, N.W. 1996. Analysis of diarrhetic shellfish poisoning toxins and metabolites in plankton and shellfish by ion-spray liquid chromatography-mass spectrometry. In *Biochemical and Biotechnological Applications of Electrospray Ionization Mass Spectrometry*, ed. Snyder, A.P. Washington, DC: American Chemical Society, , 351–364.



- Quilliam, M.A., Vale, P., and Sampayo, M.A.M. 2003. Direct detection of acyl esters of OA and DTX2 in Portuguese shellfish by LC-MS. In *Molluscan Shellfish Safety*, ed. Villalba, A., Reguera, B., Romalde, J.R., and Beiras, R. Santiago de Compostela, Spain: Consellería de Pesca e Asuntos Marítimos da Xunta de Galicia and IOC of UNESCO, 67–73.
- Schmitz, F.J., Prasard, R.S., Gopichand, Y., Houssain, M.B., van der Helm, D., and Schmidt, P. 1981. Acanthifolicin, a new episulfide-containing polyether carboxylic acid from extracts of the marine sponge *Pandarus acanthifolium*. *J Am Chem Soc* 103, 2467–2469.
- Suárez-Gómez, B., Souto, M.L., Cruz, P.G., Norte, M., and Fernández, J.J., 2005. New targets in diarrhetic shellfish poisoning control. *J Nat Prod* 68(4), 596–599.
- Suzuki, T., Beuzenberg, V., Mackenzie, L., and Quilliam, M.A. 2004. Discovery of okadaic acid esters in the toxic dinoflagellate *Dinophysis acuta* from New Zealand using liquid chromatography/tandem mass spectrometry. *Rapi Commun Mass Spectrom* 18, 1131–1138.
- Suzuki, T., and Mitsuya, T. 2001. Comparison of dinophysistoxin-1 and esterified dinophysistoxin-1 (dinophysistoxin-3) contents in the scallop *Patinopecten yessoensis* and the mussel *Mytilus galloprovincialis*. *Toxicon* 39(6), 905–908.
- Suzuki, T., Mitsuya, T., Imai, M., and Yamasaki, M. 1997. DSP toxin contents in *Dinophysis fortii* and scallops collected at Mutsu Bay, Japan. *J Appl Phycol* 8: 509–515.
- Suzuki, T., Ota, H., and Yamasaki, M. 1999. Direct evidence of transformation of dinophysistoxin-1 to 7-O-acyl-dinophysistoxin-1 (dinophysistoxin-3) in the scallop *Patinopecten yessoensis*. *Toxicon* 37(1), 187–198.
- Tachibana, K., Scheuer, P.J., Tsukitani, Y., Kikuchi, H., Engen, D.V., Clardy, J., Gopichand, Y., and Schmitz, F.J. 1981. Okadaic acid, a cytotoxic polyether from two marine sponges of the genus *Halichondria*. *J Am Chem Soc* 103, 2469–2471.
- Takai, A., Bialojan, C., Troschka, M., and Ruegg, J.C. 1987. Smooth muscle myosin phosphatase inhibition and force enhancement by black sponge toxin. *FEBS Letts* 217, 81–84.
- Takai, A., Murata, M., Torigoe, K., Isobe, M., Mieskes, G., and Yasumoto, T. 1992. Inhibitory effect of okadaic acid derivatives on protein phosphatases. *Biochem J* 284, 539–544.
- Taleb, H. 2005. Phycotoxines paralysantes (PSP) et diarrhéiques (DSP) le long des cotes marocaines: évolution spatio-temporelle, profil toxinique et cinétique de décontamination. Ph.D. thesis. Casablanca, Morocco: Université Hassan II, Faculté des Sciences Ain Chok.
- Torgersen, T., Aasen, J., and Aune, T. 2005. Diarrhetic shellfish poisoning by okadaic acid esters from Brown crabs (*Cancer pagurus*) in Norway. *Toxicon* 46, 572–578.
- Vale, P., 2004. Differential dynamics of dinophysistoxins and pectenotoxins between blue mussel and common cockle: a phenomenon originating from the complex toxin profile of *Dinophysis acuta*. *Toxicon* 44(2), 123–134.
- . 2006. Differential dynamics of dinophysistoxins and pectenotoxins, part II: offshore bivalve species. *Toxicon*, in press.
- Vale, P., and Sampayo, M.A.M. 1999. Esters of okadaic acid and dinophysistoxin-2 in Portuguese bivalves related to human poisonings. *Toxicon* 37(8), 1109–1121.
- . 2002. First confirmation of human diarrhoeic poisonings by okadaic acid esters after ingestion of razor clams (*Solen marginatus*) and green crabs (*Carcinus maenas*) in Aveiro Lagoon, Portugal and detection of okadaic acid esters in phytoplankton. *Toxicon* 40(7), 989–996.
- van Egmond, H.P., Speijers, G.J.A., and van den Top, H.J. 1992. Current situation on worldwide regulations for marine phycotoxins. *J Nat Toxins* 1(1), 69–85.
- Yasumoto, T., Murata, M., Lee, J., and Torigoe, K. 1989. Polyether toxins produced by dinoflagellates. In *Mycotoxins and Phycotoxins '88*, ed. Natori, S., Hashimoto, K., and Ueno, T. Amsterdam, Elsevier, 375–382.
- Yasumoto, T., Murata, M., Oshima, Y., Matsumoto, K., and Clardy, J. 1984. Diarrhetic shellfish poisoning. In *Seafood Toxins*, ACS Symposium Series 262, ed. Ragelis, E.P. Washington, DC: American Chemical Society, 207–214.
- Yasumoto, T., Murata, M., Oshima, Y., Sano, M., Matsumoto, G.K., and Clardy, J. 1985. Diarrhetic shellfish toxins. *Tetrahedron* 41(6), 1019–1025.
- Yasumoto, T., Oshima, Y., Sugawara, W., Fukuyo, Y., Oguri, H., Igarashi, T., and Fujita, N. 1980. Identification of *Dinophysis fortii* as the causative organism of diarrhetic shellfish poisoning. *Bull Japan Soc Sci Fish* 46(11), 1405–1411.
- Yasumoto, T., Oshima, Y., and Yamaguchi, M. 1978. Occurrence of a new type of shellfish poisoning in the Tohoku district. *Bull Japan Soc Sci Fish* 44(11), 1249–1255.



## 13 The Molecular and Integrative Basis to Domoic Acid Toxicity

John S. Ramsdell

### Introduction

Domoic acid, a relatively unknown tricarboxylic acid isolated from macroalgae in 1966, was identified as an environmental neurotoxin after a 1987 poisoning of 145 individuals in the Quebec area after consumption of Prince Edward Island mussels. This event triggered rapidly paced investigations of domoic acid toxicity, without any further evidence of human intoxication. The presence of domoic acid in seabirds and shellfish on the west coast of the United States in 1991, along with nearly annual sea lion epizootics attributed to domoic acid accumulation in planktivorous fish, firmly established domoic acid as a prominent environmental neurotoxin by 1998. Yet, domoic acid is not a highly potent toxin, as toxicokinetics limit its oral effectiveness to well over parts per thousand levels of exposure. It is poorly absorbed by the gut, poorly penetrates the central nervous system, and has a very short half life in most tissue compartments. At the level of the receptor, domoic acid binds to kainate subtypes of ionotropic glutamate receptors with high affinity (parts per billion) but is only a partial agonist. The unique molecular interactions with the receptor, which induce partial ion conductivity, prevent normal inactivation of channel opening resulting in ion conduction well beyond that achieved by natural glutamatergic transmitters. A level of excitotoxicity is reached from an integrative action on both sides of the synapse. Domoic acid activates presynaptic kainate receptors leading to depolarization and release of glutamate into the synapse. It also activates postsynaptic kainate receptors leading to depolarization that acts in coincidence with released glutamate to activate NMDA ionotropic receptors. The huge concentration of kainic acid receptors in the CA3 region of the hippocampus thus targets domoic acid, where its action overrides a signaling pathway normally propagated through closed loop, seizure-prone circuitry in the medial temporal lobe of the brain. Excitotoxicity in CA3 leads to cellular and ultrastructural damage to pathways responsible for the learning and recall of sequences underlying spatial memory and the restraint of seizure circuitry that kindles temporal lobe epilepsy. The molecular and integrative basis to mammalian domoic acid toxicity is the focus of this chapter, which reviews the primary biochemical, physiological, and toxicological literature relevant to domoic acid from 1965 to 2005. An additional valuable source is a collection of papers from the 1989 symposium on domoic acid toxicity that summarizes multiple facets of the human exposure to domoic acid, several of which did not ultimately reach the primary literature (Hynie and Todd 1990). Updated publications on toxicology of domoic acid are maintained on the Domoic Acid and Pseudo-nitzschia Reference Database (Bates 2003).

### *Domoic Acid*

*A water-soluble tricarboxylic acid with a unique large carboxylic side chain.*

Red macroalgae (Rhodophyta) have been reported as folk medicines with efficacy for the treatment of round worm disease as early as the ninth century. Kainic acid was isolated as the

anthelmintic principal from *Digenea simplex* (Murakami 1953). Another red macroalgae (*Chondria armata*) known as *doumoi* was utilized on the Japanese island of Tokunoshima for ring worm disease and the neighboring island of Yakushima to control flies. Domoic acid was isolated as the anthelmintic principal from *C. armata* (Takemoto and Daigo 1958; Daigo 1959a, 1959b) and later analyzed for its insecticidal properties (Maeda et al. 1984; Maeda et al. 1987a). Complete characterization of domoic acid was very much limited by the scarcity and depletion of its known biological source at that time. Following an unusual human shellfish poisoning in 1987, high concentrations (exceeding 10 ppt) were found in blue mussels (*Mytilus edulis*), in which the domoic acid was determined to have originated from the diatom *Pseudo-nitzschia pungens* (Wright et al. 1989) and since been found in several different species of *Pseudo-nitzschia*. This cosmopolitan diatom serves to distribute domoic acid broadly through the benthic and pelagic marine food web (Lefebvre et al. 2002).

Domoic acid is a crystalline water-soluble acidic amino acid with three carboxylic acids originally described by Takemoto (Takemoto and Daigo 1958) (Fig. 13.1). Because of the limited amount of natural sample available, a total synthesis of domoic acid was completed for further analysis (Ohfuné and Tomita 1982) and X-ray crystallography confirmed the stereochemistry of the large carboxylic side chain that extends from position 4 on the pyrrolidine ring (Nomoto et al. 1992). Initial analysis of domoic acid and the kainic acid analogues indicated that the  $\pi$  electron group with appropriate *cis*-planar orientation versus the C2-carboxyl group is essential for high affinity binding to the receptor (Slevin et al. 1983). The imizadole nitrogen and carboxylic oxygens originating from positions 2 and 3 of the pyrrolidine ring have subsequently been modeled as essential to bind to all classes of ionotropic glutamatergic receptors (Nanao et al. 2005). However, the carboxylic acid of the side chain confers subtype specificity to domoic acid action. The carboxyl groups have pKa's of 2.10, 3.72, 4.97, and the amino group 9.82, leading to five potential charge states of the molecule (Walter et al. 1992). At physiological pH the predominant species of domoic acid is deprotonated at all three carboxyl groups and protonated at the amino group leading to a net charge of negative 2 (Fig. 13.2). The degree of protonation of domoic acid affects its toxicity to animals with the CO<sub>2</sub><sup>-</sup> charged species found at physiological pH being most potent by intraparenteal administration. However, this *in vivo* approach may more reflective of absorption of toxin rather than intrinsic action at the level of the receptor (Nijjar and Madhyastha 1997). Eleven isomers of domoic acid (isodomoic acids A-G; domoic lactone A & B and 5'-epidomoic acid) have been isolated in trace amounts from various sources (Maeda et al. 1986, 1987b; Wright et al. 1990; Walter et al. 1994; Zaman et al. 1997; Holland et al. 2005). The domoic acid isomers A-G are of substantially lower potency than domoic acid and at least some of the isomers appear to be products of photo-isomerism (Hampson et al. 1992). The domoic acid lactones are inactive and the 5'-epidomoic acid is reported near equipotent to domoic acid.

*Disposition: Poorly absorbed by the gut, poorly penetrates the brain and rapidly eliminated.*

Domoic acid exposure to mammals occurs orally in a matrix of shellfish to human consumers, planktivorous fish and benthic invertebrates to marine mammals, and perhaps zooplankton and chained diatoms to whales. Analysis of the consumed mussels from the 1987 exposure indicated that 1 mg/kg was sufficient to induce gastrointestinal symptoms and 4.5 mg/kg could induce neurological effects in humans (Perl et al. 1990). Experimental studies in monkeys, rats and mice have utilized oral gavage, intraparenteal, and intravenous exposure routes and determined that oral gavage is about ten times less effective than the other routes of exposure (Iverson et al. 1990). Humans appear much more sensitive than either monkeys or rats, which when dosed orally have no observable adverse effect levels (NOAEL) at 5 and 28 mg/kg, respectively. Experimental animals have permitted evaluation of different dose scenarios. A daily NOAEL oral gavage of domoic acid to rats for

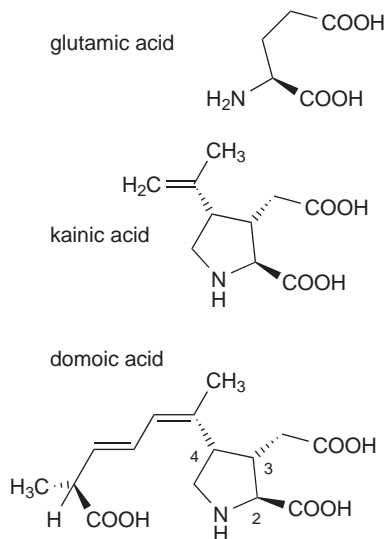


**Figure 13.1.** Structure of glutamate, kainic acid and domoic acid.

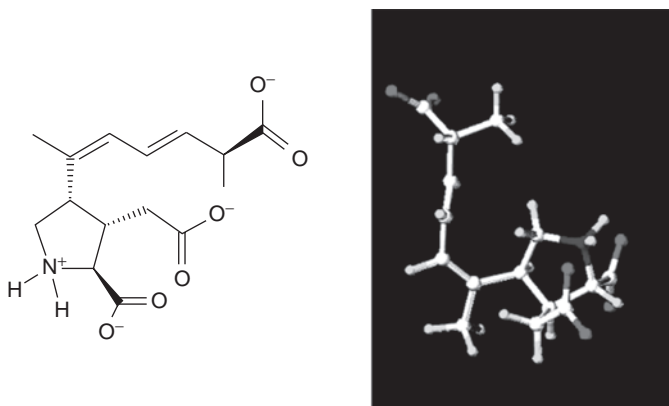


**Figure 13.2.** (A) Predicted predominant charge form of domoic acid at physiological pH. (B) Minimized structure. Reprinted with permission of from S. Pilesky, Cranfield University, © 2005.

64 days or to monkeys for 32 days showed no observable symptoms or neuropathological effects (Truelove et al. 1996, 1997). Likewise an independent repeated dose scenario using NOAEL, lowest observable adverse effect level (LOAEL) and highest tolerable nonlethal dose indicated that mice show no additional acute symptomatic toxicity, persistent effects on memory nor neurodegeneration with up to four consecutive doses (Peng et al. 1997; Clayton et al. 1999).

The low pK<sub>a</sub> of domoic favors its rapid absorption as a neutral acid in the stomach; however, overall oral absorption of domoic acid is very low with nearly the entire oral dose eliminated from rats and mice in the feces (Iverson et al. 1989). A subsequent study indicated that approximately 2%

of an oral dose is eliminated in the urine in rats (Truelove et al. 1996); whereas 4%–7% of the oral dose is eliminated in the urine of monkeys (Truelove and Iverson 1994). It is noted that effectiveness of oral exposure is quite variable, even with consideration given to the presence or absence of food extract in the administered bolus or the degree of preadministration food restriction. Hence gut absorption represents a potential mechanism of predisposition, in which gastric lesions represent one preexisting factor.

Domoic acid poorly penetrates the brain, where the endothelial cells of brain capillaries restrict the entry of all but the smallest of ions from blood through tight junctions, lack of pinocytosis and active efflux pumps. Domoic acid initially enters the brain slowly via pinocytosis at the level of capillaries, with a transfer constant of 12  $\mu\text{g}/\text{kg}$  for a low level exposure to radiotracer domoic acid (Preston and Hynie 1991). This experimental data has been used to generate a physiologically-based pharmacokinetic model for low dose domoic acid uptake into the brain (Kim et al. 1998) with constraints on the brain compartment for membrane-limited entry across capillary endothelial cells and elimination into the cerebral spinal fluid via organic anion pumps in the choroid plexus. This model determined domoic acid enters several brain regions without selectivity, reaching near equilibrium tissue levels of 50–75  $\text{pg}/\text{g}$  by one hour. Effective levels were re-estimated up to seven times higher based upon restriction of the toxin to the extracellular fluid space, reaching nearly receptor active concentrations of 0.5  $\text{ng}/\text{ml}$ . Beyond the design of this study are the circumventricular regions of the brain that have capillaries lacking the restrictive mechanisms of this barrier. One such region is the area postrema, which is responsible for the emetic response, the most sensitive neurological response to domoic acid in primates (Tryphonas et al. 1990a). Additionally, higher excitotoxic doses can enhance blood-brain permeability of domoic acid through the onset of seizures, which are documented to enhance capillary endothelial cell pinocytosis (Petito et al. 1977). This effect is also observed for excitotoxins like kainic acid, which can feedback and exasperate this effect in regions of the limbic system (Nitsch et al. 1986). Such a mechanism is likely to promote the steep dose response curve for domoic acid.

Domoic acid is eliminated rapidly by renal filtration. Clearance studies following intraperitoneal administration to rats indicate that domoic acid remains largely intact and is cleared rapidly by the kidneys with a renal clearance of 10  $\text{ml}/\text{minute}/\text{kg}$  (Suzuki and Hierlihy 1993). By contrast, monkeys have a clearance rate about ten times less than that of rats (Truelove and Iverson 1994). The clearance of domoic acid in the kidneys is resistant to probenecid, an inhibitor of reabsorption of organic acids in renal tubules, indicating that domoic acid is cleared largely by glomerular filtration (Suzuki and Hierlihy 1993). An earlier study indicated probenecid increased both the plasma levels of domoic acid and neuroexcitation (Robertson et al. 1992); however, the strength of evidence from the Suzuki and Hierlihy study is substantial. It is possible that probenecid in the earlier study may have inhibited the efflux of domoic acid from the brain compartment by inhibition of the organic anion pump in the choroid plexus.

## Receptor Interaction

### *High affinity, non-deactivating partial agonist of kainate subtype receptors.*

The structural similarity of kainic acid with glutamate lead Shinozaki and Konishi to identify an excitatory action of kainic acid on the mammalian central nervous system (Shinozaki and Konishi 1970). Olney's laboratory four years later identified kainic acid as a glutamatergic neurotoxin in rats (Grimmelt et al. 1990) sparking intense investigation of kainic acid and its use as a pharmacologic tool in the mammalian central nervous system. Shinozaki's laboratory subsequently characterized

kainic acid and domoic acid as a glutamatergic agonist in crayfish motorneurons (Shinozaki and Ishida 1976; Shinozaki and Shibuya 1976). Kainic acid and domoic acid were independently identified by Biscoe's laboratory as excitatory amino acids on frog and rat motor neurons (Biscoe et al. 1975, 1976). Application of a radiolabeled kainic acid receptor assay provided the first evidence that domoic binds a kainate receptor site that mediates its neurotoxic effects (Slevin et al. 1983). Subsequently, Hampson characterized the binding of domoic acid to kainate and AMPA binding sites in rat brain and determined that domoic acid, unlike kainic acid, binds a subpopulation of AMPA sites with low nanomolar affinity (Hampson et al. 1992). The contribution of AMPA receptors to domoic acid toxicity still remains to be determined.

The discovery of a superfamily of glutamate receptor genes coding for ionic channels led to greater discrimination of the actions of domoic acid on glutamate receptors. Originally distinguished by selectivity of the synthetic analog NMDA, two classes of receptors (NMDA and non-NMDA) were found having approximately 30% homology. Within the non-NMDA receptors, one family of receptors is selective for AMPA (GluR1–4) and two families are selective for kainic acid (GluR5–7 and KA 1&2) (Fig. 13.3). Seeburg's and Heinemann's laboratories used domoic acid to characterize the cloned receptor subunits expressed as homomeric receptors. Domoic acid was found to be less potent than kainic acid at the KA 1&2 homomeric receptors (Lothman and Collins 1981) and more potent at the homomeric GluR 5–7 (Lomeli et al. 1992; Sommer et al. 1992) (Fig. 13.4). Formation of an ionotropic receptor requires assembly of homomers into two pairs of dimers yielding a tetrameric structure. Functional channels in the brain are usually a mixture of two different homomers, with the KA1 and KA2 subunits requiring association with members of the GluR5–7 family.

The resolution of the topology of the GluR6 receptor has provided insight into the molecular interaction with the binding pocket of the receptor. Ionotropic glutamatergic receptors share a common structure which is comprised of two cytoplasmic domains (S1 and S2) and four membrane domains (M1–4), the second of which is not transmembrane but rather re-enters the cytoplasm (Fig. 13.5). Insight into the domoic acid binding site on the GluR6 has been obtained by first developing a fusion product of the S1 and S2 domains, then utilizing molecular modeling with existing data for the GluR4 and GluR2 receptors (Nanao et al. 2005). This binding pocket for domoic acid requires hydrophilic contacts with both S1 and S2 and sits between a cleft amid an upper and lower

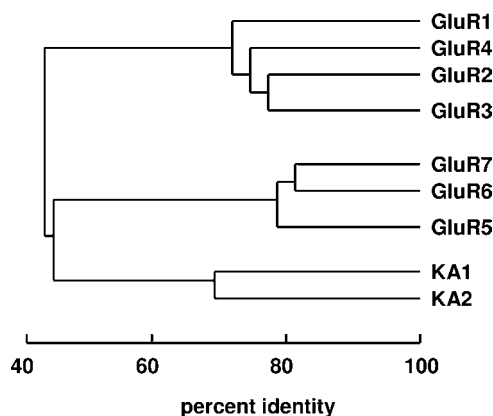


**Figure 13.3.** Homology of non-NMDA ionotropic glutamatergic receptors.

	GluR1   GluR2   GluR3   GluR4	GluR5   GluR6   GluR7	KA1   KA2
	AMPA sites	low affinity kainate sites	high affinity kainate sites
Binding Affinity	AMPA>GLU>DA>KA	DA>KA>GLU>>AMPA	KA>DA>GLU>>AMPA
Agonist Potency	AMPA~DA>GLU>KA	DA>KA>GLU>>AMPA	no activation of homomers
	AMPA Receptors	Kainate Receptors	

**Figure 13.4.** Glutamate receptor subtypes and relative affinity to glutaminergic agonists.

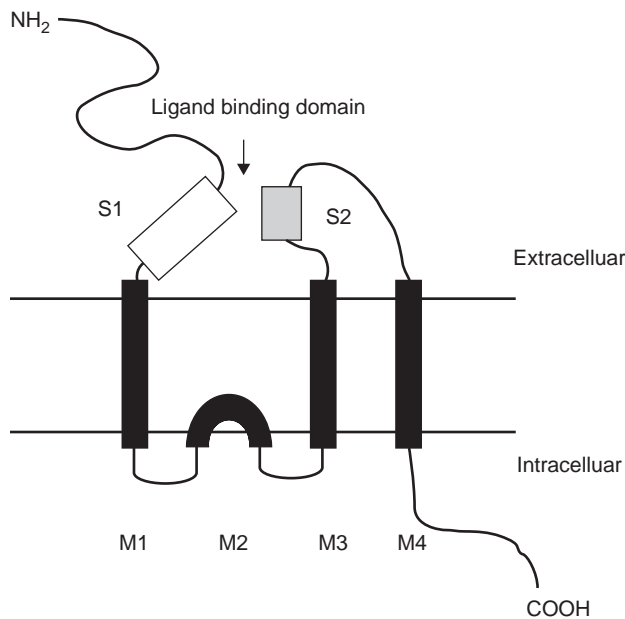


**Figure 13.5.** Schematic of ionotropic glutamatergic receptor.

lobe of the extracellular domain of the receptor (Fig. 13.6). Conductance studies indicate that both kainic acid and domoic acid are partial agonists. Structural analysis of the binding to the GluR6 receptor demonstrates that domoic acid has an intermediate effect between glutamate, which opens the binding cleft between the top and bottom lobes of the receptor, and the antagonist DNQX, which closes the binding cleft (Nanao et al. 2005). This process is believed to cause conformational changes leading to the varying degree of channel pore opening by kainic acid and domoic acid.

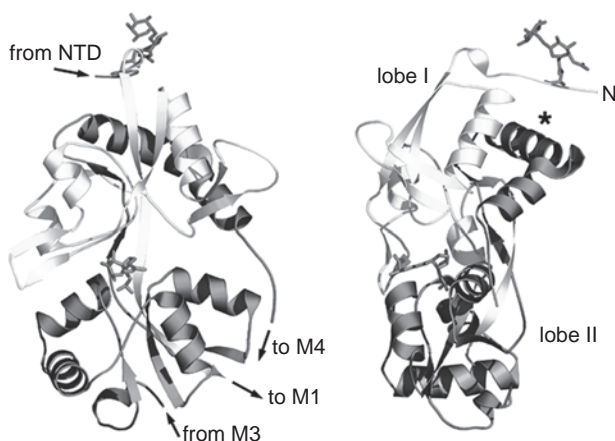


**Figure 13.6.** Minimized structure of GluR6 S1-S2 fusion protein with bound domoic acid. Reprinted with permission from Nanao et al. (2005), © National Academy of Sciences, USA.

Domoic acid has high efficacy at ionotropic receptors, causing only partial opening of the ion-conducting pore that fails to deactivate. AMPA and kainate receptors are noted for their rapid desensitization after activation by glutamate, which limits the open time of the channel to a few milliseconds and effectively closes the channel. AMPA receptors upon binding glutamate form a pair of dimers within their tetrameric structure and the stability of this conformational change keeps the channel in an open configuration. However, the conformation associated with the open pore is believed to in turn disrupt the agonist binding pocket leading to a new configuration of the dimer and a desensitized closed channel (Bowie and Lange 2002). Partial agonists such as domoic and kainic acids are believed to resist this new arrangement of the dimer, preventing the desensitized state. The precise desensitization mechanism for the GluR6 receptor is presently unresolved. The GluR6 receptor does not share the same molecular contacts between the dimer interface (Nanao et al. 2005). Nonetheless, point mutations in the GluR6 receptor away from the binding pocket increase desensitization after domoic acid exposure (Swanson et al. 1997). Kainate receptors differ from AMPA receptors by having a four- versus a two-phase desensitization (Bowie and Lange 2002). This suggests that the domoic acid nondesensitizing action on GluR6 receptors does result from its efficacy to resist conformational changes in the extracellular domain of the receptor after partial opening of the pore. Hence, the efficacy of domoic acid as a partial agonist on pore opening is substantially overcome by preventing the channel from rapid desensitization.

## Signal Transduction

### *Integrative action on both sides of the synapse.*

The neurotoxicity of domoic acid is due to more than its high affinity for the binding site of the ionotropic receptor and its efficacy as result of nondesensitization of the channel. The mechanisms of domoic toxicity have been determined to involve synergy with endogenous excitatory amino acids such as glutamate. Glutamate is the key factor in the excitotoxin hypotheses. Glutamate was originally recognized as a neurotoxicant by Olney (1969) and its toxic action, in some instances, was later determined to be mediated by NMDA receptors (Choi 1994). Olney also determined that kainic



acid acts as an excitotoxin by initiating glutamate excitotoxicity (Olney et al. 1979). Based upon structural similarity to kainic acid and the seizure behavior associated with amnesic shellfish poisoning, a number of investigators quickly surmised that domoic acid also causes an excitotoxic syndrome (Glavin et al. 1989a, 1989b; Stewart et al. 1990; Auer 1991).

Debonnel's laboratory provided the first experimental evidence that domoic acid is neurotoxic (Debonnel et al. 1989a). They determined that domoic acid was three times more potent than kainic acid and was most potent on the CA3 field, a region with high concentrations of kainate receptors (Fig. 13.7). A lesion of glutamatergic dentate granule cell axons (mossy fibers) that project to the CA3 pyramidal cells largely eliminates both kainate receptors in the CA3 area (Represa et al. 1987) and the excitatory response to domoic acid (Debonnel et al. 1989b). Domoic acid was shortly afterwards determined to release glutamate from synaptosomes of mossy fibers (Terrian et al. 1991) providing an initial basis for domoic acid as a glutamatergic excitotoxin.

Novelli's laboratory determined that the neurotoxic effect of domoic acid on cultured cerebellar granule cells was potentiated by glutamate (Novelli et al. 1992a). Additionally a shellfish extract containing domoic acid and naturally occurring excitatory amino acids showed tenfold greater toxicity relative to domoic acid concentration, and this extract was fully neutralized by NMDA receptor antagonists (Novelli et al. 1992b). The following year Nijjar provided the anticipated link between domoic acid neurotoxicity and calcium, demonstrating that domoic acid increased the uptake of neurotoxic levels of calcium by an ATP dependent mechanism in brain tissue slices (Nijjar 1993).

Subsequently, several studies have provided more detailed information on domoic acid action as an excitotoxin. The presynaptic action of domoic acid to induce glutamate release was extended to include other excitatory and inhibitory neurotransmitters and linked to the entry of calcium through voltage operated calcium channels, suggesting that domoic acid toxicity may involve multiple transmitters (Brown and Nijjar 1995; Duran et al. 1995a; Malva et al. 1996). Domoic acid effects on intracellular calcium were next characterized by FURA-2 imaging of the hilar region of individual

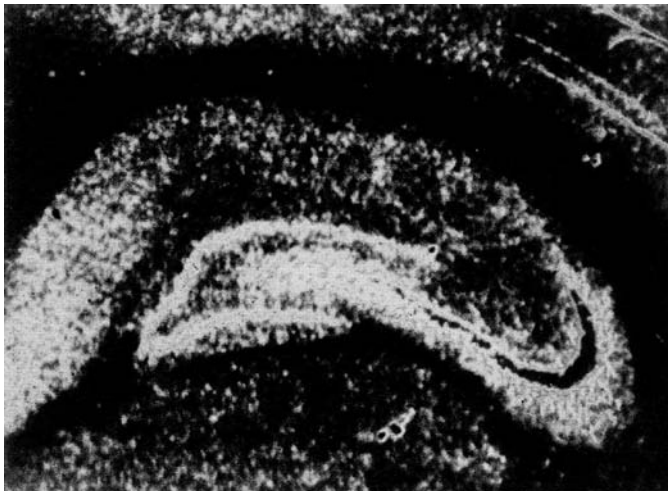


**Figure 13.7.** Autoradiogram of kainic acid binding sites in hippocampus. Reprinted with permission from Monaghan and Cotman (1982), © Elsevier.

hippocampal cells (Xi and Ramsdell 1996), indicating that domoic acid induced entry of calcium was mediated by type-L voltage dependent calcium channels and not by NMDA receptors. Research by Murray's laboratory carefully optimized conditions to re-investigate glutamate toxicity in cultured cerebellar granule cells and determined that domoic acid induced cytotoxicity is primarily mediated by the release of glutamate and glutamate activation of NMDA receptors (Berman and Murray 1996; Berman and Murray 1997). Subsequent analysis of domoic acid induced calcium entry in cerebellar granule cells demonstrated that calcium entry was by multiple mechanisms, which include NMDA receptors, reversed operation of the  $\text{Na}^+/\text{Ca}^{++}$  exchanger and voltage dependent calcium channels (Berman et al. 2002). Taken together, one mechanism of domoic acid toxicity, at least for cerebellar granule cells, involves a coordination of pre- and post-synaptic receptors and a coincidence detection mechanism involving glutamate and voltage-dependent activation of NMDA receptors, all leading to sustained elevation of intracellular calcium (Fig. 13.8). However, domoic acid excitotoxicity in other *in vitro* systems, such as hippocampal cell culture and chick retina, involves a different mechanism (Olney 1990) with a stronger contribution from voltage dependent calcium channels, release of intracellular stores of calcium and  $\text{Na}^+/\text{Ca}^{++}$  exchanger (Nijjar and Nijjar 2000). Yet overall, the case for involvement of NMDA receptors in domoic acid neurotoxicity *in vivo* is compelling as discussed later in this chapter.

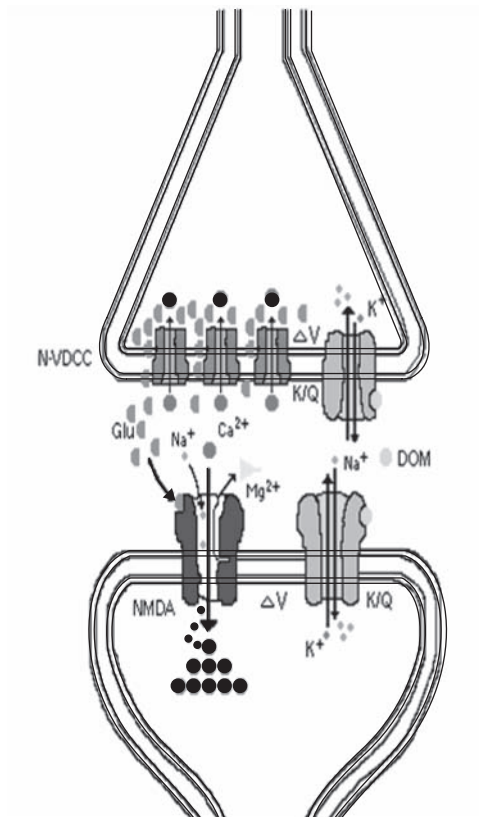


**Figure 13.8.** Schematic of pre- and post-synaptic actions of domoic acid.

Extension of *in vitro* signal transduction studies to intact animal models has supported a role for NMDA receptors and induction of genes consistent with glutamatergic excitation. Tasker's laboratory has evaluated the role of NMDA receptors on domoic acid induced observable symptoms. The first study revealed some of the complexities with extending *in vitro* to *in vivo* studies, as only one (3-(2-carboxypiperazine-4-yl)propyl-1-phosphonic-CCP) of five NMDA antagonists caused a significant, yet small (<20%) inhibition of domoic acid toxicity (Tasker et al. 1996). A subsequent study with the same experimental model demonstrated clear synergy between domoic acid and the agonist NMDA and a complete inhibition of this synergy with CCP (Tasker and Strain 1998). Several steps downstream of calcium entry is a rapid and transient induction of the immediate early response gene *c-fos* in mouse brain, an effect clearly localized to the dentate granule cells and hippocampal pyramidal cells (Peng et al. 1994). The induction of *c-fos* occurs at or below doses at the lowest observable effect level, indicating that this response is more likely the result of its action to elevate calcium rather than from extensive seizure activity (Peng and Ramsdell 1996). The induction of *c-fos* in rats is blocked by the NMDA antagonist AP-5, consistent with the involvement on NMDA receptors (Xi et al. 1997). Mouse brain mRNA microarray analysis, after acute exposure to domoic acid, has identified several panels of acute response genes based on temporal expression profiles (Ryan et al. 2005). Of prominence are the AP-1 transcription factors (primarily *c-fos* and *jun-B* and to a lesser extent *fos-B* and *c-jun*), *Nxf*, a novel seizure responsive gene in mice, and the early growth response (EGR) family of transcription factors. The inducible form of cyclooxygenase (COX-2), the key enzyme that converts arachidonic acid (AA) to prostaglandins (PGs), is rapidly and strongly induced by domoic acid. This enzyme has important roles to augment NMDA-mediated actions in the hippocampus, thus promoting formation of long term potentiation (LTP), and also participates in the inflammatory response to injury of the central nervous system. Another notable inducible gene was serum and glucocorticoid inducible kinase 1 (Sgk1), implicated in the consolidation of memory. The panel of genes showing differential expression in response to domoic acid is highly conserved with those expressed during glutamatergic excitotoxicity and those induced by other neurotoxic events such as ischemia.

### **Neuroexcitation**

*Overrides a signaling pathway designed for strong activation of spatially defined signals that propagate through a closed loop, seizure-prone circuitry.*

The adverse effects of domoic acid were readily apparent after the 1987 human exposure. From an overall perspective, Teitelbaum et al. described the neurological effects as an acute neuroexcitatory phase followed by a loss of function in those regions susceptible to excitotoxic degeneration (Teitelbaum et al. 1990). Subsequently, more thorough characterization of domoic acid toxicity has relied upon primate and rodent studies guided by existing knowledge of kainic acid, as well as repeated annual domoic acid poisonings of sea lions in California. These investigations include analysis of seizure behaviors, electroencephalography, and induction of the immediate early response gene *c-fos*, ultimately revealing a preference of domoic acid for the glutamatergic excitatory pathways in the seizure prone circuitry of the limbic system.

Seizure behavior and observable convulsions were described in victims of the 1987 exposure and were characterized in fourteen of the more severely affected patients. Behaviors of purposeless chewing and grimacing were common. These behaviors, along with observable seizures and convulsions, developed from several days to more than a week after exposure. The seizures ranged from generalized myoclonus to partial complex (psychomotor) and generalized seizures, developing into

partial status epilepticus and, in several cases, coma (Teitelbaum et al. 1990). Three laboratories characterized both toxic shellfish extracts and purified domoic acid in rodents by describing a set of seizure behavioral responses (Iverson et al. 1989; Grimmelt et al. 1990; Tryphonas and Iverson 1990; Tryphonas et al. 1990a; Tasker et al. 1991). Rodents display a characteristic set of pre-ictal signs after domoic acid exposure similar to those described for kainic acid (Lothman and Collins 1981). They begin with a period of quiescence followed by purposeless exploratory behavior, staring spells, and a hallmark stereotypic behavior of repeated bilateral scratching sessions of skin below the ear with the ipsilateral hind paw. This leads to the onset of an ictal phase of limbic seizure behaviors, including head nodding, mastication, salivation, paw claspings (Figs. 13.9A–13.9D) and fine generalized tremors. More severe limbic seizures progress to status epilepticus with characteristic postural behaviors, culminating in ataxia, falling status and extreme rigidity leading to a “crab

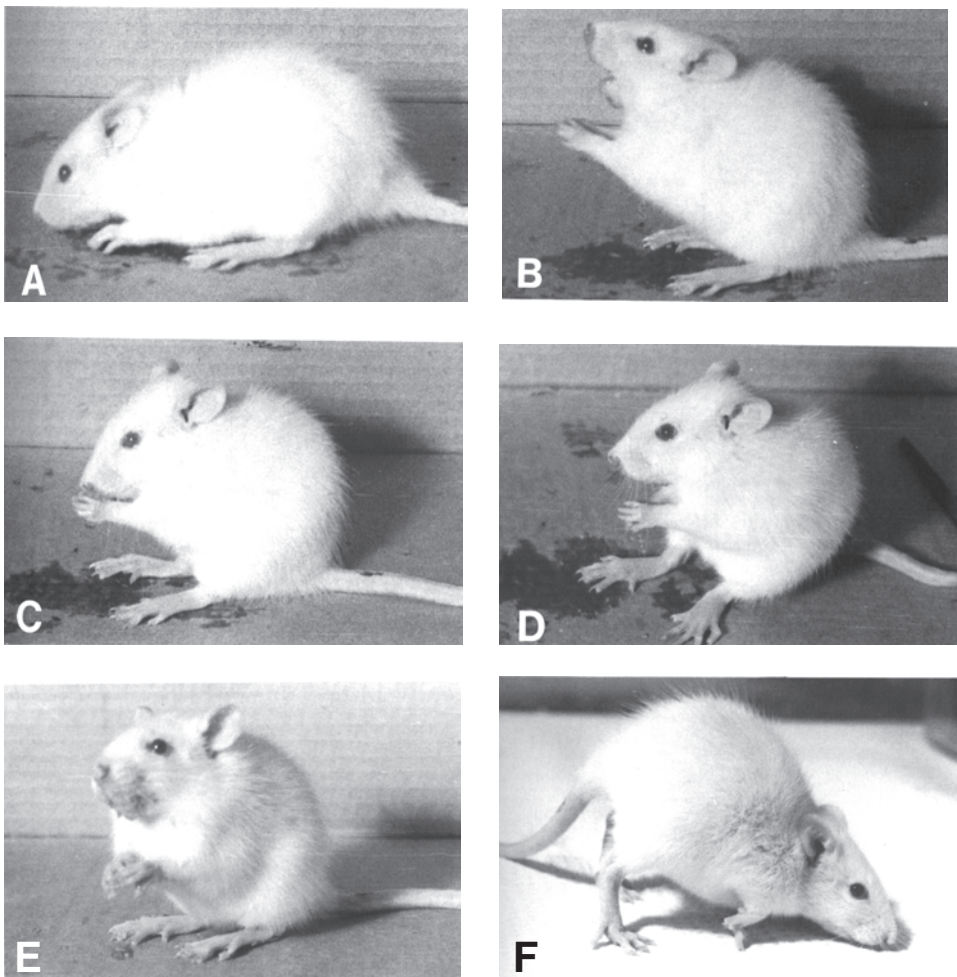


**Figure 13.9.** Domoic acid induced seizure behavior in rats. Reprinted from Tryphonas and Iverson (1990), © 1990 with permission from *Toxicology Pathology*.

like walking” (Figs. 13.9E and 13.9F). Muscular effects include forelimb and generalized tremors. Parallel studies in cynomolgus monkeys were conducted using purified domoic acid extracts and toxic mussel extracts, which both produced intense early effects of gagging and vomiting (Tryphonas et al. 1990a; Scallet et al. 1993). Seizure behaviors included lip smacking and mastication, scratching, ataxia, and loss of balance. Muscular effects included generalized fine tremors and rigidity of movements. The sea lion epizootic of 1998 documented clinical signs of ataxia, head weaving, tremors and coma, as well as the characteristic scratching behavior (Gulland et al. 2002). A prolonged post-ictal phase of seizure behavior in the sea lions included noticeable unresponsiveness in addition to rolling and back rubbing behavior.

Electroencephalographic analysis has defined the development and localization of seizure activity in response to domoic acid. Limited electroencephalograms of seven human patients within the first week of exposure showed a generalized slowing of background activity and one patient (discussed further in section on epilepsy) showed periodic lateralized epileptiform discharges in the frontotemporal region (Teitelbaum et al. 1990; Cendes et al. 1995). A subsequent study in rats thoroughly characterized domoic acid induction of seizures and EEG activity (Fujita et al. 1996). At a LOAEL of 1.0 mg/kg, an initial locus of reoccurring eliptiform EEF activity appears in the hippocampus within 1 hour, which spreads to the sensorimotor cortex regions by 2 hours, subsides at 6 hours and reaches normal activity by 24 hours. At a lethal (8–10 hour time of death) dose (5 mg/kg), the initial locus of hippocampal activity appears sooner with longer chains of reoccurring (every 5–10 minutes) activity (Fig. 13.10, top panel). The animals progressed to limbic seizure status with sensorimotor cortex activity at 2 hours with the prototypical rodent seizure behavior (Fig. 13.10, middle panel and refer to Fig. 13.9 for behavior). By 4 hours, the animals progress to generalized status epilepticus and tonic seizures (Fig. 13.10, bottom panel). Histological analysis was used to correlate these effects with specific regions. At the LOAEL only mild shrinkage of pyramidal cell nuclei in the CA3 region was observed, whereas at the lethal dose of 5 mg/ml more severe effects were observed in the CA3 and CA1. A higher dose of 10 mg/kg led to more rapid progression of seizure activity and histological damage that extended into the CA4 and cerebral cortex. These results indicate that seizure activity likely results from neuroexcitation in the CA3 and spreads to the sensorimotor cortex as a function of time and dose.

Curran’s laboratory discovered that the immediate response gene *c-fos* can be used to map seizure activity in the brain (Morgan et al. 1987). The rapid kinetics of *c-fos* and the localization of its translation product Fos to the nucleus provided an optimal means for histochemical localization of neuroexcitatory events within specific brain regions. These principals were applied to develop Fos histochemistry in the brain and characterize Fos localization after kindling induced seizures, ultimately determining that domoic acid and kainic acid induced similar localized patterns of expression (Dragunow et al. 1987; Dragunow and Robertson 1987; Robertson et al. 1992). Of particular note is the strong neuroexcitatory effect of domoic acid on dentate granule cells, which show a two stage degree of staining intensity relative to dose (Peng and Ramsdell 1996) (Fig. 13.11). Strong Fos immunoreactivity in response to domoic acid is also observed in the hippocampal pyramidal cells, lateral septum, and the granule cell layer of the olfactory bulb (Peng et al. 1994; Scallet et al. 2004). These studies have also utilized Fos immunohistochemistry in parallel with cupric silver histochemistry to distinguish neuroexcitatory and neurodegenerative effects of domoic acid, which also revealed several prominent targets of domoic acid neuroexcitation that are protected from necrotic damage (Scallet et al. 1993; Peng et al. 1994; Peng and Ramsdell 1996; Scallet et al. 2004, 2005). For example, the dentate granule cells, which are likely the initial target for domoic acid, are seldomly lost to necrosis. This is likely the result of recurrent or lateral GABA inhibition on the cells. A similar mechanism also likely occurs in mitral cells of the olfactory bulb.



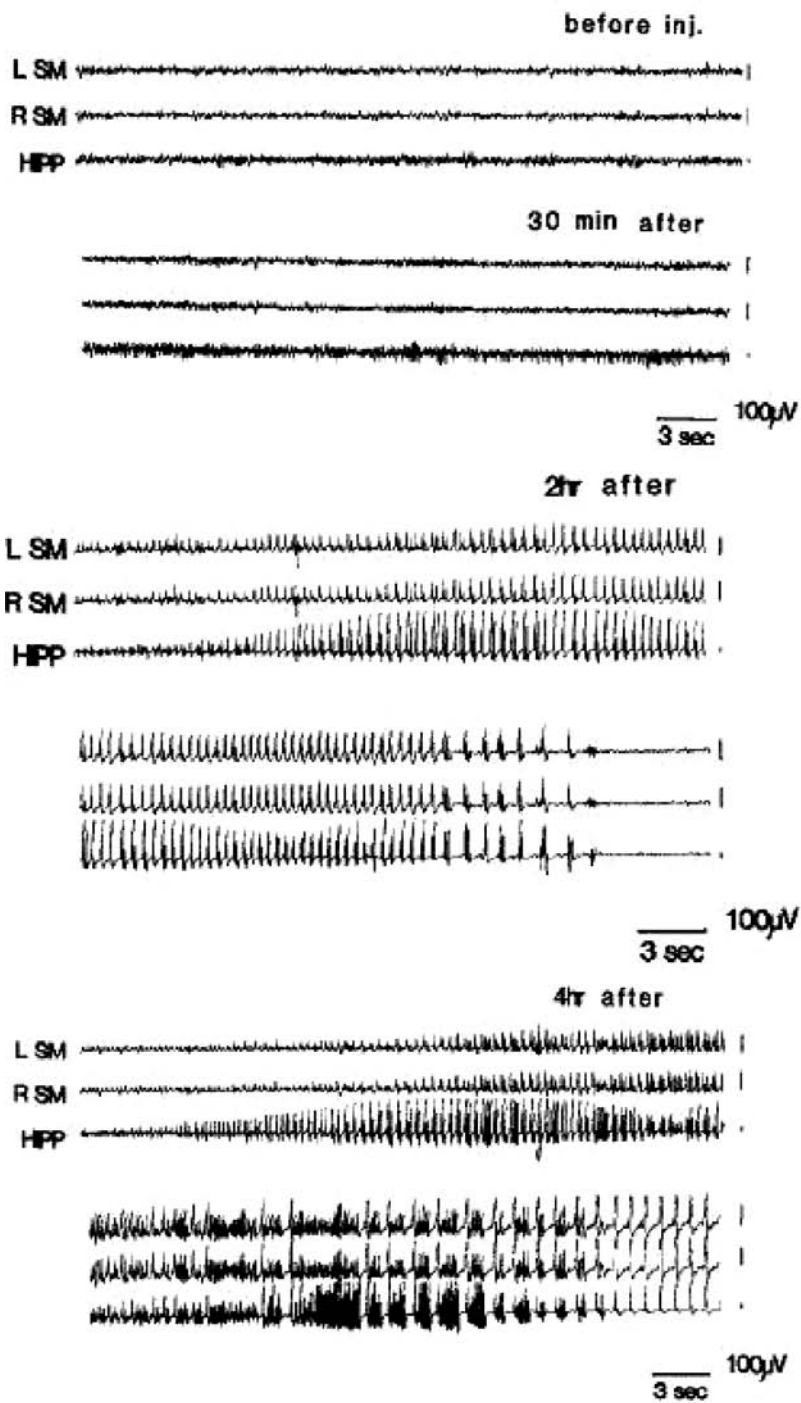


**Figure 13.10.** Domoic acid effects on EEG activity in rats. Reprinted with permission from Fujita et al. (1996), © Elsevier.

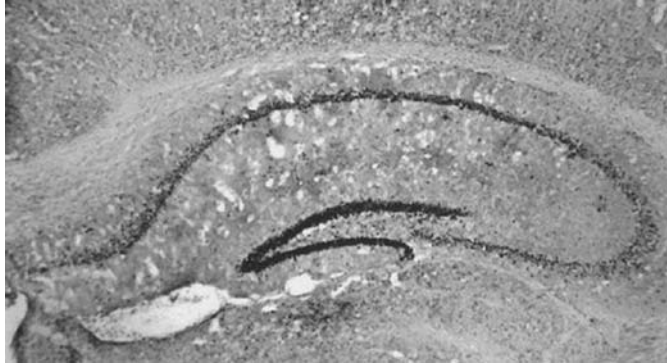


**Figure 13.11.** Domoic acid induction of Fos in the hippocampus.

Central to domoic acid excitation of the limbic system damage is the CA3 region of the hippocampus, known to have one of the highest concentrations of kainate receptors in the brain (Monaghan and Cotman 1982). Kainate receptors are found at multiple sites and serve complex roles in the CA3 region as described below. The pyramidal cells of the CA3 receive both a direct and indirect presynaptic input from entorhinal cell layers II and IV via the perforant path (Fig. 13.12). The indirect perforant input is mediated by dentate granule cells whose mossy fibers containing high densities of kainate receptors project to the CA3 pyramidal cells. Debonnel et al. demonstrated that the mossy fiber-CA3 synapses were unique within the hippocampus in showing a high degree (20-fold) of selectivity for domoic acid over kainic acid (Debonnel et al. 1989a).

The dentate granule cells are a primary target for domoic acid and show a strong induction of Fos. Careful time course studies using the pilocarpine seizure model shows Fos immunoreactivity within 15 minutes throughout the dentate granule cell layer, clearly preceding expression in other regions of the hippocampal formation (Peng and Houser 2005). Furthermore, expression of Fos in dentate granule cells precedes seizures after systemic administration of kainic acid (Willoughby et al. 1997). The induction of Fos, which is restricted to the soma, is generally considered the result of repetitive granule cell firing rather than terminal depolarization. The dentate granule cells are powerful excitatory neurons that have giant presynaptic terminals filled with glutamate. Activation of the dentate granule cells by domoic acid is likely to release massive amounts of glutamate, which in turn is toxic to the pyramidal cells. Indeed, pyramidal cells are the first reported to show morphological damage in response to systemic domoic acid (Strain and Tasker 1991). The release of glutamate is accomplished by presynaptic action of domoic acid on GluR6/KA2 heteromeric channels which provide a direct depolarization of both the axon itself and “autoreceptors,” which independently facilitate glutamate release via a cAMP-dependent protein kinase A pathway (Schmitz et al. 2001; Contractor et al. 2003; Rodriguez-Moreno and Sihra 2004). Glutamate release leads to a potentially damaging positive feedback loop of glutamate promoting its own release and hyperstimulation of the pyramidal cells. The importance of the GluR6 subunit in the process of neuroexcitation is evident in the absence of systemically induced kainic acid seizures, expression of Fos related antigen genes and damage in the CA3 region in GluR6 knockout mice (Mulle et al. 1998).

Beyond the CA3 region, many other regions of the hippocampal formation are activated in large part by links in the hippocampal circuitry. The CA4/dentate hilus mossy cells (distinct from the



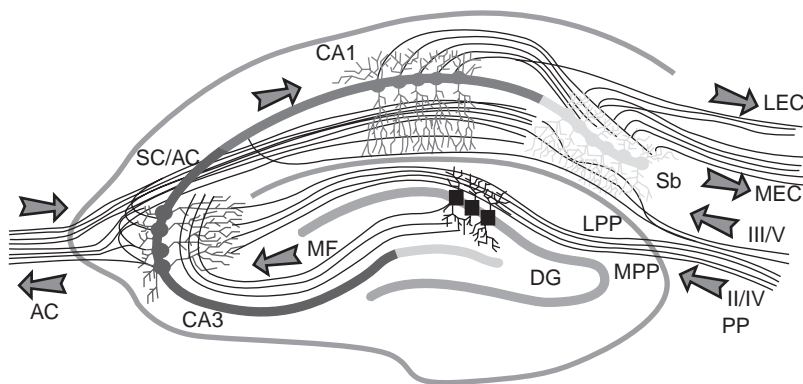


**Figure 13.12.** Afferent and efferent pathways of the hippocampus. Reprinted with permission of MRC Centre for Synaptic Plasticity, University of Bristol, © 2005.

mossy fibers of granule cells) receive projections from the dentate granule cells in a manner similar to the CA3 pyramidal cells. Additionally, the CA4/dentate hilus mossy cells are believed to integrate firing of the CA3 pyramidal cells. These CA3 pyramidal cells send Schaffer collaterals to pyramidal cells in the CA1 region, which also receive a perforate pathway from the entorhinal III layer (again refer to Fig. 13.12). The CA1 pyramidal cells project a commissural pathway to the cingulate pyramidal cells and the cingulum sends input back to the entorhinal cortex to close the loop. Furthermore, the cingulum sends input to the septal nucleus and olfactory bulb extrahippocampal areas that project back to the entorhinal cortex and amygdala, each of which respond to domoic acid with induction of Fos followed by neurodegeneration (Scallet et al. 1993; Peng et al. 1994; Scallet et al. 2004; Colman et al. 2005). Generally, excitation of these pathways is believed to result from activation of neurons proximal in the circuitry and enhanced by the returning excitatory input. However, neuroexcitation in these regions by domoic acid may also involve direct synaptic action of domoic acid to varying degrees. For example, a dose response study indicated that domoic acid induced Fos in the olfactory bulb at concentrations below those that induced Fos in the dentate granule cells (Scallet et al. 2004).

Fos histochemistry and degeneration analysis of domoic acid action in the olfactory bulb identifies granule cells of the olfactory bulb as targets of degeneration (Peng et al. 1994). The granule cells are interneurons with cell bodies just below the mitral cell layer, and dendritic trees extend through this layer to make dendrodendritic contacts (Fig. 13.13). Interestingly, granule cells are excited by release of glutamate from mitral cells (Wellis and Kauer 1993). Release of glutamate at these synapses activates postsynaptic receptors on the dendritic spines of granule cells, as well as presynaptic autoreceptors in the mitral cell membrane using a GABA mediated lateral inhibition for processing of odor discrimination (Montague and Greer 1999; Sassoe-Pognetto and Ottersen 2000; Isaacson 2001). In these respects, the interaction between glutamatergic mitral cells and granule cells of the olfactory bulb has similarities to the interaction between granule cells and CA3 pyramidal cells of the hippocampus. Accordingly, the mitral cells may represent an independent target for domoic acid excitation that involves autoreceptors for release of glutamate with a facilitating toxic action on the olfactory granule cells. The suggestion that DA action on the olfactory bulb may facilitate damage to the hippocampus is supported by the recent finding that bulbectomy actually reduces kainic acid induced damage to the hippocampus (Gary et al. 2002).

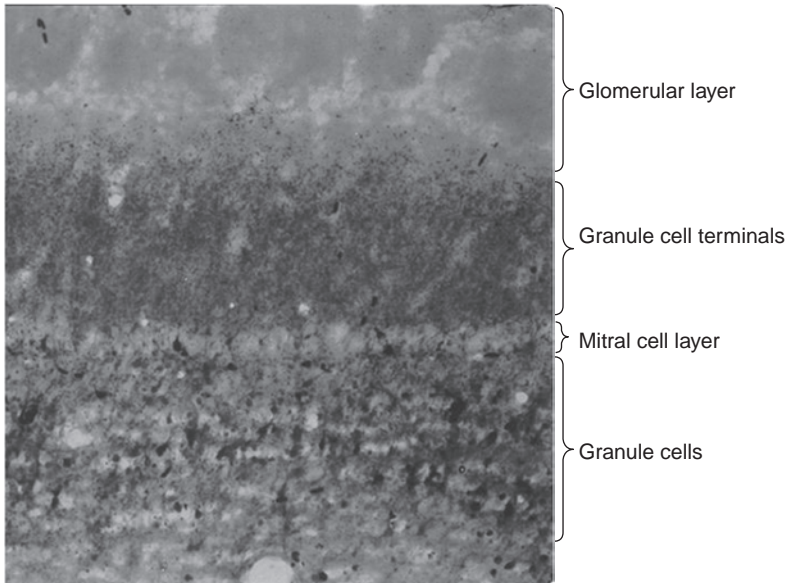


**Figure 13.13.** Domoic acid damage to olfactory bulb assessed by cupric-silver histochemistry.

### Structural Damage

*Permanent damage to the targets of glutamatergic neurons forming closed-loop circuits in the limbic system.*

Extensive structural damage to the hippocampus and limbic structures is a hallmark finding of high dose domoic acid toxicity. Damage to the central nervous system corresponds more closely to the distribution of NMDA rather than kainate receptor subtypes and is more reflective of observable seizure behavior rather than a given dosage of domoic acid (Appel et al. 1997a). Several reports indicate that the downstream action of domoic acid, like that of other excitotoxins, activates biochemical pathways associated with apoptosis, but ultimately results in necrotic neuronal cell death. Ultrastructural analysis of degenerated neurons indicates swollen morphology along with shrunken electron-dense cells characteristic of necrotic neurons (Strain and Tasker 1991; Ananth et al. 2001). Analyses of caspase-3, an enzyme used as a functional marker of apoptosis, by immunohistochemistry or enzymatic activity, have failed to show induction of apoptosis by domoic acid in the hippocampus or in cultured hippocampal cells (Ananth et al. 2001; Roy and Sapolsky 2003); however, caspase-3 activity has been reported to be enhanced in a hippocampal slice preparation (Erin and Billingsley 2004). Interestingly, the study on hippocampal cells indicates that two caspase inhibitors reduce cytotoxic effects of domoic acid and lower mitochondrial membrane potential and ATP levels (Roy and Sapolsky 2003). Another apoptotic marker named Bcl-2, a pore forming protein that shuttles to mitochondria and endoplasmic reticulum to deplete internal stores of calcium (Schendel et al. 1997), is induced early on by domoic acid but is later down regulated, corresponding with necrosis (Ananth et al. 2001; Erin and Billingsley 2004). Domoic also leads to rapid and strong activation of astrocytes, which has been well documented by immunohistochemistry of glial fibrillary acidic proteins (Stewart et al. 1990; Strain and Tasker, 1991; Appel et al. 1997a; Ananth et al. 2003a; Scallet et al. 2005) and benzodiazepine receptor

expression (Kuhlmann and Guilarte 1997). The astrocytes normally show an extensive response because of their syncytial network. This network serves to protect neurons through glutamate uptake,  $K^+$  buffering, and elimination of free radicals; all functions that are susceptible to excitotoxic damage and one that can turn toxic through release of glutamate and production of free radicals (Ananth, Gopalakrishnakone, and Kaur 2003). Domoic toxicity also leads to an inflammatory response of microglia cells, which has been documented by lectin histochemistry, as well as immunohistochemistry of CR3 phagocytic receptors and MHC II antigens (Appel et al. 1997a; Ananth et al. 2001). These effects appear subsequent to neuronal damage and relate to the processing of neuronal antigens and phagocytosis of damaged neuronal debris.

Post mortem analyses of four subjects from the 1987 exposure identified consistent damage in all hippocampal fields, other than the CA2 equivalent, as well as damage to the amygdala, septum, secondary olfactory areas, claustrum, and nucleus acumbens. Three of the patients had damage to the dentate granule cells and insular and subfrontal cortex while two had damage in the dorsal medial thalamus (Teitelbaum et al. 1990). Expanded analysis was reported of a fifth patient three years after the event. This patient, who recovered and then exhibited temporal lobe epilepsy one year later, was found to have “a complete neuronal loss in CA1 and CA3 with near total loss in CA4 and moderate loss in CA2. Dentate cells were focally diminished in numbers. The amygdala showed patch neuronal loss in medial and basal portions with neuronal loss and gliosis in the overlying cortex. Mild to moderate neuronal loss and gliosis were seen in the dorsal and ventral septal nuclei, the secondary olfactory areas and the nucleus accumbens” (Cendes et al. 1995). Histopathological analysis of the 1998 sea lion epizootic showed many similarities to the human study, with major damage to the hippocampus, dentate gyrus, amygdala and limbic regions, including the olfactory bulb (Silvagni et al. 2005). The pathology of human and marine mammal exposures has been largely consistent with more detailed analyses in laboratory animals (Stewart et al. 1990; Tryphonas et al. 1990a, 1990b; Bruni et al. 1991; Strain and Tasker 1991; Scallet et al. 1993; Peng et al. 1994; Schmued et al. 1995; Appel et al. 1997b); however, some differences are observed due to the steep dose threshold, response time post-exposure for analysis and differential effects on various brain cell types, neurons, astrocytes and microglia (Peng et al. 1994; Schmued et al. 1995; Appel et al. 1997a).

Fine resolution of neuronal damage in response to domoic acid has been characterized with the DeOlmos cupric-silver method (DeOlmos and Ingram 1971) in mice (Peng et al. 1994), rats (Appel et al. 1997a), and cynomolgus monkeys (Scallet et al. 1993; Schmued et al. 1995). These studies led to the clarification of brain regions showing neuronal damage and provided discrimination of damaged cell bodies, axons and dendritic fields. Scallet noted widespread damage to pyramidal neurons and axon terminals of CA4, CA3, CA2, CA1, and subiculum subfields of the monkey hippocampus (Scallet et al. 1993). A more extensive analysis of these samples indicated neuronal damage to a subset of subicular targets including hippocampus, septum, dorsal lateral nucleus of the thalamus and the piriform and entorhinal cortex (Schmued et al. 1995). A similar study in mice reported extensive domoic acid damage to the hippocampus, septum and secondary olfactory regions (Peng et al. 1994). An extensive analysis involving the mapping of cupric silver impregnated cells, axons, and dendritic fields has been performed and these data were reconstructed into a three dimensional image of the mouse brain (Colman et al. 2005).

### **Functional Effects**

*Outcome of damage to pathways responsible for controlling generalized seizures and the learning and recall of spatial memory.*

The loss of neurological function after domoic acid exposure may manifest in the development of epilepsy and in deficits of learning and memory. Although structural damage to hippocampal pyramidal cells and many of their projections in the limbic circuit is an obvious factor in loss of function, much attention is also directed to the dentate granule cells themselves, a primary target of domoic acid neuroexcitation which are largely resistant to overt structural damage.

A one year followup of a patient from the 1987 poisoning indicated reoccurrence of seizures and the development of epilepsy (Cendes et al. 1995). This patient initially showed generalized convulsions, complex partial status epilepticus and epileptiform discharges developing to slow wave abnormalities over the frontotemporal regions. One year later, after EEG activity had been normal for several months, complex partial seizures reoccurred, with bilateral EEG activity over temporal lobes and a MRI indicative of bilateral atrophy of the hippocampus, which was confirmed postmortem as hippocampal sclerosis. This case report provides rare evidence of toxin induced epilepsy in humans and is well supported by the rat kainic acid epilepsy model (Ben-Ari 1985).

Dentate cells are not only at the heart of the acute action of domoic acid to induce seizures but are also implicated in the sustained effect of temporal lobe epilepsy development. In this capacity, the dentate has been viewed as a restrictive gate or control point preventing excitation of other hippocampal regions (Heinemann et al. 1992; Lothman et al. 1992). Although dentate granule cells are strongly excitatory to many target cells, they follow Eccles hypothesis of lateral inhibition, yielding focused excitation well delineated by GABAergic inhibition via collaterals and interneurons. Indeed, these cells show a strong domoic acid induced excitatory response but rarely show signs of degeneration (Scallet et al. 1993; Peng et al. 1994), with the unusual exception noted in sea lions (Silvagni et al. 2005).

Hippocampal sclerosis is regularly accompanied by extensive neurodegeneration in the CA4 region, also known as at the dentate hilus. The cells affected are known as mossy cells. Like the CA3 pyramidal cells, the mossy cells of CA4 receive a branch of large glutamatergic excitatory mossy fibers originating from the dentate granule cells. Hence, the mossy cells are highly vulnerable to dentate granule cell excitation in much the same way as the CA3 pyramidal cells. The mossy cells project back to the dentate molecular layer to excite GABAergic interneurons that inhibit granule cells and do so in a way that projects laterally to inhibit beyond their lamellar plane. One causal theory of temporal lobe epilepsy is that degeneration of mossy cells will cause disinhibition of wide tracks of dentate granule cells, leading to synchronous multilaminar discharges in response to cortical stimuli (Sloviter 1994). This theory has been challenged by findings that mossy cell lesions failed to induce an epileptic state. An alternative theory is that several days to weeks after excitation, dentate granule cells undergo new axonal sprouting, changing GABAergic inhibitory connections to excitatory connections between granule cells (Buckmaster et al. 2002). Regardless of the mechanism, domoic acid does lead to damaged cells in the CA4 region and extensive loss of terminals in the molecular layer of the dentate gyrus (Colman et al. 2005), both of which may provide a basis for the toxin induced epilepsy.

Domoic acid induced damage to the hippocampal formation is strongly correlated to memory deficits in humans and experimental animals. The predominant neurological manifestation from the human amnesic shellfish poisoning event is anterograde memory loss (Teitelbaum et al. 1990; Zatorre 1990). The effects observed in humans revealed a substantial degree of selectivity. Language function (assessed by an Object Naming test), verbal comprehension (assessed by the Token test) and concept formation (assessed with the Wisconsin Card Sorting test) were within normal range. Verbal (Wechsler Memory Scale) and visuospatial (Rey complex figure test) memory were both impaired, but only for delayed recall and not immediate recall (Teitelbaum et al. 1990). Hence, the

memory deficit appeared to involve retention and/or retrieval of new information after the subject had passed out of consciousness (Zatorre 1990). Experimental studies using rats and mice have also assessed memory loss following domoic acid exposure. Several studies have been conducted on domoic acid's effects on visuospatial memory, and have reported deficits using both radial arm maze and Morris water maze tests (Sutherland et al. 1990; Nakajima and Potvin 1992; Petrie et al. 1992; Kuhlmann and Guilarte 1997). Domoic acid has also been reported to impair a delayed matching-to-sample working memory water maze task, another type of memory test based upon the ability to utilize mental representation for goal-directed behaviors (Clayton et al. 1999). This test depended on intact hippocampal formation as well as its connections with the prefrontal cortex.

Domoic acid targets neuronal pathways and synaptic mechanisms along with biochemical mechanisms known to mediate memory and learning. The hippocampus and the temporal lobe, so strongly implicated in seizure formation, were also discovered to play an essential role in short term declarative memory, as evident in the anterograde amnesia that developed after surgical ablation of this region in the noted epileptic patient H.M. (Scoville and Miller 1957). It appears that the key role of the hippocampus in spatial learning is the synthesis of the configuration of spatial cues, a process requiring the integrity of connections between the hippocampus, subiculum, and cortical areas. The discovery of long term potentiation (LTP) in the dentate granule cells after perforant path stimulation identified a mechanism for synaptic strengthening that is consistent with ultrastructural changes for memory formation (Bliss and Collingridge 1993). The critical event initiating the LTP is the entry of calcium into the postsynaptic spine, an event that often involves the coincident activation of the NMDA receptor by glutamate and membrane depolarization. The calcium influx through NMDA is detected by calcium-calmodulin dependent protein kinase II, which translocates from the cytoplasm to bind the NMDA receptor, where it undergoes autophosphorylation generating an "intramolecular memory." Calcium-calmodulin-activated adenylate cyclase is an additional detector for NMDA mediated calcium entry and leads to activation of the cAMP-dependent protein kinase A pathways. An important result of activation of these kinase pathways is the "AMPAfication" of the postsynaptic density, which occurs from enhancement of AMPA receptor conductance via phosphorylation mediated changes in conductance and increased biosynthesis and/or recruitment to the postsynaptic membrane (Shi 2001). Increased AMPA conductance is key to strengthening transmission across defined synapses.

The biochemical mechanism by which domoic acid causes memory deficits is not clear. One obvious mechanism would be due to cell loss resulting from excitotoxic damage to the pathways needed for memory formation. However, studies of aging (Rapp and Gallagher 1996) and observation of domoic acid memory impairment without evidence of damage to cells or terminals in the hippocampus (Rapp and Gallagher 1996; Clayton et al. 1999) indicates that neurodegeneration is not a prerequisite to memory deficit. Alternatively, the adverse effects on memory may involve ultrastructural reorganization of dendritic connections within the dentate gyrus that follows excitation of granule cells as described for the etiology of epilepsy. In this regard, the reciprocal circuitry between the dentate granule cells, mossy cells, and the CA3 pyramidal cells is essential for auto and heteroassociative memories that underlie both the learning and recall of sequences believed critical for visual spatial memory (Lisman et al.). Effects on the synaptic plasticity of these dentate-CA3 circuits, impairing AMPAfication, would disrupt the generation of delayed spatial memory. Beyond terminal damage and resprouting of excitatory, in place of inhibitory, contacts, changes in physical characteristics of the postsynaptic membrane may result from acute inflammatory responses to domoic acid. Neuronal COX-2 is rapidly induced by domoic acid (Ryan et al. 2005). This enzyme is regulated by neuronal activity, is expressed at its highest levels in dentate granule cells and associated with the



development of LTP (Yamagata et al. 1993). COX-2 expression potentiates kainic acid excitotoxicity and age-induced deficits in spatial learning, as evidenced in mice in a Morris water maze (Kelley et al. 1999; Andreasson et al. 2001). The production of prostaglandins by COX-2 and production of cytokines during inflammation are likely to impair enhancement of plasticity at both sides of the synapse, thus decreasing glutamate content in mossy fibers or altering AMPAfication of the pyramidal cell terminals.

### *Toxicity to Other Regions of the Nervous System*

#### *Excitotoxic effects on the gut, heart and spinal motoneurons.*

The human ASP exposure of 1987 identified gastrointestinal and neurological effects of domoic acid. The gastrointestinal effects included severe vomiting, nausea, abdominal cramping, and diarrhea. These symptoms were the most commonly reported and occurred at lower levels of intoxication (Perl et al. 1990). Likewise, studies with primates show a gagging and vomiting response which is associated with cell swelling and damage to the emetic center, the area postrema (Tryphonas et al. 1990a). A subsequent study utilizing Fos histochemistry determined that domoic acid induced Fos in both the area postrema as well as in the adjacent nucleus solitarius without neuronal damage, as assessed by degeneration specific cupric silver histochemistry (Peng et al. 1994). The effect of domoic acid on Fos in the nucleus solitarius was restricted to the medial division subnucleus. This subnucleus area regulates general visceral function and is proposed to mediate gastrointestinal symptoms of domoic acid such as abdominal cramping. The human exposure also reported gastrointestinal bleeding, and studies in mice have also shown evidence of gastric and duodenal lesions and bleeding (Glavin et al. 1990).

The human exposure of 1987 also identified cardiac instability and arrhythmias as symptoms of amnesic shellfish poisoning (Perl et al. 1990). Although this response might be attributed to effects on the brainstem, domoic acid does induce c-fos in the heart of mice (Peng et al. 1994). Subsequently, Pulido's laboratory has characterized glutamate receptors in the conduction system of the rat and monkey heart and provided evidence of GluR5/6/7 and NMDAR1 subtypes that can mediate a neurotoxic action of domoic acid (Gill et al. 2000; Mueller et al. 2003). Evidence for lesions to the myocardium and myocarditis has been reported in sea lions exposed to domoic acid (Gulland et al. 2002), while domoic acid has also been proposed as a risk factor for myocarditis and dilated cardiomyopathy in sea otters (Kreuder et al. 2005).

Domoic acid is well recognized to target spinal cord motoneurons (Biscoe et al. 1975, 1976). Domoic acid effects on ventral horn motoneurons have been characterized by perfusion in isolated spinal cord (Ishida and Shinozaki 1988). This is consistent with muscle weakness observed in several patients from the 1987 exposure and is manifest as hemiparesis (Teitelbaum et al. 1990). Additionally, domoic acid activates dorsal horn sensory C fibers and their dorsal root ganglion cells with greater potency than observed in the central nervous system (Huettner 1990; Ishida and Shinozaki 1991). Here the effects show evidence of different glutamate receptors. Agonist rank order of potency and efficacy of conduction as a full agonist with high currents which desensitize may reflect an action on AMPA receptors. Neurotoxic action of domoic acid at the anterior horn or dorsal root ganglion is consistent with electromyographic and concentric needle examination results from patients from the 1987 exposure. Up to four months post exposure, these tests showed degenerative changes suggestive of spinal column effects at the level of the anterior horn or dorsal root (Teitelbaum et al. 1990). Domoic acid has reported to have neurotoxic action on both dendritic structures in the dorsal horn and ventral motoneurons based upon perfusion studies with isolated cord (Stewart et al. 1991).

A systemic exposure of neonatal rats identified damaged neurons were largely in the ventral and intermediate gray matter (Wang et al. 2000). Accordingly, domoic acid can cause excitation and damage to sensory and motorneurons in the spinal cord.

The eye is also a target for domoic acid toxicity. Indeed the seminal observation for the glutamate excitotoxicity hypothesis originated in observations of glutamate damage to the inner retinal layer in newborn mice (Lucas and Newhouse 1957). Domoic acid has been demonstrated to cause swelling of outer plexiform and inner plexiform layers and cellular damage to the inner nuclear layer of the retina, both in chick retinal explants and after systemic administration of domoic acid in mice (Stewart et al. 1990; Tryphonas et al. 1990b). The effects of domoic acid on cultured chick retinal cells are consistent with calcium mediated effects of neuroexcitation (Alfonso et al. 1994; Duran et al. 1995b); however, evidence exists that at least some of the actions of domoic acid in the retina are mediated by AMPA receptors (Ferreira et al. 1998; Szikra and Witkovsky 2001). Muscle weakness was observed in several patients from the 1987 exposure, manifested as ophthalmoplegia, and therefore consistent with domoic acid causing excitation and damage to motor neurons innervating the eye (Teitelbaum et al. 1990).

### *Age- and Sex-Related Toxicity*

*Risk to domoic acid poisoning may also reflect status of neuroprotective mechanisms.*

The most severe cases of human amnesic shellfish poisoning occurred in males of advanced age, which originally suggested that age and sex are predisposing factors (Perl et al. 1990). However, the age-related predisposition is, at least in part, the result of renal impairment (Teitelbaum et al. 1990) and is supported by several experimental studies (Suzuki and Hierlihy 1993; Truelove and Iverson 1994; Xi et al. 1997). Nonetheless, advanced age may enhance susceptibility in other ways to domoic acid. Electric field potential analysis of hippocampal slices determined that aged rats differed from younger rats in that they did not exhibit preconditioned tolerance to domoic acid (Kerr et al. 2002). This was interpreted that the older rats may be deficient in neuroprotective mechanisms.

The sea lion epizootic revealed substantial domoic reproductive toxicity manifest in spontaneous abortion (Gulland et al. 2002). Part of this is likely the result of uterine excitation, as evident in lesions and protrusions to the uterine wall, and might represent a synergy between domoic acid and oxytocin. On the other hand, a rat neonatal study of daily in utero domoic acid exposure between gestational days 7–16 failed to show a consistent decrease in litter size, even in surviving dams given a LD50 dose (Khera et al. 1994). However, in utero exposure of rats to subsymptomatic doses of domoic acid has been demonstrated to reduce seizure threshold to postnatal domoic acid exposure. This is associated with delayed damage at postnatal day (PND) 14 to the CA3 and dentate gyrus, damage at PND 20 to the CA4 and decreased brain GABA/increased glutamate levels (Dakshinamurti et al. 1993). The alteration in brain GABA/glutamate levels is consistent with the change from GABA to glutaminergic regulation of dentate granule cells which is suggested to result from damage to CA4 mossy cells in the proposed etiology of epilepsy. Intrauterine exposure to domoic acid also increases susceptibility of rats grown to adults to the amnesic effects of the muscarinic acetylcholine scopolamine, suggesting that early life exposure to domoic acid reduces functional reserve with which to solve memory tasks (Levin et al. 2005). Additionally, these animals lacked the normal sex difference in spatial learning, suggesting that domoic acid disrupts an early hormone imprinting of differences in the hippocampus that manifest later in life.

Neonatal rats are substantially more susceptible to domoic acid than adults, showing signs of seizure behavior that progressively matures to the characteristic patterns observed in adults (Xi et al. 1997;



Doucette et al. 2000). At lower doses neonates show delayed effects on eye opening and olfactory conditioned place preference (Doucette et al. 2003). The latter supports the high sensitivity of the mitral-granule cells to domoic acid as described earlier. Evidence indicates that the sensitivity of the neonates results from insufficient renal clearance of toxin, allowing increased bioavailability in the blood (Xi et al. 1997). Domoic acid has been detected in the blood of neonates, transmitted via milk from lactating mother rats previously exposed to domoic acid, but at levels appearing to be well below symptomatic doses (Maucher and Ramsdell 2005).

Differential age- and sex-related sensitivity to domoic acid may also involve mechanisms that limit damage after toxin exposure. Possible protective pathways may counteract domoic acid induced release of glutamate and nitric oxide from neurons or microglia, such as those pathways sensitive to pyridoxine and the antioxidant neurohormone melatonin (Ananth, Gopalakrishnakone, and Kaur 2003; Dakshinamurti et al. 2003). Perhaps most intriguing of all is the neuroprotective role of estrogen. Using castrated mice, aromatase knockout mice, and the aromatase inhibitor fadrozole, Azcoitia et al. (2001) convincingly demonstrated that manipulations which reduce brain estrogens greatly enhance sensitivity to domoic acid induced damage to the hippocampus. Hence, the integrity of neuroprotective mechanisms may play an important role in defining susceptibility to domoic acid at both the level of brain regions and individual characteristics such as age and sex.

## Disclaimer

This chapter does not constitute an endorsement of any commercial product or intend to be an opinion beyond scientific or other results obtained by the National Oceanic and Atmospheric Administration (NOAA). No reference shall be made to NOAA, or this publication furnished by NOAA, to any advertising or sales promotion which would indicate or imply that NOAA recommends or endorses any proprietary product mentioned herein, or which has as its purpose an interest to cause the advertised product to be used or purchased because of this publication.

## References

- Alfonso, M., Duran, R., and Duarte, C.B. 1994. Domoic acid induced release of [3H]GABA in cultured chick retina cells. *Neurochem Internat* 24, 267–274.
- Ananth, C., Dheen, S.T., Gopalakrishnakone, P., and Kaur, C. 2001. Domoic acid-induced neuronal damage in the rat hippocampus: changes in apoptosis related genes (Bcl-2, Bax, Caspase-3) and microglial response. *J Neurosci Res* 66, 177–190.
- . 2003. Distribution of NADPH-diaphorase and expression of nNOS, N-methyl-D-aspartate receptor (NMDAR1) and non-NMDA glutamate receptor (GlutR2) genes in the neurons of the hippocampus after domoic acid-induced lesions in adult rats. *Hippocampus* 13, 260–272.
- Ananth, C., Gopalakrishnakone, P., and Kaur, C. 2003. Protective role of melatonin in domoic acid-induced neuronal damage in the hippocampus of adult rats. *Hippocampus* 13, 375–387.
- Andreasson, K.I., Savonenko, A., Vidensky, S., Goellner, J. J., Zhang, Y., Shaffer, A., Kaufmann, W. E., Worley, P. F., Isakson, P. and Markowska, A. L., 2001. Age-Dependent Cognitive Deficits and Neuronal Apoptosis in Cyclooxygenase-2 Transgenic Mice. *J Neurosci* 21, 8198–8209.
- Appel, N.M., Rapoport, S.I. and O'Callaghan, J.P. 1997a. Sequelae of parenteral domoic acid administration in rats: comparison of effects on different anatomical markers in brain. *Synapse* 25, 350–358.
- Appel, N.M., Rapoport, S.I., O'Callaghan, J.P., Bell, J.M., and Freed, L.M. 1997b. Sequelae of parenteral domoic acid administration in rats: comparison of effects on different metabolic markers in brain. *Brain Res* 754, 55–64.
- Auer, R.N. 1991. Excitotoxic mechanisms, and age-related susceptibility to brain damage in ischemia, hypoglycemia and toxic mussel poisoning. *Neurotoxicology* 12, 541–546.

- Azcoitia, I., Sierra, A., Veiga, S., Honda, S., Harada, N., and Garcia-Segura, L.M. 2001. Brain aromatase is neuroprotective. *J Neurobiol* 47, 318–329.
- Bates, S.S. 2003. Domoic acid and Pseudo-nitzschia References. Department of Fisheries and Oceans Canada.
- Ben-Ari, Y. 1985. Limbic seizure and brain damage produced by kainic acid: mechanisms and relevance to human temporal lobe epilepsy. *Neuroscience* 14, 375–403.
- Berman, F.W., LePage, K.T., and Murray, T.F. 2002. Domoic acid neurotoxicity in cultured cerebellar granule neurons is controlled preferentially by the NMDA receptor Ca(2+) influx pathway. *Brain Res* 924, 20–29.
- Berman, F.W., and Murray, T.F. 1996. Characterization of glutamate toxicity in cultured rat cerebellar granule neurons at reduced temperature. *J Biochem Toxicol* 11, 111–119.
- . 1997. Domoic acid neurotoxicity in cultured cerebellar granule neurons is mediated predominantly by NMDA receptors that are activated as a consequence of excitatory amino acid release. *J Neurochem* 69, 693–703.
- Biscoe, T.J., Evans, R.H., Headley, P.M., Martin, M., and Watkins, J.C. 1975. Domoic and quisqualic acids as potent amino acid excitants of frog and rat spinal neurones. *Nature* 255, 166–167.
- . 1976. Structure-activity relations of excitatory amino acids on frog and rat spinal neurones. *Br J Pharmacol* 58, 373–382.
- Bliss, T.V., and Collingridge, G.L. 1993. A synaptic model of memory: long-term potentiation in the hippocampus. *Nature* 361, 31–39.
- Bowie, D., and Lange, G.D. 2002. Functional Stoichiometry of Glutamate Receptor Desensitization. *J Neurosci* 22, 3392–3403.
- Brown, J.A., and Nijjar, M.S. 1995. The release of glutamate and aspartate from rat brain synaptosomes in response to domoic acid (amnesic shellfish toxin) and kainic acid. *Mol Cell Biochem* 151, 49–54.
- Bruni, J.E., Bose, R., Pinsky, C., and Glavin, G. 1991. Circumventricular organ origin of domoic acid-induced neuropathology and toxicology. *Brain Res Bull* 26, 419–424.
- Buckmaster, P.S., Zhang, G.F., and Yamawaki, R. 2002. Axon Sprouting in a Model of Temporal Lobe Epilepsy Creates a Predominantly Excitatory Feedback Circuit. *J Neurosci* 22, 6650–6658.
- Cendes, F., Andermann, F., and Carpenter, S. 1995. Temporal lobe epilepsy caused by domoic acid intoxication: evidence for glutamate receptor-mediated excitotoxicity in humans. *Annals Neurology* 37, 123–126.
- Choi, D.W. 1994. Glutamate receptors and the induction of excitotoxic neuronal death. *Prog Brain Res* 100, 47–51.
- Clayton, E.C., Peng, Y.-G., and Ramsdell, J.S. 1999. Working memory deficits induced by single but not repeated exposures to domoic acid. *Toxicol* 37, 1025–1039.
- Colman, J.R., Nowocin, K.J., Switzer, R.C., Trusk, T.C., and Ramsdell, J.S. 2005. Mapping and reconstruction of domoic acid-induced neurodegeneration in the mouse brain. *Neurotoxicol Teratol*.
- Contractor, A., Sailer, A.W., Darstein, M., Maron, C., Xu, J., Swanson, G.T., and Heinemann, S.F. 2003. Loss of Kainate Receptor-Mediated Heterosynaptic Facilitation of Mossy-Fiber Synapses in KA2-/- Mice. *J Neurosci* 23, 422–429.
- Daigo, K. 1959a. Studies on the Constituents of Chondria armata. I. Detection of the Anthelmintical Constituents. *J Pharm Soc Japan* 79, 350–353.
- . 1959b. Studies on the Constituents of Chondria armata. II. Isolation of an Anthelmintical Constituent. *J Pharm Soc Japan* 79, 353–356.
- Dakshinamurti, K., Sharma, S.K., and Geiger, J.D. 2003. Neuroprotective actions of pyridoxine. *Biochim Biophys Acta* 1647, 225–229.
- Dakshinamurti, K., Sharma, S.K., Sundaram, M., and Watanabe, T. 1993. Hippocampal changes in developing postnatal mice following intrauterine exposure to domoic acid. *J Neurosci* 13, 4456–4495.
- Debonnel, G., Beauchesne, L., and de Montigny, C. 1989a. Domoic acid, the alleged “mussel toxin,” might produce its neurotoxic effect through kainate receptor activation: an electrophysiological study in the dorsal hippocampus. *Can J Physiol Pharmacol* 67, 29–33.
- Debonnel, G., Weiss, M., and de Montigny, C. 1989b. Reduced neuroexcitatory effect of domoate following mossy fibre denervation of the rat dorsal hippocampus: further evidence that toxicity of domoic acid involves kainate receptor activation. *Can J Physiol Pharmacol* 67, 904–908.
- DeOlmos, J.S., and Ingram, W.R. 1971. An improved cupric-silver method for impregnation of axonal and terminal degeneration. *Brain Res* 33, 523–529.
- Doucette, T.A., Bernard, P.B., Yuill, P.C., Tasker, R.A., and Ryan, C.L. 2003. Low doses of non-NMDA glutamate receptor agonists alter neurobehavioural development in the rat. *Neurotoxicology and Teratology* 25, 473.
- Doucette, T.A., Strain, S.M., and Tasker, R.A.R. 2000. Comparative behavioural toxicity of domoic acid and kainic acid in neonatal rats. *Neurotoxicol Teratol* 22, 863–869.
- Dragunow, M., Peterson, M.R., and Robertson, H.A. 1987. Presence of c-fos-like immunoreactivity in the adult rat brain. *Eur J Pharmacol* 135, 113–114.

- Dragunow, M., and Robertson, H.A. 1987. Kindling stimulation induces c-fos protein(s) in granule cells of the rat dentate gyrus. *Nature* 329, 441–442.
- Duran, R., Arufe, M.C., Arias, B., and Alfonso, M. 1995a. Effect of domoic acid on brain amino acid levels. *Rev Esp Fisiol* 51, 23–27.
- Duran, R., Reis, R.A., Almeida, O.M., de Mello, M.C., and de Mello, F.G. 1995b. Domoic acid induces neurotoxicity and ip3 mobilization in cultured cells of embryonic chick retina. *Braz J Med Biol Res* 28, 100–107.
- Erin, N., and Billingsley, M.L. 2004. Domoic acid enhances Bcl-2-calcineurin-inositol-1,4,5-trisphosphate receptor interactions and delayed neuronal death in rat brain slices. *Brain Research* 1014, 45.
- Ferreira, I.L., Duarte, C.B., and Carvalho, A.P. 1998. Kainate-induced retina amacrine-like cell damage is mediated by AMPA receptors. *Neuroreport* 9, 3471–3475.
- Fujita, T., Tanaka, T., Yonemasu, Y., Cendes, F., Cashman, N.R., and Andermann, F. 1996. Electroclinical and pathological studies after parenteral administration of domoic acid in freely moving nonanesthetized rats: an animal model of excitotoxicity. *J Epilepsy* 9, 87–93.
- Gary, D.S., Getchell, T.V., Getchell, M.L., and Mattson, M.P. 2002. Olfactory bulbectomy protects hippocampal pyramidal neurons against excitotoxic death. *Exp Neurol* 176, 266–268.
- Gill, S.S., Mueller, R.W., McGuire, P.F., and Pulido, O.M. 2000. Potential target sites in peripheral tissues for excitatory neurotransmission and excitotoxicity. *Toxicol Pathol* 28, 277–284.
- Glavin, G.B., Pinsky, C., and Bose, R. 1989a. Mussel poisoning and excitatory amino acid receptors. *Trends Pharmacol Sci* 10, 15–16.
- . 1989b. Toxicology of mussels contaminated by neuroexcitant domoic acid. *Lancet* 336, 506–507.
- . 1990. Domoic acid-induced neurovisceral toxic syndrome: characterization of an animal model and putative antidotes. *Brain Res Bull* 24, 701–703.
- Grimmelt, B., Nijjar, M. S., Brown, J., MacNair, N., Wagner, S., Johnson, G.R., and Amend, J.F. 1990. Relationship between domoic acid levels in the blue mussel (*Mytilus edulis*) and toxicity in mice. *Toxicol* 28, 501–508.
- Gulland, F.M., Haulena, M., Fauquier, D., Langlois, G., Lander, M.E., Zabka, T., and Duerr, R. 2002. Domoic acid toxicity in Californian sea lions (*Zalophus californianus*): clinical signs, treatment and survival. *Vet Rec* 150, 475–480.
- Hampson, D.R., Huang, X.P., Wells, J.W., Walter, J.A., and Wright, J.L. 1992. Interaction of domoic acid and several derivatives with kainic acid and AMPA binding sites in rat brain. *Eur J Pharmacol* 218, 1–8.
- Heinemann, U., Beck, H., Dreier, J.P., Ficker, E., Stabel, J., and Zhang, C.L. 1992. The dentate gyrus as a regulated gate for the propagation of epileptiform activity. *Epilepsy Res Suppl* 7, 273–280.
- Holland, P.T., Selwood, A.I., Mountfort, D.O., Wilkins, A.L., McNabb, P., Rhodes, L.L., Doucette, G.J., Mikulski, C.M., and King, K.L. 2005. Isodomoic acid C, an unusual amnesic shellfish poisoning toxin from *Pseudo-nitzschia australis*. *Chem Res Toxicol* 18, 814–816.
- Huettnner, J.E. 1990. Glutamate receptor channels in rat DRG neurons: activation by kainate and quisqualate and blockade of desensitization by Con A. *Neuron* 5, 255–266.
- Hynie, I., and Todd, E.C.D. 1990. Proceedings of a symposium on domoic acid toxicity. *Can Diseases Weekly Rep* 16, 1–123.
- Isaacson, J.S. 2001. Mechanisms governing dendritic [gamma]-aminobutyric acid (GABA) release in the rat olfactory bulb. *Proceedings of the National Academy of Sciences of the United States of America* 98, 337.
- Ishida, M., and Shinozaki, H. 1988. Acromelic acid is a much more potent excitant than kainic acid or domoic acid in the isolated rat spinal cord. *Brain Res* 474, 386–389.
- . Novel kainate derivatives: potent depolarizing actions on spinal motoneurons and dorsal root fibres in newborn rats. *Br J Pharmacol* 104, 873–878.
- Iverson, F., Truelove, J., Nera, E., Tryphonas, L., Campbell, J., and Lok, E. 1989. Domoic acid poisoning and mussel-associated intoxication: preliminary investigations into the response of mice and rats to toxic mussel extract. *Food Chem Toxicol* 27, 377–384.
- . 1990. The toxicology of domoic acid administered systematically to rodents and primates. *Canada Diseases Weekly Report* 16S1E, 15–19.
- Kelley, K.A., Ho, L., Winger, D., Freire-Moar, J., Borelli, C.B., Aisen, P.S., and Pasinetti, G.M. 1999. Potentiation of Excitotoxicity in Transgenic Mice Overexpressing Neuronal Cyclooxygenase-2. *Am J Pathol* 155, 995–1004.
- Kerr, D.S., Razak, A., and Crawford, N. 2002. Age-related changes in tolerance to the marine algal excitotoxin domoic acid. *Neuropharmacology* 43, 357–366.
- Khera, K.S., Whalen, C., Angers, G., and Arnold, D.L. 1994. Domoic acid: a teratology and homeostatic study in rats. *Bull Environ Contam Toxicol* 53, 18–24.
- Kim, C.S., Ross, I.A., Sberg, J.A., and Preston, E. 1998. Quantitative low-dose assessment of seafood toxin, domoic acid, in the rat brain: application of physiologically-based pharmacokinetic (PBPK) modeling. *Environ Toxicol Pharmacol* 6, 49–58.

- Kreuder, C., Miller, M.A., Lowenstine, L.J., Conrad, P.A., Carpenter, T.E., Jessup, D.A., and Mazet, J.A. 2005. Evaluation of cardiac lesions and risk factors associated with myocarditis and dilated cardiomyopathy in southern sea otters (*Enhydra lutris nereis*). *Am J Vet Res* 66, 289–299.
- Kuhlmann, A.C., and Guilarte, T.R. 1997. The peripheral benzodiazepine receptor is a sensitive indicator of domoic acid neurotoxicity. *Brain Res* 751, 281–288.
- Lefebvre, K.A., Bargu, S., Kieckhefer, T., and Silver, M.W. 2002. From sanddabs to blue whales: the pervasiveness of domoic acid. *Toxicol* 40, 971–977.
- Levin, E.D., Pizarro, K., Pang, W.G., Harrison, J., and Ramsdell, J.S. 2005. Persisting behavioral consequences of prenatal domoic acid exposure in rats. *Neurotoxicology and Teratology* 27, 719.
- Lisman, J.E., Talamini, L.M., and Raffone, A. Recall of memory sequences by interaction of the dentate and CA3: A revised model of the phase precession. *Neural Networks*, in press, corrected proof.
- Lomeli, H., Wisden, W., Kohler, M., Keinänen, K., Sommer, B., and Seeburg, P.H. 1992. High-affinity kainate and domoate receptors in rat brain. *FEBS Lett* 307, 139–143.
- Lothman, E.W., and Collins, R.C. 1981. Kainic acid induced limbic seizures: metabolic, behavioral, electroencephalographic and neuropathological correlates. *Brain Res* 218, 299–318.
- Lothman, E.W., Stringer, J.L., and Bertram, E.H. 1992. The dentate gyrus as a control point for seizures in the hippocampus and beyond. *Epilepsy Res Suppl* 7, 301–313.
- Lucas, D.R., and Newhouse, J.P. 1957. The toxic effect of sodium L-glutamate on the inner layers of the retina. *AMA Arch Ophthalmol* 58, 193–201.
- Maeda, M., Kodama, T., Saito, M., Tanaka, T., Yoshizumi, H., Nomoto, K., and Fujita, T. 1987a. Neuromuscular action of insecticidal domoic acid on the American cockroach. *Pesticide Biochemistry and Physiology* 28, 85–92.
- Maeda, M., Kodama, T., Tanaka, T., Ohfune, Y., Nomoto, K., Nishimura, K., and Fujita, T. 1984. Insecticidal and neuromuscular activities of domoic acid and its related compounds. *J Pesticide Sci* 9, 27–32.
- Maeda, M., Kodama, T., Tanaka, T., Yoshizumi, H., Takemoto, T., Nomoto, K., and Fujita, T. 1986. Structures of isodomoic acids A, B and C, novel insecticidal amino acids from the red alga *Chondria armata*. *Chem Pharm Bull* 34, 4892–4895.
- . 1987b. Structures of domoic acid lactone A and B, novel amino acids from the red alga. *Tetrahedron Letters* 28, 633.
- Malva, J.O., Carvalho, A.P., and Carvalho, C.M. 1996. Domoic acid induces the release of glutamate in the rat hippocampal CA3 subregion. *Neuroreport* 7, 1330–1334.
- Maucher, J.M., and Ramsdell, J.S. 2005. Domoic acid transfer to milk: evaluation of a potential route of neonatal exposure. *Environ Health Perspect* 113, 461–464.
- Monaghan, D.T., and Cotman, C.W. 1982. The distribution of [<sup>3</sup>H]kainic acid binding sites in rat CNS as determined by autoradiography. *Brain Res* 252, 91–100.
- Montague, A.A., and Greer, C.A. 1999. Differential distribution of ionotropic glutamate receptor subunits in the rat olfactory bulb. *Journal of Comparative Neurology* 405, 233.
- Morgan, J.I., Cohen, D.R., Hempstead, J.L., and Curran, T. 1987. Mapping patterns of c-fos expression in the central nervous system after seizure. *Science* 237, 192–197.
- Mueller, R.W., Gill, S.S., and Pulido, O.M. 2003. The monkey (*Macaca fascicularis*) heart neural structures and conducting system: an immunochemical study of selected neural biomarkers and glutamate receptors. *Toxicol Pathol* 31, 227–234.
- Mulle, C., Sailer, A., Perez-Otano, I., Dickinson-Anson, H., Castillo, P.E., Bureau, I., Maron, C., Gage, F. H., Mann, J.R., Bettler, B., and Heinemann, S.F. 1998. Altered synaptic physiology and reduced susceptibility to kainate-induced seizures in GluR6-deficient mice. *Nature* 392, 601–605.
- Murakami, S., Takemoto, T., and Simizu, Z. 1953. Studies on the Effective Principles of *Digenea simplex* Ag. I. Separation of the Effective Fraction by Liquid Chromatography. *J Pharm Soc Japan* 73, 1026–1029.
- Nakajima, S., and Potvin, J.L. 1992. Neural and behavioral effects of domoic acid, an amnesic shellfish toxin, in the rat. *Can J Psychol* 46, 569–581.
- Nanao, M.H., Green, T., Stern-Bach, Y., Heinemann, S.F., and Choe, S. 2005. Structure of the kainate receptor subunit GluR6 agonist-binding domain complexed with domoic acid. *PNAS* 102, 1708–1713.
- Nijjar, M.S. 1993. Effects of domoate, glutamate and glucose deprivation on calcium uptake by rat brain tissue in vitro. *Biochem Pharmacol.* 46, 131–138.
- Nijjar, M.S., and Madhyastha, M.S. 1997. Effect of pH on domoic acid toxicity in mice. *Mol Cell Biochem* 167, 179–185.
- Nijjar, M.S., and Nijjar, S.S. 2000. Domoic acid-induced neurodegeneration resulting in memory loss is mediated by Ca<sup>2+</sup> overload and inhibition of Ca<sup>2+</sup> + calmodulin-stimulated adenylate cyclase in rat brain (review). *Int J Mol Med* 6, 377–389.
- Nitsch, C., Goping, G., and Klatzo, I. 1986. Pathophysiological aspects of blood-brain barrier permeability in epileptic seizures. *Adv Exp Med Biol* 203, 175–189.

- Nomoto, K., Takemoto, T., and Maeda, M. 1992. Conformational feature of neuroactive domoic acid: X-ray structural comparison with isodomoic acid A and alpha-kainic acid. *Biochem Biophys Res Commun* 187, 325–331.
- Novelli, A., Fernández-Sánchez, M.T., Kispert, J., Torreblanca, A., Gascón, S., and Zitko, V. 1992a. The amnesic shellfish poison domoic acid enhances neurotoxicity by excitatory amino acids in cultured neurons. *Amino Acids* 2, 233–244.
- Novelli, A., Kispert, J., Fernández-Sánchez, M.T., Torreblanca, A., and Zitko, V. 1992b. Domoic acid-containing toxic mussels produce neurotoxicity in neural cultures through a synergism between excitatory amino acids. *Brain Res* 577, 41–48.
- Ohfune, Y., and Tomita, M. 1982. Total synthesis of (–)domoic acid. *J Am Chem Soc* 104, 3511–3512.
- Olney, J.W. 1969. Brain lesions, obesity, and other disturbances in mice treated with monosodium glutamate. *Science* 164, 719–721.
- . 1990. Excitotoxicity: an overview. *Can Dis Wkly Rep* 16 Suppl 1E, 47–57; discussion 57–48.
- Olney, J.W., Fuller, T., and de Gubareff, T. 1979. Acute dendrotoxic changes in the hippocampus of kainate treated rats. *Brain Res* 176, 91–100.
- Peng, Y.G., Clayton, E.C., and Ramsdell, J.S. 1997. Repeated independent exposures to domoic acid do not enhance symptomatic toxicity in outbred or seizure-sensitive inbred mice. *Fundamental Appl Toxicol* 40, 63–67.
- Peng, Y.G., and Ramsdell, J.S. 1996. Brain fos induction is a sensitive biomarker for the lowest observed neuroexcitatory effects of domoic acid. *Fundamental Appl Toxicol* 31, 162–168.
- Peng, Y.G., Taylor, T.B., Finch, R.E., Switzer, R.C., and Ramsdell, J.S. 1994. Neuroexcitatory and neurotoxic actions of the amnesic shellfish poison, domoic acid. *NeuroReport* 5, 981–985.
- Peng, Z., and Houser, C.R. 2005. Temporal patterns of fos expression in the dentate gyrus after spontaneous seizures in a mouse model of temporal lobe epilepsy. *J Neurosci* 25, 7210–7220.
- Perl, T.M., Bédard, L., Kosatsky, T., Hockin, J.C., Todd, E., and Remis, R.S. 1990. An outbreak of toxic encephalopathy caused by eating mussels contaminated with domoic acid. *New England J Med* 322, 1775–1780.
- Petito, C.K., Schaefer, J.A., and Plum, F. 1977. Ultrastructural characteristics of the brain and blood-brain barrier in experimental seizures. *Brain Res* 127, 251–267.
- Petrie, B. F., Pinsky, C., Stish, N. M., Bose, R., and Glavin, G.B. 1992. Parenteral domoic acid impairs spatial learning in mice. *Pharmacol Biochem Behav* 41, 211–214.
- Preston, E., and Hynie, I. 1991. Transfer constants for blood-brain barrier permeation of the neuroexcitatory shellfish toxin, domoic acid. *Can J Neurol Sci* 18, 39–44.
- Rapp, P.R., and Gallagher, M. 1996. Preserved neuron number in the hippocampus of aged rats with spatial learning deficits. *PNAS* 93, 9926–9930.
- Represa, A., Tremblay, E., and Ben-Ari, Y. 1987. Kainate binding sites in the hippocampal mossy fibers: localization and plasticity. *Neuroscience* 20, 739–748.
- Robertson, H., Renton, K., Kohn, J., and White, T. 1992. Patterns of Fos expression suggest similar mechanisms of action for the excitotoxins domoic and kainic acid. *Ann NY Acad Sci* 648, 330–334.
- Rodriguez-Moreno, A., and Sihra, T.S. 2004. Presynaptic kainate receptor facilitation of glutamate release involves protein kinase A in the rat hippocampus. *J Physiol* 557, 733–745.
- Rosenmund, C., and Mansour, M. 2002. Ion channelsHow to be desensitized. *Nature* 417, 238.
- Roy, M., and Sapolsky, R.M. 2003. The neuroprotective effects of virally-derived caspase inhibitors p35 and crmA following a necrotic insult. *Neurobiology of Disease* 14, 1.
- Ryan, J.C., Morey, J.S., Ramsdell, J.S., and Van Dolah, F.M. 2005. Acute phase gene expression in mice exposed to the marine neurotoxin domoic acid. *Neuroscience*.
- Sassoe-Pognetto, M., and Ottersen, O.P. 2000. Organization of Ionotropic Glutamate Receptors at Dendrodendritic Synapses in the Rat Olfactory Bulb. *J Neurosci* 20, 2192–2201.
- Scallet, A.C., Binienda, Z., and Caputo, F.A. 1993. Domoic acid-treated cynomolgus monkeys (M. ascicularis): effects of dose on hippocampal neuronal and terminal degeneration. *Brain Res* 627, 307–313.
- Scallet, A.C., Kowalke, P.K., Rountree, R.L., Thorn, B.T., and Binienda, Z.K. 2004. Electroencephalographic, behavioral, and c-fos responses to acute domoic acid exposure. *Neurotoxicol Teratol* 26, 331–342.
- Scallet, A.C., Schmued, L.C., and Johannessen, J.N. 2005. Neurohistochemical biomarkers of the marine neurotoxicant, domoic acid. *Neurotoxicol Teratol*.
- Schendel, S.L., Xie, Z., Montal, M. O., Matsuyama, S., Montal, M., and Reed, J.C. 1997. Channel formation by antiapoptotic protein Bcl-2. *PNAS* 94, 5113–5118.
- Schmitz, D., Mellor, J., Frerking, M., and Nicoll, R.A. 2001. Presynaptic kainate receptors at hippocampal mossy fiber synapses. *PNAS* 98, 11003–11008.
- Schmued, L.C., Scallet, A.C., and Slikker, W., Jr. 1995. Domoic acid-induced neuronal degeneration in the primate forebrain revealed by degeneration specific histochemistry. *Brain Res* 695, 64–70.



- Scoville, W., and Miller, B. 1957. Loss of recent memory after bilateral hippocampal lesions. *J Neurol Neurosurg Psychiatry* 20, 11–21.
- Shi, S.-H. 2001. Essay: Amersham Biosciences and Science Prize: AMPA Receptor Dynamics and Synaptic Plasticity. *Science* 294, 1851–1852.
- Shinozaki, H., and Ishida, M. 1976. Inhibition of quisqualate responses by domoic or kainic acid in crayfish opener muscle. *Brain Res* 109, 435–439.
- Shinozaki, H., and Konishi, S. 1970. Actions of several anthelmintics and insecticides on rat cortical neurones. *Brain Research* 24, 368.
- Shinozaki, H., and Shibuya, I. 1976. Effects of kainic acid analogues on crayfish opener muscle. *Neuropharmacol* 15, 145–147.
- Silvagni, P.A., Lowenstine, L.J., Spraker, T., Lipscomb, T.P., and Gulland, F.M. 2005. Pathology of domoic acid toxicity in California sea lions (*Zalophus californianus*). *Vet Pathol* 42, 184–191.
- Slevin, J.T., Collins, J.F., and Coyle, J.T. 1983. Analogue interactions with the brain receptor labeled by [3H]kainic acid. *Brain Res* 265, 169–172.
- Sloviter, R.S. 1994. The functional organization of the hippocampal dentate gyrus and its relevance to the pathogenesis of temporal lobe epilepsy. *Ann Neurol* 35, 640–654.
- Sommer, B., Burnashev, N., Verdoorn, T. A., Keinanen, K., Sakmann, B., and Seeburg, P.H. 1992. A glutamate receptor channel with high affinity for domoate and kainate. *Embo J* 11, 1651–1656.
- Stewart, G.R., Olney, J. W., Pathikonda, M., and Snider, W.D. 1991. Excitotoxicity in the embryonic chick spinal cord. *Ann Neurol* 30, 758–766.
- Stewart, G.R., Zorumski, C.F., Price, M.T., and Olney, J.W. 1990. Domoic acid: a dementia-inducing excitotoxic food poison with kainic acid receptor specificity. *Exp Neurol* 110, 127–138.
- Strain, S.M., and Tasker, R.A.R. 1991. Hippocampal damage produced by systemic injections of domoic acid in mice. *Neuroscience* 44, 343–352.
- Sutherland, R.J., Hoising, J.M., and Wishaw, I.Q. 1990. Domoic acid, an environmental toxin induces hippocampal damage and severe memory impairment. *Neuroscience Lett* 120, 221–223.
- Suzuki, C., and Hierlihy, S. 1993. The renal clearance of domoic acid in the rat. *Food Chem Toxicol* 31, 701–706.
- Swanson, G.T., Gereau, R.W.T., Green, T., and Heinemann, S.F. 1997. Identification of amino acid residues that control functional behavior in GluR5 and GluR6 kainate receptors. *Neuron* 19, 913–926.
- Szikra, T., and Witkovsky, P. 2001. Contributions of AMPA- and kainate-sensitive receptors to the photopic electroretinogram of the *Xenopus* retina. *Vis Neurosci* 18, 187–196.
- Takemoto, T., and Daigo, K. 1958. Constituents of *Chondria armata*. *Chem Pharmaceutical Bull* 6, 578–580.
- Tasker, R.A., Strain, S.M., and Drejer, J. 1996. Selective reduction in domoic acid toxicity in vivo by a novel non-N-methyl-D-aspartate receptor antagonist. *Can J Physiol Pharmacol* 74, 1047–1054.
- Tasker, R.A.R., Connell, B.J., and Strain, S.M. 1991. Pharmacology of systemically administered domoic acid in mice. *Can J Physiol Pharmacol* 69, 378–382.
- Tasker, R.A.R., and Strain, S.M. 1998. Synergism between NMDA and domoic acid in a murine model of behavioural neurotoxicity. *Neurotoxicol Teratol* 19, 593–597.
- Teitelbaum, J.S., Zatorre, R.J., Carpenter, S., Gendron, D., Evans, A.C., Gjedde, A., and Cashman, N.R. 1990. Neurologic sequelae of domoic acid intoxication due to the ingestion of contaminated mussels. *New England J Med* 322, 1781–1787.
- Terrian, D.M., Conner-Kerr, T.A., Privette, T.H., and Gannon, R.L. 1991. Domoic acid enhances the K(+)-evoked release of endogenous glutamate from guinea pig hippocampal mossy fiber synaptosomes. *Brain Res* 551, 303–307.
- Truelove, J., and Iverson, F. 1994. Serum domoic acid clearance and clinical observations in the Cynomolgus monkey and Sprague-Dawley rat following a single IV-dose. *Bull Environ Contam Toxicol* 52, 479–486.
- Truelove, J., Mueller, R., Pulido, O., and Iverson, F. 1996. Subchronic toxicity study of domoic acid in the rat. *Food Chem Toxicol* 34, 525–529.
- Truelove, J., Mueller, R., Pulido, O., Martin, L., Fernie, S., and Iverson, F. 1997. 30-day oral toxicity study of domoic acid in cynomolgus monkeys: lack of overt toxicity at doses approaching the acute toxic dose. *Natural Toxins* 5, 111–114.
- Tryphonas, L., and Iverson, F. 1990. Neuropathology of excitatory neurotoxins: the domoic acid model. *Toxicologic Pathology* 18, 165–169.
- Tryphonas, L., Truelove, J., and Iverson, F. 1990a. Acute parenteral neurotoxicity of domoic acid in cynomolgus monkeys. *Toxicologic Pathology* 18, 297–303.
- Tryphonas, L., Truelove, J., Nera, E., and Iverson, F. 1990b. Acute neurotoxicity of domoic acid in the rat. *Toxicologic Pathology* 18, 1–9.

- Walter, J.A., Falk, M., and Wright, J.L.C. 1994. Chemistry of the shellfish toxin domoic acid: characterization of related compounds. *Can J Chem* 72, 430.
- Walter, J.A., Leek, D.M., and Falk, M. 1992. NMR study of the protonation of domoic acid. *Can J Chem* 1156–1160.
- Wang, G.J., Schmued, L.C., Rews, A.M., Scallet, A.C., Slikker, W., and Binienda, Z. 2000. Systemic administration of domoic acid-induced spinal cord lesions in neonatal rats. *J Spinal Cord Med* 23, 31–39.
- Wellis, D.P., and Kauer, J.S. 1993. GABAA and glutamate receptor involvement in dendrodendritic synaptic interactions from salamander olfactory bulb. *J Physiol (Lond)* 469, 315–339.
- Willoughby, J.O., Mackenzie, L., Medvedev, A., and Hiscock, J.J. 1997. Fos induction following systemic kainic acid: early expression in hippocampus and later widespread expression correlated with seizure. *Neuroscience* 77, 379–392.
- Wright, J.L.C., Boyd, R.K., de Freitas, A.S.W., Falk, M., Foxall, R.A., Jamieson, W.D., Laycock, V., McCulloch, A.W., McInnes, A.G., Odense, P., Pathak, V., Quilliam, M.A., Ragan, M.A., Sim, P.G., Thibault, P., Walter, J.A., Gilgan, M., Richard, D.J.A., and Dewar, D. 1989. Identification of domoic acid, a neuroexcitatory amino acid, in toxic mussels from eastern Prince Edward Island. *Can J Chem* 67, 481–490.
- Wright, J.L.C., Falk, M., McInnes, A.G., and Walter, J.A. 1990. Identification of isodomoic acid D and two new geometrical isomers of domoic acid in toxic mussels. *Can J Chem* 68, 22–25.
- Xi, D., Peng, Y.G., and Ramsdell, J.S. 1997. Domoic acid is a potent neurotoxin to neonatal rats. *Natural Toxins* 5, 74–79.
- Xi, D., and Ramsdell, J.S. 1996. Glutamate receptors and calcium entry mechanisms for domoic acid in hippocampal neurons. *NeuroReport* 26, 1115–1120.
- Yamagata, K., Andreasson, K.I., Kaufmann, W.E., Barnes, C.A., and Worley, P.F. 1993. Expression of a mitogen-inducible cyclooxygenase in brain neurons: Regulation by synaptic activity and glucocorticoids. *Neuron* 11, 371.
- Zaman, L., Arakawa, O., Shimosu, A., Onoue, Y., Nishio, S., Shida, Y., and Noguchi, T. 1997. Two new isomers of domoic acid from a red alga, *Chondria armata*. *Toxicon* 35, 205–212.
- Zatorre, R.J. 1990. Memory loss following domoic acid intoxication from ingestion of toxic mussels. *Can Dis Wkly Rep* 16 Suppl 1E, 101–103; discussion 103–104.



## 14 Hepatotoxic Cyanobacteria

Ana Gago-Martinez

### Hepatotoxic Cyanobacteria

#### *Introduction*

The incidence of toxic episodes in freshwaters due to the presence of toxic cyanobacteria has considerably increased over the last few years. There is also increasing evidence that low levels of exposure may have chronic effects in humans and therefore strict and reliable control of these toxins should be carried out in order to prevent serious public health problems. It is known that cyanobacteria have been implicated in a number of episodes of human illnesses worldwide (Falconer 1983; Tisdale 1931a, 1931b; Veldee 1931; Dillenberg and Dehnel 1960; Lippy and Erb 1976; Billings 1981; Turner 1990; Zilberg 1966). It was also an important toxic event in Brazil in which dialysis patients died from water contaminated with cyanotoxins (Jochimsen 1998; Azevedo 2002). Also a possible link between cyanobacteria and cancer has been considered as a result of epidemiological evidence from China (Yu 1994; Ueno 1996). A further exposure route may be through the consumption of contaminated foods such as freshwater mussels (Vasconcelos 1995), fish (Carbis 1997), and edible plants (Codd 1999), cyanobacteria produce several toxins, including the neurotoxins, (anatoxins and saxitoxins), hepatotoxins, cylindrospermopsin, and lipopolysaccharide (LPS) endotoxins (Carmichael and Falconer 1993; Carmichael 1997). A summary of the toxins produced by the various species of cyanobacteria is given by Sivonen and Jones (1999).

Among the cyanobacterial toxins, the hepatotoxic *Microcystis* have been the most extensively studied and reported recently. These toxins present a large number of variants but despite this and the lack of standards a large number of methods have been developed for their evaluation in different matrices such as water, cells, tissues, etc. The toxicological studies carried out for these toxins have led the WHO to set guidelines for the control of these toxins establishing a regulatory level of 1 µg per litre in drinking waters. The methods currently developed for microcystins are also suitable for some other hepatotoxic toxins such as nodularins, although these toxins are more commonly present in brackish waters. *Microcystis* and *Nodularins* enter hepatocytes through the bile acid transport mechanism. The molecular basis of the toxicity of these toxins is by inhibition of protein phosphatases 1 and 2A in a manner similar to okadaic acid and have a tumour promoting activity on rat liver. The intoxication routes of concern for human health include intraperitoneal, intravenous, and oral exposition. These aspects will be later discussed. These intoxications not only involve drinking waters containing cyanobacterial toxins but also the consumption of toxin-containing animal or plant tissues. Dietary supplements made from cyanobacteria have been also reported as a possible source for the mentioned cyanobacterial toxins. Low level chronic exposure is probably more important than the rare acute lethal poisonings.

An extensive work has been developed for the control of microcystins but not much effort has been made for the development of methods for the detection of other cyanobacterial toxins such as anatoxins or cylindrospermopsins despite their important acute toxicity as occurs in the case of the

neurotoxic anatoxin, nevertheless interest in the method of development for these toxins has been considerably increased in the last few years.

This chapter focuses on hepatotoxic cyanobacteria, including microcystins, nodularins, and cylindrospermopsins. General aspects of these toxins as well as the analytical methods for their detection will be discussed, taking into account the increased interest on the development of biochemical approaches.

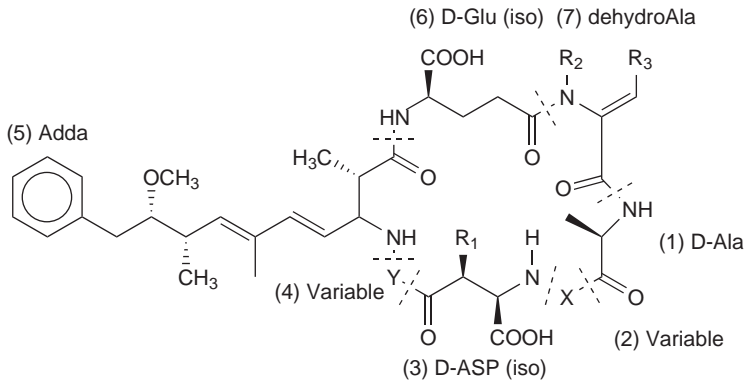
### *Peptide Hepatotoxins (Microcystins and Nodularin)*

The most extensively studied group of cyanobacterial toxins are the hepatotoxic cyclic peptides, which include the microcystins and nodularins, microcystins being the most frequently encountered. These toxins are commonly produced by *Microcystis aeruginosa* but also by other species of *Microcystis* and other genera such as *Planktothrix (Oscillatoria)*, *Anabaena*, *Nostoc*, *Anabaenopsis*, and *Hapalosiphon* (Sivonen and Jones 1999). Another similar cyclic pentapeptide is the nodularin, whose toxicity is similar to the most toxic microcystins (Rinehart 1988) and is usually produced by *Nodularia spumigena*, a brackish water cyanobacteria. The cyclic peptides are comparatively large natural products, molecular weight (m.w.) ranging from 800 to 1,000, although small compared with many other cell oligopeptides and polypeptides (proteins) (m.w. > 10,000). They contain either five (nodularins) or seven (microcystins) amino acids, with the two terminal amino acids of the linear peptide being condensed to form a cyclic compound. They are water soluble and most of them are unable to penetrate directly the lipid membranes of animal, plant, and bacterial cells. In aquatic environments, these toxins usually remain contained within the cyanobacterial cells and are only released in substantial amounts on cell lysis. Along with their high chemical stability and their water solubility, this containment has important implications for their environmental persistence and exposure to humans in surface water bodies. The first chemical structures of cyanobacterial cyclic peptide toxins were identified in the early 1980s and the number of fully characterized toxin variants has greatly increased during 1990s.

### *Microcystins*

The microcystins are a group of over 70 structurally related monocyclic heptapeptides containing seven peptide-linked aminoacids with the general structure of Cyclo-(D-alanine<sup>1</sup>-X<sup>2</sup>-D-MeAsp<sup>3</sup>-Y<sup>4</sup>-Adda<sup>5</sup>-D-glutamate<sup>6</sup>-Mdha<sup>7</sup>), in which X and Y are variable L aminoacids, D-MeAsp<sup>3</sup> is D-erythro-β-methylaspartic acid and Mdha is N-methyldehydroalanine (Fig. 14.1).

One of the invariant amino acids is a unique β-amino acid called Adda (2S,3S,8S,9S)-3; amino-9-methoxy-2,6,8-trimethyl-10-phenyldeca-4,6-dienoic acid is the most unusual structure in this group of cyanobacterial cyclic peptide toxins). A two-letter suffix (XY) is ascribed to each individual toxin to denote the two variant amino acids (Carmichael 1988). X is commonly leucine, arginine, or tyrosine. Y is arginine, alanine, or methionine. Variants of all the “invariant” amino acids have now been reported, e.g., desmethyl amino acids and/or replacement of the 9-methoxy group of Adda by an acetyl moiety. Currently there are in excess of 60 variants of microcystin that have been characterized (Rinehart 1994; Sivonen and Jones 1999). Of these 60 compounds, microcystin-LR would appear to be the microcystin most commonly found in cyanobacteria. It is also common for more than one microcystin to be found in a particular strain of cyanobacterium (Namikoshi 1992; Lawton 1995). The microcystin variants may also differ in toxicity (Carmichael 1993). The literature indicates that hepatotoxic blooms of *M. aeruginosa* containing microcystins occur commonly worldwide.



Structures of microcystins and their derivatives

Microcystin derivatives	Abbreviation	R <sub>1</sub> (3)	X (3)	Y (4)	R <sub>2</sub> (7)	R <sub>3</sub> (7)
Microcystin-LR	MC-LR	CH <sub>3</sub>	Leu	Arg	CH <sub>3</sub>	H
Microcystin-RR	MC-RR	CH <sub>3</sub>	Arg	Arg	CH <sub>3</sub>	H
Microcystin-YR	MC-YR	CH <sub>3</sub>	Tyr	Arg	CH <sub>3</sub>	H
Microcystin-LA	MC-LA	CH <sub>3</sub>	Leu	Ala	CH <sub>3</sub>	H
Microcystin-LW	MC-LW	CH <sub>3</sub>	Leu	Trp	CH <sub>3</sub>	H
Microcystin-LF	MC-LF	CH <sub>3</sub>	Leu	Phe	CH <sub>3</sub>	H
Microcystin-WR	MC-WR	CH <sub>3</sub>	Trp	Arg	CH <sub>3</sub>	H
Microcystin-LY	MC-LY	CH <sub>3</sub>	Leu	Tyr	CH <sub>3</sub>	H
3-Demethylmicrocystin-LR	[D-Asp <sup>3</sup> ]MC-LR	H	Leu	Arg	CH <sub>3</sub>	H
3-Demethylmicrocystin-RR	[D-Asp <sup>3</sup> ]MC-RR	H	Arg	Arg	CH <sub>3</sub>	H
3-Demethylmicrocystin-HTyrR	[D-Asp <sup>3</sup> ]MC-HTyrR	H	homoTyr	Arg	CH <sub>3</sub>	H
3-Demethyl-7-dehydrobutyrine-microcystin-RR	[D-Asp <sup>3</sup> ,Dhb <sup>7</sup> ]MC-RR	H	Arg	Arg	H	CH <sub>3</sub>

Figure 14.1. Structures of microcystins and their derivatives.

### Nodularin

This cyclic pentapeptide acts identical to microcystins, as they are structurally very similar. The chemical structure of Nodularin is cyclo-(D-MeAsp<sup>1</sup>-L-arginine<sup>2</sup>-Adda<sup>3</sup>-D-glutamate<sup>4</sup>-Mdhb<sup>5</sup>), in which Mdhb is 2-(methylamino)2-dehydrobutyric acid (Fig. 14.2). Nodularin contains amino acids similar or identical to those found in microcystins, namely arginine, glutamic acid, β-methylaspartic acid, N-methyldehydrobutyrine, and also Adda (Rinehart 1988). A few naturally occurring variations of nodularins have been found, two demethylated variants, one with D-Asp<sup>1</sup> instead of D-MeAsp<sup>1</sup>, the other with DMAdda<sup>3</sup> instead of Adda<sup>3</sup>, and the nontoxic nodularin, which has the 6Z-stereoisomer of Adda<sup>3</sup> (Namikoshi 1994). The equivalent 6Z- Adda<sup>3</sup> stereoisomer of microcystins is also nontoxic. In the marine sponge *Theonella swinhoei*, a nodularin analogue called motuporin has been found; in its structure it has arginine replaced by valine (de Silva 1992). In [L-Har2]-nodularin, arginine is replaced by homoarginine (Beattie 2000; Saito 2001).

### Cylindrospermopsin

This hepatotoxin first appeared in tropical and subtropical waters of Australia, resulting in an alkaloid hepatotoxin with a completely different mechanism of toxicity. The possible incidence of this cyanobacteria toxin was first reported by Byth (1980). An outbreak of hepatoenteritis occurred in 1979 at Palm Island, Queensland, Australia, when the population was supplied with drinking water from a

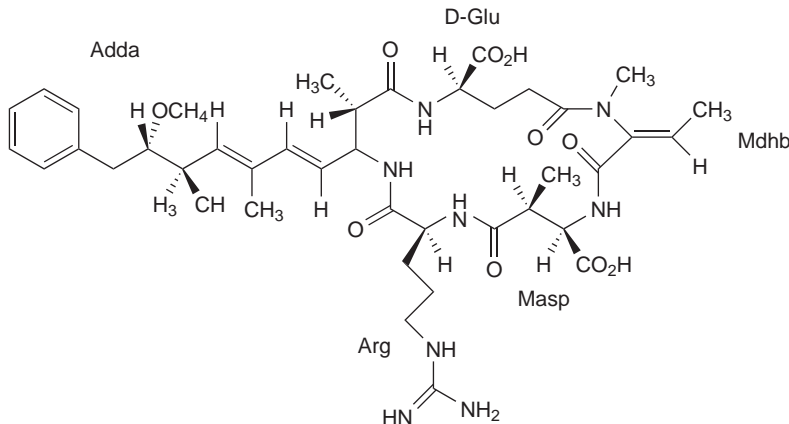


**Figure 14.2.** Structure of nodularin.

dam that had been treated with copper sulphate to kill a heavy bloom of algae. Subsequent research on *Cylindrospermopsis raciborskii* from this source showed it to produce toxicological effects in animals consistent with the symptoms observed at Palm Island. On this basis, it was subsequently suggested that the 1979 outbreak was caused by toxic *C. raciborskii*. This species has also been responsible for cattle deaths in Queensland (Saker 1999). *C. raciborskii* is predominantly a tropical and subtropical species which has been increasingly encountered also in temperate regions (Fastner 2003).

The toxin isolated from *C. raciborskii* was a hepatotoxic cyclic guanidine alkaloid named cylindrospermopsin (Ohtani 1992) with a molecular weight of 415. In pure form, cylindrospermopsin mainly affects the liver, although crude extracts of *C. raciborskii* injected or given orally to mice also induce pathological symptoms in the kidneys, spleen, thymus, and heart. Recently new structural variants of cylindrospermopsin have been isolated from an Australian strain of *C. raciborskii*, with one being identified as demethoxy-cylindrospermopsin (Chiswell 2001).

The same toxin has been subsequently isolated from the cyanobacterium *Umezakia natans* in Japan (Harada 1994) and *Aphanizomenon ovalisporum* in both Australia (Shaw 1999) and Israel (Banker 1997). An analogue of cylindrospermopsin such as 7-epicylindrospermopsin has been recently characterized as a toxic minor component of a strain of *Aph. ovalisporum* from Israel (Banker 2000). See Fig. 14.3.

### Toxicology and Pharmacology of Hepatotoxins

The safe levels of hepatotoxins in food and drinking waters have been evaluated in terms of tolerable daily intake (TDI). This value should be ideally taken as a result of human studies, but often such studies are inadequate or nonexistent. Alternatively, they are often obtained after animal studies, although the variability in sensitivity between animals and humans that makes necessary the establishment of safety factors to deal with this uncertainty should be taken into account.

A common problem with animal studies is related to the routes of exposure. Many toxins are more toxic when they are administered intravenously (i.v.) or intraperitoneally (i.p.) than by the oral route. This difference is evident when LD<sub>50</sub> values are examined for various routes of exposure. The toxicological studies using i.v. or i.p. routes of administration require much less toxin and in addition

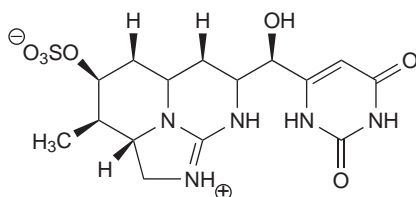


**Figure 14.3.** Structure of cylindrospermopsin.

can give information about the mechanism of toxicity, but for some natural toxins like cyanotoxins it is not always easy to find pure compounds to carry out controlled experiments; therefore, most of the studies are made using contaminated algal extracts rather than pure toxins. An advantage of this is that in this case the extract more closely mimics the real environmental situation, but the disadvantage is that some other toxins can be present in these extracts, affecting the reliability of the results. The experiments carried out to date revealed that there is no sufficient information for the calculation of TDI for most cyanotoxins. While for MC-LR more data exist and consequently a provisional value could be derived, not enough data are available for the calculation of TDI for other MCs. The toxicology and pharmacology of hepatotoxins have been extensively reviewed in *Toxic Cyanobacteria in Water* (Chorus and Bartram 1999).

### Microcystins and Nodularins

There have been no pharmacokinetic studies with orally administered microcystins. After i.v. or i.p. injection of sublethal doses of various microcystins in mice and rats, about 70% of the toxin was rapidly localized in the liver (Falconer 1983), and it is evident that the liver plays a large role in the detoxification of microcystins.

Microcystin-LR does not readily cross cell membranes and hence does not enter most tissues. After oral uptake, it is transported across the ileum into the bloodstream through a bile acid type transporter present in hepatocytes and cells lining the small intestine. Some other microcystins congeners are more hydrophobic than microcystin-LR and may cross cell membranes by other mechanisms.

Regarding to the acute toxicity, MC-LR is highly toxic ( $LD_{50}$  25–50  $\mu\text{g kg}^{-1}$  by i.p. route); the oral  $LD_{50}$  is 5000  $\mu\text{g Kg}^{-1}$  in mice. Yoshida (1997) has indicated that even by the oral route, microcystin-LR displays acute toxicity in rodents. There is no evidence of hydrolysis of microcystins by peptidases in the stomach, and it is apparent that a significant amount of microcystin-LR passes the intestinal barrier and is absorbed. The i.p.  $LD_{50}$  of several of the common occurring microcystins (MC-LA,-YR,-YM) are similar to that of MC-LR but for MC-RR is tenfold higher; however, because of differences in lipophilicity and polarity between the different microcystins, it cannot be presumed that the i.p.  $LD_{50}$  will predict toxicity after oral administration.

Microcystins are primarily hepatotoxins, after acute exposure severe liver damage is caused. Other organs affected are the kidneys and lungs and the intestines (Falconer 1999).

To assess the possible chronic effects in humans, several studies with repeated oral administration of pure microcystins to mice at various dose levels were carried out, and the results obtained showed chronic liver injury in most cases.

Carcinogenesis has been also evaluated through experiments with mice. The results obtained for MC-LR after i.p. injection in mice demonstrated the presence of neoplastic liver nodules (Ito 1997).

The same study shows that mice orally administered microcystin-LR at higher dose showed no evidence of liver injury or nodule formation.

Microcystin-LR was found to be a potent inhibitor of eukaryotic protein serine/threonine protein phosphatases 1 and 2A both in vitro (Honkanen 1994; MacKintosh 1990) and in vivo, which can induce hepatocyte necrosis and hemorrhage (Bhattacharya 1997; Kuiper-Goodman 1999). This protein phosphatase inhibition effect has become the basis of one of the bioassays to detect its presence. Nodularin acts in a similar way, inducing hepatocyte necrosis and hemorrhagic diathesis and inhibiting protein phosphatases 1 and 2A with the same potency as microcystin-LR. From the several toxicological studies carried out with nodularin, it can be concluded that its toxicity is similar to microcystin-LR; therefore, it may be appropriate to consider nodularin in a similar state of microcystins in terms of human health risk assessment. In any case, the protein phosphatases serve an important regulatory role to maintain homeostasis in the cell and results in the balance toward higher phosphorylation of target proteins, such as tumour suppresser proteins.

Recent studies have been carried out to a deeper evaluation of the toxicology and pharmacology of hepatotoxins. The oral exposure to Microcystis and its effects on the liver were evaluated (Li 2005). Lipid peroxidation and the antioxidant enzymes superoxide dismutase, catalase, and glutathione peroxidase, were evaluated in the liver of loach (*Misgurnus mizolepis*) that were orally exposed to a low dose of microcystis through dietary supplementation with bloom scum. Antioxidant enzymatic activity and lipid peroxidation were measured after termination of exposure. The activities of antioxidant enzyme were significantly increased in the livers of toxin-exposed loach after 28 days of exposure, as compared to control fish. However, lipid peroxidation remained stable in both groups. These results suggest that antioxidant enzymes were able to eliminate oxidative stress induced by low concentrations of microcystins and to prevent increased lipid peroxidation in the liver of loach (Lankoff 2001). The activity of cathepsins D and L, arginine aminopeptidase, dipeptidase II, and dipeptidase IV was determined in the lysosomal, microsomal, and cytoplasmatic fractions and in the complete homogenate of the mouse hepatocytes following injection of microcystin-YR and nodularin. The effect of both toxins depended on the time of action and on the fraction of cell cytoplasm. Microcystin-YR inhibited the synthesis of the studied proteases and caused a labialization of lysosomal membranes, whereas nodularin induced the synthesis of the enzymes and destabilised the reticulum endoplasmatic membranes. Chen (2005) investigated the immunomodulation by MC-LR of BALB/c mice peritoneal macrophages. This study has been carried out in vitro on mRNA levels of induced nitric oxide synthase and multiple cytokines by reverse-transcription polymerase chain reaction (RT-PCR). The results showed that expression of mRNA decreased significantly compared to the positive control (LPS only). These results have suggested the need for the establishment of a survey of the immunotoxicity of microcystins. An evaluation of the biological activities of several cyanobacteria including 21 anabaena, calothrix, nodularia, nostoc, and phormidium strains isolated from benthic littoral habitats of the Baltic Sea was carried out (Surakka 2005). This study showed whether benthic cyanobacterial extracts caused cytotoxicity by necrosis or induced apoptosis in two mammalian cell lines, a human leukemia cell line (HL-60,) and a mouse fibroblast cell line(3T3 Swiss), and examined potential hepatotoxin (microcystin and nodularin) production. Neither the microcystin synthetase E (mcyE) nor the nodularin synthetase F (ndaF) gene was amplified by PCR, and no microcystins or nodularins were detected by the protein phosphatase inhibition assay from the cyanobacterial strains included in this study. This indicates that benthic Baltic cyanobacteria contain potentially harmful cytotoxic compounds even though they do not produce microcystins or nodularins. These cytotoxic compounds remain to be characterized, and the mechanisms of cytotoxicity need to be studied further.



Chemoprotectant studies have indicated that membraneactive antioxidants such as vitamin E may offer protection against microcystin toxicity.

The effect of vitamin E supplementation on microcystin toxicity in the mouse liver was investigated by Gehringer et al. (2003). Groups of mice were fed vitamin E supplements (8.33 or 33.3 U/mouse/day) for 4 weeks, with intraperitoneal doses of MC-LR extract (70% LD<sub>50</sub>) every 3 days from day 8. The potential benefits of vitamin E were evaluated based on lipid peroxidation, alanine transaminase (ALT), and glutathione S-transferase (GST) levels. Vitamin E supplementation offered some protection against lipid peroxidation induced by repeated exposure to MC-LR extract and limited both the toxin-induced increase in ALT leakage and decrease in GST activity. Increased vitamin E supplementation significantly increased the time to death and reduced the increase in liver percentage body weight induced in mice given a lethal dose challenge of MC-LR extract. Therefore, vitamin E, taken as a dietary supplement, may have a protective effect against chronic exposure to MC-LR.

### *Cylindrospermopsin*

The toxicological studies carried out by i.p. injection of the lysed organism (*Cylindrospermopsis raciborskii*) to mice resulted in a progressive tissue injury with cell necrosis in the liver, kidneys, adrenals, lung, heart, spleen, and thymus (Hawkins 1997). In mice, the i.p.LD<sub>50</sub> at 24 hours was equivalent to 300 µg kg<sup>-1</sup> whereas after seven days the LD<sub>50</sub> was reduced to 180 µg kg<sup>-1</sup>. In vitro studies with pure cylindrospermopsin have shown its potential to inhibit glutathione synthesis and protein synthesis in general (Runnegar 1995; Terao 1994). In mouse liver after i.p. administration, major changes were observed in the hepatocytes. No data on the oral toxicity of cylindrospermopsin are available.

Cylindrospermopsin resulted in a hepatotoxic alkaloid that is capable of inhibiting protein synthesis, and it appears to have a progressive effect on several other vital organs such as the kidney in addition to the liver (Terao 1994; Falconer 1999). Cylindrospermopsin was shown to be a potent inhibitor of protein synthesis. The same studies described the liver as the main target of this phycotoxin, with four consecutive phases of the pathological changes in the liver: protein synthesis inhibition, membrane proliferation, fat droplet accumulation, and cell death.

## **Chemical and Biochemical Considerations for Detection of Hepatotoxins**

The harmful effects of the cyanobacteria toxins for human health after the consumption of water in which they are present have made necessary the establishment of some drinking waters guidelines (WHO 1998; NHMRC/ARMCANZ 2001), and a limit of 1 µg of microcystin-LR per liter has been recommended. To ensure the compliance of these guidelines as well as to control the amounts of toxins present in the contaminated water, minimizing the risk to human health through exposure to microcystins, reliable and accurate quantitative analytical methods are required. These methods range from biological based screening to more sophisticated analytical techniques.

The mouse bioassay, which is still the official method used for some natural toxins present in the marine environment, has been used as a routine screening method for a few years, but this method has been recently replaced in many laboratories worldwide with a more sensitive method such as an enzyme-linked-immunosorbent assay (Nagata 1995). Protein phosphatase assays (Metcalf 2001) have been also used but more details on these methods will be discussed later.

An exhaustive work has been carried out in the development of instrumental methods mostly using reversed-phase high-performance liquid chromatography (HPLC) combined with UV detection and



the potential of mass spectrometry for identification and confirmation has made this technique the most powerful approach for the analysis of these toxins especially when they are present in complex matrices, often affected by the presence of interferent compounds, which may compromise the reliability of the results obtained. Mass spectrometry is also useful because of the lack of standard and reference materials for these toxins, which makes the use of these confirmation techniques highly recommended. Alternative separation techniques such as high-performance capillary electrophoresis have been also used with UV or MS detection. The complexity of the matrix also plays an important role in the efficiency of the analytical methods as well as in the reliability of the results obtained especially when no further confirmation is carried out. Tedious and time-consuming sample pretreatment protocols must therefore be used for this purpose, and the efficiency of the different steps involved in such protocols also plays an important role in the mentioned reliability, which is mostly compromised by inefficient and nonselective extraction and clean-up procedures, responsible for false identifications leading to the strict need of further confirmation by mass spectrometry. Several extraction and clean-up procedures have arisen, mostly involving solid phase extraction using different solid supports, which in addition to the interferences removal have also preconcentration aims, being particularly useful when toxins are present at trace levels. A novel SPE approach using immunoaffinity chromatography will be also discussed in this chapter. The selectivity and in some cases specificity of the antigen-antibody interaction makes this solid-phase extraction procedure highly promising and efficient and even in some cases make unnecessary the further use of sophisticated and expensive confirmatory techniques, such as MS, being considered as useful sample pre-treatment approaches for efficient and reliable analysis in routine.

Different analytical methods will be discussed in this chapter and updated information about the most recent analytical developments and improvements will be provided also.

### *Biological Methods*

Toxicity tests and bioassays usually offer a rapid and simple screening of samples based on the overall toxic effects. The biological methods that have been reported for microcystins can be classified in three different categories: whole organism bioassays, biochemical assays, and immunological assays. These methods have been recently reviewed by McElhiney and Lawton (2005). Before discussing the different biological methods, it would be important to consider that minor differences in the structure of these toxins can lead to big differences in toxicity (Meriluoto 2005). Examples of this are reported for demethylmicrocystin-RR ( $LD_{50}$  180–250  $\mu\text{g kg}^{-1}$ ) and microcystin -RR ( $LD_{50}$  600  $\mu\text{g kg}^{-1}$ ), while the  $LD_{50}$  for demethylmicrocystin-LR ( $LD_{50}$  90–300  $\mu\text{g kg}^{-1}$ ) is less toxic than microcystin-LR ( $LD_{50}$   $\mu\text{g kg}^{-1}$ ). These structural variations in the toxicological activity have been evaluated using naturally occurring toxin variants or by introducing modifications at different sites of the toxins. Toxicity variations due to saturation or removal of the ADDA structure on Mc-LR resulted in a loss of toxicity of the derivative and other structural-related issues such as the need of the presence of a free carboxylic acid group in the D-Glu unit for toxicity and also the cyclic structure of the toxins being crucial for toxicity.

### *Bioassays*

Mouse bioassays have been used in most laboratories to analyse microcystins in samples. The main drawbacks associated with these bioassays are related with the lack of sensitivity and specificity as well as a high variability on the results (Falconer 1993). Mouse bioassay has been used primarily to

determine the toxicity of bloom material, and from the toxic response the identity of the class of toxin can be inferred. It has generally been used in a qualitative manner to determine a bloom as "toxic" or "nontoxic." However, as dose determines the toxic effect, a cut-off point in terms of toxicity should be defined. Everything is toxic if the dose is sufficient, even the salts that may be present in a sample highly concentrated by evaporation. In terms of symptoms, the peptide hepatotoxins (microcystins and nodularin) generally cause death within 4 hours with symptoms of a liver engorged with blood. This assay, although it can potentially be calibrated against a specific toxin such as microcystin-LR, and therefore produce a result in terms of microcystin-LR toxicity equivalents, does not have the sensitivity or precision to be applicable to water samples. It is not practicable to use for water samples with concentrations around 1–2 µg/L, the approximate range of the guideline for microcystins, as a significant concentration factor is required. For microcystin-LR with an LD<sub>50</sub> of 50 µg/kg, the lethal dose is around 1 µg for a 20 g mouse, which requires a 1 L sample to be concentrated to 1 ml for intraperitoneal injection to produce a lethal response.

It is also impracticable and unacceptable from the point of view of number of mice required to obtain a quantitative result when a number of samples require analysis.

The ethics of animal toxicity testing, together with the practical issues associated with the mouse bioassay, has led to toxicity assays with other organisms. These assays may be toxin specific, and are discussed under the specific toxins. Hiripi (1998) reported an assay using the African locust. All classes of toxins elicited a toxic response. As it was not possible to discriminate between the classes of toxins, this assay could not then be used as a monitoring tool for specific toxins. The use of several invertebrates, including *Daphnia melanogaster* and mosquito larvae, have been recently investigated for their ability to detect the presence of microcystins, nevertheless these assays have not been fully validated for routine monitoring. A simple and inexpensive alternative to the mouse bioassay has been developed using brine shrimp (Kiviranta 1991). This assay is a useful and simple toxicity screen. The shrimp larvae are exposed to different concentrations of test samples and the toxicity is expressed as the LC<sub>50</sub>. The main problem of this assay is the lack of specificity for microcystins and also that it can be heavily influenced by sample matrix effects. However, in general it would appear that these assays are also neither sufficiently sensitive nor specific to be applicable for measuring toxins at low levels in water.

Other bioassays reported in the literature using rat (Aune and Berg 1986; Heinze 1996; Fladmark 1998) or salmon (Fladmark 1998) hepatocytes have been proposed as a monitoring tool for the peptide hepatotoxins. However, operational difficulties in water testing laboratories (e.g., preparation of cell suspensions) and limitations of sensitivity in the case of rat hepatocytes preclude their use on a routine basis for water samples. Responses in these systems may well correlate with mammalian toxicity, thereby producing a measure of toxicity in microcystin-LR toxicity equivalents if microcystin-LR were used for calibration. They may, therefore, be an attractive option in the future with further development.

### Biochemical Assays

The use of biochemical assays for microcystins and some other cyanobacterial toxins has been considerably increased in the last few years. These assays are based on the exploitation of the biochemical properties.

Assays based on the ability of these toxins to inhibit protein phosphatases are a good example of this and are particularly useful since they can provide an indication of the biochemical activity of these toxins. These assays are rapid and sensitive and involve the measuring of the inhibitory effect of microcystins on the release of phosphate from phosphorylated protein substrates (Bell 1994).

Different assays have been developed using both PP1 and PP2, although the reaction of microcystin with PP1 is almost 50 times less sensitive than with PP2A (Honkanen 1994). Protein phosphatase assays are sufficiently sensitive to detect microcystins below the WHO guidelines without additional preconcentration strategies, and the assay is also useful for a large variety of matrices (Rapala 2002; Heresztyn 2001). The use of radiometric assays provided a higher sensitivity; nevertheless, these assays are not feasible in many laboratories due to the restrictions to use radioactive materials. The colorimetric protein phosphatase assay is simple to use, and the results obtained correlate well with the ones obtained by HPLC in water and cyanobacterial samples (Rapala 2002). An alternative assay using the fluorogenic substrates 4-methylumbelliferyl-phosphate (MUP) and 6,8-difluoro-4-methylumbelliferylphosphate (DiFMUP) has been recently developed by Bouaïcha (2002). In this assay, the activity of the enzyme PP2A is indicated by the formation of fluorescent derivatives from MUP and DiFMUP. This substrate provides increased sensitivity and reproducibility. The main problem encountered with the protein phosphatase assay is the variability of response in terms of sensitivity for the different microcystins variants. Furthermore, the reaction is not selective for microcystins when other environmental protein phosphatase inhibitors are present. However, the ability of the assay to indicate overall toxicity makes it a useful approach for a pre-screening prior to the application of physicochemical techniques (Rivasseau 1999).

A combination of PPIA and microcystin immunoassay was proposed by Carmichael et al. (1999) to indicate the potential toxicity of a bloom sample and the concentration of the microcystins. A combined assay, consistent with this principle, was developed by Metcalf et al. (2001); this includes preexposure of the sample to microcystin antibodies, to make microcystins/nodularins that are present biounavailable to the subsequent addition of protein phosphatase enzyme, before assaying for protein phosphatase inhibitory activity. The resulting assay, termed the colorimetric immunoprotein phosphatase inhibition assay (CIPPIA), was found to be specific for microcystins and nodularins since the microcystin antibodies protect the protein phosphatase from inhibition by the toxins. Complete protection from inhibition of protein phosphatase by the antibodies indicates that the inhibition of the protein phosphatase in the sample was due to the cyanobacterial toxins. These colorimetric assays showed a good correlation with the HPLC analysis of extracts cyanobacteria. Immunoassays can also be combined with physicochemical methods such as HPLC (Zeck 2001b). In this case, the HPLC method separates the microcystins according to their hydrophobicity and the resulting fractions are analyzed by immunoassay.

A highly sensitive bioassay relying on the specific inhibition of the human protein phosphatase 2A was developed by Robillot and Hennion (2004) and applied to the quantification of microcystins. A systematic approach based on the rational testing of seven purified mcyst variants as well as characterized environmental samples pointed out the limits and experimental bias associated with this assay. All the seven microcystin variants known as microcystins RR, YR, LR, LY, LA, LW, and LF strongly inhibited the enzyme with IC<sub>50</sub> ranging between  $0.29 \pm 0.02$  nM and  $0.84 \pm 0.07$  nM for microcystins LW and YR, respectively. Using the model system of *Microcystis aeruginosa* PCC7820 axenic cultures and within the 1-year study of a *Planktothrix agardhii* bloom, the PP2A assay was shown to be strongly correlated to high-performance liquid chromatography (HPLC) coupled to UV diode array detection. However, the slope of the linear regression was significantly influenced by the sample composition, as confirmed by HPLC coupled to electrospray ionization mass spectrometry. A model based on pure additivity of mcyst effects was established to describe PP2A inhibition by standard mcyst mixtures, and fully agreed with experimental observations.

The results obtained with a protein phosphatase assay and a HPLC/UV/MS method are compared with the results obtained with a bioluminescence assay, which is successfully introduced here for

nodularin determination (Dahlmanna 2001). A statistical evaluation of the three applied methods revealed a good comparability with the detected toxin content. The methods were evaluated, taking into consideration the parameters handling, efficiency, sensitivity and selectivity. The detection limit in the protein phosphatase assay is highest (0.05 ng nodularin) and lowest (250 ng nodularin) in the bioluminescence assay; it was determined with 5 ng (MS) and 25 ng (UV) for the HPLC/UV/MS methods. The different selectivities and sensitivities are critically discussed, and an analytical pathway for the determination of the biotoxin nodularin from nodularia samples is proposed.

## *Immunological Assays*

### *Immunoassays*

The immunoassays are finding increasing application for the analysis of a wide range of contaminants. These methods are currently the most promising screening methods that are based in the use of antibodies. An application of these immunoassays has been developed for cyanobacteria. Immunoassays are usually more sensitive than any other analytical methods. However, several additional performance criteria are required to be examined in the assessment of antibodies and immunomethods for the detection of cyanobacteria. An extensive review on immunoassays for cyanobacteria toxins has been reported by Metcalf and Codd (2003). The pioneering work described by Kfir (1985, 1986) resulted in the production of monoclonal antibodies against microcystin-LA using an immunoconjugate produced by a carbodiimide conjugation protocol at pH 5. The subsequent immunoassay was developed and tested with seven purified microcystins, all of which were found to cross-react with equal affinity and, of the clones produced, 15 out of 220 were found to produce antibodies specific for microcystin-LA. Unfortunately, this promising lead was not developed. Further monoclonal antibodies were produced using carbodiimide conjugation (Brooks 1988; Chu 1989; Nagata 1995) that identified clone-producing monoclonal antibodies, which resulted in a specific sensitive ELISA. McDermott (1995) immunized chickens using a similar conjugate and isolated antibodies from the yolks of laid eggs, removing the need to harvest blood and cause animal distress. Other monoclonal antibodies produced against microcystin-LR and nodularin have used conjugation methods directed through the methyldehydroalanine moiety of these toxins (Mikhailov 2001). This approach has yielded clones with antibodies directed against other epitopes of microcystin and nodularin than had previously been developed using the carbodiimide methods first reported (Kfir 1996). Monoclonal antibodies specific for 4-R microcystins have been developed using the carrier molecule SATP (succinimidyl acetylthiopropionate) reacting through the methyldehydroalanine unit of microcystin-LR. Other monoclonal antibodies to microcystins have been produced specifically for analytical detection and as potential vaccines. These have included the use of both anti-idiotypic and anti-anti-idiotypic antibodies and the production of antibodies against an immune complex of microcystin plus anti-microcystin antibodies (Nagata 1999). More recently, monoclonal antibodies have been produced against specific regions of the microcystin molecule, in particular the conserved Adda moiety using synthesized immunogens (Fischer 2001) and modified Adda (Zeck 2001c).

To improve the specific response against microcystin immunoconjugates, synthetic lipopeptides were used as adjuvants and were found to invoke a greater immune response than the use of classical adjuvants such as Freund's adjuvant. However, an ELISA for the detection of free microcystin was not developed using these antibodies. Cross-reactivities of various microcystin variants and nodularin with monoclonal antibodies have been found affecting to the specificity of these antibodies for the recognition of the mentioned toxins. The number of purified microcystin variants that have been tested by ELISA using monoclonal antibodies shows marked differences between methods,

although, with the exception of the nodularins, the majority of these variants possess either L-leucine or L-arginine at the variable amino acid positions. Although microcystin-LR was the immunizing microcystin variant in the majority of cases, microcystin-LR is generally not the variant with the highest affinity for the produced antibodies, and this was found in only one case for monoclonal antibodies (Nagata 1995).

Furthermore, as for the polyclonal antibodies generated specifically against Adda, the monoclonal antibodies used in ELISA were not tested with 6Z-Adda-containing microcystin variants (Fischer 2001; Zeck 2001c), and these antibodies were hypothesized as being potentially suitable for the analysis of linearized microcystin. Carmichael (1999) recommended that for microcystin analysis, a combination of PPIA and microcystin immunoassay was preferable, to indicate the potential toxicity of a bloom sample and the concentration of the microcystins contained within. A combined assay, consistent with this principle, was developed (Metcalf 2003). This includes preexposure of the sample to microcystin antibodies, to make microcystins/nodularins that are protein phosphatase enzyme, before assaying for protein phosphatase inhibitory activity. Control assays are run without preexposure to microcystin antibodies to provide a microcystin/nodularin-based toxicity assessment of the sample. The resulting assay, termed the colorimetric immunoprotein phosphatase inhibition assay (CIPPIA), was found to be specific for microcystins and nodularins since the microcystin antibodies protect the protein phosphatase from inhibition by the toxins. Complete protection from inhibition of protein phosphatase by the antibodies (defined as a protective index, PI, approaching a value of 1) indicates that the inhibition of the protein phosphatase in the sample was due to the cyanobacterial toxins. Assessment of CIPPIA with seven purified microcystins and nodularin gave PIs of 0.8 or greater, as compared to PIs for the protein phosphatase inhibitors, calyculin A, tautomycin, and okadaic acid, of 0.18 or less.

A novel conjugation method was developed by Metcalf and Codd (2003) by linking the hapten, the cyanobacterial hepatotoxin microcystin-LR, via 2-mercaptoethylamine to keyhole limpet haemocyanin. Polyclonal antisera were raised against this conjugate and an indirect competitive immunoassay (ELISA) developed that can detect purified microcystin-LR and the toxin in extracts of cyanobacteria from fresh, brackish, and marine waters. The cross-reactivity of the microcystin-LR antibodies was investigated with a range of purified microcystin variants (-LR, -LA, -LY, -LW, LF, -D-Asp3-RR, and -Asp3(Z)-Dhb7-HtyR) and nodularin. The antibodies cross-reacted well with all microcystin and nodularin variants. The microcystin-LA was the most readily detectable, followed by microcystins-LR, -LF, -LW, -D-Asp3-RR, -LY, nodularin, and microcystin-Asp3(Z)-Dhb7-HtyR. Extracts from several genera of cyanobacteria were investigated by the ELISA, and the results compared to high-performance liquid chromatography with diode array detection (HPLC/DAD). Analysis of microcystin-LR equivalents by ELISA and HPLC/DAD showed good correlation.

Pyo (2005) reported on the development of a new competitive enzyme-linked immunosorbent assay (ELISA) based on monoclonal antibodies. New monoclonal antibodies against the microcystin leucine-arginine variant (MCLR) were prepared from cloned hybridoma cell lines. They used keyhole limpet haemocyanin (KLH)-conjugated MCLR as an immunogen for the production of mouse monoclonal antibody. The immunization, cell fusion, and screening of hybridoma cells producing anti-MCLR antibody were conducted. In the ELISA test, a microtiter plate coated with MCLR-bovine serum albumin conjugate was incubated with standard microcystin samples. The amount of antibody bound was determined by the reaction of peroxidase-labeled anti-mouse IgG with its substrate, 3,3',5,5'-tetramethyl benzidine (TMB). Since the ELISA test was highly sensitive, the newly developed ELISA can be suitable for the trace analysis of cyanobacterial hepatotoxins and microcystins in



water. The linear responses of monoclonal antibodies with different concentrations of microcystin LR were established between 30 and 1,600 pg/mL.

Immunoassays can also be combined with physicochemical methods such as HPLC, whereby the HPLC method separates the microcystins according to their hydrophobicity and the resulting fractions are analyzed by immunoassay. Immunoaffinity columns containing microcystin antibodies (Rivasseau 1999a) can also be used to confer specificity to the PPIA for the analysis of the cyanobacterial toxins. Lin and Chu (1994) reported that polyclonal antibodies raised against microcystin-LR could successfully be used to protect PP2A from the action of microcystin *in vitro*.

The main problems associated with the immunoassays are caused by insufficient sensitivity, unfavourable cross-reactivities and difficult availability. The most favorable immunoassay would be one of broad reactivity toward all microcystins, allowing a global measurement of the concentration of the toxins involved, which would be very useful for regulatory purposes (Weller 2001).

The production and characterization of a monoclonal antibody (clone (MC10E7)) with extraordinary sensitivity and high selectivity for [4-arginine]microcystins is described by (Zeck 2001a). The immunogen used for the production of the antibody was synthesized using a novel coupling chemistry to bind microcystin-LR(MC-LR) via dehydroalanine to the carrier protein. High sensitivity has been achieved, being the detection limit for MC-LR 6 ng/L. All [4-arginine]microcystins show similar IC<sub>50</sub> values and detection limits, whereas other MCs such as MC-LA are not recognized. The cross-reactivities of MC variants containing another amino acid than arginine in position 4 of the cyclic peptide ring are at least three orders of magnitude lower. Nodularin contains an arginine next to the amino acid Adda and shows an intermediate cross-reactivity. The amino acid residues at position 2 of the MCs seem to be much less important to the binding by the antibody, concluding that the new monoclonal antibody is highly selective for those MCs containing arginine at position 4 and showing very high affinity constants for these MCs.

### *Enzyme-Linked Immunosorbent Assays (ELISA)*

Analytical techniques based on enzyme linked immunosorbent assays (ELISA) show high sensitivity; however, the cross-reactivity of the various microcystins and nodularin depends upon the similarity in chemical structure to the microcystin against which antibodies have been raised (generally microcystin-LR) and not toxicity. Therefore, an issue to be considered in the application of these antibodies to a sample with an unknown or complex mixture of microcystins is the potential for poor reaction with some components. Depending on both the cross-reactivity and the toxicity of a microcystin, ELISAs can over- or underestimate the toxin concentration in terms of microcystin-LR toxicity equivalents. In cases where the mixture of toxins is well characterized (e.g., given a water body with ongoing or regular contamination with toxic *Microcystis* with a consistent toxin profile) the use of ELISA for ongoing monitoring is quite acceptable. However, as ELISA techniques can greatly over- or underestimate the concentration with some variants, they cannot be relied on as quantitative assays. They are however, useful screening tools.

To date, four commercially available kits have been developed. Two ELISAs, the SDI EnviroGard ELISA (Strategic Diagnostics Ltd., Hampshire, U.K.) and the EnviroLogix ELISA (Crop Enhancement Systems Ltd., Norfolk, U.K.), are based on the polyclonal antibodies used by Chu (1989). The Mitsubishi ELISA kit, produced by Wako Chemicals, Japan (Wako Chemicals, Neuss, Germany), incorporates monoclonal antibodies (Nagata 1995). Most recently, an immunoassay kit for microcystins based on Adda antibodies has been developed by Abraxis LLC (Pennsylvania, USA), and a monoclonal antibody generated against 4-R-microcystins is also commercially available (Alexis

Biochemicals, Nottingham, U.K.). All are advocated by the manufacturers for the analysis of microcystins in water, and several microcystin variants have been tested using these systems.

An ELISA test using monoclonal antibodies against microcystin-LR has been used by Ueno (1996b) to analyze the microcystin concentration in environmental samples from ponds, lakes, reservoirs, and rivers in Japan, Thailand, Germany, and Portugal. Although microcystins are mainly associated with freshwater cyanobacteria, these results are relevant to the analysis of microcystins and particularly nodularins in brackish water environments.

ELISA for microcystins was used to analyze water samples from Haimen City, Jiansu Province, and Fusui County, Guangxi Province, China. Over two years, a high incidence of microcystins in ponds, ditches, and rivers was found although water from shallow and deep wells showed relatively little microcystin contamination (Ueno 1996a). Another ELISA test has been developed using antibodies specific for 4-R microcystins. This ELISA has been used to analyze microcystins in water and does not detect microcystins that lack arginine at position 4 (e.g., microcystin-LA); nevertheless, a sensitive response was obtained in water samples spiked with microcystin-LR, and the antibodies were found to be stable to the action of humic acids, pH, salt, surfactants, and organic solvents (Zeck 2001b).

*Antibodies produced against a synthetic 6E-Adda moiety were also used to develop an ELISA method, with good detection limits and good immunocross-reactivities for the microcystin variants tested (LR, RR; YR; LW; LF; desmethyl RR, nodularin, microcystin desmethyl-LR (Fischer 2001).*

## **Chromatographic Methods**

### ***Thin-Layer Chromatography (TLC)***

TLC procedures for the separation of microcystins have been reported in the literature (Poon 1987; Ojanpera 1995; Pelander 1996, 1998) using different detection systems. UV detection has been used to identify the separated components. From their characteristic UV spectra, microcystins can be identified in a similar way as it is detected in HPLC with diode array detection (DAD). This has been considered a screening procedure, and quantitative results are not yet provided. More development is still required.

### ***Gas Chromatography***

A gas chromatographic (GC) method has been described in the literature. GC is based on the oxidation of microcystins which splits the Adda side chain to produce 3-methoxy-2-methyl-4-phenylbutyric acid (MMPB), which is then determined, either by GC or GC/MS (as its methyl ester) (Sano 1992; Kaya and Sano 1999) or by HPLC/fluorescence detection (after conversion to a fluorescent derivative) (Sano 1992). GC/MS has been used to monitor microcystins in Japanese lakes (Tanaka 1993) and in sediments (Tsuji 2001). A similar method was developed by Harada (1996), but in this case the MMPB was determined directly without derivatization using GC/MS or LC/MS. The results of this approach are given in terms of total toxin concentration, which then can be expressed in terms of microcystin-LR. However, individual toxins are not determined and consequently it is not possible to produce a result in terms of microcystin-LR toxicity equivalents. This procedure cannot therefore be used to monitor water samples in relation to the proposed guideline.

### ***High-Performance Liquid Chromatography***

Several HPLC methods coupled with different detection modes have been used for the determination of hepatotoxins. An intensive review of these method has been carried out by Harada (1996) and Meriluoto (1996, 1997).



The HPLC method most widely used has been a reversed phase chromatography, with diode array detection enabling the detection of all microcystins bases in their UV spectra (Lawton 1994). This method offers a good separation of microcystins under the gradient elution conditions; nevertheless, the lack of standards and certified reference materials makes necessary that the quantitation of these toxins had to be carried out based on purified MC-LR to give MC-LR equivalence.

The improvement of sample pretreatment protocols plays an important role in the improvement of the sensitivity, selectivity, and efficiency of these HPLC methods. Efficient extraction and sample clean-up procedures are therefore critical for such analytical improvements. These concentration and clean-up procedures have been usually carried out using C18 solid phase extraction cartridges. The hydrophobicity of the individual toxins can affect their recoveries and on the other hand these recoveries can be also affected by the type of C18 cartridge and this makes the evaluation of the cartridges strictly necessary to ensure their efficiency. Solid-phase extraction based on immunoaffinity chromatography (IAC) has been also proposed as an alternative for a selective/specific extraction and clean-up. These approaches provide a selective/specific interference removal thanks to the specificity of the antigen-antibody interactions, which are the basis of the IAC principle. An SPE/IAC method has been proposed (Lawrence 2001) and this method was applied for the clean-up of different matrices contaminated with microcystins, resulting in a very promising alternative to concentrate samples and selectively remove interferences contributing to a significant increase of the sensitivity and selectivity of the HPLC method; nevertheless, some limitations especially regarding to binding capacity, cross reactivity, and volumes load still need to be overcome. An exhaustive evaluation and optimization on the application of these IAC/SPE clean-up has been carried out (Leao 2006). The immunoaffinity columns used in this study have been manufactured by Abkem Iberia S.L. (Spain) using monoclonal antibodies clone (MC10E7) developed by (Zeck 2001a), which show extraordinary sensitivity and high selectivity for [4-arginine]microcystins. The main features of these antibodies have been described in the section on immunological methods in this chapter. As it was already mentioned, the main drawback of using these antibodies is the lack of specificity for MCs such as MC-LA, and the cross-reactivities have been also described in this section; nevertheless, the effectivity and efficiency of these columns for the specific removal of compounds interfering [4-arginine]microcystins under the optimized conditions are clearly shown in this work.

The most common detection mode used in HPLC is by UV absorbance. Most microcystins and nodularin have a UV absorption maximum at 238 nm (Lawton 1994, 1995). However, those with aromatic amino acid constituents such as microcystin-LW, which contains tryptophan, have absorbance maxima at lower wavelengths, 222 nm. HPLC with diode array detection has been also used and provided very useful information through the characteristic spectra.

Fluorescence has been also selected as a detection mode for an improved sensitivity and selectivity in the HPLC determination of microcystins and nodularin (James and James 1991). This method uses a post-column system, whereby the arginine residue of microcystin-LR was derivatized with a fluorescent reagent. This approach obviously limits the application to toxins containing arginine, e.g., microcystin-LR, and toxins such as microcystin-LA.

Harada (1997) reported derivatization of microcystins with a fluorescent dienophile, DMEQ-TAD. These products were also separated by HPLC and detected by fluorescence with a high degree of sensitivity. Other detection methods include electrochemical detection but the sensitivity with microcystins not containing arginine, tryptophan, or tyrosine is likely to be very poor (Meriluoto 1998). Thus, microcystin-LA again will not be detected.

HPLC has been also widely used for the analysis of cylindrospermopsin using different chromatographic conditions.

The effect of organic solvents on the high-performance liquid chromatography (HPLC) analysis of cylindrospermopsin using photodiode array detection was examined by Metcalf (2002). Increasing concentrations of methanol resulted in an increase in the UV absorbance of purified cylindrospermopsin according to spectrometry, but a marked decrease during HPLC analysis when the concentration of this solvent was greater than 50% methanol, or when acetonitrile concentrations exceeded 30% (v/v). Precipitation of cylindrospermopsin at these high concentrations of organic solvents was not observed. Solid-phase extraction methods were developed to recover the toxin from spent extracellular growth medium after laboratory culture of *Cylindrospermopsis raciborskii* strain CR3 as an aid to toxin purification and from spiked environmental water samples.

Improvements in the selectivity of the separation of microcystins and nodularin have been achieved by selecting the most efficient stationary phase, with this aim (Spoof 2002) compared a monolithic C-bonded silica rod column (Merck Chromolith) to particle-based C and amide C 18 16 sorbents in the HPLC separation of eight microcystins and nodularin-R. Two gradient mobile phases of aqueous trifluoroacetic acid modified with acetonitrile or methanol, different flow-rates, and different gradient lengths were tested. The performance of the Chromolith column measured the resolution of some microcystin pairs. The selectivity, efficiency (peak width), and peak asymmetry equalled, or exceeded, the performance of traditional particle-based columns. The Chromolith 21 column allowed a shortening of the total analysis time to 4.3 minutes with a flow rate of 4 ml/minute.

Welkera (2002) developed an HPLC method to analyze environmental samples for their content of cylindrospermopsin (CYL) based on HPLC with photo diode array detection as an alternative to costly LC-MS approaches. A gradient from 0% to 50% aqueous methanol(+0.05% trifluoroacetic acid) in 20 minutes proved to be highly reproducible with respect to peak height, peak area, and retention time of purified CYL. Good linearity of peak area response was found for 1–300 ng CYL on column. For a good performance, the duration of equilibration prior to individual runs was crucial. Extraction from cell material (culture and bloom) was efficiently done with pure water in one extraction step, and CYL contents determined matched well with results previously obtained by LC-MS.

The data presented show a limitation of HPLC-PDA analysis for trace amounts of CYL in environmental samples but also underline the potential of an inexpensive and fast analysis for various purposes.

Cylindrospermopsin can be directly determined in water samples using LC/MS/MS with a detection limit of around 1µg/L. This is the method of choice as it has not been demonstrated that conventional HPLC with UV or PDA detection has the specificity to be applied to water samples containing low levels of cylindrospermopsin.

The results obtained after an interlaboratory study of HPLC methods to evaluate the amount of cylindrospermopsin in lyophilized cyanobacterial cells were reported (Törökne 2004). The HPLC methods were satisfactory on the basis of statistical evaluation. Further comparison of all the extraction methods allowed researchers to obtain the best conditions for an efficient extraction from interferences.

Mass spectrometry as a detection method following HPLC separation provides a much better solution to the problem of unequivocally identifying microcystins, as microcystins produce characteristic ions in their mass spectra (Namikoshi 1992; Kondo 1992; Rinehart 1994; Lawton 1995; Yuan 1998, 1999).

LC/MS with various interfaces and different ionization modes has been reported for the determination of microcystins (Poon 1993; Lawton 1995; Kondo 1992, 1995; Bateman 1995). Derivatization of microcystins prior to LC/MS analysis has also been reported as a technique to assist in identifying microcystins (Sherlock 1997).

A microcystin can be identified according to its mass spectrum, as long as a standard is available. In MS/MS, the fragmentation pattern can be used to greatly assist in determining the identities of unknown microcystins (Bateman 1995; Lawton 1995; Yuan 1998, 1999). However, the problem of the lack of standards is still present as with any other analytical procedure since standards are necessary for accurate quantification. In addition toxicity data are required in order that toxicity equivalents can be calculated.

This will be a limitation with any method that determines the concentration of individual toxins. While LC/MS systems are not yet particularly common in routine analytical laboratories, they are now increasingly available from a number of manufactures and appear sufficiently robust and relatively cheap to be used for the routine determination of these toxins.

In MS, the total ion current depends markedly on the particular microcystin. Thus concentrations of unknown microcystins, or microcystins for which standards are not available, cannot be reliably estimated with this method.

A simple, specific, and sensitive procedure for determining microcystins RR,LR, YR, LA, and LW and nodularin, in fish muscle tissue has been proposed (Bogialli 2005). This method is based on the matrix solid-phase dispersion with heated water as extractant followed by liquid chromatography tandem mass spectrometry, equipped with an electrospray ion source. On the basis of a signal-to-noise ratio of 10, limits of quantification were estimated to range between 1.6 and 4.0 ng/g. The effects of temperature and volume of the extractant on the analyte recovery were studied (Maizels 2004). The cyanobacteria toxins anatoxin-a, microcystin-LR, microcystin-RR, microcystin-YR, and nodularin were separated in less than 30 minutes on several reversed-phase liquid chromatography columns, and their electrospray mass spectra were measured using injections of 50 ng or less with a benchtop time-of-flight (TOF) mass spectrometer. New data from this work include the impact of acetic acid concentrations in the methanol-water mobile phase on measured ion abundances; the performance of the electrospray-TOF mass spectrometer as an LC detector; the accuracy and precision of exact  $m/z$  measurements after LC separation with a routinely used mass spectrometer resolving power of 5,000; and recoveries of the five toxins from reagent water, river waters, and sewage treatment plant effluent samples extracted with C-18 silica particles enmeshed in thin Teflon membrane filter disks. This technique has the potential of providing a relatively simple and reasonable-cost sample preparation and LC/MS method that provides the sensitivity, selectivity, reliability, and information content needed for source and drinking water occurrence and human exposure studies.

### *High-Performance Capillary Electrophoresis*

Other separation techniques such as capillary electrophoresis (CE) must be also considered for the separation and quantification of the peptide hepatotoxins using different CE modes (Boland 1993; Onyewuenyi and Hawkins 1996; Bouaicha 1996; Bateman 1995; John 1997; Siren 1999). One of the main disadvantages of using CE is its poor sensitivity compared with HPLC due to the lower sample volumes injected, and this has been the main limitation for its use for routine monitoring of microcystins when they are present in very low levels. Further improvements of this technique by using either preconcentration strategies or optimized alternative electrophoretic modes, such as micellar electrokinetic chromatography have been carried out with the aim of improving the sensitivity and selectivity and the results obtained are presented (Aguete 2001, 2003). These improvements make this technique very promising for a simple and fast analysis of microcystins at the required regulatory levels without further development. CE might also not yet be considered to be sufficiently robust for use in a routine analytical laboratory. Sensitivity has been also increased by

CE separation of fluorescently derivatised microcystins and detection using a laser-induced fluorescent detector (Li 1999); however, an evaluation of this method is still required.

## References

- Aguete E.C., Gago-Martinez A., Leao J.M., Rodriguez Vazquez J. A., Menard C., and Lawrence J.F. 2003. HPLC and HPCE analysis of microcystins RR, LR and YR present in cyanobacteria and water by using immunoaffinity extraction. *Talanta* 59:697–705.
- Aguete E.C., Gago-Martinez A., Rodriguez Vazquez J. A., O'Connell, S., C. Moroney, C., and James, K.J. 2001. Application of HPLC and HPCE to the Analysis of Cyanobacterial Toxins. *Chromatographia* 53:254
- Aune, T., and Berg, K. 1986. Use of freshly prepared rat hepatocytes to study toxicity of blooms of the blue-green algae *Microcystis aeruginosa* and *Oscillatoria agardhii*. *Journal of Toxicology Environmental Health* 19:325–336.
- Azevedo, S.M.F.O., Carmichael, W.W., Jochimsen, E.M., Rinehart, K.L., Lau, S., Shaw, G.R., Eaglesham, G.K. 2002. Human intoxication by microcystins during renal dialysis treatment in Caruaru-Brazil. *Toxicology*, 181–182, 441–446.
- Banker, R., Carmeli, S., Hadas, O., Teltsch, B., Porat, R. and Sukenik, A. 1997. Identification of cylindrospermopsin in *Aphanizomenon ovalisporum* (Cyanophyceae) isolated from Lake Kinneret, Israel. *Journal Phycology* 33:613–616.
- Banker, R., Teltsch, B., Sukenik, A. and Carmeli, S. 2000. 7-epicylindrospermopsin, a toxic minor metabolite of the cyanobacterium *Aphanizomenon ovalisporum* from Lake Kinneret, Israel. *Journal of Natural Products* 63: 387–389.
- Bateman, K.P., Thibault, P., Douglas, D.J., and White, R.L. 1995. Mass spectral analyses of microcystins from toxic cyanobacteria using on-line chromatographic and electrophoretic separations. *Journal of Chromatography A* 712:253–268.
- Beattie, K.A., Kaya, K., and Codd, G.A. 2000. The cyanobacterium *Nodularia* PCC 7804, of freshwater origin, produces [L-Har2]nodularin. *Phytochemistry* 54:57–61.
- Bell, S.G., and Codd, G.A. 1994. Cyanobacterial toxins and human health. *Rev Med Microbiology* 5:256–264.
- Bhattacharya, R., Sugendran, K., Dangi, R.S., and Rao, P.V. 1997. Toxicity evaluation of freshwater cyanobacterium *Microcystis aeruginosa* PCC7806:II. Nephrotoxicity in rats. *Biomedical and Environmental Sciences* 10:93–101.
- Billings, W.H. 1981. Water-associated human illness in northeast Pennsylvania and its suspected association with blue-green algae blooms. In *The Water Environment: Algal Toxins and Health*, ed. Carmichael, W.W. New York: Plenum Press, 243–255.
- Boglialli, S., Milena, B., Curini, R., di Corcia, A., Lagana, A., Mari, B. 2005. Simple assay for analyzing five microcystins and nodularin in fish muscle tissue: hot water extraction followed by liquid chromatography-tandem mass spectrometry. *Journal of Agricultural and Food Chemistry* 53:6586–6592.
- Boland, M.P., Smillie, Chen, D.Z.X. and Holmes, C.F.B. 1993. A unified bioscreen for the detection of diarrhetic shellfish toxins and microcystins in marine and freshwater environments. *Toxicon* 31:1393–1405.
- Bouaïšcha, N., Maatouk, I., Vincent, G., and Levi, Y. 2002. A colorimetric and fluorometric microplate assay for the detection of microcystin-LR in drinking water without preconcentration. *Food and Chemical Toxicology* 40:1677–1683.
- Bouaicha, N., Rivasseau, C., Hennion, M.C. and Sandra, P. 1996. Detection of cyanobacterial toxins (microcystins) in cell extracts by micellar electrokinetic chromatography. *Journal of Chromatography B* 685:53–57.
- Brenton C. Nicholson, Michael D. Burch. 2001. *Evaluation of Analytical Methods for Detection and Quantification of Cyanotoxins in Relation to Australian Drinking Water Guidelines*.
- Brooks, W. P., and Codd, G. A. 1988. Immunoassay of hepatotoxic cultures and water blooms of cyanobacteria using *Microcystis aeruginosa* peptide toxin polyclonal antibodies. *Environ Technol Lett* 9, 1343–1348.
- Byth, S. 1980 Palm Island mystery disease. *Med. J. Aust.* 2:40–42.
- Carbis, C.R., Rawlin, G.T., Grant, P., Mitchell, G.F., Anderson, J.W., and McCauley, I. 1997. A study of feral carp *Cyprinus Carpio* exposed to *Microcystis aeruginosa* at Lake Mokoan, Australia and possible implication in fish health. *J Fish Dis* 20:81–91.
- Carmichael, W.W., and An, J. 1999. Using an enzyme linked immunosorbent assay (ELISA) and a protein phosphatase inhibition assay for the detection of microcystins and nodularins. *Nat Toxins* 7:377–385.
- Carmichael, W.W., Beasley, V., Bunner, D.L., Eloff, J.N., Falconer, I., Gorham, P., Harada, K.-I., Krishnamurthy, T., Min-Juan, Y., Moore, R.E., Rinehart, K., Runnegar, M., Skulberg, O.M., and Watanabe, M. 1988. Naming of cyclic heptapeptide toxins of cyanobacteria (blue-green algae). *Toxicon* 26:971–973.
- Carmichael, W.W., Evans, W.R., Yin, Q.Q., Bell, P. and Moczydlowski, E. 1997. Evidence for paralytic shellfish poisons in the freshwater cyanobacterium *Lyngbya wollei* (Farlow ex Gomont. comb. nov.) *Appl Environ Microbiol* 63:3104–3110.

- Carmichael, W.W., and Falconer, I.R. 1993. Diseases related to freshwater blue-green algal toxins, and control measures. In *Algal Toxins in Seafood and Drinking Water*, ed. Falconer, I.R. London: Academic Press, 187–209.
- Chen, T., Shen, P., Zhang, J., and Hua, Z. 2005. Effects of microcystin-LR on patterns of iNOS and cytokine mRNA expression in macrophages in vitro. *Wiley Periodicals Inc Env Toxicol* 20:85–91.
- Chiswell, R.K., Shaw, G.R., Eaglesham, G.K., Smith, M.J., Norris, R.L., Seawright, A.A., and Moore, M.R. 2001. Stability of cylindrospermopsin, the toxin from the cyanobacterium *Cylindrospermopsis raciborskii*. Effects of pH, temperature, and sunlight on decomposition. *Environ Toxicol* 16:460–467.
- Chorus, I., and Bartram, J., eds. 1999. *Toxic Cyanobacteria in Water: A Guide to their Public Health Consequences, Monitoring and Management*. London: E. & F.N. Spon.
- Chu, F. S., Huang, X., Wei, R.D., and Carmichael, W.W. 1989. Production and characterisation of antibodies against microcystins. *Appl Environ Microbiol* 55:1928–1933.
- Codd, G.A. Metcalf, J.S., and Beattie, K.A. 1999. Retention of *Microcystis aeruginosa* and microcystin by salad lettuce (*Lactuca sativa*) after spray irrigation with water containing cyanobacteria. *Toxicon* 37:1181–1185.
- Dahlmann, J., RuÈhla, A., Hummert, C., Liebezeit, G., Carlsson, P., and Graneàic, E. 2001. Different methods for toxin analysis in the cyanobacterium *Nodularia spumigena* (Cyanophyceae). *Toxicon* 39:1183–1190.
- De Silva, E.D., Williams, D.E., Andersen, R.J., Klix, H., Holmes, C.F.B. and Allen, T.M. 1992. Motuporin, a potent protein phosphatase inhibitor isolated from the Papua New Guinea sponge *Theonella swinhoei* Gray. *Tetrahedron Lett* 33:1561–1564.
- Dillenberg, H.O. and Dehnel, M.K. 1960. Toxic waterbloom in Saskatchewan, 1959. *Can Med Assoc J* 83:1151–1154.
- Falconer, I.R. 1993. Measurement of toxins from blue-green algae in water and foodstuffs. In *Algal Toxins in Seafood and Drinking Water*, ed. Falconer, I.R. London: Academic Press, 165–175.
- Falconer, I.R., Beresford, A.M., and Runnegar, M.T.C. 1983. Evidence of liver damage by toxin from a bloom of the blue-green alga, *Microcystis aeruginosa*. *Med J Aust* 1:511–514.
- Falconer, I.R., Hardy, S.J., Humpage, A.R., Frosco, S.M., Tozer, G.J., and Hawkins, P.R. 1999. Hepatic and renal toxicity of the blue-green alga (cyanobacterium) *Cylindrospermopsis raciborskii* in male Swiss albino mice. *Environ Toxicol* 14:143–150.
- Fastner, J., Heinze, R., Humpage, A.R., Mischke, U., Eaglesham, G.K., and Chorus, L. 2003. Cylindrospermopsin occurrence in two German lakes and preliminary assessment of toxicity and toxin production of *Cylindrospermopsis raciborskii* (Cyanobacteria) isolates. *Toxicon* 42:313–321.
- Fischer, W.J., Garthwaite, I., Miles, C.O., Ross, K.R., Aggen, J.B., Chamberlin, A.R., Towers, N.R., and Dietrich, D.R. 2001. Congener-independent immunoassay for microcystins and nodularins. *Environ Sci Technol* 35:4849–4856.
- Fladmark, K.E., Serres, M.H., Larsen, N.L., Yasumoto, T., Aune, T., and Doskeland, S.O. 1998. Sensitive detection of apoptogenic toxins in suspension cultures of rat and salmon hepatocytes. *Toxicon* 36:1101–1114.
- Gehring, M.M., Govender, S., Shah, M., and Downing, T.G. 2003. An investigation of the role of vitamin E in the protection of mice against microcystin toxicity. *Wiley Periodicals Environ Toxicol* 18:142–148.
- Harada, K., Murata, H., Qiang, Z., Suzuki, M., and Kondo, F. 1996a. Mass spectrometric screening method for microcystins in cyanobacteria. *Toxicon* 34:701–710.
- Harada, K.-I., Ohtani, I., Iwamoto, K., Suzuki, M., Watanabe, M.F., Watanabe, M., and Terao, K. 1994. Isolation of cylindrospermopsin from a cyanobacterium *Umezakia natans*. *Toxicon* 32(1):73–84.
- Harada, K.-I., Oshikata, M., Shimada, T., Nagata, A., Ishikawa, N., Suzuki, M., Kondo, F., Shimizu, M. and Yamada, S. 1997. High performance liquid separation of microcystins derivatized with a highly fluorescent dienophile. *Natural Toxins* 5:201–207.
- Harada, K.-I., Tsuji, K., Watanabe, M.F., and Kondo, F. 1996b. Stability of microcystins from cyanobacteria—III. Effect of pH and temperature. *Phycologia* 35 (Suppl. 6), 83–88.
- Hawkins, P.R., Chandrasena, N.R., Jones, G.J., Humpage, A.R., and Falconer, I.R. 1997. Isolation and toxicity of *Cylindrospermopsis raciborskii* from an ornamental lake. *Toxicon* 35:341–346.
- Heinze, R., (1996). A biotest for hepatotoxins using primary rat hepatocytes. *Phycologia* 35 (Suppl. 6), 89–93.
- Heresztyn, T., Nicholson, B.C. 2001. Determination of cyanobacterial hepatotoxins directly in water using a protein phosphatase inhibition assay. *Water Res* 13: 3049–3056.
- Hiripi, L., Nagy, L., Kalmár, T., Kovács, A., and Voros, L. 1998. Insect (*Locusta migratoria migratorioides*) test monitoring the toxicity of cyanobacteria. *Neurotoxicol* 19:605–608.
- Honkanen, R.E., Codispoti, B.A., Tse, K., Boynton, A.L., and Honkanen, R.E. 1994. Characterization of natural toxins with inhibitory activity against serine/threonine protein phosphatases. *Toxicon* 32(3):339–350.
- Ito, E., Kondo, F., Terao, K., and Harada, K. 1997. Neoplastic nodular formation in mouse liver induced by repeated intraperitoneal injection of microcystin-LR, *Toxicon* 35(9):1453–1457.



- James, H.A. and James, C.P. 1991. *Development of an Analytical Method for Blue-Green Algal Toxins (Report FR0224)*. Marlow, Buckinghamshire: Foundation for Water.
- Jochimsen, E.M., Carmichael, W.W., An, J.S., Cardo, D.M., Cookson, S.T., and Holmes, C.E.M. 1998. Liver failure and death after exposure to microcystins at a hemodialysis center in Brazil. *New England Journal of Medicine* 338:873–878.
- John, W., Raynor, M.W., and Rae, B. 1997. Micellar electrokinetic capillary chromatography of algal toxins. *J High Res Chromatog* 20:34–38.
- Kaya, K. and Sano, T. 1999. Total microcystin determination using erythro-2-methyl-3-(methoxy-d(3))-4-phenylbutyric acid (MMPB-d(3)) as the internal standard. *Anal Chim Acta* 386:107–112.
- Kfir, R., Johannsen, E., and Botes, D.P. 1985. Preparation of anti-cyanoginosen-LA monoclonal antibody. In *Mycotoxins and Phycotoxins: Papers from the Sixth International IUPAC Symposium on Mycotoxins and Phycotoxins*, ed. Steyn, P.S., and Vleggar, R. Pretoria, South Africa, 377–385.
- . 1986. Monoclonal antibodies specific for cyanoginosen-LA: preparation and characterisation. *Toxicon* 30:1143–1156.
- Kiviranta, J., Sivonen, K., and Niemela, S.I. 1991. Detection and toxicity of cyanobacteria by *Artemia salina* bioassay. 1991. *Environ Toxicol Water Qual* 6:423–426.
- Kondo, F., Ikai, Y., Oka, H., Ishikawa, N., Watanabe, M.F., Watanabe, M., Harada, K.-I., and Suzuki, M. 1992. Separation and identification of microcystins in cyanobacteria by fritfast atom bombardment liquid chromatography/mass spectrometry. *Toxicon* 30:227–237.
- Kondo, F., Ikai, Y., Oka, H., Matsumoto, H., Yamada, S., Ishikawa, N., Tsuji, K., Harada, K.-I., Shimada, T., Oshikata, M., and Suzuki, M. 1995. Reliable and sensitive method for determination of microcystins in complicated matrices by frit-fast atom bombardment liquid chromatography/mass spectrometry. *Natural Toxins* 3:41–49.
- Lankoff, A. and Kolataj A. 2001. Influence of microcystin-YR and nodularin on the activity of some proteolytic enzymes in mouse liver. *Toxicon* 39:419–423.
- Lawrence, J.F. and Menard, C. 2001. Determination of microcystins in blue-green algae, fish and water using liquid chromatography with ultraviolet detection after sample clean-up employing immunoaffinity chromatography. *Journal of Chromatography A* 992: 111–117.
- Lawton, L.A., Edwards, C., Beattie, K.A., Pleasance, S., Dear, G.J., and Codd, G.A., 1995. Isolation and characterization of microcystins from laboratory cultures and environmental samples of *Microcystis aeruginosa* and from an associated animal toxicosis. *Natural Toxins* 3:50–57.
- Lawton, L.A., Edwards, C. and Codd, G.A. 1994. Extraction and high-performance liquid chromatographic method for the determination of microcystins in raw and treated waters. *Analyst* 119:1525–1530.
- Leão Martins, J.M., García, V., Reis Costa, P., Barbi Perez, L., Rivera Vila, S., de la Iglesia, P., and Gago-Martínez, A. 2006. Immunoaffinity chromatography: An alternative method for the sample clean-up of algal toxins present in biological matrices. *JAOAC Int*, in press.
- Li, P.C.H., Hu, S., and Lam, P.K.S. 1999. Development of a capillary zone electrophoretic method for the rapid separation and detection of hepatotoxic microcystins. *Mar Pollut Bull* 39:250–254.
- Li, X.-Y., Chung, I.-K., Kim, J.-I., and Lee, J.A. 2005. Oral exposure to microcystin increases activity-augmented antioxidant. *Comp Biochem Physiol C Toxicol Pharmacol* 141(3):292–296.
- Lin, J.R., and Chu, F.S. 1994. In vitro neutralisation of the inhibitory effect of microcystin-LR to protein phosphatase 2A by antibody against the toxin. *Toxicon* 32:605–613.
- Lippy, E.C. and Erb, J. 1976. Gastrointestinal illness at Sewickley, Pa. *J Am Water Works Assoc* 88:606–610.
- MacKintosh, C., Beattie, K.A., Klumpp, S., Cohen, P., and Codd, G.A. 1990. Cyanobacterial microcystin-LR is a potent inhibitor of protein phosphatases 1 and 2A from both mammals and higher plants. *FEBS Lett* 264:187–192.
- Maizels, M., Budde, W.L. 2004. A LC/MS method for the determination of cyanobacteria toxins in water. *Analytical Chemistry* 76:1342–1351.
- McDermott, C. M., Feola, R., and Plude, J. 1995. Detection of cyanobacterial toxins (microcystins) in waters of northeastern Wisconsin by a new immunoassay technique. *Toxicon* 33:1433–1442.
- McElhiney J., Lawton L. A. 2005. Detection of cyanobacterial hepatotoxins microcystins. *Toxicology and Applied Pharmacology* 203:219–230.
- Meriluoto, J. 1997. Chromatography of microcystins. *Anal Chim Acta* 352–298.
- Meriluoto J., and Codd G.A., eds. 2005. *Toxic: Cyanobacterial Monitoring and Cyanotoxin Analysis*. Abo: Abo Akademy University Press.
- Meriluoto, J.A.O., and Eriksson, J.E., 1988. Rapid analysis of peptide toxins in cyanobacteria. *J Chromatog* 438:93–99.
- Meriluoto, J.A.O., Härmälä-Braskén, A.-S., Eriksson, J.E., Toivola, D.M., and Lindholm, T. 1996. Choosing analytical strategy for microcystins. *Phycologia* 35:125–132.

- Meriluoto J., Kinkaid, B., Smith, M.R., and Wasberg, M. 1998. Electrochemical detection of microcystins, cyanobacterial peptide hepatotoxins, following High Performance Liquid Chromatography. *Journal of Chromatography A* 810:226–230.
- Metcalf, J.S., Beattie, K.A., Saker, M.L., and Codd, G.A. 2002. Effects of organic solvents on the high performance liquid chromatographic analysis of the cyanobacterial toxin cylindrospermopsin and its recovery from environmental eutrophic waters by solid phase extraction. *FEMS Microbiology Letters* 216:159–164.
- Metcalf, J.S., Bell, S.G., and Codd, G.A. 2001. Colorimetric immuno-protein phosphatase inhibition assay for specific detection of microcystins and nodularins of cyanobacteria. *Appl Environ Microbiol* 67:904–909.
- Metcalf J.S., and Codd G.A. 2003. Analysis of cyanobacterial toxins by immunological methods. *Chem Res Toxicol* 16(2):104–112.
- Mikhailov, A., Harmala-Brasken, A.S., Meriluoto, J., Sorokina, Y., Dietrich, D., and Eriksson, J.E. 2001. Production and specificity of mono and polyclonal antibodies against microcystins conjugated through *N*-methyldehydroalanine. *Toxicol* 39:377–483.
- Nagata, S., Soutome, H., Tsutsumi, T., Hasegawa, A., Sekijima, M., Sugamata, M., Harada, K. I., Suganuma, M., and Ueno, Y. 1995. Novel monoclonal antibodies against microcystin and their protective activity for hepatotoxicity. *Nat Toxins* 3, 78–86.
- Nagata, S., S., Tsutsumi, T., Yoshida, F., and Ueno, Y. 1999. A new type sandwich immunoassay for microcystin: production of monoclonal antibodies specific to the immune complex formed by microcystin and an anti-microcystin monoclonal antibody. *Natural Toxins* 7, 49–55.
- Naminoski, M., Choi, B.W., Sakai, R., Sun, F., Rinehart, K.L., Carmichael, W.W., Evans, W.R., Cruz, P., Munro, M.H.G., and Blunt, J.W. 1994. New nodularins, a general method for structure assignment. *Journal Organic Chemistry* 55:6135–6139.
- Namikoshi, M., Rinehart, K.L., Sakai, R., Stotts, R.R., Dahlem, A.M., Beasley, V.R., Carmichael, W.W., and Evans, W.R. 1992. Identification of 12 hepatotoxins from a Homer Lake bloom of the cyanobacteria *Microcystis aeruginosa*, *Microcystis viridis*, and *Microcystis wesenbergii*: Nine new microcystins. *Journal Organic Chemistry* 57:866–872.
- Ohtani, I., Moore, R.E., and Runnegar, M.T.C. 1992. Cylindrospermopsin: a potent hepatotoxin from the blue green algae *Cylindrospermopsis raciborskii*. *Journal of American Chemical Society* 114:7941–7942.
- Ojanpera, I., Pelander, A., Vuori, E., Himberg, K., Waris, M., and Niinivaara, K. 1995. Detection of cyanobacterial hepatotoxins by TLC. *Journal of Planar Chromatog* 8:69–72.
- Onyewuenyi, N., and Hawkins, P. 1996. Separation of toxic peptides (microcystins) in capillary electrophoresis, with the aid of organic mobile phase modifiers. *Journal of Chromatography A* 749:271–278.
- Pelander, A., Ojanpera, I., Sivonen, K., Himberg, K., Waris, M., Niinivaara, K., and Vuori, E. 1996. Screening for cyanobacterial toxins in bloom and strain samples by thin layer chromatography. *Water Research* 30:1464–1470.
- Pelander, A., Ojanpera, I., and Vuori, E. 1998. Analysis of cyanobacterial hepatotoxins by overpressured layer chromatography. *Journal of Planar Chromatography*. 11:365–369.
- Poon, G.K., Griggs, L.J., Edwards, C., Beattie, K.A., and Codd, G.A. 1993. Liquid chromatography-electrospray ionization mass-spectrometry of cyanobacterial toxins. *Journal of Chromatography* 628:215–233.
- Poon, G.K., Priestley, I.M., Hunt, S.M., Fawell, J.K., and Codd, G.A. 1987. Purification procedure for peptide toxins from the cyanobacterium *Microcystis aeruginosa* involving high-performance liquid chromatography. *Journal of Chromatography* 387:551–555.
- Pyo, D., Lee, J., and Choi, E. 2005. Trace analysis of microcystins in water using enzyme-linked immunosorbent assay. *Microchemical Journal* 80:165–169.
- Rapala, J., Erkomaa, K., Kukkonen, J., Sivonen, K., and Lahti K. 2002. Detection of microcystins with protein phosphatase inhibition assay, high performance liquid chromatography-UV detection and enzymelinked immunosorbent assay. Comparison of methods. *Analytica Chimica Acta* (466):213–231.
- Rinehart, K.L., Harada, K.-I., Namikoshi, M., Chen, C., Harvis, C.A., Munro, M.H.G., Blunt, J.W., Mulligan, P.E., Beasley, V.R., Dahlem, A.M., and Carmichael, W.W. 1988. Nodularin, microcystin, and the configuration of Adda. *Journal of American Chemical Society* 110:8557–8558.
- Rinehart, K.L., Namikoshi, M., and Choi, B.W. 1994. Structure and biosynthesis of toxins from blue-green algae (cyanobacteria). *Journal of Applied Phycology* 6:159–176.
- Rivasseau, C., and Hennion M.C. 1999. Potential of immunoextraction coupled to analytical and bioanalytical methods (liquid chromatography, ELISA kit and phosphatase inhibition test) for an improved environmental monitoring of cyanobacterial toxins. *Anal Chim Acta* 399(13):75–87.
- Robillot, C., and Hennion, M.C. 2004. Issues arising when interpreting the results of the protein phosphatase 2A inhibition assay for the monitoring of microcystins. *Analytica Chimica Acta* 512:339–346.
- Runnegar, M.T.C., King, S.M., Zhong, Y.Z., and Lu, S.C. 1995. Inhibition of reduced glutathione synthesis by cyanobacterial alkaloid cylindrospermopsin in cultured rat hepatocytes. *Biochemistry and Pharmacology* 49(2):219–225.



- Saito, K., Konno, A., Ishii, H., Saito, H., Nishida, F., Abe, T., and Chen, C.Y. 2001. Nodularin-Har: A new nodularin from *Nodularia*. *Journal of Natural Products* 64:139–141.
- Saker, M.L., Thomas, A.D., and Norton, J.H. 1999. Cattle mortality attributed to the toxic cyanobacterium *Cylindrospermopsis raciborskii* in an outback region of north Queensland. *Environmental Toxicology* 14:179–182.
- Sano, T., Nohara, K., Shiraiishi, F., and Kaya, K. 1992. A method for micro-determination of total microcystin content in waterblooms of cyanobacteria (blue-green algae). *International Journal of Environmental Analytical Chemistry* 49:163–170.
- Shaw, G.R., Sukenik, A., Livne, A., Chiswell, R.K., Smith, M.J., Seawright, A.A., Norris, R.L., Eaglesham, G.K., and Moore, M.R. 1999. Blooms of the cylindrospermopsin containing cyanobacterium, *Aphanizomenon ovalisporum* (Forti), in newly constructed lakes, Queensland, Australia. *Environmental Toxicology* 14:167–177.
- Sherlock, I.R., James, K.J., Caudwell, F.B., and MacKintosh, C. 1997. The first identification of microcystins in Irish lakes aided by a new derivatisation procedure for electrospray mass spectrometric analysis. *Natural Toxins* 5:247–254.
- Siren, H., Jussila, M., Liu, H.W., Peltoniemi, S., Sivonen, K., and Riekkola, M.L. 1999. Separation, purity testing and identification of cyanobacterial hepatotoxins with capillary electrophoresis and electrospray mass spectrometry. *J Chromatog A* 839:203–215.
- Sivonen, K., and Jones, G. 1999. Cyanobacterial toxins. In *Toxic Cyanobacteria in Water: A Guide to their Public Health Consequences, Monitoring and Management*, ed. Chorus, I., and Bartram, J. London: E. & F.N. Spon., 41–111.
- Spoof, L., and Meriluoto, J. 2002. Rapid separation of microcystins and nodularin using a monolithic silica C column 18. *Journal of Chromatography A* 947:237–245.
- Surakka A., Sivonen, L.M., J. M. Lehtimäki J. M., Wahlsten, M., Vuorela P., and Sivonen K. 2005. Cyanobacteria from the Baltic Sea contain cytotoxic anabaena, nodularia, and nostoc strains and an apoptosis-inducing phormidium strain. *Wiley Periodicals Environ Toxicol* 20: 285–292.
- Tanaka, Y., Takenaka, S., Matsuo, H., Kitamori, S., and Tokiwa, H. 1993. Levels of microcystins in Japanese lakes. *Toxicological Environmental Chemistry* 39:21–27.
- Terao, K., Ohmori, S., Igarashi, K., Ohtani, I., Watanabe, M.F., Harada, K.I., Ito, E., and Watanabe, M. 1994. Electronmicroscopic studies on experimental poisoning in mice induced by cylindrospermopsin isolated from the blue-green alga *Umezakia natans*. *Toxicon* 32:833–844.
- Tisdale, E.S. 1931a. Epidemic of intestinal disorders in Charleston, W. Va., occurring simultaneously with unprecedented water supply conditions. *American Journal of Public Health* 21:198–200.
- . 1931b. The 1930–1931 drought and its effect upon public water supply. *American Journal of Public Health* 21:1203–1218.
- Törökne, A., Asztalos, M., Bánkiné, M., Bickel, H., Borbély, G., Carmeli, S., Codd, G.A., Fastner, J., Huang, Q., Humpage, A., Metcalf, J.S., Rábai, E., Sukenik, A., Surányi, G., Vasas, G., and Weiszfeilera, V. 2004. Interlaboratory comparison trial on cylindrospermopsin measurement. *Analytical Biochemistry* 332:280–284.
- Tsuji, K., Masui, H., Uemura, H., Mori, Y., and Harada, K. 2001. Analysis of microcystins in sediments using MMPB method. *Toxicon* 39:687–692.
- Turner, P.C., Gammie, A.J., Hollinrake, K., and Codd, G.A. 1990. Pneumonia associated with cyanobacteria. *Brit Med J* 300:1440–1441.
- Ueno, Y., Nagata, S., Tsutsumi, T., Hasegawa, A., Watanabe, M. F., Park, H.-D., Chen, G.-C., Chen, G., and Yu, S.-Z. 1996a. Detection of microcystins, a blue-green algal hepatotoxin, in drinking water sampled in Haimen and Fusui, endemic areas of primary liver cancer in China, by highly sensitive immunoassay. *Carcinogenesis* 17:1317–1321.
- Ueno, Y., Nagata, S., Tsutsumi, T., Hasegawa, A., Yoshida, F., Suttajit, M., Mebs, D., Putsch, M., and Vasconcelos, V. 1996b. Survey of microcystins in environmental water by a highly sensitive immunoassay based on monoclonal antibody. *Nat Toxins* 4:271–276.
- Vasconcelos, V.M. 1995. Uptake and depuration of the heptapeptide toxin microcystin-LR in *Mytilus galloprovincialis*. *Aquatic Toxicology* 32:227–237.
- Veldee, M.V. 1931. An epidemiological study of suspected water-borne gastroenteritis. *American Journal of Public Health* 21:1227–1235.
- Welkera M., Bickel, H., and Fastner, J. 2002. Technical note HPLC-PDA detection of cylindrospermopsin—opportunities and limits. *Water Research* 36:4659–4663.
- Weller, M.G. Zeck, A., Eikenberg, A., Nagata, S., Ueno, Y. and Niessner, R. 2001. Development of a direct competitive microcystin immunoassay of broad specificity. *Analytical Sciences* 17:1445–1448.
- Yoshida, T., Makita, Y., Nagata, S., Tsutsumi, T., Yoshida, F., Sekijima, M., Tamura, S., and Ueno, Y. 1997. Acute oral toxicity of microcystin-LR, a cyanobacteria hepatotoxin, in mice. *Natural Toxins* 5:91–95.

- Yu, S.-Z. 1994. Blue-green algae and liver cancer. In *Toxic Cyanobacteria: Current Status of Research and Management*, ed. Steffensen, D.A., and Nicholson, B.C., 75–85.
- Yuan, M., Namikoshi, M., Otsuki, A., and Sivonen, K. 1998. Effect of amino acid side-chain on fragmentation of cyclic peptide ions: differences of electrospray ionization collision-induced decomposition mass spectra of toxic heptapeptide microcystins containing ADMAdda instead of Adda. *Eur Mass Spectrom* 4:287–298.
- Yuan, M., Namikoshi, M., Otsuki, A., Watanabe, M.F., and Rinehart, K.L. 1999. Electrospray ionization mass spectrometric analysis of microcystins, cyclic heptapeptide hepatotoxins: Modulation of charge states and  $[M+H]^+$  to  $[M+Na]^+$  ratio. *Journal of American Society of Mass Spectrometry* 10:1138–1151.
- Zeck, A., Eikenberg, A., Weller, M. G., and Niessner, R. 2001a. Highly sensitive immunoassay based on a monoclonal antibody specific for [4-arginine]microcystins. *Analytica Chimica Acta* 441:1–13.
- Zeck, A., Weller, M. G., Bursill, D., and Niessner, R. 2001c. Generic microcystin immunoassay based on monoclonal antibodies against Adda. *Analyst* 126:2002–2007.
- Zeck, A., Weller, M.G., and Niessner, R. 2001b. Multidimensional biochemical detection of microcystins in liquid chromatography. *Analytical Chemistry* 73:5509–5517.
- Zilberg, B. 1966. Gastroenteritis in Salisbury European children—a five-year study. *Centr Afr J Med* 12:164–168.

## 15 Polycavernosides

Leo A. Paquette and Mari Yotsu-Yamashita

### Discovery of the Polycavernosides

#### Isolation

Fatal human intoxication resulting from the ingestion of the edible red alga *Gracilaria edulis* (*Polycavernoside tsudai*) occurred in Guam in late April 1991. Three people out of thirteen patients were killed by this incident. Polycavernoside A (PA, 1) (0.4 mg) and polycavernoside B (PB) (0.2 mg) (Fig. 15.1) were isolated by Yasumoto and his colleagues (Yotsu-Yamashita, Haddock, and Yasumoto 1993) as the causative toxins from *G. edulis* (2.6 kg) collected on June 4, 1991, at Tanguisson Beach, Guam, where the causative alga had previously been collected. Other minor analogues such as polycavernoside A2 (PA2) (0.1 mg), A3 (PA3) (0.4 mg), and B2 (PB2) (0.1 mg), together with PA (0.4 mg), were isolated from the same alga collected at the same beach on June 11, 1992 (Yotsu-Yamashita et al. 1995). These toxins were extracted from the alga with acetone or CH<sub>2</sub>Cl<sub>2</sub>-MeOH (2:1), and the extract was partitioned between 80% aqueous MeOH and hexane

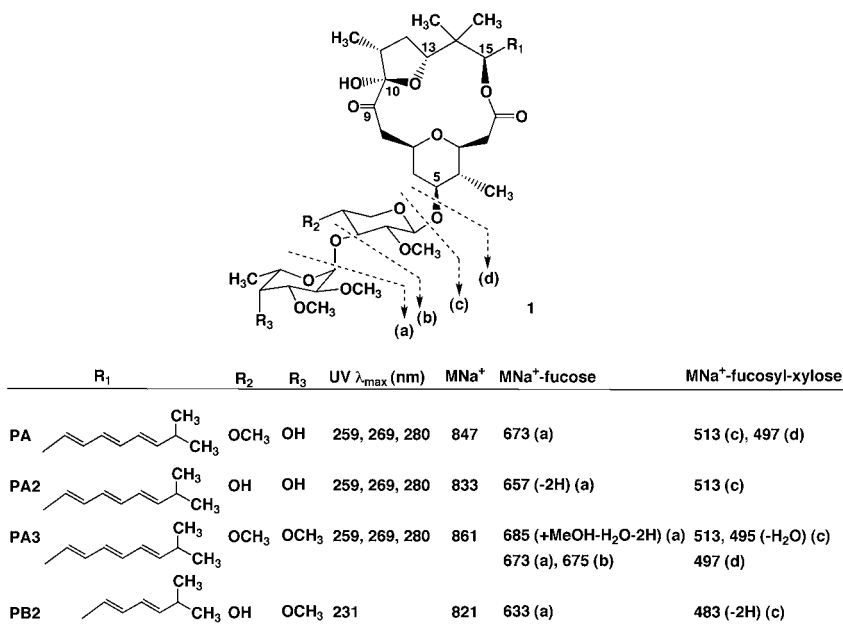


**Figure 15.1.** The structures, UV λ<sub>max</sub> wave lengths, MNa<sup>+</sup> ions, and the prominent fragmentations by ESI-MS/MS of polycavernosides (PA, PA2, PA3 and PB2).

(toxins in the aqueous phase), and then between  $\text{CH}_2\text{Cl}_2$  and  $\text{H}_2\text{O}$  (toxins in the organic phase). PA and PB present in the organic phase were separated by chromatography on silica gel with  $\text{CH}_2\text{Cl}_2/\text{MeOH}$  [1:0, 99:1 (PB), and 9:1 (PA)], and further purified by successive reverse phase chromatography on ODS-Q3 and Develosil ODS-7 with  $\text{CH}_3\text{CN}/\text{H}_2\text{O}$  85:15, and on Cosmosil 5C18-AR with  $\text{CH}_3\text{CN}/\text{H}_2\text{O}$  4:1. PA, PA2, PA3 and PB2 were isolated by chromatography on ODS-Q3 with  $\text{CH}_3\text{CN}/\text{H}_2\text{O}$  [3:1 (PA, PA2, PB2), and 9:1 (PA3)], and on Develosil ODS-5 with  $\text{CH}_3\text{CN}/\text{H}_2\text{O}$  [65:35–100:0 gradient].

## Structures

The planar structure of PA and the relative configurations of its tetrahydrofuran and tetrahydropyran rings, as well as those of the sugar moieties were determined by HR-FABMS, IR, UV, and NMR (COSY, TOCSY, HMQC, HMBC,  $^{13}\text{C}$ , NOESY, ROESY, NOE difference) data (Yotsu-Yamashita, Haddock, and Yasumoto 1993). The polycavernosides are characterized by the presence of a macrolide structure possessing side chains containing a conjugated diene or triene moiety, and an *O*-methylated or *O*-acetylated fucosyl-xylose. Fujiwara and Murai determined the relative configuration of the sequence of the L-fucosyl-D-xylose and bottom half of the macrolactone synthetically (Fujiwara, Amano, and Murai 1995a, 1995b). Paquette and co-workers also synthesized the corresponding disaccharide (Johnston and Paquette 1995). Finally, the total synthesis of (–)-PA (1) was achieved by Murai and Fujiwara et al. in 1998 (Fujiwara et al. 1998), Paquette et al. in 1999 (Paquette, Barriault, and Pissarnitski 1999), and White et al. in 2001 (White et al. 2001; Blakemore et al. 2005). The CD spectrum of the synthesized (–)-PA agreed well with that of the natural PA, thereby completely establishing its absolute configuration (Fujiwara et al. 1998). Further,  $\text{LD}_{50}$  (240–360  $\mu\text{g}/\text{kg}$ ) in mice by intraperitoneal injection (i.p.) of the synthesized PA was almost comparable to that of natural PA (200–400  $\mu\text{g}/\text{kg}$ ), strongly supporting the notion that PA was the causative agent of the human intoxication. The structures of PA2, PA3, PB, and PB2 were deduced as shown in Fig. 15.1 by comparison of FABMS, UV spectra, and  $^1\text{H}$ - $^1\text{H}$  COSY among these analogues and PA (Yotsu-Yamashita et al. 1995). PA2 and PA3 were suggested to share the common aglycone with PA, whereas PB and PB2 were suggested to possess isopropyl substituted conjugated dienes (*E,E*) in the C15 side chains. The presence of fucosyl-xylose moieties was suggested in all four analogs. The position of the methylated or acetylated hydroxyl groups in the sugars were determined by comparison of the chemical shifts of the  $^1\text{H}$  NMR signals and the fragmentation patterns shown on the FAB/MS/MS spectra of these congeners.

## Analytical Methods

Polycavernoside poisoning had not been reported for 11 years since the outbreak in Guam in 1991. However, during 2002–2003, three fatal poisonings occurred by ingestion of *G. edulis* and another edible red alga, *Acanthophora specifera*, in the Philippines. In these three events, 8 victims died from among 38 patients. Analytical methods were developed for polycavernosides, and PA was identified from the causative *G. edulis* collected on December 2, 2002, at the beach in Luna, La Union, Philippines (Yotsu-Yamashita et al. 2004).

The semipurified toxic fraction obtained from this alga and selected on the basis of a mouse bioassay was applied to LC-diode array detection (LC-DAD) and LC/electrospray-MS (LC/ESI-MS) analysis. The UV absorption  $\lambda_{\text{max}}$  at 259, 269, and 280 nm due to the conjugated triene of PA, PA2, and PA3, and  $\lambda_{\text{max}}$  at 231 nm due to the conjugated diene of PB2 were used to detect them by

LC-DAD (Fig. 15.2). To separate these congeners, LC was performed using a column of 0.2 cm  $\times$  15 cm Mightysil RP-18 GP (5  $\mu$ m, Kanto Chemical, Tokyo, Japan) with an aqueous solution containing 80% MeCN as the mobile phase at a flow rate of 0.2 mL/min at 26°C. Both LC-DAD (Fig. 15.2) and LC/MS chromatograms (Fig. 15.3) of this toxic fraction suggested the presence of PA by comparison with authentic PA. The amount of PA in the alga was estimated as 84 and 72 nmol/kg wet alga by using the standard calibration curves for LC-DAD and for LC/ESI-MS in the single ion monitoring (SIM) mode, respectively. Other polycavernoside congeners such as PA2, PA3, and PB2 were below the detection limit (2 nmol/kg wet alga). In ESI-MS/MS, authentic polycavernosides showed the

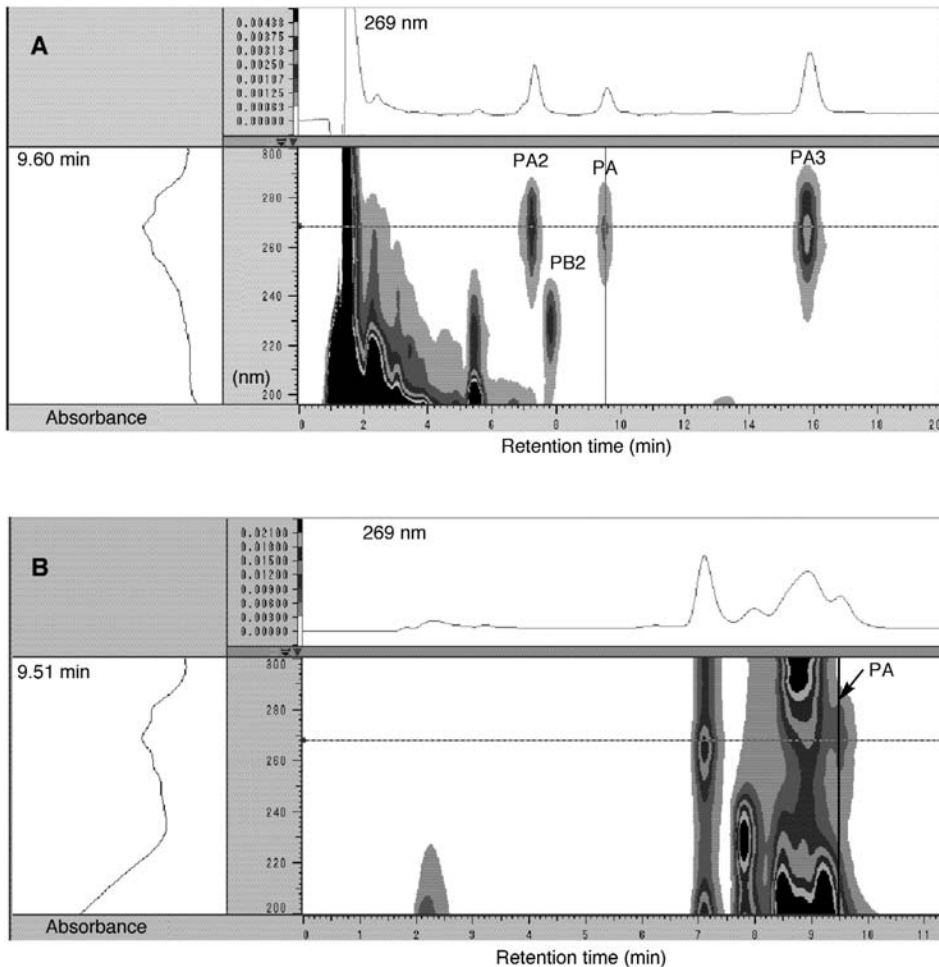


**Figure 15.2.** LC-DAD 3D chromatograms are shown with the sliced chromatograms at 269 nm (above), and UV spectra for the peaks at 9.60 minutes (A) and 9.51 minutes (B) (left). (A) A volume of 10  $\mu$ l of the polycavernosides standard mixture containing 25 pmol of PA, 25 pmol of PA2, 75 pmol of PA3, and 125 pmol of PB2. (B) An aliquot of the semi-purified toxic fraction obtained from the causative *G. edulis* collected in Luna, Philippines, on December 2, 2002. The chromatographic conditions: 0.2  $\times$  15 cm Mightysil RP-18GP 5  $\mu$ m, aqueous MeCN 8%, 0.2 ml/minutes, 26°C.

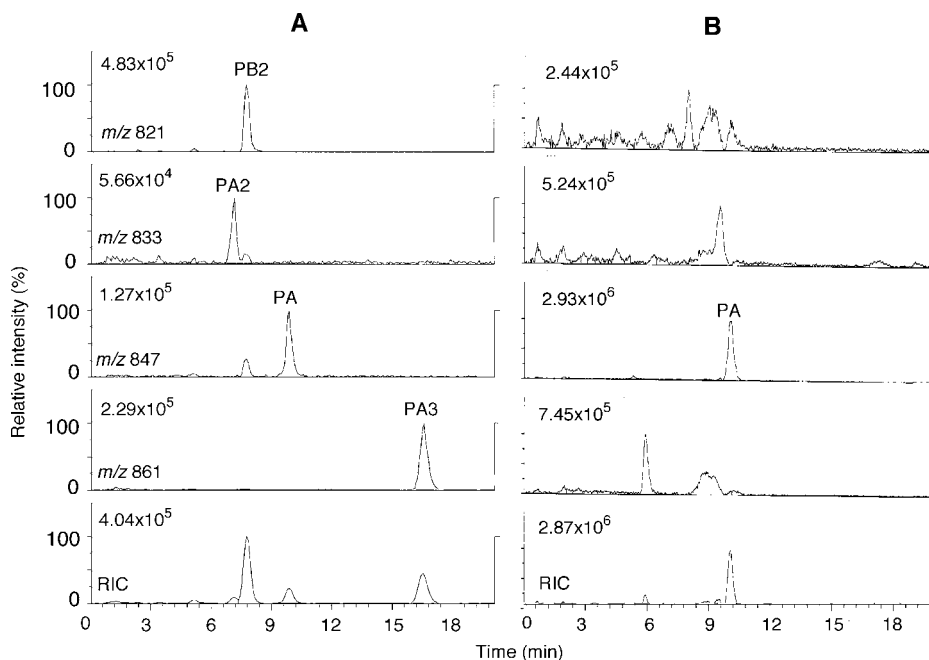


**Figure 15.3.** LC/ESI-MS SIM chromatograms of polycavernosides at  $m/z$  821 (PB2), 833 (PA2), 847 (PA), and 861 (PA3) and a reconstructed ion current (RIC). (A) A volume of 10  $\mu$ l of the standard mixture containing 50 pmol of PA, 25 pmol of PA2, and 75 pmol of PA3 and 125 pmol of PB2. (B) A volume of 10  $\mu$ l of the semi-purified toxic fraction (total 0.6 ml) eluted from a Cosmosil 5C18-AR-II column, obtained from the *G. edulis*. The ion intensity of the base peak 100% relative intensity was indicated in each mass chromatogram. The chromatographic condition was the same as that in Figure 15.2.

daughter ions corresponding to the sequential loss of fucosyl-xylose residues (Fig. 15.1). These fragmentations were applied to LC/ESI-MS/MS in the selective reaction monitoring (SRM) mode. Where SRM mass chromatograms are concerned, the toxic fraction from the alga showed the peaks corresponding to PA, supporting the identification of PA as the cause of poisoning by *G. edulis* on this occasion (Fig. 15.4). The detection limit of PA by LC/DAD, LC/ESI-MS (SIM), and LC/ESI-MS/MS (SRM) were 0.4 pmol, 2 pmol, and 10 pmol, respectively ( $s/n = 2$ ).

### Biological Activity

PA and PB caused diarrhea, hypersalivation, lachrymatory effects, muscle spasm, and cyanosis in mice (Yotsu-Yamashita, Haddock, and Yasumoto, 1993). These symptoms were comparable to those observed in the patients involved in the Guam case according to Dr. R. Roos at the Guam Memorial Hospital (Haddock and Cruz 1991).  $LD_{99}$  values in mice (i.p.) were determined to be 0.2–0.4 mg/kg for both PA and PB (Yotsu-Yamashita, Haddock, and Yasumoto 1993). Further pharmacological studies on polycavernosides were severely hampered by the lack of materials. However, Murai and Fujiwara (Fujiwara et al. 1998) and Paquette et al. (Paquette, Barriault, and Pissarnitski 1999) have independently completed total syntheses of the natural levorotatory enantiomer, thereby making available additional quantities of PA for more extensive investigation. Further, Paquette and

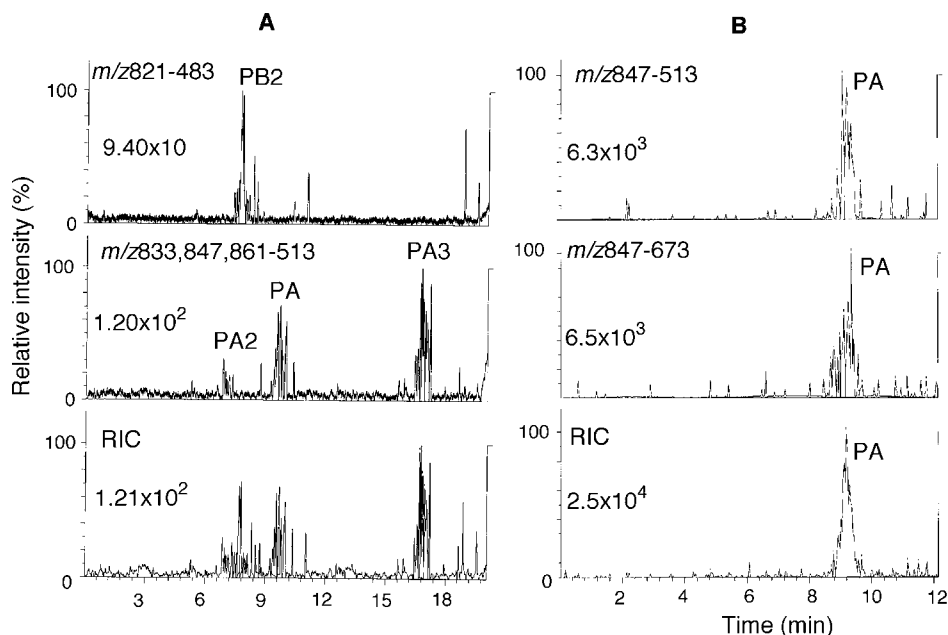


**Figure 15.4.** LC/ESI-MS/MS SRM chromatograms of authentic polycavernosides and the semi-purified toxic fraction from *G. edulis*. (A) A volume of 10  $\mu$ l of the standard mixture containing 120 pmol of PA, 60 pmol of PA2, and 180 pmol of PA3 and 300 pmol of PB2 ( $m/z$  821–483, 833–513, 847–513, 861–513). (B) An aliquot of the semi-purified toxic fraction obtained from the causative *G. edulis* ( $m/z$  847–513, 847–673 for PA). The ion intensity of the base peak (100% relative intensity) was indicated in each mass chromatogram. The chromatographic condition was the same as that in Figure 15.2.

co-workers (Barriault et al. 1999) synthesized the four derivatives 3–6 of PA (Fig. 15.5), which possess different structures, including  $\beta$ -styrenyl (3), isopropyl diene (4), isopropyl substituted enyne (5), and cyclohexyl diene (6) in the C-15 side chain instead of the isopropyl triene of PA. In addition, vinyl iodide 7 and PA aglycone 8 synthesized by Murai and Fujiwara were also subjected to bioassay in mice. The toxicities of these analogs to male mice (ddY strain, 12–15 g body weight) were determined by i.p. injection and the mice were observed 24 hours after injection. The minimal lethal dose values are shown in Fig. 15.5. The analogues 3, 6, and 7 showed significantly lower activities compared to other analogues, and the aglycone of PA (8) still retained reduced activity. However, the symptoms caused in mice by 8 were rather different from those of PA, suggesting that the macrocyclic core and triene side chain are required for toxicity. The analogues that possess an isopropyl group in the side chain (4, 5, and 8) showed high levels of toxicity. The closely related structures 4 and PB share the same aglycone including the C15 side chain. The differences in the toxicity levels of 4 and PB may arise because of the availability of a free hydroxyl substituent in the sugar component of 4.

We have also determined the cytotoxicities of natural PA and the synthetic analogues 3–6 in the mouse neuroblastoma cells, Neuro-2a. Due to the limitation of availability of the compounds, the cytotoxicities were tested only at 12  $\mu$ M by counting the viable cells treated with toxins for 24 h. We observed that 5 and 6 elicited more than 90% death responses, whereas PA elicited only 20% death responses, and 3 and 4 did not show cytotoxicity at this level, suggesting this cytotoxicity not to be comparable to that in mice. We proved that 5 induced apoptosis in Neuro-2a at 12  $\mu$ M within



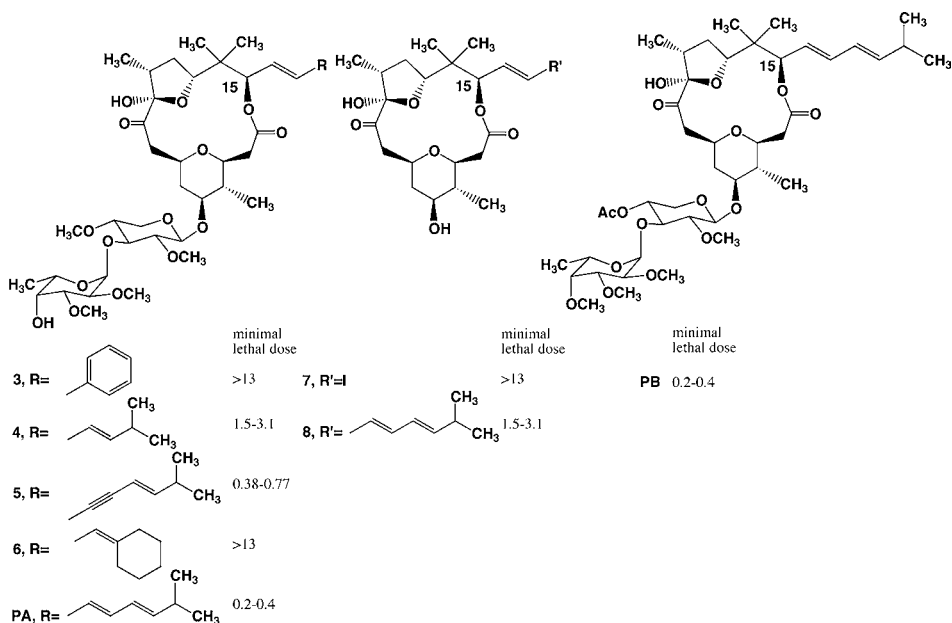


**Figure 15.5.** The structures of synthesized analogues (3–8), PA and PB, and their minimal lethal dose values in mice expressed as mg/kg (11).

24 hours following treatments to activate caspase-3/7, nucleosomal DNA fragmentation, and TUNEL (TdT-mediated dUTP-biotin nick end labeling) staining (Gavrieli, Sherman, Ben-Sasson 1992). Further pharmacological study of PA is highly demanded to develop the method for the purpose of curing the patients of the poisoning.

### Comparison with Other Seaweed Toxins

Outbreaks of seaweed poisoning are rather rare and widely spread over the Pacific area. In the Hawaii case of 1994, Nagai and co-workers identified the potent tumor promoters, aplysiatxin and debromoaplysiatoxin from *G. coronopifolia* as the causative agents (Nagai, Yasumoto, and Hokama 1996). Further, prostaglandins were identified from *G. vercosa* and *G. chorda* by Fusetani and Hashimoto (1984) and by Noguchi et al. (1994) as viable candidates for the causative agents of fatal human intoxication resulting from consumption of these algae that occurred in 1980, 1982, and 1993 in Japan. One person was killed in each incident. All of these algae are commonly eaten species.

The microbial origin of polycavernosides has been speculated on the basis of the sudden and transient occurrence of poisonous algae, as well as their structural features. Some structurally similar glycosidic macrolides possessing methylated sugars have been isolated from marine cyanobacteria; for example, lynglouiloside from *Lyngbya bouillonii* by Gerwick and co-worker (Tan Marquez and Gerwick 2002) and lyngbyaloside and lyngaloside B (Lueschet al. 2002) from *Lyngbya* sp. by Moore and Paul.

## Synthesis of Polycavernoside A

As delineated above, the isolation and characterization of polycavernoside A (1) was undertaken in urgent response to the appreciable human toxicity discovered following the ingestion of the red alga *Polycavernosa tsudai* (Yotsu-Yamashita, Haddock and Yasumoto 1993). Although several analogues of PA were subsequently identified (Yotsu-Yamashita et al. 1995), the A factor was soon targeted for synthesis because of its confirmed lethality and very limited availability. On the basis of detailed  $^1\text{H}$  and  $^{13}\text{C}$  NMR studies, the Sendai group succeeded in deducing the molecular structure of the A factor to be constituted of a novel macrolide disaccharide. Since the production of these toxins is seasonal and they are expressed in vanishingly small quantities, only a planar representation could be originally defined. Therefore there remained the companion need to unravel the absolute configuration of the numerous stereogenic centers including those residing in the disaccharide unit.

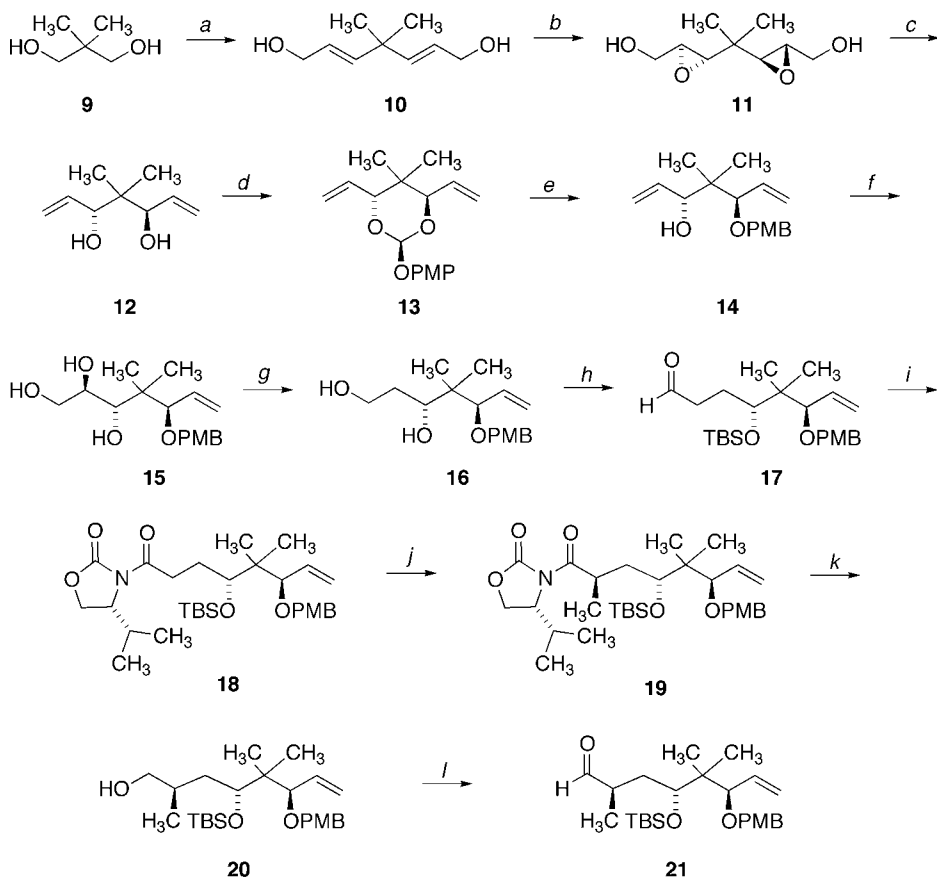
The key structural information provided by Yasumoto indicated the 3,5,7,13,15-pentahydroxy-9,10-dioxotricosanoic acid backbone of 1 to be unprecedented. On the other hand, the smaller trioxatridecane ring has features similar to those found in the aplysiatoxins (Kato and Scheuer 1974). The absence of unsaturation within the macrolide ring is quite atypical, as is the polyene appendage whose role is presumably to serve as a "lipophilic anchor" to cell membranes. The extensive degree of *O*-methylation of the disaccharide component is indicative of the algal origin of this metabolite.

Deduction of the absolute stereochemistry of 1 awaited the independent synthesis of several building blocks. Ultimately, three successful enantioselective routes have been completed to the present time by the Murai, Paquette, and White research groups. In order to facilitate comparison of the tactical design elements unique to each accomplishment, the construction of each structural sector is dealt with individually.

### Routes to the Tetrahydrofuran Subunit

Murai's pioneering effort to deduce the stereochemistry along C10–C16 of the target began with the twofold homologation of diol 9 to the symmetrical bisallylic alcohol 10 (Scheme 15.1) (Hayashi et al. 1994). The exhaustive Sharpless epoxidation of this substrate proved to be notably efficient in delivering 11 (91% yield, >98% ee), thereby setting the stage for convenient arrival at the regio-reversed diol 12. The  $C_2$ -symmetric nature of this intermediate was broken as in 14 by sequential reductive cleavage of the *p*-methoxybenzylidene acetal and regioselective dihydroxylation of only one olefinic terminus. At this point, the primary hydroxyl group was protected with TBDPSCl in a maneuver designed to allow for removal of the neighboring OH group. The transformation of 15 into 16 was effected by formation of the monotosylate and reductive cleavage with  $\text{LiAlH}_4$ . The homologation of 1,3-diol 16 to aldehyde 17 was brought about by  $S_N2$  displacement involving the tosylate with cyanide ion in advance of reduction with Dibal-H. Oxidation to the carboxylic acid level and introduction of the enantiopure oxazolidinone moiety as in 18 made possible installation of the last methyl substituent on the way to 21.

The Paquette team proceeded ahead in the expectation that aldehyde 31 would outperform other chiral C10–C17 subunits (Paquette, Pissarnitski, and Barriault 1998). Their routing began with oxirane 22, which is readily available from (*R*)-(-)-pantolactone (Scheme 15.2). After *O*-silylation, 23 was reacted with dilithioacetate in dimethoxyethane to induce nucleophilic ring cleavage with follow-up cyclization. The resulting lactone 24 could be successfully monomethylated under closely

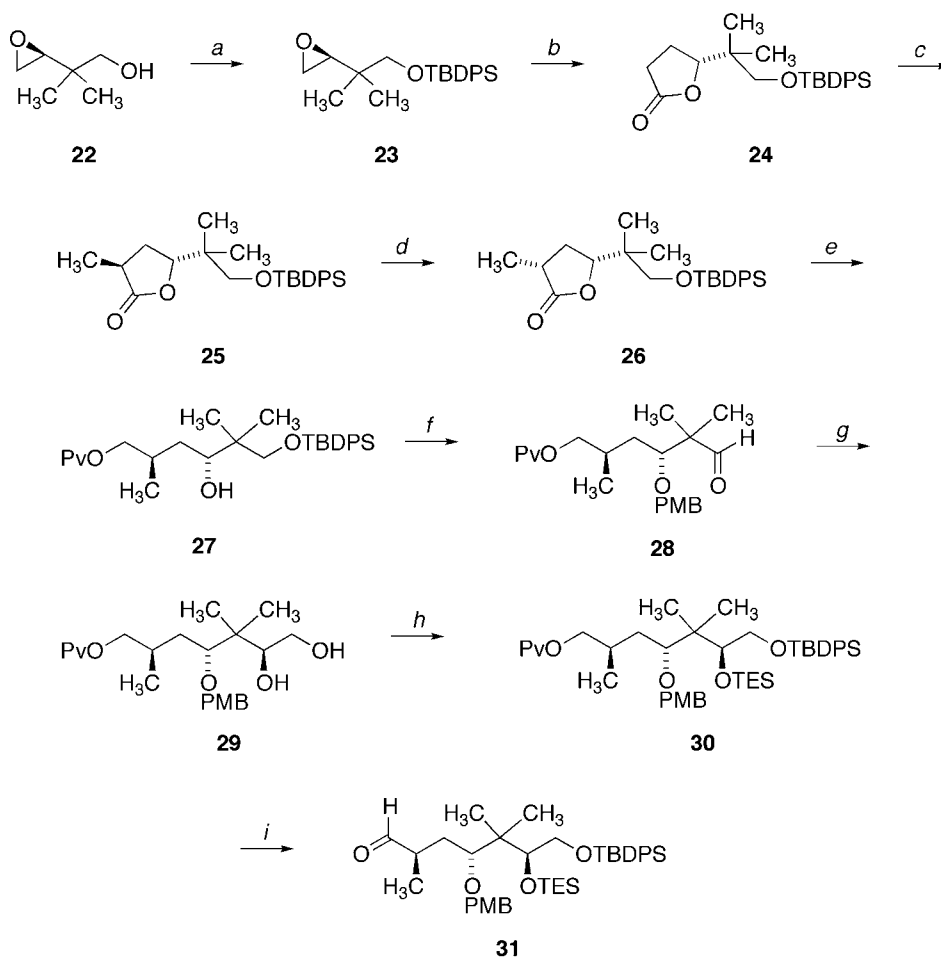


<sup>a</sup> DMSO, (COCl)<sub>2</sub>, CH<sub>2</sub>Cl<sub>2</sub>, -78 °C, 1 h, then Et<sub>3</sub>N, 20 °C, 30 min; Ph<sub>3</sub>P=CHCOOCH<sub>3</sub>, C<sub>6</sub>H<sub>6</sub>, reflux, 2.5 days (56%); Dibal-H, CH<sub>2</sub>Cl<sub>2</sub>, -78 °C, 3.5 h (84%). <sup>b</sup> (+)-DET, Ti(O*i*-Pr)<sub>4</sub>, *t*-BuOOH, MS 4A, CH<sub>2</sub>Cl<sub>2</sub>, -20 °C, 2 days (91%). <sup>c</sup> Ph<sub>3</sub>P, I<sub>2</sub>, imid, THF, 20 °C, then sat. Na<sub>2</sub>S<sub>2</sub>O<sub>3</sub>/H<sub>2</sub>O, 20 °C (83%). <sup>d</sup> *p*-Methoxybenzaldehyde, PPTS, C<sub>6</sub>H<sub>6</sub>, Δ (93%). <sup>e</sup> Dibal-H, CH<sub>2</sub>Cl<sub>2</sub>, -20 °C (100%). <sup>f</sup> OsO<sub>4</sub>, NMO, 1:3 dioxane-H<sub>2</sub>O, 20 °C (75%). <sup>g</sup> TBDPSCI, imid, DMF, 20 °C (96%); MsCl, Et<sub>3</sub>N, CH<sub>2</sub>Cl<sub>2</sub>, 0 °C; LiAlH<sub>4</sub>, THF, 20 °C (54%). <sup>h</sup> TsCl, Et<sub>3</sub>N, DMAP, CH<sub>2</sub>Cl<sub>2</sub>, 0 °C (98%); TBSOTf, 2,6-lutidine, CH<sub>2</sub>Cl<sub>2</sub>, 0 °C; KCN, DMSO, 20 °C (92%); Dibal-H, CH<sub>2</sub>Cl<sub>2</sub>, -78 °C; Rochelle's salt, H<sub>2</sub>O (96%). <sup>i</sup> NaClO<sub>2</sub>, NaH<sub>2</sub>PO<sub>4</sub>, 2-Me-2-butene, *t*-BuOH, H<sub>2</sub>O, 0 °C; PvCl, Et<sub>3</sub>N, Et<sub>2</sub>O, 0 °C, then lithio-(4*R*)-4-isopropyl-2-oxazolidinone, THF, -78 °C (100%). <sup>j</sup> LDA, CH<sub>3</sub>I, THF, -25 °C (69%). <sup>k</sup> LiAlH<sub>4</sub>, THF, 0 °C (100%). <sup>l</sup> Swern oxid (90%).

Scheme 15.1.

monitored conditions. This step proceeds with high β-selectivity. The same inherent steric bias can be relied upon to invert configuration at this center as in 26 by protonating the enolate anion of 25 with NH<sub>4</sub>Cl. The desired stereodisposition of the two chiral centers in 26 was thereby achieved.

The reduction of 26 with lithium borohydride provided a diol whose monoesterification with pivaloyl chloride materialized at the site of the primary hydroxyl (Paquette, Barriault and



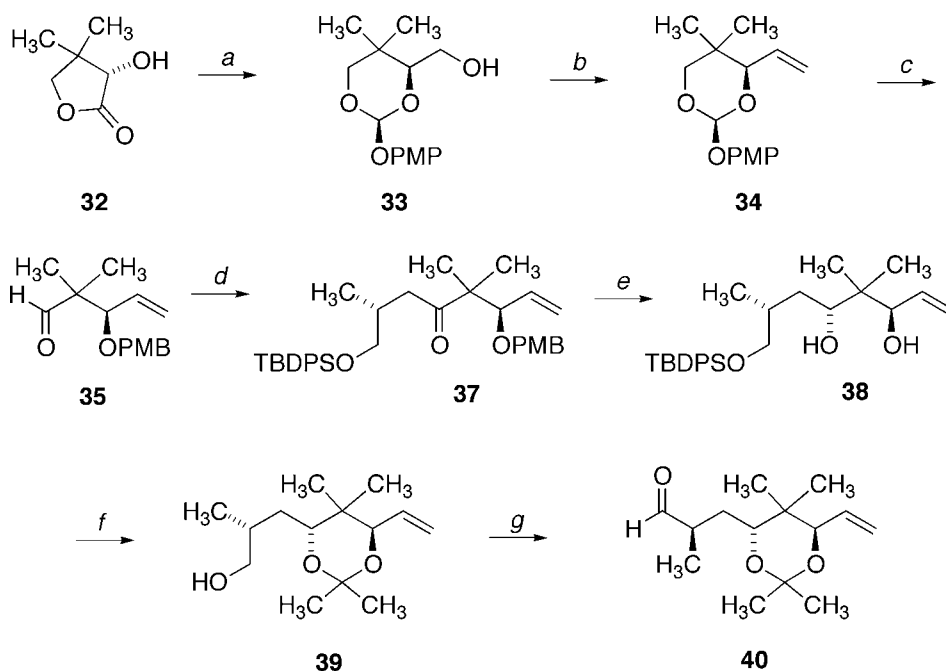
<sup>a</sup> TBDPSCl, imid, CH<sub>2</sub>Cl<sub>2</sub> (95%). <sup>b</sup> CH<sub>2</sub>=C(OLi)OLi (9 equiv), DME, reflux; H<sub>3</sub>O<sup>+</sup> (72%).  
<sup>c</sup> LiHMDS, THF, -78 °C; CH<sub>3</sub>I (81%). <sup>d</sup> LDA, THF, -78 °C; NH<sub>4</sub>Cl (81%). <sup>e</sup> LiBH<sub>4</sub>, ether, CH<sub>3</sub>OH (93%); PvCl, py, CH<sub>2</sub>Cl<sub>2</sub> (96%). <sup>f</sup> 4-CH<sub>3</sub>OC<sub>6</sub>H<sub>4</sub>CH<sub>2</sub>OC(=NH)CCl<sub>3</sub>, (TfOH), ether (81%); TBAF, THF (94%); Swern oxid (89%). <sup>g</sup> Ph<sub>3</sub>P=CH<sub>2</sub>, THF (89%); OsO<sub>4</sub>, (DHQ)<sub>2</sub>PYR, K<sub>3</sub>Fe(CN)<sub>6</sub>, K<sub>2</sub>CO<sub>3</sub>, *t*-BuOH, H<sub>2</sub>O, 0 °C (99%). <sup>h</sup> TBDPSCl, imid, THF; TESCl, imid, DMAP, DMF (82%). <sup>i</sup> Dibal-H, THF, -30 °C (79%); TPAP, NMR, 4A MS, CH<sub>2</sub>Cl<sub>2</sub> (89%).

Scheme 15.2.

Pissarnitski 1999; Paquette, Barriault, Pissarnitski and Johnson 2000). The application of trichloroacetimidate technology to 27 was instrumental in making possible appropriate chain extension of the derived nonepimerizable aldehyde 28. This structural feature minimized the level of care and attention to detail that was required during deployment of the Wittig olefination. Reagent-controlled dihydroxylation with (DHQ)<sub>2</sub>PYR provided diol 29, the stereochemical assignment to which was confirmed indirectly by oxidative cyclization of an independently prepared diastereomer

to a 1,3-dioxolane, and detailed NOE analysis of its all-equatorial (and therefore non-dynamic) conformation. Regioselective introduction of two different silyl protecting groups as in 30, reductive cleavage of the pivaloyl group with Dibal-H, and ultimate perruthenate oxidation gave rise to the fully elaborated aldehyde 31.

The White approach to construction of the C10-C16 fragment began with the conversion of (*S*)-pantolactone (32) to acetal 33 via a four-step, previously reported sequence (Scheme 15.3) (White et al. 2001; Blakemore et al. 2005). Reduction of 34 with Dibal-H proceeded with anticipated regioselectivity to afford a lone PMP ether, and from that point the aldehyde 35 by Swern oxidation. The securing of 35 was followed by Julia coupling to the *S* enantiomer of sulfone 36 via its lithio anion. The interim goal of arriving at 37 was realized by sequential oxidation to a pair of keto sulfones with the Dess-Martin periodinane and desulfonylation with samarium diiodide. Removal of the PMB ether from 37 gave rise to a  $\beta$ -hydroxy ketone whose reduction with tetramethylammonium triacetoxyborohydride proceeded with high stereoselectivity to make available the anti 1,3-diol 38. Once the acetonide was generated, the siloxy group was unmasked, and the primary hydroxyl so exposed in 39 was oxidized straightforwardly to make aldehyde 40 available.

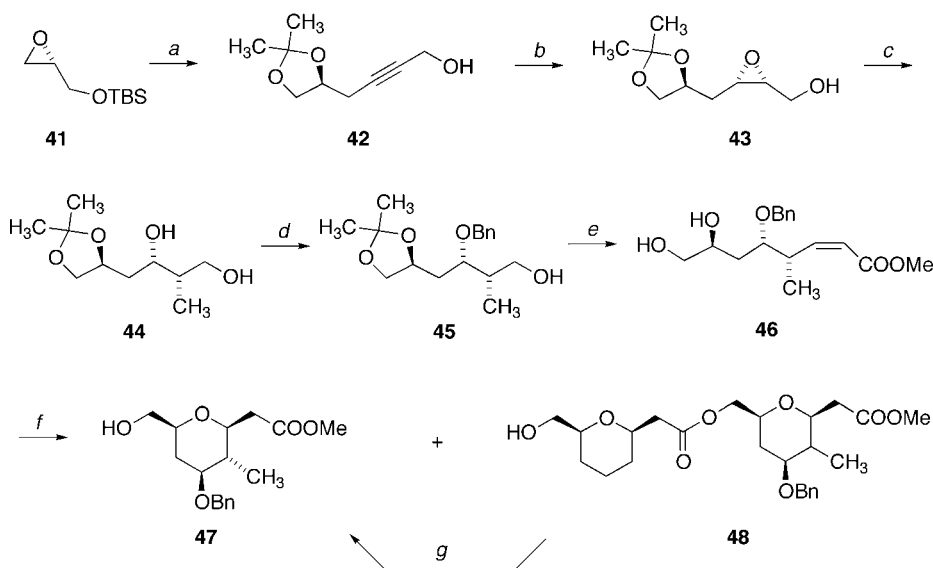


*a*  $\text{LiAlH}_4$ , THF, 0 °C;  $\text{PMPCH}(\text{OCH}_3)_2$ , CSA,  $\text{CH}_2\text{Cl}_2$ , rt (92%). *b* Swern;  $\text{Ph}_3\text{P}=\text{CH}_2$ , THF (86%). *c* Dibal-H,  $\text{CH}_2\text{Cl}_2$ , -78 °C  $\rightarrow$  rt (100%); Swern oxid (96%).  
*d* (*S*)- $\text{TBDPSOCH}_2\text{CH}(\text{CH}_3)\text{CH}_2\text{SO}_2\text{Ph}$  (**36**), *n*-BuLi, THF, -50 °C; Dess-Martin periodinane,  $\text{CH}_2\text{Cl}_2$ , rt;  $\text{SmI}_2$ , THF, -78 °C (90%). *e*  $\text{Me}_4\text{NBH}(\text{OAc})_3$ , HOAc/ $\text{CH}_3\text{CN}$  (1:1), -20 °C;  $\text{Me}_2\text{C}(\text{OMe})_2$ , (PPTS),  $\text{CH}_2\text{Cl}_2$ , rt (76%). *f* TBAF, THF, rt (94%). *g* Dess-Martin periodinane,  $\text{CH}_2\text{Cl}_2$ , rt (76%).

Scheme 15.3.

### Elaboration of the Tetrahydropyran Sector

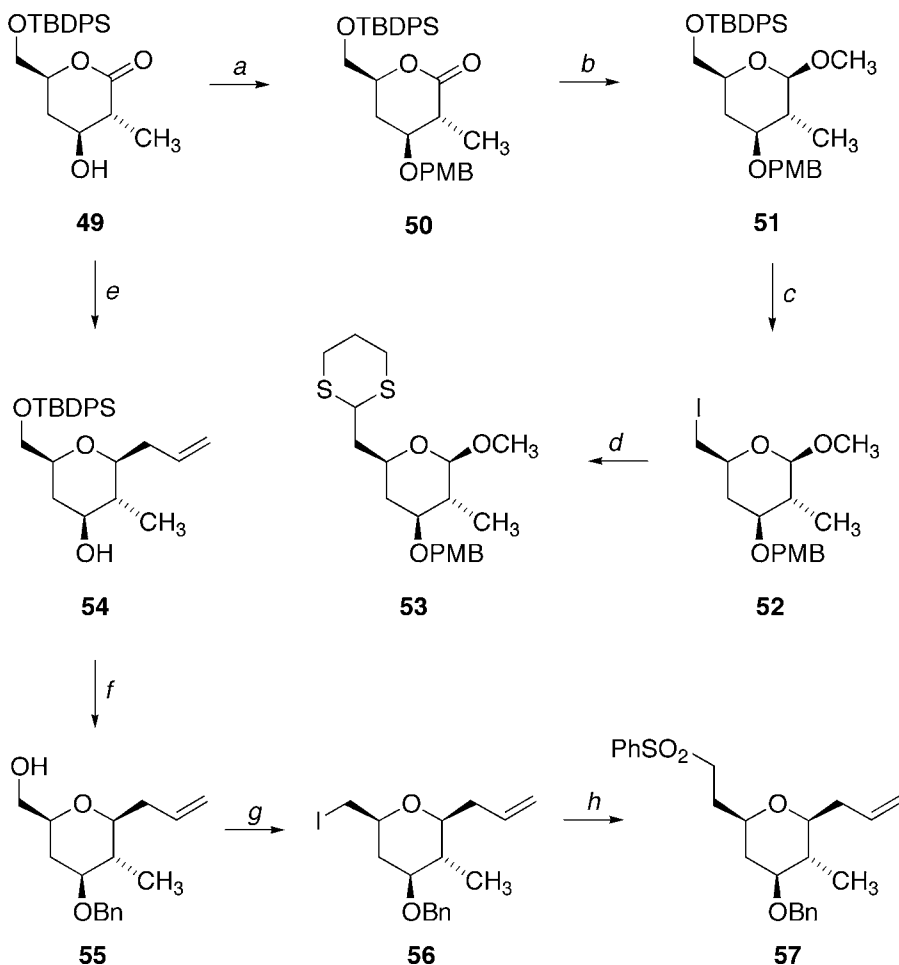
In the Murai laboratories, the thrust to fashion a route to the lower C1-C8 half of the polycavernoside macrolactone began with the silylation of (*R*)-(+)-glycidol with TBSCl to give 41 (Scheme 15.4) (Fujiwara et al. 1994). Coupling of 41 to the lithiated tetrahydropyranyl ether of propargyl alcohol in the presence of boron trifluoride etherate occurred in good yield to furnish 42. This step allowed partial reduction in Lindlar fashion and Sharpless epoxidation of the resulting dihydro product in the presence of (-)-diethyl tartrate to be carried out. The resulting 2,3-epoxy alcohol underwent subsequent regiodirected oxirane cleavage in the presence of lithium dimethylcuprate. A three-step sequence was necessary to transform 42 to the monobenzylated derivative 45. The role of 45 was to serve as a precursor to the aldehyde, which was immediately subjected to homologation under Wadsworth-Emmons conditions to afford predominantly 46 (*Z*:*E* = 5:1). The *Z* isomer was chromatographically purified, its acetonide protecting group was removed with PPTS, and cyclization studies involving 47 were undertaken. This step proved initially to be highly problematic. In the final analysis, the desired intramolecular ring closure could be brought about with potassium *tert*-butoxide in THF at 30°C within minutes. The co-formation of dimer 48 proved not to be a serious drawback since its conversion to the targeted tetrahydropyran could be implemented on demand under closely comparable conditions.



<sup>a</sup>  $\text{HC}\equiv\text{CCH}_2\text{OTHP}$ , *n*-BuLi,  $\text{BF}_3\cdot\text{OEt}_2$ , THF, -78 °C;  $\text{TsOH}\cdot\text{H}_2\text{O}$ , MeOH,  $\Delta$ ; 2,2-dimethoxypropane,  $\text{TsOH}\cdot\text{H}_2\text{O}$ ,  $\text{CH}_2\text{Cl}_2$ -MeOH (4:1), 20 °C (71%). <sup>b</sup>  $\text{H}_2$ , Lindlar catalyst, quinoline,  $\text{C}_2\text{H}_2\text{OH}$ ; (-)-DET,  $\text{Ti}(\text{O}-i\text{Pr})_4$ , *t*-BuOOH, MS 4A,  $\text{CH}_2\text{Cl}_2$ , -20 °C. <sup>c</sup>  $\text{CH}_3\text{Li}$ , CuI, THF-ether (2.3:1), -20 °C;  $\text{NaIO}_4$ , THF- $\text{H}_2\text{O}$  (2:1), 69%. <sup>d</sup> TBSCl, DMAP,  $\text{Et}_3\text{N}$ ,  $\text{CH}_2\text{Cl}_2$ , 0 °C (91%);  $\text{KO}^t\text{-Bu}$ , BnBr, TBAI, THF, 0 °C (95%); TBAF, THF, 20 °C (79%). <sup>e</sup> Swern oxid;  $(\text{MeO})_2\text{POCH}_2\text{COOMe}$ , KH, 18-cr-6, THF, 0 °C (78% *Z*-olefin). <sup>f</sup>  $\text{KO}^t\text{-Bu}$  (8 mol %), THF, -20 °C (92%). <sup>g</sup>  $\text{KO}^t\text{-Bu}$  (1 eq), MeOH, 25 °C (91%).

Scheme 15.4.

Paquette's early attempts to arrive at a suitably functionalized pyran focused on gaining access to the dithiane 53 whose role it was to provide a nucleophilic site at C9. The substructure of 53 was recognized to correspond well from the functionality and stereochemistry standpoints to the pattern resident in Fukui's lactone (49), which is readily available from L-malic acid. To enable proper structural modification, the hydroxyl group in 49 was first masked as the PMB ether by implementation of the trichoroacetimidate process (Scheme 15.5).



<sup>a</sup> PMBOC(=NH)CCl<sub>3</sub>, (TfOH), ether (77%). <sup>b</sup> Dibal-H, CH<sub>2</sub>Cl<sub>2</sub>, -78 °C; Ag<sub>2</sub>O, CH<sub>3</sub>I, reflux (62%). <sup>c</sup> TBAF, THF (97%); CH<sub>3</sub>SO<sub>2</sub>Cl, Et<sub>3</sub>N, CH<sub>2</sub>Cl<sub>2</sub>, -10 °C (95%); (*n*-Bu)<sub>4</sub>N<sup>+</sup> I<sup>-</sup>, C<sub>6</sub>H<sub>6</sub>, reflux (95%). <sup>d</sup> 1,3-dithiane, *n*-BuLi/KO<sup>t</sup>-Bu (1:1), 2:1 THF-hexane, -78 °C. <sup>e</sup> CH<sub>2</sub>=CHCH<sub>2</sub>MgBr, THF, -78 °C; Et<sub>3</sub>SiH, SnCl<sub>4</sub>, CH<sub>2</sub>Cl<sub>2</sub>, -78 °C → -30 °C (71%). <sup>f</sup> NaH, BnBr, NaI, THF, Δ (87%); TBAF, THF (98%). <sup>g</sup> Ph<sub>3</sub>P, I<sub>2</sub>, imid, C<sub>6</sub>H<sub>6</sub> (94%). <sup>h</sup> LiCH<sub>2</sub>SO<sub>2</sub>Ph, THF, HMPA, rt (69%).

Scheme 15.5.



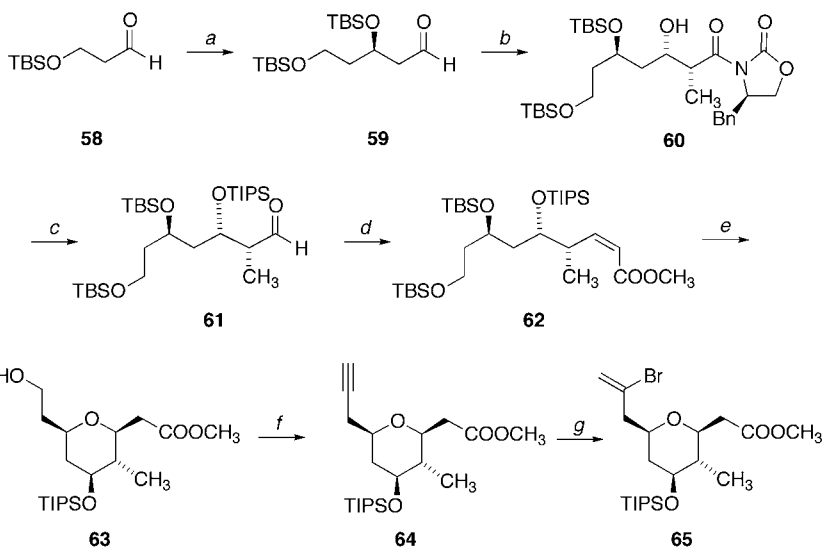
Conversion to methyl glycoside 51 was effected by sequential Dibal-H reduction and reaction with silver(I) oxide and methyl iodide (Paquette, Pissarnitski and Barriault 1998). Side chain functionalization was next entertained. Following the desilylation of 51, the preferred means for generating iodide 52 proved to involve  $S_N2$  displacement by iodide ion of the sulfonate ester in the mesylate. The intermediacy of 52 was valued since its condensation with lithio 1,3-dithiane as promoted by Schlosser's base proceeded well to deliver 53. However, it was soon recognized that attempts to bring about the union of 53 with lactone 26 could not be realized without the onset of degradation. An alternative tactical means for merging these chiral segments was therefore given consideration.

As matters unfolded, use was made of the same disconnection and the role of 49 as a key building block was left unchanged. As seen in Scheme 15.5, its hydroxyl group could be left unprotected during condensation with an excess of allylmagnesium bromide at  $-78^\circ\text{C}$  (Paquette, Barriault and Pissarnitski 1999; Paquette et al. 2000). Although the resulting hemiacetal proved expectedly to be sensitive, its direct ionic reduction with triethylsilane and stannic chloride served well to orient the allyl substituent in 54 equatorially. There followed a very efficient series of transformations to provide iodide 56. As with 52, the response of 56 to nucleophilic displacement was enhanced as reflected in the conversion to 57 (68%) stemming from alkylation with lithiated methyl phenyl sulfone.

White's retrosynthesis of the C1–C9 subunit of 1 led back to aldehyde 58 (Scheme 15.6). Subjection of this starting material to Brown asymmetric allylation in the presence of (–)-diisopinylcamphenylmethoxyborane delivered the (*S*)-homoallylic alcohol whose hydroxyl group was silylated prior to ozonolytic cleavage of the terminal  $\pi$ -bond (White et al. 2001; Blakemore et al. 2005). Following arrival at 59 in this manner, the chain extension process was continued by aldol reaction with the di-*n*-butylboron enolate of (*R*)-4-benzyl-3-propionyloxazolidin-2-one. The labile 60 was directly transformed into its Weinreb amide, silylated with triisopropylsilyl triflate, and reduced with Dibal-H to generate 61. The  $\alpha,\beta$ -unsaturated ester 62 became the next interim goal. This advanced intermediate was reached by application of the Gennari-Still phosphonate coupling. Once the TBS protecting groups present in 62 were removed, cyclization to tetrahydropyran 63 could be realized cleanly in the presence of methanolic potassium carbonate. The chain extension that ensued involved sequential oxidation with the Dess-Martin periodinane, alkyne generation with the Ohira reagent, and final treatment with 9-bromo-9-borabicyclo[3.3.1]nonane. As discussed below, vinyl bromide 65 so formed proved to be fully serviceable as a building block for macrolactone construction.

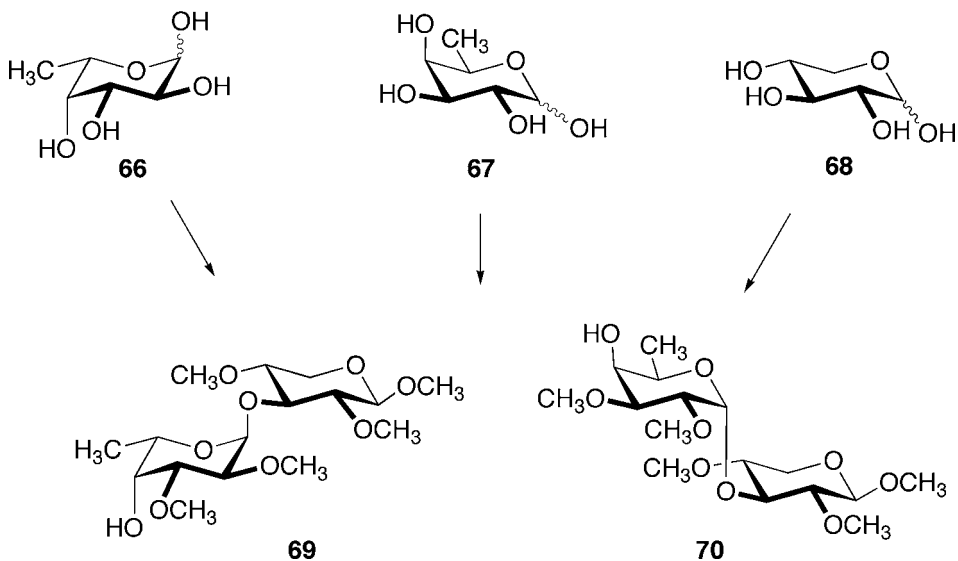
### *Enantioselective Acquisition of the Disaccharide Component*

Confirmation was now needed of the working premise that the glycosidic residue in 1 was constituted of a 2,3-di-*O*-methyl- $\alpha$ -L-fucopyranose linked "1 to 3" to a 2,4-di-*O*-methyl- $\alpha$ -D-xylopyranose. An enantioselective synthesis of disaccharide 82 and its close relatives would provide proper verification of the absolute configuration of polycavernoside A. Murai and co-workers accepted the challenge of carrying natural L-fucose (66), unnatural D-fucose (67), and natural D-xylose (68) through independent routes to 69 and 70 (Scheme 15.7) (Fujiwara, Amano, and Murai 1995). Direct  $^1\text{H}$  NMR comparison of these two disaccharides with 1 revealed the chemical shifts and splitting patterns of the manifold signals in 69 to be very closely matched. This was not the situation with 70. On this basis, the conclusion was reached "that the disaccharide moiety of 1 might consist of a combination of D-xylose and L-fucose or their enantiomers." The conclusion that the natural form of these sugars was indeed involved did indeed prove to be correct.



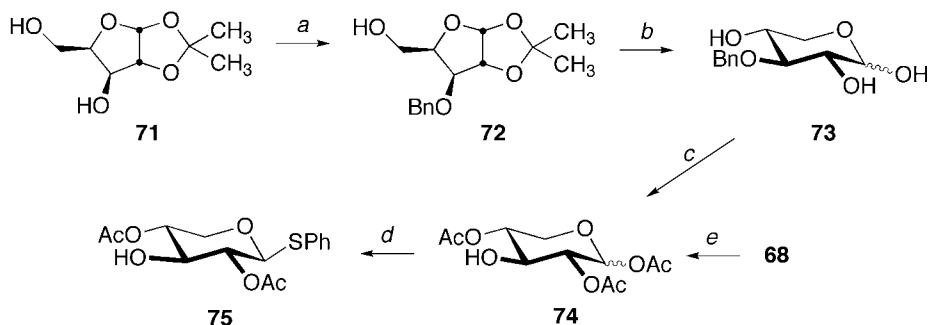
<sup>a</sup>  $\text{CH}_2=\text{CHCH}_2\text{MgBr}$ , (-)-Ipc<sub>2</sub>BOMe, ether -100 °C → -78 °C (82%; 85% ee); TBSCl, imid, DMF, rt (90%); O<sub>3</sub>, CH<sub>2</sub>Cl<sub>2</sub>, -78 °C, then Ph<sub>3</sub>P (93%). <sup>b</sup> (4*R*)-Benzyl-3-propionyloxazolidin-2-one, *n*-Bu<sub>2</sub>BOTf, Et<sub>3</sub>N, -78 °C → rt. <sup>c</sup> MeNH(OMe)·HCl, Me<sub>3</sub>Al, CH<sub>2</sub>Cl<sub>2</sub>, 0 °C → rt (75%); TIPSOTf, 2,6-lutidine, CH<sub>2</sub>Cl<sub>2</sub>, -78 °C → 0 °C (100%); Dibal-H, THF, -78 °C (81%). <sup>d</sup> (CF<sub>3</sub>CH<sub>2</sub>O)<sub>2</sub>P(O)CH<sub>2</sub>COOMe, KHMDS, 18-cr-6, THF, -78 °C → rt (94%). <sup>e</sup> PPTS, MeOH-THF, 55 °C, then K<sub>2</sub>CO<sub>3</sub> (70%). <sup>f</sup> Dess-Martin periodinane, CH<sub>2</sub>Cl<sub>2</sub>, rt (85%); MeCOC(N<sub>3</sub>)PO(OMe)<sub>2</sub>, K<sub>2</sub>CO<sub>3</sub>, MeOH, rt (84%). <sup>g</sup> 9-Br-9-BBN, CH<sub>2</sub>Cl<sub>2</sub>, 0 °C → rt (77%).

Scheme 15.6.



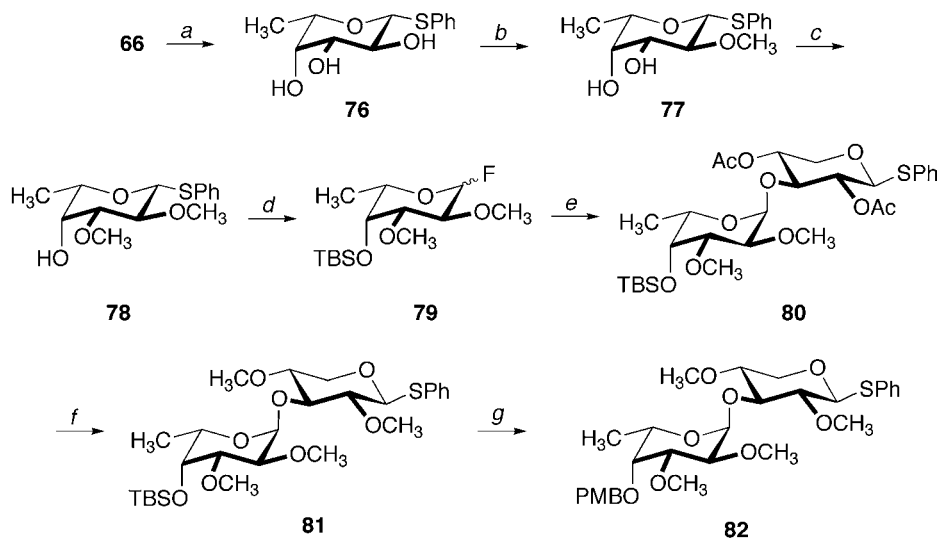
Scheme 15.7.

Of the options explored by Paquette, those outlined in Schemes 15.8 and 15.9 were demonstrated to be entirely workable (Johnston and Paquette 1995). Two routes were developed to approach the acceptor glycoside 75, with that originating from commercially available 71 proving to be the more efficient. Benzyl protection of the more hindered secondary hydroxyl in this diol was realized via a three-step sequence involving highly regioselective *O*-tritylation in advance of reaction with sodium



<sup>a</sup> TrCl, Et<sub>3</sub>N, (DMAP), DMF; BnBr, NaH, Bu<sub>4</sub>N<sup>+</sup> I<sup>-</sup>, DMF; (TsOH), CH<sub>3</sub>OH, ether, H<sub>2</sub>O (81%).  
<sup>b</sup> 50% aq HOAc, 100 °C. <sup>c</sup> Ac<sub>2</sub>O, DMAP (85%); H<sub>2</sub>, Pd/C, EtOAc (96%). <sup>d</sup> PhSSiMe<sub>3</sub>, SnCl<sub>4</sub>, C<sub>6</sub>H<sub>6</sub> (60%). <sup>e</sup> Ac<sub>2</sub>O, py, -35 °C (21%).

Scheme 15.8.



<sup>a</sup> Ac<sub>2</sub>O, (DMAP), py; PhSH, SnCl<sub>4</sub>, C<sub>6</sub>H<sub>6</sub>; KOH, MeOH (91%). <sup>b</sup> ZnCl<sub>2</sub>, (H<sub>3</sub>PO<sub>4</sub>), acetone; NaH, CH<sub>3</sub>I, DMF, 0 °C; 50% aq HOAc, 90 °C (83%). <sup>c</sup> (*n*-Bu)<sub>2</sub>SnO, MeOH, Δ; CH<sub>3</sub>I, CsF, DMF (99%). <sup>d</sup> TBSOTf, imid, (DMAP), DMF, 80 °C (77%); Et<sub>2</sub>NSF<sub>3</sub>, NBS, CH<sub>2</sub>Cl<sub>2</sub>, 0 °C (88%).  
<sup>e</sup> 74, SnCl<sub>2</sub>, AgClO<sub>4</sub>, ether (64%). <sup>f</sup> KOH, MeOH; NaH, CH<sub>3</sub>I, DMF (84%). <sup>g</sup> TBAF, THF (95%); PMBCl, NaI, NaH, THF (96%).

Scheme 15.9.

hydride and benzyl bromide followed by detritylation. The ensuing deacetalization of 72 allowed for equilibration to the pyranose form 73, the direct acylation of which furnished 74 after hydrogenolysis. Exposure of 74 to phenylthiotrimethylsilane and  $\text{SnCl}_4$  in dry benzene allowed for smooth conversion to 75.

The alternative route to 74 took advantage of a previously recognized ability to perform the controlled acetylation of D-xylose (68). However, under conditions that came to be regarded as optimized, the yield of 74 from this direction was only 21%.

The first step designed to access the glycosyl donor 79 from L-fucose (66) took advantage of the ease with which peracetylated L-fucose responds to site-selective exchange with thiophenol at the anomeric center. Subsequent saponification provided 76 efficiently. The time had now been reached when advantage was taken of the capability of the *O*-stannylacetal to experience equatorial *O*-methylation selectively. Arrival at 78 was preceded by acetonide formation within 76 to guide regiocontrolled introduction of the first methoxy group. The subsequent conversion to 78 was uneventful. The remaining axial alcohol was next protected as the TBS ether, thus making possible the formation of fluoride 79 with diethylaminosulfur trifluoride and *N*-bromosuccinimide.

Admixing 79 with 75 under Mukaiyama conditions resulted in conversion to disaccharide 80, which proved to be the only isomer produced. Once the final methoxyl group was installed as in 81, the OTBS substituent was replaced by OPMB to skirt potential problems with later desilylation that was revealed during the course of ensuing probe experiments.

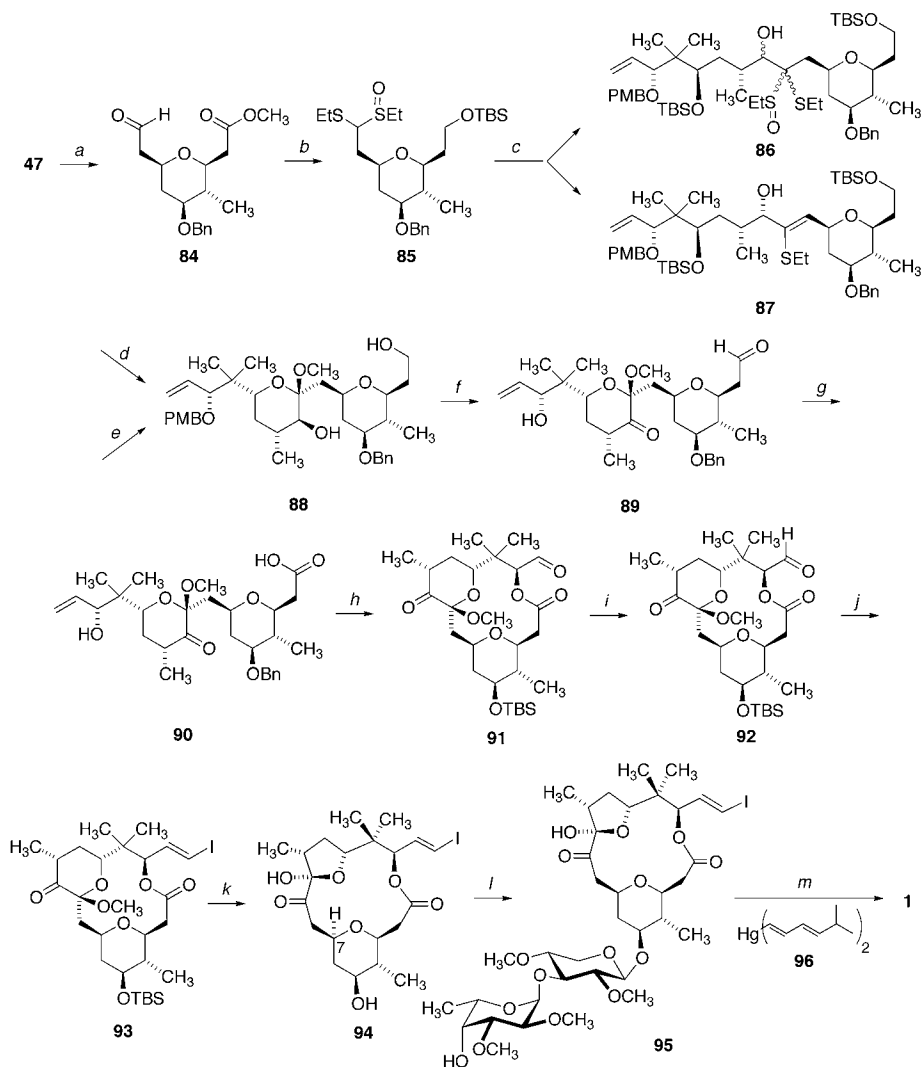
The disaccharide employed by White was the corresponding benzyl ether of 82. This reactant is the anomer of the compound earlier deployed by the Murai team (structure 83).

## *Definition of Absolute Configuration and Completion of the Total Syntheses*

### *The Murai Route*

The successful development of a stereoselective protocol for the construction of 1 that was undertaken in Japan began with a seven-step conversion of hydroxy ester 47 to the dithioacetal monoxide 85 (Scheme 15.10) (Fujiwara et al. 1998). This sequence of steps began with a Swern oxidation, Wittig olefination to provide an enol ether, and mild acidic hydrolysis to generate the aldehyde 84. The further developments involved application of the Evans thioacetalization protocol and reduction of the methyl ester to the alcohol in advance of TBS protection. Oxidation with MCPBA afforded monosulfoxide 85 in a move designed to allow regioselective deprotonation at C9. Addition of aldehyde 21 to this anion gave rise to 86 as a mixture of stereoisomers and vinyl sulfide 87 as a single isomer. Since both of these intermediates were convertible predominantly to 88 by hydrolysis with *p*-toluenesulfonic acid, it proved possible to bring about direct acyclic acetal formation in a single laboratory maneuver. Compound 88 was oxidized under Swern conditions and freed of its PMB group, thereby generating 91.

The synthesis progressed by way of seco acid 90 and lactonization with generation of a 12-membered ring as in 91 by application of the modified Yamaguchi method. At this point, considerable thought and experimentation were devoted to selecting the proper sequence of steps. The conclusion was reached that the trans vinyl iodide moiety had best be elaborated at this stage. To this end, the olefinic bond in 91 was dihydroxylated and the resulting diol cleaved with sodium periodate. Next to be faced was the replacement of benzyl by TBS, and ultimately Takai iodovinylation. With 93 now available, equilibration of its 6-membered cyclic acetal to the desired 5-membered isomer 94 was implemented under mild conditions. Covalent bonding of 94 to disaccharide 83 was accomplished by the Nicolaou method.



<sup>a</sup> Swern oxid;  $\text{Ph}_3\text{P}=\text{CHOCH}_3$ , THF,  $-78^\circ\text{C}$  (90%);  $\text{CF}_3\text{COOH}$ , THF,  $\text{H}_2\text{O}$ ,  $20^\circ\text{C}$  (92%). <sup>b</sup>  $\text{Me}_3\text{SiSEt}$ ,  $\text{ZnI}_2$  (cat),  $\text{CH}_2\text{Cl}_2$ ,  $20^\circ\text{C}$ ;  $\text{LiAlH}_4$ , THF,  $0^\circ\text{C}$ ; TBSCl, imid, DMF,  $0^\circ\text{C}$ ; MCPBA (1 equiv),  $\text{CH}_2\text{Cl}_2$ ,  $-60^\circ\text{C}$  (93%). <sup>c</sup> LDA, THF,  $-78^\circ\text{C}$ , then **21** (46% of **86**, 33% of **87**). <sup>d</sup>  $\text{TsOH}\cdot\text{H}_2\text{O}$ , MeOH,  $(\text{MeO})_3\text{CH}$  (50%). <sup>e</sup>  $\text{TsOH}\cdot\text{H}_2\text{O}$ , MeOH,  $(\text{MeO})_3\text{CH}$  (65%). <sup>f</sup> Swern oxid; DDQ,  $\text{CH}_2\text{Cl}_2$  (92%). <sup>g</sup>  $\text{NaClO}_2$ ,  $\text{NaH}_2\text{PO}_4$ , 2-methyl-2-butene, *t*-BuOH,  $\text{H}_2\text{O}$ ,  $0^\circ\text{C}$  (100%). <sup>h</sup> 2,4,6-trichlorobenzoyl chloride,  $\text{Et}_3\text{N}$ , THF, then DMAP, toluene,  $60^\circ\text{C}$  (>75%). <sup>i</sup>  $\text{OsO}_4$ , NMO, dioxane,  $\text{H}_2\text{O}$ , then  $\text{NaIO}_4$ ;  $\text{H}_2$ , Pd/C, MeOH; TBSOTf, 2,6-lutidine,  $\text{CH}_2\text{Cl}_2$ ,  $0^\circ\text{C}$  (>95%). <sup>j</sup>  $\text{CrCl}_2$ ,  $\text{CH}_3\text{I}$ , THF,  $0^\circ\text{C}$  (>80%). <sup>k</sup>  $\text{CF}_3\text{COOH}$ , THF,  $\text{H}_2\text{O}$  (>95%). <sup>l</sup> **82**, NBS, MS4A,  $\text{CH}_3\text{CN}$ ,  $-20^\circ\text{C}$  (>50%); DDQ,  $\text{CH}_2\text{Cl}_2$ ,  $\text{H}_2\text{O}$ ,  $20^\circ\text{C}$  (>70%). <sup>m</sup> **96** (excess),  $\text{Pd}(\text{PPh}_3)_4$ , THF,  $0-20^\circ\text{C}$  (>75%).

Scheme 15.10.

In the final phase of the synthesis, it was necessary to effect debenzoylation and to isolate 95 in advance of exposing this vinyl iodide to 96 and the palladium dichloride bis(acetonitrile) complex in cold THF. The synthetic polycavernoside A obtained in this manner was identical in all respects to the natural material.

### *The Paquette Pathway*

The alternative end-game scenario played out at Ohio State began with the coupling of sulfone 57 to aldehyde 31 (Scheme 15.11) (Paquette, Barriault, and Pissarnitski 1999; Paquette et al. 2000). Once the hydroxyl group introduced in this manner was oxidized to a ketone functionality as in 97, it was time to bring about chemoselective desilylation under acidic conditions and crafting of an acetaldehyde side chain from the pendant allyl functionality. Following the chemoselective oxidation of 98 to the carboxylic acid level with sodium chlorite, the opportunity to achieve macrolactonization was grasped to generate 99 in good yield. This key intermediate lent itself well to introduction of a vinyl iodide segment by one-carbon homologation. As before, recourse to the Takai reagent functioned reliably without evidence of detectable epimerization. Equally dependable was the oxidative desulfonation that transformed 100 to the  $\alpha$ -diketone. The lability of this product dictated that its OPMB substituent be immediately removed to produce 101 as a single diastereomer.

There ensued an NBS-promoted glycosidation with the activated disaccharide 82 to deliver exclusively the  $\beta$ -anomer 102. This step and a subsequent Stille coupling involving dienylstannane 104 proved particularly conducive to the delivery of 1, which exhibited a negative optical rotation of  $-34.5$ , a value closely comparable to that recorded for the natural marine toxin.

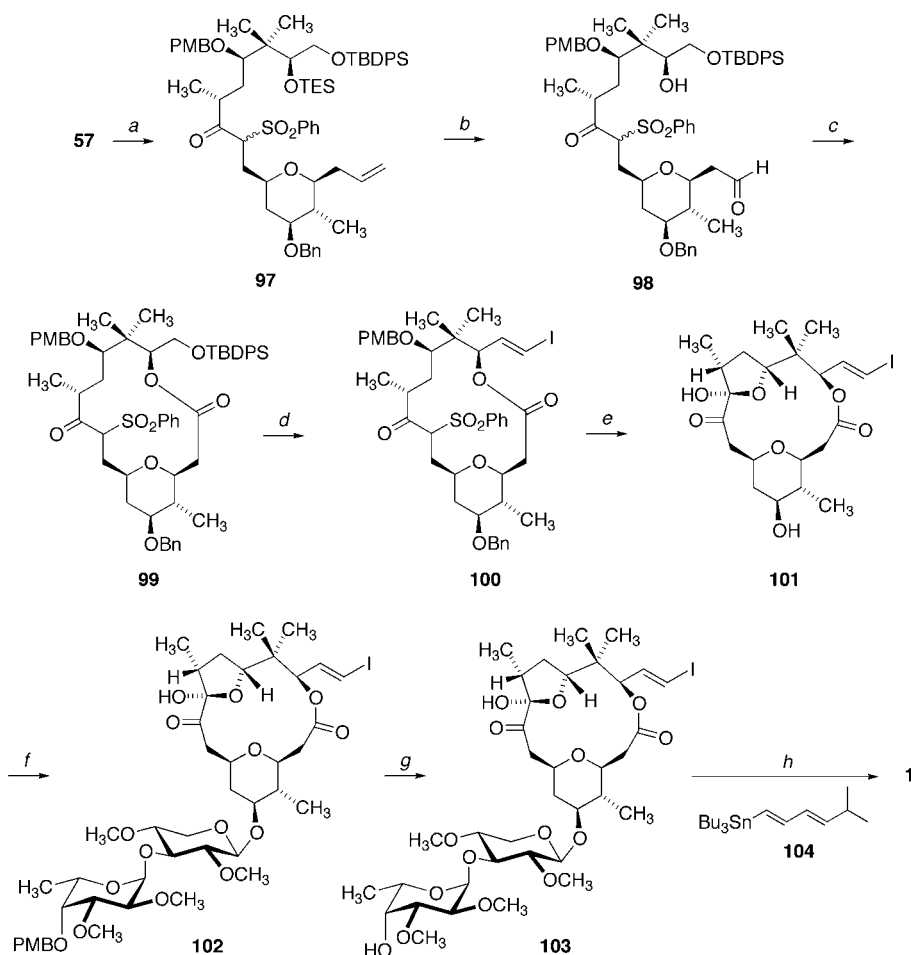
### *White's Successful Strategy*

In the case at hand, it proved feasible to couple 40 to 65 with  $\text{CrCl}_2$  in the presence of catalytic  $\text{NiCl}_2$  under Nozaki-Hiyama-Kishi conditions. This process gave rise to 105 as a 1:1 mixture of epimers. Fortunately, these alcohols were chromatographically separable, thereby allowing the less polar  $\beta$ -isomer to be carried forward to 106 and beyond. Notwithstanding the elevated level of functionalization resident in trihydroxycarboxylic acid 106, recourse to the Yamaguchi macrolactonization protocol was rewarded by the exclusive involvement of the C15 carbinol. This high level of selectivity was in agreement with molecular modeling calculations that indicated the formation of nine- and twelve-membered lactones to involve higher energy reaction trajectories. Protection as the bis-triethylsilyl ether 107 followed (Scheme 15.12).

The stage was now set for ozonolytic cleavage to reach the keto aldehyde 108, which served conveniently as a precursor to the homologated vinyl iodide. The C10 hydroxyl group in this intermediate was next unmasked selectively with acidic methanol to provide 109. The latter was treated with the hydrogen fluoride-pyridine complex, these conditions resulting in twofold desilylation and cyclization to form hemiketal 101. This substance proved to be identical in all respects to the late-stage intermediate independently generated in the earlier two syntheses. The formality of completing the end game with arrival at 1 was executed via 103 under entirely similar conditions.

### *Synthesis of Analogs of the Toxin*

The final step in two of the synthetic approaches to polycavernoside A (1) involved a notably clean palladium-catalyzed cross-coupling of vinyl iodide 103 to the dienylstannane reagent 104. This

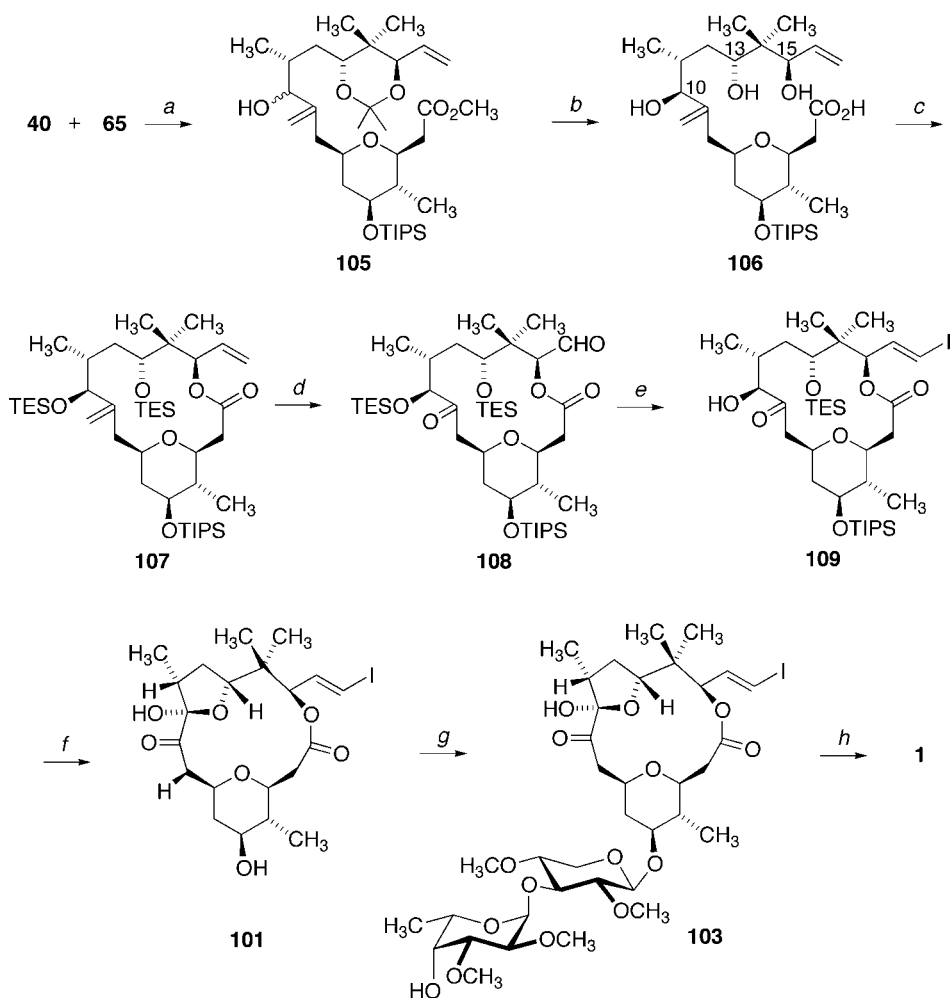


<sup>a</sup> *n*-BuLi, THF, then **31** (76%); Dess-Martin periodinane, CH<sub>2</sub>Cl<sub>2</sub> (99%). <sup>b</sup> TsOH, CH<sub>3</sub>OH, CH<sub>2</sub>Cl<sub>2</sub> (97%); OsO<sub>4</sub>, NMO, THF, H<sub>2</sub>O then NaIO<sub>4</sub> (85%). <sup>c</sup> NaClO<sub>2</sub>, NaH<sub>2</sub>PO<sub>4</sub>, 2-methyl-2-butene, *t*-BuOH, H<sub>2</sub>O, 0 °C (88%); 2,4,6-trichlorobenzoyl chloride, Et<sub>3</sub>N, THF, 25 °C; DMAP, toluene, 110 °C (82%). <sup>d</sup> HF·py, py, THF (90%); Dess-Martin periodinane, CH<sub>2</sub>Cl<sub>2</sub> (90%); CrCl<sub>2</sub>, CH<sub>3</sub>I, THF (77%). <sup>e</sup> KO<sup>t</sup>Bu, 2-(phenylsulfonyl)-3-phenyloxaziridine, THF, 0 °C; DDQ, CH<sub>2</sub>Cl<sub>2</sub>, H<sub>2</sub>O (73%). <sup>f</sup> NBS, 4A MS, **82**, CH<sub>3</sub>CN (49%). <sup>g</sup> DDQ, CH<sub>2</sub>Cl<sub>2</sub>, H<sub>2</sub>O (76%). <sup>h</sup> PdCl<sub>2</sub>(CH<sub>3</sub>CN)<sub>2</sub>, **104**, DMF, rt (87%).

Scheme 15.11.

positive characteristic and the diversity of available vinyl-, aryl-, and alkynylstannanes placed second-generation analogues of **1** well within reach (Barriault et al. 1999). By this route, 3–6 were made available. It will be recognized that the length and extent of conjugation in the C15 side chain has been systematically varied. The minimal lethal doses in mice exhibited by these macrocyclic lactones suggest that terminal isopropyl group on this appendage provides for maximum lethality.





<sup>a</sup> CrCl<sub>2</sub>, (NiCl<sub>2</sub>), DMF, rt, dr 1:1 (79%). <sup>b</sup> PPTS, MeOH, 35 °C, then NaOH (86%). <sup>c</sup> 2,4,6-trichlorobenzoyl chloride, Et<sub>3</sub>N, THF, then DMAP, toluene, Δ (75%); TESOTf, 2,6-lutidine, CH<sub>2</sub>Cl<sub>2</sub>, 0 °C (95%). <sup>d</sup> O<sub>3</sub>, CH<sub>2</sub>Cl<sub>2</sub>/MeOH (3:1), -78 °C; then Ph<sub>3</sub>P (81%). <sup>e</sup> CHI<sub>3</sub>, CrCl<sub>2</sub>, THF, 0 °C → rt (76%); PPTS, MeOH/CHCl<sub>2</sub> (4:1), rt (88%). <sup>f</sup> Dess-Martin periodinane, py/CH<sub>2</sub>Cl<sub>2</sub>, 0 °C, then HF·py, THF (88%). <sup>g</sup> Anomer of **83**, NBS, CH<sub>3</sub>CN, -35 °C → rt (27%); DDQ, CH<sub>2</sub>Cl<sub>2</sub>/H<sub>2</sub>O (20:1), rt (70%). **104**, PdCl<sub>2</sub>(CH<sub>3</sub>CN)<sub>2</sub>, DMF (74%).

Scheme 15.12.

## Acknowledgments

We thank Eli Lilly and Company and the Astellas USA Foundation for their financial support (L.A.P.). This work was supported by grants-in-aid for Scientific Research on Priority Areas (no.17035011) from MEXT, (no.17580091) from JSPS, and Yamada Foundation (M.Y.Y.).

## References

- Barriault, L., Boulet, S.L., Fujiwara, K., Murai, A., Paquette, L.A., and Yotsu-Yamashita, M. 1999. Synthesis and Biological Evaluation of Analogs of the Marine Toxin Polycavernoside A. *Bioorganic & Medicinal Chemistry Letters* 7(9), 2069–2072.
- Blakemore, Paul R., Browder, Cindy C., Hong, Jian, Lincoln, Christopher M., Nagornyy, Pavel A., Robarge, Lonnie A., Wardrop, Duncan J. and White, James D. 2005. Total Synthesis of Polycavernoside A, A Lethal Toxin of the Red Alga *Polycavernosa tsudai*. *Journal of Organic Chemistry* 70(14), 5449–5460.
- Fujiwara, K., Amano, S., and Murai, A. 1995a. Relative Configuration of a Marine Toxin Polycavernoside-A. *Chemistry Letters* 9, 855–856.
- . 1995b. Synthesis and Relative Configuration of the Sugar Part of a Marine Toxin Polycavernoside-A. *Chemistry Letters* 3, 191–192.
- Fujiwara, K., Amano, S., Oka, T., and Murai, A. 1994. Synthesis of the Tetrahydropyran Ring Part of a Marine Toxin Polycavernoside-A. *Chemistry Letters* (11), 2147–2150.
- Fujiwara, K., Murai, A., Yotsu-Yamashita, M., and Yasumoto, T. 1998. Total Synthesis and Absolute Configuration of Polycavernoside A. *Journal of the American Chemical Society* 120(41), 10770–10771.
- Fusetani, N., and Hashimoto, K. 1984. Prostaglandin E<sub>2</sub>: A Candidate for Causative Agent of Ogonori Poisoning. *Bulletin of the Japanese Society of Scientific Fisheries* 50(3), 465–469.
- Gavrieli, Y., Sherman, Y., and Ben-Sasson, S.A. 1992. Identification of Programmed Cell Death in situ via Specific Labeling of Nuclear DNA Fragmentation. *Journal of Cell Biology* 119(3), 493–501.
- Haddock, R.L., and Cruz, O.L.T. 1991. Foodborne Intoxication Associated with Seaweed. *Lancet* 338(8760), 195–196.
- Hayashi, N., Mine, T., Fujiwara, K., and Murai, A. 1994. Synthesis of the Tetrahydrofuran Ring Part of a Marine Toxin Polycavernoside A. *Chemistry Letters* 11, 2143–2146.
- Johnston, J.N., and Paquette, L.A. 1995. Studies Directed toward the Total Synthesis of Polycavernoside A. Enantioselective Synthesis of the Disaccharide Component. *Tetrahedron Letters* 36(25), 4341–4344.
- Kato, Y., and Scheuer, P.J. 1974. Aplysiatoxin and Debromoaplysiatoxin, Constituents of the Marine Mollusk *Stylocheilus longicauda* (Quoy and Gaimard). *Journal of the American Chemical Society* 96(7), 2245–2246.
- Luesch, H., Yoshida, W.Y., Harrigan, G.G., Doom, J.P., Moore, R.E., and Paul, V.J. 2002. Lyngbyalyside B, a New Glycoside Macrolide from a Palauan Marine Cyanobacterium, *Lyngbya* sp. *Journal of Natural Products* 65(12), 1945–1948.
- Nagai, H., Yasumoto, T., and Hokama, Y. 1996. Aplysiatoxin and Debromoaplysiatoxin as the Causative Agents of a Red Alga *Gracilaria coronopifolia* Poisoning in Hawaii. *Toxicon* 34(7), 753–761.
- Noguchi, T., Matsui, T., Miyazawa, K., Asakawa, M., Iijima, N., Shida, Y., Fuse, M., Hosaka, Y., Kirigaya, C., Watabe, K., Usui, S., and Fukagawa, A. 1994. Poisoning by the Red Alga 'Ogonori' (*Gracilaria verrucosa*) on the Nojima Coast, Yokohama, Kanagawa Prefecture, Japan. *Toxicon* 32(12), 1533–1538.
- Paquette, L.A., Barriault, L., and Pissarnitski, D. 1999. A Convergent Total Synthesis of the Macrolactone Disaccharide Toxin (-)-Polycavernoside A. *Journal of the American Chemical Society* 121(18), 4542–4543.
- Paquette, L.A., Barriault, L., Pissarnitski, D., and Johnston, J.N. 2000. Stereocontrolled Elaboration of Natural (-)-Polycavernoside A, a Powerfully Toxic Metabolite of the Red Alga *Polycavernosa tsudai*. *Journal of the American Chemical Society* 122(4), 619–631.
- Paquette, L.A., Pissarnitski, D., and Barriault, L., 1998 A Modular Enantioselective Approach to Construction of the Macrolactone Core of Polycavernoside A. *Journal of Organic Chemistry* 63(21), 7389–7398.
- Tan, L.T., Marquez, B.L., and Gerwick, W.H. 2002. Lyngbouilloside, a Novel Glycosidic Macrolide from the Marine Cyanobacterium *Lyngbya bouillonii*. *Journal of Natural Products* 65(6), 925–928.
- White, J.D., Blakemore, P.R., Browder, C.C., Hong, J., Lincoln, C.M., Nagornyy, P.A., Robarge, L.A., and Wardrop, D.J. 2001. Total Synthesis of the Marine Toxin Polycavernoside A via Selective Macrolactonization of a Trihydroxy Carboxylic Acid. *Journal of the American Chemical Society* 123(35), 8593–8595.

- Yotsu-Yamashita, M., Haddock, R.L. and Yasumoto, T. 1993. Polycavernoside A: A Novel Glycosidic Macrolide from the Red Alga *Polycavernose tsudai Gracilaria edulis*, *Journal of the American Chemical Society* 115(3), 1147–1148.
- Yotsu-Yamashita, M., Seki, T., Paul, V.J., Naoki, H., and Yasumoto, T. 1995. Four New Analogs of Polycavernoside A. *Tetrahedron Letters* 36 (31), 5563–5566.
- Yotsu-Yamashita, M., Yasumoto, T., Yamada, S., Bajarias, Fe Farida A., Formelozsa, Mirriam, A., Romero, M.L., and Fukuyo, Y. 2004. Identification of Polycavernoside A as the Causative Agent of the Fatal Food Poisoning Resulting from Ingestion of the Red Alga *Gracilaria Edulis* in Philippines. *Chemical Research in Toxicology*, 17(9), 1265–1271.

## 16 Structural Assignment and Total Synthesis of Azaspiracid-1

Michael O. Frederick, Kevin P. Cole, Goran Petrovic, Eriketi Loizidou, and K. C. Nicolaou

### Introduction

In 1995, a report of human illness with diarrhetic shellfish poisoning (DSP)-like symptoms in the Netherlands was eventually found to result from the consumption of poisoned mussels (*Mytilus edulis*) harvested from Killary Harbour, Ireland (McMahon 1996). Yasumoto, Satake, and co-workers eventually isolated and proposed a structure for the causative agent of this condition: azaspiracid-1 (1a, Fig. 16.1). The unique polyether structure of azaspiracid-1 (1a) is characterized by several spirocyclic systems, including an azaspiro ring fused to a 2,9-dioxabicyclo[3.3.1]nonane system and a terminal carboxylic acid. In total, there are nine rings and twenty stereogenic centers within the structure proposed by Yasumoto and co-workers in 1998 (Satake 1998). This structure was based primarily on NMR spectroscopic data and did not include absolute stereochemistry, nor did it specify relative stereochemistry between the ABCDE and FGHI domains.

Since the isolation of azaspiracid-1, several other related compounds have been isolated and structurally assigned based on extensive NMR and mass spectrometric analysis (James 2003, Ofuji 1999, Ofuji 2001). Thus, structures were proposed for azaspiracids-2 to -11 (2a–11a, Table 16.1) by analogy to the proposed structure of azaspiracid-1 (1a). Our group synthesized the proposed structure of azaspiracid-1 (1a) in 2003 and proved that it was not correct (Nicolaou 2003a). Through a subsequent collaborative effort between us and the Satake group, the correct structure of azaspiracid-1 (1) was determined, and thence constructed in our laboratory in 2004 (Nicolaou 2004a, 2004b). In this chapter, we summarize the major synthetic pursuits toward the structural determination and total synthesis of azaspiracid-1.

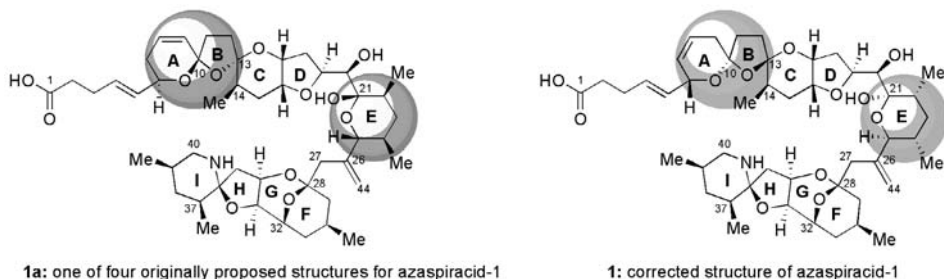


**Figure 16.1.** Originally proposed structure of azaspiracid-1 (1a, relative stereochemistry between ABCDE and FGHI domains and absolute stereochemistry unknown) and the corrected structure of azaspiracid-1 (1).

**Table 16.1.** Molecular structures of azaspiracids-2 to -11

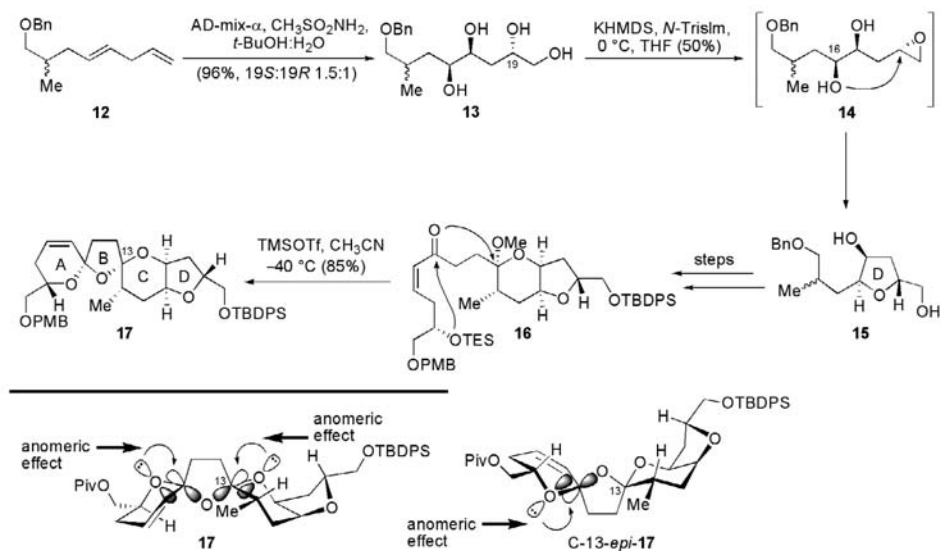
Originally proposed structures <sup>a</sup>					Revised structures <sup>b</sup>				
	R <sup>1</sup>	R <sup>2</sup>	R <sup>3</sup>	R <sup>4</sup>		R <sup>1</sup>	R <sup>2</sup>	R <sup>3</sup>	R <sup>4</sup>
2a: azaspiracid-2	H	Me	Me	H	2: azaspiracid-2	H	Me	Me	H
3a: azaspiracid-3	H	H	H	H	3: azaspiracid-3	H	H	H	H
4a: azaspiracid-4	OH	H	H	H	4: azaspiracid-4	OH	H	H	H
5a: azaspiracid-5	H	H	H	OH	5: azaspiracid-5	H	H	H	OH
6a: azaspiracid-6	H	Me	H	H	6: azaspiracid-6	H	Me	H	H
7a: azaspiracid-7	OH	H	Me	H	7: azaspiracid-7	OH	H	Me	H
8a: azaspiracid-8	H	H	Me	OH	8: azaspiracid-8	H	H	Me	OH
9a: azaspiracid-9	OH	Me	H	H	9: azaspiracid-9	OH	Me	H	H
10a: azaspiracid-10	H	Me	H	OH	10: azaspiracid-10	H	Me	H	OH
11a: azaspiracid-11	OH	Me	Me	H	11: azaspiracid-11	OH	Me	Me	H

<sup>a</sup>See: James 2003, Ofuji 1999, Ofuji 2001. <sup>b</sup>See: Nicolaou 2004b.

## Synthetic Studies Toward the ABCD Domain of Azaspiracid-1

The proposed structure of azaspiracid-1 (1a) is composed of three main structural motifs: the ABCD, the E, and the FGHI domains, as shown in Fig. 16.1. Two logical disconnections, those between the ABCD and the E rings, and the E and FGHI rings served well to disassemble the molecule retrosynthetically, generating three key building blocks, the ABCD, the E, and the FGHI domains as suitable starting points for a projected total synthesis.

The first pursuit of the ABCD domain of azaspiracid-1 was reported by Forsyth and co-workers (Dounay 2001). A key feature of their synthesis was the initial construction of the D-ring, a task accomplished by first treating racemic diene 12 with AD-mix- $\alpha$ , resulting in tetraol 13 as a separable 1.5:1 mixture of C-19 epimers (Scheme 16.1). Treatment of tetraol 13 with KHMDS and *N*-triisopropylsulfonylimidazole (*N*-TrisIM) formed the primary sulfonate, which was converted to epoxide 14 by base-induced intramolecular displacement of the sulfonate group. This epoxide (14) was found to be short-lived, as the C-16 hydroxyl group initiated an intramolecular attack that resulted in the formation of the desired D-ring furan system 15 as a single diastereomer and in 50% overall yield. Further elaboration of this intermediate (15) afforded the C<sub>5</sub>–C<sub>20</sub> fragment 16, setting the stage for the next key reaction in the sequence leading to the ABCD ring fragment, namely an acid-catalyzed deprotection-ring closure. Treatment of advanced intermediate 16 with TMSOTf in CH<sub>3</sub>CN at –40°C resulted in the formation of the A and B rings, giving rise to ABCD tetracycle 17 in 85% yield, as a single stereoisomer. Unfortunately, the stereochemistry at the C-13 spirocenter was opposite to that reported in the originally proposed structure of azaspiracid-1. Furthermore, treatment with various Lewis or protic acids failed to provide the desired stereochemistry through epimerization. The difficulty in obtaining the desired stereochemistry of the proposed ABC bis-spiroacetal ring juncture had been suspected from the outset. Examination of the inset in Scheme 16.1 reveals that the obtained product (17) benefits nicely from a double anomeric effect in the ABC ring junction, while the desired product, C-13-*epi*-17, does not enjoy such stabilization,

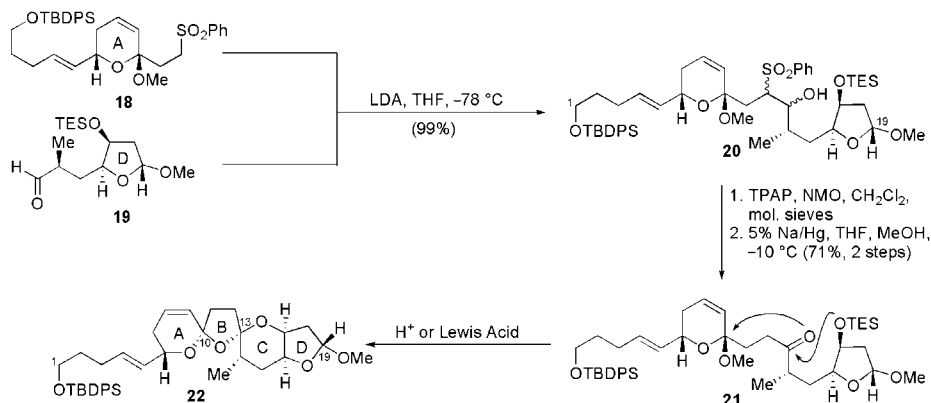


**Scheme 16.1.** Construction of the ABCD backbone, providing an undesired diastereomer (**17**) instead of the desired isomer *C-13-epi-17* (Dounay 2001).

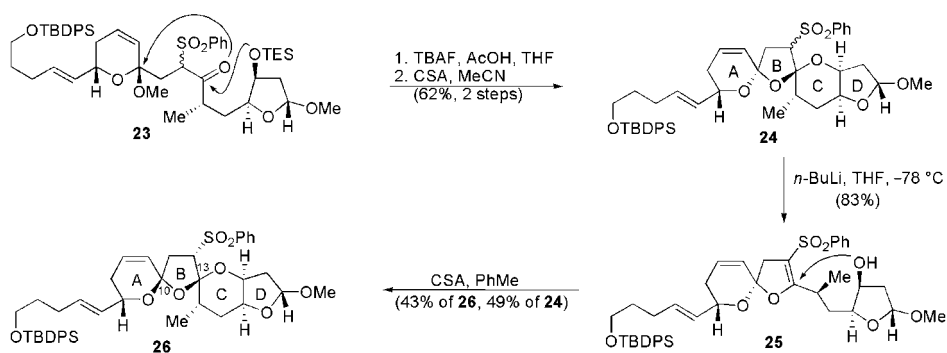
making it a higher energy intermediate. A new approach had to be devised in order to counteract this thermodynamic instability.

The Carter group would be the next to report their synthetic forays into the ABCD domain of azaspiracid-1 (Carter 2001). In their efforts (shown in Scheme 16.2), deprotonation of A-ring sulfone **18** with LDA allowed its smooth addition to the D-ring aldehyde **19**, affording  $\text{C}_1\text{-C}_{19}$  secondary alcohol **20** (99% yield). TPAP oxidation of secondary alcohol **20**, followed by Na/Hg-mediated reductive removal of the sulfonyl group resulted in the formation of ketone **21** in 71% yield over the two steps, setting the stage for their key deprotection-polycyclization cascade. Treatment of the latter compound (**21**) with various Lewis and protic acids afforded the ABCD tetracyclic product **22** as a single isomer, but with the wrong stereochemistry at C-13, which could not be epimerized to the desired product, just as was encountered by the Forsyth group.

Confronted with this failure to produce the desired C-13 stereocenter, the Carter group resorted to other tactics (Scheme 16.3). They reasoned that by retaining the sulfone moiety on their previously synthesized  $\text{C}_1\text{-C}_{19}$  fragment **23**, they could possibly direct the cyclization event providing at least some of the desired C-13 epimer. Unfortunately, treatment of this compound (**23**) with TBAF and AcOH, and subsequent exposure to CSA in  $\text{CH}_3\text{CN}$  resulted in the formation of tetracycle **24** once again with the undesired C-13 stereochemistry, which could not be equilibrated to the desired product. Treatment of the latter compound (**24**) with  $n\text{-BuLi}$  resulted in opening of the C ring, yielding vinyl sulfone **25** in 83% yield. Subsequent treatment of the latter compound (**25**) with CSA in toluene effected the formation of two tetracyclic products. One of these products was the C-13 epimeric compound **24** (obtained in 49% yield) and the other was a new product, **26** (obtained in 43% yield), which now had the correct stereochemistry at C-13, but the wrong stereochemistry at C-10, which could not be equilibrated to the desired configuration.



**Scheme 16.2.** Construction of the undesired C1–C19 azaspiracid-1 backbone (22, ABCD ring system) (Carter 2001).

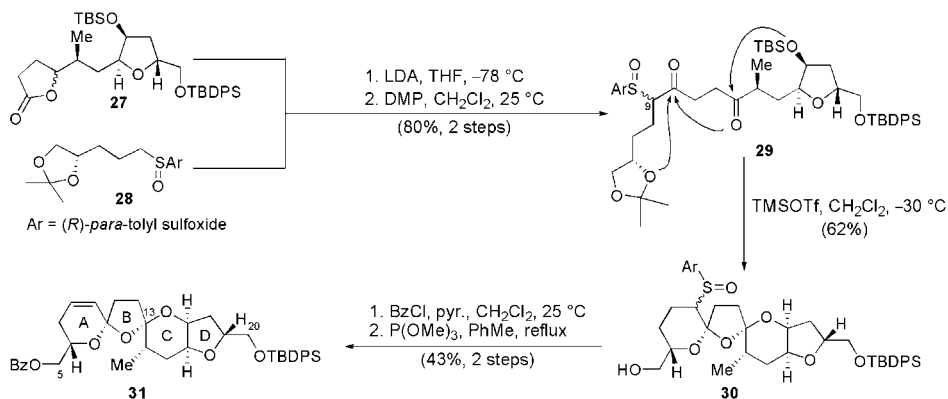


**Scheme 16.3.** Attempts to construct the ABCD backbone of azaspiracid-1 (1a), resulting in the undesired diastereomer (26) (Carter 2001).

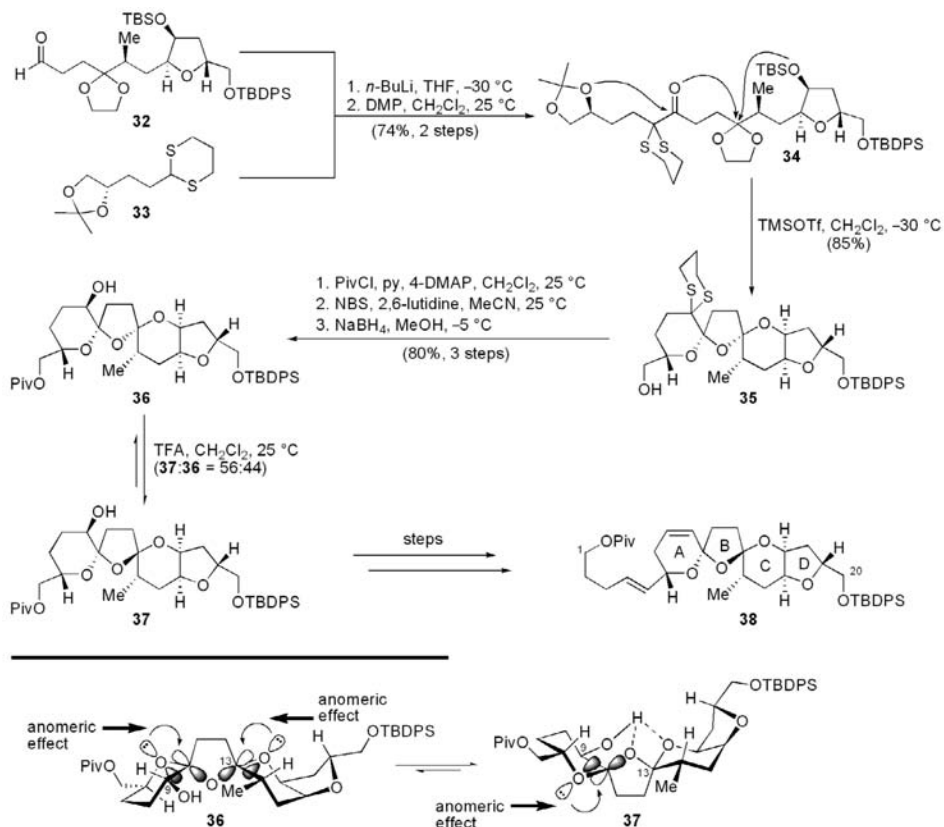
In order to avoid the thermodynamic trap of the C-13 stereocenter, we opted for a different strategy than those of previous workers in the field. Inspired by the reports of Williams (1982), we reasoned that the placement of a chiral sulfoxide on C-9 would bias the proposed ring closure, providing the desired ABCD diastereomer with the correct stereochemistry at C-13 (Scheme 16.4) (Nicolaou 2001b). To test this hypothesis, we reacted lithiated chiral sulfoxide 28 with lactone 27, affording, after Dess-Martin periodinane (DMP) oxidation, C<sub>5</sub>–C<sub>20</sub> diketone 29 in 80% yield over the two steps. Treatment of the latter compound (29) with TMSOTf in CH<sub>2</sub>Cl<sub>2</sub> at -30 °C resulted in the formation of tetracycle 30 (62%) as a 1:1 mixture of sulfoxide diastereomers, whose stereochemical details were not determined at this point. Proceeding forward, protection of the primary alcohol as the benzoate (BzCl, pyridine), followed by thermolysis of the sulfoxide moiety, afforded alkene 31 (43% over two steps) as a single isomer. Much to our disappointment, however, this compound (31) was proven to possess the wrong C-13 stereochemistry, and as in the case of the previous investigations by Forsyth and Carter, could not be isomerized to the desired stereoisomer.

We then set out to attempt a more daring approach to forge the desired ABCD tetracycle. Inspection of manual molecular models, and as seen in the inset in Scheme 16.5, a hydroxyl group at





**Scheme 16.4.** Unsuccessful attempt to construct the correct ABCD azaspiracid-1 backbone using a chiral sulfoxide (Nicolaou 2001a).



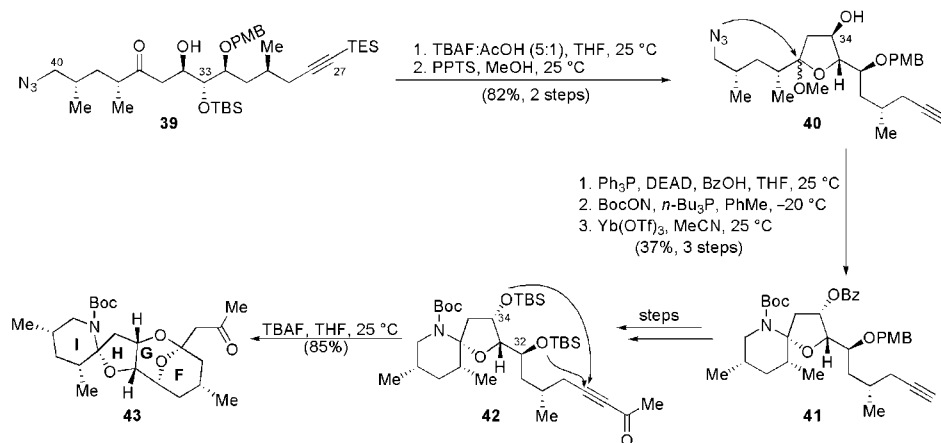
**Scheme 16.5.** Construction of the originally proposed ABCD core structure of azaspiracid-1 through exploitation of intramolecular hydrogen bonding (Nicolaou 2001b).

C-9 could potentially improvise for a hydrogen bond with both the B and C ring ether oxygen atoms. It was hoped that such hydrogen bonding would override the double anomeric effect present within 36, and could, in principle, lead to the desired product 37 stabilized by the hydrogen bonds and the single anomeric effect as shown (Scheme 16.5). In order to construct the appropriate substrate to test this hypothesis, we added the lithium anion of dithiane 33 to aldehyde 32, affording, after DMP oxidation, the C<sub>5</sub>–C<sub>20</sub> cyclization precursor 34 (74% for the two steps). Treatment of the latter compound (34) with TMSOTf in CH<sub>2</sub>Cl<sub>2</sub> at –40°C resulted in tetracycle 35 with the undesired stereochemistry at C-13 as expected. The desired C-9 alcohol (36) was then synthesized by a three-step sequence: first pivaloate protection (PivCl, pyridine, 4-DMAP) of the primary alcohol, followed by oxidative dithiane removal (NBS, 2,6-lutidine) and reduction of the resultant ketone (NaBH<sub>4</sub>, 80% over the three steps). Exposure of this compound (36) to TFA delightfully yielded a 56:44 separable mixture in favor of the desired tetracyclic product 37, now possessing the correct stereochemistry at C-13. The latter compound (37) was then smoothly elaborated to the complete C<sub>1</sub>–C<sub>20</sub> domain of the originally proposed structure of azaspiracid-1 (1a).

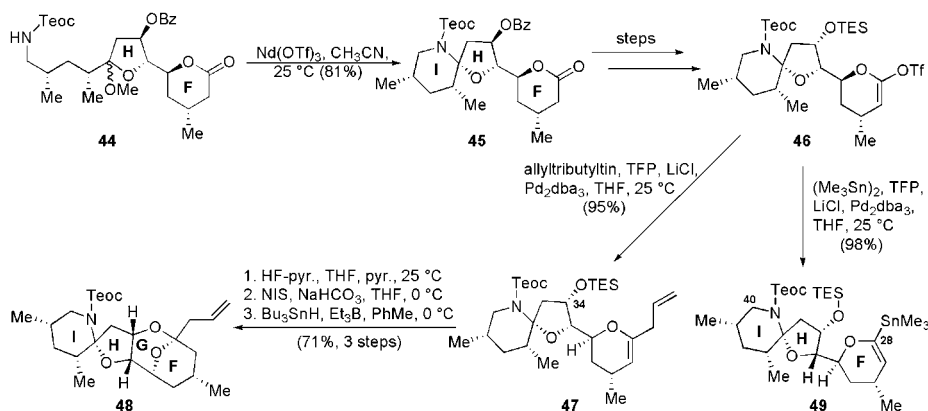
### Synthetic Efforts Toward the FGHI Domain of Azaspiracid-1

The Forsyth group reported the first route to the FGHI segment (Scheme 16.6) (Forsyth 2001). Using relatively straightforward chemistry, they were able to procure the C<sub>27</sub>–C<sub>40</sub> straight-chained fragment 39. Treatment of 39 with TBAF resulted in the cleavage of both silicon protecting groups from the molecule, furnishing the corresponding acetylenic diol, which, upon treatment with catalytic amounts of PPTS in MeOH, afforded methyl acetal 40 (82% yield, two steps) through cyclization to form ring H. Because the alcohol at C-34 was of the wrong stereochemistry, inversion through a Mitsunobu reaction (Ph<sub>3</sub>P, DEAD, BzOH) was necessary, resulting in the corresponding inverted benzoate. Staudinger reaction (*n*-Bu<sub>3</sub>P), followed by in situ trapping of the primary amine as the corresponding Boc carbamate, set the stage for the Yb(OTf)<sub>3</sub>-mediated spiroaminal (I ring) forming reaction, providing bicycle 41 (37% yield over three steps). The latter compound (41) was then elaborated into ynone 42, a species primed for a double intramolecular hetero-Michael addition to form the intramolecular bridged ketal (FG ring system). Treatment of this compound (42) with TBAF removed the TBS groups at C-32 and C-34 allowing the resulting hydroxyl groups to add into the ynone, affording the desired FGHI tetracycle (43) in 85% yield, as a single stereoisomer.

Our route to the FGHI domain of azaspiracid-1 is shown in Scheme 16.7 (Nicolaou 2001a). Treatment of key intermediate 44 (with the F and H rings formed) with Nd(OTf)<sub>3</sub> resulted in spiroaminal formation, providing FHI tricycle 45 in 81% yield. This compound (45) was then elaborated into vinyl triflate 46, a key compound that was employed in two different ways. The first purpose was as a model system for the G ring formation, a task accomplished by first converting vinyl triflate 46 into diene 47 (allyl(*n*-Bu)<sub>3</sub>Sn, TFP, LiCl, Pd<sub>2</sub>dba<sub>3</sub>, 95% yield). The G ring was then successfully formed by first treating the latter compound (47) with HF•py to reveal the C-34 alcohol. Treatment of the resulting secondary alcohol with NIS and NaHCO<sub>3</sub> formed the G ring through an iodoetherification reaction, leaving behind an extraneous iodide residue, which was then reductively removed with *n*-Bu<sub>3</sub>SnH and Et<sub>3</sub>B providing tetracycle 48 (71% over three steps). Intermediate 46 was also converted into vinyl stannane 49 [(Me<sub>3</sub>Sn)<sub>2</sub>, TFP, LiCl, Pd<sub>2</sub>dba<sub>3</sub>, 98% yield, Scheme 16.7], a substance that was intended for our total synthesis of azaspiracid-1, through a Stille coupling reaction.



**Scheme 16.6.** Construction of the FGHI rings of azaspiracid-1 using a double intramolecular hetero-Michael addition (Forsyth 2001).

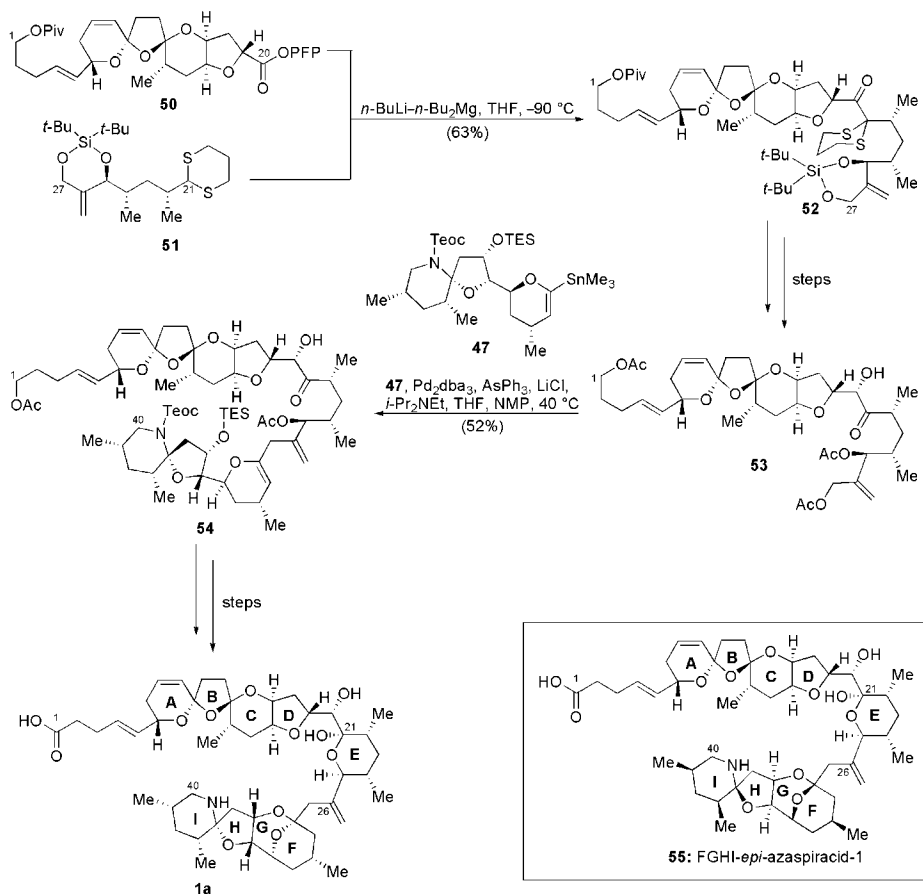


**Scheme 16.7.** Construction of the FGHI model system 48 and coupling partner 49 (Nicolaou 2001a).

## Synthesis of the Originally Proposed Structure of Azaspiracid-1

With the key ABCD and FGHI fragments synthesized in our laboratories, the next step was to join them and complete the synthesis of azaspiracid-1 (1a) (Nicolaou 2003a, 2003b). To complete the total synthesis of azaspiracid-1, there were two key bond-forming reactions to be accomplished, specifically, the C<sub>20</sub>–C<sub>21</sub> bond between the ABCD and E ring domains, and the C<sub>27</sub>–C<sub>28</sub> bond between the E and FGHI domains. To form the C<sub>20</sub>–C<sub>21</sub> bond, a dithiane coupling was employed. Lithiation of dithiane 51 with *n*-BuLi–*n*-Bu<sub>2</sub>Mg at 25 °C, followed by the addition of

pentafluorophenol (PFP) ester **50** to the solution at  $-90^{\circ}\text{C}$ , resulted in the formation of  $\text{C}_1\text{-C}_{27}$  ketone **52** in 63% yield. Elaboration of ketone **52** into triacetate **53** set the stage for the next key bond forming reaction, a Stille coupling. Addition of vinyl stannane **47** to a solution of triacetate **53**, in the presence of  $\text{Pd}_2\text{dba}_3$ ,  $\text{AsPh}_3$ ,  $\text{LiCl}$ , and  $i\text{-Pr}_2\text{NEt}$  resulted in the formation of  $\text{C}_1\text{-C}_{40}$  fragment **54** (52% yield). With the carbon backbone of azaspiracid-1 in place, all that was left to arrive at one of the originally proposed structures of azaspiracid-1 (**1a**) were a few functional group manipulations. Unfortunately, synthesis of originally proposed azaspiracid-1 (**1a**) led to disappointment, as it was not identical to the natural sample of azaspiracid-1 ( $R_f$  and  $^1\text{H}$  NMR). Because the relative stereochemistry between the ABCDE and FGHI domains was not assigned, we also targeted **55** (Scheme 16.8), the FGHI diastereomer of **1a**. Unfortunately, synthesis of **55** proved that this was also not the structure of azaspiracid-1.

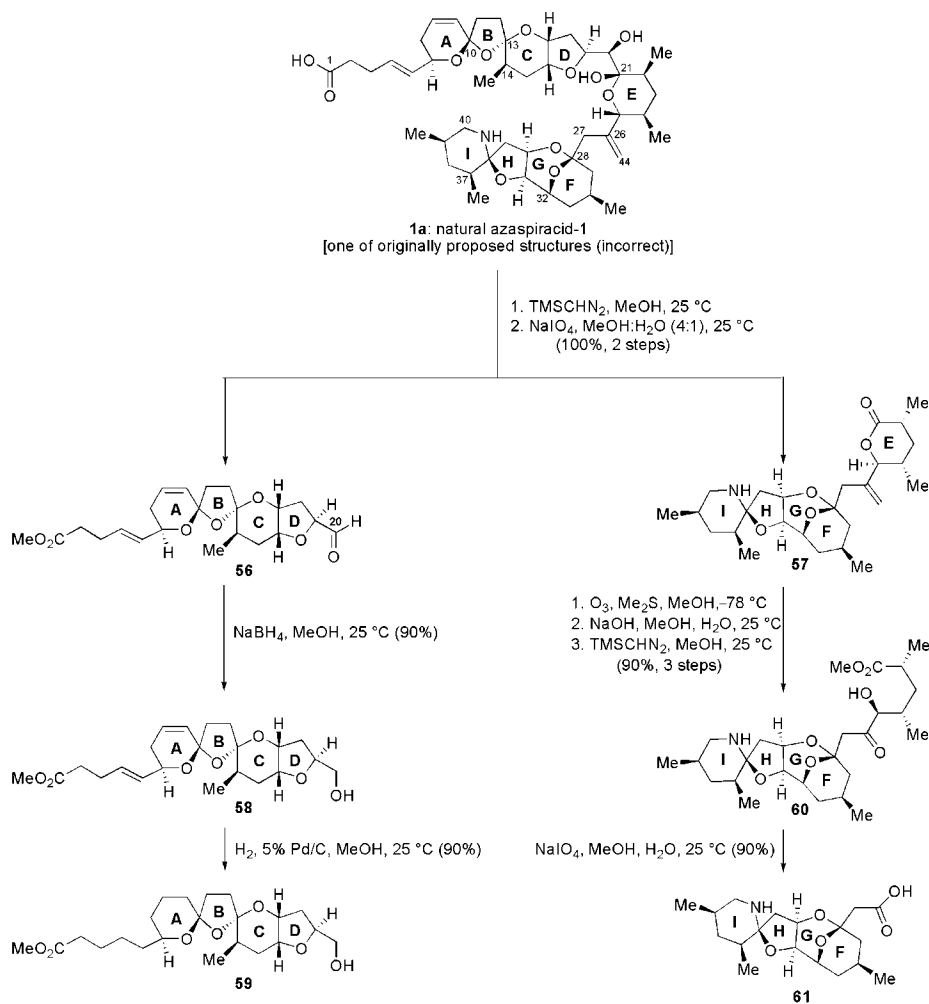


**Scheme 16.8.** Strategies toward the originally proposed structures of azaspiracid-1 (**1a**) and FGHI-epi-azaspiracid-1 (**55**) (Nicolau 2003a, 2003b).

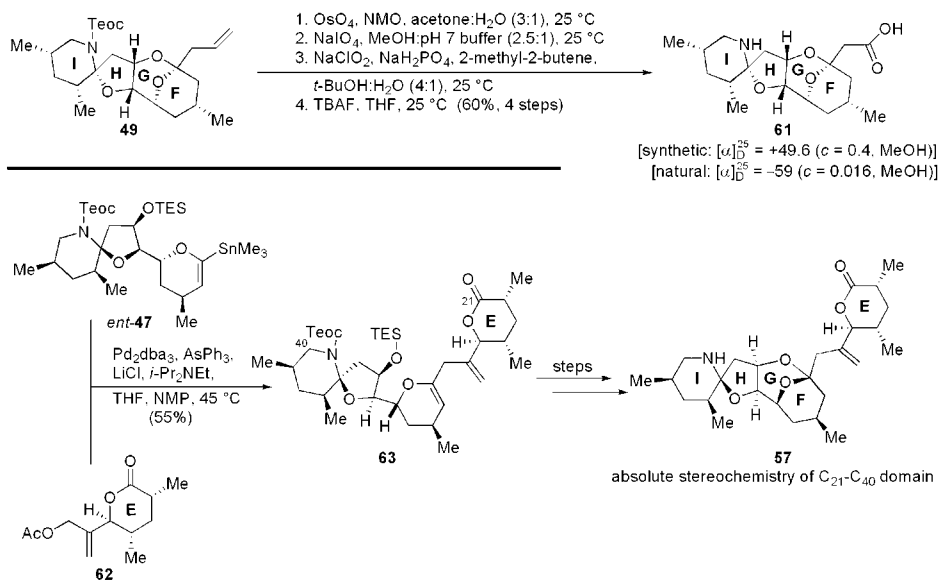
## Degradation and Match-up Studies

Unsure of how to proceed along the lines of total synthesis, we resorted to new tactics in order to discover the true structure of azaspiracid-1 (Nicolau 2004a, 2004b). It was requested that the Satake group attempt a chemical degradation of natural azaspiracid-1, a task that was admirably carried out as shown in Scheme 16.9, to produce 56–61. The Satake group then obtained  $^1\text{H}$  NMR spectra of these compounds (58, 59, 57, and 61) and we set out to synthesize them in order to confirm their structures.

Our synthesis of the originally proposed FGHI carboxylic acid 61 is summarized in Scheme 16.10. Thus, terminal alkene 49 was converted to the corresponding carboxylic acid through a three-step procedure ( $\text{OsO}_4$ -mediated dihydroxylation,  $\text{NaIO}_4$  cleavage to the aldehyde, and  $\text{NaClO}_2$  oxidation to the carboxylic acid) from which the Teoc protecting group was removed with TBAF to



**Scheme 16.9.** Degradation of natural azaspiracid-1 (Nicolau 2004a).



**Scheme 16.10.** Proof of the relative and absolute stereochemistries of the EFGHI fragment of azaspiracid-1 through comparison of synthetic and naturally derived materials (Nicolaou 2004b).

provide the desired FGHI carboxylic acid fragment (61). This synthetic material matched the degradation product by <sup>1</sup>H NMR spectroscopy, but its optical rotation was of the opposite sign to that found by Satake with the natural material [synthetic:  $[\alpha]_D = +49.6$  ( $c = 0.4$ , MeOH); natural:  $[\alpha]_D = -59$  ( $c = 0.016$ , MeOH)]. This observation meant that the absolute stereochemistry of the FGHI segment was opposite to that depicted by 61.

The next goal was to determine the absolute stereochemistry of the EFGHI domain 57. Stille coupling between vinyl stannane *ent*-47 and E ring allylic acetate 62 (Pd<sub>2</sub>dba<sub>3</sub>, AsPh<sub>3</sub>, LiCl, *i*-Pr<sub>2</sub>NEt) afforded C<sub>21</sub>-C<sub>40</sub> fragment 63, which was elaborated into EFGHI lactone 57. Fortunately, lactone 57 was identical by <sup>1</sup>H NMR spectroscopy to the naturally derived material (Scheme 16.10). These studies proved that the original assignments by Yasumoto and co-workers (Satake 1998) for the EFGHI domain of azaspiracid-1 were correct, and that the errors were in the ABCD domain of the structure.

Deciphering the structure of the ABCD domain required the synthesis of several structures (see Fig. 16.2). The first synthesis was of the originally proposed ABCD domain 58, which, as expected, did not match the originally proposed structure by <sup>1</sup>H NMR spectroscopy. Key differences in the <sup>1</sup>H NMR spectra revolved around the A-ring. And when comparing these chemical shifts to those of another natural product, lissoketal (64) (Hopman 1997), we found striking similarities. These similarities, which extended over to nOe correlations, suggested that the double bond in azaspiracid-1 was in the wrong location within ring A. We then proceeded to synthesize the structure 65, with the double bond shifted by one position. Although the spectra were more in agreement, in particular with regards to A-ring, this compound (65) was still not identical to the naturally derived material. Still troubled by the thermodynamic instability of the ABC bis-spiroacetal ring system, we reasoned that the stereochemistries

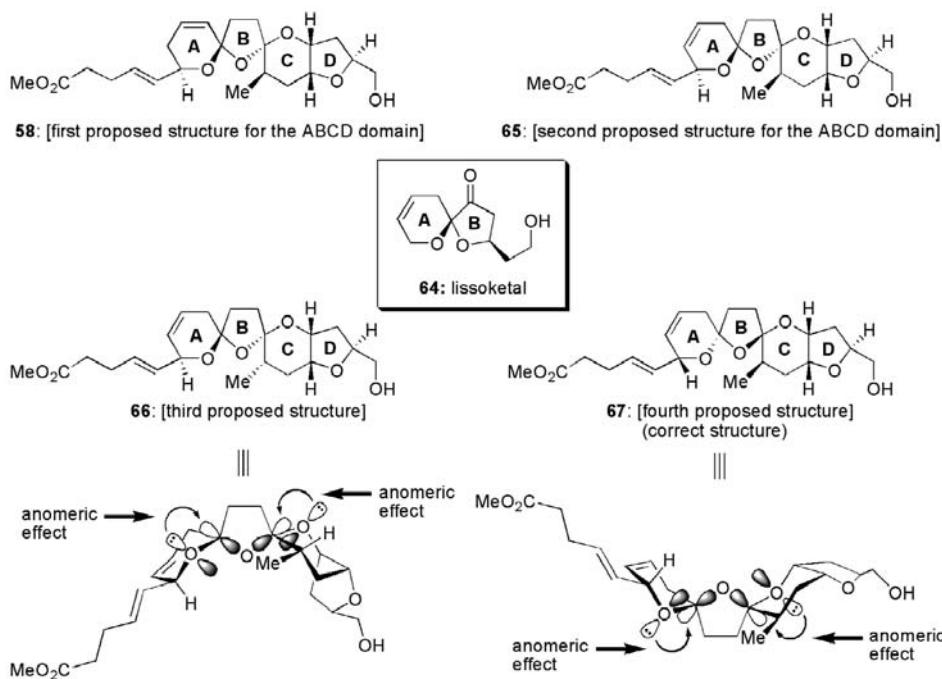
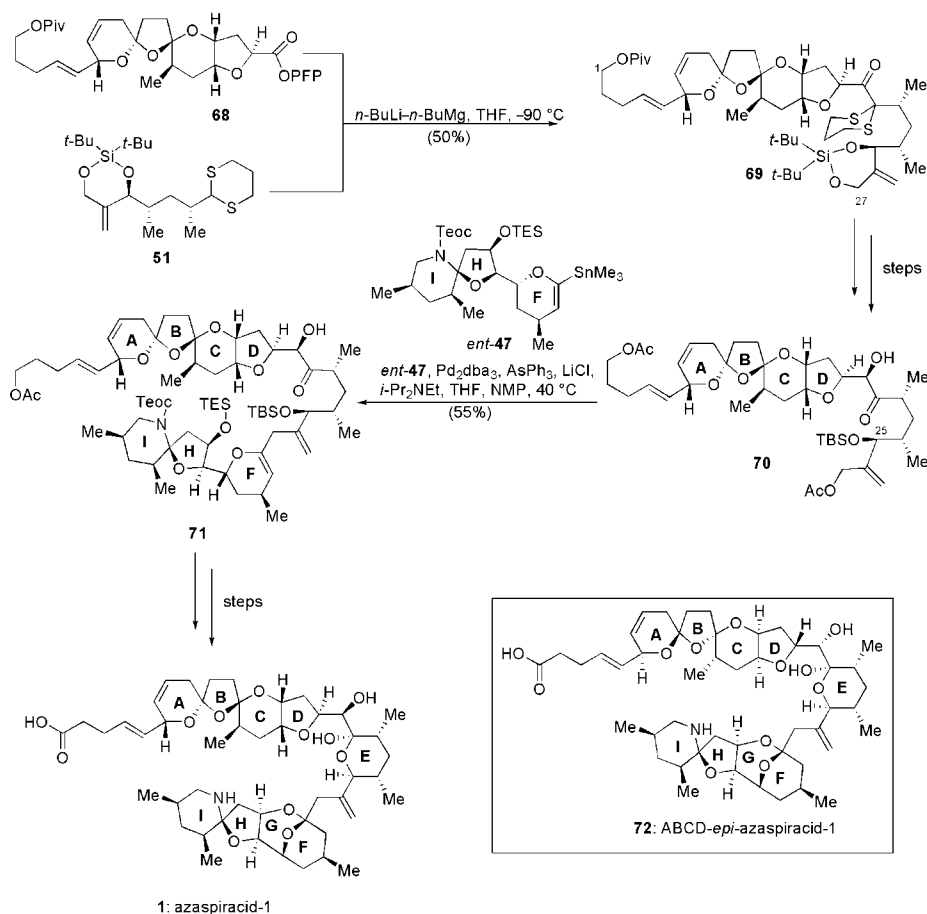


Figure 16.2. Molecular structures of azaspiracids-2 to -11.

assigned for the ring junctures were incorrect. At this point, it was speculated that the actual structure would, in fact, take advantage of the double anomeric effect within the ABC ring framework and manifest itself in the natural product. Keeping the rest of the stereochemistry the same, this would lead to either structure 66 or 67 as the correct isomer. While we determined that the third proposed structure (66) was incorrect, the synthesis of the ABCD structure 67 confirmed its identity to the naturally-derived material by  $^1\text{H}$  NMR spectroscopy. With this accomplishment the relative stereochemistry of the ABCD domain was now known, but because of the small quantities of natural material obtained, a measurement of optical rotation was not possible and, therefore, its absolute stereochemistry remained in question. This deficiency meant that both ABCD diastereomers of azaspiracid-1 would have to be synthesized in order to determine its true structure.

Scheme 16.11 shows the completion of the total synthesis of azaspiracid-1, which followed, with slight modifications, the synthesis of the originally proposed structure of azaspiracid-1 (1a). This chemistry was also carried out with the corresponding ABCD enantiomer in similar yields. Thus, lithiation of dithiane 51 ( $n\text{-BuLi}-n\text{-Bu}_2\text{Mg}$ ) followed by addition into pentafluorophenol ester 68 resulted in  $\text{C}_1\text{-C}_{27}$  ketone 69 (50% yield). Ketone 69 was then elaborated into diacetate 70, this time as the TBS ether at C-25, as this protecting group was easier to remove than the acetate used in the earlier work directed toward the original structure (see Scheme 16.8). Stille coupling of this allylic acetate (70) then proceeded smoothly, as before, affording the complete  $\text{C}_1\text{-C}_{40}$  backbone 71, which was successfully elaborated to the correct structure of azaspiracid-1 (1), identical in all measured physical properties ( $^1\text{H}$  NMR,  $^{13}\text{C}$  NMR, Rf,  $[\alpha]_D$ ) to the natural material.





**Scheme 16.11.** The completion of the total synthesis of azaspiracid-1 (Nicolaou 2004a).

## Conclusions

The isolation of azaspiracid-1 from poisonous mussels (*Mytilus edulis*) by Yasumoto and Satake was an admirable and Herculean accomplishment. Its originally proposed structure by these investigators stimulated considerable efforts to synthesize it in the laboratory. The efforts in our laboratory led first to the demise of the originally proposed structures and subsequently to the proposal and total synthesis of the correct structure of this fascinating natural product.

## Acknowledgments

Financial support for this work was provided by The Skaggs Institute for Chemical Biology and a predoctoral fellowship from the National Science Foundation (to M. O. F.). A general acknowledgement is given to the National Institutes of Health (USA) for their support over the years.

## References

- Carter, R.G., and Graves, D.E. 2001. Studies directed toward the total synthesis of azaspiracid. Construction of the C<sub>1</sub>–C<sub>19</sub> carbon backbone and synthesis of the C<sub>10</sub>, C<sub>13</sub> nonnatural transoidal bisspirocyclic ring system. *Tetrahedron Lett* 42(35):6035–6039.
- Dounay, A.B., and Forsyth, C.J. 2001. Synthetic studies toward the C5–C20 domain of the azaspiracids. *Org Lett* 3(7):975–978.
- Forsyth, C.J., Hao, J.L., and Aiguade, J. 2001. Synthesis of the (+)-C26–C40 domain of the azaspiracids by a novel double intramolecular hetero-Michael addition strategy. *Angew Chem Int Ed* 40(19):3663–3667.
- Hopman, C., and Faulkner, D.J. 1997. Lissoketal, a spiroketal from the Palauan ascidian *Lissoclinum voeltzkowi*. *Tetrahedron Lett* 38(2):169–170.
- James, K.J., Diaz Sierra, M., Lehane, M., Magdalena, A.B., and Furey, A. 2003. Detection of five new hydroxyl analogues of azaspiracids in shellfish using multiple tandem mass spectrometry. *Toxicon* 41:277–283.
- McMahon, T., and Silke, J. 1996. Winter toxicity of unknown aetiology in mussels. *Harmful Algae News* 14:2.
- Nicolaou, K.C., Chen, David Y.-K., Li, Y.W., Qian, W.Y., Ling, T.T., Vyskocil, S., Koftis, T.V., Govindasamy, M., and Uesaka, N. 2003a. Total synthesis of the proposed azaspiracid-1 structure, part 2: Coupling of the C1–C20, C21–C27, and C28–C40 fragments and completion of the synthesis. *Angew Chem Int Ed* 42(31):3649–3653.
- Nicolaou, K.C., Koftis, T.V., Vyskocil, S., Petrovic, G., Ling, T.T., Yamada, Y.M.A., Tang, W.J., and Frederick, M.O. 2004a. Structural revision and total synthesis of azaspiracid-1, part 2: definition of the ABCD domain and total synthesis. *Angew Chem Int Ed* 43(33):4318–4324.
- Nicolaou, K.C., Li, Y.W., Uesaka, N., Koftis, T.V., Vyskocil, S., Ling, T.T., Govindasamy, M., Qian, W.Y., Bernal, F., and Chen, D.Y.-K. 2003b. Total synthesis of the proposed azaspiracid-1 structure, part 1: construction of the enantiomerically pure C1–C20, C21–C27, and C28–C40 fragments. *Angew Chem Int Ed* 42(31):3643–3648.
- Nicolaou, K.C., Pihko, P.M., Diedrichs, N., Zou, N., and Bernal, F. 2001a. Synthesis of the FGHI ring system of azaspiracid. *Angew Chem Int Ed* 40(7):1262–1265.
- Nicolaou, K.C., Qian, W.Y., Bernal, F., Uesaka, N., Pihko, P.M., and Hinrichs, J. 2001b. Synthesis of the ABCD ring system of azaspiracid. *Angew Chem Int Ed* 40(21):4068–4071.
- Nicolaou, K.C., Vyskocil, S., Koftis, T.V., Yamada, Y.M.A., Ling, T.T., Chen, D.Y.-K., Tang, W.J., Petrovic, G., Frederick, M.O., Li, Y.W., and Satake, M. 2004b. Structural revision and total synthesis of azaspiracid-1, part 1: intelligence gathering and tentative proposal. *Angew Chem Int Ed* 43(33):4312–4318.
- Ofuji, K., Satake, M., McMahon, T., James, K.J., Naoki, H., Oshima, Y., and Yasumoto, T. 2001. Structures of azaspiracid analogs, azaspiracid-4 and azaspiracid-5, causative toxins of azaspiracid poisoning in Europe. *Biosci Biotechnol Biochem* 65(3):740–742.
- Ofuji, K., Satake, M., McMahon, T., Silke, J., James, K.J., Naoki, H., Oshima, Y., and Yasumoto, T. 1999. Two analogs of azaspiracid isolated from mussels, *Mytilus edulis*, involved in human intoxication in Ireland. *Nat Toxins* 7(3):99–102.
- Satake, M., Ofuji, K., Naoki, H., James, K.J., Furey, A., McMahon, T., Silke, J., and Yasumoto, T. 1998. Azaspiracid, a new marine toxin having unique spiro ring assemblies, isolated from Irish mussels, *Mytilus edulis*. *J Am Chem Soc* 120(38):9967–9968.
- Williams, D.R., Barner, B.A., Nishitani, K., and Phillips, J.G. 1982. Total synthesis of milbemycin β<sub>3</sub>. *J Am Chem Soc* 104(17):4708–4710.

## 17 Biochemistry of Azaspiracid Poisoning Toxins

Natalia Vilariño

### Introduction

The occurrence of toxic algal blooms has increased in the last decades. Not only the number of toxic blooms has multiplied and their geographical distribution has spread all over the world, but also new toxins and new toxic algae species have been described. Azaspiracids are the most recently identified class of marine toxins present in shellfish. Only known since 1997, azaspiracid and its analogues have awakened both public health concern and scientific interest.

### Azaspiracid Toxic Blooms and Accumulation in Shellfish

The first reported azaspiracid toxic episodes occurred in 1995 in the Netherlands due to ingestion of mussels from Killary Harbor, Ireland (McMahon et al. 1996, Satake et al. 1998a) and in 1997 in Arranmore Island, Ireland (McMahon et al. 1998, Ofuji et al. 1999a). Since then, several outbursts of azaspiracid toxic molluscs have been described in shellfish cultivated in Ireland, England, Norway (James et al. 2002a), France, and Spain (Magdalena et al. 2003a).

The main toxin present in the mussels that originated the first toxic episode was isolated in 1997 by Satake et al. (1998a) and named azaspiracid-1 (Fig. 16.1, Chapter 16). As discussed previously in this book, the initial chemical structure proposed in that first publication for azaspiracid-1 has been revised (Nicolaou et al. 2003a, 2003b), and 11 different analogues have been described as present in natural samples since then (azaspiracids 1–11) (Fig. 16.2, Chapter 16) (James et al. 2003b; Ofuji et al. 2001; Ofuji et al. 1999a; Satake et al. 1998a; Volmer et al. 2002).

A source of azaspiracid toxins has been recently identified as the dinoflagellate species *Protoperidinium crassipes* (Fig. 17.1) (James et al. 2003a), which is part of the trophic chain of many shellfish species. Most likely other species of this genus—more than 60 have been described (Jeong et al. 1994; Latz et al. 1996)—are also able to contain the toxin. However, it is not completely clear yet if this species synthesizes the toxin itself. Due to its predator habits, it would be possible that it acquired the toxin feeding from other plankton species. The toxins detected in *Protoperidium* cell extracts were azaspiracids-1, -2, and -3 (James et al. 2003a). It has been suggested that some of the analogues described to date may be a product of modification of these three compounds by shellfish metabolism, for example, azaspiracid-4 and -5 being a product of azaspiracid-3 oxidation (FAO, 2004). However, there is no experimental evidence to support this hypothesis yet.

After an azaspiracid toxic bloom, toxicity of shellfish is thought to last for months (James et al. 2000; Ofuji et al. 1999b). Although all the toxic episodes reported in humans were related to mussel (*Mytilus edulis*) consumption, azaspiracids have been recently detected in comparable levels in oysters (*Crassostrea gigas*) (Furey et al. 2003; Magdalena et al. 2003b). Clams (*Tapes philippinarium*), scallops (*Pecten maximum*) cockles (*Cardium edule*), razor fish (*Ensis siliqua*), and another species



**Figure 17.1.** *Protoperdinium crassipes*. Average dimensions  $0.1 \times 0.12$  mm. Reprinted from James et al. 2003, with permission from Elsevier.

of mussel (*Mytilus galloprovincialis*) also accumulate the toxin; however, the amounts detected in these species were lower than in mussels (Furey et al. 2003; Hess et al. 2001; Magdalena et al. 2003a). Very recently a European Union rapid alert was released in week 47, year 2005 after Norway notified that azaspiracid toxins had been found in crabs (*Cancer pagurus*) (RASFF 2005).

The distribution of toxins in shellfish tissues and culture areas should be considered when sampling shellfish for toxin detection. Although previous studies suggested that the distribution of azaspiracids in mussel body differed from other lipophilic shellfish toxins, with only 0%–40% of azaspiracids being located to the hepatopancreas and the rest being located to other parts of the shellfish body (James et al. 2002b), more recent studies suggest otherwise. In a 2005 study the amount of toxin/g of tissue was fivefold higher in mussel hepatopancreas than in the whole body both in fresh and cooked samples (Hess et al. 2005). Considering that around 18% of the mussel body weight is hepatopancreas, the results strongly suggest that the toxin is almost exclusively located to the hepatopancreas. Another report on the distribution of toxin in scallops showed that about 85% of the toxin concentrates in the hepatopancreas in this species (Magdalena et al. 2003b). The apparent toxin distribution to other tissues in the initial report could be the result of sample manipulation preceding extraction, where manoeuvres such as freezing or dissection, may be responsible for the contamination of adjacent shellfish tissues. It could be argued also that seasonal variations such as time of sample collection after the onset of the toxic bloom affected toxin distribution to other shellfish tissues. However, this unusual distribution was not observed over three seasons in the recent Hess et al. study. It is important to note for sampling purposes that there is a high variability of toxin content among sites within a culture area and among mussel individuals within the same sample (James et al. 2002b).

Another common feature with other shellfish toxins is that heat does not destroy azaspiracids either (EU/SANCO 2001; Hess et al. 2005). Therefore, cooking does not eliminate the toxicity of shellfish due to an azaspiracid toxic bloom. Overall, these compounds seem to be quite stable during storage (EU/SANCO 2001), although there are some concerns about their stability in certain organic solvents and alkaline conditions (James et al. 2002b; Satake et al. 1998b).

## Azaspiracid Poisoning Syndrome

The clinical symptoms caused by azaspiracid poisoning in humans are similar to diarrhetic shellfish poisoning and to bacterial enterotoxin poisoning. Because of the similarity of the gastrointestinal symptoms induced by this new toxin and the well characterized DSP (diarrhetic shellfish poisoning) toxins in humans, azaspiracids have been classified at times in the diarrhetic toxin group. However, when the chemical structure of this new toxin was identified as a completely different molecule from DSP toxins, this toxic syndrome was named azaspiracid poisoning (AZP).

Azaspiracid poisoning symptoms in humans include nausea, vomiting, diarrhea, stomach cramps, and headache. The symptoms appear 3 to 18 hours after eating contaminated shellfish, and the recovery is complete within 2 to 5 days (James et al. 2004; McMahon et al. 1996).

Diagnosis of AZP in humans relies on identification of the symptoms, since there are no available laboratory tests. The only way to achieve a specific diagnosis is, if possible, to test the suspected contaminated seafood. In any case, the specific diagnosis is not necessary for treatment since no antidote is known for shellfish toxins. The therapy is symptomatic, supported by monitoring of fluid and electrolyte levels in cases of severe intoxication.

## Azaspiracid Toxicity to Experimental Animals and Humans

The minimum lethal dose to mice by oral administration that has been reported is 0.25 mg/kg; however, lethality fluctuates depending on individuals and age (Ito et al. 2002). Interestingly, the intraperitoneal and oral lethal doses in mice are fairly close for azaspiracid-1, which is not the case for other groups of marine toxins (Ito et al. 2002; Ito et al. 2000). The relative toxic potency for different analogues is only known for azaspirazids-1 to -5, and the comparison is based in mouse lethal doses by intraperitoneal injection. Azaspiracids-1, -2, and -3 are the more toxic forms, with mouse lethal doses of 0.2 mg/kg, 0.11 mg/kg, and 0.14 mg/kg, respectively (Ofuji et al. 1999a; Satake et al. 1998a), followed by azaspiracid-4 (0.47 mg/kg) and the less toxic azaspiracid-5 (approximately 1.0 mg/kg) (Ofuji et al. 2001).

Toxicity to humans was initially estimated to be 15 µg/person (mean value) based on the toxin content of the mussels from the blooms that originated the first two toxic episodes, 0.6 µg/g of meat (Killary Harbour) and 1.36 µg/g of meat (Arranmore) (equivalent to 0.15 and 0.4 mouse units/g, respectively) (Ofuji et al. 1999b; Satake et al. 1998a, 1998b). However, recent data showed that azaspiracid concentration is not reduced by heat (EU/SANCO 2001; Hess et al. 2005), which had been a parameter for initial calculations. Therefore, the lowest observed adverse effect level (LOEL) has been re-estimated to be within the range of 23 to 86 µg/person, with a mean value of 51.7 µg/person (EU/SANCO 2001; FAO 2004). The non-observable adverse effect level (NOEL) was consequently calculated to be 80 µg/kg of shellfish meat, considering a safety factor of 3, which should account for individual variations, a maximum intake of 100 g per person and the lowest value in the LOEL range.

European regulations set the limit for azaspiracid toxins content in shellfish that is to be destined to human consumption in 160 µg of azaspiracid equivalents/kg in the whole body or any part edible separately (EU 2002). This limit has a higher value than the NOEL to allow for detection by mouse bioassay, the most commonly used method due to the lack of standards for chemical analysis.

## Pathology

Since there have not been any human casualties due to AZP, the existing pathology data has been collected from experimental animals.

Toxicity studies performed in mice showed several organs affected by azaspiracid poisoning. By p.o. administration, acute lesions to the small intestine consisted of small accumulation of fluid, vacuolization, and degeneration of epithelial cells, atrophic lamina propria that becomes spatially separated from the epithelium (Fig. 17.2) and shortening and erosion of villi (Ito et al. 2000). The first significant pathological signs in the small intestine were detected 4 hours after the administration of 300  $\mu\text{g}/\text{kg}$  azaspiracid-1. Lesions to the intestine progressed in intensity up to 8 hours, at doses of 600–700  $\mu\text{g}/\text{kg}$  and the recovery was not complete after 24 hours (Ito et al. 2000). When severe damage to the intestine was induced by azaspiracid administration, lesions persisted for 3 months (Ito et al. 2002). Interestingly, a comparative study of okadaic acid-induced lesions to the intestine

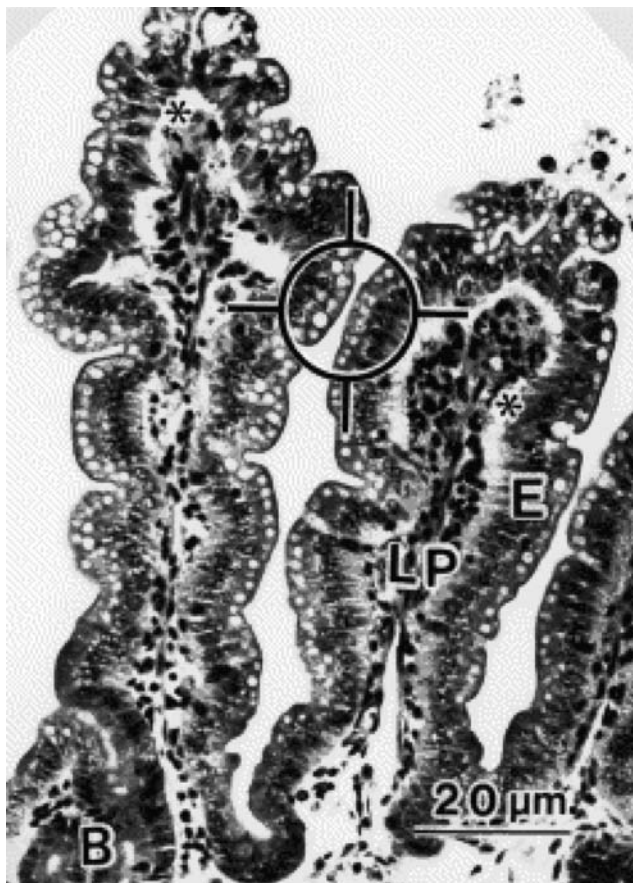


**Figure 17.2.** Vertical section of villi 4 hours after p.o. administration of azaspiracid at 300  $\mu\text{g}/\text{kg}$ . Vacuole degeneration of epithelial cells (circle) and atrophy of lamina propria (LP) are shown. Spaces (\*) are left between epithelial cells (E) and lamina propria. Reprinted from Ito et al. 2000, with permission from Elsevier.



showed a fast accumulation of liquid in the gut (30 minutes). Lesions consisted in erosion and shortening of villi with a peak around 2 hours, and recovery was already prominent by 4–8 hours depending on the dose (Ito et al. 2000).

The liver is also typically affected after acute azaspiracid intoxication, showing accumulation of fat droplets in a microscopic analysis at 1 hour after p.o. administration. Fatty liver was observed macroscopically after 4 hours, inducing the typical change in liver color (Ito et al. 2000). After severe lesions to the liver, recovery lasted for 20 days (Ito et al. 2002).

Lymphoid organs, including spleen, thymus, and Peyer's patches showed necrosis of T and B lymphocytes, the onset of lesions depending on the dose (Ito et al. 2000). Again, recovery of severe injuries to lymphoid organs was slow taking a period of 10 days (Ito et al. 2002).

When administered by intraperitoneal injection, azaspiracid caused similar lesions to those reported for oral administration. Besides fatty liver and necrosis of lymphoid tissues, i.p. administration to mice induced neurologic symptoms that included spasm and paralysis of the limbs (Ito et al. 1998).

Data related to chronic effects of natural toxins are extremely relevant in order to evaluate possible health risks for consumers. Chronic p.o. administration of low doses of azaspiracid-1 (1–50 µg/kg, twice a week for 145 days) induced shortened small intestinal villi, interstitial pneumonia, and appearance of lung tumour in 20% of the animals (Ito et al. 2002). These last data suggest that azaspiracid might be a tumour inducer raising serious concerns of public health due to the possibility of co-occurrence in toxic blooms with okadaic acid (James et al. 2002a; McMahan et al. 1996), a well-known tumour promoter (Fujiki et al. 1994, 1990).

## Toxicologic Mechanism

The toxicologic mechanism of azaspiracid toxins is not known yet. However, there is enough evidence accumulated that suggests that the mechanism of action of azaspiracid differs from that of the well characterized DSP toxins, okadaic acid, and dinophysistoxin. The first data that pointed to a different mechanism were the symptoms observed during mouse bioassay tests. After intraperitoneal injection in mice, azaspiracid containing extracts caused not only accumulation of fluid in the intestine but also neurological symptoms, the latter not appearing during DSP bioassay (Ito et al. 2000; Ito et al. 1998). More evidence suggesting a different mechanism at the molecular level was published recently showing that azaspiracid-1 does not inhibit protein phosphatase 2A (PP2A) activity, which is potently inhibited by DSP toxins (Twiner et al. 2005).

In vitro studies on the effect of azaspiracids on different cellular types have revealed some aspects of cellular biology affected by azaspiracids. However, the mechanism of action of this toxin remains elusive.

Azaspiracid-1 has been shown to be cytotoxic to several cell lines at doses in the nanomolar range and long incubation times (48 hours) (Twiner et al. 2005). Interestingly, Jurkat cells, a T lymphocyte cell line, were especially sensitive to azaspiracid induced cytotoxicity, in agreement with the pathologic findings in mouse toxicity assays where damage to lymphocytes was prominent. Likely, the mechanism of cytotoxicity is not apoptosis, since concentrations as high as 10 µM did not induce any change in mitochondrial membrane voltage, a sign of apoptotic death (Roman et al. 2002).

In human lymphocytes azaspiracid-1 has been shown to have an effect on the intracellular calcium signal by inducing a small, but gradual and steady, increase in the intracellular calcium concentration (Roman et al. 2002). Azaspiracid-2 and -3 also increased the intracellular calcium concentration, azaspiracid-3 by itself, similarly to azaspiracid-1, and azaspiracid-2 enhancing the intracellular



calcium rise induced by pharmacologic means (Roman et al. 2004). Opposite to azaspiracids-1, -2 and -3 that had a positive effect on the calcium signal, azaspiracid-4 diminished the calcium increase induced by an external stimulus (Alfonso et al. 2005; Roman et al. 2004). Intracellular pH does not seem to be affected by the presence of the toxin. This toxin group has also been shown to increase intracellular cAMP levels in lymphocytes (Roman et al. 2002; Roman et al. 2004). The mechanism and relevance to toxicology of both signaling effects is still unknown.

Several studies suggest an involvement of azaspiracid-1 in the regulation of microfilament cytoskeleton. In Jurkat T cells azaspiracid treatment induced a reduction in the number of pseudopodia (plasmatic membrane protrusions) per cell (Twiner et al. 2005). Additionally, high doses of azaspiracid-1 seemed to reduce the amount of polymerized actin in neuroblastoma cells (Roman et al. 2002). Very recent results obtained in our lab have shown that lower doses of azaspiracid-1 (10–50 nM) induced a reduction in the number of neurites (cell projections) in neuroblastoma cells (Fig. 17.3) and a disorganization of the basal actin cytoskeleton in caco-2 cells (an enterocyte cell line), without affecting the amount of polymerized actin (Vilariño et al. 2006).

Another effect of azaspiracid-1 that has been recently reported is the teratogenicity to finfish embryos (Colman et al. 2005). Microinjection of azaspiracid-1, a technique that has been used to mimic the effects of maternally transferred toxins (Colman et al. 2004; Kimm-Brinson et al. 2001) induced development retardation and death or hatching failure. Although the presence of azaspiracids in finfish tissues has not been described, these results suggest that azaspiracids might be toxic to fish population affecting embryo development and changing the balance of species in the environment, even though these toxins might not have a toxic effect on adult fish.

## Summary

A great effort has been made by the scientific community during the last 10 years to increase the available knowledge regarding azaspiracid toxins. The results of this effort have allowed the detection

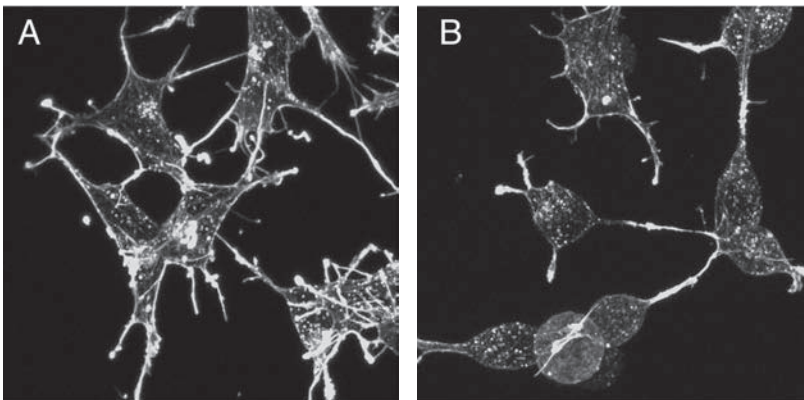


**Figure 17.3.** Neuroblastoma cells (BE(2)-M17 cell line) treated with azaspiracid-1 (50 nM) for 48 hours show a rearrangement of their microfilament cytoskeleton and adopt a round morphology compared to the more flattened controls. (A) Carrier control (DMSO). (B) Azaspiracid-1. Microfilaments (F-actin) were labelled with Oregon Green Phalloidin (Molecular Probes) and pictures were taken using a Nikon Eclipse TE2000-E confocal microscope.

and localization of azaspiracid toxic blooms, the identification of a dinoflagellate species that contains the toxin and the characterization of toxin distribution in shellfish body and culture areas, information extremely useful in the protection of consumer health. Toxicologic studies have helped in the estimation of the azaspiracid NOEL and in the awareness of possible pathologic consequences of azaspiracid intoxication that causes injuries with very slow recovery compared to other marine toxins and may be potentially tumorigenic. In vitro studies have focussed on the elucidation of azaspiracid toxicity mechanism and the identification of its molecular target, which is still unknown.

## References

- Alfonso, A., Roman, Y., Vieytes, M.R., Ofuji, K., Satake, M., Yasumoto, T., and Botana, L.M. 2005. Azaspiracid-4 inhibits Ca<sup>2+</sup> entry by stored operated channels in human T lymphocytes. *Biochem Pharmacol* 69, 1627–1636.
- Colman, J.R., Dechraoui, M.Y., Dickey, R.W., and Ramsdell, J.S. 2004. Characterization of the developmental toxicity of Caribbean ciguatoxins in finfish embryos. *Toxicon* 44, 59–66.
- Colman, J.R., Twiner, M.J., Hess, P., McMahon, T., Satake, M., Yasumoto, T., Doucette, G.J., and Ramsdell, J.S. 2005. Teratogenic effects of azaspiracid-1 identified by microinjection of Japanese medaka (*Oryzias latipes*) embryos. *Toxicon* 45, 881–890.
- EU. 2002. Commission decision 2002/225/EC of 15 March 2002 laying down detailed rules for the implementation of council directive 91/492/EEC as regards the maximum levels and the methods of analysis of certain marine biotoxins in bivalve molluscs, echinoderms, tunicates and marine gastropods. *OJ L75*, 62–64.
- EU/SANCO. 2001. Report of the meeting of the working group on toxicology of DSP and AZP 21 to 23rd May 2001, Brussels.
- FAO. 2004. Food and nutrition paper on marine biotoxins.
- Fujiki, H., Suganuma, M., Komori, A., Yatsunami, J., Okabe, S., Ohta, T., and Sueoka, E. 1994. A new tumor promotion pathway and its inhibitors. *Cancer Detect Prev* 18, 1–7.
- Fujiki, H., Suganuma, M., Nishiwaki, S., Yoshizawa, S., Winyar, B., Sugimura, T., and Schmitz, F. J. 1990. A new pathway of tumor promotion by the okadaic acid class compounds. *Adv Second Messenger Phosphoprotein Res* 24, 340–344.
- Furey, A., Moroney, C., Brana-Magdalena, A., Saez, M.J., Lehane, M., and James, K.J. 2003. Geographical, temporal, and species variation of the polyether toxins, azaspiracids, in shellfish. *Environ Sci Technol* 37, 3078–3084.
- Hess, P., Nguyen, L., Aasen, J., Keogh, M., Kilcoyne, J., McCarron, P., and Aune, T. 2005. Tissue distribution, effects of cooking and parameters affecting the extraction of azaspiracids from mussels, *Mytilus edulis*, prior to analysis by liquid chromatography coupled to mass spectrometry. *Toxicon* 46, 62–71.
- Ito, E., Satake, M., Ofuji, K., Higashi, M., Harigaya, K., McMahon, T., and Yasumoto, T. 2002. Chronic effects in mice caused by oral administration of sublethal doses of azaspiracid, a new marine toxin isolated from mussels. *Toxicon* 40, 193–203.
- Ito, E., Satake, M., Ofuji, K., Kurita, N., McMahon, T., James, K., and Yasumoto, T. 2000. Multiple organ damage caused by a new toxin azaspiracid, isolated from mussels produced in Ireland. *Toxicon* 38, 917–930.
- Ito, E., Terao, K., McMahon, T., Silke, J., and Yasumoto, T. 1998. Acute pathological changes in mice caused by crude extracts of novel toxins isolated from Irish mussels. Ed. Reguera, B., Blanco, J., Fernandez, M.L., and Wyatt, T. Santiago de Compostela, Spain: IOC of UNESCO and Xunta de Galicia, 588–589.
- James, K.J., Fidalgo Saez, M.J., Furey, A., and Lehane, M. 2004. Azaspiracid poisoning, the food-borne illness associated with shellfish consumption. *Food Addit Contam* 21, 879–892.
- James, K.J., Furey, A., Lehane, M., Ramstad, H., Aune, T., Hovgaard, P., Morris, S., Higman, W., Satake, M., and Yasumoto, T. 2002a. First evidence of an extensive northern European distribution of azaspiracid poisoning (AZP) toxins in shellfish. *Toxicon* 40, 909–915.
- James, K.J., Furey, A., Satake, M., and Yasumoto, T. 2000. Azaspiracid Poisoning (AZP): A new shellfish toxic syndrome in Europe. Abstract for the 9th International Conference on Algal Blooms, Tasmania, Australia.
- James, K.J., Lehane, M., Moroney, C., Fernandez-Puente, P., Satake, M., Yasumoto, T., and Furey, A. 2002b. Azaspiracid shellfish poisoning: unusual toxin dynamics in shellfish and the increased risk of acute human intoxications. *Food Addit Contam* 19, 555–561.
- James, K.J., Moroney, C., Roden, C., Satake, M., Yasumoto, T., Lehane, M., and Furey, A. 2003a. Ubiquitous “benign” alga emerges as the cause of shellfish contamination responsible for the human toxic syndrome, azaspiracid poisoning. *Toxicon* 41, 145–151.

- James, K.J., Sierra, M.D., Lehane, M., Brana Magdalena, A., and Furey, A. 2003b. Detection of five new hydroxyl analogues of azaspiracids in shellfish using multiple tandem mass spectrometry. *Toxicon* 41, 277–283.
- Jeong, H.J., and Latz, M.I. 1994. Growth and grazing rates of the heterotrophic dinoflagellate, *Protoperidinium*, on red tide dinoflagellates. *Mar Ecol Prog Ser* 106, 173–185.
- Kimm-Brinson, K.L., and Ramsdell, J.S. 2001. The red tide toxin, brevetoxin, induces embryo toxicity and developmental abnormalities. *Environ Health Perspect* 109, 377–381.
- Latz, M.I., and Jeong, H.J. 1996. Effect of red tide dinoflagellate diet and cannibalism on the bioluminescence of the heterotrophic dinoflagellates *Protoperidinium* spp. *Mar Ecol Prog Ser* 132, 275–285.
- Magdalena, A.B., Lehane, M., Kryst, S., Fernandez, M.L., Furey, A., and James, K.J. 2003a. The first identification of azaspiracids in shellfish from France and Spain. *Toxicon* 42, 105–108.
- Magdalena, A.B., Lehane, M., Moroney, C., Furey, A., and James, K.J. 2003b. Food safety implications of the distribution of azaspiracids in the tissue compartments of scallops (*Pecten maximus*). *Food Addit Contam* 20, 154–160.
- McMahon, T., and Silke, J. 1996. Winter toxicity of unknown aetiology in mussels. *Harmful Algae News* 14, 2.
- . 1998. Re-occurrence of winter toxicity. *Harmful Algae News* 17, 12–16.
- Nicolaou, K.C., Chen, D.Y., Li, Y., Qian, W., Ling, T., Vyskocil, S., Koftis, T.V., Govindasamy, M., and Uesaka, N. 2003a. Total synthesis of the proposed azaspiracid-1 structure, part 2: coupling of the C1–C20, C21–C27, and C28–C40 fragments and completion of the synthesis. *Angew Chem Int Ed Engl* 42, 3649–3653.
- Nicolaou, K.C., Li, Y., Uesaka, N., Koftis, T.V., Vyskocil, S., Ling, T., Govindasamy, M., Qian, W., Bernal, F., and Chen, D.Y. 2003b. Total synthesis of the proposed azaspiracid-1 structure, part 1: construction of the enantiomerically pure C1–C20, C21–C27, and C28–C40 fragments. *Angew Chem Int Ed Engl* 42, 3643–3648.
- Ofuji, K., Satake, M., McMahon, T., James, K.J., Naoki, H., Oshima, Y., and Yasumoto, T. 2001. Structures of azaspiracid analogs, azaspiracid-4 and azaspiracid-5, causative toxins of azaspiracid poisoning in Europe. *Biosci Biotechnol Biochem* 65, 740–742.
- Ofuji, K., Satake, M., McMahon, T., Silke, J., James, K. J., Naoki, H., Oshima, Y., and Yasumoto, T. 1999a. Two analogs of azaspiracid isolated from mussels, *Mytilus edulis*, involved in human intoxication in Ireland. *Nat Toxins* 7, 99–102.
- Ofuji, K., Satake, M., Oshima, Y., McMahon, T., James, K. J., and Yasumoto, T. 1999b. A sensitive and specific determination method for azaspiracids by liquid chromatography mass spectrometry. *Nat Toxins* 7, 247–250.
- RASFF. 2005. Rapid Alert System for Food and Feed. Week 47, 2005.
- Roman, Y., Alfonso, A., Louzao, M. C., de la Rosa, L.A., Leira, F., Vieites, J.M., Vieytes, M.R., Ofuji, K., Satake, M., Yasumoto, T., and Botana, L.M. 2002. Azaspiracid-1, a potent, nonapoptotic new phycotoxin with several cell targets. *Cell Signal* 14, 703–716.
- Roman, Y., Alfonso, A., Vieytes, M.R., Ofuji, K., Satake, M., Yasumoto, T., and Botana, L.M. 2004. Effects of Azaspiracids 2 and 3 on intracellular cAMP, [Ca<sup>2+</sup>], and pH. *Chem Res Toxicol* 17, 1338–1349.
- Satake, M., Ofuji, K., Naoki, H., James, K., Furey, A., McMahon, T., Silke, J., and Yasumoto, T. 1998a. Azaspiracid, a New Marine Toxin Having Unique Spiro Ring Assemblies, Isolated from Irish Mussels, *Mytilus edulis*. *J Am Chem Soc* 120, 1200–1201.
- Satake, M., Ofuji, K., James, K., Furey, A. and Yasumoto, T. 1998b. New toxic event caused by Irish mussels. Ed. Reguera, B., Blanco, J., Fernandez, M., and Wyatt, T. Xunta de Galicia and IOC of UNESCO, 468–469.
- Twiner, M.J., Hess, P., Dechraoui, M.Y., McMahon, T., Samons, M.S., Satake, M., Yasumoto, T., Ramsdell, J.S., and Doucette, G.J. 2005. Cytotoxic and cytoskeletal effects of azaspiracid-1 on mammalian cell lines. *Toxicon* 45, 891–900.
- Vilariño, N., Nicolaou, K.C., Frederick, M.O., Cagide, E., Ares, I.R., Louzao, M.C., Vieytes, M.R., and Botana, L.M. 2006. Cell growth inhibition and actin cytoskeleton disorganisation induced by azaspiracid-A. Structure-activities studies. *Chem. Res. Toxicol* 19, 1459–1466.
- Volmer, D.A., Brombacher, S., and Whitehead, B. 2002. Studies on azaspiracid biotoxins. I. Ultrafast high-resolution liquid chromatography/mass spectrometry separations using monolithic columns. *Rapid Commun Mass Spectrom* 16, 2298–2305.

## 18 Cyclic Imines: An Insight into this Emerging Group of Bioactive Marine Toxins

Jordi Molgó, Emmanuelle Girard, and Evelyne Benoit

### Introduction

Poisoning by toxins of marine origin is a substantial worldwide hazard that may occur by the ingestion of contaminated finfish and shellfish, and through water or aerosol exposure (Molgó et al. 1999; Van Dolah 2000; Whittle and Gallaher 2000). The main source of these toxins is confirmed or believed to be marine micro-organisms, including phytoplankton species of unicellular algae. Under a favorable environment, these unicellular algae proliferate during certain periods of the year or in certain geographical areas, and produce these non-proteinaceous compounds. The genetic and environmental factors that favour the occurrence of toxic phytoplankton species and production of toxins are yet to be fully understood. Several environmental and climatic factors have been implicated in explaining the apparent increase in harmful algal blooms worldwide (Garthwaite 2000; Cembella 2003). Shellfish constitute a worldwide rich food resource that may be contaminated by toxins produced by harmful microalgae upon which filter-feeding bivalve molluscs (such as clams, mussels, oysters, or scallops) feed. Shellfish can concentrate these phycotoxins in their edible tissues and act as vectors for transferring these toxic chemical compounds to fish, crabs, birds and humans. The increased frequency and wide distribution of toxic algal blooms has become a major environmental and economic problem that menaces wildlife and human health.

This brief chapter is intended to review an emerging group of novel marine toxins, the cyclic imines, all of which share a functional imine group as a part of a cyclic ring system within their molecular framework, and to detail, when available, their pharmacological activity and toxicity. As the result of their significant and specific biological effects, some of the cyclic imines are often useful as drugs or biological probes for physiological studies.

### Gymnodimines: Nicotinic Acetylcholine Receptor Ligands

In 1994 along the east coast of the South Island of New Zealand, dredge oysters (*Tiostrea chilensis*) displayed neurotoxic shellfish poisoning (NSP) features in a mouse bioassay for detecting lipid-soluble marine biotoxins. The unusual NSP-type of toxicity was related to a new marine toxin, named gymnodimine, of unprecedented structure isolated from both New Zealand oysters and a gymnodinoid dinoflagellates, within the *Gymnodinium mikimotoi/nagasakiense* species complex, collected during this outbreak (Seki et al. 1995, 1996; MacKenzie et al. 1995). The toxicity was also noted in many other species of shellfish widespread around the New Zealand coastline including greenshell mussel (*Perna canaliculus*), blue mussel (*Mytilus galloprovincialis*), scallops (*Pecten novaezelandiae*), Pacific oyster (*Crassostrea gigas*), cockle (littleneck clam, *Austrovenus stutchburyi*, and a surfclam, *Paphies subthangulata*), and New Zealand abalone (*Haliotis iris*) (MacKenzie et al. 1996; Stirling 2001). Gymnodimine has been reported to persist in oysters for several years after the initial contamination events indicating that it is not readily depurated, and for months in

other shellfish like *P. canaliculus*, where it concentrates in tissues outside the digestive gland (MacKenzie et al. 2002). Although published reports on the presence of gymnodimine in shellfish were initially restricted to New Zealand, subsequent studies revealed its presence in clams harvested in Tunisia (Biré et al. 2002; Biré 2004), and it has been unequivocally detected in shellfish from European and North American coasts.

Gymnodimine is produced by the planktonic dinoflagellate *Karenia selliformis* (formerly named *Gymnodinium selliforme*), a new species from the genus *Karenia* (*Dinophyceae*) (Haywood et al. 2004). Distinguishing morphological characters for the genus *Karenia* include a smooth theca and a linear apical groove. Molecular analyses of rDNA sequence alignments revealed that the new species is phylogenetically distinct, but closely related to *K. mikimotoi* and *K. brevis*.

The chemical structure of gymnodimine was initially elucidated by NMR spectroscopy (Seki et al. 1995) and later confirmed by X-ray crystallographic analysis of its *p*-bromobenzamide derivative, which revealed its absolute stereochemistry (Stewart et al. 1997). As shown in Fig. 18.1, gymnodimine and analogues exhibit unusual structural features, including a spirocyclic imine ring system and a trisubstituted tetrahydrofuran embedded within a 16-membered macrocycle. The presence of the spirocyclic imine places this marine toxin in the same family with the spirolides, pinna-toxins, pteriatoxins, and prorocentrolides (see below). Two new analogues, gymnodimine B and gymnodimine C (Fig. 18.1), have been isolated from extracts of cell cultures of the dinoflagellate *K. selliformis* (Miles et al. 2000, 2003). Gymnodimine B is similar in structure to gymnodimine, but contains an exocyclic methylene at C17 and an allylic hydroxyl group at C18, while gymnodimine C is oxidized analogue of gymnodimine and was found to be isomeric with gymnodimine B at C18.

Several studies have been carried out for the synthesis of gymnodimine-components (Ahn et al. 2001; White et al. 2003; Johannes et al. 2005; Kong et al. 2005), but the total synthesis has yet to be achieved. The synthesis and production of intermediate components of gymnodimine appears essential for providing immunogens that will help its toxic monitoring in shellfish by methods other than the mouse bioassay.

Gymnodimine elicits highly toxic effects when administered either by intraperitoneal (Biré et al. 2002; Munday et al. 2004), subcutaneous or intracerebroventricular injection to mice (Kharrat et al. 2006). Symptoms after intraperitoneal injection included hyperactivity, jumping, curled tail, paralysis of the hind legs, severe dyspnea, followed by rapid death within 6–15 minute of injection. The mean LD<sub>50</sub> after intraperitoneal of highly purified gymnodimine was found to be 96 µg kg<sup>-1</sup> (Munday et al.

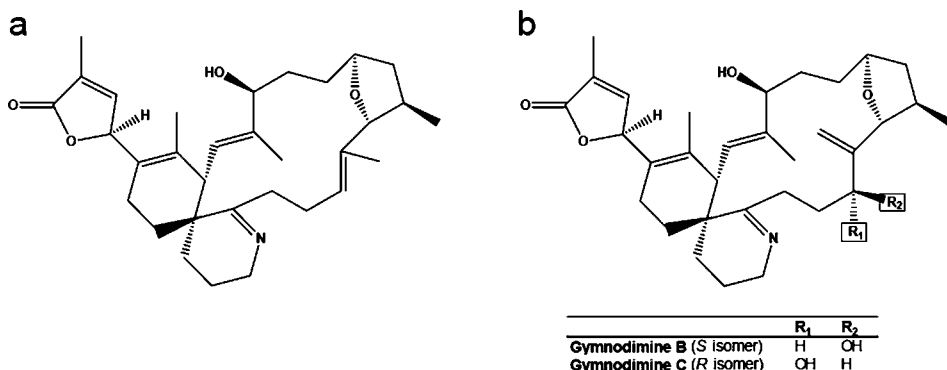


**Figure 18.1.** Chemical structures of gymnodimine (a) and gymnodimine B and C (b).

2004) and  $80 \text{ mg kg}^{-1}$ , while after intracerebroventricular injection it was  $3 \text{ mg kg}^{-1}$  (Kharrat et al. 2006). Thus, gymnodimine appears to be about 30 times more potent when administered by intracerebroventricular than by intraperitoneal injection indicating that it acts on the central nervous system (Kharrat et al. 2006). Interestingly, gymnodimine was less toxic when administered orally by gavage to mice (Munday et al. 2004).

Some of the symptoms observed after the intraperitoneal injection of gymnodimine resemble those produced by tubocurarine, a competitive inhibitor of nicotinic acetylcholine receptors in skeletal muscles. Interestingly, pre-treatment of mice with acetylcholinesterase inhibitors (neostigmine or physostigmine) was found to protect against gymnodimine toxicity (Munday et al. 2004). This can be explained by the fact that acetylcholinesterase inhibitors increase the concentration of acetylcholine in the synaptic cleft and displace the competitive binding of tubocurarine to nicotinic acetylcholine receptors (Nguyen et al. 2005). Therefore, it was hypothesized by Munday et al. (2004) that gymnodimine exerts its toxic effects via blockade of nicotinic acetylcholine receptors at the neuromuscular junction.

Direct evidence that gymnodimine produced a concentration- and time-dependent blockade of twitch responses evoked by nerve stimulation, without affecting directly evoked twitches, has been obtained in amphibian and mammalian isolated neuromuscular preparations (Kharrat et al. 2006). In addition, the neuromuscular blockade produced by gymnodimine was completely reversed by 4-aminopyridine and 3,4-diaminopyridine, well-known potassium channel blockers (Molgó et al. 1977, 1980) that enhance acetylcholine release from motor nerve terminals. Furthermore, the phyco toxin was found to block the current responses evoked by constant and brief iontophoretical acetylcholine pulses applied to the surface of skeletal muscle cells. These data support the view that gymnodimine blocks muscle nicotinic acetylcholine receptors of the neuromuscular junction. However, these data cannot explain the high toxicity of gymnodimine when applied directly to the central nervous system by intracerebroventricular injection. Competition-binding assays revealed that gymnodimine is a powerful ligand interacting with subnanomolar affinities not only with muscular, but also homopentameric and heteropentameric neuronal nicotinic acetylcholine receptors of various animal species (Kharrat et al. 2006). Therefore, it can be concluded that gymnodimine broadly targets nicotinic acetylcholine receptors. Further appropriate toxicological studies must be developed in order to assess the risk of gymnodimine to human health.

### **Spirolides: Muscarinic and/or Nicotinic Acetylcholine Receptor Ligands?**

Novel seafood toxins were discovered in 1991, during routine toxin monitoring of bivalve mollusks at aquaculture sites along the eastern shore of Nova Scotia, in Canada. These toxins, called spirolides, are macrocyclic compounds that exist in various toxic groups. Spirolides B and D were first isolated from the digestive glands of mussels (*Mytilus edulis*) and scallops (*Pacopecten magellanicus*) harvested from aquaculture sites (Hu et al. 1995; Cembella et al. 2000). Further investigations afforded spirolides A, C, 13-desmethyl-C (Hu et al. 2001) and the biologically inactive spirolides E and F (Hu et al. 1996a). Spirolides A-D contain an unusual 5,5,6-bis-spirocetal moiety together with a 6,7-spirocyclic imine (Fig. 18.2). Spirolides E and F are keto amine hydrolysis derivatives resulting from the ring opening of the cyclic imine. The spirolide group of toxins has grown over the years to include several isomers and compounds with slightly modified structures like spirolide 13,19-didesmethyl-C, spirolide G and spirolide 20,methyl-G (Fig. 18.2; Aasen et al. 2005). The relative and absolute stereochemistry of these molecules has not been established to date, but a tentative assignment based on NMR studies has been reported (Falk et al. 2001). Synthesis of



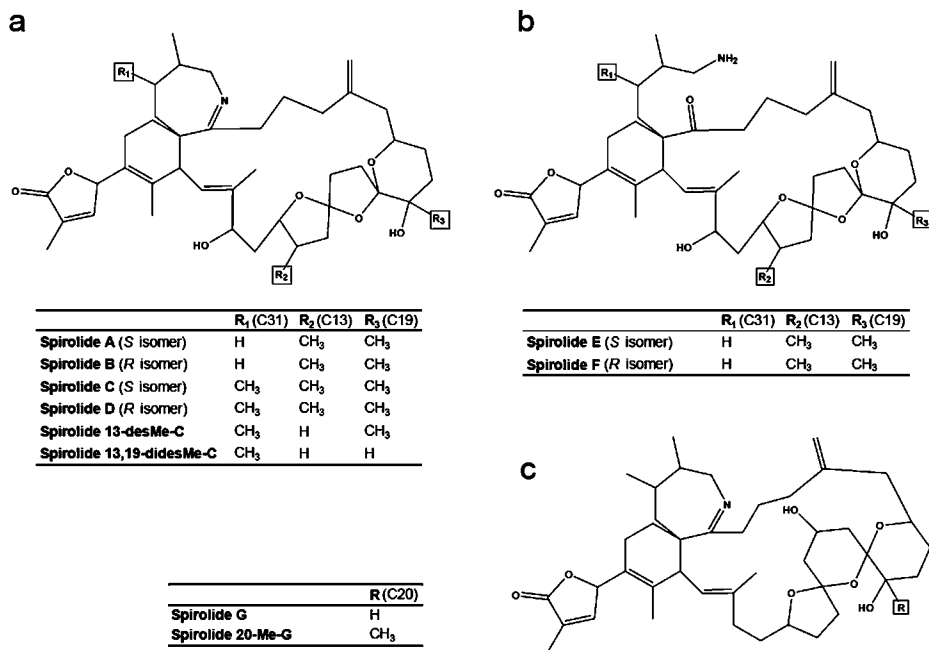


**Figure 18.2.** Chemical structures of spirolides.

the spirocentres of spirolides B and D has been reported (Brimble and Furkert 2004). All spirolide compounds display “fast-acting” toxicity in the traditional mouse bioassay used for monitoring shellfish, and this is related to the presence of a cyclic imine function in all these compounds. Those spirolides containing a vicinal dimethyl group in the seven-membered ring are resistant to oxalic acid hydrolysis, whereas those that do not are readily hydrolyzed. These observations suggest that the extra methyl group on the seven-membered imine ring blocks the process of imine hydrolysis, perhaps by stereochemical interference.

The causative micro-organism producing spirolide toxins has been unequivocally identified as the dinoflagellate *Alexandrium ostenfeldii* (Cembella et al. 1998, 1999, 2000, 2001) a species that is widely distributed (Balech and Tangen 1985; Moestrup and Hansen 1988; McKenzie et al. 1996; Aasen et al. 2005). *A. ostenfeldii* can form temporary cysts, which may function to resist unfavorable short-term environmental conditions, but available for germination and bloom initiations (McKenzie et al. 1996; Toth et al. 2004). Important differences in spirolides content and profiles have been reported for dinoflagellate strains from different coastal regions (Cembella et al. 2000). Spirolide production by toxic strains of the dinoflagellate *A. ostenfeldii* has been suggested to be governed by light-dependent events during the cell division cycle (John et al. 2000).

The identification of the toxic dinoflagellate *A. ostenfeldii* is currently done by microscopic examination (Fig. 18.3), which requires a broad taxonomic knowledge, expensive equipment (electron scanning microscope), and is very time consuming. The co-occurrence of the toxic dinoflagellate *Alexandrium tamarense*, a known producer of potent neurotoxins associated with paralytic shellfish poisoning, and *A. ostenfeldii* in Scottish coastal waters has been reported (John et al. 2003). In mixed phytoplankton assemblages, these two *Alexandrium* species are difficult to discriminate accurately



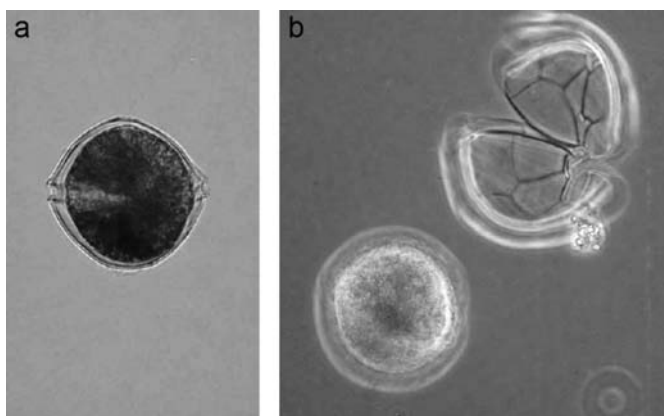


**Figure 18.3.** *Alexandrium ostenfeldii* dinoflagellate obtained from a phytoplankton sample collected in France (bouchot de Loire, May 28, 2004) by Elisabeth Nezan (Ifremer, Nantes). Whole cell (a), and after dissection (b).

by conventional light microscopy. New techniques are being used with species-specific rRNA probes based upon 18S and 28S ribosomal DNA sequences for *A. ostenfeldii* and tested by dot-blot and fluorescence *in situ* hybridization (FISH) techniques (John et al. 2003). Recently, to facilitate *A. ostenfeldii* identification, an inexpensive and easy-to-handle DNA-biosensor has been developed and detailed (Metfies et al. 2005).

Spirolides induce a fast lethal toxic effect when administered by intraperitoneal injection to both mice and rats, and are less toxic by oral administration. Mice administered with lethal doses of desmethyl spirolide C became lethargic, with decreased movements and exploratory behavior, exhibited piloerection, and displayed uncoordinated movements and jerky locomotion progressing from generalized tremors to rapid violent flexion with extension of the hind limbs in splayed fashion. Moderate exophthalmia, with lachrymaton were also evident. Abdominal breathing was characteristic, indicating respiratory distress, followed by mouth breathing and tremors that involved the whole body resembling a seizure, just before the respiratory arrest (Richard et al. 2001; Gill et al. 2003). Usually, mice receiving lethal doses of spirolide died between 3 and 20 minutes after intraperitoneal injection. The time to death was reported to be accelerated when atropine and other acetylcholine muscarinic receptor antagonists were used (Richard et al. 2001; Gill et al. 2003). Neither macroscopic nor histological changes have been detected in the retina, skeletal muscle, peripheral nerves, heart, liver, kidney, spleen, lungs, adrenals, or gastrointestinal tract of mice receiving lethal doses of desmethyl spirolide C (Pulido et al. 2001; Gill et al. 2003). Interestingly, no histological changes were observed in the brains of rats that received spirolides. However, widespread neuronal damage was seen in mouse brains, particularly in the brain stem and hippocampus and a clear relationship was observed between the dose and the severity of the lesions (Pulido et al. 2001; Gill et al. 2003). Early injury markers such as c-jun and HSP-72 both showed a twofold increase in spirolide-treated animals when compared to controls (Gill et al. 2003). Furthermore, transcriptional analysis revealed that muscarinic receptor subtypes (mAChR1, mAChR4 and mAChR5) and nicotinic receptors (nAChR $\alpha$  2 and nAChR $\beta$  4) showed an upregulation of gene expression (Gill et al. 2003). This suggested that the muscarinic and nicotinic receptors may be the targets for spirolides. In contrast, the glutamate receptors (KA2 and NMDAR1), which are known to be involved in excitotoxicity (Gill and

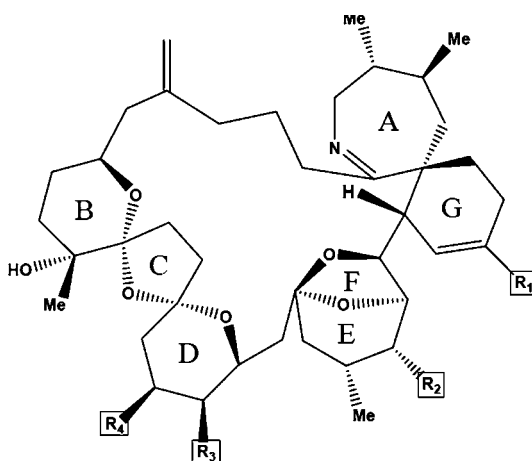
Pulido 2001), appeared not to be involved since there were no transcriptional differences between controls and spirolide-treated animals (Gill et al. 2003). It is clear that further studies are needed to define the molecular targets for this growing number of phycotoxins.

### Pinnatoxins and Pteriatoxins: Ca<sup>2+</sup> Channel Activators?

Shellfish of the genus *Pinna* live mainly in shallow waters of the temperate and tropical zones of the Indian and Pacific Oceans (Rosewater 1961). The adductor muscle of this bivalve is eaten in Japan and China, and this particularly tasty morsel has been the culprit of a frequently occurring sea-food poisoning, characterized mainly by gastrointestinal disorders (Zheng et al. 1990). Indeed, several outbreaks of poisoning were reported in Japan between 1975 and 1991 after the consumption of *P. pectinata* (Chou et al. 1996b), and toxicity from *P. attenuata* was recorded in China in 1980 and 1989 (Uemura et al. 1995). Although toxic compounds referred to as pinnatoxins, pinnaic acids and pinnamine were isolated from *Pinna* sp., solid evidence for human intoxication by these compounds (i.e., the association between toxicity of shellfish and the presence of toxins) therein has not, however, been established. In addition, the fact that extracts from the digestive glands of several *Pinna* sp. (including *P. muricata*, *P. attenuata* and *P. atropupurea*) produced the same symptoms of poisoning in mice, strongly suggests that *Pinna* shellfish obtain their toxins from feeding on toxic organisms such as dinoflagellates (for a review, see Kuramoto et al. 2004).

Four pinnatoxins (A-D) have been isolated and purified from the Okinawan bivalve *Pinna muricata*, and their structures solved by NMR experiments and positive ion ESI MS/MS spectra (Uemura et al. 1995; Chou et al. 1996a, 1996b; Takada et al. 2001a). More recently, three pteriatoxins (A-C) have been isolated and characterized from another Okinawan bivalve, *Pteria penguin*, (Takada et al. 2001b). Structurally, pinnatoxins and pteriatoxins consist of a 27-membered carbocyclic backbone composed of a [6,7]-spiro-linked imine moiety (AG ring), a [5,6]-bicycloketal (EF ring) and a [6,5,6]-dispiroketal (BCD ring), and represent variations in the substitution pattern at C21, C22, C28, and C33 (Fig. 18.4). It is worth noting a homologous 6,7-spirocyclic imine ring system is also present in the related macrocyclic toxins, the spirolides A-D (see above). This unusual backbone poses a significant challenge for synthesis of pinnatoxins and pteriatoxins. Indeed, since the pioneering total synthesis of pinnatoxin A achieved by McCauley et al. in 1998, a number of insightful studies directed toward a new approach to the total synthesis of pinnatoxins and pteriatoxins have been undergone, leading to an efficient, highly stereoselective synthesis of the molecules (Suthers et al. 1998; Nagasawa 2000; Ishihara et al. 2002; Nakamura et al. 2002; Sakamoto et al. 2004; Pelc and Zakarian 2005).

Although an early study has reported that a toxic extract from *Pinna attenuata*, referred to as pinnatoxin, is a Ca<sup>2+</sup> channel activator (Zheng et al. 1990), there is, at present, no information on the mechanism(s) of action of pinnatoxins and pteriatoxins and on the specific molecular sites targeted by these marine iminium alkaloids (but see Kita and Uemura 2005). In contrast, the acute toxicity of intraperitoneal administration of pinnatoxins and pteriatoxins to mice has been systematically addressed, although the symptoms of intoxication were not reported. The data, summarised in Table 18.1, show that natural (+)-pinnatoxin A exhibited potent acute toxicity against mice whereas synthetic (-)-pinnatoxin A had no toxicity at a dose of 5,000 µg/kg (Uemura et al. 1995; McCauley et al. 1998; Kuramoto et al. 2004). Similarly, pteriatoxin A exhibits significant acute toxicity against mice (Takada et al. 2001b). Moreover, these data permit some comment on structure-activity relationships among pinnatoxins A-C, on one hand, and pteriatoxins A-C, on the other hand, since these



	R <sub>1</sub> (C33)	R <sub>2</sub> (C28)	R <sub>3</sub> (C22)	R <sub>4</sub> (C21)
<b>Pinnatoxin A</b>	COO <sup>-</sup>	OH	OH	H
<b>Pinnatoxin B</b> (C34 <i>S</i> isomer)	CH(NH <sub>3</sub> <sup>+</sup> )-COO <sup>-</sup>	OH	OH	H
<b>Pinnatoxin C</b> (C34 <i>R</i> isomer)	CH(NH <sub>3</sub> <sup>+</sup> )-COO <sup>-</sup>	OH	OH	H
<b>Pinnatoxin D</b>	CO-CH <sub>2</sub> -CH <sub>2</sub> -COO <sup>-</sup>	H	H	CH <sub>3</sub>
<b>Pteriatoxin A</b>	CH(OH)-CH <sub>2</sub> -S-CH <sub>2</sub> -CH(NH <sub>3</sub> <sup>+</sup> )-COO <sup>-</sup>	OH	OH	H
<b>Pteriatoxin B</b> ( <i>S</i> isomer)	CH(CH <sub>2</sub> OH)-S-CH <sub>2</sub> -CH(NH <sub>3</sub> <sup>+</sup> )-COO <sup>-</sup>	OH	OH	H
<b>Pteriatoxin C</b> ( <i>R</i> isomer)	CH(CH <sub>2</sub> OH)-S-CH <sub>2</sub> -CH(NH <sub>3</sub> <sup>+</sup> )-COO <sup>-</sup>	OH	OH	H

**Figure 18.4.** Chemical structures of pinnatoxins and pteriatoxins.

**Table 18.1.** Acute toxicity of pinnatoxins and pteriatoxins by intraperitoneal administration to mice

	LD <sub>99</sub> (μg/kg) <sup>1</sup>	References	LD <sub>50</sub> (μg/MU) <sup>1</sup>	References
(+)-Pinnatoxin A	180	Uemura et al. 1995		
(-)-Pinnatoxin A	135	McCauley et al. 1998	2.70	Kuramoto et al. 2004
(-)-Pinnatoxin A	>5,000	McCauley et al. 1998		
Pinnatoxins B and C <sup>2</sup>	22	Takada et al. 2001a	0.99	Kuramoto et al. 2004
Pinnatoxin D	400	Chou et al. 1996a	>10.00	Kuramoto et al. 2004
Pteriatoxin A	100	Takada et al. 2001b		
Pteriatoxins B and C <sup>2</sup>	8	Takada et al. 2001b		

<sup>1</sup>LD<sub>99</sub> (μg/kg body weight) and LD<sub>50</sub> (μg/mouse unit) are doses of toxins that produced lethality of 99% and 50% of animals, respectively. <sup>2</sup>1:1 mixture of toxins B and C (stereoisomers)

molecules differ only in the nature of the substitute at position C33 (see Fig. 18.4). Hence, a 1:1 mixture of pinnatoxins B and C, which are stereoisomers and have a glycine residue at C33, was between 3 to 8 times more toxic to mice than (+)-pinnatoxin A, which has a carboxyl group at this site (Takada et al. 2001a; Kuramoto et al. 2004). The situation with pteriatoxins is even more remarkable. These compounds are derivatives of 3-(2-hydroxyethylthio)-2-aminopropanoic acid [i.e., HOCH<sub>2</sub>CH<sub>2</sub>SCH<sub>2</sub>CH(NH<sub>2</sub>)COOH], in which the macrocycle is attached at positions 2 and 1 of the

hydroxyethylthio moiety for pteriatoxin A and pteriatoxins B-C, respectively. As a consequence, a 1:1 mixture of pteriatoxins B and C was 12.5 times more toxic to mice than pteriatoxin A (Takada et al. 2001b). It is worth noting that the potency of pinnatoxins B-C and pteriatoxins B-C is comparable to that of tetrodotoxin, well-known to be responsible for pufferfish toxicity. Finally, the acute toxicity of pinnatoxin D to mice was weaker than that of the other pinnatoxins and pteriatoxins, although it showed the strongest cytotoxicity against the murine leukaemia cell line P388 (Chou et al. 1996a; Kuramoto et al. 2004).

## Pinnaic Acids and Halichlorine: Anti-inflammatory Agents

In 1996, Uemura's research group reported the isolation and purification of three novel spirocyclic marine alkaloids: pinnaic acid and tauropinnaic acid from the viscera of the Okinawan bivalve *Pinna muricata* (Tong et al. 1996), and halichlorine from the Japanese black marine sponge *Halichondria okadai* Kadota (Kuramoto et al. 1996). The gross structure of halichlorine was determined by using MS, IR, and NMR methods (Kuramoto et al. 1996), and its absolute configuration was elucidated by synthesis of an oxidative degradation product (Arimoto et al. 1998). It consists of a sterically hindered 15-membered lactone, an azabicyclo [4.4.0] ring and a [5.6]-spiro ring moiety (Fig. 18.5A). The structures of pinnaic acids, although incompletely established with NMR methods (Tong et al. 1996), reveals that both products are closely related to halichlorine since they share in common a characteristic and highly functionalized 6-azaspiro[4.5]decane ring system (Fig. 18.5B). It is thus likely that these marine natural compounds are produced by symbiotic micro-organisms.

The molecular complexities of these architecturally novel alkaloids have prompted intense studies to elaborate new and efficient methods and strategies for the synthesis of these products. Hence, several stereocontrol approaches have been developed to successfully construct the azaspirocyclic core of pinnaic acids and halichlorine, providing access to the formal total synthesis and highly stereoselectivity of these molecules (Christie et al. 2004; Zhang et al. 2005; Andrade and Martin 2005; Clive et al. 2005; and references cited therein). In particular, Danishefsky's research group has reported the first total synthesis of halichlorine (Trauner et al. 1999), supporting the previous conclusions regarding the structure of this alkaloid (Kuramoto et al. 1996; Arimoto et al. 1998), and has

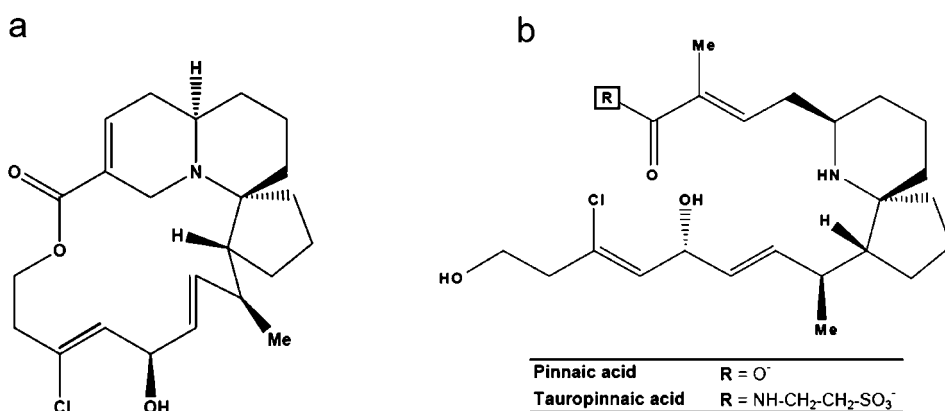


**Figure 18.5.** Chemical structures of halichlorine (a) and pinnaic acids (b).

achieved the total synthesis of pinnaic acids (Carson et al. 2001), leading to revision of the structures originally proposed (Tong et al. 1996) and unambiguously establishing the relative and absolute configurations of the molecules at C14 and C17, respectively.

Pinnaic acids and halichlorine are considered as potential drugs for the treatment of some inflammatory diseases, although they exhibit different biological activities (for a review, see Kuramoto et al. 2004). On one hand, both pinnaic acid and tauropinnaic acid have been reported to inhibit in vitro the activity of cytosolic 85-kDa phospholipase A2 (cPLA2), a phospholipase that preferentially cleaves arachidonic acid-containing phospholipids (Kramer and Sharp 1997), the former being about two times less potent than the latter (Tong et al. 1996). On the other hand, halichlorine was shown to selectively inhibit the expression of the vascular cell adhesion molecule 1 (VCAM-1), a cytokine-induced endothelial protein that binds to lymphocytes (Osborn et al. 1989), in cultured human endothelial cells (Kuramoto et al. 1996; Trauner et al. 1999). Interestingly and unexpectedly, some of the bicyclic and tricyclic compounds with the azaspiro core structure, prepared from a key intermediate used in synthetic studies on halichlorine, have been found to exhibit cytotoxic activity towards a cultured human monocytic leukaemia cell line, involving apoptotic phenomena such as induction of chromatin condensation and caspase activation (Itoh et al. 2002).

### Pinnamine: Nicotinic Acetylcholine Receptor Ligand

A seventh novel alkaloidal toxin, pinnamine, was isolated and purified from the viscera of the Okinawan bivalve *Pinna muricata* (Takada et al. 2000). Its gross structure, clarified by a detailed analysis of NMR and CD spectra, includes a 9-azabicyclo[4.2.1]nonane pharmacophoric element (Fig. 18.6A). Further synthetic studies have not only confirmed the absolute stereochemistry of the molecule, but have also allowed stereocontrolled access to a non-natural congener, 5-epi-pinnamine, of the natural product (Kigoshi et al. 2001; Hjelmggaard et al. 2005).

Pinnamine has been shown to exhibit significant acute toxicity against mice, producing characteristic excitability symptoms, such as scurrying around, before death of animals (Takada et al. 2000). Interestingly, these toxic symptoms, as well as the structure of pinnamine, resemble those of the agonists of nicotinic acetylcholine receptors (nAChR) discovered from natural sources and including anatoxin-a (Fig. 18.6B; Hjelmggaard et al. 2005), a freshwater cyanobacterial (blue-green algal) alkaloidal toxin (for a recent review, see Daly 2005). Indeed, replacement of the 9-azabicyclo[4.2.1]nonane element of pinnamine by the 8-azabicyclo[3.2.1]octane moiety of ferruginine, an alkaloidal toxin from arboreal *Darlingia* species, resulted in distinctly lower nAChR [ $(\alpha 4)_2(\beta 2)_3$  and  $\alpha 7$  subtypes] affinities than pinnamine and ferruginine (Schwarz et al. 2003).

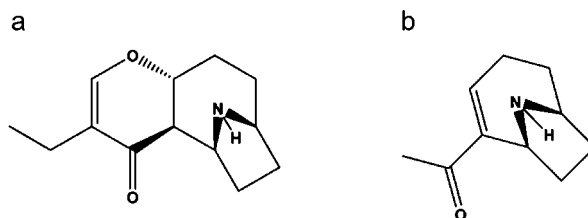


**Figure 18.6.** Chemical structures of pinnamine (a) and anatoxin-a (b).

## Prorocentrolides and Spiro-prorocentrimine: Fast-Acting Toxins with Unknown Molecular Targets

Various species of benthic marine dinoflagellates belonging to the genus *Prorocentrum* sp. are well known to be producers of diarrhetic shellfish poison (DSP) toxins, a group of lipid-soluble polyethers including okadaic acid and dinophysistoxins (for a review, see Vale et al. in the present book). In addition, two more polar lipid-soluble compounds, prorocentrolide and prorocentrolide B, have also been reported to be present in BuOH-soluble fractions of MeOH extracts from a strain of *P. lima*, common in sandy benthic sediments in British Columbia, and from the tropical dinoflagellate *P. maculosum* (originally referred to as *P. concavum*), respectively (Torigoe et al. 1988; Hu et al. 1996b). Interestingly, neither prorocentrolides nor related compounds could be identified in two DSP toxin-producing strains of *P. lima* obtained from various localities in eastern Canada (Hu et al. 1996b). This may indicate that cold water strains of *Prorocentrum* species, in contrast to those from warm-water, do not produce any of these toxins. More recently, a third novel polar lipid-soluble compound, spiro-prorocentrimine, was isolated and purified from a culture of an unknown benthic *Prorocentrum* species obtained from epiphytes of coral reef seaweeds in Taiwan (Lu et al. 2001). It is worth noting that although the involvement of DSP toxins in human intoxication has been largely documented, there is no evidence that any of the three polar compounds found in *Prorocentrum* sp. have been responsible for adverse effects in humans.

NMR and MS methods, as well as X-ray crystallography, have been used to achieve the structure elucidation of prorocentrolide, prorocentrolide B, and spiro-prorocentrimine, and to establish stereochemical details regarding some ring systems present within the structures (Torigoe et al. 1988; Hu et al. 1996b; Kusuoku et al. 1998; Lu et al. 2001). The data obtained reveal that these marine toxins all are closely related nitrogenous polyether macrocycles containing two similar macrocyclic rings, although spiro-prorocentrimine has a smaller macrolide moiety than the prorocentrolides (Fig. 18.7). The unique feature of spiro-prorocentrimine is the spiro-linked cyclic imine with an ortho, para-disubstituted cyclohexene, a distinctive functional group similar to the azaspiro[5.5]undecadiene subunit found in gymnodimines (see above). In contrast, both prorocentrolide and prorocentrolide B are characterized by a hexahydroisoquinoline ring system, sharing thus a common pharmacophore with the spirolides (see above and Wright et al. 1997). However, a sulfonyl substitution is present within

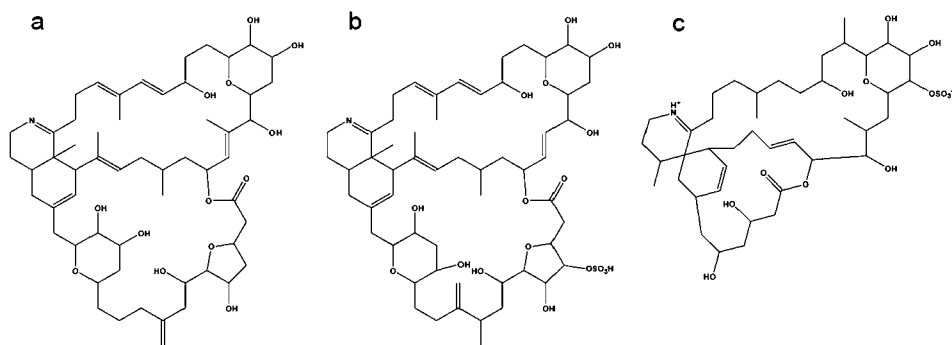


**Figure 18.7.** Chemical structures of prorocentrolide (a), prorocentrolide B (b), and spiro-prorocentrimine (c).

the structures of spiro-procentrimine and procentrolide B, on the 6-membered ether ring of the former and on the 5-membered cyclic ether within the macrolide moiety of the latter.

Procentrolide, procentrolide B and spiro-procentrimine have been shown to produce an acute toxicity by intraperitoneal administration to mice, spiro-procentrimine (LD<sub>99</sub> of 2,500 µg/kg) being about 6 times less toxic than the procentrolides (Torigoe et al. 1988; Hu et al. 1996b; Lu et al. 2001). Although no information on the symptoms of intoxication with spiro-procentrimine has been found, procentrolide and procentrolide B were reported to cause the characteristic “fast-acting” symptoms in the mouse bioassay. Hence, these polar toxins produce a rapid toxic response within a few minutes after their administration to mice, with death occurring shortly thereafter. Furthermore, these polar toxins display an “all or none” effect, since there are critical doses below which the animals recover completely. Interestingly, an earlier study has reported that the Et<sub>2</sub>O- and BuOH-soluble fractions of MeOH extracts, from the Caribbean *P. concavum*, cause different toxic responses in the mouse bioassay: the Et<sub>2</sub>O-soluble fraction killed mice in hours, whereas the more polar BuOH-soluble fraction induced a much more rapid animal death, i.e., within minutes (Tindall et al. 1984). It is likely that these two types of toxicity are accounted for by DSP toxins and procentrolides or related derivatives, respectively. Finally, procentrolide was shown to be toxic, *in vitro*, to the murine leukemia cell line L1210 but not to the fungus *Aspergillus niger*, the yeast *Candida rugosa*, or the bacterium *Staphylococcus aureus* (Torigoe et al. 1988). Although the toxicological and pharmacological effects of these fast-acting toxins are not yet understood, it is worth noting that they are not phosphatase inhibitors (Hu et al. 1996b), unlike their co-metabolites, the DSP toxins.

### Symbioimines: Inhibitors of Osteoclast Differentiation and Cyclooxygenase Activity

The symbiotic marine dinoflagellate *Symbiodinium* sp., which is a type of zooxanthellae found in a wide range of marine invertebrates (Rowan and Powers 1991), is known to produce a number of super-carbon-chain compounds, such as zooxanthellatoxins (Nakamura et al. 1995), zooxanthellamides (Onodera et al. 2004) and symbiodinolide (Washida et al. 2004). It is likely that these compounds in the symbiotic dinoflagellate may serve as a defence material which prevents digestion of their host animal. In addition, two marine iminium alkaloids, symbioimine and its congener neosymbioimine, were purified from a culture of *Symbiodinium* sp. isolated from the Okinawan marine acorn atworm *Amphiscolops* sp., and characterized (Kita et al. 2004 2005; Kita and Uemura 2005). Their structure and relative stereochemistry, deduced by spectroscopic and X-ray crystallographic analysis, show that these compounds are novel amphoteric cyclic iminium metabolites with a unique [6,6,6]-tricyclic iminium ring structure and an aryl sulfate moiety (Fig. 18.8). It is obvious, from a very recent synthetic study regarding (+/-)-deoxysymbioimine (Snider and Che 2006), that the formal synthesis and absolute stereochemistry of symbioimine and neosymbioimine molecules are in progress.

Studies related to the biological activity of symbioimine have been performed. They reveal that micromolar concentrations of this alkaloidal compound, while being not cytotoxic, exhibit potent and valuable pharmacological effects (Kita et al. 2004 2005; Kita and Uemura 2005). Indeed, symbioimine significantly inhibits the differentiation of murine monocytic cells (line RAW264) into osteoclasts, probably by neutralizing the receptor activator of nuclear factor-κB ligand. Thus, this effect makes symbioimine a potential antiresorptive agent for the prevention and treatment of osteoporosis in post-menopausal women. It is worth noting that other marine iminium alkaloids, the norzoanthamine and its



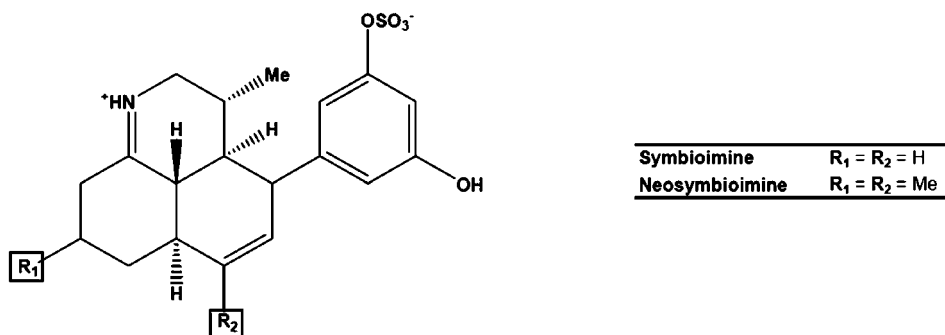


**Figure 18.8.** Chemical structures of symbioimines.

homologues isolated from the colonial zoanthid *Zoanthus* sp., were also notified to be good candidates for antiosteoporotic drugs (for reviews, see Kuramoto et al. 2004; Kita and Uemura 2005). Interestingly, on the basis of structural similarities between the molecules, a plausible precursor for these zoanthid alkaloids has been briefly reported to be zooxanthellamine, an iminium alkaloid purified from *Symbiodinium* sp. (Nakamura et al. 1998), which strongly suggests an algal origin for norzoanthamine and its homologues. Symbioimine has also been shown to inhibit, with moderate subtype specificity, the activity of cyclooxygenases (COX-1 and COX-2), the over expression of which has been linked to carcinogenesis and angiogenesis (Kita et al. 2004 2005; Kita and Uemura 2005). Thus, symbioimine may also be useful for the development of new anti-inflammatory drugs to treat COX-associated diseases, such as inflammatory diseases and cancer.

### Other Marine Cyclic Imines: Source of Potential Drugs and/or Biological Probes for Physiological Studies

The distinguishing feature of the compounds described above, i.e., the presence of a cyclic imine moiety within their molecular framework, has also been found in various toxins that occur naturally in other marine organisms, such as bacteria and sponges. Indeed, a non exhaustive list of these toxins, together with their origin and their biological activity, is given in Table 18.2. As the result of their significant and specific biological activity, most of them are often considered useful as potential drugs and/or biological probes for physiological studies.

### Conclusion

The monitoring of cyclic imines in areas where shellfish are gathered or commercially harvested appears essential for ensuring consumer's safety and confidence. To further enhance the safety of consumers, it is imperative to elucidate the mechanisms of action of a number of cyclic imines and to improve our knowledge of their metabolism, as well as their toxicological properties. Data presented in this review support this prospective approach, and this is particularly important since there is a global expansion of shellfish culture. Understanding the toxicology and pharmacology of phycotoxins containing cyclic imines will also permit identifying the risk, implement preventive measures, develop appropriate treatment strategies, and set the basis for regulation and policies.

**Table 18.2.** A nonexhaustive list of marine iminium alkaloids isolated from bacteria, sponges or ascidia, together with their biological activity

Alkaloid	Species	Behavior
A58365A and A58365B	<i>Streptomyces chromofuscus</i>	Inhibitors of angiotensin converting enzyme
Aburatubolactams	<i>Streptomyces</i> sp.	Inhibitors of superoxide anion generation
Amphotericin B	<i>Streptomyces nodosus</i>	Antifungal activity
Jenamidines A-C	<i>Streptomyces</i> sp.	Inhibitors of proliferation of myeloid leukemia cell line K-562
Salinosporamides	<i>Salinispora tropica</i>	Inhibitors of proteasome function and cytotoxic activity (tumor cells)
Tetrapetalones	<i>Streptomyces</i> sp.	Inhibitors of lipoxygenase
Anchinopeptolides A-D	<i>Anchinoe tenacior</i>	Ligands of somatostatin, bradykinin and neuropeptide Y receptors
Batzelladines A-E	<i>Batzella</i> sp.	Inhibitors of the binding of HIV gp-120 to CDA
Crambescidins	<i>Crambe crambe</i>	Antiviral and cytotoxic activities
Dysiherbaine	<i>Dysidea herbacea</i>	Agonist for non-NMDA type glutamate receptors
Ircinamine	<i>Ircinia</i> sp.	Activity is expected based on the reactivity of the thioester moiety
Manzamines	<i>Haplosclerida</i> sp./other sponges	Antiinflammatory, antifungal and anti-HIV-1 activities
Nakadomarin A	<i>Amphimedon</i> sp.	Cytotoxic and antimicrobial activities
Phloeodictines A-A1-A2	<i>Phloeodictyon</i> sp.	Antibacterial and cytotoxic activities (KB cells)
Ptilomycalin A	<i>Ptilocaulis spiculifer</i> <i>Ptilocaulis / Hemimycale</i> sp.	Inhibitor of Na <sup>+</sup> , K <sup>+</sup> , or Ca <sup>2+</sup> -ATPase Cytotoxic, antifungal, antimicrobial, and antiviral activities
Pyrinodemins A-B	<i>Amphimedon</i> sp.	Cytotoxic activity (murine leukemia and KB epidermoid carcinoma cells)
Sarains	<i>Haplosclerida</i> sp.	Anticancer, antibacterial, and insecticidal activities
Cylindricines A-K	<i>Clavelina cylindrica</i>	Cytotoxic activity

## Acknowledgements

Work in the author's laboratory has been supported in part by a grant from the European Union Sixth Framework Program FOOD-CT-2004-514055 (Detectox) and by a grant from the Direction des Systèmes de forces et de la Prospective. E. Girard was supported by a fellowship from Institut de Chimie des Substances Naturelles (ICSN-CNRS). The authors would like to thank Catherine Guilou (ICSN-CNRS, Gif-sur-Yvette) for helpful discussions, and Benoît Fleury (Institut de Chimie Moléculaire et des Matériaux d'Orsay, University of Paris-South, Orsay) for drawing the chemical structures of the present chapter.

## References

- Aasen, J., MacKinnon, S.L., LeBlanc, P., Walter, J.A., Hovgaard, P., Aune, T., and Quilliam M.A., 2005. Detection and identification of spirolides in Norwegian shellfish and plankton. *Chem Res Toxicol* 18, 509–515.

- Ahn, Y., Cardenas, G.I., Yang, J., and Romo, D. 2001. Studies toward gymnodimine: development of a single-pot Hua reaction for the synthesis of highly hindered cyclic imines. *Org Lett* 3, 751–754.
- Andrade, R.B., and Martin, S.F. 2005. Formal syntheses of (+/-)-pinnaic acid and (+/-)-halichlorine. *Org Lett* 7, 5733–5735.
- Arimoto, H., Hayakawa, I., Kuramoto, M., and Uemura, D. 1998. Absolute stereochemistry of halichlorine; a potent inhibitor of VCAM-1 induction. *Tetrahedron Lett* 39, 861–862.
- Balech, E., and Tangen, K. 1985. Morphology and taxonomy of toxic species in the tamarensis group (Dinophyceae): *Alexandrium excavatum* (Braarud) comb. nov. and *Alexandrium ostenfeldii* (Paulsen) comb. nov. *Sarsia* 70, 333–343.
- Biré, R. 2004. Contribution à l'appréciation du risque pour l'homme lié à la présence de phycotoxines neurologiques dans les coquillages—Mise en place d'un système de management de la qualité en recherche. Ph.D. thesis. University of Paris VII.
- Biré, R., Krysz, S., Frémy, J.M., Dragacci, S., Stirling, D., and Kharrat, R. 2002. First evidence on occurrence of gymnodimine in clams from Tunisia. *J Nat Toxins* 11, 269–275.
- Brimble, M.A., and Furkert, D.P. 2004. Synthesis of the 1,6,8-trioxadispiro[4.1.5.2]tetradec-11-ene ring system present in the spirolide family of shellfish toxins and its conversion into a 1,6,8-trioxadispiro[4.1.5.2]-tetradec-9-en-12-ol via base-induced rearrangement of an epoxide. *Org Biomol Chem* 2, 3573–3583.
- Carson, M.W., Kim, G., and Danishefsky, D.J. 2001. Total synthesis and proof of stereochemistry of natural and unnatural pinnaic acids: a remarkable long-range stereochemical effect in the reduction of 17-oxo precursors of the pinnaic acids. *Angew Chem Int Ed Engl* 40, 4453–4456.
- Cembella, A.D. 2003. Chemical ecology of eukaryotic microalgae in marine ecosystems. *Phycologia* 42, 420–447.
- Cembella, A.D., Bauder, A.G., and Lewis, N.I. 2001. Association of the gonyaulacoid dinoflagellate *Alexandrium ostenfeldii* with spirolide toxins in size-fractionated plankton. *J Plankton Res* 23, 1413–1419.
- Cembella, A.D., Bauder, A.G., Lewis, N.I., and Quilliam, M.A. 2001. Population dynamics and spirolide composition of the toxigenic dinoflagellate *Alexandrium ostenfeldii* in coastal embayments of Nova Scotia. In *Harmful Algal Blooms 2000*, ed. Hallegraeff, G.M., Blackburn, S.I., Bolch, C.J., and Lewis, R.J. Intergovernmental Oceanographic Commission of UNESCO, 173–176.
- Cembella, A.D., Lewis, N.I., and Quilliam, M.A. 1999. Spirolide composition of micro-extracted pooled cells isolated from natural plankton assemblages and from cultures of the dinoflagellate *Alexandrium ostenfeldii*. *Nat Toxins* 7, 197–206.
- . 2000. The marine dinoflagellate *Alexandrium ostenfeldii* (Dinophyceae) as the causative organism of spirolide shellfish toxin. *Phycologia* 39, 67–74.
- Cembella, A.D., Quilliam, M.A., Lewis, N.I., Bauder, A.G., and Wright, J.L.C. 1998. Identifying the planktonic origin and distribution of spirolides in coastal Nova Scotian waters. In *Harmful Algae*, ed. Reguera, B., Blanco, J., Fernández, M.L., and Wyatt, T. Xunta de Galicia and Intergovernmental Oceanographic Commission of UNESCO, 481–484.
- Chou, T., Haino, T., Kuramoto, M., and Uemura, D. 1996a. Isolation and structure of pinnatoxin D, a new shellfish poison from the Okinawan bivalve *Pinna muricata*. *Tetrahedron Lett* 37, 4027–4030.
- Chou, T., Kamo, O., and Uemura, D. 1996b. Relative stereochemistry of pinnatoxin A, a potent shellfish poison from *Pinna muricata*. *Tetrahedron Lett* 37, 4023–4026.
- Christie, H.S., and Heathcock, C.H. 2004. Total synthesis of (+/-)-halichlorine, (+/-)-pinnaic acid, and (+/-)-tauropinnaic acid. *Proc Natl Acad Sci USA* 101, 12079–12084.
- Clive, D.L., Yu, M., Wang, J., Yeh, V.S. and Kang, S. 2005. Synthetic chemistry of halichlorine and the pinnaic acids. *Chem Rev* 105, 4483–4514.
- Daly, J.W. 2005. Nicotinic agonists, antagonists, and modulators from natural sources. *Cell Mol Neurobiol* 25, 513–552.
- Falk, M., Burton, I.W., Hu, T., Walter, J.A. and Wright, J.L.C., 2001. Assignment of the relative stereochemistry of the spirolides, macrocyclic toxins isolated from shellfish and from the cultured dinoflagellate *Alexandrium ostenfeldii*. *Tetrahedron* 57, 8659–8665.
- Garthwaite, I., 2000. Keeping shellfish safe to eat: a brief review of shellfish toxins, and methods for their detection. *Trends Food Sci Technol* 11, 235–244.
- Gill, S., Murphy, M., Clausen, J., Richard, D., Quilliam, M., MacKinnon, S., LaBlanc, P., Mueller, R. and Pulido, O., 2003. Neural injury biomarkers of novel shellfish toxins, spirolides: a pilot study using immunochemical and transcriptional analysis. *Neurotoxicology* 24, 593–604.
- Gill, S.S., and Pulido, O. 2001. Glutamate receptors in peripheral tissues: current knowledge. *Toxicol Pathol* 29, 208–223.
- Haywood, A.J., Steidinger, K.A., Truby, E.W., Bergquist, P.R., Bergquist, P.L., Adamson, J. and Mackenzie, L., 2004. Comparative morphology and molecular phylogenetic analysis of three new species of the genus *Karenia* (Dinophyceae) from New Zealand. *J Phycol* 40, 165–179.
- Hjelmgaard, T., Sotofte, I. and Tanner, D., 2005. Total synthesis of pinnamine and anatoxin-a via a common intermediate. A caveat on the anatoxin-a endgame. *J Org Chem* 70, 5688–5697.

- Hu, T., Burton, I.W., Cembella, A.D., Curtis, J.M., Quilliam, M.A., Walter, J.A. and Wright, J.L.C., 2001. Characterization of spirolides A, C, and 13-desmethyl C, new marine toxins isolated from toxic plankton and contaminated shellfish. *J Nat Prod* 64, 308–312.
- Hu, T., Curtis, J.M., Oshima, Y., Quilliam, M.A., Walter, J.A., Watson-Wright, W.M. and Wright, J.L.C., 1995. Spirolides B and D, two novel macrocycles isolated from the digestive glands of shellfish. *J Chem Soc Chem Commun* 20, 2159–2161.
- Hu, T., Curtis, J.M., Walter, J.A. and Wright, J.L.C., 1996a. Characterization of biologically inactive spirolides E and F: identification of the spirolide pharmacophore. *Tetrahedron Lett* 37, 7671–7674.
- Hu, T., deFreitas, A.S., Curtis, J.M., Oshima, Y., Walter, J.A. and Wright, J.L., 1996b. Isolation and structure of prorocentrolide B, a fast-acting toxin from *Prorocentrum maculosum*. *J Nat Prod* 59, 1010–1014.
- Ishihara, J., Horie, M., Shimada, Y., Tojo, S. and Murai, A., 2002. Asymmetric construction of the azaspiro[5.6]dodec-9-ene system in marine natural toxins. *Synlett* 3, 403–406.
- Itoh, M., Kuwahara, J., Itoh, K., Fukuda, Y., Kohya, M., Shindo, M. and Shishido, K., 2002. Apoptosis-inducing activity of synthetic intermediates of halichlorine. *Bioorg Med Chem Lett* 12, 2069–2072.
- Johannes, J.W., Wenglowksy, S. and Kishi, Y., 2005. Biomimetic macrocycle-forming Diels-Alder reaction of an iminium dienophile: synthetic studies directed toward gymnodimine. *Org Lett* 7, 3997–4000.
- John, U., Cembella, A., Hummert, A., Elbrächter, M., Groben, R. and Medlin, L. 2003. Discrimination of the toxigenic dinoflagellates *Alexandrium tamarense* and *A. ostenfeldii* in co-occurring natural populations from Scottish coastal waters. *Eur J Phycol* 38, 25–40.
- John, U., Quilliam, M.A., Medlin, L., and Cembella, A.D. 2000. Spirolide production and photoperiod-dependent growth of the marine dinoflagellate *Alexandrium ostenfeldii*. In *Harmful Algal Blooms*, ed. Hallegraeff, G.M., Blackburn, S.I., Bolch, C.J., and Lewis, R.J. Paris: Intergovernmental Oceanographic Commission of UNESCO, 292–295.
- Kharrat, R., Servent, D., Girard, E., Ouanounou, G., and Molgó, J. 2006. Gymnodimine broadly targets nicotinic acetylcholine receptors. Submitted.
- Kigoshi, H., Hayashi, N. and Uemura, D., 2001. Stereoselective synthesis of pinnamine, an alkaloidal marine toxin from *Pinna muricata*. *Tetrahedron Lett* 42, 7469–7472.
- Kita, M., Kondo, M., Koyama, T., Yamada, K., Matsumoto, T., Lee, K.H., Woo, J.T., and Uemura, D. 2004. Symbioimine exhibiting inhibitory effect of osteoclast differentiation, from the symbiotic marine dinoflagellate *Symbiodinium* sp. *J Am Chem Soc* 126, 4794–4795.
- Kita, M., Ohishi, N., Washida, K., Kondo, M., Koyama, T., Yamada, K. and Uemura, D., 2005. Symbioimine and neosymbioimine, amphoteric iminium metabolites from the symbiotic marine dinoflagellate *Symbiodinium* sp. *Bioorg Med Chem* 13, 5253–5258.
- Kita, M., and Uemura, D. 2005. Iminium alkaloids from marine invertebrates: structure, biological activity, and biogenesis. *Chem Lett* 34, 454–459.
- Kong, K., Moussa, Z. and Romo, D., 2005. Studies toward a marine toxin immunogen: enantioselective synthesis of the spirocyclic imine of (–)-gymnodimine. *Org Lett* 7, 5127–5130.
- Kramer, R.M. and Sharp, J.D., 1997. Structure, function and regulation of Ca<sup>2+</sup>-sensitive cytosolic phospholipase A2 (cPLA2). *FEBS Lett* 410, 49–53.
- Kuramoto, M., Arimoto, H. and Uemura, D., 2004. Bioactive alkaloids from the sea: a review. *Mar Drugs* 1, 39–54.
- Kuramoto, M., Chou, T., Yamada, K., Chiba, T., Hayashi, Y. and Uemura, D., 1996. Halichlorine, an inhibitor of VCAM-1 induction from the marine sponge *Halichondria okadai* Kadota. *Tetrahedron Lett* 37, 3867–3870.
- Kusuoku, H., Murata, M. and Tachibana, K., 1998. Relative configuration of prorocentrolide. 74th National Meeting of the Chemical Society of Japan, Abstract 3E543.
- Lu, C.K., Lee, G.H., Huang, R. and Chou, H.N., 2001. Spiro-prorocentrimine, a novel macrocyclic lactone from a benthic *Prorocentrum* sp. of Taiwan. *Tetrahedron Lett* 42, 1713–1716.
- McCaulley, J.A., Nakagawa, K., Lander, P.A., Mischke, S.G., Semones, M.A. and Kishi, Y., 1998. Total synthesis of pinnatoxin A. *J Am Chem Soc* 120, 7647–7468.
- MacKenzie, L., Haywood, A., Adamson, J., Truman, P., Till, D., Seki, T., Satake, M. and Yasumoto, T., 1996. Gymnodimine contamination of shellfish in New Zealand. In *Harmful and Toxic Algal Blooms*, ed. Yasumoto T., Oshima Y., and Fukuyo Y. Paris: Intergovernmental Oceanographic Commission of UNESCO, 97–100.
- MacKenzie, L., Holland, P., McNabb, P., Beuzenberg, V., Selwood, A. and Suzuki, T., 2002. Complex toxin profiles in phytoplankton and Greenshell mussels (*Perna canaliculus*), revealed by LC-MS/MS analysis. *Toxicon* 40, 1321–1330.
- MacKenzie, A.L., Rhodes, L.L., Till, D., Chang, F.H., Kaspar, H., Haywood, A., Kapa, J. and Walker, B., 1995. A *Gymnodinium* sp. bloom and the contamination of shellfish with lipid soluble toxins in New Zealand, Jan–April 1993. In *Harmful Marine Algal Blooms*, ed. Lassus P., Arzul G., Erard-le Denn E., Gentien P., and Marcaillou-le Baut, C. Paris: Lavoisier Science Publishers, 795–800.

- McCauley, J.A., Nakagawa, K., Lander, P.A., Mischke, S.G., Semones, M.A. and Kishi, Y., 1998. Total synthesis of pinnatoxin A. *J Am Chem Soc* 120, 7467–7468.
- McKenzie, L., White, D., Yasukatsu, O., and Kapa, J. 1996. The resting cyst and toxicity of *Alexandrium ostenfeldii* (Dinophyceae) in New Zealand. *Phycologia* 35, 148–155.
- Metfies, K., Huljic, S., Lange, M. and Medlin, L.K., 2005. Electrochemical detection of the toxic dinoflagellate *Alexandrium ostenfeldii* with a DNA-biosensor. *Biosens Bioelectron* 20, 1349–1357.
- Miles, C.O., Wilkins, A.L., Stirling, D.J., and MacKenzie, A.L. 2000. New analogue of gymnodimine from a *Gymnodinium* species. *J Agric Food Chem* 48, 1373–1376.
- . 2003. Gymnodimine C, an isomer of gymnodimine B, from *Karenia selliformis*. *J Agric Food Chem* 51, 4838–4840.
- Moestrup, Ø., and Hansen, P.J. 1988. On the occurrence of the potentially toxic dinoflagellates *Alexandrium tamarense* (= *Gonyaulax excavata*) and *A. ostenfeldii* in Danish and Faroese waters. *Ophelia* 28, 195–213.
- Molgó, J., Benoit, E., Legrand, A.M. and Kreger, A.S., 1999. Bioactive agents involved in fish poisoning: an overview. In *Proceedings of the 5th Indo-Pacific Fish Conference*, ed. Noumea, S.B., and Sire, J.Y. *Soc Fr Ichtyol Paris*, 721–738.
- Molgó, J., Lemeignan, M. and Lechat, P., 1977. Effects of 4-aminopyridine at the frog neuromuscular junction. *J Pharmacol Exper Ther* 203, 653–663.
- Molgó, J., Lundh, H., and Thesleff, S. 1980. Potency of 3,4-diaminopyridine and 4-aminopyridine on mammalian neuromuscular transmission and the effects of pH changes. *Eur J Pharmacol* 61, 25–34.
- Munday, R., Towers, N.R., Mackenzie, L., Beuzenberg, V., Holland, P.T. and Miles, C.O., 2004. Toxicity of gymnodimine to mice. *Toxicon* 44, 173–178.
- Nagasawa, K.J., 2000. Total synthesis of pinnatoxin A. *J Synth Org Chem Jpn* 58, 877–886.
- Nakamura, H., Asari, T., Murai, A., Kan, Y., Kondo, T., Yoshida, K. and Ohizumi, Y., 1995. Zootoxanthellatoxin-A, a potent vasoconstrictive 62-membered lacton from a symbiotic dinoflagellate. *J Am Chem Soc* 117, 550–551.
- Nakamura, H., Kawase, Y., Maruyama, K. and Murai, A., 1998. Studies on polyketide metabolites of a symbiotic dinoflagellate, *Symbiodinium* sp.: a new C30 marine alkaloid, zootoxanthellamine, a plausible precursor for zoanthid alkaloids. *Bull Chem Soc Jpn* 71, 781–787.
- Nakamura, S., Inagaki, J., Kudo, M., Sugimoto, T., Obara, K., Nakajima, M. and Hashimoto, S., 2002. Studies directed toward the total synthesis of pinnatoxin A: synthesis of the 6,5,6-dispiroketal (BCD ring) system by double hemiketal formation/hetero-Michael addition strategy. *Tetrahedron* 58, 10353–10374.
- Nguyen-Huu, T., Dobbertin, A., Minic, J., Krejci, E., Duvaldestin, P. and Molgó, J., 2005. Cholinesterases and the resistance of the diaphragm to the effect of tubocurarine. *Anesthesiology* 103, 788–795.
- Onodera, K., Nakamura, H., Oba, Y. and Ojika, M., 2004. Zootoxanthellamide B, a novel large polyhydroxy metabolite from a marine dinoflagellate of *Symbiodinium* sp. *Biosci Biotechnol Biochem* 68, 955–958.
- Osborn, L., Hession, C., Tizard, R., Vassallo, C., Luhowskyj, S., Chi-Rosso, G. and Lobb, R., 1989. Direct expression cloning of vascular cell adhesion molecule 1, a cytokine-induced endothelial protein that binds to lymphocytes. *Cell* 59, 1203–1211.
- Pelc, M.J. and Zakarian A., 2005. An approach to the imine ring system of pinnatoxins. *Org Lett* 7, 1629–1631.
- Pulido, O., Richard, D., Quilliam, M., Clausen, J., Murphy, M., Smyth, P., Mueller, R and Gill, S., 2001. Toxicological Neuropathology from Domoic Acid to Spirolides—the Health Canada Experience. In *Proceedings of the Seventh Canadian Workshop on Harmful Marine Algae*, ed. Whyte, J.N.C. Canadian Technical Report of Fisheries Aquatic Sciences 2386, Fisheries and Oceans Canada, 36–44.
- Richard, D., Arsenault, E., Cembella, A. and Quilliam, M., 2001. Investigations into the toxicology and pharmacology of spirolides, a novel group of shellfish toxins. In *Harmful Algal Blooms 2000: Proceedings of the 9th International Conference on Harmful Microalgae*, ed. Hallegraeff, G.M., Blackburn, S.I., Bolch, C.J., and Lewis, R.J. Intergovernmental Oceanographic Commission of UNESCO, 383–386.
- Rosewater, J. 1961. The family Pinnidae in the Indo-Pacific. *Indo-Pacific Mollusca* 1, 53/501/632.
- Rowan, R., and Powers, D.A. 1991. A molecular genetic classification of zootoxanthellae and the evolution of animal-algal symbiosis. *Science* 251, 1348–1351.
- Sakamoto, S., Sakazaki, H., Hagiwara, K., Kamada, K., Ishii, K., Noda, T., Inoue, M., and Hirama, M. 2004. A formal total synthesis of (+)-pinnatoxin A. *Angew Chem Int Ed Engl* 43, 6505–6510.
- Schwarz, S., Kampchen, T., Tilotta, M.C., Gundisch, D., and Seitz, G. 2003. Synthesis and nicotinic binding studies on enantiopure pinnamine variants with an 8-azabicyclo[3.2.1]octane moiety. *Pharmazie* 58, 295–299.
- Seki, T., Satake, M., MacKenzie, L., Kaspar, H., and Yasumoto, T. 1995. Gymnodimine, a new marine toxin of unprecedented structure isolated from New Zealand oysters and the dinoflagellate, *Gymnodinium* sp. *Tetrahedron Lett* 36, 7093–7096.
- . 1996. Gymnodimine, a novel toxic imine isolated from the Foveaux Strait oysters and *Gymnodinium* sp. In *Harmful and Toxic Algal Blooms*, ed. Yasumoto, T., Oshima, Y., and Fukuyo, Y. Paris: Intergovernmental Oceanographic Commission of UNESCO, 95–498.

- Snider, B.B., and Che, Q. 2006. Synthesis of (+/-)-deoxysymbioimine using an intramolecular diels-alder reaction with an N-alkoxycarbonyl 2,3-dihydropyridinium cation as the dienophile. *Angew Chem Int Ed Engl* 45, 932–935.
- Stewart, M., Blunt, J.W., Munro, M.H.G., Robinson, W.T., and Hannah, D.J. 1997. The absolute stereochemistry of the New Zealand shellfish toxin gymnodimine. *Tetrahedron Lett* 38, 4889–4890.
- Stirling, D.J. 2001. Survey of historical New Zealand shellfish samples for accumulation of gymnodimine. *NZ J Mar Freshwat Res* 35, 851–857.
- Suthers, B.D., Jacobs, M.F., and Kitching, W. 1998. Synthesis and NMR profiling of dioxabicyclo[3.2.1]octanes related to pinnatoxin D. Confirmation of the relative stereochemistry about rings E and F. *Tetrahedron Lett.* 39, 2621–2624.
- Takada, N., Iwatsuki, M., Suenaga, K., and Uemura, D. 2000. Pinnamine, an alkaloidal marine toxin, isolated from *Pinna muricata*. *Tetrahedron Lett* 41, 6425–6428.
- Takada, N., Uemura, N., Suenaga, K., Chou, T., Nagatsu, A., Haino, T., Yamada, K., and Uemura, D. 2001a. Pinnatoxins B and C, the most toxic components in the pinnatoxin series from the Okinawan bivalve *Pinna muricata*. *Tetrahedron Lett.* 42, 3491–3494.
- Takada, N., Uemura, N., Suenaga, K., and Uemura, D. 2001b. Structural determination of pteriatoxins A, B and C, extremely potent toxins from the bivalve *Pteria penguin*. *Tetrahedron Lett* 42, 3495–3497.
- Tindall, D.R., Dickey, R.W., Carlson, R.D., and Morey-Gaines, G. 1984. Ciguatoxic dinoflagellates from the Caribbean Sea. In *Seafood Toxins*, ed. Ragelis, E.P. ACS Symposium Series 262. Washington DC: American Chemical Society, 225–240.
- Tong, C., Kuramoto, M., Otani, Y., Shikano, M., Yazawa, K. and Uemura, D., 1996. Pinnaic acid and taupinnaic acid: two novel fatty acids composing a 6-azaspiro[4.5]decane unit from the Okinawan bivalve *Pinna muricata*. *Tetrahedron Lett* 37, 3871–3874.
- Torigoe, K., Murata, M. and Yasumoto, T., 1988. Procentrolide, a toxic nitrogenous macrocycle from a marine dinoflagellate. *J Am Chem Soc* 110, 7876–7877.
- Toth, G.B., Noren, F., Selander, E. and Pavia, H., 2004. Marine dinoflagellates show induced life-history shifts to escape parasite infection in response to water-borne signals. *Proc Biol Sci* 271, 733–738.
- Trauner, D., Schwarz, J.B. and Danishefsky, S.J., 1999. Total synthesis of (+)-halichlorine: an inhibitor of VCAM-1 expression. *Angew Chem Int Ed Engl* 38, 3542–3545.
- Uemura, D., Chou, T., Haino, T., Nagatsu, A., Fukuzawa, S., Zheng, S.Z. and Chen, H., 1995. Pinnatoxin A: a toxic amphoteric macrocycle from the Okinawan bivalve *Pinna muricata*. *J Am Chem Soc* 117, 1155–1156.
- Van Dolah, F.M. 2000. Marine algal toxins: origins, health effects and their increased occurrences. *Environ Health Perspect* 108, 133–141.
- Washida, K., Ohishi, N., Kondo, M., Yamada, K., Koyama, T., Kita, M., and Uemura, D. 2004. Symbiodinolide, a novel super-carbon-chain compound isolated from the symbiotic dinoflagellate *Symbiodinium* sp. COE-RCMS Conf on Metals in Biology, Abstract P-61.
- White, J.D., Wang, G. and Quaranta, L., 2003. Studies on the synthesis of gymnodimine. Stereocontrolled construction of the tetrahydrofuran subunit. *Org Lett* 5, 4109–4112.
- Whittle, K., and Gallaher, S. 2000. Marine toxins. *Br Med Bull* 56, 236–253.
- Wright, J.L.C., Curtis, J.M., Hu, T., and Walter, J.A. 1997. The spirolides and procentrolide B: new additions to a rapidly growing group of fast-acting toxins with a common pharmacophore. 8th Int Conf on Harmful Algae, Abstract p. 215.
- Zhang, H.L., Zhao, G., Ding, Y., and Wu, B. 2005. An efficient and enantioselective approach to the azaspirocyclic core of alkaloids: formal synthesis of halichlorine and pinnaic acid. *J Org Chem* 70, 4954–4961.
- Zheng, S.Z., Huang, F.L., Chen, S.C., Tan, X.F., Zuo, J.B., Peng, J., and Xie, R.W. 1990. Pinnatoxins suspected in China. *Zhongguo Haiyang Yaowu (Chin J Mar Drugs)* 33, 33–35.



# Index

## A

Acetylacetonate, 9  
Acetylcholine, 119, 133, 142, 146–148, 243, 319, 321, 327  
Adda, ((2*S*,3*S*,8*S*,9*S*,-)3-amino-9-methoxy-2,6,8-trimethyl-10-phenyldeca-4,6-dienoic acid), 252, 253, 258, 261–264  
Alcohol, 2–9, 131, 132, 175, 290, 292, 302  
  allylic, 9  
  amino, 75, 121  
  axial, 290  
  bisallylic, 281  
  epoxy, 29, 285  
  homoallylic, 287  
  primary, 3, 5, 300, 302  
  propargyl, 285  
  secondary, 299, 302  
  tertiary, 3  
*Alexandrium*,  
  *ostenfeldi*, 322, 323  
  *tamarense*, 322  
Alkoxyallylstannane, 4  
Aminoalcohol, 75, 121  
Aminotransferase, 179  
*Anabaena*, 141–149, 252, 256  
Analysis,  
  calcium entry, 231  
  chemical, 105, 313  
  electric potential, 243  
  ELISA, 160, 261–264  
  histological, 234, 237–239, 315  
  HPLC, 89, 112, 150, 160, 174, 213, 260, 265, 266  
  Instrumental, 42  
  J-based configuration, 51, 53  
  mass spectrometry and,  
    anatoxin, 151  
    azaspiracid, 297  
    maitotoxin, 51  
    microcystin, 258  
    okadaic acid, 211  
    palytoxin, 78  
    pectenotoxin, 166, 167, 170  
    polycavernoside, 276

    yessotoxin, 196, 198  
  Mosher, 1  
  mRNA microarray, 232  
  NMR, 1, 51, 173, 327  
  NOE, 284  
  phosphatase, 263  
  pigment, 32  
  retrosynthetic, 21, 30  
  structural, 228  
  toxicological, 112  
  transcriptional, 323  
  X-Ray, 219, 224, 320  
9-anthryldiazomethane (ADAM), 205, 213, 215  
*Aphanizomenon*, 141, 254  
Apoptosis, and  
  anatoxin, 148  
  azaspiracid, 315  
  domoic acid, 238  
  maitotoxin, 66, 69, 70  
  pectenotoxin, 180, 181  
  polycavernoside, 279  
  yessotoxin, 204, 205  
Argopecten, 167  
Artemia, 106, 111, 112  
Aspergillus, 181, 329  
Austrovenus, 39, 319  
Azabicyclo, 122, 133  
Azaspiracid, 195, 199, 297–307, 311–317  
Azaspiro, 297, 326, 327, 328  
2,2'-azobisisobutyronitrile (AIBN), 3

## B

Biosynthesis, 22, 75, 160, 181  
Bis-triethylsilyl ether, 292  
Bis(trimethylsilyl)amide, 3  
Bond,  
  carbamate double, 127  
  C-C, 22, 25, 49, 129, 303, 304  
  cleavage, 51  
  C-O, 23, 25  
  covalent, 290  
  disconnection, 31



- Bond (*continued*)  
 disulfide, 55  
 double, 3, 9, 22, 49, 75, 76, 84, 128, 306  
 ether, 51  
 hydrogen, 302  
 olefinic, 290  
 reaction, 303  
 reconstruction, 51  
 terminal, 287  
 trans-double, 123  
 9-borabicyclo[3.2.1]nonane (9-BBN), 2, 287  
 Butanol, 76, 87, 110, 111, 144, 211
- C**
- Calmidazolium, 68  
*Calothrix*, 256  
 Calpain, 66, 70  
*Candida*, 181, 329  
*Cardium*, 311  
 Caspase, 66, 148, 180, 204, 205, 327  
   caspase-1, 70  
   caspase-3, 66, 69, 204, 280  
   caspase-9, 66  
 Catalyst, 4, 5, 124  
   Grubbs, 7, 131–132  
 Cell,  
   acidification, 102  
   adhesion molecule, 327  
   adhesion, 70  
   adrenal chromaffin, 148  
   breast MCF-7, 69  
   bronchial epithelial, 104  
   caco-2, 316  
   cardiac muscle, 58, 206  
   cerebellar granule (CGC), 99–103, 230, 231  
   CHO, 62, 67, 69  
   cis-platin resistant, 204  
   cyanobacterial, 266  
   death, 58, 64–70, 238, 257  
   dentate granule, 230–243  
   dinoflagellate, 112  
   Dinophysis, 160, 162, 218  
   endothelial bovine aortic, 62, 63, 66  
   endothelial, 148, 226  
   entorhinal, 236  
   epidermal, 104  
   epithelial, 205, 314  
   eukaryotic, 107, 181  
   excitable, 15, 33, 58–61, 66, 97, 99, 203  
   fibroblasts, 57, 62, 256  
   Gambierdiscus, 1, 47  
   ganglion, 242  
   glioma, 62–64, 70  
   HEK, 62, 63  
   HeLa, 204  
   hippocampal, 231–234, 238, 240  
   homeostasis, 96  
   hybridoma, 262  
   insulin secreting, 58, 62, 65  
   insulinoma HIT, 55, 58  
   intestinal, 107–110, 113, 181, 255  
   Jurkat, 315, 316  
   Karenia brevis, 19, 32, 42  
   kidney, 148  
   leukaemia, 326, 327  
   leukaemia HL-60, 62, 256  
   leukaemia P388, 326  
   liver hepatoma, 60, 65  
   liver HepG2, 180, 204, 205  
   liver KB, 180  
   liver, 41, 64  
   lymphocyte, 203, 315  
   lyophilized, 144, 145  
   macrophage BAC-1, 66, 70  
   mast cell, 38  
   membrane, 58  
   microglia, 239  
   mitral granule, 234, 244  
   monocyte, 70  
   mossy, 236, 237, 240, 241  
   mouse taste, 15, 16  
   muscle, 16, 97, 142  
   necrosis, 257  
   neuroblastoma, 13–15, 61, 70, 98, 104–108, 113,  
     180, 204, 279, 316  
   neuroendocrine GHC, 61  
   non-excitable, 58, 60, 61, 66  
   *Ostreopsis mascarenensis*, 110  
   *Ostreopsis ovata*, 87, 111, 112  
   *Ostreopsis siamensis*, 104–107  
   ouabain resistant, 98, 104  
   ovarian adenocarcinoma, 204  
   p-53 deficient, 181  
   proliferation, 58, 65  
   *Protoceratium*, 187, 188  
   *Protopteridium* 311  
   Purkinje, 205–207  
   pyramidal CA3, 230, 236–242

- rat pituitary GH3, 148
  - red blood, 55, 63, 96, 98
  - renal epithelial MDCK, 55, 59, 64
  - retinal, 243
  - skeletal muscle, 321
  - sperm, 65, 70
  - structure, 11
  - submandibular acini, 67
  - transfected, 60, 64
  - type, 55, 58, 64, 180
  - villi, 179
  - voltage-clamped, 59
  - wall, 19, 32
  - Xenopus* oocytes, 59
  - yeast, 97
  - Center, 1, 282, 290, 297, 300
  - Channel, 229
    - calcium, 38, 63–68, 97–101, 203, 230, 231, 324
    - cation, 55, 58, 62, 96, 99, 148, 227
    - heteromeric, 236
    - low-conductance, 98
    - open, 13, 95, 223, 228
    - potassium, 12, 15, 16, 321
    - sodium, 1, 12, 16, 22, 37, 38, 55, 101, 146, 203
    - stretch-activated, 65
    - voltage, 12
  - Chiral, 25, 127
    - amide, 125
    - base, 125
    - center, 76, 77, 167, 282
    - ether, 130
    - gas chromatography, 53
    - ligand, 124
    - pool, 120, 125
    - segment, 287
    - skeleton, 133
    - subunit, 281
    - sulfoxide, 300
    - syntheses, 120
  - Chirality, 124
  - Chlorotrimethylsilane, 3
  - Choline, 58, 60, 98, 103
  - Chondria, 75, 224
  - Chromatin, 148, 327
  - Chromium, 25, 133
  - Configuration, 49, 51, 53, 241, 282, 300
    - absolute and,
      - anatoxin, 120
      - cyclic imines, 326, 327
      - gambierol, 1, 4
      - maitotoxin, 53
      - pectenotoxin, 167
      - polycavernoside, 276, 281, 287, 290
      - yessotoxin, 191
    - cell-attached, 58
    - J-based, 51, 53
    - open, 37, 229
    - relative, 167, 191, 276
    - stereochemical, 120
  - Congestion, 11, 84, 147
  - Coupling, 3–6, 22–32, 51, 97, 174, 196, 263, 285
    - allosteric, 14
    - dithiane, 303
    - Gennari-Still, 287
    - Julia, 284
    - photoinduced, 22
    - Stille, 2–6, 126, 292, 303–308
    - Suzuki-Miyaura, 2, 4
  - Crassostrea*, 39, 107, 167, 311, 319
  - Cyclization, 121–131
    - 1,5 cyclooctanediol, 122
    - cyclooctene, 120, 121
    - epoxide, 25
    - hydroxydithioketal, 32
    - iminium ion, 120, 126, 129
    - ketone, 22, 123
    - transannular, 121, 123
  - Cyclooctanone, 126
  - Cyclooctene, 120, 121, 123
  - Cyclooctanediol, 122
  - Cyclooxygenase, 232, 241, 329, 330
  - Cylindrospermopsin, 251–254, 257, 265, 266
  - Cylindrospermum*, 141
  - Cytoskeleton, 107, 108, 113, 181, 316
- ## D
- Darlingia*, 327
  - Dehydrogenase, 179
  - Derivatization, 1, 215
  - Desilylation, 132, 287, 290, 292
  - Diarrhea, 10, 47, 88, 211, 242, 278, 313
  - Diastereoisomer, *see* isomer
  - Diastereomer, *see* isomer
  - 1,1-dibromoethane, 7
  - Dibromoolefin, 4
  - Diene, 5, 302
    - 1,5-cycloocta, 121
    - 2-ethoxy, 121

Diene (*continued*)

- azaspiro[5.5]undeca, 328
- conjugate, 79, 84, 276
- cyclohexyl, 279
- isopropyl, 279
- racemic, 298
- system and,
  - (*Z,Z*), 1
  - cyclic enol ether, 22, 32
- 6,8-difluoro-4-methylumbelliferylphosphate (DiFMUP), 260
- Difluorotrimethylsilicate, 4
- Digenea*, 224
- Dihydroanatoxin, 129
- Diisobutylaluminum, 4
- Dimethylsulphoxide (DMSO), 4, 6, 41, 49
- Dinophysis*, 162, 166
  - acuminata*, 160
  - acuta*, 218
  - fortii*, 160, 211, 215
  - spp.*, 160, 167, 168, 181, 213, 214, 218
- Dinophysistoxin, 159, 180, 206, 211–214, 315, 328
- Dioxirane, 7
- Dithiothreitol, 55, 58
- Duodenum, 179, 181

**E**

- ELISA, 160, 188, 196, 198, 217, 261–264
- Enantiomer, 124, 126–128, 167, 278, 284, 287, 307
- Enantioselective, 53, 120, 124, 125, 129, 281, 287
- Ensis*, 311
- Enzyme,
  - acetylcholinesterase, 119, 142, 146, 321
  - aminotransferase, 179
  - ASK, 70
  - calpain, 70
  - caspase, 66, 238
  - dehydrogenase, 66, 179
  - drug metabolism, 179
  - exonuclease, 204
  - NA-K ATPase, 95–98, 103
  - pectenotoxin hydrolysis, 162, 175
  - protease, 256
  - superoxide dismutase, 256
  - transglutaminase, 70
- Edema, 11, 147
- 7-epicylindrospersin, 254
- Exoskeleton, 111

**F**

- Fluo-3, 108
- Fura-2, 15, 66, 230
- Fura red, 108
- Furan, 298

**G**

- Gambierdiscus*, 1, 37, 47
- Gambierol, 1–16, 37
- Glutamate, 226–230, 236, 242, 243
  - efflux, 101
  - excitotoxicity, 230
  - receptor, 99–101, 223, 227, 230, 241, 242, 323
  - release, 100, 101, 223, 230, 236–239, 244
  - toxicity, 231
  - uptake, 239
- Glycoside, 6, 96, 287, 289

**H**

- Halichlorine, 326, 327
- Halichondria*, 211, 326
- Haliotis*, 319
- Hapaloshiphon*, 252
- Headache, 10, 313
- Hermodice*, 95
- Hexamethyldisilazane, 4
- Homoanatoxin, 141, 146
- Homotropane, 120, 125, 127, 133
- Hypertensión, 10

**I**

- Ileum, 255
- Iodoolefin, 5
- Iodotrimethylsilane, 4, 121, 129
- Isomer, 6, 7, 76
  - acid-catalysed, 168, 174
  - anatoxin, 125, 128, 150
  - anti, 53
  - azaspiracid, 298, 300, 302, 307
  - cis/trans, 75
  - diastereoisomer, 121, 174
  - diastereomer, 4, 8, 298, 300, 304
  - dinophysistoxin, 213

domoic acid, 224  
 endo/exo, 120  
 gymnodimine, 320  
 microcystin, 253  
 okadaic acid, 213  
 optic, 67  
 pectenotoxin, 166–177  
 photoisomer, 123  
 pinnatoxin, 325  
 polycavernoside, 285, 290, 292  
 spirolide, 321  
 stereoisomer, 3, 53, 75, 82, 128, 253, 290, 298  
 syn, 53  
 yessotoxin, 191, 198  
 Iso-propylanatoxin, 133  
 Itching, 10

## J

Jejunum, 181

## K

*Karenia*, 19, 32, 320  
 Kinase,  
   ASK, 70  
   calmodulin-dependent protein, 70  
   ERK MAP, 69, 103  
   glucocorticoid inducible, 232  
   inhibitor, 180  
   inositol-3, 64  
   JNK MAP, 103  
   MAPK, 103  
   p38 MAPK, 68, 70  
   PKA, 224–225  
   PKC, 103, 148  
   protein kinase II, 241  
   protein, 55, 103  
   Ser-Thr protein, 69, 103  
   tyrosine, 69

## L

Lactate dehydrogenase (LDH), 66, 68, 70  
 Lethal, 147, 179, 181  
   activity, 147  
   dose and,

  anatoxin, 142  
   cylindrospermopsin, 257  
   domoic acid, 234  
   gymnodimine, 320, 323  
   hepatotoxin, 257  
   homoanatoxin, 141  
   maitotoxin, 47, 55  
   mascarenotoxin, 87  
   microcystin, 255–259  
   ostreocin, 84, 105  
   palytoxin, 76  
   pectenotoxin, 178, 179  
   polycavernoside, 276, 278  
   spiro-prorocentrimine, 329  
   yessotoxin, 206  
 minimal dose, 1, 9, 177–179, 279, 293, 313  
 nonlethal, 225  
 oral dose, 313  
 sublethal, 106, 147, 151

## M

Mascarenotoxin, 87–89, 104, 110, 111  
 Metathesis, *see also* reaction  
   alkene, 131  
   cross, 131  
   enol-ether, 7  
   enyne, 120, 131  
   ring-closing, 4, 30, 131, 196  
 Methanol, and  
   anatoxin, 121, 128, 143, 144  
   brevetoxin, 20, 40, 41  
   cylindrospermopsin, 266  
   deuterated, 80  
   microcystin, 267  
   ostreocin, 84, 87  
   palytoxin, 76  
   pectenotoxin, 173, 195, 211  
   polycavernoside, 292  
 Method,  
   Ateeq and Simpkins, 133  
   Bignami, 106  
   biological, 258  
   carbodiimide, 261  
   conjugation, 261, 262  
   DeOlmos, 239  
   detection, 160, 211, 251, 252, 257, 314, 320  
   ELISA, 160, 261–264  
   extraction, 266

Method (*continued*)

- gas chromatography (GC), 264
- HPLC, 213, 217, 257, 260–268
- isolation, 51, 144, 178
- LC-MS, 151, 160, 162, 195, 213, 215, 266
- Mori, 131
- Nicolaou, 290
- NMR, 51, 326
- Pandey, 133
- PCR, 32
- purification, 168
- Rapoport, 124, 129
- Royer, 133
- Rychnovsky, 4
- sample preparation, 160
- screening, 257, 261
- SPATT, 162
- Speckamp, 131
- spectroscopic, 51
- Stjernlöf, 122
- synthesis, 5, 22, 29–32, 53, 119, 121, 174, 326
- thin layer chromatography (TLC), 264
- toxicity, 151
- Yamaguchi, 7, 290
- Methoxy-*a*-trifluoromethylphenylacetic acid (MTPA), 1
- Methylmagnesium, 3, 124
- Microcystis*, 141, 145, 251, 252, 256, 260, 263
- Motuporin, 253
- Mytilus*,
  - coruscus*, 166
  - edulis*, 107, 297, 308, 311, 321
  - galloprovincialis*, 166, 312, 319

**N**

- Nausea, 10, 37, 47, 113, 177, 211, 242, 313
- Necrosis, 66, 69, 179, 206, 234, 238, 256, 257, 315
- Nickel, 25
- N*-methylmorpholine *N*-oxide (NMO), 2
- Nodularia*, 252, 256, 261
- Nodularin, 145, 149, 251–267
- Nostoc*, 252, 256
- N*-tosylanatoxin, 129–132

**O**

- Oscillatoria*, see *Planktothrix*
- O-silylation, 281

- Ostreocin, 75, 82, 84, 87, 89, 95, 104–113
- Ostreopsis*, 76
  - heptagona*, 83, 84
  - lenticularis*, 83, 106
  - mascarenensis*, 83, 87, 88, 89, 110, 111
  - ovata*, 83, 87, 111, 112
  - siamensis*, 83, 84, 104–107, 111
  - spp.*, 82, 83, 89, 104, 106, 113
- Ouabain, 84, 87, 96–98, 104, 107, 112
- Ovatatoxin, 87
- Oxazolidinone, 281
- Oxepane, 22, 23, 25
- Oxonium, 5
- Oxonol, 13, 99, 108, 113

**P**

- Pacopecten*, 321
- Palladium, 3, 32, 123, 124, 292
- Palythoa*, 75–77, 95
  - sp.*, 79
  - toxica*, 95, 103, 111
  - tuberculosa*, 75, 82, 87
- Pandaros*, 211
- Paphies*, 319
- Paralysis, 10, 19, 33, 38, 111, 142, 315, 320
- Patinopecten*, 159, 187
- Pecten*,
  - fumatus*, 167
  - maximus*, 166, 311
  - novaezealandiae*, 107, 175, 319
- Penicillium*, 181
- Perna*, 107, 319
- Pinna*, 167, 324, 326, 327
- Phormidium*, 256
- Phosphatase, 179–180, 203, 217, 219, 251, 256–262, 315, 329
  - glucose-6, 179
- Phosphodiesterase, 63, 203
- Pinnaic acid, 324, 326, 327
- Pinnamine, 324, 327
  - 5-*epi*-, 327
- Pinnatoxin, 320, 324–326
- Piridinium, 5, 122
- Planktothrix*, 142, 144–146, 252, 260
- Platypodiella*, 95
- Polycyclization, 22
- Pteria*, 324
- Pteriatoxin, 320, 324–326
- Pyroglutamate, 127, 132
- p*-methoxybenzyl, 2

- p*-methoxybenzylidene, 281  
 Polycavernoside, 275, 276–292  
 Polycyclic,  
   backbone, 13  
   compound, 123  
   ether, 1, 4, 6, 9, 21, 30, 187, 196  
 Polyether, 12, 13, 19, 37, 211, 297, 328  
   disulphated, 188  
   ionophore, 22  
   ladder-shaped, 199  
   macrocyclic, 159  
   natural, 33  
   octacyclic, 1, 3, 5, 9  
 Prorocentrolide, 320, 328, 329  
 Prorocentrum, 111, 211, 213, 214,  
   218, 328  
 Protocol, *see also* method, *see also* reaction.  
   carbodiimide conjugation, 261  
   Ito-Saegusa, 3  
   Murai, 290  
   Takai-Utimoto, 7  
   Uenishi, 4  
   Yamaguchi, 292  
   Yamamoto, 8  
   Yasumoto, 195  
*Protoberidinium*,  
   *crassipes*, 311  
   *spp.*, 160  
*Pseudo-nitzschia*, 223, 224  
 Pyran, 25, 286  
 Pyranose, 287, 290  
 Pyridine, 4, 76, 292, 300, 301  
   4-amino, 321  
   3,4-diamino, 321
- R**
- Racemic, 120–126, 129, 130, 131, 133,  
   147, 298  
 Reaction, 4, 7, 9, 32, 125, 130, 173–174, 260–263,  
   298, *see also* method  
   acrosome, 65, 70  
   addition, 25, 29, 32  
   aldol, 287  
   allylsilane, 129  
   aminocarbonylation, 123  
   bond-forming 303, 304, *see also*  
     Stille reaction  
   cell, 69  
   contraction, 127  
   Corey-Fuchs, 3  
   cyclization, 32, 129, 130  
   cyclopropanation, 125  
   Diels-Alder, 53, 174  
   double, 30  
   energy, 292  
   enozilation, 125  
   expansion, 125  
   Horner-Wadsworth-Emmons (HWE), 25  
   hydrolysis, 175  
   iodoetherification, 302  
   lactonization, 29  
   metathesis, 4, 5, 131, 132  
   Mitsunobu, 302  
   monitoring, 278  
   neurosensory, 10  
   periodate, 49, 51  
   peroxidase, 262  
   polymerase chain (PCR), 256,  
     *see also* method  
   Reformatsky, 29  
   sequence, 128, 129  
   silver, 287  
   sodium hydride, 289  
   spiroaminal, 302  
   Staudinger, 302  
   Stille, *see* coupling  
   Suzuki-Miyaura, *see* coupling  
   Wittig, 23, 25  
   zip type, 22  
 Receptor,  
   acetylcholine, 119, 133, 146–149,  
     319, 321  
   AMPA, 227, 229, 241–243  
   autoreceptor, 236, 237  
   benzodiazepine, 238  
   domoic acid, 223, 226  
   glutamate, 99–101, 223, 227–229, 242  
   ionotropic, 223, 229  
   kainate, 223, 226–230, 236, 238  
   maitotoxin, 55, 62–70  
   muscarinic, 323  
   nicotinic, 132, 148, 327  
   NMDA, 227, 230–232, 241  
   nuclear factor- $\kappa$ B, 329  
   palytoxin, 98  
   phagocytic, 239  
   postsynaptic, 237  
   sodium channel, 12, 37  
   transient, 58, 60  
   YTX, 205

## S

- Saponin, 76  
 Scopolamine, 243  
 Silylation, 285, 287  
 Silyl, 4, 132, 284  
 Skeleton, 121–123, 126  
   bicycle, 130  
   polyether, 1  
   ring, 32, 119, 123  
   semi-rigid, 133  
 Spirolide, 206, 320–328  
 Spirocenter, 298  
 Spiro-procentrimine, 328, 329  
 Staphylococcus, 329  
 Stereocenter, 300  
 Steroid, 96, 97  
 Stereoisomer, *see* isomer  
 Stereoselectivity, 5, 284, 326  
 Structure,  
   -activity, and  
     anatoxin, 126, 133, 142, 147  
     brevetoxin, 203  
     gambierol, 9  
     pectenotoxin, 175, 177  
     yessotoxin, 196, 198, 205  
   cell, 11  
   chemical, and  
     ADDA, *see* Adda  
     anatoxin, 119–126, 130, 134, 141  
     azaspiracid, 297–308  
     brevetoxin, 19–22, 30–32  
     gambierol, 1, 4, 9, 13  
     gymnodimine, 319, 320  
     halichlorine, 326  
     maitotoxin, 49–53, 62  
     mascarenotoxin, 89, 111  
     microcystin, 252, 258, 263  
     motuporin, 253  
     nodularin, 253  
     okadaic acid, 211, 213, 219  
     ostreocin, 84, 87, 105, 107, 112  
     ovatatoxin, 87  
     palytoxin, 75–77, 89  
     pectenotoxin, 167–174  
     pinnaic acid, 326, 327  
     pinnamine, 327  
     pinnatoxin, 324  
     polycavernoside, 276, 279, 281, 286  
     procentrolide, 328, 329  
     spirolide, 321  
     spiropurocentrimine, 328, 329  
     yessotoxin, 187–191, 196, 204, 205  
   dendritic, 242  
   limbic, 238  
   mitochondria, 41  
   polyether, 12  
   tetrameric, 227, 229  
 Submucosa, 11  
 Symbioimine, 329, 330  
*Symbiodinium*, 329, 330  
 Synthesis,  
   adriatoxin, 196  
   anatoxin, 120–133, 142, 150, and  
     Campbell, 123  
     Gallagher, 134  
     Ham, 123  
     Martin, 132  
     Rapoport, 126  
     Simpkins, 125  
     Trost, 124  
   azaspiracid, 297–308  
   brevetoxin, 21, 22, 25, 29, 32, 35, and  
     Kadota, 30  
     Matsuo, 29  
     Nicolaou, 22, 31  
     polycyclic ether, 30  
 cAMP, 203  
 disaccharide, 287  
 DNA, 181  
 domoic acid, 224  
 gambierol, 1, 2, 4, and  
   ABCD-ring, 8, 9  
   diverted, 9  
   Mori, 8  
   octacycle, 3  
   Rainier, 6, 8  
   Sasaki, 2, 5  
   Yamamoto-Kadoka, 4, 8  
 glutathione, 257  
 gymnodimine, 320, 321  
 halichlorine, 326  
 ionophore, 22  
 learning, 241  
 maitotoxin, 53  
 microcystin, 256  
 palytoxin, 75–77, and  
   Kishi, 75, 82  
   protein, 103  
 pectenotoxin, 159, 160, 167, 174



pinnaic acid, 326, 327  
pinnatoxin, 324  
polycavernoside, 276, 281, 290, 292  
polyepoxides, 22  
protein, 257  
yessotoxin, 187, 196

## T

Tapes, 311  
Tachycardia, 10  
Tauropinnaic acid, 326, 327  
*Tert*-butyldimethylsilyl (TBDMS), 4  
Tetrahydrofuran, 22, 276, 281, 320  
Tetrahydropyran, 25, 276, 285, 287  
Tetramethylammonium, 98, 284  
Tetra-*n*-butylammonium fluoride (TBAF), 4  
Tetra-*n*-propylammonium perruthenate (TPAP), 2  
*Tiostrea*, 319  
Titanium, 7  
Triene,  
  conjugate, 276  
  isopropyl, 279  
  moiety, 276  
  side chain, 1, 2, 4, 5, 8, 9  
Triethylsilane, 9, 287  
Triflate, 8, 121, 196  
  enol, 27, 31, 121, 125  
  triisopropylsilyl, 287

  vinyl, 302  
  zinc, 2  
Triisopropylsilyl, 287  
Trimethylsilyldiazomethane (TMSCHN<sub>2</sub>), 120  
Trimethylsilyl enol ether, 121  
Tropane, 120, 125, 131  
Trypsin, 55

## V

Venus, 167  
Vinyl,  
  bromide, 4, 287  
  carbamate, 127  
  carbon, 129  
  ether, 125, 126  
  ethoxy-tributyltin, 126  
  iodide, 8, 279, 290, 292  
  stannane, 4, 5, 293, 302, 304, 306  
  sulfide, 290  
  sulfone, 299  
  triflate, 302  
Vomiting, 10, 38, 47, 177, 211, 234, 242, 313

## Z

Zoanthus, 95, 330